



Hashemite Kingdom of Jordan



Jordan Journal
of



Biological Sciences

An International Peer-Reviewed Scientific Journal

Financed by the Scientific Research and Innovation Support Fund



<http://jjbs.hu.edu.jo/>

المجلة الأردنية للعلوم الحياتية Jordan Journal of Biological Sciences (JJBS)

<http://jjbs.hu.edu.jo>

Jordan Journal of Biological Sciences (JJBS) (ISSN: 1995–6673 (Print); 2307-7166 (Online)): An International Peer- Reviewed Open Access Research Journal financed by the Scientific Research and Innovation Support Fund, Ministry of Higher Education and Scientific Research, Jordan and published quarterly by the Deanship of Scientific Research , The Hashemite University, Jordan.

Editor-in-Chief

Professor Atoum, Manar F.

Molecular Biology and Genetics,
The Hashemite University

Assistant Editor

Dr. Muhannad, Massadeh I.

Microbial Biotechnology,
The Hashemite University

Editorial Board (Arranged alphabetically)

Professor Al-Eitan, Laith

Biotechnology and Genetic Engineering
Jordan University of Science and Technology

Professor Al-Khateeb , Wesam M.

Plant Genetics and Biotechnology
Yarmouk University

Professor Al-Ghzawi , Abdul Latief A.

Plant biotechnology
The Hashemite University

Professor Al-Najjar , Tariq Hasan Ahmad.

Marine Biology
The University of Jordan/ Aqaba

Professor Khleifat, Khaled M.

Microbiology and Biotechnology
Mutah University

Professor Odat , Nidal

Plant biodiversity
Al Balqa Applied University

Associate Editorial Board

Professor Al-Hindi, Adnan I.

Parasitology
The Islamic University of Gaza, Faculty of Health
Sciences, Palestine

Dr Gammoh, Noor

Tumor Virology
Cancer Research UK Edinburgh Centre, University of
Edinburgh, U.K.

Professor Kasperek, Max

Natural Sciences
Editor-in-Chief, Journal Zoology in the Middle East,
Germany

Professor Krystufek, Boris

Conservation Biology
Slovenian Museum of Natural History,
Slovenia

Dr Rabei, Sami H.

Plant Ecology and Taxonomy
Botany and Microbiology Department,
Faculty of Science, Damietta University, Egypt

Professor Simerly, Calvin R.

Reproductive Biology
Department of Obstetrics/Gynecology and
Reproductive Sciences, University of
Pittsburgh, USA

Editorial Board Support Team

Language Editor

Dr. Shadi Neimneh

Publishing Layout

Eng.Mohannad Oqdeh

Submission Address

Professor Atoum, Manar F

The Hashemite University
P.O. Box 330127, Zarqa, 13115, Jordan
Phone: +962-5-3903333 ext.4147
E-Mail: jjbs@hu.edu.jo

المجلة الاردنية للعلوم الحياتية
Jordan Journal of Biological Sciences (JJBS)
<http://jjbs.hu.edu.jo>

International Advisory Board (Arranged alphabetically)

Professor Abdelaziz M. Hussein
Mansoura University, Egypt

Professor Adnan Bashir Al-lahham
German Jordanian University, Jordan

Professor Ahmed Amri
genetic resources ICARDA in Morocco, Morocco

Professor Amir Menwer Al-Hroob
Al-Hussein Bin Talal University, Jordan

Professor Elif Demirkan
Bursa Uludag University Turkey, Turkey

Professor Erhan Nurettin ÜNLÜ
Turkey Dicle University, Turkey

Professor Hassan Mohammed M. Abd El-Rahman Awad
National Research Centre, Egypt

Professor Khalid M. Al-Batayneh
Yarmouk University, Jordan

Professor Laith Abd Jalil Jawad
School of Environmental and Animal Sciences, Unitec Institute of
Technology Auckland, New Zealand

Professor Maroof A. Khalaf
Jordan University/ Aqaba, Jordan

Professor Mohammed H. Abu-Dieyeh
Biological and Environmental Sciences, Qatar University, Qatar

Professor Nour Shafik Emam El-Gendy
Egyptian Petroleum Research Institute, Egypt

Professor Omar F. Khabour
Jordan University of Science and Technology, Jordan

Professor Saleem Hmood Aladaileh
Al-Hussein Bin Talal University, Jordan

Professor Walid Al Zyoud
German Jordanian University, Jordan

Professor Abhik Gupta
School of Environmental Sciences, Assam University, India

Professor Ahmed Deaf Allah Telfah
Leibniz-Institut für Analytische Wissenschaften-, Germany

Dr. Amalia A Tsiami
University of West London, London

Professor David Modry
Masaryk University, Science Department, Czech

Professor Emad Hussein Malkawi
Yarmouk University, Jordan

Professor Gottfried Hartmut Richard Jetschke
Friedrich-Schiller-University of Jena, Germany

Professor Ihsan Ali Mahasneh
Al al-Bayt University, Jordan

Professor Khalid Majid Hameed
Dept. of Biological Sciences, Duke University, USA

Dr Maizirwan Bin Muhammad Mel
International Islamic University Malaysia, Malaysia

Professor Mohamed Emara
Chartered Management Institute, UK

Professor Nabil Joseph Awadalla Girgis
King Khalid University, Saudi Arabia

Professor Olga Anne
Marine Technology and Natural Sciences of Klaipėda University,
Lithuania

Dr Roy Hendroko Setyobudi
University of Muhammadiyah, Indonesia

Dr. Salem M Akel
St. Jude's Children's Research Hospital, USA

Professor Yacob Hassan Yacob
Al al-Bayt University, Jordan

Instructions to Authors

Scopes

Study areas include cell biology, genomics, microbiology, immunology, molecular biology, biochemistry, embryology, immunogenetics, cell and tissue culture, molecular ecology, genetic engineering and biological engineering, bioremediation and biodegradation, bioinformatics, biotechnology regulations, gene therapy, organismal biology, microbial and environmental biotechnology, marine sciences. The JJBS welcomes the submission of manuscript that meets the general criteria of significance and academic excellence. All articles published in JJBS are peer-reviewed. Papers will be published approximately one to two months after acceptance.

Type of Papers

The journal publishes high-quality original scientific papers, short communications, correspondence and case studies. Review articles are usually by invitation only. However, Review articles of current interest and high standard will be considered.

Submission of Manuscript

Manuscript, or the essence of their content, must be previously unpublished and should not be under simultaneous consideration by another journal. The authors should also declare if any similar work has been submitted to or published by another journal. They should also declare that it has not been submitted/ published elsewhere in the same form, in English or in any other language, without the written consent of the Publisher. The authors should also declare that the paper is the original work of the author(s) and not copied (in whole or in part) from any other work. All papers will be automatically checked for duplicate publication and plagiarism. If detected, appropriate action will be taken in accordance with International Ethical Guideline. By virtue of the submitted manuscript, the corresponding author acknowledges that all the co-authors have seen and approved the final version of the manuscript. The corresponding author should provide all co-authors with information regarding the manuscript, and obtain their approval before submitting any revisions. Electronic submission of manuscripts is strongly recommended, provided that the text, tables and figures are included in a single Microsoft Word file. Submit manuscript as e-mail attachment to the Editorial Office at: JJBS@hu.edu.jo. After submission, a manuscript number will be communicated to the corresponding author within 48 hours.

Peer-review Process

It is requested to submit, with the manuscript, the names, addresses and e-mail addresses of at least 4 potential reviewers. It is the sole right of the editor to decide whether or not the suggested reviewers to be used. The reviewers' comments will be sent to authors within 6-8 weeks after submission.

Manuscripts and figures for review will not be returned to authors whether the editorial decision is to accept, revise, or reject. All Case Reports and Short Communication must include at least one table and/ or one figure.

Preparation of Manuscript

The manuscript should be written in English with simple lay out. The text should be prepared in single column format. Bold face, italics, subscripts, superscripts etc. can be used. Pages should be numbered consecutively, beginning with the title page and continuing through the last page of typewritten material.

The text can be divided into numbered sections with brief headings. Starting from introduction with section 1. Subsections should be numbered (for example 2.1 (then 2.1.1, 2.1.2, 2.2, etc.), up to three levels. Manuscripts in general should be organized in the following manner:

Title Page

The title page should contain a brief title, correct first name, middle initial and family name of each author and name and address of the department(s) and institution(s) from where the research was carried out for each author. The title should be without any abbreviations and it should enlighten the contents of the paper. All affiliations should be provided with a lower-case superscript number just after the author's name and in front of the appropriate address.

The name of the corresponding author should be indicated along with telephone and fax numbers (with country and area code) along with full postal address and e-mail address.

Abstract

The abstract should be concise and informative. It should not exceed **350 words** in length for full manuscript and Review article and **150 words** in case of Case Report and/ or Short Communication. It should briefly describe the purpose of the work, techniques and methods used, major findings with important data and conclusions. No references should be cited in this part. Generally non-standard abbreviations should not be used, if necessary they should be clearly defined in the abstract, at first use.

Keywords

Immediately after the abstract, **about 4-8 keywords** should be given. Use of abbreviations should be avoided, only standard abbreviations, well known in the established area may be used, if appropriate. These keywords will be used for indexing.

Abbreviations

Non-standard abbreviations should be listed and full form of each abbreviation should be given in parentheses at first use in the text.

Introduction

Provide a factual background, clearly defined problem, proposed solution, a brief literature survey and the scope and justification of the work done.

Materials and Methods

Give adequate information to allow the experiment to be reproduced. Already published methods should be mentioned with references. Significant modifications of published methods and new methods should be described in detail. Capitalize trade names and include the manufacturer's name and address. Subheading should be used.

Results

Results should be clearly described in a concise manner. Results for different parameters should be described under subheadings or in separate paragraph. Results should be explained, but largely without referring to the literature. Table or figure numbers should be mentioned in parentheses for better understanding.

Discussion

The discussion should not repeat the results, but provide detailed interpretation of data. This should interpret the significance of the findings of the work. Citations should be given in support of the findings. The results and discussion part can also be described as separate, if appropriate. The Results and Discussion sections can include subheadings, and when appropriate, both sections can be combined.

Conclusions

This should briefly state the major findings of the study.

Acknowledgment

A brief acknowledgment section may be given after the conclusion section just before the references. The acknowledgment of people who provided assistance in manuscript preparation, funding for research, etc. should be listed in this section.

Tables and Figures

Tables and figures should be presented as per their appearance in the text. It is suggested that the discussion about the tables and figures should appear in the text before the appearance of the respective tables and figures. No tables or figures should be given without discussion or reference inside the text.

Tables should be explanatory enough to be understandable without any text reference. Double spacing should be maintained throughout the table, including table headings and footnotes. Table headings should be placed above the table. Footnotes should be placed below the table with superscript lowercase letters. Each table should be on a separate page, numbered consecutively in Arabic numerals. Each figure should have a caption. The caption should be concise and typed separately, not on the figure area. Figures should be self-explanatory. Information presented in the figure should not be repeated in the table. All symbols and abbreviations used in the illustrations should be defined clearly. Figure legends should be given below the figures.

References

References should be listed alphabetically at the end of the manuscript. Every reference referred in the text must be also present in the reference list and vice versa. In the text, a reference identified by means of an author's name should be followed by the year of publication in parentheses (e.g.(Brown,2009)). For two authors, both authors' names followed by the year of publication (e.g.(Nelson and Brown, 2007)). When there are more than two authors, only the first author's name followed by "*et al.*" and the year of publication (e.g. (Abu-Elteen *et al.*, 2010)). When two or more works of an author has been published during the same year, the reference should be identified by the letters "a", "b", "c", etc., placed after the year of publication. This should be followed both in the text and reference list. e.g., Hilly, (2002a, 2002b); Hilly, and Nelson, (2004). Articles in preparation or submitted for publication, unpublished observations, personal communications, etc. should not be included in the reference list but should only be mentioned in the article text (e.g., Shtyawy,A., University of Jordan, personal communication). Journal titles should be abbreviated according to the system adopted in Biological Abstract and Index Medicus, if not included in Biological Abstract or Index Medicus journal title should be given in full. The author is responsible for the accuracy and completeness of the references and for their correct textual citation. Failure to do so may result in the paper being withdraw from the evaluation process. Example of correct reference form is given as follows:-

Reference to a journal publication:

Bloch BK. 2002. Econazole nitrate in the treatment of *Candida vaginitis*. *S Afr Med J.* , **58**:314-323.

Ogunseitan OA and Ndoeye IL. 2006. Protein method for investigating mercuric reductase gene expression in aquatic environments. *Appl Environ Microbiol.*, **64**: 695-702.

Hilly MO, Adams MN and Nelson SC. 2009. Potential fly-ash utilization in agriculture. *Progress in Natural Sci.*, **19**: 1173-1186.

Reference to a book:

Brown WY and White SR.1985. **The Elements of Style**, third ed. MacMillan, New York.

Reference to a chapter in an edited book:

Mettam GR and Adams LB. 2010. How to prepare an electronic version of your article. In: Jones BS and Smith RZ (Eds.), **Introduction to the Electronic Age**. Kluwer Academic Publishers, Netherlands, pp. 281–304.

Conferences and Meetings:

Embabi NS. 1990. Environmental aspects of distribution of mangrove in the United Arab Emirates. Proceedings of the First ASWAS Conference. University of the United Arab Emirates. Al-Ain, United Arab Emirates.

Theses and Dissertations:

El-Labadi SN. 2002. Intestinal digenetic trematodes of some marine fishes from the Gulf of Aqaba. MSc dissertation, The Hashemite University, Zarqa, Jordan.

Nomenclature and Units

Internationally accepted rules and the international system of units (SI) should be used. If other units are mentioned, please give their equivalent in SI.

For biological nomenclature, the conventions of the *International Code of Botanical Nomenclature*, the *International Code of Nomenclature of Bacteria*, and the *International Code of Zoological Nomenclature* should be followed.

Scientific names of all biological creatures (crops, plants, insects, birds, mammals, etc.) should be mentioned in parentheses at first use of their English term.

Chemical nomenclature, as laid down in the *International Union of Pure and Applied Chemistry* and the official recommendations of the *IUPAC-IUB Combined Commission on Biochemical Nomenclature* should be followed. All biocides and other organic compounds must be identified by their Geneva names when first used in the text. Active ingredients of all formulations should be likewise identified.

Math formulae

All equations referred to in the text should be numbered serially at the right-hand side in parentheses. Meaning of all symbols should be given immediately after the equation at first use. Instead of root signs fractional powers should be used. Subscripts and superscripts should be presented clearly. Variables should be presented in italics. Greek letters and non-Roman symbols should be described in the margin at their first use.

To avoid any misunderstanding zero (0) and the letter O, and one (1) and the letter l should be clearly differentiated. For simple fractions use of the solidus (/) instead of a horizontal line is recommended. Levels of statistical significance such as: $^*P < 0.05$, $^{**}P < 0.01$ and $^{***}P < 0.001$ do not require any further explanation.

Copyright

Submission of a manuscript clearly indicates that: the study has not been published before or is not under consideration for publication elsewhere (except as an abstract or as part of a published lecture or academic thesis); its publication is permitted by all authors and after accepted for publication it will not be submitted for publication anywhere else, in English or in any other language, without the written approval of the copyright-holder. The journal may consider manuscripts that are translations of articles originally published in another language. In this case, the consent of the journal in which the article was originally published must be obtained and the fact that the article has already been published must be made clear on submission and stated in the abstract. It is compulsory for the authors to ensure that no material submitted as part of a manuscript infringes existing copyrights, or the rights of a third party.

Ethical Consent

All manuscripts reporting the results of experimental investigation involving human subjects should include a statement confirming that each subject or subject's guardian obtains an informed consent, after the approval of the experimental protocol by a local human ethics committee or IRB. When reporting experiments on animals, authors should indicate whether the institutional and national guide for the care and use of laboratory animals was followed.

Plagiarism

The JJBS hold no responsibility for plagiarism. If a published paper is found later to be extensively plagiarized and is found to be a duplicate or redundant publication, a note of retraction will be published, and copies of the correspondence will be sent to the authors' head of institute.

Galley Proofs

The Editorial Office will send proofs of the manuscript to the corresponding author as an e-mail attachment for final proof reading and it will be the responsibility of the corresponding author to return the galley proof materials appropriately corrected within the stipulated time. Authors will be asked to check any typographical or minor clerical errors in the manuscript at this stage. No other major alteration in the manuscript is allowed. After publication authors can freely access the full text of the article as well as can download and print the PDF file.

Publication Charges

There are no page charges for publication in Jordan Journal of Biological Sciences, except for color illustrations,

Reprints

Ten (10) reprints are provided to corresponding author free of charge within two weeks after the printed journal date. For orders of more reprints, a reprint order form and prices will be sent with article proofs, which should be returned directly to the Editor for processing.

Disclaimer

Articles, communication, or editorials published by JJBS represent the sole opinions of the authors. The publisher shoulders no responsibility or liability what so ever for the use or misuse of the information published by JJBS.

Indexing

JJBS is indexed and abstracted by:

DOAJ (Directory of Open Access Journals)

Google Scholar

Journal Seek

HINARI

Index Copernicus

NDL Japanese Periodicals Index

SCIRUS

OAJSE

ISC (Islamic World Science Citation Center)

Directory of Research Journal Indexing
(DRJI)

Ulrich's

CABI

EBSCO

CAS (Chemical Abstract Service)

ETH- Citations

Open J-Gat

SCImago

Clarivate Analytics (Zoological Abstract)

Scopus

AGORA (United Nation's FAO database)

SHERPA/RoMEO (UK)

المجلة الأردنية للعلوم الحياتية
Jordan Journal of Biological Sciences (JJBS)
ISSN 1995- 6673 (Print), 2307- 7166 (Online)

<http://jjbs.hu.edu.jo>

The Hashemite University
Deanship of Scientific Research
TRANSFER OF COPYRIGHT AGREEMENT

Journal publishers and authors share a common interest in the protection of copyright: authors principally because they want their creative works to be protected from plagiarism and other unlawful uses, publishers because they need to protect their work and investment in the production, marketing and distribution of the published version of the article. In order to do so effectively, publishers request a formal written transfer of copyright from the author(s) for each article published. Publishers and authors are also concerned that the integrity of the official record of publication of an article (once refereed and published) be maintained, and in order to protect that reference value and validation process, we ask that authors recognize that distribution (including through the Internet/WWW or other on-line means) of the authoritative version of the article as published is best administered by the Publisher.

To avoid any delay in the publication of your article, please read the terms of this agreement, sign in the space provided and return the complete form to us at the address below as quickly as possible.

Article entitled:-----

Corresponding author: -----

To be published in the journal: Jordan Journal of Biological Sciences (JJBS)

I hereby assign to the Hashemite University the copyright in the manuscript identified above and any supplemental tables, illustrations or other information submitted therewith (the "article") in all forms and media (whether now known or hereafter developed), throughout the world, in all languages, for the full term of copyright and all extensions and renewals thereof, effective when and if the article is accepted for publication. This transfer includes the right to adapt the presentation of the article for use in conjunction with computer systems and programs, including reproduction or publication in machine-readable form and incorporation in electronic retrieval systems.

Authors retain or are hereby granted (without the need to obtain further permission) rights to use the article for traditional scholarship communications, for teaching, and for distribution within their institution.

- ☐ I am the sole author of the manuscript
- ☐ I am signing on behalf of all co-authors of the manuscript
- ☐ The article is a 'work made for hire' and I am signing as an authorized representative of the employing company/institution

Please mark one or more of the above boxes (as appropriate) and then sign and date the document in black ink.

Signed: _____ Name printed: _____
Title and Company (if employer representative) : _____
Date: _____

Data Protection: By submitting this form you are consenting that the personal information provided herein may be used by the Hashemite University and its affiliated institutions worldwide to contact you concerning the publishing of your article.

Please return the completed and signed original of this form by mail or fax, or a scanned copy of the signed original by e-mail, retaining a copy for your files, to:

Hashemite University
Jordan Journal of Biological Sciences
Zarqa 13115 Jordan
Fax: +962 5 3903338
Email: jjbs@hu.edu.jo

EDITORIAL PREFACE

Jordan Journal of Biological Sciences (JJBS) is a refereed, quarterly international journal financed by the Scientific Research and Innovation Support Fund, Ministry of Higher Education and Scientific Research in cooperation with the Hashemite University, Jordan. JJBS celebrated its 12th commencement this past January, 2020. JJBS was founded in 2008 to create a peer-reviewed journal that publishes high-quality research articles, reviews and short communications on novel and innovative aspects of a wide variety of biological sciences such as cell biology, developmental biology, structural biology, microbiology, entomology, molecular biology, biochemistry, medical biotechnology, biodiversity, ecology, marine biology, plant and animal biology, plant and animal physiology, genomics and bioinformatics.

We have watched the growth and success of JJBS over the years. JJBS has published 14 volumes, 60 issues and 800 articles. JJBS has been indexed by SCOPUS, CABI's Full-Text Repository, EBSCO, Clarivate Analytics- Zoological Record and recently has been included in the UGC India approved journals. JJBS Cite Score has improved from 0.7 in 2019 to 1.4 in 2021 (Last updated on 6 March, 2022) and with Scimago Institution Ranking (SJR) 0.22 (Q3) in 2021.

A group of highly valuable scholars have agreed to serve on the editorial board and this places JJBS in a position of most authoritative on biological sciences. I am honored to have six eminent associate editors from various countries. I am also delighted with our group of international advisory board members coming from 15 countries worldwide for their continuous support of JJBS. With our editorial board's cumulative experience in various fields of biological sciences, this journal brings a substantial representation of biological sciences in different disciplines. Without the service and dedication of our editorial; associate editorial and international advisory board members, JJBS would have never existed.

In the coming year, we hope that JJBS will be indexed in Clarivate Analytics and MEDLINE (the U.S. National Library of Medicine database) and others. As you read throughout this volume of JJBS, I would like to remind you that the success of our journal depends on the number of quality articles submitted for review. Accordingly, I would like to request your participation and colleagues by submitting quality manuscripts for review. One of the great benefits we can provide to our prospective authors, regardless of acceptance of their manuscripts or not, is the feedback of our review process. JJBS provides authors with high quality, helpful reviews to improve their manuscripts.

Finally, JJBS would not have succeeded without the collaboration of authors and referees. Their work is greatly appreciated. Furthermore, my thanks are also extended to The Hashemite University and the Scientific Research and Innovation Support Fund, Ministry of Higher Education and Scientific Research for their continuous financial and administrative support to JJBS.

Professor Atoum, Manar F.
March, 2021

CONTENTS

Original Articles

- 171 – 179 Characterization of Qualitative and Quantitative Traits of Four Types of Indonesian Native Chickens as Ancestor of New Strains of Local Super Laying Hens
Suyatno Suyatno, Sujono Sujono, Aris Winaya, Lili Zalizar and Mulyoto Pangestu
- 181 – 187 The Response of Some Cassava Clones to Red Mite - *Tetranychus urticae*
Sri Wahyuni Indiaty, Kartika Noerwijati, Sumartini Sumartini, and Nguyen van Minh
- 189 – 197 Morphometric Diversity and Genetic Relationship of “Bangkok” Chicken (Thai Game Fowl) in East Java, Indonesia
Aris Winaya, Deni Insan Fahmiady, Suyatno Suyatno, Abdul Malik, Ali Mahmud, and Ravindran Jaganathan
- 199 – 206 Inhibitory Effect of Partially Purified Compounds from Pomegranate Peel and Licorice Extracts on Growth and Urease Activity of *Helicobacter pylori*
Sereen M.B. Bataineh, Bara’ah A. Abu Dalo, Bayen S. Mahawreh, Homa Darmani and Abdul-Karim J. Sallal
- 207 – 221 Agronomic Characters and Quality of Fruit of Salak cv. Gulapasir Planted in Various Agro-Ecosystems
I Ketut Sumantra, I Ketut Widnyana, Ni Gusti Agung Eka Martingsih, I Made Tamba, Praptiningsih Gamawati Adinurani, Ida Ekawati, Maizirwan Mel, and Peeyush Soni
- 223 – 232 Impact of Maternal Exposure to Lead Acetate before Pregnancy Through Lactation Period on the Testicular histomorphologic Indices of Male Offspring of Wistar Rats, A Stereological Study
Ehsan Roomiani, Hassan Morovvati, Saeid Keshkar, Sareh Najaf Asaadi, Shaker Shayestehnia and Arash alaeddini
- 233 – 242 Bioefficacy of *Bacillus cereus* and its Three Mutants by UV Irradiation Against *Meloidogyne incognita* and Gene Expression in Infected Tomato Plants
Gazeia M. Soliman, Sameh M. El-Sawy, Rasha G. Salim, Ghada M. El-Sayed and Walaa A. Ramadan
- 243 – 248 Skin-Cancer Protective Effect of *Ziziphus Spina-christi* Leaf Extract: *In vitro* and *in Vivo* Models
Omar F. Khabour, Karem H. Alzoubi, Ahmad S. Alkofahi, Rafat M. Al-Awad
- 249 – 258 Induced Toxicity and Bioaccumulation of Chromium (VI) in Cluster Bean: Oxidative Stress, Antioxidative Protection Strategy, Accumulation and Translocation of Certain Nutrient
Kamlesh Kumar Tiwari, Manoj Kumar Bidhar, Naveen Kumar Singh
- 259 – 266 Antifungal and Antiamoebic Activities, Cytotoxicity, and Toxicity of Aqueous and Ethanolic Extracts of Propolis Produced by Brunei Stingless Bees
Nadzirah Zulkiflee, Fatimah Hashim, Hussein Taha, Anwar Usman
- 267 – 277 Chemical and Functional Properties of Myofibrillar Protein from Selected Species of Trash Fish
Choirul Anam, Manar Fayiz Mousa Atoum, Noor Harini, Damar Damar, Roy Hendroko Setyobudi, Ahmad Wahyudi, Agustia Dwi Pamujiati, Nita Kuswardhani Yuli Witono, Rusli Tonda, Hendro Prasetyo, Ida Ekawati, Endang Dwi Purbajanti, Zane Vincēviča-Gaile, Taavi Liblik, Ahmad Fauzi, Hadinoto Hadinoto, Nico Syahputra Sebayang, Eni Suhesti, Asgami Putri, and Fasal Munsif
- 279 – 288 Biogenic Synthesis of Chitosan/Silver Nanocomposite by *Escherichia coli* D8 (MF062579) and its Antibacterial Activity
Mohamed M. El-Zahed, Zakaria A. M. Baka, Mohamed I. Abou-Dobara, and Ahmed K.A. El-Sayed
- 289 – 295 Plastic Particles in the Gastrointestinal Tract of Some Commercial Fish Species Inhabiting in the Gulf of Bejaia, Algeria
Z. Zeghdani, S. Mehdioui, Y. Mehdioui, R. Gherbi and Z. Ramdane

- 297 – 305 Peptides from Casein Extend the Survival Rate and Protect *Drosophila melanogaster* from Oxidative Stress Via Interacting with the Keap1-Nrf2 Pathway
Idris Zubairu Sadiq, Babangida Sanusi Katsayal, Rashidatu Abdulazeez, Odunola Safiyyah Adedoyin, Yakubu Fatimat Omengwu, Abdullahi Garba Usman
- 307 – 321 The Impact of Selected Ecological Factors on the Growth and Biochemical Responses of Giza Faba Bean (*Vicia faba* L.) Seedlings
Mohammad Abo Gamar, Riyadh Muhaidat, Tareq Fhely, Fatima Abusahyoun, and Taghleb Al-Deeb
- 323 – 327 Investigation of Seagrass-Associated Fungi as Antifouling Candidates with Anti-Bacterial Properties
Wilis Ari Setyati, Sri Sedjati, Alun Samudra, and Dafit Ariyanto
- 329 – 334 *Moringa oleifera* (Lam) Root Extracts Elevate Catecholamine Levels in Experimental Rats: Potential Role of Ethnopharmacology in Combating Depressive Conditions
Auwal Adamu, Mahmoud S. Jada, Umar Saidu, Yahaya I. Usha, Emmanuel G. Favour and Mohammed N. Shuaibu
- 335 – 343 Carbon Footprint Calculation of Net CO₂ in Agroforestry and Agroindustry of Gayo Arabica Coffee, Indonesia
Rahmat Pramulya, Tajuddin Bantacut, Erliza Noor, Mohamad Yani, Moh Zulfajrin, Yudi Setiawan, Heru Bagus Pulunggono, Sudrajat Sudrajat, Olga Anne, Shazma Anwar, Praptiningsih Gamawati Adinurani, Kiman Siregar, Hendro Prasetyo, Soni Sisbudi Harsono, Elida Novita, Devi Maulida Rahmah, Nguyen Ngoc Huu, Devi Agustia, and Maya Indra Rasyid
- 345 – 352 Immunomodulatory Effects of Unripe Sapodilla (*Manilkara zapota*) Fruit Extract Through Inflammatory Cytokine Regulation in Type 1 Diabetic Mice
Fikriya Novita Sari, Rizky Senna Samoedra, Setyaki Kevin Pratama, Sri Rahayu, Aris Soewondo, Yoga Dwi Jatmiko, Muhammad Halim Natsir2, Hideo Tsuboi, Muhaimin Rifa'i
- 353 – 361 Activity of lactic acid-producing *Streptomyces* strain CSK1 against *Staphylococcus aureus*
Shahad Al Nuaimi, Ismail Saadoun, Ban Al Joubori, and Sofian Kanan
- 363 – 369 *Bacteroides fragilis* Induce Apoptosis and subG1/G1 Arrest Via Caspase and Nrf2 Signaling Pathways in HT-29 Cell Line
Samin Loniakan, Aras Rafiee, Alireza Monadi
- 371 – 377 Effects of Spirulina on Some Oxidative Stress Parameters and Endurance Capacity in Regular and Strenuous Exercises
Mehmet OZ, Hakkı GOKBEL

Characterization of Qualitative and Quantitative Traits of Four Types of Indonesian Native Chickens as Ancestor of New Strains of Local Super Laying Hens

Suyatno Suyatno¹, Sujono Sujono¹, Aris Winaya^{1,*}, Lili Zalizar¹ and Mulyoto Pangestu²

¹Department of Animal Science, Faculty of Agriculture and Animal Science, University of Muhammadiyah Malang, Jl. Raya Tlogomas No. 246 Malang 65145, East Java, Indonesia; ²Department of Obstetrics and Gynaecology, Faculty of Medicine, Nursing and Health Sciences, Blok F, Level 5 Monash Medical Centre 246 Clayton Road, Clayton VIC 3168, Monash University, Australia.

Received: Sep 29, 2022; Revised: March 6, 2023; Accepted Mar 16, 2023

Abstract

An important aspect that determines the productivity of native chickens is the genetic factor. Improving the genetic quality of chickens can be done through a breeding program which involves the selection and arrangement of mating lines. The objective of the research project is to find basic information on the ancestor's qualitative and quantitative traits to produce a new Indonesian native chicken laying-hens strain. The ancestors used as the genetic source are four native chicken lines: White, Lurik, Wareng, and Ranupane (male and female). Qualitative traits were analyzed using descriptive statistics, and quantitative data were analyzed with ANOVA of a two-level Nested Classification followed by the Least Significant Difference test. The results showed differences in plumage and shank color in each chicken line. In cocks, there were differences ($P < 0.05$) in body weight, wing length, tail length, head circumference, and front-body width. The height, body circumference, shank length, and beak length differed ($P < 0.05$) between hen lines. Qualitative characteristics (plumage and shank colors) can be used as a marker for native chicken lines. They can be used as a reference for selection according to the objectives of the breeding program. Body conformation (weight and height) can be used as selection criteria for ancestors (male and female) to produce new strains of laying native hens.

Keywords: Breeding native chicken, *Gallus gallus domesticus* (Linnaeus, 1758), Improve genetic quality, Increase productivity, Laying native hens, Morphology, Morphometric, Produce superior lines

1. Introduction

Native chickens have several advantages, including being good foragers, efficient mothers, and requiring minimal care to grow (Sankhyan *et al.*, 2013). Moreover, the meat and eggs of Indonesian native chickens are preferred by consumers because of their better taste. In addition, native chickens are more disease-resistant, cheaply fed, and having simple housing (Sujionohadi and Hendriawan, 2013), simple farming, and being used as a side farm business (Permadi *et al.*, 2020). Eggs of native chicken are sought after because consumers believe they could increase stamina and vitality as they are widely used in herbal medication (Hendriyanto, 2019). Multipurpose indigenous village chickens (IVCs), besides meat and eggs, produce decorative feathers, play a recreational role such as cockfighting, and are used for ritual practices and to fulfil social obligations (Desta, 2020). Apart from having several advantages, native chickens still have many disadvantages. One of drawbacks of native chickens in Indonesia is that they generally have lower growth rates and egg production compared to commercial breeds, which can limit their potential as a source of meat and eggs for

the market. Their productive performances and reproductive rates are low, yet improvements of native chickens would be beneficial for the development of economic growth in Indonesia (Yuwanta, 2010). The productivity of native chickens is low due to extensive farming, and the chickens are allowed to find their feed, inadequate management, and lack of disease prevention (Suprijatna and Natawihardja, 2005; Tonda *et al.*, 2023). In addition, they are more susceptible to diseases and have lower feed conversion efficiency, which can boost production costs.

Native chickens have great potential to be developed as an ancestor of superior lines. Adapting to a tropical environment, which can provide higher income for farmers, is advantageous for local chickens (Kartika *et al.*, 2017). The productivity of native chickens is low, but they are essential as a genetic source because of their excellent adaptability in poor farming conditions (Agarwal *et al.*, 2020). The genetic diversity of local chickens also has excellent potential in the selection program and genetic engineering efforts to produce superior lines (Depison, 2009). The preservation of genetic diversity becomes a target in the future to improve genetic quality in breeding programs, especially selection activities to produce

* Corresponding author. e-mail: winaya@umm.ac.id.

superior native chicken lines (Habiburahman *et al.*, 2020). Increasing the productivity of local chickens requires careful attention to breeding, nutrition, and health (Manyelo *et al.*, 2020). Many studies have been carried out to increase the productivity of native chickens from the aspect of feed, among others by Widodo *et al.* (2019, 2021) who gave *Curcuma xanthorrhiza* Roxb., and Tonda *et al.* (2022, 2023) with dried rice leftover treatment to improve the performance of native chickens.

Researches on breeding aspects to produce new final stock (FS) of native chickens have not been widely carried out in Indonesia. After all this time, only a few researchers have been diligent in researching to produce super native chicken strains, such as the KUB (Agriculture Research and Development Agency) line, the IPB D1 strain produced by researchers from Bogor Agricultural University, and the SenSi-1 Agrinak strain produced by produced by researchers from the Bogor Livestock Research, whereas the breeding aspect contributes in determining the productivity of native chicken eggs. Therefore, the authors conducted a study aiming to produce new strains of super-laying native hens through a selection program and mating line arrangement. The ancestors used four native chicken lines as a genetic source from the primary population: White, Lurik, Wareng, and Ranupane native chickens.

Performance improvement in native chickens requires basic information regarding the traits to be selected. The initial selection steps included characterizing several qualitative and quantitative traits. Characterization is the first step in breeding livestock to identify critical economic characteristics such as body weight and growth or characteristics of the relevant livestock family. The application of morphometrics is not only carried out on chickens but also on other livestock such as what was done by Brahantiyo *et al.* (2021) who applied morphometrics to characterize several types of rabbits. Morphometrics are not only performed on livestock, but also on other species, as done by Rahman *et al.* (2019) who used morphometric as the key to identify catfish. Characterization of traits in native chickens can be carried out through morphometric identification of quantitative traits that can be used as selection criteria to increase productivity (Putri *et al.*, 2020). Although several previous research results state that morphology contributes very little to morphometrics and production (Shuaibu *et al.*, 2020), it is essential to identify the morphology and morphometrics to support the selection program to produce new native chicken lines, which have high egg and meat productivity.

2. Materials and Methods

This research was conducted starting July 2020 at the Native Chicken Breeding House, Experimental Farm Animal Husbandry Study Program, University of Muhammadiyah Malang, East Java, Indonesia. The native chicken used as a genetic source is White Native Chicken

and Wareng (from Malang), Lurik Chicken (from Jombang Regency) and Ranupane Chicken (from the highlands around Bromo-Tengger-Semeru), both male and female. White native chickens have advantages in terms of body resistance from disease attacks. The advantages of Wareng chickens are that they have high egg productivity and are disease resistant. Lurik chickens have advantages in the aspect of good egg production, while Ranupane chickens have a good body composition as a characteristic of laying hens. All of these traits will be combined to produce a new final stock of super-laying native hens.

Chickens were reared in experimental cages with a male: female ratio = 1:5 to keep egg fertility high. This sex ratio refers to research conducted by Singh *et al.* (2020). Management of rearing and feeding were given uniformly to eliminate environmental factors and keep genetic factors as determinants of phenotype.

2.1. Identification of qualitative traits (morphology)

Visual morphological observations were carried out by applying the observation method issued by the FAO: "Draft Guidelines on Phenotypic Characterization of Animal Genetic Resources: Chicken Descriptors" with modifications according to local conditions. The qualitative traits (morphology) observed were in accordance with El-Safty (2012), where the ones stated are coat color, shank color, comb type, head shape, presence of earlobe, and color of earlobe as well as plumage color (body, neck, wings, tail), wattle type, and skin color. The variable of qualitative traits was analyzed using descriptive statistics and compared as percentages to measure the distribution of each qualitative trait (FAO, 2011).

2.2. Identification of quantitative traits (morphometric)

The measured quantitative traits (morphometrics) were: Ten linear body size (chest circumference, wings span, shank length, shank circumference, comb length, comb height, sternum length, beak length, wattle length and body length) and body weight morphometric data (Tareke *et al.*, 2018). The data were analyzed by simple statistical ($\bar{x} \pm \sigma$) and ANOVA of two Levels Nested Classification followed by the Least Significant Difference (LSD 5 %) test to determine which line was better for each trait (Adinurani, 2016, 2022; Tribudi and Prihandini, 2020). This research was conducted with the Description of Ethical Approval No.5.a/048.a/KEPK-UMM/III/2022 issued by the Faculty of Medicine, University of Muhammadiyah Malang.

3. Result and Discussion

3.1. Qualitative traits

3.1.1. The plumage pattern

The results of the plumage color pattern analysis of native chickens are presented in Figure 1, and the distribution data are presented in Table 1 and Table 2.



Figure 1. Physical performance of four lines native chicken as genetic sources

Table 1. Plumage colors of White and Lurik native chickens

Traits	White Chicken		Lurik Chicken	
	Cocks (%)	Hens (%)	Cocks (%)	Hens (%)
Body	White (100.00)	White (100.00)	Red black brown (100.00)	Brown-black spots (100.00)
Wings	White (100.00)	White (100.00)	Red black (100.00)	Brown-black spots (100.00)
Neck	White (100.00)	White (100.00)	Red (100.00)	Yellow (100.00)
Head	White (100.00)	White (100.00)	Red (100.00)	Brown (100.00)
Tail	White (100.00)	White (100.00)	Black red (100.00)	Brown black (100.00)

Table 1 shows that for the cocks, the color of white chicken plumage can be used as a marker because it is 100 % white plumage and very different from other chickens. For the cocks Lurik, Wareng, and Ranupane, the color of the plumage cannot be used as a single marker, but it is necessary to look at the type of comb and the color of the shank. All male Lurik chicken comb is the single and wide type with greenish gray shank. In contrast to the

Wareng and Ranupane chickens, the comb types are single, pea and walnut. The color of the shank in male Ranupane is yellow (> 80 %), while the color of male Wareng shank is white (> 70 %). Other characteristics such as wattle, neck and wing plumage color, beak, and skin cannot be used as a marker in cocks, because the relative color patterns spread equally between the lines.

Table 2. Plumage colors of Wareng and Ranupane native chickens

Traits	Wareng Chicken		Ranupane Chicken	
	Cocks (%)	Hens (%)	Cocks (%)	Hens (%)
Body	Red black (80.00)	Black (70.59)	Black yellow (20.00)	Light brown (40.91)
	Red black brown (20.00)	Black brown spots (70.59)	Red black (80.00)	Light brown black (31.82)
				Light brown white (22.73) Dark brown black (4.54)
Wings	Red black (60)	Black (82.35)	Yellow black (20.00)	Black brown (9.09)
	Red black brown (40)	Black brown spots (17.65)	Red black (60.00)	Light brown black (63.64)

Continued on the next page

Table 2. Continued

Traits	Wareng Chicken		Ranupane Chicken	
	Cocks (%)	Hens (%)	Cocks (%)	Hens (%)
Neck			Red black white (20.00)	Light brown white (9.09)
				Light brown white black (9.09)
				Light brown black yellow (4.54)
				Red black (4.54)
				Black brown spots (22.73)
	Red (60.00)	Black (52.94)	Yellow (20.00)	Light brown black (45.45)
	Red black (20.00)	Black red (17.65)	Red black (20.00)	Brown white (9.09)
Head	Red black white (20.00)	Black white (17.65)	Red (20.00)	Brown black white (4.54)
		Black brown (11.76)		Red (9.09)
				Light brown (9.09)
	Red (100.00)	Black (100.00)	Yellow (20.00)	Black (9.09)
			Red (80.00)	Black brown (54.54)
Tail				Black brown white (27.27)
	Black (40.00)	Black (100)	Black (60.00)	Red (9.09)
	Black white (60.00)		Black brown (20.00)	Black brown (95.45)
			Black red white (20.00)	Black red (4.55)

Table 2 shows that for the hens, the overall plumage color can be used as a marker between lines because the plumage color of the hens of the four strains is strikingly different. The comb type is only specific to female Lurik chickens, a 100 % single type. The color of the shank can also be used as a marker for Lurik (100 % greenish-gray) and Wareng (80 % blackish-gray) chickens. Other

characteristics, such as the color of the beak, shank, and skin, cannot be used as a marker for the hens.

3.1.2. The comb type

The types of comb found in all lines are single, pea, and walnut, both male and female (Table 3 and Figure 2).

Table 3. Comb and wattle types in native chicken

Traits	White		Lurik		Wareng		Ranupane		Overall
	Cocks	Hens	Cocks	Hens	Cocks	Hens	Cocks	Hens	
Comb									
Pea (%)	40.00	4.00			100.00				8.83
Walnut (%)	20.00	60.00				76.47		59.09	43.75
Single (%)	40.00	36.00	100.00	100.00		23.53	100.00	40.91	47.92
Wattle									
Small (%)	40.00	38.00			40.00	29.41		40.91	29.16
Medium (%)		20.00			20.00	23.53		4.54	11.46
Large (%)	40.00	12.00	100.00	100.00	20.00		100.00	27.27	35.42
No wattle (%)	20.00	40.00			20.00	47.06		27.27	23.96

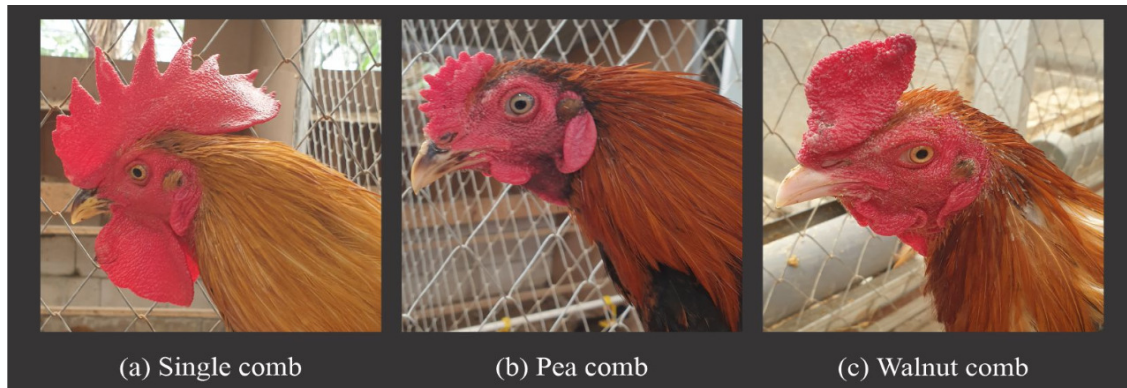


Figure 2. Comb and wattle types in native chicken

Table 3 shows the overall mean of all male and female lines obtained by pea (8.83 %), walnut (43.75 %), and single (47.92 %). Male and female Lurik chickens and male Ranupane chickens have uniform comb types, 100 % single combs. The results of this study are in line with those reported (Bugiwati *et al.*, 2020a) that Gaga chickens (South Sulawesi) have more single comb types (males > 86 %), while the hens are more walnut type. Several studies of local chickens abroad reported (Agarwal *et al.*, 2020; Bibi *et al.*, 2021; Machete *et al.*, 2021; Shuaibu *et al.*, 2020; Wario *et al.*, 2021) that the single comb type is most commonly found in local chickens. The results of this study differ from the research reported (Iskandar and Sartika, 2018) in that the pea comb type is more commonly found in male and female Agrinak chickens (> 89 %), and the rest are single types. Research conducted (Abadi, 2020) on local chickens in Lasusua Sub-District, North Kolaka District, South Sulawesi also produced different percentages, where the most common types of combs are pea (42 %), followed by single (35.5 % and rose 22.5 %).

Most wattle types (Table 3) are large (35.42 %), followed by small (29.16 %), no-wattle (23.96 %), and medium (11.46 %). This wattle size differs from the research results (Mahmood *et al.*, 2017) on Pakistani Aseel chickens that the no-wattle type is the most common (male: 80.3 % and female: 97 %). Similar results are reported by (Qureshi *et al.*, 2018) that most Aseel chickens have a no-wattle type. Comb and wattle size have a relationship with body weight. Ovariectomized chickens showed a larger size of the body, comb, and wattle (Guo *et al.*, 2017). Comb and wattle are essential traits for selection in laying hens because they can reflect egg production. Healthy, normally, and bright red combs and wattles reflect a healthy, rich variety and high egg productivity.

3.1.3. The beak, shank and skin color

The results of the beak, shank and skin color analysis of native chickens are presented in Table 4 and Figure 3.

Table 4. Beak, shank and skin color in native chicken

Traits	White		Lurik		Wareng		Ranupane	
	Cocks	Hens	Cocks	Hens	Cocks	Hens	Cocks	Hens
Beak Color								
White (%)	60	32			20			
Yellow (%)	40	68	25				40	40.91
Black (%)			25	23.08		58.82		
Black white (%)				76.92		5.88		
White black (%)			50					
White brown (%)								36.36
Yellow black (%)					40		60	4.54
Yellow brown (%)					40			
Brown (%)						5.88		13.64
Black yellow (%)						17.65		
Black brown (%)						11.76		
Shank Color								
White (%)	100	100						45.45
Greenish-grey (%)			100	100				
Blackish-grey (%)					100	100		9.1
Yellow (%)							100	45.45
Skin Color								
White (%)					20			
Dark white (%)	20	40	50	76.92	60	76.48	60	68.18
Red (%)	80	40	50	23.08				
Light red (%)		20				11.76	40	22.73
Dark-red (%)					20	11.76		9.09

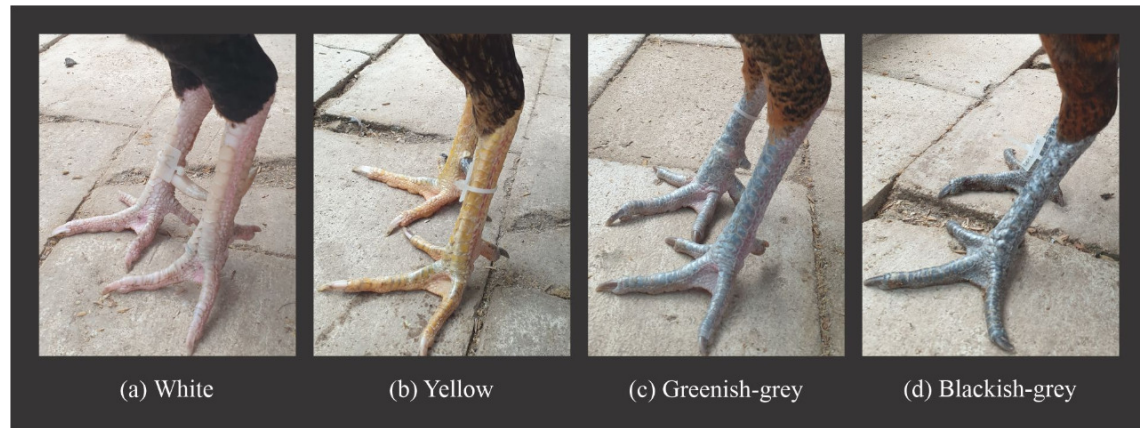


Figure 3. Shank color in native chicken

Table 4 above shows that beak color is varied and is not strain-specific. The color of the shank obtained different results between the lines (Figure 3): 100 % white (White chicken), 100 % greenish-grey (Lurik), and 100 % blackish-grey (Wareng). The shank color of the male Ranupane is 100 % yellow, while the color of the shank varies (white 45.45 %, yellow 45.45 %, and blackish-grey 9.10 %). Skin color contrasted in all strains, so it is not specific to any distinct strain. The skin colors are white, dark white, red, dark red, and bright red. The color

of the shank and skin is an essential characteristic of native chickens and is significantly related to consumer preference. Shen *et al.* (2019) stated that shank color in local chickens plays an essential role in market competition.

3.2. Quantitative traits

The measurements of several quantitative traits are presented in Table 5 (cocks) and Table 6 (hens).

Table 5. The average of quantitative traits (morphometric) of cocks native chickens

Quantitative Traits	White	Lurik	Wareng	Ranupane	Overall*
BW (kg) **	2.00±0.47 ^a	1.96±0.39 ^{ab}	1.59±0.24 ^b	2.31±0.22 ^{ab}	1.97±0.33 ^s
BH (cm)	29.84±3.00	28.00±5.28	27.24±2.99	31.20±3.51	29.07±3.70 ^{ns}
BL (cm)	20.60±2.19	19.75±1.32	19.30±2.28	21.50±2.40	20.29±2.05 ^{ns}
BC (cm)	26.40±7.27	26.13±1.65	28.50±2.35	30.10±1.14	27.78±3.10 ^{ns}
WL (cm) **	17.75±2.18 ^{ab}	19.00±1.00 ^b	17.10±1.67 ^a	21.50±1.73 ^{ab}	18.84±1.65 ^s
SL (cm)	23.54±3.54	22.13±3.07	20.40±0.65	23.40±1.52	22.37±2.19 ^{ns}
TL (cm)	13.40±2.16	12.25±2.50	10.80±0.76	11.50±0.91	11.99±1.58 ^{ns}
BeL (cm)	2.80±0.37	2.90±0.18	2.86±0.22	2.84±0.40	2.85±0.29 ^{ns}
HC. (cm) **	12.50±1.06 ^{ab}	10.95±1.20 ^c	11.22±0.54 ^b	12.60±1.14 ^a	11.82±0.99 ^s
TC (cm)	10.70±0.97	11.50±1.35	11.02±1.58	12.30±1.57	11.38±1.37 ^{ns}
NL (cm)	12.40±2.88	12.25±3.40	13.50±2.32	13.80±3.25	12.99±2.96 ^{ns}
NC (cm)	11.60±1.82	10.88±0.85	10.30±1.04	12.20±0.91	11.24±1.15 ^{ns}
HL (cm)	5.30±0.67	4.88±0.25	4.70±0.76	5.20±0.45	5.02±0.53 ^{ns}
HW (cm)	3.45±0.34	3.30±0.25	3.23±0.23	3.47±0.26	3.36±0.27 ^{ns}
BeW (cm)	1.44±0.27	1.22±0.23	1.58±0.06	1.60±0.30	1.46±0.21 ^{ns}
TaL (cm) **	27.66±8.93 ^{ab}	20.63±3.59 ^b	30.40±7.31 ^{ab}	38.60±10.57 ^a	29.32±7.60 ^s
FBW(cm) **	5.54±0.57 ^{ab}	4.66±0.97 ^b	6.25±0.78 ^{ab}	5.48±0.51 ^a	5.48±0.71 ^s
RBW(cm)	7.57±0.26	7.70±0.93	7.07±0.96	7.64±0.90	7.50±0.76 ^{ns}

* s: significant ($P < 0.05$); ns: non-significant ($P > 0.05$).

** different letters (a, b, and c) in the same row are significant (LSD test, $P < 0.05$).

BW: body weight; **BH:** body height; **BL:** body length; **WL:** wing length; **SL:** shank length; **TL:** thigh length; **BEL:** beak length; **HC:** head circumference; **TC:** thigh circumference; **BC:** body circumference; **NL:** neck length; **NC:** neck circumference; **HL:** head length; **HWT:** head width; **BEW:** base-beak width; **TAL:** tail length; **FBW:** front-body width; **RBW:** rear-body width.

For the cocks, the ANOVA results show that the characteristics of body weight, wing length, head circumference, tail length, and front-body width are significantly different between lines ($P < 0.05$). Other traits are relatively the same between lines ($P > 0.05$). The body weight is relatively the same, except for Wareng chickens, which show the lowest body weight and differ

from the other three strains. Ranupane chickens have longer wings and a larger head circumference than other chickens. Based on the appearance of several quantitative characteristics, the body conformation of the cocks can be described because Wareng chickens tend to be shorter and have wider bodies. In contrast, Lurik cocks are taller and narrower.

Table 6. The average of quantitative traits (morphometric) of hens native chickens

Quantitative Traits	White	Lurik	Wareng	Ranupane	Overall*
BW (kg)	1.45±0.28	1.75±0.28	1.42±0.28	1.45±0.29	1.52±0.28 ^{ns}
BH (cm)**	25.16±1.50 ^a	22.52±4.97 ^b	23.74±2.01 ^b	24.11±2.28 ^b	23.88±2.69 ^S
BL (cm)	18.74±1.95	16.94±2.25	17.96±1.82	18.30±2.13	17.99±2.04 ^{ns}
BC (cm)**	26.35±2.02 ^a	24.48±2.27 ^b	26.47±2.63 ^a	26.78±2.39 ^a	26.02±2.33 ^S
WL (cm)	16.08±2.06	15.88±1.78	17.09±1.99	16.72±1.77	16.44±1.90 ^{ns}
SL (cm)**	19.88±1.28 ^b	18.81±1.70 ^c	21.09±1.73 ^a	21.14±1.64 ^a	20.23±1.59 ^S
TL (cm)	11.51±1.34	10.62±1.06	11.28±1.10	11.25±1.15	11.16±1.16 ^{ns}
BeL (cm)**	2.80±0.39 ^a	2.40±0.37 ^b	2.64±0.31 ^{ab}	2.73±0.31 ^a	2.64±0.35 ^S
HC. (cm)	11.10±1.20	10.72±1.00	11.00±0.88	10.92±0.65	10.94±0.93 ^{ns}
TC (cm)	10.43±2.57	8.58±1.29	9.10±2.25	9.23±2.23	9.33±2.08 ^{ns}
NL (cm)	12.02±2.12	11.65±2.45	12.56±2.16	12.81±1.81	12.26±2.14 ^{ns}
NC (cm)	8.54±1.03	7.77±1.11	8.18±1.17	8.11±1.09	8.15±1.10 ^{ns}
HL (cm)	4.74±0.67	4.36±0.70	4.71±0.88	4.83±0.75	4.66±0.75 ^{ns}
HW (cm)	3.13±0.34	3.31±1.13	3.10±0.26	3.13±0.30	3.17±0.51 ^{ns}
BeW (cm)	1.34±0.19	1.35±0.17	1.43±0.19	1.49±0.24	1.40±0.20 ^{ns}
TaL (cm)	15.24±2.56	15.42±0.79	16.15±1.84	15.78±2.06	15.65±1.81 ^{ns}
FBW(cm)	5.55±0.81	4.73±0.47	5.06±0.59	5.24±0.58	5.14±0.61 ^{ns}
RBW(cm)	7.53±0.70	11.70±18.50	6.97±0.64	6.78±0.80	8.24±5.16 ^{ns}

* s: significant ($P < 0.05$); ns: non-significant ($P > 0.05$).

** different letters (a, b, and c) in the same row are significant (LSD test, ($P < 0.05$)).

BW: body weight; **BH:** body height; **BL:** body length; **WL:** wing length; **SL:** shank length; **TL:** thigh length; **BEL:** beak length; **HC:** head circumference; **TC:** thigh circumference; **BC:** body circumference; **NL:** neck length; **NC:** neck circumference; **HL:** head length; **HWT:** head width; **BEW:** base-beak width; **TAL:** tail length; **FBW:** front-body width; **RBW:** rear-body width.

For the hens, almost all the quantitative characteristics of hens are not different ($P > 0.05$) between lines, except for body height, shank length, beak length, and body circumference, which show differences ($P < 0.05$) between lines. The size of the White chicken is the highest and different ($P < 0.05$) from other strains. The Shank length of Ranupane and Wareng chickens is higher ($P < 0.05$) than White and Lurik chickens. The body circumference of Lurik chicken is the smallest and most different ($P < 0.05$) compared to other lines.

Identification of quantitative traits in native chickens has been mostly carried out by previous researchers with genetic sources from local Indonesian chickens (Abadi, 2020; Bugiwati, 2020b; Iskandar and Sartika, 2018; Rofii *et al.*, 2020; Sophian *et al.*, 2020; Zurahmah, 2019), as well as local chickens from other countries (Agarwal *et al.*, 2020; Brito *et al.*, 2021; Mahmood *et al.*, 2017; Perini *et al.*, 2020; Qureshi *et al.*, 2018; Shuaibu *et al.*, 2020; Wario *et al.*, 2021). The average bodyweight of the four strains of native chicken from the study (male: 1.97 kg \pm 0.33 kg and female 1.52 kg \pm 0.28 kg) is relatively the same as reported (Rofii *et al.*, 2020) in Kedu and Bali chickens, with an average of 1.05 kg \pm 1.15 kg. The average body weight of

this study is lower than that of several local chicken lines outside Java: Manokwari-Papua local chickens 2 368.5 g \pm 626.3 g (male) and 1 876 g \pm 413.8 g (female) (Zurahmah, 2019); local chicken Kolaka 1 681.92 g \pm 342.76 g (male) and 1 305.45 g \pm 410.93 g (female) (Abadi, 2020), and local chicken Gorontalo 1.33 kg \pm 1.79 kg (Sophian *et al.*, 2020). However, the weight of some local chickens from abroad is higher than the results of this study. Some data on the weight of local foreign chickens include female Aseel chickens 1.96 kg \pm 0.8 kg (Qureshi *et al.*, 2018), female Pakistani Aseel chickens 2.0 kg \pm 0.9 kg (Mahmood *et al.*, 2017), local Portuguese chickens 2 852 g and female 2 066 g (Brito *et al.*, 2021), local chickens Nigerian normal feathers 1.72 kg \pm 0.11 kg (Shuaibu *et al.*, 2020), Spanish native chickens 1 293.3 g \pm 219.2 g (female) and 1 695 g \pm 128.1 g (male) (Perini *et al.*, 2020), and Ethiopian local chicken 1.313 kg \pm 0.186 kg (female) and 1.23 kg \pm 0.229 kg (male) (Wario *et al.*, 2021).

The main trait used as selection criteria for hens is egg production, but information on weight, height and other quantitative traits is also required. The layer native chicken lines that will be made have high egg production and a

healthy body condition and are efficient in using the feed. These quantitative traits are needed as supporting selection criteria because they are related to productivity. As the primary line used by ancestors, the quantitative trait performance must be reasonable and reflect healthy chickens and high productivity. This selected hen as a parent depends on the ability of the egg production of the offspring.

4. Conclusion and Recommendation

Qualitative traits of Indonesian native chickens, especially the plumage pattern, comb type, beak color, shank color, and skin color show differences between lines. In the same chicken lines, the variation in the appearance of qualitative traits was relatively low. Several important quantitative traits indicate differences between lines. Based on the conformation of the body, Lurik and Wareng chickens can be recommended as the female line while White and Ranupane chickens should be the male line to produce the Parent Stock of laying hens.

Acknowledgments

The authors gratefully thank the Rector University of Muhammadiyah Malang, Indonesia, for the support and the permission to conduct the research. This research is part of the National Research Project funded by the Ministry of Research and Technology / National Research Agency, the Republic of Indonesia, in 2020 by contract number: 7/EI/II/PRN/2020.

References

Abadi M. 2020. Characteristics of qualitative and quantitative properties of chicken village in the Sub-District Lasusua, North Kolaka District. *Anjoro: International Journal of Agriculture and Business*, **1**(2):64–74. <https://doi.org/10.31605/anjoro.v1i2.766>.

Adinurani PG. 2016. **Design and Analysis of Agrotorial Data: Manual and SPSS**. Plantaxia, Yogyakarta, Indonesia

Adinurani PG. 2022. **Non-Parametric Statistics (Agricultural Applications, Manuals and SPSS)**. Deepublish Publisher, Yogyakarta, Indonesia,

Agarwal S, Prasad S, Kumar R, Naskar S, Kumari S, Chandra S and Agarwal BK. 2020. Phenotypic characterization and economic traits of native chicken of Chotanagpur plateau of Jharkhand. *J. Entomol. Zool. Stud.*, **8**(5):2328–2333.

Bibi S, Khan MF, Noreen S, Rehman A, Khan N, Mahmood S and Shah M. 2021. Morphological characteristics of native chicken of village Chhajjian, Haripur Pakistan. *Poult. Sci.*, **100**(3):1–6. <https://doi.org/10.1016/j.psj.2020.11.022>

Brahmantioy B, Nuraini H, Putri AW, Mel M and Hidayat C. 2021. Phenotypic and morphometric characterization of hycole, hyla and New Zealand white rabbits for KUAT hybrid (tropical adaptive and superior rabbit). *Sarhad J. Agric.*, **37**(1):09–15. <https://dx.doi.org/10.17582/journal.sja/2021/37.s1.09.15>

Brito NV, Lopes JC, Ribeiro V, Dantas R and Leite JV. 2021. Biometric characterization of the Portuguese autochthonous hens breeds. *Animals*, **11**(2):498–511. <https://doi.org/10.3390/ani11020498>.

Bugiwati SRA, Dagong MIA and Tokunaga T. 2020a. Crowing characteristics of native singing chicken breeds in Indonesia. *IOP Conf. Ser.: Earth Environ. Sci.*, **492**(012100):1–7. <https://doi.org/10.1088/1755-1315/492/1/012100>

Bugiwati SRA, Syakir A and Dagong MIA. 2020b. Phenotype characteristics of Gaga chicken from Sidrap regency, South Sulawesi. *IOP Conf. Ser.: Earth Environ. Sci.*, **492**(012103):1–8. <https://doi.org/10.1088/1755-1315/492/1/012103>.

Depison D. 2009. Quantitative and qualitative characteristics of crosses of several local chickens. *Jurnal Ilmiah Ilmu-Ilmu Peternakan*, **12**(1):7–13. <https://doi.org/10.22437/jiip.v0i0.484>

Desta T. 2020. Indigenous village chicken production: A tool for poverty alleviation, the empowerment of women, and rural development. *Trop. Anim. Health Prod.*, **53**(1):1–16. <https://doi.org/10.1007/s11250-020-02433-0>

El-Safty SA. 2012. Determination of some quantitative and qualitative traits in Libyan native fowls. *Egypt. Poult. Sci. J.*, **32**(II): 247–258.

Food and Agriculture Organization (FAO). 2011. **Draft Guidelines on Phenotypic Characterization of Animal Genetic Resources: Annex 3, Chicken Descriptors**. pp. 63–66. <http://www.fao.org/3/am651e/am651e.pdf>.

Guo X, Ma C, Fang Q, Zhou B, Wan Y and Jiang R. 2017. Effects of ovariectomy on body measurements, carcass composition, and meat quality of Huainan chickens. *Anim. Prod. Sci.*, **57**(5):815–820. <https://doi.org/10.1071/AN15815>.

Habiburahman R, Darwati S and Sumantri C. 2020. Egg production and quality of chicken eggs IPB D-1 G7 and estimation of ripitability value. *Jurnal Ilmu Produksi dan Teknologi Hasil Peternakan*, **8**(2):97–101. <https://doi.org/10.29244/jipthp.8.2.97-101>.

Hendriyanto W. 2019. **Guide to Breeding & Doing Village Chicken Business**. Laksana, Yogyakarta, Indonesia.

Iskandar S and Sartika T. 2018. Qualitative and quantitative characteristics of Sensi-1 Agrinak chicken. *Jurnal Ilmu Ternak dan Veteriner*, **22**(2):68–79. <http://dx.doi.org/10.14334/jitv.v22i2.1605>.

Kartika AA, Widayati KA, Burhanuddin, Ulfah M and Farajallah A. 2017. Exploration of community preferences on the use of local chicken in Bogor Regency, West Java. *Jurnal Ilmu Pertanian Indonesia*, **21**(3):180–185. <https://doi.org/10.18343/jipi.21.3.180>.

Machete JB, Kgwatalala PM, Nsoso SJ, Moreki JC, Nthoiwa PG and Aganga AO. 2021. Phenotypic characterization (qualitative traits) of various strains of indigenous Tswana chickens in Kweneng and Southern districts of Botswana. *Int. J. Livest. Prod.*, **12**(1):28–36. <https://doi.org/10.5897/IJLP2020.0745>

Mahmood S, Rehman AU, Khan MS, Lawal RA and Hanotte O. 2017. Phenotypic diversity among indigenous cockfighting (Aseel) chickens from Pakistan. *J. Anim. Plant Sci.*, **27**:1126–1132.

Manyelo TG, Selaledi L, Hassan ZM and Mabalebele M. 2020. Local chicken breeds of Africa: Their description, uses and conservation methods. *Animals*, **10**(12- 2257):1–18. <https://doi.org/10.3390/ani10122257>.

Perini F, Cendron F, Lasagna E and Cassandro M. 2020. Morphological and genetic characterization of 13 Italian local chicken breeds. *Acta Fytotech. Zootech.*, **23**(5):137–143. <https://doi.org/10.15414/afz.2020.23.mi-fpap.137-143>

Permadi ANN, Kurnianto E and Sutiyono S. 2020. Morphometric characteristics of male and female Kampung Chickens in Tirtomulyo Village, Plantungan District, Kendal Regency, Central Java. *Jurnal Peternakan Indonesia*, **22**(1):11–20. <https://doi.org/10.25077/jpi.22.1.11-20.2020>.

Putri ABSRN, Gushairiyanto G and Depison D. 2020. Body weight and morphometric characteristics of several local chicken

- breeds. *Jurnal Ilmu dan Teknologi Peternakan Tropis*, **7(3)**:256–264. <https://doi.org/256.10.33772/jitro.v7i3.12150>.
- Qureshi M, Qadri AH, and Gachal GS. 2018. Morphological study of various varieties of Aseel chicken breed inhabiting district Hyderabad. *J. Entomol. Zool. Stud.*, **6(2)**:2043–2045.
- Rahman MA, Hasan MR, Hossain MY, Islam MA, Khatun D, Rahman O, Mawa Z, Islam MS, Chowdhury AA, Parvin MF and Khatun H. 2019. Morphometric and meristic characteristic of the Asian Stinging Catfish *Heteropneustes fossilis* (Bloch, 1794): A key for identification. *Jordan J Biol Sci.*, **12(4)**:467–470.
- Rofii A, Saraswati TR and Yuniwati EYW. 2020. Phenotypic characteristics of Indonesian native chickens. *J. Anim. Behav. Biometeorol.*, **6(3)**:56–61. <http://dx.doi.org/10.31893/2318-1265jabb.v6n3p56-61>.
- Sankhyan V., Katoch S., Thakur YP, Dinesh K, Patial S and Bhardwaj N. 2013. Analysis of characteristics and improvement strategies of rural poultry farming in north western Himalayan state of Himachal Pradesh, India. *Livest. Res. Rural Dev.*, **25(12)**. <http://www.lrrd.org/lrrd25/12/sank25211.html>
- Shen X, Wang Y, Cui C, Zhao X, Li D, Zhu Q, Jiang X, Yang C, Qiu M, Yu C, Li Q, Du H, Zhang Z and Yin H. 2019. Detection of SNPs in the Melanocortin 1-Receptor (MC1R) and its association with shank color trait in Hs Chicken., *Braz. J. Poult. Sci.*, **21(3)**:1–9. <https://doi.org/10.1590/1806-9061-2018-0845>.
- Shuaibu A, Ma'aruf BS, Maigado AI, Abdu I, Ibrahim Y and Mijinyawa A. 2020. Phenotypic characteristics of local chickens in Dass and Tafawa Balewa local government areas of Bauchi State, Nigeria. *Niger. J. Anim. Sci.*, **22(2)**:19–31.
- Singh, DN, Shukla, PK, Bhattacharyya and Amitav. 2020. Effect of sea buckthorn leaf meal on production performance and immunity in Coloured Breeder Chicken during summer season. *Rassa J. Of Sci. For Soc.*, **2(3)**:129–133.
- Sophian A, Abinawanto, Nisa UC and Fadhillah. 2021. Morphometric analysis of Gorontalo (Indonesia) native chickens from six different regions. *Biodiversitas*, **22(4)**:1757–1763. <https://dx.doi.org/10.13057/bio-div/d220420>.
- Sujionohadi K and Setiawan AI. 2013. **Laying Native Chicken**. Niaga Swadaya, Jakarta, Indonesia.
- Suprijatna E and Natawihardja D. 2005. Growth of reproductive organs and its effect on laying performance of medium type layer due to different levels of dietary protein in the growing period. *Jurnal Ilmu Ternak dan Veteriner*, **10(4)**:260–267. <https://dx.doi.org/10.14334/jitv.v10i4.451>
- Tareke M, Assefa B, Abate T and Tekletsadik E. 2018. Evaluation of morphometric differences among indigenous chicken populations in Bale zone, Oromia Regional State, Ethiopia. *Poult. Sci. J.*, **6(2)**: 181–190. <https://doi.org/10.22069/psj.2018.14974.132>
- Tonda R, Zalizar L, Widodo W, Setyobudi RH, Hermawan D, Damat D, Endang Dwi Purbajanti ED, Prasetyo H, Ekawati I, Jani Y, Burlakovs J, Wahono SK, Anam C, Pakarti TA, Susanti MS, Mahnunin R, Sutanto A, Sari DK, Hilda H, F Ahmad, Wirawan W, Sebayang NS, Hadinoto H, Suhesti E, Amri U and Busa Y. 2022. Potential utilization of dried rice leftover of household organic waste for poultry functional feed. *Jordan J. Biol. Sci.*, **15(5)**: 879–886. <https://doi.org/10.54319/jjbs/150517>
- Tonda R, Manar FMA, Setyobudi RH, Zalizar L, Widodo W, Zahoor M, Hermawan D, Damat D, Fauzi A, Putri A, Zainuddin Z, Yuniati S, Hawayanti E, Rosa I, Sapar S, Adil A, RA DS, Supartini N, Indriatiningtias R, Kalsum U, Iswahyudi I, and Pakarti TA. 2023. Food waste product for overcoming heat stress in broilers. *E3S Web Conf.*, **374(00031)**:1–14. <https://doi.org/10.1051/e3sconf/202337400031>
- Tribudi YA and Prihandini PW. 2020. **Experimental Design Procedures for Animal Husbandry**. UI Publishing, Jakarta, Indonesia
- Wario DD, Tadesse Y and Yadav SBS. 2021. On-farm phenotypic characterization of indigenous chicken, in Dire and Yabello Districts, Borena Zone, Oromia Regional State, Ethiopia. *J. Genet. Resour.*, **7(1)**:36–48. <https://dx.doi.org/10.22080/jgr.2020.19954.1211>
- Widodo W, Rahayu ID, Sutanto A, Setyobudi RH and Mel M. 2019. The effectiveness of curcuma (*Curcuma xanthorrhiza* Roxb.) addition in the feed toward super Kampong chicken performances. *Proc. Pak. Acad. Sci.: B*, **56(4)**: 39–46
- Widodo W, Rahayu ID, Sutanto A, Anggraini AD, Sahara H, Safitri S and Yaro A. 2021. *Curcuma xanthorrhiza* Roxb. as feed additive on the carcass and fat weight percentage, meat nutrient, and nutrient digestibility of super kampong chicken. *Sarhad J. Agric.*, **37(1)**:41–47. <https://dx.doi.org/10.17582/journal.sja/2021/37.s1.41.47>.
- Yuwanta T and Fujihara. T. 2000. Indonesian native chickens: Production and reproduction potentials and future development. *Br. Poult. Sci.* **41(sup001)**:1–25. <https://doi.org/10.1080/00071660050148624>
- Zurahmah N. 2019. Performance of the local chickens on traditional management in Manokwari District, West Papua Province. Proceedings International Seminar on Tropical Animal Production. Universitas Gadjah Mada, Yogyakarta, Indonesia. pp. 216–219.

The Response of Some Cassava Clones to Red Mite - *Tetranychus urticae*

Sri Wahyuni Indiaty^{1,2,*}, Kartika Noerwijati^{1,2}, Sumartini Sumartini^{1,2}, and
Nguyen van Minh³

¹Research Center for Food Crops, BRIN, Jl. Raya Jakarta-Bogor No.46, Cibinong, Cibinong- Bogor 16911, West Java, Indonesia;

²Indonesian Legumes and Tuber Crops Research Institute, Jl. Raya Kendalpayak No.66, Malang 65162, East Java, Indonesia; ³Faculty of Agriculture and Forestry, Tay Nguyen University, 567 Le Duan St. Buon Ma Thuot City, Dak Lak Province, Vietnam, 63100

Received: Feb 2, 2023; Revised: March 25, 2023; Accepted Mar 26, 2023

Abstract

The red spider mite *Tetranychus urticae* (C.L. Koch, 1836) is an essential cassava pest, particularly in dry regions, which may cause a considerable yield loss. To reduce the damage of this pest, chemicals are applied in the field, possibly leading to adverse environmental effects. Therefore, using resistant cultivars is considered an effective and environment-friendly alternative. The study was conducted on 11 cassava clones and four cultivars (as control) during the 2016 planting season to identify the resistant clones to red spider mites in a greenhouse, producing a high yield in the field. The greenhouse experiment was conducted at ILETRI (Indonesian Legumes and Tubers Crop Research Institute). In contrast, the field experiments were explored at the Jambegede research station, Malang district, East Java Province, Indonesia. Both trials were arranged in a randomized block design with three replications. The results showed that there were four clones (CMM 03036-7, CMM 03036-5, CMM 03038-7, and CMM 02040-1), and one cultivar (Adira 4) in cluster 3 were categorized as moderately resistant and resistant groups to mites and had high tuber yields (above the average yield, > 41.12 t ha⁻¹). At a high mite population, all clones or cultivars will be attacked by mite pests; however, the clones (CMM 03036-7, CMM 03036-5, CMM 03038-7, and CMM 02040-1) exhibited the tolerance to red mite attacks. These results indicate that these clones are promising approaches for collecting resistant cassava cultivars against red mites.

Keywords: Environmentally friendly, High yielding, *Manihot esculenta* Crantz., Manioc, Pest control, Red spider mites, Resistant cultivar, *Tetranychus urticae* Koch, 1836

1. Introduction

Cassava (*Manihot esculenta* Crantz), one of the most important root crops, is widely grown in Africa, Southeast Asia, and Latin America. Apart from rice, corn, and soybeans, cassava is a priority food-crop commodity and has become the third-largest carbohydrate source. With a total production of 23 900 000 t in Indonesia, 64 % of cassava is used for food while the rest is for starch raw materials, animal feed, and export industries (BBPOPT 2013).

The red mite, *Tetranychus urticae* (Koch, 1836), is always found in cassava plantations around the world, and it is one of the factors causing the low productivity of cassava (Bellotti *et al.*, 2012; Graziosi *et al.*, 2016) and decreasing the quality of the yield, such as physical damage, chemical toxins, disease vectors, increased production costs, and social, environmental, and consumer rejection. In Indonesia, red mite infestation usually occurs during the dry season. According to Indiaty (2012), yield reduction due to red mite attack can reach 20 % to 53 %, depending on the age of the plant when the attack occurs. At severe levels of damage, yield loss can get 95 % (Santoso and Astuti. 2019). Therefore, comprehensive

control efforts are needed to reduce yield loss due to red mite attacks.

In general, mite control can be done in several ways, such as using resistant cultivars, biological control by relying on natural enemies in the field, mechanical control by spraying water on the underside of leaves so that mites are washed away with the water flow, planting cassava at the beginning of the rainy season, and chemical control. In Indonesia, the control of red mites on cassava plants has yet to be carried out optimally by farmers. This is closely related to cassava's relatively low economic value, so applying insecticides to control red mites needs to be properly applied to cassava plants. Using 2 mL L⁻¹ dicofol in the field did not affect the intensity of mite attacks. However, the tuber yield in the plots controlled by dicofol 2 mL L⁻¹ was 14 % higher than in the plots without control (Indiaty, 2012). Chemical control should be applied only in emergencies because of the increased control cost and the negative environmental effect. To overcome this problem, it is necessary to look for alternative control methods, for example, by using resistant cultivars to pest attack (Wani *et al.*, 2022), organic pesticides (Ekawati and Purwanto, 2013; Ikhwan *et al.*, 2021; Roeswitawati *et al.*, 2021), and pests' natural enemies in the form of insect pathogens (Jones *et al.*, 2022). Radhakrishnan *et al.* (2015)

* Corresponding author. e-mail: tika_iletri@yahoo.com; kart012@brin.go.id.

stated that low-input or chemical-free pest control is particularly suitable for cassava, as it is grown by smallholders throughout resource-poor tropical developing countries on small plots or degraded land.

Planting resistant cultivars is a solution to long-term problems in pest and disease control because it is economical, easy to use, can be combined with other control methods, and does not pollute the environment (Douglas, 2018). Using resistant crops with other control components in pest management suits agricultural agroecosystems. Planting resistant cultivars is a cheap, easy control technique and does not pollute the environment. Eight cassava cultivars are somewhat resistant to red mite attacks such as Adira 1, Adira 2, Adira 4, Malang 1, Malang 4, Malang 6, LITBANG UK-2, UK-1 Agritan have been released by the Ministry of Agriculture (Balitkabi, 2016). Planting resistant cassava cultivars can inhibit the development rate of mite populations, reduce the intensity of mite attacks, and reduce cassava yield losses. A series of selection activities have been carried out to obtain promising cassava clones with high yield and starch content, but the response to the red mite attack has yet to be discovered. Therefore, this study aimed to identify the resistant clones of red spider mites in a greenhouse, producing a high yield in the field.

2. Materials and Methods

2.1. Study area

The greenhouse experiment was carried out at ILETRI. The coordinates are -8° 2' 51" S and 112° 37' 30" E, with an altitude of 436 m above sea level. The field experiment was done at the Jambegede research station in Malang district, East Java province, Indonesia. It is located at the coordinates -8° 10' 20" S and 112° 33' 43" E, at 335 m above sea level. The Jambegede research station has a climate type of C3, with rainfall of 1 600 mm to 2 600 mm yr⁻¹, and the soil type Alfisols is associated with Inceptisols.

2.2. Procedures

The greenhouse experiment was conducted from June to October 2016. The study used a randomized block design with 11 cassava clones and four cultivars as treatments and was repeated three times. The materials used were cassava cuttings, red mite imago, soil as a medium, and NPK fertilizer. Cassava cuttings consisted of 11 clones (CMM 03025-43, CMM 03036-7, CMM 03036-5, CMM 03038-7, CMM 03094-12, CMM 03094-4, CMM 03095-5, CMM 02040-1, CMM 02033-1, CMM 02035-3, and CMM 02048-6) and four cultivars as control (UJ 5, Malang 6, Malang 4, and Adira 4), UJ5 as the negative control, and Adira 4 as the positive control. Cassava cuttings of 25 cm in length were planted in pots (one cutting per pot) with a diameter of 30 cm (volume 5 kg of soil). Fertilization is applied at the time of planting, with up to 10 g of NPK fertilizer per pot mixed with soil. Watering occurs three times a week, while weeding is done as needed.

The intensity of the mite attack was observed on each plant aged 1 wk after infestation (WAI), 2 WAI, 3 WAI, 4 WAI, 5 WAI, 6 WAI, 7 WAI, and 8 WAI. The intensity of the mite attack was calculated based on Equation (1)

$$I = \sum \frac{nxv}{NxV} \times 100 \% \quad (1)$$

Note:

I = intensity of the attack

N = number of leaves in 1 plant

V = the highest score (in this case, 5)

n = number of leaves in each category score

v = category score (0 to 5)

Leaf damage scores due to mite attacks are categorized in Table 1.

Table 1. The red mite *T. urticae* damage index classification on the cassava leaf surface score

Score	Description
0	Healthy leaves (no spotting)
1	There is yellowish spots (about 10 %) on some lower leaves and or middle leaves
2	Yellowish spots (11 % to 20 %) on the lower and middle leaf.
3	Clear damage; lots of yellow spots (21 % to 50 %), few areas have necrotic (< 20 %), especially the lower and middle leaves are slightly shrunk; a number of leaves become yellow and fall out.
4	Severe damage (51 % to 75 %) at the lower and middle leaves, abundant population of mites and found white threads such as spider webs
5	Total leaf loss; plant shoots shrink; more white threads; plant death.

Source: Wahyuningsih *et al.* (2021).

The field experiment was conducted in the 2016 rainy season at the Jambegede research station, Malang district, East Java Province, Indonesia. The experiment used a randomized block design, repeated three times. The research materials consisted of 15 genotypes of cassava, consisting of 11 promising clones, namely CMM 03025-43, CMM 03036-7, CMM 03036-5, CMM 03038-7, CMM 03094-12, CMM 03094-4, CMM 03095-5, CMM 02040-1, CMM 02033-1, CMM 02035-3, and CMM 02048-6, and four superior cultivars as controls, namely Adira 4, UJ 5, Malang 4, and Malang 4 and Malang 6.

Cassava stem cuttings about 25 cm in length were planted vertically on plots measuring 5 m × 6 m with a spacing of 100 cm × 80 cm. Fertilization and weeding are performed 1 mo to 3 mo after planting. The first fertilization was (46 kg N, 36 kg P2O5, and 60 kg K2O) ha⁻¹, and the second was 46 kg N ha⁻¹. The repair of the mounds is carried out at the same time as fertilization. Cassava shoots should be removed by leaving two shoots at 2 mo after planting. Harvesting is done at the age of 10 mo. Observations were made on small tuber weight, big tuber weight, small tuber number, big tuber number, and fresh tuber yield.

The data obtained were analyzed using analysis of variance; if there was a significant difference, it was continued with the 5 % DMRT test (Adinurani, 2016, 2022). In addition, cluster analysis among the observed variables was also carried out.

2.3. Mass rearing of red mite

The test insect in the greenhouse experiment was the adult red mite *T. urticae* obtained from the Muneng research station, Probolinggo, East Java field. The mites

obtained are maintained and propagated in screen houses on peanut leaves or cassava plants. Peanut and cassava plants used for mite propagation are made by planting peanut seeds of the Kancil varieties or UJ5 cassava cuttings in pots with a diameter of 30 cm (volume 5 kg of soil). Fertilization is applied at the time of planting, with up to 10 g of NPK fertilizer per pot. Watering is done as needed. After the cassava plants tested were 1 mo old, each plant was infested with 15 adult red mites from mite propagation in the greenhouse.

2.4. Mite infestation

A red mite infestation was carried out artificially by infesting 15 adult red mites per pot on the 1-month-old test plant. The infestation was carried out by attaching peanut leaves containing 15 adult red mites to each fourth or fifth lower surface of the cassava leaf from the shoot.

2.5. Data analysis

The severity of the damage caused by the red mite attack on the cassava plant was then used to determine the cassava clones' resistance level. The level of resistance to mites was determined based on the mean and the Standard Deviation (SD) method developed by Sholihin *et al.* (2022) as follows: **HR** (high resistance): $I < (R-2SD)$; **R** (resistance): $(R-2SD) < I < (R-SD)$; **MR** (moderate resistance): $(R-SD) < I < (R+SD)$; **S** (susceptible): $I > (R+SD)$. Note: R = average mite infestation intensity; I = intensity of red mite attack; SD = standard deviation

3. Results and Discussion

3.1. The greenhouse experiment

The symptoms of a red mite attack on cassava begin with the appearance of yellow spots along the leaf bones. Symptoms of a mite attack will be seen in two weeks. The symptoms then spread, and brown necrosis occurs on the affected leaves. Severe infestations cause the leaves to dry and fall off. The initial attack of the red mite occurs on the plant's lower leaves, then spreads to the upper part of the plant. Mite-infested leaves turn reddish brown or dark brown, then dry and eventually fall off.

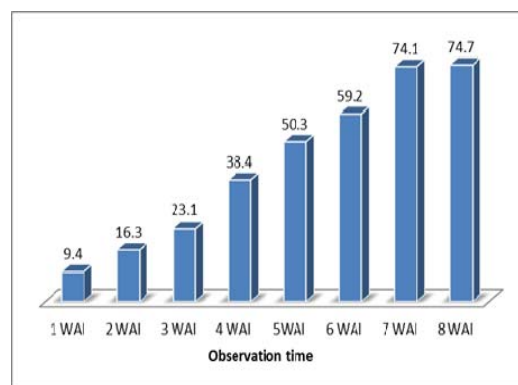
Red mites attack plants by destroying mesophyll cells and sucking cell contents, including chlorophyll. As a result, the rate of photosynthesis decreases, transpiration increases, and the chlorophyll content is low (Rioja *et al.*, 2017; Silva *et al.*, 2016). Damage to plants due to mite attacks causes the photosynthetic ability of plants to decrease; nutrient production decreases; tuber size decreases; and yields also decrease (Indiati, 2012; Sobha, 2017). Severe mite attacks can cause the death of cassava plants (Indiati, 2012; Pramudianto and Sari, 2016).

3.1.1. Intensity of mite attack on cassava

Attacks by red mites on cassava begin in 1 WAI and increase until 8 WAI (Table 2). All cassava cultivars and clones were not significantly different at 1 WAI; the leaf damage intensity was still relatively low (3.88 % to 14.58 %). However, the intensity of red mite attacks on 2 WAI and 3 WAI significantly differed between clones/cultivars. At 2 WAI, the attack intensity started to creep up from 9 % to 24 %, and CMM02035-3 showed the

lowest intensity equivalent to the positive control cultivar (Adira 4). On CMM02035-3 and Adira-4, all the leaves still looked green, and yellowish spots were found (about 10 %) on some of the lower and middle leaves, while the remaining clones and cultivars showed yellowish spots around 11 % to 20 % on the lower and middle leaves. Even CMM 02048-6 showed apparent damage, characterized by many yellow spots and few necrotic areas (< 20 %), especially on the lower leaves. At 3 WAI, the damage intensity increases to 40 % (Table 2). The most down attack occurred on CMM 03038-7 and was not significantly different from Adira 4 (positive control). Besides CMM 03038-7, there are one cultivar and three clones with lower damage intensity than Adira 4 as positive controls. All the leaves on these clones and cultivars still looked green; only yellowish spots (about 10 %) were found on some of the lower and middle leaves.

From 4 WAI to 7 WAI, crop damage continued to increase, averaging 38.44 % in 4 WAI, 50.75 % in 5 WAI, 59.18 % in 6 WAI, and 74.12 % in 7 WAI (Figure 1). The differences among the tested clones were not significantly different. At 5 WAI, 6 WAI, and 7 WAI, the lowest plant damage occurred at CMM 02033-1, while the most significant damage occurred at CMM 03094-12. Both clones were stable at the lowest and highest damage intensities. At 8 WAI, the intensity of plant damage decreased by an average of 74.66 %, which was caused by most of the test clones experiencing severe leaf loss. In these observations, there were seven clones with increasing attack intensity (leaf fall has not yet occurred), including Malang 6, CMM 03025-43, CMM 03036-7, CMM 02040-1, CMM 02033-1, CMM 02035-3, and CMM 02048-6, with the lowest attack occurring at CMM 02035-3 (69.8 %). A severe mite infestation in the greenhouse will cause high leaf loss in some cassava clones. Resistant cassava clones were characterized by low leaf loss over some time (Indiati, 2012). According to Poovizhiraja *et al.* (2018), host plants' morphological and chemical components, especially plant nutrients, cause severe crop damage and yield losses.



Note: WAI = week after infestation

Fig. 1. Development of mite attack intensity on cassava from 1 WAI to 8 WAI. ILETRI greenhouse, dry season 2016.

Table 2. The intensity of red mite attack on several cassava clones/cultivars in greenhouse conditions.

Clones/cultivars	Observation schedule (WAI) (%)									
	1	2	3	4	5	6	7	8		
UJ 5	6.62	13.97	abc	26.49	ab	31.45	45.35	61.67	78.46	78.67
Malang 6	10.17	19.14	cdef	22.48	ab	45.03	60.98	65.86	77.98	80.74
Malang 4	8.29	15.66	abcd	18.54	ab	32.91	55.28	63.68	79.69	76.57
Adira 4	3.88	9.98	a	19.02	ab	31.44	46.89	56.25	72.88	67.11
CMM 03025-43	10.26	21.68	def	26.01	ab	44.51	49.28	63.35	77.84	80.25
CMM 03036-7	9.30	17.52	bcde	21.74	ab	33.31	41.62	53.71	66.41	74.95
CMM 03036-5	7.80	10.54	a	17.72	ab	34.22	48.75	56.93	76.02	74.47
CMM 03038-7	9.65	11.35	ab	14.87	a	34.41	50.76	54.60	75.22	74.36
CMM 03094-12	11.34	20.49	def	30.40	bc	53.37	61.97	67.70	80.75	67.73
CMM 03094-4	12.69	22.67	ef	25.63	ab	49.09	56.67	62.29	78.54	69.63
CMM 03095-5	13.48	18.70	cdef	26.63	ab	46.69	52.07	60.49	75.35	73.46
CMM 02040-1	8.72	15.57	abcd	18.20	ab	32.88	45.63	55.97	73.18	79.39
CMM 02033-1	9.21	13.19	abc	17.82	ab	22.75	38.34	49.03	58.79	72.65
CMM 02035-3	4.30	9.94	a	20.96	ab	31.28	46.50	52.30	62.96	69.85
CMM 02048-6	14.58	24.36	f	39.62	c	52.69	55.05	63.93	77.71	80.00
Mean	9.35	16.32		23.08		38.44	50.75	59.18	74.12	74.66
Sd	3.0	4.8		6.3		9.3	6.7	5.5	6.5	4.6
DMRT	ns	5.64		11.46		ns	ns	ns	ns	ns
CV (%)	22.33	19.37		17.36		24.16	13.38	9.26	8.71	6.18

Note: WAI = weeks after infestation; ns = not significant

Numbers in the same column followed by the same letter are not significantly different based on the DMRT test at 5 %.

3.1.2. Category of resistance of cassava to red mites

Table 3. Resistance criteria of 15 cassava clones/cultivars to the red mite. ILETRI greenhouse, dry season 2016.

Clones/Cultivars	Observation Schedule (WAI)						
	1	2	3	4	5	6	7
UJ 5	MR	MR	MR	MR	MR	MR	MR
Malang 6	MR	MR	MR	MR	S	S	MR
Malang 4	MR	MR	MR	MR	MR	MR	MR
Adira 4	R	R	MR	MR	MR	MR	MR
CMM 03025-43	MR	S	MR	MR	MR	MR	MR
CMM 03036-7	MR	MR	MR	MR	R	MR	R
CMM 03036-5	MR	R	MR	MR	MR	MR	MR
CMM 03038-7	MR	R	R	MR	MR	MR	MR
CMM 03094-12	MR	MR	S	S	S	S	S
CMM 03094-4	S	S	MR	S	MR	MR	MR
CMM 03095-5	S	MR	MR	MR	MR	MR	MR
CMM 02040-1	MR	MR	MR	MR	MR	MR	MR
CMM 02033-1	MR	MR	MR	R	R	R	HR
CMM 02035-3	R	R	MR	MR	MR	R	R
CMM 02048-6	S	S	S	S	MR	MR	MR

Note: HR: high resistance, R: resistance, MR: moderate resistance, S: susceptibility

The resistance level of cassava was determined based on the standard deviation method, which was calculated based on the intensity of mite attacks per observation. The

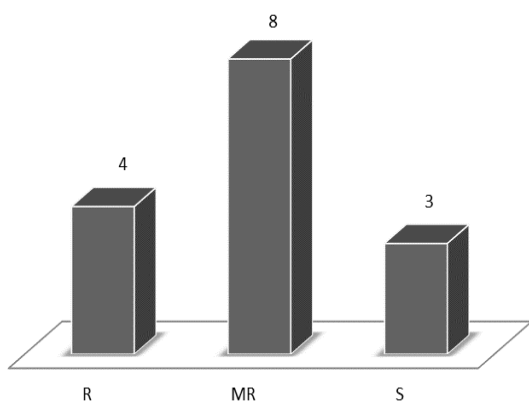
resistance response of each cassava clone or cultivar to a red mite attack is different, depending on genetics and the environment. Therefore, in each compliance, the resistance response of each clone depended on the mean severity of the attack and the value of the standard deviation of the set of tested cassava clones.

Overall, from 1 WAI to 7 WAI, there was one clone, CMM 02035-3, which consistently had better resistance than the Adira 4 (resistant check cultivar) (Table 3). In addition, this clone has the characteristics of dense leaves that do not fall off easily, so it is resistant to red mite attacks.

In high mite populations, all cultivars with different levels of resistance will be attacked by mites. Still, the period from the appearance of initial symptoms to severe symptoms is other. Resistance and susceptible cultivars take longer (Indiati, 2012). Based on the description above, the classification of the resistance of cassava clones to mite attack will be based on the intensity of plant damage at 2 WAI, with the following category: Eight clones/cultivars (UJ 5, Malang 6, Malang 3; CMM 03036-7, CMM 03094-12, CMM 03095-5, CMM 02040-1, CMM 02033-1) were tested including the MR category, four clones including the R category (Adira 4, CMM 03036-5, CMM 03038-7, CMM 02035-3); and three clones (CMM 03025-43, CMM 03094-4, and CMM 02048-6) including susceptible (S); UJ-5 as a sensitive check was included in the moderately resistant (MR) category, and Adira 4 was included in the resistant (R) category (Figure 2) against the red mite.

The presence of severe mite attacks will cause plants to grow less optimally. In heavily infected plants, fine cobweb-like threads between the cassava leaves serve as a bridge for transferring mites from one leaf to another or from one plant to another. The line also helps to protect mites from predators (Iwasa and Osakabe, 2015; Sato *et al.*, 2016).

The response of different cassava cultivars to mite attack can be influenced by various factors, including leaf morphology (leaf shape, leaf color, leaf thickness, and cuticle thickness) (Radhakrishnan *et al.*, 2015). In addition to differences in leaf morphology, the content of chemical compounds or nutrients in cassava leaves can also affect the level of mite attack on leaves (Poovizhiraja *et al.*, 2018). Santoso and Astuti (2019) reported that every cultivar showed different resistance against *T. kanzawai*. The Manggu cultivar showed the lowest damage, while the Mentega cultivar showed the highest. On the Manggu cultivar, *T. kanzawai* had the most extended life cycle and lowest fecundity. The Manggu cultivar was more resistant to the attack of the red mite *T. kanzawai* than other cultivars.



Note: R = resistance, MR = moderately resistant, S = susceptible.

Figure 2. Distribution of resistance groupings of 15 cassava clones to red mite attack. ILETRI greenhouse, dry season 2016.

In other host plants, several different resistance mechanisms are responses to the red mites' attacks. In citrus plants, the mechanism of host plant resistance to red mites is associated with flavonoid content (Agut *et al.*, 2014), leaf trichoma (Olbricht *et al.*, 2014), increased peroxidase and polyphenol oxidase activities in melon—*Cucumis melo* L. (Shoorooei *et al.*, 2013), and antibiosis and antixenosis in lima beans—*Phaseolus lunatus* L. (França *et al.*, 2018). De Oliveira *et al.* (2018) reported that tomato (*Solanum lycopersicum* L.) genotypes with high zingiberene (ZGB) content are a potential gene source for resistance to the mite *T. urticae* and possibly other pests in tomato breeding programs.

The phytochemical content of plants influences the red pest mites. But, the mechanism of cassava resistance to red mites is not yet known with certainty. Indiati (2012) stated that trichomes on cassava shoots are not the only factor determining cassava's resistance to mites. The cassava leaf buds of M4-p, OMM 0915-11, and UJ5d50-207-3, which were attacked by mites with the lowest intensity, did not have trichomes (Indiati, 2012; Sholihin *et al.*, 2022). However, low mite infestation was found in clones and cultivars with leaves with more than 70 % moisture

content. In addition, the HCN content in leaves was also not significantly correlated with mite attacks (Indiati, 2012). Yang *et al.* (2020) reported that the mite-resistant cassava genotype (XX048) had thicker abaxial epidermis and palisade tissue than the susceptible genotype (GR4). The mite damage index of XX048 was lower than GR4. XX048 had synthesized more secondary metabolites in the leaves than GR4. XX048 accumulated higher levels of secondary metabolites, potentially contributing to its higher mite resistance.

3.2. The field experiment

The results of the analysis of variance for yield variables and components showed that all variables showed significant differences except for the number of small tubers. The weight of small tubers ranged from (0.51 kg to 1.41 kg) plant⁻¹, with an average of 0.91 kg plant⁻¹. The weight of large tubers ranged from (2.37 kg to 7.29 kg) plant⁻¹, with an average of 4.32 kg plant⁻¹. The one with the highest significant tuber weight was clone CMM 03094-4. Small tubers range from 2.53 to 6 tuber plant⁻¹, with an average of 3.9 small tuber plant⁻¹. The number of large tubers ranged from 2.67 to 7.47 plant⁻¹. The tuber yield per ha ranged from 21.26 t ha⁻¹ to 62.41 t ha⁻¹ (average 41.12 t ha⁻¹). Six promising clones had tuber yields above the average: CMM 03036-7, CMM 03036-5, CMM 03038-7, CMM 03094-4, CMM 02040-1, and CMM 02048-6 (Table 4).

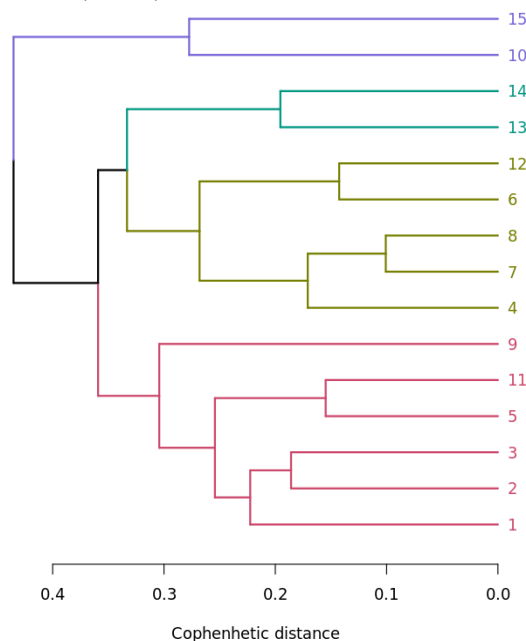


Figure 3. Cluster analysis using tuber yield, yield components, and intensity of mite infestation variable

Cluster analysis formed four groups (Figure 3). Cluster 1 consisted of two clones, namely clones 10 and 15 (CMM 03094-4 and CMM 02048-6), cluster 2 also consisted of two clones, namely clones 13 and 14 (CMM 02033-1 and CMM 02035-3), cluster 3 consisted of five clones/cultivars, namely clones 4, 6, 7, 8, and 12 (Adira 4, CMM 03036-7, CMM 03036-5, CMM 03038-7, and CMM 02040-1), while cluster 4 consisted of six clones, namely clones 1, 2, 3, 5, 9, and 11 (UJ 5, Malang 6, Malang 4, CMM 03025-43, CMM 03094-12, CMM 03095-5, CMM 030) (Figure 3). The CMM 03094-4 and CMM 02048-6

clones in cluster 1 were high-yielding clones (62.41 t ha⁻¹ and 50.94 t ha⁻¹, respectively), but based on the greenhouse test, the two clones were classified as sensitive to red mites. It is suspected that during the field experiment, the red mite attack was not too severe, so it did not affect the decrease in yield. In the glass house experiment, five clones in cluster 3 were categorized as

moderately and highly resistant to mites and had high tuber yields (above the average yield) in the field experiment. These clones (CMM 03036-7, CMM 03036-5, CMM 03038-7, and CMM 02040-1) had a high chance of being released as high-yielding cassava cultivars that were resistant to red mites.

Table 4. Yield and yield components of 15 cassava genotypes. Jambegede Research Station, 2016.

No.	Genotypes	Small tuber weight (kg)	Big tuber weight (kg)	Small tuber number	Big tuber number	Tuber yield (t ha ⁻¹)
1	UJ5	0.74 d	3.45 defg	4.53 abcd	4.67 bcde	34.25 e
2	Malang 6	0.81 d	4.39 cde	3.53 bcd	4.80 bcde	42.70 d
3	Malang 4	0.67 d	4.61 bcde	2.53 d	4.60 bcde	50.20 cd
4	Adira 4	0.80 d	4.86 bcde	3.27 cd	5.13 bcd	45.81 bc
5	CMM 03025-43	0.86 bcd	3.13 fg	3.87 abcd	3.33 bcde	24.07 fg
6	CMM 03036-7	1.41 a	5.39 bc	5.60 abc	5.40 abc	46.97 cd
7	CMM 03036-5	0.77 d	6.23 ab	2.80 d	5.47 ab	58.63 a
8	CMM 03038-7	0.93 a-d	4.90 bcd	3.40 cd	5.27 bc	56.64 ab
9	CMM 03094-12	0.51 e	3.19 efg	2.40 d	3.27 cde	29.59 ef
10	CMM 03094-4	1.33 abc	7.29 a	6.00 a	7.47 a	62.41 a
11	CMM 03095-5	0.83 cd	2.37 g	4.47 abcd	2.67 e	22.71 g
12	CMM 02040-1	1.35 ab	4.41 cde	5.87 ab	4.40 bcde	45.60 cd
13	CMM 02033-1	0.67 e	2.49 g	3.07 d	4.07 bcde	25.07 fg
14	CMM 02035-3	0.87 bcd	2.55 g	3.07 d	3.07 de	21.26 g
15	CMM 02048-6	1.15 abcd	5.61 bc	4.53 abcd	5.33 abc	50.94 bc
	Average	0.91	4.32	3.90	4.59	41.12
	F test	*	**	ns	*	**
	CV (%)	33.74	23.14	37.64	27.76	9.99
	LSD (5%)	0.51	1.67	2.45	2.13	6.87

Note: the number of columns followed by the same letter is not significantly different in the 5 % DMRT test. ns = non-significant

4. Conclusion

In the greenhouse experiment, eight clones/cultivars tested belonged to the moderately resistant (MR) category (UJ 5, Malang 6, Malang 4, CMM 03036-7, CMM 03094-12, CMM 03095-5, CMM 02040-1, and CMM 02033-), four clones/cultivar were categorized as resistant (R) (Adira 4, CMM 03036-5, CMM 03038-7, and CMM 02035-3), and three clones (CMM 03025-43, CMM 03094-4, and CMM 02048-6) as susceptible (S).

Four clones (CMM 03036-7, CMM 03036-5, CMM 03038-7, and CMM 02040-1) and one cultivars (Adira 4) in cluster 3 had high tuber yields (above the average yield, > 41.12 t ha⁻¹) and categorized as moderately resistant and resistant groups to mites. Therefore, these clones (CMM 03036-7, CMM 03036-5, CMM 03038-7, and CMM 02040-1) have a high chance of being released as high-yielding cassava cultivars that are resistant to red mites.

From 1 WAI to 7 WAI, there was one clone, CMM 02035-3, which consistently had better resistance than the Adira 4. In addition, this clone has the characteristics of dense leaves that do not fall off easily, so it can be used as a parent in the breeding process for high-yielding cassava cultivars resistant to red mites.

Until now, cassava cultivars free from red mites have not been found. Red mites will attack all clones or cultivars in high mite populations. Incubation time for severe red mite infestation on resistant clones is more extended than on susceptible clones.

Acknowledgments

The authors are thankful to the Director of the Indonesian Legumes and Tuber Crops Research Institute (ILETRI), the Indonesian Agency for Agricultural Research and Development (IAARD), and the Ministry of Agriculture of the Republic of Indonesia for providing funding for this research (No. 1807115002052).

References

- Adinurani PG. 2016. **Design and Analysis of Agrotorial Data: Manual and SPSS**. Plantaxia, Yogyakarta, Indonesia
- Adinurani PG. 2022. **Agrotechnology Applied Statistics (compiled according to the semester learning plan)**. Deepublish, Yogyakarta, Indonesia
- Agut B, Gamir J, Jacas JA, Hurtado M and Flors V. 2014. Different metabolic and genetic responses in citrus may explain relative susceptibility to *Tetranychus urticae*. *Pest Manag. Sci.*, **70**(11): 1728–1741.
- Balitkabi. 2016. **Description of Superior Varieties of Various Beans and Tubers**. Balai Penelitian Tanaman Aneka Kacang dan Umbi. Badan Litbang Pertanian. <http://balitkabi.litbang.pertanian.go.id/wp-content/uploads/2016/09/ubikayu.pdf>

- BBPOPT - Center for forecasting plant pests. 2013. Evaluation report on the prediction of the main pest attacks of rice, corn, soybeans and cassava for the 2013 planting season on the incidence of April-July 2013. Ministry of Agriculture, Directorate of Food Crops. <http://bbpopt.info/berita/97-evaluation-ramal>.
- Bellotti AC, Arias BV, Vargas OH, Rejes JAQ and Guerrero GM. 2012. Insects and mites that attack cassava, and their control in Cassava in the third millennium. In: Ospina B and Veballos H (Eds.) **Modern Production, Processing, Use, and Marketing Systems**. CIAT, Colombia, pp. 213–250.
- de Oliveira JRF, de Resende JTV, Maluf WR, Lucini T, de Lima Filho RB, de Lima IP and Nardi C. 2018. Trichomes and allelochemicals in tomato genotypes have antagonistic effects upon behavior and biology of *Tetranychus urticae*. *Front. Plant Sci.*, **9**(1132):1–9. <https://doi.org/10.3389/fpls.2018.01132>.
- Douglas AE. 2018. Strategies for enhanced crop resistance to insect pests. *Annu. Rev. Plant Biol.*, **69**: 637–660. <https://doi.org/10.1146/annurev-arplant-042817-040248>.
- Ekawati I and Purwanto Z. 2013. Transfer of local resource-based vegetable pesticide technology to rice farmers. *Cemara*, **10**(1): 36–40.
- França SM, Silva PRR, Gomes-Neto AV, Gomes RLF, Silva MJW and Breda MO. 2018. Resistance of lima bean (*Phaseolus lunatus* L.) to the red spider mite *Tetranychus neocaledonicus* (Acari: Tetranychidae). *Front. Plant Sci.*, **9**(1466):1–8. <https://doi.org/10.3389/fpls.2018.01466>.
- Graziosi I, Minato N, Alvarez E, Ngo DT, Trinh XH, Aye TM, Pardo JM, Wongtiem P and Wyckhuys KAG. 2016. Emerging pests and diseases of south-east Asian cassava: A comprehensive evaluation of geographic priorities, management options and research needs. *Pest Manag. Sci.*, **72**(6): 1071–1089. <https://doi.org/10.1002/ps.4250>.
- Ikhwan A, Indratni D, Hasanah F, Atoum MFM and Iqar I. 2021. Analysis of metabolites from purple cleome extract (*Cleome rutidosperma* Linn.) as potential organic fungicides. *Sarhad J. Agric.*, **37**(Special issue 1): 115–121. <https://dx.doi.org/10.17582/journal.sja/2021/37.s1.115.121>.
- Indiati SW. 2012. Resistance of early age cassava varieties/clones to red mite. *Jurnal Penelitian Pertanian Tanaman Pangan*, **31**(1):54–59.
- Iwasa T and Osakabe M. 2015. Effects of combination between web density and size of spider mite on predation by a generalist and a specialist phytoseiid mite. *Exp. Appl. Acarol.*, **66**(2): 219–225. <https://doi.org/10.1007/s10493-015-9902-7>.
- Jones IJ, Sokolow SH and Leo GAD. 2022. Three reasons why expanded use of natural enemy solutions may offer sustainable control of human infections. *People Nature*, **4**(1):32–43. <https://doi.org/10.1002/pan3.10264>.
- Olbricht K, Ludwig A, Ulrich D, Spangenberg R, Guenther M and Neinhuis C. 2014. Leaf morphology and anatomy in the genus *Fragaria*: Implications for resistances. *Acta Hort.*, **1049**: 269–273. <https://doi.org/10.17660/ActaHortic.2014.1049.34>.
- Poovizhiraja B, Chinniah C and Kumar AR. 2018. Influence of nitrogen and phosphorus on the biological parameters of TSSM *T. urticae* Koch. on cassava, french bean and pumpkin. *J. Entomol. Zool. Stud.*, **6**(1): 757–762. <https://www.entomoljournal.com/archives/2018/vol6issue1/PartK/5-4-374-484.pdf>.
- Pramudianto and Sari KP. 2016. Red mite (*Tetranychus urticae* Koch) on cassava plants and how to control it. *Palawija Bulletin*, **14**(1): 36–48.
- Radhakrishnan AS, Girija S and Anil AT. 2015. Organic vs conventional management in cassava: Growth dynamics, yield and soil properties. *J. Root Crops*, **39**(2):93–99.
- Rioja C, Zhurov V, Bruinsma K, Grbic M and Grbic V. 2017. Plant-herbivore interactions: A case of an extreme generalist, the two-spotted Spider Mite *Tetranychus urticae*. *Mol. Plant Microbe Interact.*, **30**: 935–945. <https://doi.org/10.1094/MPMI-07-17-0168-CR>.
- Roeswitawati D, Kristova I, Muhidin M, Endarto O, Atoum MFM, Iqar I and Shah LA. 2021. Assessment of three natural pesticide concentration on the imago phase red mites persistency. *Sarhad J. Agric.*, **37**(Special issue 1): 153–158. <https://doi.org/10.17582/journal.sja/2021.37.s1.153.158>.
- Santoso S and Astuti W. 2019. Resistance of four cassava cultivars against *Tetranychus kanzawai* Kishida (Acari: Tetranychidae). *Agrovigor*, **12**(2): 87–93.
- Sato Y, Alba JM, Egas M and Sabelis MW. 2016. The role of web sharing, species recognition and host-plant defence in interspecific competition between two herbivorous mite species. *Exp Appl Acarol.*, **70**(3): 261–274. <https://doi.org/10.1007/s10493-016-0079-5>.
- Sholihin, Indiati SW, Noerwijati K, Wahyuni TS, Kuswantoro K, Suhartina, Soehendi R, Bayu MSI, Sutanto GWA, Mejaya MJ and Budiono R. 2022. Improving the genetics of tuber yield and resistance to mite to avoid mite incident and to increase the productivity of cassava (*Manihot esculenta* Crantz). *Scientifica*, **2022**(6309679):1–9. <https://doi.org/10.1155/2022/6309679>.
- Shoorooei M, Lotfi M, Nebipour A, Mansouri AI, Kheradmand K, Zalom FG, Madadkhah E and Parsafar A. 2013. Antixenosis and entibiosis of some melon (*Cucumis melo*) genotypes to the Two-Spotted Spider Mite (*Tetranychus urticae*) and a possible mechanism for resistance. *J. Hortic. Sci. Biotechnol.*, **88**(1): 73–78. <https://doi.org/10.1080/14620316.2013.11512938>.
- Silva CAD and Junior MGCG. 2016. First record and characteristics of damage caused by the spider mite *Tetranychus neocaledonicus* André on peanuts in the State of Paraíba, Brazil. *Bragantia*, **75**(3):331–334. <http://dx.doi.org/10.1590/1678-4499.483>.
- Sobha TR, Ummukulsoom OP and Shabana TP. 2017. Impact of climatic factors on the population density of vegetable spider mite, *Tetranychus neocaledonicus* (Acari: Tetranychidae) infesting cassava. *Int. J. Adv. Res.*, **5**(7): 2174–2178. <http://dx.doi.org/10.21474/IJAR01/4956>.
- Wahyuningsih S, Indriani FC, Restuono J, Noerwijati K, Taufiq A, Baliadi Y, Budiono R, Minh NV, Soni P. 2021. Growth and productivity of four cassava cultivars on several levels of mixed fertilizers. *Jordan J. Biol. Sci.*, **14**(5): 939–944. <https://doi.org/10.54319/jjbs/140509>.
- Wani SH, Choudhary M, Barmukh R, Bagaria PK, Samantara K, Razzaq A, Jaba J, Ba MN and Varshney RK. 2022. Molecular mechanisms, genetic mapping, and genome editing for insect pest resistance in field crops. *Theor Appl Genet.*, **135**: 3875–3895. <https://doi.org/10.1007/s00122-022-04060-9>.
- Yang Y, Luo X, Wei W, Fan Z, Huang T and Pan X. 2020. Analysis of leaf morphology, secondary metabolites and proteins related to the resistance to *Tetranychus cinnabarinus* in cassava (*Manihot esculenta* Crantz). *Sci Rep.*, **10**(14197):1–13. <https://doi.org/10.1038/s41598-020-70509-w>.

Morphometric Diversity and Genetic Relationship of “Bangkok” Chicken (Thai Game Fowl) in East Java, Indonesia

Aris Winaya^{1,2,*}, Deni Insan Fahmiady¹, Suyatno Suyatno¹, Abdul Malik¹, Ali Mahmud¹, and Ravindran Jaganathan³

¹Department of Animal Science, Faculty of Agriculture and Animal Science, University of Muhammadiyah Malang, Kampus III, Jl. Raya Tlogomas No. 246 Malang 65144, East Java, Indonesia; ²Center for Biotechnology Development, University of Muhammadiyah Malang, Indonesia; ³Department of Preclinical, Microbiology Unit, Faculty of Medicine, Royal College of Medicine, Universiti Kuala Lumpur, Ipoh-30450, Perak, Malaysia

Received: Feb 4, 2023; Revised: March 24, 2023; Accepted Mar 26, 2023

Abstract

Commercial chickens that were selected for both meat and egg production were domesticated from the descendants of red junglefowl (*Gallus gallus*) species that have been widely spreading in Asia, including Indonesia. There were an estimated 32 strains of local chicken in Indonesia with high morphological diversity. The one of contributors to the diversity of Indonesian local chicken is called “Bangkok” chicken. As a reference to the name of the chicken, it is a suspected descendent of Thai game fowl (*Gallus gallus domesticus* Linnaeus, 1758) which was introduced in Thailand region many years ago. The objective of this study was to explore the existence of this chicken related to the genetic relationship with the Indonesian local chicken. This study was conducted in East Java Province which covered sample areas Banyuwangi, Pasuruan, and Madiun Regencies. The materials were “Bangkok” chicken offspring with a total of 450 birds. The observed variables consisted of qualitative and quantitative morphological characters, both male and female of adult chickens (1 yr to 1.5 yr old). The highest frequency of the comb shape was Single comb (36.9 %) and the lowest was Rose shape (11.8 %). While the highest frequency of shank colour was blackish-yellow (45.6 %) and the white color (3.6 %) was the lowest. The closest genetic distance base on morphometric diversity was between Pasuruan and Banyuwangi chickens (96.04). It was suspected due to the distance area between Pasuruan and Banyuwangi closer than Madiun and Banyuwangi, while Madiun and Pasuruan was the farthest genetic distance (682.03). Hence, the breeding program of Bangkok chicken based on the genetic distance needs further consideration to prevent inbreeding from occurring. Otherwise, the closest distance should be called for to upgrade the purity of the Bangkok chicken ancestor.

Keywords: Cock, Comb, *Gallus gallus domesticus* (Linnaeus, 1758), Genetic distance, Morphological character, Native chicken, Shank color

1. Introduction

Native chickens are included in the chicken family and there is no comprehensive information on strains or breeds. These local chickens are raised by farmers and generally have a large phenotypic diversity (FAO, 2012). However, this animal diversity is important for the life and food security of small-holder farmers (Widodo *et al.*, 2019). The genetic potential of native chicken to meet changing environmental conditions is a potential source of genes related to resistance or tolerance among emerging diseases and is compatible with consumer preferences for meat and egg products (Carbales, 2013); while the ancestor of Indonesia's local chicken was also descendent from *Gallus gallus* species. Hence, chicken has been one of the genetic resources of animal biodiversity in Indonesia. The Indonesian local chickens have different appearance characteristics that were found around 32 types of local chickens in Indonesian, namely Ayunai, Balenggek, Banten, Bangkok, Burgo, Bekisar, Cangehgar

(or Cukir or Alas), Cemani, Ciparage, Gaok, Jepun, Kampung, Kasintu, Kedu (Black and White Kedu), Pelung, Lamba, Maleo, Malay, Merawang, Nagrak, Nunukan, Nusa Penida, Olagan, Rintit or Walik, Sedayu, Sentul, Siem, Sumatra, Tolaki, Tukung and Wareng (Nataamijaya, 2010; Iskandar 2012; Widodo *et al.*, 2022). However, Rusdin *et al.* (2011) reported that were found around 31 local chicken strains in Indonesia with different morphological diversity.

The total population of Indonesia's local chickens was about 312×10^6 birds in 2019 (BPS, 2020). While, by 2020, the world's chicken population has reached more than 33×10^9 birds and about 46 % of them were in the Asian continent (FAO 2022). Therefore, the potency of native chicken is high, which can be important to fulfil protein demand. Sulandari *et al.*, (2008) reported that Indonesia is the one of main centres of chicken domestication in the world. The one contributor to the genetic diversity of Indonesia local chicken is “Bangkok” chicken or Thai game fowl chicken. This chicken was presumably developed genetically in part of Thailand

* Corresponding author. e-mail: winaya1964@gmail.com.

region as a reference to the name and then famous as a fighting chicken. While having a variety of colors ranging from solid white to grey, black, and even brown, Thai chicken is recognized by their black feathers with metallic green sheen and blood red back feathers, and neck hackles. This is a stereotypical depiction of Thai game birds, as most of them have been acknowledged based on this particular bird (Duengkae *et al.*, 2021; Oocities.org, 2009). Thus, when this chicken was introduced to Indonesia, it was popular as a fighting cock and the popularity is suitable with the culture of cockfighting in some Indonesian communities and areas as well.

“Bangkok” chicken was suspected to have been introduced to Indonesia firstly in the city of Tuban, East Java Province of Indonesia around 1980. This chicken was introduced by the people that like this chicken in that area. However, it is not clear who was the first person to introduce and develop this chicken in Indonesia (Tika, 2017). Therefore, a study to determine the potential of “Bangkok” chicken offspring is important since the potential of additive genes introduced to Indonesia local chickens can be utilized to improve the genetic quality.

The objective of this study was to determine the morphometric characteristics of Thai game fowl chicken offspring in East Java related to finding the genetic variation and its relationship among chickens that was spreading in East Java Province. Also, the genetic data and distance will be useful for the genetic selection of filial Bangkok chicken related to meat and egg productivity. The morphometric and meristic characteristics can help in the recognition and classification of the species (Hossain *et al.*, 2016; Nawar *et al.*, 2017). This data is very useful in the preparation of a superior future Bangkok chicken breeding program. This study can also use additional information that the East Java area is the center of Thai game fowl offspring chicken in Indonesia.

2. Materials and methods

2.1. Sampling area

The sampling materials were taken from three areas of East Java Province, consisting of Pasuruan, Madiun, and Banyuwangi Regencies (Figure 1). This province is located in the coordinates of 1110 4' to 1140 4' E and 7012' to 804' S. The total area is 47 963 km² which includes two main parts, namely East Java mainland and the Madura Islands. The mainland area is 88.70 % or 42 541 km², while Madura Island area is 11.30 % or 5 422 km². The total population in 2020 reached 39 886 288 inhabitants (BPS Jatim, 2020), while the total local chicken population in 2019 was estimated 39 291 778 birds (Dispet Jatim, 2020); and East Java Province is the second largest local chicken population in Indonesia with 36 609 094 birds after Central Java by 40 633 383 heads (BPS, 2020).



Figure 1. Map of sampling chicken area in East Java Province, Indonesia (red color). The regencies of sampling area are as follows (1) Madiun, (2) Pasuruan and (3) Banyuwangi.

2.2. Sampling materials and equipment

A total of 450 chickens were chosen for analysis in the study area. Each regency area sampled about 150 chickens. The study area was determined by considering based on chicken population number, agroecology, and socioeconomic that supported chicken growth. The geographical map of the study area is illustrated in Figure 1, while the observation and measurement of chicken morphology were applied on adult layer female and male chickens by around 2 yr old.

The main equipment used in this study consisted of i) measuring tools for quantitative traits, including measuring tape with a scale of 150 cm, digital hanging scales with a capacity of 10 kg, and a metal ruler; and ii) supporting tools for activities in the field such as baskets, gloves, masks, stationery, GPS and documentations kits. The main activity of this study was to collect the existing data, primarily on phenotypic data, including quantitative and qualitative data obtained directly from the study area. The phenotypic data were then tabulated and followed by data analyzed using descriptive analysis, nested design, and discriminant analysis.

The data source was phenotypic variables including quantitative and qualitative characters of chickens that were recorded following the FAO (2012) standard descriptor. A physical descriptors list was determined to record both quantitative and qualitative morphological characters. In each study area, the selected household owner of chicken was identified as having experience in rearing “Bangkok” or Thai game fowl chicken for more or less than one and a half years. Furthermore, the selected chicken owners were depth interviewed to describe the family's historical rearing “Bangkok” chicken and the history of chicken origin.

2.3. Morphological data collection

Quantitative traits of body morphological characters were obtained from chickens aged around one and a half to 2 yr old. Body weight was weighed using a scale, while chicken morphological measures cover back length (taken when the chicken is standing, then taken from the curve of the chicken's neck to the end of the tailbone), beak length (from the tip of the beak to the base of the beak), shank length (from the hock joint to the spur of either leg), chest width (from the tip of the right chest to the tip of the left chest horizontally), chest circumference (circular from the tip of the pectus [hind breast] to the of front chest), wing length (the distance between the tips of right and left wings when fully stretched) and the 3rd finger length (from the tip of the chicken's 3rd toe to its base) (Figure 2). The qualitative variables observed were the shape of the comb and the color of the shank (Figure 3). Body morphological measurements and photography of chickens (front, side, and back) were carried out by placing the chicken on its two legs and placing it on a flat surface withholding it; hence, the chicken did not escape.

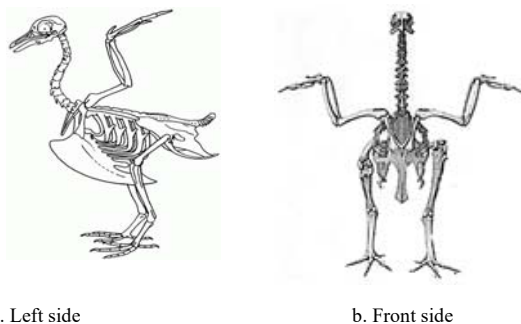


Fig. 2. The topological morphology measurement on Thai game fowl chicken (picture modified from Bell, 2002; Mustefa *et al.*, 2021)

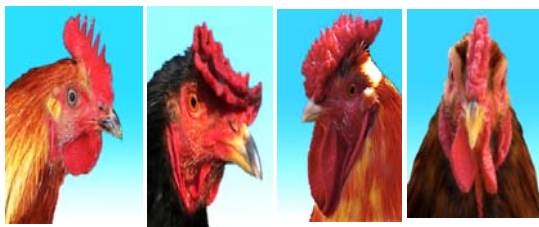


Figure 3. The comb shape found in "Bangkok" chicken (a. Single comb; b. Pea comb; c. Rose comb; and d. Walnut / Strawberry comb) (adapted from Imsland *et al.*, 2012)

2.4. Data analysis

The data measurement from chicken morphometric variables, both quantitative and qualitative data, was analyzed using descriptive analysis, based on frequency and cross-tabulation for comparisons between study areas. Nested analysis was applied to determine the differences between "Bangkok" chickens that were nested in the three sampling areas. The linear mathematical model for the two-staged nested design (Adinurani, 2022; Montgomery, 2008) in Equation (1):

$$Y_{ijk} = \mu + \tau_i + \beta_{(i)} + \varepsilon_{K(ij)} \quad \begin{cases} i = 1, 2, \dots, a \\ j = 1, 2, \dots, b \\ k = 1, 2, \dots, n \end{cases} \quad (1)$$

Where;

Y_{ijk} = an observation factor a at level $-i_{th}$; factor b at level $-j_{th}$; and repetition $-k_{th}$

μ = mean value

τ_i = effect of group $-i_{th}$

$\beta_{(i)}$ = effect of sub-group $-j_{th}$ in group $-i_{th}$

$\varepsilon_{K(ij)}$ = error of sub group $-j_{th}$ in group $-i_{th}$ with repetition $-k_{th}$

Furthermore, to calculate the genetic distance and the morphometric genetic similarity relationship, the discriminant function was applied by calculating the genetic distance from Mahalanobis and the quadratic minimum distance function is calculated using the Nei formula (Fatmarischaet *et al.*, 2014), in Equation (2):

$$D^2 = (m - x)^T \cdot C^{-1} \cdot (m - x) \quad (2)$$

Where,

D^2 is the square of the Mahalanobis distance for genetic distance between Bangkok chicken

x is the vector of the observation (row in data set for quantitative and qualitative variables of chicken)

m is the vector of the mean values of independent variables (mean of each column for quantitative and qualitative variables of chicken)

C^{-1} is the inverse covariance matrix of independent variables

Several procedure analyses were performed by SAS platform. From the analysis, it is expected that the morphological variations and genetic relationship among Thai game fowl offspring chickens will identify in the selected sampling area. This research was conducted with the Description of Ethical Approval No.5.a/048.a/KEPK-UMM/III/2022 issued by the Faculty of Medicine, University of Muhammadiyah Malang.

3. Results and discussions

3.1. The qualitative traits of "Bangkok" chicken offspring

The qualitative traits determined in this study consisted of the comb shape and shank color of chickens. The comb shape that was mostly found in "Bangkok" chicken offspring was a Single (36.9 %) (Fig. 3.a, Fig. 4 c and Table 1), then followed by Walnut or Strawberry comb (32.7 %), Pea (18.7 %) and Rose (11.8 %). This result corresponds to Rafian *et al.*, (2017) study on the local chicken "Burgo" from Bengkulu Province, Sumatra, and Arlina *et al.*, (2015) on Kokok Balenggek, a local chicken from West Sumatra Province, Indonesia with a single comb was the dominant comb. The major single comb of Indonesian native chicken was also found by Maharani *et al.* (2018; 2021) with a dominantly black color on the chest feather, whereas Permadi *et al.* (2020) study showed that people of Tirtomulyo Village, Kendal Regency of Central Java preferred raising single comb (53.3 %) for their backyard chicken. Another study by Asmara *et al.* (2019) stated that Pelung chicken, a local chicken from

West Java, has single comb dominantly. The majority of single-combed local chicken was also found in Saral village of Chhajjian valley, Haripur district in Khyber Pakhtunkhwa, a province in Pakistan, by 92.50 % (Bibi *et al.*, 2021), in “Zoar” – chicken native to Mizoram, India – by 74.63 % (Lalhlimpuia *et al.*, 2021), and even in Black-bone chicken – a native to Thailand – by 100 % (Buranawit *et al.*, 2016). The type of combs in chicken is supposedly related to climate adaptability; for instance, single comb complies with warm temperature. Single comb is the wild type of native chicken genetic with recessive genotype (*rr pp*) (Imsland *et al.*, 2012), and its existence may be the result of genetic selection activities correlated with certain cultural and religious practices. For example, in some areas of the Muslim religion in Ethiopia single comb type was commonly found, while the pea and walnut type was commonly found in non-Muslim religious areas, even in Vietnam (Desta *et al.*, 2013). Nevertheless, the consistency of this finding should be followed by exploring the correlation between comb-type with religion and traditional activities.



a. Pea b. Rose c. Single d. Walnut/Strawberry

Figure 4. The comb shape of “Bangkok” chicken from sample area of East Java Province, Indonesia.

Table 1. The frequency of comb shape on Bangkok chicken offspring

Comb shape	Frequency	Percentage (%)	Total cumulative
Pea	84	18.7	18.7
Rose	53	11.8	30.4
Walnut	147	32.7	63.1
Single	166	36.9	100.0
Total	450	100.0	

The analysis of the shank color of “Bangkok” chicken offspring from 450 samples showed that the highest frequency was blackish yellow by 205 chickens (45 %)

and the lowest was blackish white by seven chickens 1.6 %). This finding was in line with Arlina *et al.* (2015); Maharani *et al.* (2018); and Tamsil *et al.* (2020) that yellow and white or a mixture of these color were the dominant shank color found in Indonesia native chicken. Similar studies found that white and yellow were dominant in native chicken shanks in Bangladesh (Sharker *et al.*, 2014), in South-Western Ethiopia (Bayou *et al.*, 2022; Tadele *et al.*, 2018), in Eastern and Western Samar of the Philippines (Godinez *et al.*, 2020), and in transboundary area of Jammu and Kashmir in India (Singh *et al.*, 2022).

From an economic viewpoint, the shank color is a very important trait due to the different consumer preferences prevalent in different areas of Korea (Jin *et al.*, 2014). The pigmentation of non-feathered or plumage tissue, in this case, is body skin and shank involving carotenoids and melanin which are responsible for yellow and black color respectively (Gowda *et al.*, 2020). The white color of chicken skin is carried by the dominant allele while the yellow color is homozygous for the recessive allele (Lalhlimpuia *et al.*, 2021). The finding of a low proportion of white skin color in this recent study indicated that there was a small frequency for the dominant allele. In addition, skin color is a genetic trait related to carotenoid pigments and is also related to the type of nutrition, adaptive fitness, and health conditions (Lalhlimpuia *et al.*, 2021). The high frequency of yellow color in this study suggested that the availability of feed sources was almost uniform in the rearing system besides breeder selection practiced towards specific characters related to fighting cocks. Skin pigmentation in chicken such as shank color is related to the levels of carotenoid and melanin (Jin *et al.*, 2014). In addition, an SNP study of Korean native chicken stated that the strong candidate for pigmentation was *MC1R* gene or equivalent with *E* locus.

Table 2. Frequency of shank color on “Bangkok” chicken offspring

Shank color	Frequencies	Percentage (%)	Comulatif
Black	13	2.9	2.9
Blackish white	7	1.6	4.4
Yellow	190	42.2	46.7
Blackish yellow	205	45.6	92.2
Yellowish white	19	4.2	96.4
White	16	3.6	100
Total	450	100	



Figure 5. The variation color shank of “Bangkok” chicken offspring in East Java, Indonesia

3.2. Morphometric measurements of “Bangkok” chicken offspring

In the rearing of “Bangkok” chicken offspring, farmers' practices vary from free range to semi-intensive system. However, the coefficient of variation (CV) of body measurements was still acceptable. Aronhime *et al.* (2014) defined reproducibility parameters as excellent when CV is $\leq 10\%$, good when CV is between 10% to 20% , acceptable when CV is between 20% to 30% , and poor when CV is 30% . The coefficient of the diversity of body

measurements in Banyuwangi Regency was the highest score by 7% to 25% (Table 3). This was presumably due to the rearing chicken practical gap between breeders. The field observations showed that some breeders applied intensive rearing for selected superior male chickens to fight cock beside the free-range system. This different rearing system also affected the diversity of body measurements, like body weight in each regency. However, feeding and health management could also

Table 3. The body measurements parameter of “Bangkok” chicken between sample areas

Body measurement	Region			Total
	Banyuwangi	Madiun	Pasuruan	
	$\bar{x} \pm \text{sd}$ (% CV)	$\bar{x} \pm \text{sd}$ (% CV)	$\bar{x} \pm \text{sd}$ (% CV)	$\bar{x} \pm \text{sd}$ (% CV)
Sample number (birds)	150	150	150	450
Body weight (g)	1 781.46 \pm 536.47 (25)	2 366.74 \pm 749.46 (19)	2 463.19 \pm 549.65 (18)	2 203.60 \pm 667.36 (10.03)
Shank length (cm)	9.74 \pm 1.35 (12)	11.21 \pm 1.75 (10)	11.33 \pm 1.46 (10)	10.760 \pm 1.69 (5.32)
Beak length (cm)	1.99 \pm 0.12 (7)	2.00 \pm 0.15 (7)	2.04 \pm 0.19 (7)	2.03 \pm 0.15 (3.56)
Breast depth (cm)	8.69 \pm 1.09 (12)	9.42 \pm 1.30 (11)	10.965 \pm 1.20 (19)	9.69 \pm 1.53 (5.17)
Brisket length (cm)	21.24 \pm 2.36 (10)	23.54 \pm 3.12 (9)	23.42 \pm 2.06 (9)	22.73 \pm 2.76 (4.76)
Breast circumference (cm)	29.67 \pm 4.51 (11)	34.20 \pm 4.16 (9)	34.17 \pm 3.19 (9)	32.68 \pm 4.52 (4.90)
Wing length (cm)	20.16 \pm 2.33 (8)	21.44 \pm 2.60 (8)	18.88 \pm 2.89 (9)	20.16 \pm 2.81 (4.22)
Third toe length (cm)	6.59 \pm 1.04 (14)	8.46 \pm 1.37 (11)	8.54 \pm 1.01 (11)	7.86 \pm 1.46 (5.70)

impact chicken performance. According to Prasetyo (2017) and Tonda *et al.* (2022, 2023) the variation in body weight could be influenced by several factors, like rearing management, feeding, and health management. The coefficient of variance (CV) of body measurements between sexes was ranged from 7% to 24% . This score also allowed for data analysis since it was in the range of normal distribution. The body weight of the female showed was higher than male chicken as shown in Table 4. According to Daikwo *et al.* (2011), male body weight

is higher than females due to the dimorphism sexual of chickens that are regulated by genetic mechanisms. Body weight in male chickens can grow faster than in females because of their genetic capability (Kalita *et al.*, 2017). According to Petkov *et al.* (2020), the existence of male chickens in a group begins to accumulate negative effects from the age of 28 d after hormonal changes, sex competition, and sexual dimorphism which began to appear at the age of 35 d. Thus, in this period females will experience male-dominated stage which could affect stress and decreasing feed consumption.

Table 4. The variation of body measurement between “Bangkok” chicken offspring based on sex

Body measurements	Sex	
	Male $\bar{x} \pm sd$ (% CV)	Female $\bar{x} \pm sd$ (% CV)
Sample number (chickens)	225	225
Body weight (g)	2 580.71 \pm 695.75 (17)	1 826.88 \pm 423.37 (24)
Shank length (cm)	11.68 \pm 1.72 (10)	9.84 \pm 1.03 (12)
Beak length (cm)	2.05 \pm 0.18 (7)	1.98 \pm 0.11 (7)
Breast depth (cm)	10.21 \pm 1.59 (10)	9.18 \pm 1.27 (11)
Brisket length (cm)	23.66 \pm 2.59 (9)	21.81 \pm 2.26 (10)
Breast circumference (cm)	34.56 \pm 4.37 (9)	30.79 \pm 3.83 (10)
Wing length (cm)	21.54 \pm 2.62 (8)	18.78 \pm 2.28 (9)
Third toe length (cm)	8.52 \pm 1.20 (11)	7.2 \pm 1.41 (12)

3.3. Genetic distance between “Bangkok” chicken offspring

The analysis of similarity and admixture within and between regency of local chickens (Table 5) showed similarity rates ranging from 80.7 % to 86 %. The highest percentage of similarities among area was Pasuruan (86 %), followed by Banyuwangi (80.7%) and the lowest was Madiun regency (72%).

Table 5. Percentage of similarity and admixture within and between sampling area

Area (Regency)	Area (Regency)			Total
		Banyuwangi	Madiun	Pasuruan
Banyuwangi	N	121	26	3
	%	80.7	17.3	2
Madiun	N	25	108	17
	%	16.7	72	11.3
Pasuruan	N	6	15	129
	%	4	10	86

Notes: N = number of chicken

The diversity of chicken species in the population can be caused by many reasons, but mostly by genetic factors. Segregation of genetic traits in native chickens was influenced by uncontrolled genetic selection practices for a long time resulting in unique traits and providing materials for genetic map study (Wragg *et al.*, 2012). Hence, the genetic structure provides an opportunity to study the effects of artificial selection and ecological influences on the morphological structure of domestic chickens (Desta *et al.*, 2013).

Native chicken populations are greatly genetic variation due to their long-term adaptation in response to varying agroecological zones. Native chickens have unique adaptive traits that enable them to survive and reproduce under harsh conditions, like climate, nutrition, and management which are usually associated with low input–output production systems (Maw *et al.*, 2015). Thus, the difference between the area of “Bangkok” chicken

offspring in this recent study can lead to the variation of chicken traits.

The genetic distance matrix between areas ranged from 96.04 to 682.03 (Table 6), and the closest genetic distance was between Pasuruan and Banyuwangi (96.04). This was presumably because the distance area between Pasuruan and Banyuwangi is close compared with Madiun and Banyuwangi. On the other side, the distance between Madiun and Pasuruan is far, thus the genetic distance was farther. According to Fatmarischa *et al.* (2014), the estimating of genetic distance through body measurement can be useful for an initial step in determining of genetic relationship between geographical areas, and the length of genetic distance was suspected caused by the slow deployment of chickens from one site to another of geographic location.

Since domestication, chickens have been distributed across countries, continents and cultures. Breeds originating from the same geographical area are spread across a spectrum of genetic diversity, especially breeds of European and Asian types. When based on sampling area, genetic diversity can be correlated with geographic distance to the wild type fowl of chicken, *Gallus gallus* within Asian breeds. The pattern of genetic diversity in a population can be better explained by the geographic expansion of its ancestor groups, which correlates with genetic differentiation. Genetic distance between domesticated chicken populations and their wild relatives can predict the genetic diversity of domesticated chicken populations.

Table 6. The genetic distance matrix between sampling area

Sampling Area	Sampling Area		
	Banyuwangi	Madiun	Pasuruan
Banyuwangi	0.000		
Madiun	586.03	0.000	
Pasuruan	96.04	682.03	0.000

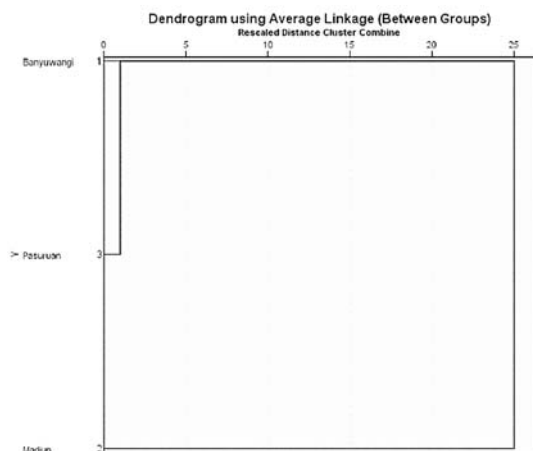


Figure 6. The dendrogram of genetic distance of “Bangkok” chicken between sampling area

The dendrogram which confirms genetic distance matrix of “Bangkok” chicken offspring between areas (Table 6) is shown in Figure 6. The genetic distance between Banyuwangi and Madiun was farther than between Banyuwangi and Pasuruan regency. The overall genetic diversity might be the result of population-specific events, such as mutation, natural selection that favors adaption to the current environment, and/or artificial selection (for example for certain production traits) and population genetic drift as well (Malomane *et al.*, 2021). Many local breeds were developed due to the diversity of geographical conditions and the lack of gene flow. For poultry, the genetic flow should be made possible by carrying eggs from one area to another (Bao *et al.*, 2009).

In the case of the “Bangkok” offspring chicken which assumed that the ancestor was originated from Thailand's native chicken was related to the practice of crossbreeding between captured Jungle fowl and native chicken for cockfighting and sports game bird in Thailand and Philippines (Maw *et al.*, 2015). Native chickens of Thailand, Myanmar and Laos were low in genetic diversity when compared to other Asia chickens (Indonesia, China, Nepal, and Vietnam), leading to low diversity based on egg white protein polymorphism. From the center(s) of domestication in Asia, chickens colonized the world through human migration and terrestrial and maritime trading routes (Lawal and Hannote, 2021).

4. Conclusions

The study of “Bangkok” offspring chickens in Indonesia that spread over the East Java region has generally high similarity (72 % to 80 %) based on morphological variables. Thus, the genetic variation is low. Although geographically separated, the similarity is still high. This correlated with the previous studies that local chickens in the ASEAN region, including Indonesia, generally tend to have high similarity although they are separated geographically. Genetic diversity can change more rapidly within genes associated with protein transport and lipid metabolic processes. Thus, these genes are thought to be flexible or elastic to changes according to the needs of the population. For further studies, it is necessary to identify gene-based traits that are relevant to the environmental adaptation.

Acknowledgment

The authors gratefully thank the Rector University of Muhammadiyah Malang, Indonesia for the support and research permissions. This research is part of the National Research Project funded by the Ministry of Research and Technology / National Research Agency, the Republic of Indonesia in 2020 by contract number: 7/EI/II/PRN/2020-2021.

References

- Adinurani P.G. 2022. **Non-Parametric Statistics (Agricultural Applications, Manuals and SPSS)**. Deepublish, Yogyakarta, Indonesia
- Arlina F, Abbas H, Anwar S and Jamsari. 2015. Qualitative and quantitative traits of Kokok Balenggek chicken, the rare indigenous chicken in West Sumatera. Proceeding the 6th International Seminar on Tropical Animal Production (ISTAP). Integrated Approach in Developing Sustainable Tropical Animal Production. Universitas Gadjah Mada Yogyakarta, Indonesia. pp. 453–457.
- Aronhime S, Calcagno C, Jajamovich GH, Dyvorne HA, Robson P, Dieterich D, Fiel MI, Martel-Laferrriere V, Chatterji M, Rusinek H and Taouli B. 2014. DCE-MRI of the liver: Effect of linear and nonlinear conversions on hepatic perfusion quantification and reproducibility. *J Magn Reson Imaging*, **40**(1):90–98. <https://doi.org/10.1002/jmri.24341>
- Asmara, IY, Garnida D, Tanwiriah W and Partasasmita R. 2019. Qualitative morphological diversity of female Pelungchickens in West Java, Indonesia. *Biodiversitas*, **20**(1):126–133. <https://doi.org/10.13057/biodiv/d200115>
- Bao WB, Shu JT, Wu XS, Musa HH, Ji CL and Chen GH. 2009. Genetic diversity and relationship between genetic distance and geographical distance in 14 Chinese indigenous chicken breeds and red jungle fowl. *Czech J. Anim. Sci.*, **54**(2):74–83. <https://doi.org/10.17221/1666-CJAS>
- Bayou Y, Bayou E, Genzebu D and Assefa H. 2022. Phenotypic characterization of indigenous chicken ecotypes in selected districts of Bench Maji Zone, South West Ethiopia. *Int. J. Food Sci. Agric.*, **6**(3):293–300.
- Bell DD. 2002. Anatomy of the chicken. In: Bell DD and Weaver WD (Eds). *Commercial Chicken Meat and Egg Production*. Springer, Boston, USA. https://doi.org/10.1007/978-1-4615-0811-3_4
- Bibi S, Fiaz Khan M, Noreen S, Rehman A, Khan N, Mehmood S and Shah M. 2021. Morphological characteristics of native chicken of village Chhajjian, Haripur Pakistan. *Poult Sci.*, **100**(3): 1–6. <https://doi.org/10.1016/j.psj.2020.11.022>
- BPS (Badan Pusat Statistik Indonesia - Central Statistics Bureau). 2020. Population of Indonesian native chicken by province 2009–2019. Indonesian Ministry of Agriculture. <https://www.bps.go.id/subject/24/peternakan.html#subjekViewTab3>.
- BPS Jatim (Badan Pusat Statistik Provinsi Jawa Timur - Central Statistics Bureau of East Java). 2020. The population number of East Java Province in 2018–2020. <https://jatim.bps.go.id/indikator/12/375/1/jumlah-penduduk-provinsi-jawa-timur.html>.
- Buranawit K, Chailungka C, Wongsunri Cand Laenoi W. 2016. Phenotypic characterization of Thai native black-bone chickens indigenous to Northern Thailand. *Thai J. Vet. Med.*, **46**(4):547–554.

- Caballes JC. 2013. Production potentials of native chickens (*Gallus gallus domesticus* L.) of Western Visayas, Philippines. *Trop Anim Health Prod* **45**: 405–410. <https://doi.org/10.1007/s11250-012-0230-1>
- Daikwo IS, Okpe AA, and Ocheja JO. 2011. Phenotypic characterization of local chickens in Dekina. *Int. J. Poultry Sci.*, **10**:444–447. <https://doi.org/110.3923/ijps.2011.444.447>
- Desta T, Dessie T, Bettridge J, Lynch S, Melese K, Collins M, Christley RM, Wigley P, Kaiser P, Terfa Z, Mwacharo JM and Hanotte O. 2013. Signature of artificial selection and ecological landscape on morphological structures of Ethiopian village chickens. *Anim. Genet. Res.*, **52**:17–29. <https://doi.org/10.1017/S2078633613000064>
- Dispet Jatim (Dinas Peternakan Provinsi Jawa Timur - Animal Husbandry Agency of East Java Province) 2020. Statistics of animal husbandry population. http://disnak.jatimprov.go.id/web/data/datastatistik/statistikpopulasi_siternak.
- Duengkae P, Chaiwatana S, Chamchumroon W, Suzuki T, Koonawootrittrirong S, Matsuda Y and Srikulnath K. 2021. Origin and evolutionary history of domestic chickens inferred from a large population study of Thai red jungle fowl and indigenous chickens. *Sci Rep* **11**(2035): 1–15 <https://doi.org/10.1038/s41598-021-81589-7>
- FAO (Food and Agriculture Organization). 2022. Gateway to poultry production and products. <https://www.fao.org/poultry-production-products/production/poultry-species/chickens/en/>.
- Fatmarischa N, Sutopo and Johari S. 2014. Genetic distance and differentiating factors of male and female ducks through morphometric analysis approach. *Jurnal Peternakan Indonesia*, **16**(1):33–39. <https://doi.org/10.25077/jpi.16.1.33-39.2014>
- Gowda V, Jayanaik BG, Nagaraja CS, Veeregowda M, Krishnamurthy TN, Jayashree R, Kotresh AM, Gouri MD and Basavarajiah DM. 2020. Phenotypic characterization of indigenous chicken of Belagaum Division of Karnataka State, India. *Int. J. Curr. Microbiol. App. Sci.*, **9**(04):1304–1312.
- Godinez CJP, Nishibori M and Espina DM. 2020. Qualitative traits and genetic characterization of native chicken (*Gallus gallus domesticus*) in selected areas of Eastern and Western Samar, Philippines. *Ann. Trop. Res.* **42**(2): 52–70. <https://doi.org/10.32945/atr4225.2020>
- Hossain MY, Hossen MA, Islam MM, Pramanik MNU, Nawer F, Paul AK, Hameed HMA, Rahman MM, Kaushik G, Bardoloi S. 2016. Biometric indices and size at first sexual maturity of eight alien fish species from Bangladesh. *Egypt J Aquat. Res.* **42**: 331–339. <https://doi.org/10.1016/j.ejar.2016.09.001>
- Imsland F, Feng C, Boije H, Bed'hom B, Fillon V, Dorshorst B, Rubin CJ, Liu R, Gao Y, Gu X, Wang Y, Gourichon D, Zody MC, Zecchin W, Vieaud A, Tixier-Boichard M, Hu X, Hallböök F and Li NAL. 2012. The rose-comb mutation in chickens constitutes a structural rearrangement causing both altered comb morphology and defective sperm motility. *PLoS Genet.* **8**(6): 1–12. <https://doi.org/10.1371/journal.pgen.1002775>
- Iskandar S. 2012. Optimally of protein and ration energy for increasing meat production of local chicken. *Pengembangan Inovasi Pertanian*, **5**(2):96–107. <http://203.190.37.42/publikasi/ip052123.pdf>
- ITIS [Integrated Taxonomic Information System] 2020. *Gallus gallus* (Linnaeus, 1758). https://www.itis.gov/servlet/SingleRpt/SingleRpt?search_topic=T&search_value=176086#null.
- Jin S, Park H and Seo D. 2014. Association of MCR1 genotype with shank color traits in Korean native chicken. *Livest. Sci.*, **170**:1–7. <https://doi.org/10.1016/j.livsci.2014.10.001>
- Kalita S, Kalita K, Kalita N, Mahanta J, Ahmed H and Islam R. 2017. Effect of sex separate rearing on uniformity of commercial broiler chicken reared in deep litter system. *Int. J. Livest.*, **8**(1):79–83. <http://dx.doi.org/10.5455/ijlr.20170630041851>
- Lalhlimpua C, Singh NS, Mayengbam P, Chaudhary JK and Tolengkomba TC. 2021. Phenotypic characterization of native chicken 'Zoar' of Mizoram, India in its home tract. *J. Entol. Zool. Studies*, **9**(1):1756–1759.
- Lawal, RA and Hanotte, O. 2021. Domestic chicken diversity: Origin, distribution, and adaptation. *Anim. Genet.*, **52**: 385–394. <https://doi.org/10.1111/age.13091>
- Malomane DK, Weigend S, Schmitt AO, Weigend A, Reimer C and Simianer H. 2021. Genetic diversity in global chicken breeds in relation to their genetic distances to wild populations. *Genet. Sel. Evol.*, **53**:36 <https://doi.org/10.1186/s12711-021-00628-z>
- Maharani D, Insani GA and Adinda L. 2018. Phenotypic characterizations of Indonesia native chicken with different combs. Proceedings the 1st International Conference on Food and Agriculture (ICoFA): Current Innovation and Implementation of Modern Technology in Food and Sustainable Agriculture., Nusa Dua, Bali, Indonesia. Universitas Gadjah Mada, Indonesia
- Maharani D, Mustofa F, Sari APZNL, Fathoni A, Sasongko H and Hariyono DNH. 2021. Phenotypic characterization and principal component analyses of indigenous chicken breeds in Indonesia. *Vet. Word*, **14**(6):1665–1676. <https://doi.org/10.14202/vetworld.2021.1665-1676>
- Maw AA, Kawabe K, Shimogiri T, Rerkamnuaychoke W, Kawamoto Y, Masuda S and Okamoto S. 2015. Genetic diversity and population structure in native chicken populations from Myanmar, Thailand and Laos by using 102 indels markers. *Asian-Australas J Anim Sci.*, **8**(1):14–19. <https://doi.org/10.5713/ajas.14.0212>
- MontgomeryDC. 2008. **Design and Analysis of Experiments**. 7th ed. Wiley Publisher, USA
- Mustefa A, Kenfob H, Belayhuna T, Hailua A and Assefaa A. 2021. Morphometric and morphological characterization of chicken resources adapted to pastoral and agropastoral areas of southern Ethiopia. *Genetic Resources* **2**(4): 72–84. <https://doi.org/10.46265/genresj.NDFM2712>
- Nataamijaya AG. 2010. The development of local chicken potency for supported increasing farmers welfare. *Jurnal Litbang Pertanian* **29**(4): 131–138. <http://ejurnal.litbang.pertanian.go.id/index.php/jppp/article/view/7759/6723>
- Nawer F, Hossain MY, Hossen MA, Khatun D, Parvin MF, Ohtomi J and Islam MA. 2017. Morphometric relationships of the endangered Ticto barb *Pethia ticto* (Hamilton, 1822) in the Ganges River (NW Bangladesh) through multi linear dimensions. *Jordan J. Biol. Sci.*, **10**(3): 199–203.
- Oocities.org. 2009. Thai game fowl. <http://www.oocities.org/xyoojaviaries/thaigamefowl.html..>
- Petkov E, Ignatova M and Popova T. 2020. Effect of the sex separate and straight-run type of rearing on the performance, carcass and meat chemical composition in fast growing broilers. *Bulgarian J. Agric. Sci.*, **26**(3):652–658.
- Permadi ANN, Kurnianto E and Sutiyono. 2020. Morphometrical characteristics of male and female native chickens in Tirtomulyo Village, Plantungan sub-district, Kendal districts, Central Java *Jurnal Peternakan Indonesia*, **22**(1):11–20. <https://doi.org/10.25077/jpi.22.1.11-20.2020>
- Prasetyo D. 2017. Phenotypic variance analysis of civet (*Paradoxurus hermaphroditus*) in Bali Province as the basis identification of genetic variation. Undergraduate thesis. University of Muhammadiyah Malang, Indonesia. <https://eprints.umm.ac.id/36780/>

- Rafian T, Jakaria J and Ulupi N. 2017. Qualitative phenotype diversity of Burgo chicken in Bengkulu Province. *Jurnal Sains Peternakan Indonesia*, **12**(1): 47–54. <https://doi.org/10.31186/jspi.id.12.1.47-54>
- Rusdin M, Nafiu LO, Saili T and Aku AS. 2011. Characteristic of phenotype qualitative traits of Tolaki chicken from Konawe Regency, South Sulawesi. *Agriplus*, **21**(03): 248–256.
- Sarker NR, Hoque A, Faruque S, Islam N and Bhuiyan FH. 2014. An ex-situ study on body characteristics and effect of plumage color on body weight of indigenous chicken (*Gallus domesticus*) in Bangladesh. *Acta Sci. - Anim. Sci.*, **36**(1): 79–84. <https://doi.org/10.4025/actascianimsi.v36i1.20118>
- Singh S, Taggar RK, Chakraborty D, Kumar D, Kumar N, and Azad MS. 2022. Characterization of local chicken of transboundary region of Jammu and Kashmir (India). *Research Square*. <https://doi.org/10.21203/rs.3.rs-1568349/v1>
- Sulandari S, Zein MSA and Sartika T. 2008. Molecular characterization of Indonesian indigenous chickens based on mitochondrial DNA displacement (D)-loop sequences. *Hayati*, **15**(4): 145–154. <https://doi.org/10.4308/hjb.15.4.145>
- Tadele A, Melesse A and Taye M. 2018. Phenotypic and morphological characterizations of indigenous chicken populations in Kaffa Zone, south-western Ethiopia. *Anim. Husb. Dairy Vet. Sci.*, **2**(1): 1–9. <https://doi.org/10.15761/AHDVS.1000128>
- TikaE. 2017. The simple six ways of bangkok chicken raising for the beginner. Ilmu Budaya. Com. <https://ilmubudidaya.com/cara-budidaya-ayam-bangkok>
- Tamzil MH, Indarsih B, Ichsan M and Jaya INS. 2020. Phenotypic characteristics of super kampung chickens raised as meat producers. *Int. J. Poult. Sci.*, **19**:524–530. <https://doi.org/10.3923/ijps.2020.524.530>
- Tonda R, Zalizar L, Widodo W, Setyobudi RH, Hermawan D, Damat D, Endang Dwi Purbajanti ED, Prasetyo H, Ekawati I, Jani Y, Burlakovs J, Wahono SK, Anam C, Pakarti TA, Susanti MS, Mahnunin R, Sutanto A, Sari DK, Hilda H, Fauzi A, Wirawan W, Sebayang NS, Hadinoto H, Suhesti E, Amri U and Busa Y. 2022. Potential utilization of dried rice leftover of household organic waste for poultry functional feed. *Jordan J. Biol. Sci.*, **15**(5): 879–886. <https://doi.org/10.54319/jjbs/150517>
- Tonda R, Atoum MFM, Setyobudi RH, Zalizar L, Widodo W, Zahoor M, Hermawan D, Damat D, Fauzi A, Putri A, Zainuddin Z, Yuniati S, Hawayanti E, Rosa I, Sapar S, Adil A, RA Dodi S, Supartini N, Indriatiningtias R, Kalsum U, Iswahyudi I and Pakarti TA. 2023. Food waste product for overcoming heat stress in broilers. *E3S Web Conf.*, **374**(00031):1–14. <https://doi.org/10.1051/e3sconf/202337400031>
- Widodo W, Rahayu ID, Sutanto A, Setyobudi RH and Mel M. 2019. The effectiveness of curcuma (*Curcuma xanthorrhiza* Roxb.) addition in the feed toward super Kampung chicken performances. *Proc. Pak. Acad. Sci.-B.*, **56**(4): 39–46
- Widodo W, Winaya A, Zalizar L, Anggraini AD, Malik A, Suyatno S, Zahoor M, and Mel M. 2022. Protein level efficacy in improving meat nutritional contents in cross-bred local chickens aged 0 month to 2 month. *Jordan J Biol Sci.* **15**(5): 893–896. <https://doi.org/10.54319/jjbs/150519>
- Wragg D, Mwacharo JM, Alcalde JA, Hocking PM and Hanotte O. 2012. Analysis of genome-wide structure, diversity and fine mapping of Mendelian traits in traditional and village chickens. *Heredity*, **109**:6–18. <https://doi.org/10.1038/hdy.2012>

Inhibitory Effect of Partially Purified Compounds from Pomegranate Peel and Licorice Extracts on Growth and Urease Activity of *Helicobacter pylori*

Screen M.B. Bataineh*, Bara'ah A. Abu Dalo, Bayen S. Mahawreh, Homa Darmani and Abdul-Karim J. Sallal

Department of Biotechnology and Genetic Engineering, Faculty of Science and Arts, Jordan University of Science and Technology, Irbid 22110, Jordan. * Received: Oct 10, 2022; Revised: March 27, 2023; Accepted Mar 29, 2023

Abstract

Helicobacter pylori (*H. pylori*) is the main causative agent responsible for chronic gastritis, peptic ulcer, and gastric cancer in humans. An important virulence factor of *H. pylori* is urease that converts urea into ammonia, producing a neutral micro-environment, which allows colonization and survival in the stomach lining. Although various therapies have been introduced for the treatment of *H. pylori* infection, the eradication failure rate stays as high as 5–20% along with frequent recurrence of gastric ulcers even after complete healing. Looking for an alternative mode of treatment using natural products, we investigated the effects of pomegranate peel and licorice extracts that had been fractionated using ethyl acetate and methanol into 4 fractions (F1-F4) on the growth (disc diffusion and minimum inhibitory concentration - MIC) and urease activity of this pathogen. We found that all fractions had antimicrobial activity with the maximum activity observed with the F1 fraction of both pomegranate peel and licorice extracts with growth inhibitory zones of 33 mm and 26 mm, and MICs of 2 and 1 mg/ml, respectively. The F2 and F4 fractions of licorice extract, and F3 of pomegranate peel extract showed MIC values of 4 mg/mL, whereas the F4 fraction of pomegranate peel extract and F3 of licorice extract showed MIC values of 8 mg/ml. The F1 and F2 fractions of pomegranate peel caused 80 and 91% inhibition of urease activity and the F1 fraction of licorice caused total inhibition (100%) of *H. pylori* urease activity at MIC values. In conclusion, these results indicate that both pomegranate and licorice contain important bioactive compounds against *H. pylori* and should be examined further to help in the fight against this important pathogen.

Keywords: *Helicobacter pylori*, Pomegranate peel, Licorice, Urease, Gastritis

1. Introduction

Helicobacter pylori (*H. pylori*) is an important pathogen that selectively colonizes the epithelium of the stomach and duodenum (Ruggiero, 2010), which leads to gastritis, peptic ulcer, and gastric cancer in humans (Sokolova & Naumann, 2022; Abu-Ahmad *et al.*, 2011). The key virulence factor produced by *H. pylori* is urease (Valenzuela-Valderrama *et al.*, 2019), which converts urea into ammonia and enables the microorganism to colonize the stomach lining (Bansil *et al.*, 2013). Other virulence factors include cytotoxin-associated gene A (*cagA*) and vacuolating cytotoxin (*vacA*) proteins (Wen & Moss, 2009) which are responsible for the pathogenicity of *H. pylori* (Radosz-Komoniewska *et al.*, 2005). *CagA*-positive *H. pylori* strains have been associated with interleukin-8 (IL-8) induction in gastric epithelium. Increased production of IL-8 causes neutrophilic infiltration into gastric epithelium leading to epithelial inflammation and disruption of the tight junctions and cell integrity of the stomach (Huang *et al.*, 2014). The *vacA* gene encodes VacA protein which can remain on the bacterial surface (Foegeding *et al.*, 2016) and cause cell death (Chauhan *et al.*, 2019).

Triple therapy with a proton pump inhibitor (PPI) and the antimicrobials amoxicillin and clarithromycin is a recent therapeutic regimen for *H. pylori* eradication (Puig *et al.*, 2016). It was found to be highly effective in the long-term treatment of disease in 80% of the patients (Juergens *et al.*, 2010). Although this mode of therapy shows some related side effects such as diarrhea, colitis (Cremonini *et al.*, 2002), and low eradication of *H. pylori* (Perri *et al.*, 2001), it led to the absence of the pathogen (Moss and Calam, 1992). However, it failed to exterminate the bacteria in 10-20% of patients (Choi *et al.*, 2012) due to strains resistant to clarithromycin.

Quadruple therapy was then introduced as a better regimen for treating *H. pylori* infection (Kanizaj and Kunac, 2014) with amoxicillin, metronidazole, omeprazole, and bismuth subnitrate (Lu *et al.*, 2013). Quadruple therapy is usually associated with high levels of antibiotic resistance (Ndip *et al.*, 2008; Tanih *et al.*, 2010), although it is reported to be 90% effective (Tanih *et al.*, 2010). However, the eradication failure rate stays as high as 5–20% along with frequent recurrence of gastric ulcers even after complete healing. The problem of incomplete/partial treatment that occurs with triple and quadruple therapy, in addition to the possible side effects (Li *et al.*, 2005), has led to the search for new chemical

* Corresponding author. e-mail: smbataineh3@just.edu.jo.

compounds with bacteriostatic or bactericidal effects against *H. pylori* (González *et al.*, 2019) in order to overcome these challenges. There is growing interest in looking at alternative treatments using natural products that are relatively nontoxic and cheap (Ayala *et al.*, 2014).

Several natural materials are used in folk medicine for the treatment of bacterial infections and examples of different natural compounds that exhibit activity against *H. pylori* include broccoli, curcumin, *Nigella sativa* or black caraway, olive oil and mume (Muraliet *et al.*, 2014). Many of these natural products have been shown to have phenolic phytochemicals such as cinnamic acids, cinnamaldehydes, coumarins, phenolic acids, capsaicin, flavonoids, and tannins (Tabak *et al.*, 1996; Jones *et al.*, 1997; Bae *et al.*, 1999; Graham *et al.*, 1999; Tabak *et al.*, 1999; Yanagawa *et al.*, 2003).

Pomegranate (*Punica granatum* L.) belongs to the genera *Punica* and the family *Punicaceae* (Chen *et al.*, 2019), and the fruits, leaves, flowers, and bark of this plant have been used in various fields of traditional medicine (Mekni *et al.*, 2013) of the Middle East, India, China, Pakistan, and many other countries (Zhicen, 1987; Kapoor, 1990). It has been used as an antiparasitic agent, and to treat various illnesses including diarrhea, diabetes (Moghaddam *et al.*, 2013), rheumatism, sore throats and to decrease inflammation (Arun and Singh, 2012). In addition, pomegranate has been used to treat infections caused by *Salmonella*, *Shigella*, *Proteus*, *Klebsiella*, *Escherichiacoli*, *Pseudomonas*, *Vibrio cholerae*, and *Staphylococcus aureus*. Moreover, pomegranate exocarp anthocyanin methanol extract combined with metronidazole has been shown to significantly decrease the colonization of *H. pylori* in rats (Ragab, A.E. *et al.*, 2022). Pomegranate peels represent approximately 40% of the whole fruit and contain several phytochemicals including punicalin, punicalagin, granatin B, gallagylidilactone, punicalagin, pedunculagin, and tellimagrandin (Cerdeira *et al.*, 2003; Seeram *et al.*, 2005; Jurenka, 2008; Magangana *et al.*, 2020). The antioxidant activity of pomegranate peels has been linked with its phenolic components such as gallotannins, anthocyanins, ellagitannins, gallagyl esters, hydroxycinnamic acids, dihydroflavonol and hydroxybenzoic acids (Fischer *et al.*, 2011).

Licorice (*Glycyrrhizauralensis*) is another important medicinal plant, and the roots, stolons and rhizomes of this plant have also been used in traditional medicine. The major phenolic compounds of licorice include glycosides of liquiritigenin (4,7-dihydroxyflavanone) and isoliquiritigenin (2,4,4-trihydroxychalcone) (Bethapudi *et al.*, 2022). Licorice extract has been investigated as a substitute to bismuth that is normally used in quadruple therapy (Li *et al.*, 2018). Bismuth protects against acid and pepsin secretions by covering the location of the lesion and promoting mucous secretion (Sreeja *et al.*, 2020).

Given the activities and benefits of pomegranate peel and licorice, in the current study we investigated the effect of pomegranate peel and licorice on the growth and urease activity of *H. pylori*.

2. Materials and Methods

2.1. Organism and growth conditions

Helicobacter pylori was obtained from American Type Culture Collection (ATCC 700392). Columbia blood agar base enriched with 7% horse serum and Brucella broth were used to grow and maintain *H. pylori* cultures. Incubation was done under microaerophilic conditions using a campygen pack at 37 °C for 48-72 hours

2.2. Pomegranate peel and licorice extraction procedure

Pomegranate peel was dried at room temperature for 7 days and then grinded to a powder. Licorice powder was purchased from local markets in Jordan. The plant extraction method was a modification of the protocol used by Ajaikumar *et al.* (2005). Twenty grams of both powdered pomegranate peel and licorice were extracted with 200 ml of methanol and then mixed using a magnetic hot plate at 45 °C for 3 hr. A rotary evaporator was used at 45 °C to concentrate the extract to 100 mg and dissolve it in 1 ml dimethylsulfoxide (DMSO). Fractionation of concentrated extract was performed depending on the polarity of their compounds using methanol and ethyl acetate solvents by Isolera Prime™ Flash Purification System at flow rates 18 ml /min, followed by drying it using nitrogen gas then stored in the refrigerator until use. Each fraction (0.1 g) was dissolved in 1 ml of DMSO in an Eppendorf tube. Doubling dilutions were performed for each crude extract using DMSO as the following 1:1, 1:2, 1:4 and 1:8. Thin layer chromatography (TLC) was used to determine the number of fractions (F) that found in pomegranate peel and licorice extracts using methanol solvent. The partially purified fractions were dissolved in DMSO (0.1 g of each fraction was dissolved in 1 ml of DMSO).

2.3. Bacterial growth inhibition

The Disk diffusion method was performed to investigate the bacterial growth inhibition to determine the effect of pomegranate peel and licorice crude extracts and their fractions on *H. pylori* activities *In vitro* according to Zhang *et al.* (2013).

H. pylori suspension (0.1 ml in liquid Brucella medium) (1×10^8 CFU/ml) was inoculated on the Columbia agar surface. Sterile paper disks (6 mm) were impregnated with 10 µl of different concentrations from each crude extract of pomegranate peel and licorice. The negative control used was the DMSO and the positive control was ampicillin (100 mg/ml). All test plates were incubated in a microaerophilic atmosphere. The inhibitory zone around each disk was measured

2.4. Determination of minimum inhibitory concentration (MIC) and minimum bactericidal concentration (MBC) of the partially purified fractions against *Helicobacter pylori*

The MIC and MBC were determined using a broth microdilution method (Weseler *et al.*, 2005). The partially purified fractions of pomegranate peel and licorice were diluted in sterile water to obtain a series of concentrations for each fraction 32.0, 16.0, 8.0, 4.0, 2.0, and 1.0 mg/ml. Separately, 100 µl of each concentration was added to 96 well plates containing 100 µl of *H. pylori* (1×10^8 CFU/ml) supplemented with 7% horse serum. Plates were incubated

under the microaerophilic condition at 37 °C for a period of 20±2 h. A tetrazolium salt p-iodonitrophenyltetrazolium violet (INT) was used as an indicator of bacterial growth in which INT reduced to violet color formazan. The MICs were determined as the lowest concentration of each fraction showed no detectable *H. pylori* growth. After an incubation period, 10 µl from each fraction was spread onto the surface of the Columbia agar plate to determine the MBC values. The MBCs were determined as the lowest concentration of each fraction that showed no detectable *H. pylori* growth.

2.5. Growth curve of *Helicobacter pylori*

The partially purified fractions of pomegranate peel and licorice at their MIC concentrations were evaluated for their impact on *H. pylori* growth. Briefly, separately 100 µl of each concentration was added into a 96-well plate containing 100 µl of *H. pylori* (1×10⁸ CFU/ml) supplemented with 7% horse serum. Brucella broth was used as a negative control. Plates were incubated under the microaerophilic condition at 37 °C, then optical density (OD) at 600 nm was measured at different intervals.

2.6. Effect of partially purified compounds on urease activity of *Helicobacter pylori*

Forty ml broth cultures (1×10⁸ CFU/ml) were harvested by centrifugation at 5000 rpm for 10 min at 4 °C. Cells were suspended in 4 ml phosphate buffer pH 7.4 containing 5 mg protease inhibitor. This suspension was disrupted by four 15-sec periods of ultrasonication punctuated with 15-sec rest periods in an ice bath. Following centrifugation at 5000 rpm for 10 minutes at 4 °C, the supernatant was filtered using 0.2 µm membrane filters. Protein concentrations in filtrated solution were determined using the Bradford protein assay (Bardford, 1976).

Ammonia production was used to assess the inhibition of partially purified compounds on urease activity of *H. pylori* (Matsubara *et al.*, 2003 and Shin *et al.*, 2003): using 96 well plates, 30 µl of each purified fraction was mixed with 30 µl of urease reaction solution (final concentration 200 µg/ml) and incubated at 37 °C for 10 min, distilled water was also used as control. Fifty µl of urea reagent (2% urea and 0.03% phenol red in phosphate-buffered saline, pH 6.8) was added to initiate the urease reaction. Ammonia concentration was determined by measuring the absorbance at 520 nm.

Inhibition rate was calculated using the formula: (Inhibition rate) % = ((OD520 control - OD520 sample)/OD520 control) * 100.

2.7. Statistical analysis

All assays were performed in triplicate and the results were expressed as the mean value. Results of the growth inhibition assay, MIC and MBC, and urease assay were analyzed using a one-sample students T-test. Growth curve effects for partially purified fractions were analyzed using one-way analysis of variance (ANOVA) by performing the Least Significant Difference (LSD) multiple comparison tests on the data means. The Statistical Package for the Social Sciences (SPSS) version 20.0 software was used for the statistical analyses. *P*-value ≤ 0.05–0.01 was considered significant and *P*-value ≤ 0.01 was considered highly significant in all data analyses.

3. Results

Crude extracts of pomegranate peel and licorice at different concentrations were found to inhibit the growth of *H. pylori* using the disk diffusion method (*P*-value= 0.005 and *P*-value= 0.001 for pomegranate peel and licorice, respectively). The maximum inhibition zone was found at 100 mg/ml for both pomegranate peel and licorice crude extracts (Table 1). Pomegranate peel extract showed an inhibition zone of about 29 mm, whereas the inhibition zone for licorice was 21 mm. DMSO and ampicillin were used as negative and positive controls, respectively (Table 1).

Table 1: Growth inhibition zone of crude extracts of pomegranate peel and licorice against *H. pylori*.

Concentrations	Inhibition zone of pomegranate peel (mm)*	Inhibition zone of Licorice (mm)**
100 mg/ml	29.3	21.3
1:1	28.7	19
1:2	20.7	18.3
1:4	16.7	16
1:8	10	13.6
Ampicillin	78.3	78.3
DMSO	0	0

**P*-value= 0.005

***P*-value= 0.000

Pomegranate and licorice extracts were fractioned using ethyl acetate and methanol solvents by Isolera Prime™ Flash Purification System. Four fractions (F1-F4) for each licorice and pomegranate peel were obtained according to their polarity. These fractions were evaluated for their inhibitory influence on *H. pylori* growth by using the disk diffusion method. The diameters of inhibitory zones of the partially purified fractions are shown in Table 2, and it can be seen that the maximum antimicrobial activity was found with the F1 fraction for both pomegranate peel and licorice. The F1 fraction of pomegranate peel extract showed an inhibition zone of 34 mm, whereas that of licorice showed an inhibition zone of 27 mm. The negative control, DMSO, did not affect the growth of *H. pylori*.

Table 2: Growth inhibition zone of pomegranate peel and licorice fractions and DMSO against *H. pylori*.

Pomegranate peel and Licorice fractions	Inhibition zone of pomegranate peel (mm)*	Inhibition zone of Licorice (mm)*
F1	33.7	26.7
F2	24	13.7
F3	20.7	12
F4	15.7	16
Ampicillin	78.3	78.3
DMSO	0	0

**P*-value= 0.008

**P*-value= 0.014

Table 3 shows the results of the MIC and MBC for the partially purified compounds that were determined using the microdilution method. The F1 fraction of licorice extract showed the lowest MIC value of 1 mg/mL, whereas the F1 fraction of pomegranate peel extract showed an

MIC value of 2 mg/ml. However, the F2 and F4 fractions of licorice extract, and F3 fraction of pomegranate peel extract showed MIC values of 4 mg/ml, whereas F4 of pomegranate peel extract and F3 of licorice extract showed MIC values of 8 mg/ml. The DMSO that was used to dissolve the isolated active compounds showed no interference with the MIC results. There were no significant differences between the fractions of both pomegranate peel and licorice (P -value= 0.094 for pomegranate peel fractions at their MIC and MBC values and P -value= 0.06 and 0.074 for licorice fractions at their MIC and MBC values respectively).

Table 3. Minimum inhibitory concentration (MIC) and Minimum bactericidal concentration (MBC) of the partially purified fractions on *Helicobacter pylori* growth(mg/ml)

Fraction	Pomegranate peel		Licorice	
	MIC	MBC	MIC	MBC
F1	2	4	1	1
F2	16	32	4	8
F3	4	8	8	16
F4	8	16	4	8

P -value= 0.094

P -value= 0.06(MIC) and 0.074(MBC)

The F1 fractions of both pomegranate peel and licorice at their MIC values inhibited the growth of *H. pylori* (Figures 1 and 2). Complete (100%) growth inhibition of *H. pylori* using both pomegranate peel and licorice was obtained after 24-hour incubation under microaerophilic conditions.

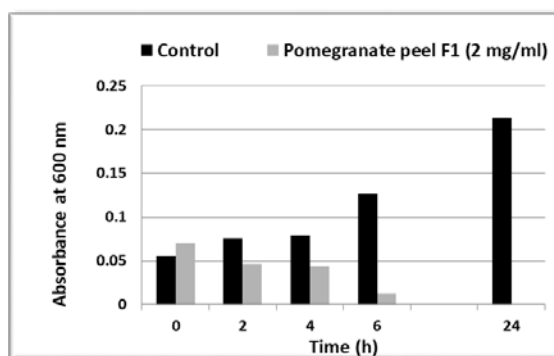


Figure 1. The effect of F1 from pomegranate peel on the growth of *Helicobacter pylori* (P -value= 0.00)

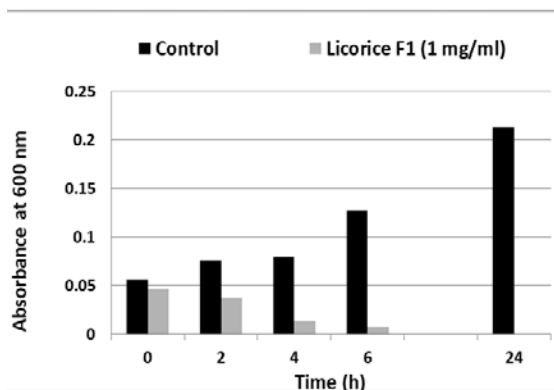


Figure 2. The effect of F1 from licorice on the growth of *Helicobacter pylori* (P -value= 0.019)

The effects on inhibition of *H. pylori* urease activity using different fractions of pomegranate peel and licorice at their MIC values are shown in Table 4. The F2 fraction

of pomegranate peel caused 91% inhibition while F1 of licorice caused 100% enzyme inhibition (Table 4). However, the F1 fraction of pomegranate peel inhibited the enzyme by 80%.

Table 4. Percentage inhibition of *H. pylori* urease enzyme using pomegranate peel and licorice fractions.

Fractions	Urease inhibition (%) Pomegranate peel	Urease inhibition (%) Licorice
F1	79.6	100
F2	91	20.1
F3	8.8	43.9
F4	4.8	55.7

*Urease activity of *H. pylori* =

4. Discussion

With increasing problems associated with antimicrobial resistance together with the added challenges of currently available eradication therapies of *H. pylori* infections, such as high cost and poor compliance of patients, it is of utmost importance to develop novel antibacterial treatments using natural materials against this very important pathogen. A variety of natural compounds have been reported to exhibit antimicrobial activity against *H. pylori* including olive oil, *Nigella sativa*, broccoli, mume, and curcumin (Murali *et al.*, 2014), pomegranate (Hajimahmoodi *et al* 2011; Moghaddam, 2011) and licorice (Fukai *et al* 2001). Indeed, both pomegranate and licorice have been used in traditional medicine throughout history to provide relief from various gastrointestinal problems ranging from diarrhea, epigastric pain to peptic ulcers. This encouraged us to study the effects of these phytotherapeutic agents on the growth and urease production of *H. pylori*. Our results indicate that indeed, crude extracts of both pomegranate peel and licorice were active against *H. pylori*. The crude extract of pomegranate peel showed a greater degree of inhibition (29mm) of growth of *H. pylori* than that of licorice (21mm). Our results agree with those of Hajimahmoodi *et al* (2011) who reported that crude extracts of pomegranate peel showed inhibition zone diameters ranging from 16 to 40 mm. Another study showed that the highest inhibition zone of pomegranate peel was 27.96 mm at 2 mg of crude extract/disc (Moghaddam, 2011). In addition, Fukai *et al* (2001) reported that licorice fractions showed inhibition diameters ranging from 11.5 to 19 mm, which is slightly less than the growth inhibitory zones reported in the results of the current study.

In addition, we found that all of the four different isolated methanolic fractions inhibited the growth of *H. pylori* and interestingly the F1 fractions from both pomegranate peel and licorice showed greater activity producing larger growth inhibitory zones (33.7 and 26.7 mm, respectively) than the crude extracts. We also found that the F1 fraction of pomegranate peel and licorice exhibited the highest bacteriostatic and bactericidal activity (MIC and MBC of 2mg/ml and 4mg/ml, respectively for pomegranate; 1mg/ml for licorice) in comparison to the other fractions tested, using the modified broth dilution method. Moghaddam (2011), on the other hand, reported that the MIC and MBC for pomegranate peel was much lower (312.5 µg/ml and 338.5

µg/ml, respectively) using the agar dilution method. In contrast to our results, Jafarian and Ghazvini, (2007) reported that MIC for licorice against *H. pylori* was much higher than the results of the current study (range of 50-400 mg/ml, compared to 1mg/ml for the F1 fraction in the current study).

H. pylori is known for its high activity of urease enzyme which protects the bacterium from gastric secretions. Both pomegranate peel and licorice were found to inhibit urease activity. The F1 and F2 fractions of pomegranate peel showed the greatest inhibitory effects with 80 and 91% inhibition of enzyme activity, respectively at MIC values of 2mg/ml. Nabati *et al.* (2012) reported that a crude extract of pomegranate peel causes almost total inhibition (99.9%) of urease activity of this pathogen. This effect may be due to the presence of ellagic acid derivatives such as the ellagitannins, punicalagin, and punicalin (Cerdeira *et al.*, 2003; Larrosa *et al.*, 2006) and catechins (Julie Jurenka, 2008). Furthermore, we found that the F1 fraction of licorice at its MIC value had the strongest activity with 100% inhibition of urease activity. This effect may be due to the presence of flavonoid compounds (Eloff *et al.*, 1998; Cowan *et al.*, 1999). Complete or partial inhibition of urease activity would result in decreased ability of *H. pylori* to survive the acidity of the gastric secretions.

As a vital factor of virulence, the effects of pomegranate peel and licorice on inhibition of urease activity in the current study are of particular significance. Without this vital enzyme, the ability of *H. pylori* to establish infection would be totally compromised. Indeed, in a gnotobiotic piglet model, *H. pylori* mutants that were unable to produce urease could not colonize the gastric mucosa and were unable to cause infection (Eaton *et al.* 1991). It comes as no surprise that the production of urease has been suggested an important target for innovative alternate antimicrobial regimens to thwart the unending problem of drug resistance of this important pathogen (Tarsia *et al.* 2018). Urease activity is not only important in allowing *H. pylori* to colonize and infect the gastric mucosa but the resulting increased pH also decreases the viscoelastic properties of the gastric mucus which would permit greater mobility of *H. pylori* and allow easier penetration and attachment to the host epithelial cells (Celli *et al.* 2009).

The results of the current study clearly indicate that exposure of *H. pylori* to extracts of pomegranate and licorice resulted in inhibition of growth and urease activity of this pathogen. One limitation of the current study is that the isolated fractions of both plants were not characterized further. This needs to be done in order to identify the component(s) responsible for the observed inhibitory effects. Furthermore, future studies should focus on *in vivo* testing of these extracts in animal models of *H. pylori* infection to correlate these *in vitro* findings.

In addition to the bactericidal effects and urease inhibiting properties, pomegranate peel and licorice possess other properties that promote gastric health. For example, pomegranate possesses antineoplastic effects since it inhibits proliferation of cancer cells causing cell cycle disruption and apoptosis of cancer cells, and also inhibits angiogenesis (Lansky *et al.*, 2007; Amin *et al.*, 2009; Adhami *et al.*, 2009). Indeed, it has been reported to be effective against different types of cancer including

colon cancer (Amin *et al.*, 2009), and this has been attributed to the antioxidant and anti-proliferative effects (Amin *et al.*, 2009; Adhami *et al.*, 2009). The antioxidant properties of pomegranate peel (Iqbal *et al.*, 2008) would prevent lipid peroxidation which results in the formation of reactive oxygen species and free radicals that are associated with carcinogenesis (Shahidi, 1997; Siddhuraju and Becker, 2003). Furthermore, the flavonoid-rich fractions of licorice not only exhibit anti-*H. pylori* activity (Eloff *et al.*, 1998; Cowan *et al.*, 1999), but also anti-ulcer activity (Aly *et al.*, 2005; Shibata and Saitoh, 1973) due to their antioxidant, anti-inflammatory, and anticarcinogenic effects (Park *et al.* 2014). Not surprisingly, licorice has been used for many decades to treat gastric ulcers based on three lines of evidence that confirm that licorice-derived compounds have ulcer healing ability (Duke 1985). Firstly, licorice-derived products induce increases in prostaglandin levels in the digestive system and have been reported to enhance increased secretion of protective gastric mucin. Secondly, licorice is thought to play a role in increasing the life span of superficial gastric cells and thus slowing down the process of gastric lesion development. Thirdly, it has pepsin inhibitory properties which would lead to less damage to the gastric epithelium. Indeed, the licorice-derived carbenoxolone has been used to promote healing of gastric ulcers since its development in the 1960s (Dehpour 1994). In addition, the many flavonoids with one or more isoprenoid groups that have been isolated from *Glycyrrhiza* species contribute to the anti-*H. pylori* activity of licorice (Nomura and Fukai, 1998; Yamada *et al.*, 1998; Krause *et al.*, 2004).

5. Conclusion

Taken together, the results of the current study and the findings reported in the available literature indicate that both pomegranate peel and licorice not only kill *H. pylori*, but have protective effects on the gastric mucosa. Our results are of significance in highlighting the promising potential of pomegranate and licorice as safe sources to control *H. pylori* infections. Furthermore, pomegranate peel and licorice fractions can be further fractionated to determine the most active chemical compound(s) and test them against *H. pylori* both *In vivo* and *In vitro* and compare the effectiveness with the antibiotics in use.

Acknowledgment

Thanks go to the Deanship of Scientific Research, Jordan University of Science and Technology for funding this research, grant No. 358.

References

- Abu-Ahmad NM, Odeh A and Sallal A-KJ, 2011. Prevalence of *Helicobacter pylori* Gastritis at the North of Jordan. *Jordan J Biol Sci.*, (4) 2: 71-76.
- Adhami VM, Khan N and Mukhtar H. 2009. Cancer Chemoprevention by Pomegranate: Laboratory and Clinical Evidence. *Nutr Cancer.*, 61(6): 811- 815.
- Ajaikumar, KB, Asheef, M, Babu, BH, Padikkala, J. 2005. The inhibition of gastric mucosal injury by *Punicagranatum* L. (pomegranate) methanolic extract. *J. Ethnopharmacol.*, 96: 171-176.

- Aly AM, Al-Alousi L and Salem HA. 2005. Licorice: A possible anti-inflammatory and anti-ulcer drug. *AAPS PharmSciTech.*, **6**(1): E74 – E82.
- Amin AR, Kucuk O, Khuri FR and Shin DM. 2009. Perspectives for cancer prevention with natural compounds. *J. Clin. Oncol.*, **27**: 2712 – 2725.
- Arun N and Singh DP. 2012. Punica granatum: a review on pharmacological and therapeutic properties. *Int J Pharm Sci Res.*, **3**(5): 1240.
- Ayala G, Escobedo-Hinojosa WI, de la Cruz-Herrera CF, Romero I. 2014. Exploring alternative treatments for *Helicobacter pylori* infection. *World J. Gastroenterol.*, **20**(6): 1450.
- Bae EA, Han MJ and Kim DH. 1999. *In vitro* anti-*Helicobacter pylori* activity of some flavonoids and their metabolites. *Planta Med.*, **65**(5): 442 – 3.
- Bansil R, Celli J, Hardcastle J and Turner B. 2013. The influence of mucus microstructure and rheology in *Helicobacter pylori* infection. *Front immunol.*, **4**: 310.
- Bradford MM. 1976. A rapid and sensitive method for the quantitation of microgram quantities of protein utilizing the principle of protein-dye binding. *Anal. Biochem.*, **72**: 248 – 254.
- Bethapudi B, Murugan SK, Nithyanantham M, Singh VK, Agarwal A and Mundkinajeddu D. 2022. Gut health benefits of licorice and its flavonoids as dietary supplements. In *Nutrition and Functional Foods in Boosting Digestion, Metabolism and Immune Health*, Academic Press., 377 - 417.
- Celli JP, Turner BS, Afdhal NH, Keates S, Ghiran I *et al.* *Helicobacter pylori* moves through mucus by reducing mucin viscoelasticity. *Proc Natl Acad. Sci. U.S.A.*, 2009;**106**:14321–14326.
- Cerda B, Ceron JJ, Tomas-Barberan FA and Espin JC. 2003. Repeated oral administration of high doses of the pomegranate ellagitannins punicalagin to rats for 37 day is not toxic. *J. Agric. Food Chem.*, **51**: 3493 – 3501
- Chauhan N, Tay ACY, Marshall BJ and Jain U. 2019. *Helicobacter pylori* VacA, a distinct toxin exerts diverse functionalities in numerous cells: An overview. *Helicobacter.*, **24**(1): e12544.
- Chen M, Zhang TK and Yuan ZH. 2019. Evolution and classification of pomegranate. *Acta Hortic.*, **1254**: 41- 48.
- Choi HS, Chun HJ, Park SH, Keum B, Seo YS, Kim YS and Ryu HS. 2012. Comparison of sequential and 7-, 10-, 14-d triple therapy for *Helicobacter pylori* infection. *World J. Gastroenterol.*, **18**(19): 2377.
- Cowan MM. 1999. Plant products as antimicrobial agents. *Clin. Microbiol. Rev.*, **12**: 564 – 582.
- Cremonini F, Di Caro S, Covino M, Armuzzi A, Gabrielli M, Santarelli L and Gasbarrini A. 2002. Effect of different probiotic preparations on anti-*Helicobacter pylori* therapy-related side effects: a parallel group, triple blind, placebo-controlled study. *Am. J. Gastroenterol.*, **97**(11): 2744 -2749.
- Duke JA. **Handbook of Medicinal Herbs**. Boca Raton, FL: CRC Press; 1985.
- Dehpour AR. The protective effect of licorice components and their derivatives against gastric ulcer induced by aspirin in rats. *J Pharm Pharmacol.* 1994;**46**:148-152.
- Eaton KA, Brooks CL, Morgan DR, Krakowka S. Essential role of urease in pathogenesis of gastritis induced by *Helicobacter pylori* in gnotobiotic piglets. *Infect. Immun.*, 1991;**59**:2470–2475.
- Eloff JN. 1998. Which extraction should be used for screening and isolation of antimicrobial components from plants. *J Ethnopharmacol.*, **60**: 1- 8.
- Fischer UA, Carle R and Kammerer DR. 2011. Identification and quantification of phenolic compounds from pomegranate (*Punica granatum* L.) peel, mesocarp, aril and differently produced juices by HPLC-DAD-ESI/MSn. *Food chem.*, **127**(2): 807- 821.
- Foegeding NJ, Caston RR, McClain MS, Ohi MD and Cover TL. 2016. An overview of *Helicobacter pylori* VacA toxin biology. *Toxins.*, **8**(6): 173.
- Fukai T, Cai BS and Nomura T. 2001. Flavonoids from Kirghiz licorice (*Glycyrrhiza glabra*). *Nat. Med.*, **55** (6): 311.
- González A, Salillas S, Velázquez-Campoy A, Angarica VE, Fillat MF, Sancho J and Lanas Á. 2019. Identifying potential novel drugs against *Helicobacter pylori* by targeting the essential response regulator HsrA. *Sci. rep.*, **9**(1): 1-13.
- Graham DY, Anderson SY and Lang T. 1999. Garlic or jalapeno peppers for treatment of *Helicobacter pylori* infection. *Am. J. Gastroenterol.*, **94**(5): 1200 – 2.
- Hajimahmoodi M, Shams-Ardakani MP, SanieeSiavoshi F, Mehrabani M, Hosseinzadeh H, Foroumadi P, Safavi M, Khanavi M, Akbarzadeh T, Shafiee A and Foroumadi A. 2011. *In vitro* antibacterial activity of some Iranian medicinal plant extracts against *Helicobacter pylori*. *Nat. Prod. Res.*, **25** (11): 1059 – 1066.
- Huang HL, Ko CH, Yan YY and Wang CK. 2014. Antiadhesion and anti-inflammation effects of noni (*Morindacitrifolia*) fruit extracts on AGS cells during *Helicobacter pylori* infection. *J. Agric. Food Chem.*, **62**(11): 2374-2383.
- Iqbal S, Haleem S, Akhtar M, Zia-ul-Haq M and Akbar J. 2008. Efficiency of pomegranate peel extracts in stabilization of sunflower oil under accelerated conditions. *Food Res. Int.*, **41**: 194 – 200.
- Jafarian M k and Ghazvini K. 2007. *In vitro* susceptibility of *Helicobacter pylori* to licorice extract. *Iran J Pharm Res.*, **6** (1): 69 – 72.
- Jones NL, Shabib S and Sherman PM. 1997. Capsaicin as an inhibitor of the growth of the gastric pathogen *Helicobacter pylori*. *FEMS Microbiol. Lett.*, **146**(2): 223 – 7.
- Juergens A, Pels H, Rogowski S, Fließbach K, Glasmacher A, Engert A and Schlegel U. 2010. Long-term survival with favorable cognitive outcome after chemotherapy in primary central nervous system lymphoma. *Ann. of Neuro: Official Journal of the American Neurological Association and the Child Neurology Society.*, **67**(2): 182-189.
- Julie Jurenka MT. 2008. Therapeutic applications of pomegranate (*Punica granatum* L). *Altern. Med. Rev.* **13**(2): 128 -144.
- Kanizaj TF and Kunac N. 2014. *Helicobacter pylori*: future perspectives in therapy reflecting three decades of experience. *World J. Gastroenterol.*, **20**(3): 699.
- Kapoor LD. 1990. **CRC Handbook of Ayurvedic Medicinal Plants**, 1st ed, CRC Press: Boca Raton, Florida.
- Krausse R, Bielenberg J, Blaschek W and Ullmann U. 2004. *In vitro* anti-*Helicobacter pylori* activity of Extractumliquiritiae, glycyrrhizin and its metabolites. *J. Antimicrob. Chemother.*, **54**: 243 – 6.
- Lansky EP and Newman RA. 2007. Punica granatum (pomegranate) and its potential for prevention and treatment of inflammation and cancer. *J. Ethnopharmacol.* **109**(2): 177 – 206.
- Larrosa M, Gonzalez-Sarrias A, Garcia-Conesa MT, Tomas-Barberan FA and Espin JC. 2006. Urolithins, ellagic acid-derived metabolites produced by human colonic microflora, exhibit estrogenic and antiestrogenic activities. *J. Agric. Food Chem.*, **54**: 1611 – 1620

- Lei L, Meng F, Zhu S, Guo S, Wang Y, Zhao X and Zhang S. 2018. Efficacy and safety of Wei Bi Mei, a Chinese herb compound, as an alternative to bismuth for eradication of *Helicobacter pylori*. *Evid. Based Complementary Altern. Med.*, 2018.
- Li Y, Xu C, Zhang Q, Liu JY and Tan RX. 2005. *In vitro* anti-*Helicobacter pylori* action of 30 Chinese herbal medicines used to treat ulcer diseases. *J. Ethnopharmacol.*, 98, 329 -333.
- Lu H, Zhang W and Graham DY. 2013. Bismuth-containing quadruple therapy for *Helicobacter pylori*: lessons from China. *Eur. J. Gastroenterol. Hepatol.*, 25(10).
- Machado T, Pinto A, Pintov M, Leal I, Silva M, Amaral A, Kuster R and NettodosSantos K. 2003. *In vitro* activity of Brazilian medicinal plants, naturally occurring naphthoquinones and their analogues, against methicillin-resistant *Staphylococcus aureus*. *Int. J. Antimicrob. Agents.*, 21: 279 – 284.
- Magangana TP, Makunga NP, Fawole OA and Opara UL. 2020. Processing factors affecting the phytochemical and nutritional properties of pomegranate (*Punica granatum* L.) peel waste: A review. *Molecules.*, 25(20): 4690.
- Mekni M, Azez R, Tekaya M, Mechri B and Hammami M. 2013. Phenolic, non-phenolic compounds and antioxidant activity of pomegranate flower, leaf and bark extracts of four Tunisian cultivars. *J. Med. Plants Res.*, 7(17): 1100 – 1107.
- Moghaddam G, Sharifzadeh M, Hassanzadeh G, Khanavi M and Hajimahmoodi M. 2013. Anti-ulcerogenic activity of the pomegranate peel (*Punica granatum*) methanol extract. *Food Sci. Nutr.*, 4(10A): 43.
- Moghaddam MV. 2011. *In vitro* Inhibition of *Helicobacter pylori* by some species and medicinal plants used in Iran. *Glob. J. Pharmacol.*, 5(3): 176-180.
- Moss S and Calam J. 1992. *Helicobacter pylori* and ulcer: the present position. *Gut.*, 33: 289 -292.
- Murali BR, Naveen SV, Son GC and Raghavendran HRB. 2014. Current knowledge on alleviating *Helicobacter pylori* infections through the use some commonly known natural products: bench to bedside. Integrative Medicine Research. *Gastroenterology.*, 133(3): 926 – 936.
- Nabati F, Mojab F, Habibi-Rezaei M, Bagherzadeh K, Amanlou M and Yousefi B. 2012. Large scale screening of commonly used Iranian traditional medicinal plants against urease activity. *J. Pharm. Sci.*, 20: 72.
- Ndip RN, Alertia EMT, Ojongokpoko JEA, Luma HN, Malongue A, Akoachere JFTK, Ndip LM, MacMillan M and Weaver LT. 2008. *Helicobacter pylori* isolates recovered from gastric biopsies of patients with gastro-duodenal pathologies in Cameroon: current status of antibiogram. *Trop. Med. Int. Health.*, 13(6): 848 – 854.
- Nomura T and Fukai T. 1998. Phenolic constituents of licorice (*Glycyrrhiza* species). In: Herz, W., Kirby, G.W., Moore, R.E., Steglich, W. and Tamm, Ch. (Eds.) **Progress in the Chemistry of Organic Natural Products**. 73: 1 – 140.
- Park JM, Park SH, Hong KS, Han YM, Jang SH, Kim EH, Hahm KB. Special licorice extracts containing lowered glycyrrhizin and enhanced licochalcone A prevented *Helicobacter pylori*-initiated, salt diet-promoted gastric tumorigenesis. *Helicobacter.*, 2014 19(3): 221-36.
- Perri F, Villani MR, Festa V, Quitadamo M and Andriulli A. 2001. Predictors of failure of *Helicobacter pylori* eradication with the standard 'Maastricht triple therapy. *Aliment. Pharmacol. Ther.*, 15(7): 1023-1029.
- Puig I, Baylina M, Sanchez-Delgado J, Lopez-Gongora S, Suarez D, Garcia-Iglesias P and Calvet X. 2016. Systematic review and meta-analysis: triple therapy combining a proton-pump inhibitor, amoxicillin and metronidazole for *Helicobacter pylori* first-line treatment. *J. Antimicrob. Chemother.*, 71(10): 2740-2753.
- Radosz-Komoniewska H, Bek T, Jóźwiak J and Martirosian G. 2005. Pathogenicity of *Helicobacter pylori* infection. *Clin. Microbiol. Infect.*, 11(8): 602-610.
- Ragab, AE, Al-Madboly, LA, Al-Ashmawy, GM, Saber-Ayad, M, Abo-Saif, MA. 2022. Unravelling the *In vitro* and *In vivo* Anti-*Helicobacter pylori* Effect of Delphinidin-3-O-Glucoside Rich Extract from Pomegranate Exocarp: Enhancing Autophagy and Downregulating TNF-and COX2. *Antioxidants.*, 11, 1752.
- Ruggiero P. 2010. *Helicobacter pylori* and inflammation. *Curr. Pharma. des.*, 16(38): 4225 - 4236.
- Seeram NP, Adams LS, Henning SM, Niu Y, Zhang Y and Nair MG. 2005. *In vitro* antiproliferative, apoptotic and antioxidant activities of punicalagin, ellagic acid and a total pomegranate tannin extract are enhanced in combination with other polyphenols as found pomegranate juice. *J. Nutr. Biochem.*, 16(6): 360-367.
- Shahidi F. 1997. (Ed.). Natural antioxidants: An overview. In: Natural antioxidants, chemistry, health effects and applications, *J. Am. Oil Chem. Soc.*, 1- 11.
- Shibata S and Saitoh T. 1973. Chemical Studies on the Oriental Plant Drugs. Structure of Licoricone, a New Isoflavone from Licorice Root. *Chem. Pharm. Bull.*, 21(6): 1338-1341.
- Shin JH, Nam SW, Kim JT, Yoon JB, Bang WG and Roe IH. 2003. Identification of immunodominant *Helicobacter pylori* proteins with reactivity to H.pylori -specific egg-yolk immunoglobulin. *J. Med. Microbiol.*, 52: 217– 222.
- Siddhuraju P and Becker K. 2003. Antioxidant properties of various solvent extracts of total phenolic constituents from three different agroclimatic origins of Drumstick tree (*Moringaoleifera* Lam.) leaves. *J. Agric. Food Chem.*, 51: 2144 – 2155.
- Sokolova, O,Naumann, M. 2022. Matrix Metalloproteinases in *Helicobacter pylori*–Associated Gastritis and Gastric Cancer. *Int. J. Mol. Sci.*, 23, 1883.
- Sreeja PS, Arunachalam K and Thangaraj P. 2020. Evaluation of Anti-ulcer Potential of *Sphenodesme involucrata* var. *paniculata* (CB Clarke) Munir Leaves on Various Gastric Aggressive Factors. In **Phytomedicine, 1st ed**, CRC Press, 203-216.
- Tabak M, Armon R and Neeman I. 1999. Cinnamon extracts inhibitory effect on *Helicobacter pylori*. *J. Ethnopharmacol.*, 67(3): 269 – 77.
- Tabak M, Armon R, Potasman I and Neeman I. 1996. *In vitro* inhibition of *Helicobacter pylori* by extracts of thyme. *J. Appl. Bacteriol.*, 80(6): 667- 7.
- Tanih NF, Okeleye BI and Naido N. 2010. Marked susceptibility of South African *Helicobacter pylori* strains to ciprofloxacin and amoxicillin: clinical implication. *S. Afr. Med. J.*, 100(1): 45-48.
- Tarsia C, Danielli A, Florini F, Cinelli P, Ciarli S and Zambelli B. 2018. Targeting *Helicobacter pylori* urease activity and maturation: In-cell high-throughput approach for drug discovery. *Biochim. Biophys. Acta Gen. Subj.*, 1862(10): 2245–2253.
- Wen S and Moss S.F. 2009. *Helicobacter pylori* virulence factors in gastric carcinogenesis. *Cancer lette.*, 282(1): 1-8.
- Weseler A, Geiss HK, Saller R and Reichling J. 2005. A novel colorimetric broth microdilution method to determine the minimum inhibitory concentration (MIC) of antibiotics and essential oils against *Helicobacter pylori*. *Pharmazie.*, 60: 498 – 502.

- Valenzuela-Valderrama M, Cerda-Opazo P, Backert S, González MF, Carrasco-Véliz N, Jorquera-Cordero C and Quest AF. 2019. The *Helicobacter pylori* urease virulence factor is required for the induction of hypoxia-induced factor-1 α in gastric cells. *Cancers.*, **11**(6): 799.
- Voravuthikunchai S, Lortheeranuwat A, Jeeju W, Srirak T, Phongpaichit S and Supawita T. 2004. Effective medicinal plants against enterohaemorrhagic *Escherichia coli* O157:H7. *J. Ethnopharmacol.*, **94**: 49 – 54.
- Yamada M, Murohisa B, Kitagawa M, Takehira Y, Tamakoshi K, Mizushima N, Nakamura T, Hirasawa K, Horiuchi T, Oguni I, Harada N and Hara Y. 1998. Effects of tea polyphenols against *Helicobacter pylori*. In: Shibamoto T, Terao J and Osawa T. (Eds.) *Functional Foods for Disease Prevention I, Fruits, Vegetables, and Teas*. ACS Symposium Series, **701**: 217 – 38.
- Yanagawa Y, Yamamoto Y, Hara Y and Shimamura TA. 2003. Combination effect of epigallocatechin gallate, a major compound of green tea catechins, with antibiotics on *Helicobacter pylori* growth *In vitro*. *Curr. Microbiol.*, **47**(3): 244 – 9.
- Zhang X, MeiGu H, ZhuLi X, NanXu Z, ShengChen Y and YangLi. 2013. Anti-*Helicobacter pylori* compounds from the ethanol extracts of *Geranium wilfordii*. *J. Ethnopharmacol.*, **147**: 204 – 207.
- Zhichen L. 1987. *Colour Atlas of Chinese Traditional Drugs*. Science Press, Beijing, People's Republic of China, **1**: 75 – 76.

Agronomic Characters and Quality of Fruit of Salak cv. Gulapasir Planted in Various Agro-Ecosystems

I Ketut Sumantra^{1,2,*}, I Ketut Widnyana^{1,2}, Ni Gusti Agung Eka Martingsih³,
I Made Tamba³, Praptiningsih Gamawati Adinurani⁴, Ida Ekawati⁵,
Maizirwan Mel^{6,7}, and Peeyush Soni⁸

¹Department of Agrotechnology, Faculty of Agriculture and Business University of Mahasaraswati Denpasar Jl. Kamboja 11 A, Denpasar 80233, Bali, Indonesia; ²Masters Program in Regional Development Planning and Environmental Management, University of Mahasaraswati Denpasar, Bali.; ³Department of Agribusiness, Faculty of Agriculture and Business, University of Mahasaraswati, Denpasar, Bali, Indonesia; ⁴Department of Agrotechnology, Faculty of Agriculture, Merdeka University of Madiun, Jl. Serayu No.79, Madiun 63133, East Java, Indonesia; ⁵Department of Agribusiness, Faculty of Agriculture, Universitas Wiraraja, Jl. Raya Pamekasan KM. 05, Sumenep 69451, East Java, Indonesia; ⁶Department of Chemical Engineering and Sustainability, Faculty of Engineering, International Islamic University Malaysia, 50728 Kuala Lumpur, Malaysia; ⁷Postgraduate School, Program Study of Biology, Menara Universitas Nasional, Jl. RM. Harsono No.1, Special Region of Jakarta 12550, Indonesia ; ⁸Department of Agricultural and Food Engineering, Indian Institute of Technology Kharagpur, 721302, Kharagpur, West Bengal, India

Received: Jan 29, 2023; Revised: Apr 2, 2023; Accepted Apr 4, 2023

Abstract

Salak [*Salacca zalacca* (Gaertn.) Voss] var. amboinensis cv. Gulapasir has been officially released by the Minister of Agriculture of the Republic of Indonesia since 1994. Salak 'Gulapasir' is one of five types of fruit that have been designated as the superior fruit of the Bali Province. Salak 'Gulapasir' is preferred by consumers due to its specific fruit flesh taste. Salak 'Gulapasir' was propagated using seeds so that a new type of salak emerged. However, the characters of this new type of salak 'Gulapasir' are not yet known. The research objective was to obtain the superior products of Salak 'Gulapasir' both in quantity and quality. The research used a Randomized Block Design with three replications. The non-independent variable was the three of Salak 'Gulapasir' (SGP): SGP var. angka (N), SGP var. nenas (NS), SGP var. gondok (G), and six sites, namely Karangasem: (K < 560 m asl, K 560 m to 650 m asl, and K > 650 m asl) and Tabanan: (T < 560 m asl, T 560 m to 650 m asl, T > 650 m asl). Observations were made on the agronomic characters and fruit quality. Data were analyzed using variance analysis, and if the planting location and varieties show a difference, then it is followed by the LSD test at the 5 % level. The results showed that different varieties caused different fruit weights, fruit bunches, TSS, and total acid ratio. In Karangasem and in Tabanan, SGP var. angka grows ideally at an altitude of 560 m to 650 m asl with fruit weight per tree of 1.62 kg⁻¹ and 1.29 kg⁻¹, respectively. SGP var. nenas and SGP var. gondok are ideal for cultivating at an altitude of < 560 m asl both in Karangasem and Tabanan, but the fruit production of SGP var. nenas and SGP var. gondok is higher, respectively 19.29 % and 15.31 % when planted in Karangasem, while the SGP var. nenas showed the highest number of fruit bunches⁻¹ in six locations. Further research can be applied using sustainable salak organic agriculture to maintain soil fertility.

Keywords: Altitude, Improve soil fertility, Organic potassium fertilizer, Organic salak, *Salacca zalacca* (Gaertn.) Voss, Salak sustainable agriculture, Snake fruit, Tropical fruit

1. Introduction

Salak [*Salacca zalacca* (Gaertn.) Voss] var. amboinensis cv. Gulapasir is one of the essential fruits in Indonesia, and the plant can be found in most regions of Indonesia (Rai *et al.*, 2016; Ritonga *et al.*, 2018). The salak fruit belongs to the family Palmae or Arecaceae and is native to the Indonesian-Malaysian region (Hakim *et al.*, 2019; Zumaidar *et al.*, 2014). One of the extraordinary strengths of this fruit commodity for Indonesia is the possession of high genetic diversity (Budiyantri *et al.*, 2019). Also, the nutrition of salak fruit is rich in antioxidants, phenolics, vitamins, and minerals (Cepkova

et al., 2021; Mazumdar *et al.*, 2019), and a good source of income and provides livelihood opportunities on seasonal days (Khan and Idrees, 2021). Furthermore fruit flesh and peel have shown tremendous anti-inflammatory, anticancer, antidiabetic (Saleh *et al.*, 2018), and anti-aging agents (Girsang *et al.*, 2019). Antioxidants are chemical compounds that play an essential role in protecting cells due to attacks against free radicals-induced damage to biomolecules (Damat *et al.*, 2019, 2020; Puspitasari and Ningsih, 2016; Setyobudi *et al.*, 2019). Despite its incredible food and medicinal benefits, salak fruit is still underutilized and unknown globally so that this underutilized fruit remains an issue for future sustainable utilization and commercial value enhancement market

* Corresponding author. e-mail: ketut.sumantra@unmas.ac.id

(Mazumdar *et al.*, 2019). Fruit quality is an important issue, especially for products that are consumed raw and fresh. One of the problems is the lack of fruit quality because of inadequate information about superior salak (Budiyanti *et al.*, 2019; Herawati *et al.*, 2018). Therefore, it is necessary to select superior salak to meet market demand and serve community nutrition.

Salak 'Bali' is quite a lot, based on the shape, aroma, taste, and skin colour of the location where the plants are cultivated (Sumantra *et al.*, 2012, 2014; Sumantra and Martiningsih, 2016, 2018). Under the Decree of the Minister of Agriculture of the Republic of Indonesia in 1994, Balinese zalacca was grouped into two superior zalacca: Salak 'Bali' (SK Mentan, 1994a) and Salak 'Gulapasar' (SK Mentan, 1994b). The second type, the salak 'Gulapasar' (SGP) is the most superior salak because of its sweet fruit taste; even though the age of the fruit is still young, thick fruit flesh and seeds are not attached to the fruit flesh (Rai *et al.*, 2014; Sumantra *et al.*, 2016). The nature of this fruit is ideal for meeting market demands for both the domestic and export markets (Martiningsih *et al.*, 2018). Salak 'Bali' is monoecious, so crossing does not need human help (Herawati *et al.*, 2018), and can quickly develop using seeds (Sumantra and Martiningsih, 2016). Another advantage of salak plants in Indonesia compared to other fruits is harvest 2 to 3 times a year if management is good (Rai *et al.*, 2016; Warnita *et al.*, 2019). The expansion of salak 'Gulapasar' planting causes variations in phenotypic diversity. People can find two to three types of salak plants with a marker, fruit shape, aroma, flesh colour, and fruit weight (Martiningsih *et al.*, 2018). The results of this study mean that the emergence of plant diversity due to plant propagation is done by seeds so that new varieties of salak 'Gulapasar' (SGP) appear, as reported by Sumantra and Martiningsih (2016). Based on the marker that can be used as a differentiator, salak farmers give it the name of SGP var. nenas, SGP var. gondok, and SGP var. nangka. The three varieties have not yet identified their advantages in meeting market needs in line with the results of research (Sumantra and Martiningsih, 2016). The performance and produce are influenced by the characteristics of the agricultural ecosystem, particularly microclimate and endogenic factors such as carbohydrate contents, nutrient status (Adelina *et al.*, 2021a; Kumar *et al.*, 2020) and growth hormone (Prihastanti and Haryanti, 2022; Rai *et al.*, 2016).

The salak 'Gulapasar' plantation in the District of Bebandemis the main producer of salak 'Gulapasar' in Bali is located in the southern part of Mount Agung with an altitude of 450 m to 700 m above sea level (m asl). The effect of altitude on plant growth and production is related to plant adaptation to temperature (Sumantra, *et al.*, 2014), full sunlight (Sukawijaya *et al.*, 2009), water status and soil quality (Raharjo *et al.*, 2022; Rai *et al.*, 2014; Ritonga *et al.*, 2018). Salak plants are not resistant to full sun but 50 % to 70 % enough, therefore it is necessary to have shade plants (Sukawijaya *et al.*, 2009; Sumantra *et al.*, 2012). The effect of altitude on plant growth and production is related to plant adaptation to plant tolerance to temperature (Fenech *et al.*, 2019). Water status and soil quality really determine the fruit set on the salak 'Gulapasar'. Low rainfall reduces the Relative Water Content in leaves (RWC), leaf chlorophyll content, and plant nutrient uptake (Rai *et al.*, 2014). Soil quality

included the suitability of the physical, chemical and biological properties (Raharjo *et al.*, 2022). Nuary *et al.* (2019) stated that the distribution of the salak 'Pondoh' plantation area in Sleman (Yogyakarta, Special Region) was greatly influenced by temperature and rainfall. The contribution of temperature in the modelling reached 38.6 % while the rainfall was 27.8 %. Furthermore, taking into account the probability of the temperature variable, the average temperature ranges from 17.41 °C to 25.65 °C, and the ideal month's rainfall ranges from 385.24 mm to 505.01 mm.

Ascorbate content is influenced by abiotic factors, especially temperature and light (Fenech *et al.*, 2019; Setyobudi *et al.*, 2021, 2022). Therefore, variety differences may depend on growing requirements and cultivation techniques. Likewise, Puspitasari *et al.* (2016) stated that tannin content, fruit size and flesh colour of salak fruit are strongly influenced by where it grows. Other studies also explain that salak 'Gulapasar' var. nangka which is grown 570 m asl, would result in a higher quality of fruit that includes thickness of the mesocarpium, edible portion of fruit than compared to above and below 570 m asl (Sumantra *et al.*, 2014; Sumantra and Martiningsih, 2016). Meanwhile, fruit weight and fruit quality of var. gondok and var. nenas have not been reported. Therefore, one way of handling salak quality is by undertaking severe studies for factors such as land and climate and adjusting agricultural patterns according to local climate conditions (Nassar *et al.*, 2018). The success of each species to occupy the environment of an area is influenced by its ability to adapt optimally to all physical environmental factors (temperature, light, soil structure, humidity), biotic factors (interaction between species, competition, parasitism), and chemical factors including the availability of water, oxygen, pH, and nutrients (Nassar *et al.*, 2018; Widyastuti *et al.*, 2022). Moreover, a broad genetic variability would lead to wide phenotypic variability due to the effect of genetic-environment interaction (Ritonga *et al.*, 2018). The research objective was to obtain several superior salak 'Gulapasar' both in production and fruit quality (sugar and acid ratio, vitamin C and tannins) in six different agricultural ecosystems in Bali. This research was important to do to get the suitability and adaptation of the types of salak based on the altitude where it grows so that in the future, its development will be able to provide maximum results according to existing agro-ecosystem conditions.

2. Materials and Methods

2.1. Experimental site

The research was conducted in Tabanan and Karangasem Regencies. Tabanan and Karangasem were selected as research locations because the domination of salak 'Gulapasar' in these two regencies was the highest. In 2021, the salak 'Gulapasar' population in Tabanan was 84 % of all salak species, while in Karangasem Regency the dominance of the salak 'Gulapasar' was more than 63 % (Sumantra *et al.*, 2022).

The study was carried out in six different locations, three sites in Karangasem Regency and three sites in the district of Tabanan. Locations in Karangasem (K) are

lowlands ($K < 560$ m asl) which include several places, namely Telaga, Dukuh, and Karanganyar. Karangasem in the moderate plains ($K 560$ m to 650 m asl) has several areas, namely Kecing and Kutabali and highlands ($K > 650$ m asl), namely Tanah Apo and Kresek (Figure 1).

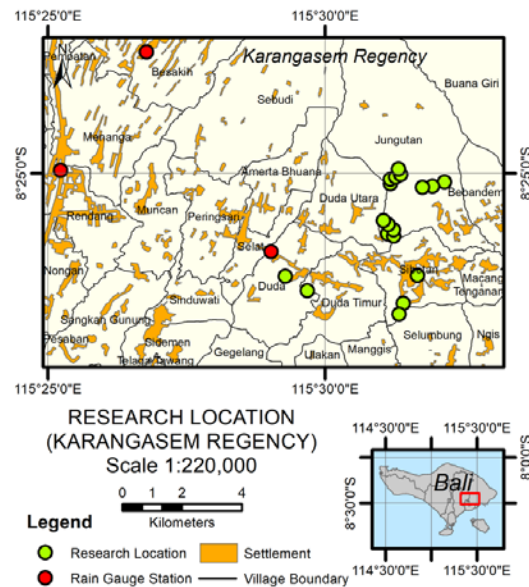


Fig. 1. Research map and sampling point in Karangasem (K)

The research location is in Tabanan (T) in the lowlands ($T < 560$ m asl), including Wanagiri, Sari Buana, and Mundeh Kauh. Tabanan in the medium lands ($T 560$ m to 650 m asl) includes several places, namely Pajahan, Kebon Jero, and Angseri. Tabanan in the highlands ($T > 650$ m asl), namely Munduk Temu, Pempatan, and Batungsel (Figure 2).

Table 1. Treatment of plant location and three varieties of 'Gulapisir' salak

No	Treatment	Explanation
1	NT < 560 m asl	Salak GP var. nangka Tabanan < 560 m asl.
2	NT 560 m to 650 m asl	Salak GP var. nangka Tabanan 560 m to 650 m asl.
3	NT > 650 m asl.	Salak GP var. nangka Tabanan > 650 m asl.
4	NK < 560 m asl.	Salak GP var. nangka Karangasem < 560 m asl.
5	NK 560 m to 650 m asl	Salak GP var. nangka Karangasem 560 m to 650m asl.
6	NK > 650 m asl.	Salak GP var. nangka Karangasem > 650 m asl.
7	GT < 560 m asl	Salak GP var. gondok Tabanan < 560 m asl.
8	GT.560 to 650 m asl	Salak GP var. gondok Tabanan 560 m to 650 m asl.
9	GT > 650 m asl	Salak GP var. gondok Tabanan > 650 m asl.
10	GK.< 560 m asl	Salak GP var. gondok Karangasem < 560 m asl.
11	GK 560 m to 650 m asl	Salak GP var. gondok Karangasem 560 m to 650 m asl.
12	GK > 650 m asl	Salak GP var. gondok Karangasem > 650 m asl.
13	NST < 560 m asl	Salak GP var. nenas Tabanan < 560 m asl.
14	NST.560 m to 650 m asl	Salak GP var. nenas Tabanan 560 m to 650 m asl.
15	NST > 650 m asl	Salak GP var. nenas Tabanan > 650 m asl.
16	NSK .< 560 m asl	Salak GP var. nenas Karangasem < 560 m asl.
17	NSK 560 m to 650 m asl	Salak GP var. nenas Karangasem 560 m to 650 m asl..
18	NSK > 650 m asl	Salak GP var. nenas Karangasem > 650 m asl.

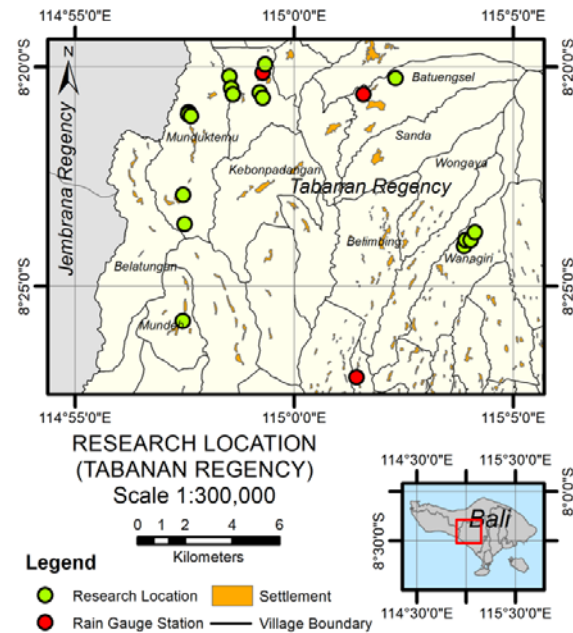


Fig 2. Research map and sampling point in Tabanan (T)

The non-independent variable was the three varieties of Salak 'Gulapisir' (SGP): SGP var. nangka (N), SGP var. nenas (NS), SGP var. gondok (G), and six sites, namely Karangasem (K): ($K < 560$ m asl, $K 560$ m to 650 m asl, and $K > 650$ m asl) and Tabanan (T): ($T < 560$ m asl, $T 560$ m to 650 m asl, $T > 650$ m). Repetition was carried out three times with the number of sample plants in each location, and cultivars were seven plants. The treatment tested is as shown in Table 1.

The study used a Composite Analysis of Variance (Andinurani, 2016, 2022) with the model determined using Equation (1) below:

$$Y_{ijk} = U + Li + \delta_{ik} + P_j + (LP)_{ij} + \varepsilon_{ijk} \quad (1)$$

Where:

Y_{ijk} = The observation value of the treatment (j) in the group (k), which is repeated at the location (i).

u = the actual average value

Li = additive effect from location i

δ_{ik} = the error effect in group k at location i

P_j = additive effect of the next treatment

$(LP)_{ij}$ = the effect of treatment (j) at the location (i)

ε_{ijk} = the effect of error from the treatment (j) in the group (k) which was carried out at the location (i).

2.2. Preparation of study materials

The material used is the salak 'Gulapasir' plant with uniform growth; plants have been fruitful with uniform on morphological, age of plants and cultivation action. The intentional practice is that the plant only receives treatment in the midrib, tillers, and weed cleaning. In this study, the plants were not fertilized. The provision of water was only from rainfall following the habits applied by salak farmers. The sample plant was maintained by trimming unproductive leaf midribs and removing young shoots. Plant material was taken from the Salak Development Centre in six locations, namely at the Centre of Salak Development in the Bebandem sub-districts, Karangasem district (K-lowland < 560 m asl, K-medium 560 m to 650 m asl and K-highland > 650 m asl), Bajre, West Slemadeg and Pupuan sub-districts, Tabanan district (T-lowland < 560 m asl, T-medium 560 to 650 m asl and T-highland > 650 m asl).

2.3. Analysis of physicochemical properties of soil sample and climate

Soil analysis was carried out to determine the physical and chemical properties of the soil. Soil sampling was carried out under sample plant trees, in a composite manner at a depth of 0 cm to 40 cm. Chemical analysis was carried out on total N (Kjeldahl method), available P by Bray I method and K_2O by the Bray I method, organic C, pH, soil physical properties in the form of texture by pipette method (Eviati and Sulaeman. 2009; Hailu *et al.*, 2015; Prasetyo *et al.*, 2022a; Rzasa and Owczarzak, 2013).

Rainfall data was taken for 5 yr from 2015 to 2019. Rainfall data has been collected from six nearby stations to the research site (Figure 1 and Figure 2). Daily temperature data was obtained from the Denpasar Meteorology Climatology Agency.

2.4. Observation of fruit and fruit quality

Salak fruit can be harvested when it is ready for consumption. Consumable ripe fruit is a fruit that is ready to be consumed, characterized by a change in skin colour from dark brown to light brown, the thorns on the skin being reduced and not sharp, and in general, at this stage, the fruit easily falling when shaken.

Observation and measurement of agronomic characters follow the method that has been done by Sumantra *et al.* (2014) including fruit weight, number of fruit bunches, the thickness of fruit flesh and fruit shape. The fruit characters from six-observed locations include the numbers of fruits

per bunch, which is calculated manually on the formed fruits. The fruit weight per fruit and the fruit weight per tree is weighed after the fruits were removed from the bunch. The thickness of the mesocarpium is obtained by measuring the mesocarpium after it is cut vertically. The length of the flower sheath is measured on the stem of the sheath from the base to the tip of the sheath.

While fruit quality includes sugar content, tannins, titrated acid, sugar content and vitamin C. Titrated acid was analyzed by titration (Sripakdee *et al.*, 2015). The fruit which was weighed 10 g of sample was added to 100 mL of distilled water, then was homogenized using a slow spin blender, and filtered using an aseptic filter. The filtrate obtained was taken as much as 25 mL, then titrated with 0.1 N NaOH solution with phenolphthalein indicator until red colour appeared. The results obtained are calculated as the percentage tartaric acid as per Equation (2) below :

$$A = \frac{\text{mL NaOH} \times N \text{ NaOH} \times P \times BM}{Y \times 1000 \times 2} \times 100 \% \quad (2)$$

where:

A = percentage of total acid

P = amount of dilution

BM = molecular weight of tartaric acid

Y = sample weight (g).

Tannins content was analyzed as done by Thakur *et al.* (2021), Setyobudi *et al.* (2022). Amount of 100 mg of the sample was homogenized by 2 mL of methanol, centrifuged for 10 min at 10 000 rpm (1 rpm = 1/60 Hz), and then the supernatant was collected. Amount of 1 mL of the aforementioned supernatant was mixed with 0.5 mL Folin's phenol reagent and 35 % Na_2CO_3 of 5 mL was added, and the mixture was kept at room temperature for 5 min. The blue colour of the reaction mixture was observed at 640 nm by UV/visible spectrophotometer (Shimadzu UV-1800, Japan). The content of tannins was calculated by calibration curve equation and determined using Equation (3) below:

$$Y = 0.0073 \times -0.0071 : R^2 = 0.9973 \quad (3)$$

Vitamin C was determined by titration like the method used by Asamara (2016), Setyobudi *et al.* (2021a, 2022). The material is weighed as much as 10 g and crushed in mortar, then put into a 250 mL volumetric flask, set to the mark and filtered. Take 25 mL of the filtrate and titrate with 0.01 N Yod solution equivalent to 0.88 mg of ascorbic acid. The calculation of ascorbic acid content per 100 g of material is determined using Equation (4) below:

$$A = \frac{\text{mL Yod } 0.01 N \times 0.88 \times P \times 100}{Y} \quad (4)$$

where: A = mg of ascorbic acid per 100 g of material

P = amount of dilution

Y = gram sample weight

Sugar content as TSS is calculated using a hand refractometer (Bellingham and Stanley Ltd., London) at 20 °C (Adinurani *et al.*, 2018). The ratio of sugar content (TSS) and total acid is calculated by the sugar content divided by the acid content multiplied by 100 %.

The materials used in this study were Folin-ciocalteu reagent (Pro Analytic, Merck), NaOH (pro analytic, Merck), Na_2CO_3 (pro analytic, Merck), Phenol reagent (pro analytic, Merck), Ascorbic acid (pro analytic, Merck), Phosphoric acid (Pro Analytic, Merck), Sodium

phosphate (pro analytic, Merck) and Ammonium molybdate (pro analytic, Merck).

The tools used in this study were analytical balances (Shimadzu ATY224, Japan), centrifuge tubes, Erlenmeyer flasks (Pyrex), dropper pipettes (pyrex), volume pipettes (Pyrex), vortex (Maxi Mix II Type 367000), measuring flask (Pyrex), water bath (Mettler), blender (Miyako), and centrifuge (Damon /IEC Division). Whatman filter paper No 1 (Sigma – Aldrich, USA), measuring cup (Pyrex, USA), micropipette (Dragon Lab, Indonesia), spectrophotometer (Biochroms 133467, UK), test tube (Pyrex, USA), vortex (Barnstead Thermolyne Type 37600 Mixer, USA), aluminum foil (Klin Pak, Indonesia).

2.5. Study design

This study used a randomized block design with the data analyzed using a Composite Analysis of Variance. If the variance test is significantly different, then it is continued with a different test with LSD at the 5 % level. Data analysis was performed using SPSS-IBM 18

(Adinurani, 2016, 2022). Each experimental treatment was repeated three times.

3. Results and Discussion

3.1. Agroclimate characteristic

The low production level and the quality of salak fruit are caused by environmental factors that do not support growth or because the physiological processes of the plant are not optimal due to insufficient nutrients and water. The suitability of climatic and soil conditions at six locations of the centres for the development of the ‘Gulapasir’ salak was evaluated. The evaluation results show that the air temperature decreases as the altitude increases. The average air temperature at the ‘Gulapasir’ salak plantation in Tabanan is 22.90 °C, while the air temperature at the Karangasem salak plantation is around 23.24 °C. (Tabel 2)

Table 2. Soil and climate characteristics of the research site in Tabanan and Karangasem in three subzones

Parameter	Tabanan (T)			Karangasem (K)		
	Lowlands (< 560 m asl)	Moderate (560 m to 650 m asl)	Highlands (> 650 m asl)	Lowlands (< 560m asl)	Moderate (560 m to 650 m asl)	Highlands (> 650 m asl)
Temp. (°C)	23.82	22.75	22.12	24.29	23.35	22.09
Rainfall (mm mo ⁻¹)	188.24	199.91	231.008	237.242	254.183	289.216
Soil texture	loamy clay	loamy clay	loamy clay	clay	Clay	sandy loam
pH (H ₂ O)	5.64 (sa)	5.75 (sa)	5.84 (sa)	6.08 (sa)	6.05 (sa)	6.03(sa)
C- organic (%)	2.94 (m)	3.40 (h)	3.25 (h)	2.77 (m)	3.63 (h)	3.32 (h)
Nutrients available						
N total (%)	0.18 (l)	0.16 (l)	0.18 (l)	0.24(m)	0.23 (m)	0.29 (m)
P ₂ O ₅ (mg g ⁻¹)	9.38 (vl)	9.12 (vl)	13.50 (l)	22.55 (m)	24.18 (m)	23.04 (m)
K ₂ O (mg g ⁻¹)	18.47 (vl)	22.05 (vl)	17.23 (vl)	24.17 (vl)	19.93 (vl)	18.37 (vl)

Notes: sa: slightly acidic; h: high; m: medium; l: low; vh: very high; h: high; asl: above sea level (The assessment criteria refer to Eviati and Sulaeman. 2009; PPT, 1983).

In addition to monthly rainfall, the average rainfall over 5 yr is presented in Figure 3. Annual rainfall in Tabanan (T < 560, T 560 to 650 and T > 650) is lower with an average of 2515.05 mm, while in Karangasem (K < 560, K 560 to 650 and K > 650) it is 3 122.05 mm. However, the six locations show a trend of increasing rainfall as altitude increases. The salak plantation area in Karangasem is in the southern part of Mount Agung. Meanwhile, in Tabanan, the dominant salak plantation area is behind Mount Batukaru with a lower elevation than Mount Agung. Mount Agung has an altitude of 3 142 m asl (Andaru and Rau, 2019), while Batukaru mountains area

of 2 250 m asl (Asmiwyati *et al.*, 2015). Mount Batukaru serves as a barrier from the rain, causing this area to be a rain shadow. Enyew and Steenveld (2014) state that rainfall in an area is influenced by topographical factors and mountain ranges. Decreasing the height of the mountains provides a reduction in the maximum level of rainfall over the mountains and foothills by 50 % (Flesch and Reuter, 2012). Topographical factors and regional weather systems have an important role in the amount and spatial pattern of rainfall in an area (Enyew and Steenveld, 2014).

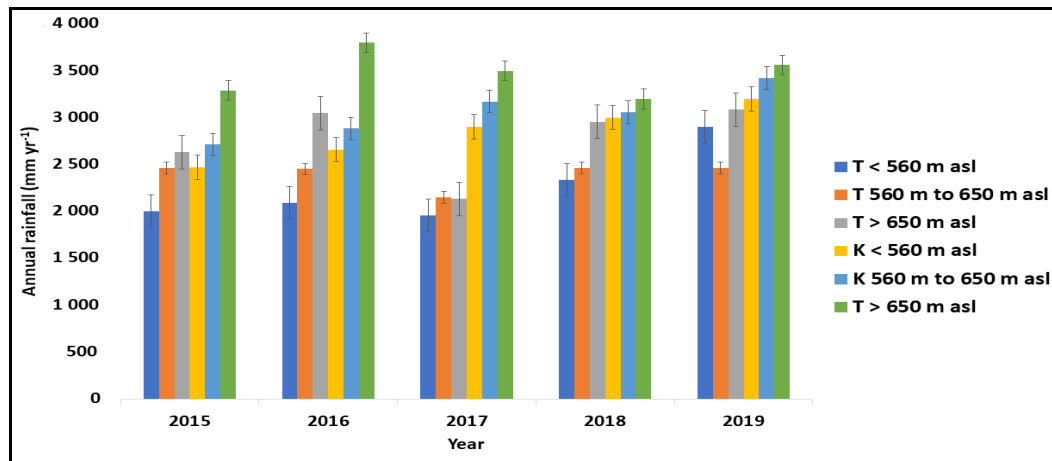


Fig. 3. The annual rainfall in the six study sites

Based on the growing requirements of salak plants, rainfall and air temperature in the six locations evaluated were in the very suitable range to support plant growth and development. A good air temperature for the growth of salak plants is between 20 °C to 30°C and an average rainfall of (200 to 400) mm mo⁻¹ (Nuary *et al.*, 2019).

Soil C-organic content in six planting sites was in the medium to high range. Availability of N and P nutrients in salak plantations in Tabanan in the lowlands, medium and highlands is of low to very low conditions. In salak planting land in Karangasem - both in the lowlands, medium and highlands - these two nutrients are available in moderate conditions (Table 3). The nutrient content of potassium available in the six planting locations that have been evaluated shows a very low value. The results of this study indicate that the cultivation techniques carried out by farmers are very low. Farmers do not apply fertilizers that only rely on litter from the pruning of salak midrib as reported by Ilmiah *et al.* (2021), Rai *et al.* (2014), and Warnita *et al.* (2019). To cultivate sustainable agriculture, especially in agroecosystems salak in Bali, the authors will discuss this issue more in the future research paragraph.

3.2. Fruit Characteristics of Salak 'Gulapasir'

The salak 'Gulapasir' his monoecious plant, namely male and female flowers arranged on the same bunches, the shape of the bunchesis compound, and the position of the flower is on the back of the midrib. The salak 'Gulapasir' is classified as special because of its sweet fruit taste and the price per unit weight is four times more expensive than the salak 'Bali' (Rai *et al.*, 2014; Sumantra *et al.*, 2012). The expansion of the cultivation of the salak 'Gulapasir' from its area of origin, Sibatana, Karangasem, has resulted in phenotypic diversity with a phenotypic similarity level of 58.62 % to 93.10 % (Sumantra and Martiningsih, 2016). In the same garden, more than one type of 'Gulapasir'salak appears, depending on fruit shape, aroma, color of fruit flesh and fruit weight (Sumantra and Martiningsih, 2016).The results of this study mean that the emergence of plant diversity due to plant propagation is done by seed, so new variants of salak 'Gulapasir' appear with local names such as salak 'Gulapasir' nenas, salak 'Gulapasir' gondok and salak 'Gulapasir' nangka. The striking difference between these three varieties lies in the shape and flesh of the fruit. The number of fruit branches of salak 'Gulapasir' nangka, 1 to 2 branches, salak

'Gulapasir' nenas amount of 2 to 4 branchesand salak 'Gulapasir' gondok the fruit bunches that do not form fruit branches. Salak 'Gulapasir', which is ready to harvest, has fruit flesh attached to the seed, and the fruit flesh is 0.63 cm thick. However, the flesh of the salak 'Gulapasir' nenas is the thinnest and the seeds are attached to the flesh. And when the salak 'Gulapasir' gondok is ready to harvest, the seeds make a sound when shaken (Figure 4 and Figure 5).



Fig. 4. The shape and the thickness of the fruit flesh of SGP.var.nenas, gondok and nangka



Figure 5. The shape of the bunch and the number of fruits of SGPvar. gondok, nenas, and nangka

3.3. Agronomic characteristics of 'Gulapafir' Salak

Analysis of variance showed that the interaction between planting locations and varieties of 'Gulapafir' salak had significant effect on the number of fruits per bunch, fruit weight per tree, fruit weight per fruit, number of fruits per bunch, the ratio of sugar and acid and vitamin C content. Meanwhile, the thick fruit flesh and tannins content was not significant (Table 4)

Table 4. Recapitulation of the effects of varieties and growing locations on agronomic and fruits quality of 'Gulapafir' salak

No.	Character agronomic and fruits quality	Planting location	Varieties	Varieties x Location
1	Length of the flower sheath	**	**	*
2	Number of fruit bunches ⁻¹	**	**	*
3	Fruit tree weight ⁻¹	**	**	*
4	Fruit weight ⁻¹	**	**	*
5	TSS ratio and total acid	**	**	**
6	Thick fruit flesh	**	**	Ns
7	Vitamin C	Ns	Ns	*
8	Tannins	Ns	Ns	Ns
9	Edible portion	**	**	Ns

Notes: *) significant $P < 0.05$, **) very significant $P < 0.01$ and Ns) not significantly different $P > 0.05$

The interaction of varieties and planting location had a significant effect on the length of the flower sheath and the number of fruit bunches⁻¹. Nenas variety grown in Tabanan ($T < 560$, $T 560$ to 650 , and $T > 650$) and Karangasem ($K < 560$, $K 560$ to 650 , and $K > 650$) showed higher sheath length and a number of fruit bunches⁻¹ than with nangka and gondok varieties (Table 5). Tabanan ($T 560$ to 650) and Karangasem ($K < 560$ m asl) are ideal conditions for flower sheath development and fruit development of nenas.

Table 5. Flower sheath length (cm) and a number of fruit bunches⁻¹ (fruit) of nangka, gondok and nenas varieties at six locations.

Treatment	Sheath length (cm)	Amount fruit bunches ⁻¹
NT < 560	27.50 ± 0.34 bcd	19.55 ± 0.82 hij
NT 560 to 650	28.83 ± 1.31 b	20.39 ± 1.00 g
NT > 650	27.17 ± 0.96 cde	19.02 ± 0.82 j
NK < 560	26.00 ± 0.82 e	21.13 ± 0.82 ef
NK 560 to 50	27.17 ± 0.14 cde	22.28 ± 2.45 c
NK > 650	26.67 ± 1.36 cde	21.13 ± 0.74 ef
GT < 560	26.67 ± 2.18 cde	20.22 ± 0.31 gh
GT 560 to 650	27.50 ± 1.22 bed	20.55 ± 0.62 fg
GT > 650	27.70 ± 1.98 bc	19.22 ± 0.74 ij
GK < 560	25.83 ± 1.41 e	21.89 ± 0.82 cd
GK 560 to 650	26.83 ± 0.75 cde	20.5 ± 1.63 fg
GK > 650	27.5 ± 0.82 bcd	21.28 ± 0.78 def
NST < 560	27.5 ± 0.82 bcd	21.41 ± 0.91 de
NST 560 to 650	27.67 ± 0.82 bc	22.00 ± 1.56 cd
NST > 650	26.17 ± 2.16 de	19.91 ± 1.36 ghi
NSK < 560	32.00 ± 1.63 a	25.27 ± 1.41 a
NSK 560 to 650	30.90 ± 2.10 a	24.00 ± 0.82 b
NSK > 650	27.00 ± 1.47 cde	21.86 ± 0.82 cde

Remarks : Numbers followed by the same letter in the same column and parameter indicate a non-significant difference in LSD 5 %.

From Table 5 above, it can be explained that the three varieties planted in six locations produced a number of fruits between 19.02 to 25.27 fruits per bunch. The nenas variety planted in Karangasem at an altitude of < 560 m asl (treatment NSK < 560) produced the highest number of fruits of 25.27 per bunch, followed by NSK 560 to 650 and NST 560 to 650 with 24.00 and 22.00 fruits per bunch. In order for the salak plants to bear much fruit, the nangka variety is ideal in Karangasem 560 to 650 m asl (NK 560 to 650), while the gondok variety is very good when planted below 560 m asl (GK < 560) although the number of fruits is not significantly different from the same altitude for NT 560 to 650 and GT < 560. The results of this study are in line with the findings of Sumantra and Martiningsih (2016) that the 'Gulapasar' salak var. nenas produces the highest number of fruits both in the on season (*gadu* season) and -off-season (*sela* season). Sumantra *et al.* (2014) reported that the emergence of new sheaths occurred on the third or fourth leaf midrib from the growing point depending on the altitude and plant conditions. The time for new sheaths to appear ranges from 129.00 d to 145.10 d with the required heat units between (1 233.62 to 1 047.90) Degree-Day (DD). The higher altitude causes the longer the sheath appears as well as the harvest time.

The interaction of varieties and planting location had a significant effect on the fruit weigh (fruit tree⁻¹ and fruit⁻¹). Nangka variety grown in Tabanan (T < 560, T 560 to 650, and T > 650) and Karangasem (K < 560, K 560 to 650, and K > 650) showed higher of weight of fruit tree⁻¹ and fruit⁻¹ than with nenas and gondok (Table 7).

Table 6. Fruit weight of nangka, gondok, and nenas varieties in six locations

Treatment	Fruit ⁻¹ (g)	Fruit tree ⁻¹ (kg)
NT < 560	45.32±1.08 cd	1.19±0.08 def
NT 560 to 650	48.56±0.71 c	1.29±0.07 cd
NT > 650	38.22±0.46 ef	1.03±0.06 ghi
NK < 560	55.84±1.37 a	1.48 ± 0.02 b
NK 560 to 650	59.43±0.71 a	1.62 ± 0.07 a
NK > 650	49.4±1.65 b	1.34 ± 0.05 c
GT < 560	40.14±0.11 e	1.11±0.09 fg
GT 560 to 650	38.67±0.55 ef	1.09 ± 0.07 fg
GT > 650	32.95±0.73 gh	0.93 ± 0.10 i
GK < 560	44.22±0.18 d	1.27 ± 0.06 cde
GK 560 to 650	38.20 ± 0.78 ef	1.16 ± 0.05 defg
GK > 650	36.20 ± 0.75 fg	1.07 ± 0.11 fgh
NST < 560	39.00 ± 1.07 ef	1.14 ± 0.11 efg
NST 560 to 650	37.79±0.65 f	1.13 ± 0.06 g
NST > 650	32.12±0.11 h	0.94 ± 0.10 hi
NSK < 560	41.80 ± 0.65 de	1.36 ± 0.08 bc
NSK 560 to 650	36.57±0.80 fg	1.18 ± 0.09 def
NSK > 650	37.10 ± 0.23 f	1.11 ± 0.07 fg

Remarks : Numbers followed by the same letter in the same column and parameter indicate a non-significant difference in LSD 5 %.

From Table 6, it can be explained that the three varieties grown in six locations produced fruit weight per tree between 0.93 kg and 1.62 kg. The salak nangka variety planted in Karangasem at an altitude of 560 to 650

m asl (NK 560 to 650) produced the heaviest fruit weight of 1.62 kg tree⁻¹, followed by NK < 560 and NT 560 to 650 with fruit weights of 1.48 and 1.29 kg, while the nenas variety produces the best fruit at altitudes < 560 m asl (NSK < 560 and NT < 560). Salak 'Gulapasar' var. gondok is ideal when planted at altitudes < 560 m asl (GK < 560 and GT < 560), although the two growing locations showed different yields.

Nenas and gondok varieties showed a trend of decreasing fruit weight in line with increasing altitude, both planted in Karangasem and Tabanan. The reverse occurred in the salak Nangka variety, an increase in altitude from 550 m asl to 650 m asl caused an increase in fruit weight and after that the fruit weight decreased when planted at altitudes > 650 m asl. This finding is in line with the results of research that have been reported by Sumantra *et al.* (2014). However, for the gondok and nenas varieties, this is a new finding.

Apart from being influenced by environmental factors, the production of salak 'Gulapasar' fruit is also influenced by internal plant factors (Adelina *et al.*, 2021b; Lestari *et al.* 2011). The effect of altitude on plant growth and production is related to plant adaptability and tolerance to temperature (Fenech *et al.*, 2019) and rainfall (Ritonga *et al.*, 2018). Altitude increases, the average daily air temperature decreases and monthly rainfall increases (Table 3). Nuary *et al.* (2019) stated that the distribution and adaptation of salak plants is strongly influenced by temperature and rainfall. It was further stated that the contribution of daily temperature accounts for nearly 38.6% while rainfall is 27.8 %. Kanzaria *et al.* (2015) reported that mango plants planted at an altitude of 229 m flowered slower than those at an altitude of 148 m and 81 m asl. The temperature regime at higher altitudes is colder than at lower altitudes. Lower temperatures accumulate less growing degree day (GDD) and may result in late flowering. Table 7 shows that the 'Gulapasar' salak planted in Karangasem produced a higher fruit weight in the three salak varieties tested. This is related to the level of soil fertility. The soil nitrogen and phosphate nutrient content at three locations in Karangasem was higher than at three locations in Tabanan. Meanwhile, the potassium content in the six research locations was low (Table 3). Therefore, it is necessary to make improvements by providing fertilizers containing elements of N, P and K to meet ideal conditions for growth, although more data is needed to fully support this conclusion (Hailu *et al.*, 2015).

3.4. Quality characteristics of salak varieties

The interaction between varieties and altitude significantly affected sugar/total acid and vitamin C content. The three varieties grown in Tabanan (T < 560, T 560 to 650 and T > 650) showed a lower TSS/acid ratio. The fruit flavour planted in three locations in Tabanan is more sour than the three locations in Karangasem. Sugar content is greatly affected by the geographical conditions. The geographical difference is usually followed by overall climate and weather differences, particularly temperature, humidity, and rainfall (Ritonga *et al.*, 2018). Table 8 also shows that the increase in altitude from 550 m to 700 m asl in Tabanan and the addition in altitude from 550 to 650 m asl in Karangasem causes the sugar/acid ratio decrease in all three varieties, and the lowest sugar/acid value occurs in nenas variety in all locations. Each salak variety has an

adaptation to an elevation closely related to plant tolerance to temperature (Sumantra and Martiningsih, 2016; 2018). Many factors influence fruit quality, but the most dominant are climate factors, especially temperature and rainfall. Rainfall has a negative correlation with fruit weight-1 ($r = -0.991^{**}$), TSS/acid ratio ($r = -0.875^{**}$) and vitamin C ($r = -1.000^{**}$). However, the air temperature has a positive and significant correlation with fruit weight¹, TSS/acid ratio, and vitamin C with correlations, respectively: $r = 0.930^{**}$, $r = 0.733^{**}$, and $r = 0.964^{**}$. High rainfall and low air temperature during the fruit ripening phase can cause the dissolved solids in the fruit to become watery so that the TSS value is low (Singh *et al.*, 2011).

Salak fruits from three different varieties grown in low lands in Karangasem (K < 560 m asl) showed the highest vitamin C content and were significantly different from the three cultivars when planted in other locations. In both areas, land increased by > 650 m asl effects to vitamin C decrease; nangka and gondok varieties showed higher levels of vitamin C between < 550 m to < 650 m asl. (Table 7).

Table 7. TSS/acid ratio and levels of vitamin C of nangka, gondok, and nenas varieties in six locations.

Treatment	TSS/T acid	Vit. C (mg 100 g ⁻¹)
NT < 560	56.20 ± 0.16 abc	27.50 ± 0.41 bde
NT 560 to 650	59.18 ± 0.82 a	25.45 ± 0.37 defgh
NT > 650	37.89 ± 0.91 f	22.52 ± 0.39 j
NK < 560	51.41 ± 0.33 cde	27.74 ± 0.47 bd
NK 560 to 650	53.52 ± 0.82 abcd	29.61 ± 0.50 ab
NK > 650	47.76 ± 0.11 de	24.25 ± 0.20 fghij
GT < 560	34.88 ± 0.72 fg	25.50 ± 0.41 defgh
GT 560 to 650	34.80 ± 0.65 fg	25.75 ± 0.20 defgh
GT > 650	30.24 ± 0.20 gh	23.34 ± 0.28 hij
GK < 560	51.28 ± 0.23 cde	30.31 ± 0.25 a
GK 560 to 650	58.44 ± 0.36 ab	27.63 ± 0.30 bd
GK > 650	53.04 ± 0.82 bcde	25.07 ± 0.33 efghi
NST < 60	31.50 ± 0.41 gh	26.71 ± 0.21 cdef
NST 560 to 650	30.44 ± 0.36 gh	25.88 ± 0.41 defg
NST > 650	26.13 ± 0.11 h	23.65 ± 0.29 ghij
NSK < 560	53.73 ± 0.60 abc	24.42 ± 0.34 fghij
NSK 560 to 650	52.63 ± 0.51 bcde	22.82 ± 0.15 ij
NSK > 650	47.60 ± 0.49 e	25.16 ± 0.13 efghi

Remarks : Numbers followed by the same letter in the same column and parameter indicate a non-significant difference in LSD 5 %.

The results showed that the varieties of the 'Gula pasir'salak need different environmental requirements to optimize yields. Ascorbate content is influenced by abiotic factors, especially temperature and light (Fenech *et al.*, 2019; Setyobudi *et al.*, 2021, 2022). Therefore, variety differences may depend on growing requirements and cultivation techniques. Vitamin C in the 'Gula pasir'salak is strongly influenced by the altitude of the land. To produce high levels of vitamin C, the nangka and gondok varieties are ideal for planting at an altitude of 560 m to 650 m asl, while the nenas variety is ideal at a land altitude of < 560 m asl. However, changes in ascorbate levels

during fruit ripening are species-dependent and environmental factors, especially temperature and light (Fenech *et al.*, 2019).

There was no interaction between varieties and altitude to the flesh thickness, edible fruit portion, and fruit sugar content. The nangka salak variety showed fruit quality, including TSS, edible parts of the fruit, and higher flesh thickness (Table 8).

Table 8. The effect of a single factor of varieties on TSS, the portion of edible flesh, and the thickness of salak fruits

Treatment	TSS (° Brix)	Edible portion (%)	Flesh thickness (cm)
Nangka	16.59a	72.50a	0.63a
Gondok	16.42a	70.66ab	0.59b
Nenas	15.64b	69.22b	0.52c

Remarks : Numbers followed by the same letter in the same column and parameter indicate a non-significant difference in LSD 5 %.

Salak grown in Karangasem both from the lowlands and the middle lands produces fruit thickness, and the edible portion of fruits is higher than plants in the highlands. This study indicates that the ideal growing place for salak plants is between 450 m to 650 m asl (Tabel 9). This study is in line with several previous studies which explained that altitude affects the flowering process and fruit enlargement (Sophie *et al.*, 2017; Spinardi *et al.*, 2019; Widyastuti *et al.*, 2022).

Table 9. The effect of a single factor of planting location on TSS, the portion of edible flesh, and the thickness of salak fruits

Treatment (m asl)	TSS (° Brix)	Edible portion (%)	Flesh thickness (cm)
T < 550	16.28a	73.13a	0.54c
T 550 to 650	16.27a	69.89a	0.58bc
T > 650	16.14a	63.87b	0.49d
K 550	16.81a	73.15a	0.61b
K 550 to 650	16.11a	72.29a	0.66a
K > 650	15.69a	72.44a	0.61b

Remarks : Numbers followed by the same letter in the same column and parameter indicate a non-significant difference in LSD 5 %.

The soil analysis results showed that the total N and P₂O₅ contents at three locations in Tabanan were very low to low, while the K₂O content at the six study sites was very low (Table 3). The low nutrient values of the three nutrients above are thought to be a factor causing the three types of salak planted in Tabanan at different altitudes to produce low fruit. The correlation results showed that N and P₂O₅ content negatively correlated with fruit weight ($r = -0.855^{**}$ and -0.992^{**}), while K₂O content had a positive and highly significant correlation ($r = 0.997^{**}$) with fruit weight. The quality of salak land is low because farmers practice very simple technique in salak cultivation, where most fertilization only uses buried salak midrib (Sumantra, *et al.*, 2014; Tamba and Sumantra, 2022). Therefore, the utilization and processing of plant waste need to be optimized to improve land quality.

Further research can be applied using sustainable salak organic agriculture (Budiasa, 2014; Handayani, 2022; Nurhidayat *et al.*, 2022; Rahmah *et al.*, 2022; Sukewijaya

et al., 2009; Wimatsari *et al.*, 2019). Table 3 shows that salak cultivation in the research location still needs to implement sustainable farming (Prasetyo *et al.*, 2022b; 2022a). There are indications on decrease in soil fertility, especially potassium availability, as the six planting locations came out with very low values. Potassium levels in Table 3 are lower than the observations of Ashari (2013) and Woran *et al.* (2018) in salak cultivation areas in Swaru – Malang (very high), Sleman – Yogyakarta (moderate), Bangkalan – Madura (very high), and Pangu – Minahasa (moderate).

The low availability of potassium (Table 3) in the nine study areas deserves attention, especially since the authors stated that the K₂O content had a positive and highly significant correlation ($r = 0.997^{**}$) with fruit weight. Potassium helps produce good fruit quality, such as bigger, heavier, and sweeter fruit. Another benefit of the nutrient potassium in plants is to increase the growth of meristem tissue and regulate the movement of stomata. Potassium also helps the development of plant roots so that plant stems can stand upright and do not collapse easily (Adinurani *et al.*, 2018; Budiono *et al.*, 2019). Therefore, Nasution (2022) recommends more K₂O fertilizer than P₂O₅ fertilizer and N fertilizer. In addition, salak needs 70 kg of K₂O because this nutrient is found in the leaves at an amount (12.2 to 14.7) mg g⁻¹ (Ashari, 2013).

The chemical fertilizers (*e.g.*, KCl) are too expensive for Salak farmers and do not support the salak organic. Therefore, the application of sustainable farming should apply local wisdom including the use of the pruning of salak midrib. Consider this policy because C organic is essential to soil fertility (Budiono *et al.* 2021; Goenadi *et al.* 2021). The success of this midrib decomposition is demonstrated by the C organic in Table 3, which is classified as medium to high. This finding supports Faizah and Fauzan (2021), Saputra *et al.* (2018) in salak plantation of Purwosari District - Pasuruan Regency, and Wonosalam District – Jombang Regency.

But, in the next stage, some of the salak midribs should be burned into ashes which can be used as a source of potassium nutrients (Ekawati and Purwanto, 2012; Vincevica-Gaile *et al.*, 2021a, 2021b). Another organic source of potassium is the pulp/husk of coffee cherries. Karangasem and Tabanan districts are coffee cultivation areas in Bali, so they should take advantage of this coffee processing waste. Several researchers stated that coffee pulp/husk contains higher potassium than nitrogen or phosphorus nutrients (Bahri *et al.*, 2016; Novita *et al.*, 2018; Setyobudi *et al.*, 2018).

Several researchers (Analianasari *et al.* 2022; Ningsih, 2020; Wachisbu, 2020) recommend soaking the pulp/husk of coffee cherries and using it as liquid organic fertilizer, which is beneficial for various plants. To develop this idea, salak farmers in Karangasem and Tabanan Regency should create biogas as household or communal scale digesters (Prespa *et al.*, 2020; Setyobudi *et al.* 2021b; Susanto *et al.*, 2020a) or use digesters from used drums (Adinurani *et al.*, 2013, 2017; Hendroko *et al.*, 2013). All household organic waste is processed in the digester, including kitchen waste, leftover food, and human excrement from pit latrines and septic tank (Anukam and Nyamukamba, 2022; Somorin, 2020; Susanto *et al.*, 2020b; Zhou *et al.*, 2022). This action has various advantages, namely reducing global warming, obtaining clean - renewable energy, and two kinds of

organic fertilizer, *i.e.*, liquid and solid (Abdullah *et al.*, 2020; Burlakovs *et al.*, 2022; Hendroko *et al.*, 2014; Prespa *et al.*, 2020; Setyobudi, *et al.*, 2018). In addition, many researchers have reported (among other things Benyahya *et al.*, 2022; Baştak and Koça, 2020; Li *et al.*, 2021) the benefits of organic fertilizers from biogas digesters.

Another measure to increase and maintain land fertility is in salak cultivation, namely the application of Plant Growth Promoting Rhizobacteria (PGPR) or biological fertilizer (Afzal *et al.*, 2017; Basu *et al.*, 2021; Ekawati, *et al.*, 2019; Nguyen *et al.*, 2020; 2022, Sukorini *et al.*, 2023). Several researchers (Adinurani *et al.*, 2021; Kumalawati *et al.*, 2021; Muhammad *et al.* 2021) have reported using mycorrhiza, which positively impacts various plants, including salak cultivation (Amnah and Friska, 2018; Dewi *et al.*, 2020; Rai *et al.*, 2021). Multiplication of mycorrhiza is relatively simple (Sportes *et al.*, 2021; Sukmawati *et al.*, 2021) and can be done by farmer groups with initial guidance from universities.

4. Conclusion and Recommendation

The SGP var. nangka in Karangasem showed higher fruit weight, vitamin C content, and sugar/acid ratio. In Karangasem and Tabanan, SGP var. nangka grows ideally at an altitude of (560 to 650) m asl with fruit weight per tree of 1.62 kg⁻¹ and 1.29 kg⁻¹, respectively, while the SGP var. nenas showed the highest number of fruit bunches⁻¹ in six locations. In contrast, SGP var. nenas and SGP var. gondok are ideal for cultivating at an altitude of < 560 m asl both in Karangasem and Tabanan, but the fruit production of SGP var. nenas and SGP var. gondok is higher, respectively, 19.29 % and 15.31 % when planted in Karangasem. In order to obtain ideal fruit production and quality, SGP var. nangka is very suitable to be planted at an altitude of 550 m to 650 m asl. In contrast, the SGP var. nenas and var. gondok are developed naturally at low altitudes < 550 m asl.

In order to enable all cultivars produce optimally, efforts to improve the cultivation system are needed through fertilization; mainly potassium is highly recommended. Further research can be applied using sustainable salak organic agriculture to maintain soil fertility.

Acknowledgements

The authors would like to thank the Head of the Regional Research and Innovation Agency of Bali Province for the funding provided for this research with contract number: B .17.027/3220/Bid.II/BaRI.

References

- Abdullah K, Uyun AS, Soegeng R, Suherman E, Susanto H, Setyobudi RH., Burlakovs J and Vincēviča-Gaile Z. 2020. Renewable energy technologies for economic development. *E3S Web of Conf.*, **188(00016)**: 1–8. <https://doi.org/10.1051/e3sconf/202018800016>
- Adelina R, Suliansyah I, Syarif A and Warnita. 2021a. Sulfate ammonium fertilizer on the off-season production of snake fruit (*Salacca sumatrana* Becc.). *Biotropia.*, **28(2)**: 156–164. <https://DOI10.11598/btb.2021.28.2.1280>

- Adelina R, Suliansyah I, Syarif A and Warnita. 2021b. Phenology of flowering and fruit set insnake fruit (*Salacca Sumatrana* Becc.). *Acta Agrobotanica*, **74(742)**: 1–12. <https://doi.org/10.5586/aa.742>
- Adinurani PG, Liwang T, Salafudin, Nelwan LO, Sakri Y, Wahono SK, Setyobudi RH. 2013. The study of two stages anaerobic digestion application and suitable bio-film as an effort to improve bio-gas productivity from *Jatropha curcas* Linn capsule husk. *Energy Procedia* **32**: 84–89. <https://doi.org/10.1016/j.egypro.2013.05.011>
- Adinurani PG. 2016. **Design and Analysis of Agrottrial Data: Manual and SPSS**. Plantaxia, Yogyakarta, Indonesia.
- Adinurani PG, Setyobudi RH, Wahono SK, Mel M, Nindita A, Purbajanti E, Harsono SS, Malala AR, Nelwan LO and Sasmito A. 2017. Ballast weight review of capsule husk *Jatropha curcas* Linn. on acid fermentation first stage in two-phase anaerobic digestion. *Proc. Pakistan Acad. Sci. B* **54(1)**: 47–57
- Adinurani PG, Rahayu S, Budi LS, Nindita A, Soni P and Mel M. 2018. Biomass and sugar content of some varieties of sorghum (*Sorghum bicolor* L. Moench) on dry land forest as feedstock bioethanol. *MATEC Web Conf.* **164(01035)**: 1–5. <https://doi.org/10.1051/mateconf/201816401035>
- Adinurani PG, Rahayu S, Purbajanti ED, Siskawardani DD, Stankeviča K and Setyobudi RH. 2021. Enhanced of root nodules, uptake NPK, and yield of peanut plant (*Arachis hypogaea* L.) using rhizobium and mycorrhizae applications. *Sarhad J. Agric.*, **37(Special issue 1)**: 16–24. <https://dx.doi.org/10.17582/journal.sja/2021/37.s1.16.24>
- Adinurani PG. 2022. **Agrotechnology Applied Statistics (compiled according to the semester learning plan)**. Deepublish, Yogyakarta, Indonesia.
- Afzal I, Iqar I, Shinwari ZK and Yasmin A. 2017. Plant growth-promoting potential of endophytic bacteria isolated from roots of wild *Dodonaea viscosa* L. *Plant Growth Regul.*, **81**:399–408. <https://doi.org/10.1007/s10725-016-0216-5>
- Amnah R and Friska M. 2018. The usage of *Arbuscular mycorrhiza* on the growth of salak Sidimpunan (*Salacca sumatrana* Becc.) seedling. *Jurnal Pertanian Tropik*. **5(3-59)**: 455–461
- Analianasari A, Kenali EW, Berliana D and Yulia M. 2022. Liquid organic fertilizer development strategy based coffee leather and raw materials to increase revenue local coffee Robusta farmers. *IOP Conf. Ser.: Earth Environ. Sci.* **1012(012047)**: 1–9. <https://doi.org/10.1088/1755-1315/1012/1/012047>
- Andaru R and Rau JY. 2019. Lava dome changes detection at Agung mountain during high level of volcanic activity using UAV photogrammetry. *Int. Arch. Photogramm. Remote Sens. Spatial Inf. Sci.*, **XLII-2/W13**: 173–179. <https://doi.org/10.5194/isprs-archives-XLII-2-W13-173-2019>
- Anukam A and Nyamukamba P. 2022. The chemistry of human excreta relevant to biogas production: A review. In: Meghvansi M., Goel AK (Eds) **Anaerobic Biodigesters for Human Waste Treatment** pp 29–38. *Environmental and Microbial Biotechnology*. Springer, Singapore. https://doi.org/10.1007/978-981-19-4921-0_2
- Ashari S. 2013. **Salak: The Snake Fruit**. UB Press, Malang, Indonesia
- Asmara AP. 2016. Analysis of vitamin C level contained in mango Gadung (*Mangifera indica* L.) with varied retention time. *Elkawnie* **2(1)**: 37–50. <http://dx.doi.org/10.22373/ekw.v2i1.658>
- Asmiwyati, IG, Mahendra S, Arifin NHS and Ichinose T. 2015. Recognizing indigenous knowledge on agricultural landscape in Bali for micro climate and environment control. *Procedia Environ. Sci.*, **28(07073)**: 623–629. <https://doi.org/10.1016/j.proenv.2015.07.073>
- Bahri S, Pratiwi D and Zulnazri. 2020. Extraction of potassium from coffee seed waste (*Coffea* sp) using the reflux method. *Jurnal Teknologi Kimia Unimal*, **9(1)**:24–31.
- Baştabak B and Koça G. 2020. A review of the biogas digestate in agricultural framework. *J Mater Cycles Waste Manag.*, **22**: 1318–1327. <https://doi.org/10.1007/s10163-020-01056-9>
- Basu A, Prasad P, Das SN, Kalam S, Sayyed RZ, Reddy MS and Enshasy HE. 2021. Plant growth promoting rhizobacteria (PGPR) as green bioinoculants: Recent developments, constraints, and prospects. *Sustainability*, **13(3-1140)**:1–20. <https://doi.org/10.3390/su13031140>
- Benyahya Y, Fail A, Alali A and Sadik M. 2022. Recovery of household waste by generation of biogas as energy and compost as bio-fertilizer—A review. *Processes.*, **10(81)**: 1–22. <https://doi.org/10.3390/pr10010081>
- Budiasa IW. 2014. Organic farming as an innovative farming system development model toward sustainable agriculture in Bali., *Asian J Agric Dev.* **11(1)**: 65–76
- Budiono R, Adinurani PG and Soni P. 2019. Effect of new NPK fertilizer on lowland rice (*Oryza sativa* L.) growth. *IOP Conf. Ser.: Earth Environ. Sci.* **293(012034)**:1–10. <https://doi.org/10.1088/1755-1315/293/1/012034>
- Budiono R, Aziz FN, Purbajanti ED, Turkadze T and Adinurani PG. 2021. Effect and effectivity of granular organicfertilizer on growth and yield of lowland rice. *E3S Web of Conf.*, **226(00039)**:1–7. <https://doi.org/10.1051/e3sconf/202122600039>
- Budiyantri T, Hadiati S and Fatria D. 2019. Evaluation and selection of salacca hybrid population based on fruit characters. *IOP Conf. Ser.: Earth and Environ. Sci.*, **497 (012005)**: 1–13. <https://doi.org/10.1088/1755-1315/497/1/012005>
- Burlakovs J, Vincevica-Gaile Z, Bisters V, Hogland W, Kriipsalu M, Zekker I, Setyobudi RH, Jani Y and Anne O. 2022. Application of anaerobic digestion for biogas and methane production from fresh beachcastbiomass. *Proceedings EAGE GET2022– 3rd Eage Global Energy Transition, The Hague, Netherlands*, pp. 1–5.
- Cepkova PH, Jagr M, Janovska D, Dvoracek V, Kozak AK, and Viehmannova I. 2021. Comprehensive mass spectrometric analysis of snake fruit: Salak (*Salacca zalacca*). *J. Food Qual.*, **Article ID 6621811**: 1–12. <https://doi.org/10.1155/2021/6621811>
- Damat D, Anggriani R, Setyobudi RH and Soni P. 2019. Dietary fiber and antioxidant activity of gluten-free cookies with coffee cherry flour addition. *Coffee Sci.*, **14(4)**:493–500.
- Damat D., Setyobudi RH, Soni P, Tain A, Handjani H, Chasanah U. 2020. Modified arrowroot starch and glucomannan for preserving physicochemical properties of sweet bread. *Cienc. e Agrotecnologia.*, **44(e014820)**:1–9. <https://doi.org/10.1590/1413-7054202044014820>
- Dewi NMK, Rai IN and Wiraatmaja IW. 2020. Fertilization response to off-season production and fruit quality of Salak Gula Pasir (*Salacca zalacca* cv. Gula Pasir) and water and chlorophyll content of leaves. *Agrotrop*, **10(1)**:88–99. <https://doi.org/10.24843/AJoAS.2020.v10.i01.p10>
- Ekawati I and Purwanto Z. 2012. Potential of agricultural waste ash as an alternative source of potassium, calcium and magnesium nutrients to support sustainable crop production. *Prosiding Seminar Nasional Kedaulatan Pangan dan Energi*. **27**: 135–139. Universitas Trunojoyo, Bangkalan, Madura, Indonesia.
- Ekawati I. 2019. Smart farming: PGPR technology for sustainable dry land agriculture. *Prosiding Seminar Nasional Ekonomi dan*

- Teknologi, pp 615–622. Universitas Wiraraja, Sumenep, Madura, Indonesia.
- Enyew BD and Steeneveld GJ. 2014. Analysing the impact of topography on precipitation and flooding on the Ethiopian highlands. *Journal of Geology & Geosciences.*, **3(6)**: 1–6. <https://doi.org/10.4172/2329-6755.1000173>
- Eviati and Sulaeman. 2009. **Technical Instructions - Chemical Analysis of Soil, Plant, Water, and Fertilizer, 2nd Edition.** Balai Penelitian Tanah, Badan Penelitian dan Pengembangan Pertanian, Departemen Pertanian Republik Indonesia.
- Faizah M and Fauzan A. 2021. Biomass technology based on salak plantation waste (*Salacca zalacca*) as compost fertilizer in Sumber village, Wonosalam district, Jombang district. *Agrifor.*, **20(2)**: 235–246. <https://doi.org/10.31293/agrifor.v20i2.5607>
- Falahuddin I, Raharjeng ARP and Harmeni L. 2016. The effect of coffee (*Coffea arabica* L.) waste organic fertilizer on the growth of coffee seeds. *Jurnal Bioilmi.*, **2 (2)**: 108–120
- Flesch TK and Reuter GW. 2012. WRF model simulation of two alberta flooding events and the impact of topography. *J. Hydrometeorol.*, **13(2)**, 695–708. <https://doi.org/10.1175/JHM-D-11-035.1>
- Fenech M, Amaya I, Valpuesta V and Botella MA. 2019. Vitamin C content in fruits: biosynthesis and regulation. *Front. Plant Sci.* **9(2006)**: 1–21. <https://doi.org/10.3389/fpls.2018.02006>
- Girsang E, Lister INE, Ginting CN, Khu A, Samin B, Widowati W, Wibowo S and Rizal R. 2019. Chemical constituents of snake fruit (*Salacca zalacca* (Gaert.) Voss) peel and in silico anti-aging analysis. *Molecular and Cellular Biomedical Sciences*, **3(2)**: 122–128. <https://doi.org/10.21705/mcbs.v3i2.80>
- Goenadi DH, Setyobudi RH, Yandri E, Siregar K, Winaya A, Damat D, Widodo W, Wahyudi A, Adinurani PG, Mel M, Zekker I, Mazwan MZ, Siskawardani DD, Purbajanti ED and Ekawati I. 2021. Land suitability assessment and soil organic carbon stocks as two keys for achieving sustainability of oil palm (*Elaeis guineensis* Jacq.). *Sarhad J. Agri.*, **37(Special issue 1)**: 184–196. <https://dx.doi.org/10.17582/journal.sja/2022.37.s1.184.196>
- Hailu H, Mamo T, Keskinen R, Karitun E and Gebrekidan H. 2015. Soil fertility status and wheat nutrient content in vertisol cropping systems of central highlands of Ethiopia. *Agric. Food Secur.* **4(19)**: 1–10. <https://doi.org/10.1186/s40066-015-0038-0>
- Hakim L, Widyorini R, Nugroho WD and Prayitno TA. 2019. Anatomical, chemical, and mechanical properties of fibrovascular bundles of salacca (snake fruit) frond. *Bioresources*, **14(4)**: 7943–7957. <http://dx.doi.org/10.15376/biores.14.4.7943-7957>
- Handayani A. 2022. Strategies to enhance the development of organic coffee to support local economic resource growth. The case of Wonokerso Village, Temanggung Regency, Central Java, Indonesia. In: Chaiechi T and Wood J. (Eds) **Community Empowerment, Sustainable Cities, and Transformative Economies.** Springer, Singapore. https://doi.org/10.1007/978-981-16-5260-8_35
- Hendroko R, Liwang T, Adinurani PG, Nelwan LO, Sakri Y and Wahono SK. 2013. The modification for increasing productivity at hydrolysis reactor with *Jatropha curcas* Linn. capsule husk as bio-methane feedstocks at two-stage digestion. *Energy Procedia*, **32**: 47–54. <https://doi.org/10.1016/j.egypro.2013.05.007>
- Hendroko R, Wahono SK, Adinurani PG, Salafudin, Yudhanto AS, Wahyudi A and Dohong S. 2014 The study of optimization hydrolysis substrate retention time and augmentation as an effort to increasing biogas productivity from *Jatropha curcas* Linn. capsule husk at two stage digestion. *Energy Procedia.*, **47**: 255–262. <https://doi.org/10.1016/j.egypro.2014.01.222>
- Herawati W, Amurwanto A, Nafi'ah Z, Ningrum AM and Samiyarsih S. 2018. Variation analysis of three Banyumas local salak cultivars (*Salacca zalacca*) based on leaf anatomy and genetic diversity. *Biodiversitas*, **19(1)**: 119–125. <https://doi.org/10.13057/biodiv/d190118>
- Ilmiah E, Sulistyarningsih and Joko T. 2021. Fruit morphology, antioxidant activity, total phenolic and flavonoid contents of *Salacca zalacca* (Gaertner) Voss by applications of goat manures and *Bacillus velezensis* B-27. *Caraka Tani*, **36(2)**: 270–282. <https://dx.doi.org/10.20961/carakatani.v36i2.43798>
- Kanzaria RS, Chovatia DK, Varu ND, Polara RL, Chitroda HN and Patel DV. 2015. Influence of growing degree days (GDD) on flowering and fruit set of some commercial mango varieties under varying climatic conditions. *Asian J. Hort.*, **10(1)**: 130–133. <https://doi.org/10.15740/HAS/TAJH/10.1/130-133>
- Khan AA and Idrees M. 2021. Factors affecting the production of stone fruit (Apricot) in district Mansehra Khyber Pakhtunkhwa, Pakistan. *Sarhad J. Agric.*, **37(2)**: 475–483. <https://dx.doi.org/10.17582/journal.sja/2021/37.2.475.483>
- Kumar N, Kumar A, Jeena N, Singh R and Singh H. 2020. Factors influencing soil ecosystem and agricultural productivity at higher altitudes. In: Goel R, Soni R and Suyal D (Eds), **Microbiological Advancements for Higher Altitude Agro-Ecosystems & Sustainability.** Rhizosphere Biology. Springer Nature, Singapore. pp.55–70. <https://doi.org/10.1007/978-981-15-1902-44>
- Kumalawati Z, Muliani S, Asmawati, Kafrawi and Musa Y. 2021. Exploration of *Arbuscular Mycorrhizal* fungi from sugarcane rhizosphere in marginal land. *Planta Tropika.*, **9(2)**: 126 – 135. <https://doi.org/10.18196/pt.v9i2.4026>
- Lestari R, Ebert G and Keil SH. 2011. Growth and physiological responses of salak cultivars (*Salacca zalacca* (Gaertn.) Voss) to different growing media. *J. Agric. Sci.* **3(4)**: 261–271. <http://doi.org/10.5539/jas.v3n4p261>
- Li C, Wang Q, Shao S, Chen Z, Nie J, Liu Z, Rogers KM and Yua Y. 2021. Stable isotope effects of biogas slurry applied as an organic fertilizer to rice, straw, and soil. *J. Agric. Food Chem.* **69(29)**: 8090–8097. <https://doi.org/10.1021/acs.jafc.1c01740>
- Martiniingsih EGAG, Sumantra IK and Sujana, P. 2018. The profile of salak gula pasir's farmer in Pajahan Village, Bali. *Int. J. Contemp. Res. Rev.* **9(8)**: 20254–20256. <https://doi.org/10.15520/ijcrr/2018/9/08/583>
- Mazumdar P, Pratama H, Lau SE, Teo CH and Harikrishna JA. 2019. Biology, phytochemical profile and prospects for snake fruit: An antioxidant-rich fruit of South East Asia. *Trends Food Sci. Technol.*, **91**: 147–158. <https://doi.org/10.1016/j.tifs.2019.06.017>
- Muhammad M, Isnatin U, Soni P and Adinurani PG. 2021. Effectiveness of mycorrhiza, plant growth promoting rhizobacteria and inorganic fertilizer on chlorophyll content in *Glycine max* (L.) cv. Detam-4 Prida. *E3S Web Conf.* **226 (00031)**: 1–5. <https://doi.org/10.1051/e3sconf/202122600031>
- Nassar JM, Khan SM, Villalva DR, Nour MM, Amani, Almuslem AS and Hussain MM. 2018. Compliant plant wearables for localized microclimate and plant growth monitoring. *npj Flex. Electron.*, **2(24)**: 1–12. <https://doi.org/10.1038/s41528-018-0039-8>
- Nasution Y. 2022. Application of N, P, K, fertilizer based on soil nutrient status support improving production and skills salak farmers and erosion prevention in the sub-district Padangsidimpuan Hutaimbaru, Padangsidimpuan city. *Jurnal Nauli*, **1(2)**: 7–11.
- Nguyen NH, Trotel-Aziz P, Villaume S, Rabenoelina F, Schwarzenberg A, Nguema-Ona E, Clément C, Baillieu F and Aziz A. 2020. *Bacillus subtilis* and *Pseudomonas fluorescens* Trigger common and distinct systemic immune responses in

- Arabidopsis thaliana depending on the pathogen life style. *Vaccines*, **8**(503): 1–18. <https://doi.org/10.3390/vaccines8030503>
- Nguyen NH, Trollet-Aziz P, Clément C, Jeandet P, Fabienne Baillieu F and Aziz A. 2022. Camalexin accumulation as a component of plant immunity during interactions with pathogens and beneficial microbes. *Planta*, **255**, 116. <https://doi.org/10.1007/s00425-022-03907-1>
- Ningsih YC. 2020. The effect of Robusta coffee liquid organic fertilizer on red chili crily productivity (*Capsicum annum* L.). Undergraduate Thesis. Universitas Islam Negeri Mataram, Indonesia.
- Novita E, Fathurrohman A and Pradana HA. 2018. The utilization of coffee pulp and coffee husk compost block as growing media. *Jurnal Agrotek.*, **2** (2): 61–72
- Nuary RB, Sukartiko AC and Machfoedz MM. 2019. Modeling the plantation area of geographical indication product under climate change: Salak Pondoh Sleman (*Salacca edulis* Reinw). *IOP Conf. Ser.: Earth Environ. Sci.* **365** (012020): 1–10. <https://doi.org/10.1088/1755-1315/365/1/012020>
- Nurhidayat O, Andayani SA and Sulaksana J. 2022. Analysis of organic and inorganic *Salacca* farming. *Journal of Sustainable Agribusiness* **1**(1):1–7. <https://doi.org/10.31949/jsa.v1i1.2761>
- PPT (Pusat Penelitian Tanah). 1983. **Term of Fertility Capability Survey Reference Land**. Departemen Pertanian, Bogor, Indonesia
- Prasetyo H, Setyobudi RH, Adinurani PA, Vincēviča-Gaile Z, Fauzi A, Pakarti TA, Tonda R, Minh NV and Mel M. 2022a. Assessment on soil chemical properties for monitoring and maintenance of soil fertility in Probolinggo, Indonesia. *Proc. Pak. Acad. Sci.: B.*, **59**(4):99–113. [http://doi.org/10.53560/PPASB\(59-4\)811](http://doi.org/10.53560/PPASB(59-4)811)
- Prasetyo H, Karmiyati D, Setyobudi RH, Fauzi A, Pakarti TA, Susanti MS, Khan WA, Neimane L and Mel M. 2022b. Local rice farmers' attitude and behavior towards agricultural programs and policies. *Pakistan Journal of Agricultural Research*, **35**(4): 663–677. <https://dx.doi.org/10.17582/journal.pjar/2022/35.4.663.677>
- Prespa Y, Gyuricza C and Fogarassy C. 2020. Farmers' attitudes towards the use of biomass renewable energy a case study from south eastern Europe. *Sustainability*, **12**(4009):1–18. <https://doi.org/10.3390/su12104009>
- Prihastanti E and Haryanti S. 2022. The combination of plant growth regulators (GA3 and *Gracilaria* sp. extract) and several fertilisers in Salak Pondoh fruit production. *Hort. Sci.*, **49**(2): 109–116. <https://doi.org/10.17221/102/2021-HORTSCI>
- Puspitasari E and Ningsih IY. 2016. Antioxidant capacity of gula pasir variant of salak (*Salacca zalacca*) fruit extract using DPPH radical scavenging method. *Pharmacy*, **13**(01): 116–126.
- Puspitasari PD, Sukartiko AC and Mulyati GT 2016. Characterizing quality of snake fruit (*Salacca zalacca* var. *zalacca*) based on geographical origin. *Foreign Agricultural Economic Report*, **101**:101–105.
- Raharjo G, Saidi D and Afany MR. 2022. Soil quality in cultivation land of snakefruit (*Salacca edulis*) in Ledoknongko, Bangunkerto Village, Turi, Sleman Yogyakarta Indonesia. *Int. J. Adv. Eng. Res. Sci.* **6**(5): 27–31.
- Rahmah DM, Putra AS, Ishizaki R, Noguchi R and Ahamed T. 2022. A life cycle assessment of organic and chemical fertilizers for coffee production to evaluate sustainability toward the energy–environment–economic nexus in Indonesia. *Sustainability*, **14**(7), 3912: 1–28. <https://doi.org/10.3390/su14073912>
- Rai IN, Wiraatmaja IW, Semarajaya CGA and Astiari NKA. 2014. Application of drip irrigation technology for producing fruit of salak Gula Pasir (*Salacca zalacca* var. *Gula Pasir*) off season on dry land. *J. Degraded Min. Lands Manag.* **2**(1): 219–222. <https://doi.org/10.15243/jdmlm.2014.021.219>
- Rai IN, Semarajaya CGA, Wiraatmaja IW and Astiari KA. 2016. Relationship between IAA, sugar content and fruit-set in snake fruit (*Zalacca zalacca*). *J. Appl. Hortic.*, **18**(3): 213–216. <https://doi.org/10.37855/jah.2016.v18i03.37>
- Rai IN, Suada IK, Wiraatmaja IW and Astiari NKA. 2021. Effectiveness of indigenous endomycorrhizal biofertilizer prototype on organic salak leaves and fruits in Bali. *Biotropia* **28**(3): 214–220. <https://doi.org/10.11598/btb.2021.28.3.1333>
- Ritonga EN, Satria B and Gustian G. 2018. Analysis of phenotypic variability and correlation on sugar content contributing phenotypes of salak (*Salacca sumatrana* Reinw var. *Sidempuan*) under various altitudes. *Int. J. Environ Agric. Biotech.* **3**(6):2103–2109. <https://dx.doi.org/10.22161/ijeab/3.6.18>
- Rzasa S and Owczarzak W. 2013. Methods for the granulometric analysis of soil for science and practice. *Pol. J. Soil Sci.* **(46)**1: 1–50.
- Saleh MS, Siddiqui MJ, Mediani A, Ismail NH, Ahmed QU, So'ad SZ and Saidi-Besbes S. 2018. *Salacca zalacca*: A short review of the palm botany, pharmacological uses and phytochemistry. *Asian Pac J Trop Med*; **11**(12): 645–652. <https://doi.org/10.4103/1995-7645.248321>
- Saputra DD, Putrantyo AR and Kusuma Z. 2018. Relationship between soil organic matter content and bulk density, porosity, and infiltration rate on salak plantation of Purwosari District, Pasuruan Regency. *Jurnal Tanah dan Sumberdaya Lahan.*, **5** (1) : 647–654
- Setyobudi RH, Wahono SK, Adinurani PG, Wahyudi A, Widodo W, Mel M, Nugroho YA, Prabowo B and Liwang T. 2018. Characterisation of Arabica coffee pulp – hay from Kintamani - Bali as prospective biogas feedstocks. *MATEC Web Conf.* **164** (01039):1–13. <https://doi.org/10.1051/mateconf/201816401039>
- Setyobudi RH, Zalizar L, Wahono SK, Widodo W, Wahyudi A, Mel M, Prabowo B, Jani Y, Nugroho YA, Liwang T and Zaebudin A. 2019. Prospect of Fe non-heme on coffee flour made from solid coffee waste: Mini Review. *IOP Conf. Ser. Earth Environ. Sci.*, **293** (012035):1–24. <https://doi.org/10.1088/1755-1315/293/1/012035>
- Setyobudi RH, Yandri E, Nugroho YA, Susanti MS, Wahono SK, Widodo W, Zalizar L, Saati EA, Maftuchah M, Atoum MFM, Massadeh MI, Yono D, Mahaswa RK, Susanto H, Damat D, Roeswitawati D, Adinurani PG and Mindarti S. 2021a. Assessment on coffee cherry flour of Mengani Arabica Coffee, Bali, Indonesia as iron non-heme source. *Sarhad J. Agric.*, **37**(Special issue 1): 171–183. <https://dx.doi.org/10.17582/journal.sja/2022.37.s1.171.183>
- Setyobudi RH, Yandri E, Atoum MFM, Nur SM, Zekker I, Idroes R, Tallei TE, Adinurani PG, Vincēviča-Gaile Z, Widodo W, Zalizar L, Van Minh N, Susanto H, Mahaswa RK, Nugroho YA, Wahono SK and Zahriah Z. 2021b. Healthy-smart concept as standard design of kitchen waste biogas digester for urban households. *Jordan J. Biol. Sci.*, **14**(3): 613 – 620. <https://doi.org/10.54319/jjbs/140331>
- Setyobudi HS, Atoum MFM, Damat D, Yandri E, Nugroho YA, Susanti MS, Wahono SK, Widodo W, Zalizar L, Wahyudi A, Saati EA, Maftuchah M, Hussain Z, Yono D, Harsono SS, Mahaswa RK, Susanto H, Adinurani PA, Ekawati I, Fauzi A and Mindarti S. 2022. Evaluation of coffee pulp waste from coffee cultivation areas in Indonesia as iron booster. *Jordan J. Biol. Sci.*, **15**(3): 475–488. <https://doi.org/10.54319/jjbs/150318>

- Singh D, Singh KVK, Ram RB and Yadava LP. 2011. Relationship of heat units (degree days) with softening status of fruits in Mango cv. Dashehari. *Plant Arch.* **11**(1): 227–230.
- SK Mentan 1994a. Decree of the Minister of Agriculture - No. 585/Kpts/TP.240/7/94, date 23 Juli 1994, on Bali salak
- SK Mentan 1994b. Decree of the Minister of Agriculture No.584/Kpts /TP.240 /7/94, date 23 Juli 1994 on Gulapisir salak
- Somarin TO. 2020. Valorisation of human excreta for recovery of energy and high-value products: A Mini-review. In: Daramola M, Ayeni A. (Eds) **Valorization of Biomass to Value-Added Commodities** pp 341–370. *Green Energy and Technology*. Springer, Cham. https://doi.org/10.1007/978-3-030-38032-8_17
- Sophie F, Stöcklin J, Hamann E and Kesselring, H. 2017. High elevation plants have reduced plasticity in flowering time in response to warming compared to low-elevation congeners. *Basic Appl Ecol.* **21**: 1–12. <https://doi.org/10.1016/j.baae.2017.05.003>.
- Spinardi, A, Cola G, Gardana CS and Mignani I. 2019. Variation of anthocyanin content and profile throughout fruit development and ripening of highbush blueberry cultivars grown at two different altitudes. *Front. Plant Sci.* **10**(1045): 1–14. https://doi.org/10.3389/fpls.2019.01045_2
- Sportes A, Hériché M, Boussageon R, Noceto PA, van Tuinen D, Wipf D and Courty PE. 2021. A historical perspective on mycorrhizal mutualism emphasizing arbuscular mycorrhizas and their emerging challenges. *Mycorrhiza.* **31**:637–653. <https://doi.org/10.1007/s00572-021-01053-2>
- Sripakdee T, Sriwicha A, Jansam N, Mahachai R and Chanthai S. 2015. Determination of total phenolics and ascorbic acid related to an antioxidant activity and thermal stability of the Mao fruit juice. *Int. Food Res. J.* **22**(2):618–624
- Sukewijaya IM, Nyoman R and Mahendra MS. 2009. Development of Salak Bali as an organic fruit. *As. J. Food Ag-Ind. Special Issue*: S37–S43
- Sukmawati S, Adnyana A, Suprpta DN, Proborini M, Soni P and Adinurani PG. 2021. Multiplication arbuscular mycorrhizal fungi in corn (*Zea mays* L.) with pots culture at greenhouse. *E3S Web Conf.* **226**(00044):1–10. <https://doi.org/10.1051/e3sconf/202122600044>
- Sukorini H, Putri ERT, Ishartati E, Sufianto S, Setyobudi RH, Nguyen Huu NN and Suwannarat S. 2023. Assessment on drought stress resistance, salinity endurance, and indole acetic acid production potential of dryland-isolated bacteria. *Jordan J. Biol. Sci.* **16**(1): 137–147. <https://doi.org/10.54319/jjbs/160117>
- Sumantra K, Ashari S, Wardiyati T and Suryanto A. 2012. Diversity of shade trees and their influence on the microclimate of agro-ecosystem and fruit production of Gulapisir Salak (*Salacca Zalacca* var. Amboinensis) fruit. *Int. J. Basic Appl. Sci.* **12**(06): 214–221.
- Sumantra K, Labek SIN and Ashari S. 2014. Heat unit, phenology and fruit quality of salak (*Salacca zalacca* var. amboinensis) cv. Gulapisir on different elevation in Tabanan regency-Bali. *Agriculture, Forestry and Fisheries.* **3**(2): 102–107. <https://doi.org/10.11648/j.aff.20140302.18>.
- Sumantra K and Martiningsih E. 2016. Evaluation of the superior characters of salak Gulapisir cultivars in two harvest seasons at the new development area in Bali. *Int. J. Basic Appl. Sci.* **16**(06):19–22.
- Sumantra K and Martiningsih E. 2018. The agroecosystem of salak Gulapisir (*Salacca zalacca* var. amboinensis) in new development areas in Bali. Proceedings of International Symposia on Horticulture (ISH), Kuta, Bali. Indonesian Center for Horticulture Research and Development pp. 19– 28.
- Sumantra K, Tamba M, Partama Y, Sukerta M and Ariati PEP. 2022. Mapping potential for superior food in Bali: Sub-study of agro-ecosystem, post-harvest and marketing chain of salak commodity. Research Report. Bali Regional Research and Innovation Agency. Bali Province.
- Susanto H, Setyobudi RH, Sugiyanto D, Nur SM, Yandri E, Herianto H, Jani Y, Wahono SK, Adinurani PA, Nurdiansyah Y and Yaro A. 2020a. Development of the biogas-energized livestock feed making machine for breeders. *E3S Web Conf.* **188**(00010): 1–13. <https://doi.org/10.1051/e3sconf/202018800010>
- Susanto H, Uyun, AS, Setyobudi, RH, Nur SM, Yandri E, Burlakovs J, Yaro A, Abdullah K, Wahono SK, and Nugroho YA. 2020b. Development of moving equipment for fishermen's catches using the portable conveyor system. *E3S Web Conf.* **190**(00014): 1–10. <https://doi.org/10.1051/e3sconf/202019000014>
- Tamba M and Sumantra K. 2022. Organic-based *Salacca zalacca* var. amboinensis farming development: An alternative to strengthening farmers' economy and food security. *IOP Conf. Ser: Earth Environ Sci.* **1107**(012074): 1–7. <https://doi.org/10.1088/1755-1315/1107/1/012074>
- Thakur A, Singh S and Puri S. 2021. Nutritional evaluation, phytochemicals, antioxidant and antibacterial activity of *Stellaria monosperma* Buch.-Ham. ex D. Don and *Silene vulgaris* (Moench) Garcke: Wild edible plants of Western Himalayas. *Jordan J. Biol. Sci.* **14**(1): 83–90. <https://doi.org/10.54319/jjbs/140111>.
- Vincevica-Gaile Z, Stankevica K, Klavins M, Setyobudi RH, Damat D, Adinurani PG, Zalazar L, Mazwan MZ, Burlakovs J, Goenadi DH, Anggriani R and Sohail A. 2021a. On the way to sustainable peat-free soil amendments. *Sarhad J. Agri.* **37**(Special issue 1):122–135. <https://dx.doi.org/10.17582/journal.sja/2021.37.s1.122.135>
- Vincevica-Gaile Z, Teppand T, Kripsalu M, Krievans K, Jani Y, Klavins M, Setyobudi RH, Grinfelde I, Rudovica V, Tamm T, Shanskiy M, Saaremaa E, Zekker I and Burlakovs J. 2021b. Towards sustainable soil stabilization in peatlands: Secondary raw materials as an alternative. *Sustainability*, **13**(126726):1–24. <https://doi.org/10.3390/su13126726>
- Wachisbu DR. 2020. Liquid organic fertilizer from coffee pulp/husk. <http://cybex.pertanian.go.id/mobile/artikel/94356/Pupuk-Organik-Cair-Dari-Kulit-Kopi/>
- Warnita I, Suliansyah, Syarif A and Adelina R. 2019. Flowering induction and formation of salak (*Salacca sumaterana* Becc) fruit with potassium and boron fertilization. *IOP Conf. Ser. Earth and Environ. Sci.* **347**(012092):1–12. <https://doi.org/10.1088/1755-1315/347/1/012092>
- Widyastuti RAD, Budiarto R, Hendarto K, Warganegara A, Listiana I, Haryanto Y and Yanfika H. 2022. Fruit quality of guava (*Psidium guajava* 'kristal') under different fruit bagging treatments and altitudes of growing location. *J. Trop.Crop. Sci.* **9**(1): 8–14.
- Wimatsari AD, Hariadi SS and Martono E. 2019. Youth of village attitudes on organic farming of snakefruit and it's effect toward their interest on farming organic. *Agraris* **5**(1):56–65. <http://dx.doi.org/10.18196/agr.5175>
- Woran RF, Nangoi R and Lengkong JE. 2018. The study of physical and land chemical properties on the green plant area (*Salacca zalacca*) in Pangu village district Southeast Minahasa). *Cocos*, **1**(1):1–15. <https://doi.org/10.35791/cocos.v1i1.19180>

Zhou X, Simha P, Perez-Mercado LF, Barton MA, Lyu Y, Guo S, Nie X, Wu F and Li Z. 2022. China should focus beyond access to toilets to tap into the full potential of its rural toilet revolution. *Resour Conserv Recycl.*, **178**, 106100. <https://doi.org/10.1016/j.resconrec.2021.106100>

Zumaidar T, Chikmawati, Hartana A, Sobir, Mogeia JP and Borchsenius F. 2014. *Salacca acehensis* (Arecaceae), A newspecies from Sumatra, Indonesia. *Phytotaxa*, **159 (4)**: 287–290. <https://doi.org/10.11646/phytotaxa.159.4.5>.

Impact of Maternal Exposure to Lead Acetate before Pregnancy Through Lactation Period on the Testicular histomorphologic Indices of Male Offspring of Wistar Rats, A Stereological Study

Ehsan Roomiani¹, Hassan Morovvati^{2,*}, Saeid Keshtkar³, Sareh Najaf Asaadi⁴, Shaker Shayestehnia⁵ and Arash alaeddini⁶

¹PhD, Graduate of Comparative Histology, Faculty of Veterinary Medicine, University of Tehran, Tehran, Iran; ² Professor in Anatomical Sciences, Department of Basic Sciences, Faculty of Veterinary, University of Tehran, Iran; ³ PhD, Graduate of Food industry biotechnology, Kaliningrad state university, Kaliningrad, Russia; ⁴ PhD, Graduate of Comparative Histology, Faculty of Veterinary Medicine, University of Tehran, Tehran, Iran; ⁵ DVM, Department of Veterinary, Faculty of Veterinary Medicine, Islamic Azad University, Iran, Karaj; ⁶ PhD student of Veterinary Microbiology, Department of Basic Sciences and Health, Faculty of Veterinary, Islamic Azad University of Tehran, Science and Research Branch, Tehran, Iran.

Received: August 11, 2022; Revised: October 19, 2022; Accepted: November 23, 2022

Abstract

Exposure to heavy metals in the products of various industries and the environment is a permanent threat to humans. Much research had shown the adverse effects of lead acetate even at low doses. The present study was conducted to investigate the effect of lead acetate on testicular histomorphologic indices of male offspring of female Wistar rats that were exposed to lead during pre-pregnancy, pregnancy and lactation periods. After adaption, rats were divided into different cages for mating (1 male to 2 females). After diagnosing pregnancy, rats were divided into three groups: pregnancy, lactation, and pregnancy until the end of lactation (PL). During the mentioned periods, 0.2% lead acetate plus 500 µl of glacial acetic acid were available in drinking water. Female rats belonging to the pre-pregnancy group had access to the mentioned compound for 3 weeks before mating. Also, females belonging to the PrePregnancy to the end of Lactation, had access to the mentioned compound for 3 weeks before pregnancy to the end of lactation. Offspring of control and sham groups also had access to drinking water and 500 µl of glacial acetic acid in drinking water, for survey of deposition of lead acetate, from the beginning to the end of the experimental period (63 days), respectively. At the end of the experiment (postnatal day: 63), adults were sacrificed and their left testicles were fixed in 10% formalin. In order to perform morphometric studies, testicular tissue was randomly divided into equal sections, and for hematoxylin-eosin staining routine tissue preparation steps were performed. Finally, the prepared slides were used for stereological examinations.

The results showed that exposure to 0.2% lead acetate had significant reduction on the volumetric density of the seminiferous tubules, the volumetric density of the epithelium of the tubules, the volumetric density of the interstitial tissue and the height of the germinal epithelium of the tubules of experimental groups compared to the control and sham groups. It should be noted that exposure to 0.2% lead acetate, despite the decreasing effects, did not cause a significant change in the length of the tubules and the epithelial surface area of these tubules. We conclude that lead, in the amount of 0.2%, has different effects on the tissue structure of testes of male offspring. Therefore, due to the increasing development of various technologies and industries that are sources of production of this harmful compound, the need to protect the mother and fetus against its adverse effects are felt more than ever.

Keywords: Stereology, Rat testis, PrePregnancy to lactation periods, Lead acetate

* Corresponding author. e-mail: hmorovvati@ut.ac.ir.

1. Introduction

The testicles are the main and important organ of the male reproductive system and are responsible for the production of sex cells (Treuting *et al.*, 2017). The activity and steps of spermatogenesis are easily affected by pollution. Therefore, in toxicological and pathological studies, the toxic effects of heavy metals on the spermatogenesis are very important (Morais *et al.*, 2012). Existing reports of reduced male fertility point to the role of exposure to toxic and environmental factors in the etiology of human infertility (Benoff *et al.*, 2000). Elgawish and Abdel Razak (2014) have stated that lead acetate is the most abundant toxic metal substance in nature. According to Restanty *et al.* (2018) lead acetate is one of the most important heavy metals clinically, and leads to physiological, biochemical, and behavioral disorders. The reproductive system (male and female) is the target tissue of lead exposure. BaSalamah *et al.* (2018) also reported that lead is an unnecessary element that can cause numerous health problems through environmental pollution.

Toxicological studies have shown that lead has negative effects on the nervous system (CNS & PNS), cardiovascular, endocrine, immune and digestive system, blood tissue, urinary system, and male and female reproductive system. It also causes chromosomal abnormalities (Altunkaynak *et al.*, 2013; Restanty *et al.*, 2018). For example, lead can cross the blood-testicular barrier and affect the testes and other accessory organs (Fair and Ricklefs, 2002; Snoeijs *et al.*, 2004). Accumulation of lead in the testes and epididymis affects sexual germ cell differentiation (Apostoli *et al.*, 1999). Lead is also an estrogenic compound that may affect fetal development by crossing the blood-placental barrier (Goyer, 1990; Baghurst *et al.*, 1991; Taupeau *et al.*, 2001).

In the present study, an effort was made to evaluate the morphometric characteristics of testicular tissue in male offspring of wistar rats maternally exposed to lead acetate using stereology. Stereology is a set of mathematical laws that interprets two-dimensional information in three dimensions using mathematical principles and statistics and geometry and provide information about the quantity of structures (Nyengaard, 1999; Dehoff, 2000). Stereology provides a set of efficient, unbiased, or minimally biased tools for quantifying functional aspects of three-dimensional morphology. These values include volume, surface area, length, and number, and can be estimated for different levels of structure, from the entire organ to the cell and molecule (Brown, 2017).

Accordingly, due to the complex mechanisms of sperm production (spermatogenesis) and how the testicle develops, the effects of lead on it are probable. So, in this study, with the help of the stereology technique (Boyce *et al.*, 2010; West, 2012), the effect of lead administration in pre-pregnancy to lactation periods on the morphometric characteristics of the testes of male offspring of Wistar rats were examined. These characteristics were: the volumetric density of seminiferous tubules, the volumetric density of tubular epithelium, the volumetric density of interstitial tissue, the surface area and height of germinal epithelium, and the length of seminiferous tubules of testis.

2. Materials and Methods

2.1. Animals

Forty-two adult Wistar rats (male and female) with 200-210 g average weight, were purchased from the Pasteur Institute, Iran and kept in the embryology laboratory under conditions of 12 hours of light, a temperature of 20-26 °C and adequate water and food. The study was done in accordance with the standard protocol for the care and use of laboratory animals (Faculty of veterinary medicine, University of Tehran, Tehran, Iran. N. 6067543). After adaptation (one week), male and female rats were considered in each cage (1 male to 2 females) for mating. After 12 hours, vaginal plaque was examined for pregnancy and the pregnant rats were randomly distributed into 5 different groups (6 rats in each group) in addition to the pre-pregnancy and the pre-pregnancy to the end of lactation groups that received lead acetate plus acetic acid 21 days before mating (overall 7 groups).

2.2. Experimental design:

Control (Cont.): animals had access to drinking water and adequate food during the experimental period.

Sham group: animals had access to acetic acid (glacial, 0.05%) in drinking water, for survey of lead acetate deposition, during the experimental period.

Pre-pregnancy (PrePreg.): animals during the pre-pregnancy period (21 days) had access to a combination of lead acetate (0.2%) and acetic acid (glacial, 0.05%) in drinking water.

Pregnancy (Preg.): animals during the pregnancy period (21 days) had access to a combination of lead acetate (0.2%) and acetic acid (glacial, 0.05%) in drinking water.

Lactation (Lac.): animals had access to lead acetate (0.2%) and acetic acid (glacial, 0.05%) in drinking water during lactation (21 days).

Pregnancy_lactation (Preg.Lac.): animals during pregnancy and lactation (42 days) had access to a combination of 0.2% lead acetate and 0.05% glacial acetic acid in drinking water.

Pre-pregnancy_pregnancy_lactation (PrePreg.Preg.Lac.): animals had access to a combination of lead acetate (0.2%) and acetic acid (glacial, 0.05%) in drinking water during the pre-pregnancy, pregnancy, and lactation period (63 days).

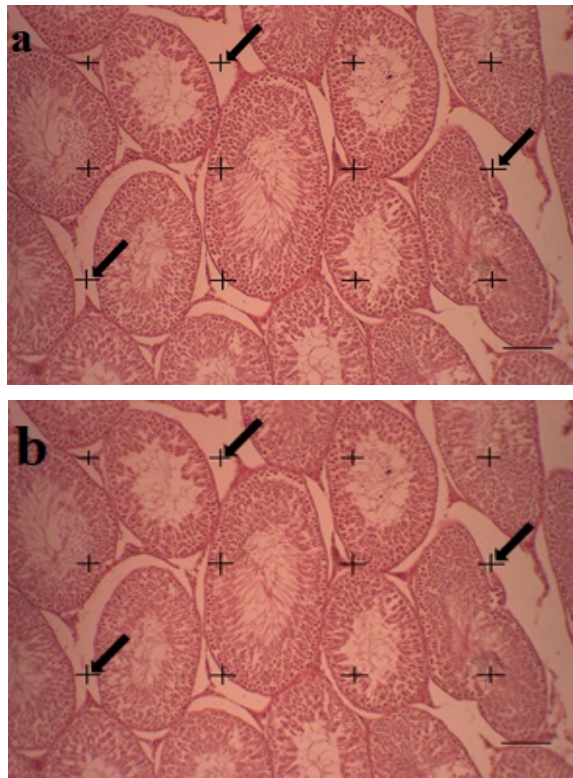
All experimental animals, after the mentioned period, except control group, had access to a combination of 0.05% glacial acetic acid in drinking water to the end of the study. Lead was administered as a 0.2% lead-acetate in drinking water (Barkur and Bairy, 2016). Then, to prevent lead-acetate deposition, 0.05% glacial acetic acid was added to it (Jaco-Movits *et al.*, 2005; Heidmets *et al.*, 2006; Barkur and Bairy, 2016). No deaths were recorded during the experimental period. Also, water consumption was checked daily, and no rejection of water was observed.

2.3. Sampling and Quantitative survey:

To evaluate the stereological features of the testes, samples were taken from the 5 male offspring (left testicle) on day 63 (postnatal day: 63). After fixation of the samples in 10% formalin, sampling was done by the isotropic

random uniform method. Briefly, the testes were first embedded in agar and then placed on the first circle, which consisted of 10 equal parts. In the next step, a random number between 0 and 10 was selected, and the sample in the direction of the selected number was divided into two equal parts. The incision surface of both halves of the testis was placed on the second circle, which also had 10 equal parts. Then, a random number was selected (between 0 - 10) and the samples were cut in the direction of the selected number so that 8 to 10 equal pieces were obtained from each testicle (Sadeghinezhad *et al.*, 2021). Samples were prepared for microscopic study. The samples were then embedded in paraffin and 5 µm thickness sections were prepared for Hematoxylin-eosin staining. To perform stereological examinations, images of testicular tissue sections were taken by using of CX40 Jenu (China) light microscope connected to Is1000 Jenu (China) camera. Then, the images were analyzed using Image j software and dedicated plugins for stereology.

The following equation was used to calculate the



absolute volume of the testis (Howard and Reed, 2005):

$$V = \frac{M}{d}$$

V: Total structure (testis) volume

M: Testicular weight

d: Testicular density

The following formulas were used to calculate the volumetric parameters of the testis, including the volumetric density of the seminiferous tubules, the volumetric density of the interstitial tissue, and the volumetric density of the germinal layer by point grades (Gundersen *et al.*, 1988) (Fig. 1):

$$V_v(\text{structure}) = \frac{\sum P_{\text{structure}}}{\sum P_{\text{testis}}}$$

V (structure) = $V_v(\text{structure}) \times V(\text{testis})$

Vv: Volumetric density of the structure

$\sum P_{\text{structure}}$: The sum of the points of collision with structure

$\sum P_{\text{testis}}$: The sum of the points of impact on the testis

Figure 1. A point grid for calculating the volumetric density of the seminiferous tubules - the volumetric density of the epithelium of the tubules and the volumetric density of the interstitial tissue in the testes of 63-day-old male offspring rats. The arrow signs (at the top right of each point) indicate the count of that point (hematoxylin-eosin, scale; 50 µm).

The following equation was used to calculate the length of testicular seminiferous tubules (Howard and Reed, 2005) (Fig. 2).

$$Lv = 2 \times \frac{\sum Q}{\sum (\text{frame}) \times a(\text{frame})}$$

Lv: Density of length of seminiferous tubules

$\sum Q$: Number of profiles counted

$\sum (\text{frame})$: The number of frames counted

a: The area of the frame surface

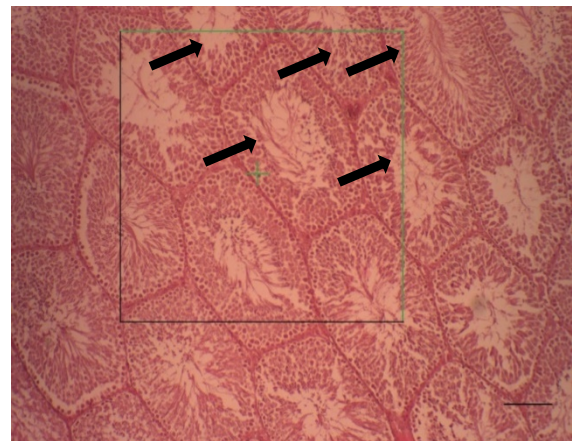


Figure 2. Counting the number of seminiferous tubules (arrow sign) to calculate the length of tubules in the testes of 63-day-old male offspring rats, hematoxylin-eosin, scale; 50µm)

The surface area of the germinal epithelium of tubules was also estimated using a linear probe by the following equation (Howard and Reed, 2005) (Fig. 3).

$$S_v = \frac{2 \times \Sigma I}{l/p \times \Sigma P}$$

$$S = S_v \times V_{\text{Germinal layer}}$$

S_v : The surface density of the germinal epithelium of the seminiferous tubules

ΣI : The sum of the points of collision of the probe with the edge of the germinal epithelium

l/p : linear probe length per grid point

ΣP : Number of points of contact with the germinal epithelium

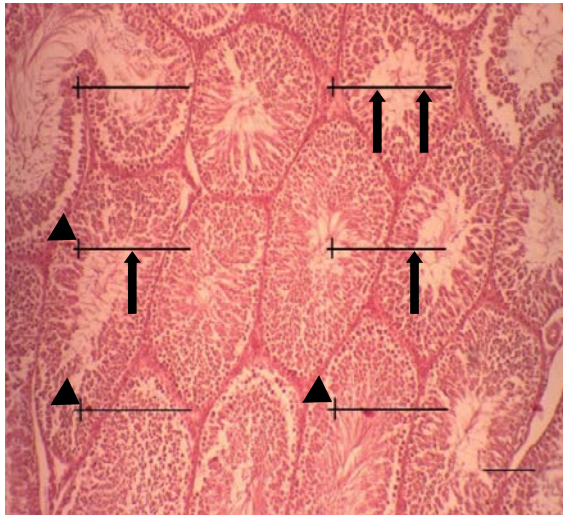


Figure 3. A linear probe to calculate the surface area of the germinal epithelium of tubules of a 63-day-old male offspring rats. The arrow mark indicates countable points for calculating the points of collision at the edge of the germinal epithelium (ΣI) and the arrowhead indicates countable points for calculating the point of impact on the germinal epithelium (ΣP) (hematoxylin-eosin, scale; 50 μ m).

The height of the germinal epithelium was calculated from the following formula (Nyengaard, 1999).

$$H = \frac{V_v (\text{Germinal layer})}{S_v (\text{Germinal layer})}$$

V_v : The density of the germinal epithelium

S_v : surface density of germinal epithelium

2.4. Statistical analysis

Data were analyzed using SPSS software version 22 and expressed as mean \pm standard deviation. The normal distribution of data was evaluated using the Kolmogorov-Smirnov test, and comparison between groups was performed by one-way ANOVA and $P < 0.05$ was regarded as a significant level.

3. Results

3.1. Absolute weight and volume of the testis

Statistically, for testicular weight index, a significant increase was observed in control and sham groups compared with pregnancy, lactation, and pregnancy-lactation groups ($P < 0.05$). Among the experimental

groups, the means obtained from the pre-pregnancy group was significantly increased compared with the means obtained from the lactation and pregnancy-lactation groups ($P < 0.05$). Finally, the mean of the samples of the pregnancy-lactation group was significantly increased from the mean obtained for the pre-pregnancy-pregnancy-lactation group ($P < 0.05$) (fig. 4). Regarding the absolute volume of the testis, the obtained results were similar to the mentioned results for the testicular weight (fig. 5)

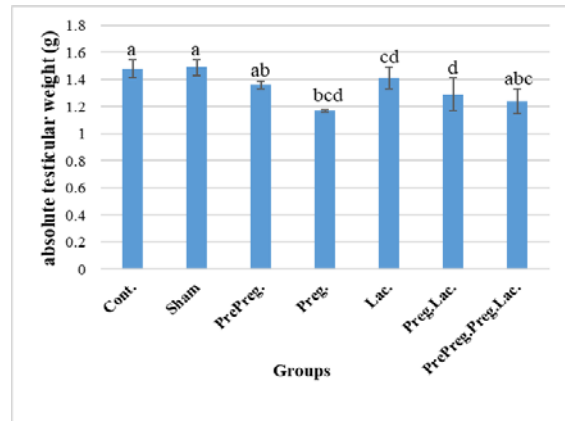


Figure 4. Indicates the results of data on the absolute weight of the testis of 63-day-old male offspring rats exposed to 0.2% lead acetate orally. The results are expressed as Mean \pm Std. Heterogeneous letters indicate a significant difference.

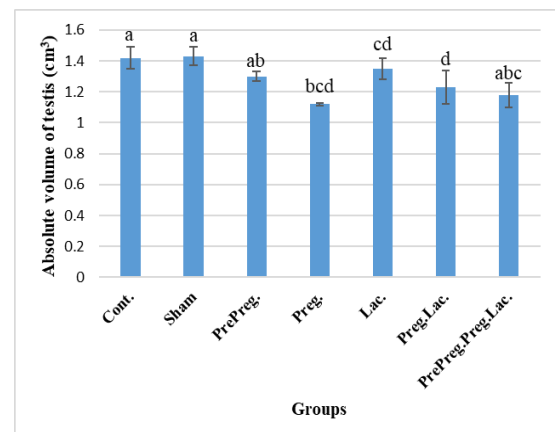


Figure 5. Indicates the results of data on the absolute volume of the testis of 63-day-old male offspring rats exposed to 0.2% lead acetate orally. The results are expressed as Mean \pm Std. Heterogeneous letters indicate a significant difference.

3.2. The volume of seminiferous tubules, epithelium of tubules, interstitial tissue, and length of seminiferous tubules

A comparison of the means related to the volume of seminiferous tubules and the volume of epithelium showed that there was a significant difference, increase, between control and sham groups with all experimental groups except the lactation group. Between experimental groups, a significant decrease was recorded in pregnancy group than lactating group ($P < 0.05$) (fig. 6 & 7). The interstitial tissue volume in the testis of the experimental male rat offspring showed only a significant increase in pre-pregnancy group obtained means compared with the control and sham groups ($P < 0.05$) (fig. 8). Comparison of data related to the length of seminiferous tubules in the

testes of 63-day-old offspring of the studied rats did not show a significant difference ($P > 0.05$) (fig. 9).

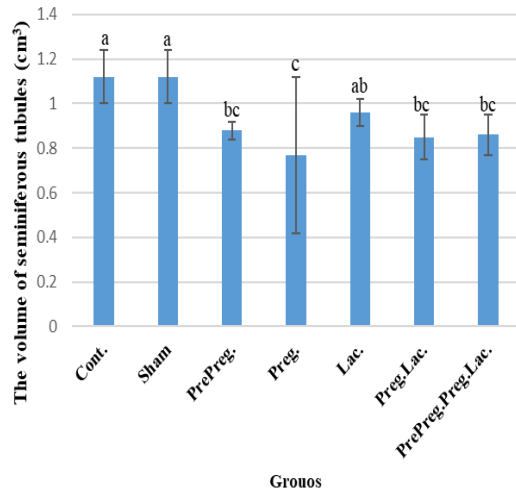


Figure 6. Indicates the results of data related to the volume of seminiferous tubules in the testes of 63-day-old male offspring rats exposed to 0.2% lead acetate orally. The results are expressed as Mean \pm Std. Heterogeneous letters indicate a significant difference.

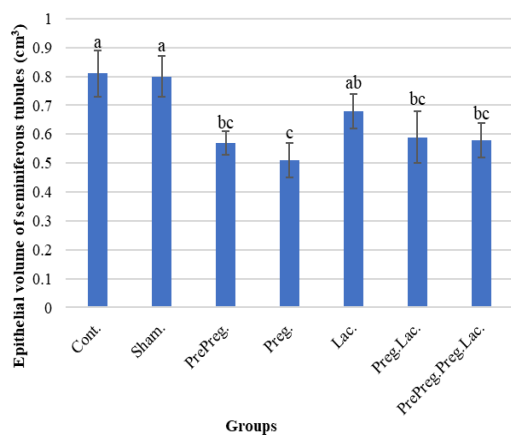
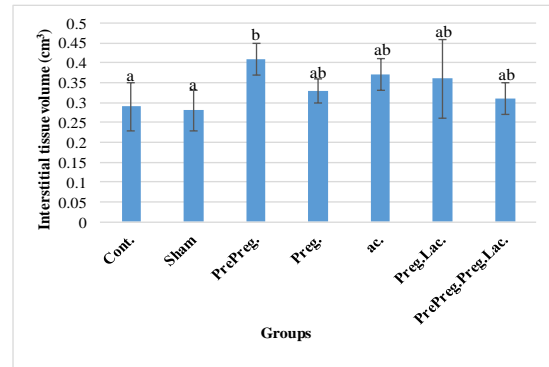


Figure 7. Indicates the results of data on the epithelial volume of the seminiferous tubules in the testes of 63-day-old male offspring rats exposed to 0.2% lead acetate orally. The results are expressed as Mean \pm Std. Heterogeneous letters indicate a significant difference.

Figure 8. Indicates the results of data on the interstitial tissue



volume of the testis of 63-day-old male offspring rats exposed to 0.2% lead acetate orally. The results are expressed as Mean \pm Std. Heterogeneous letters indicate a significant difference.

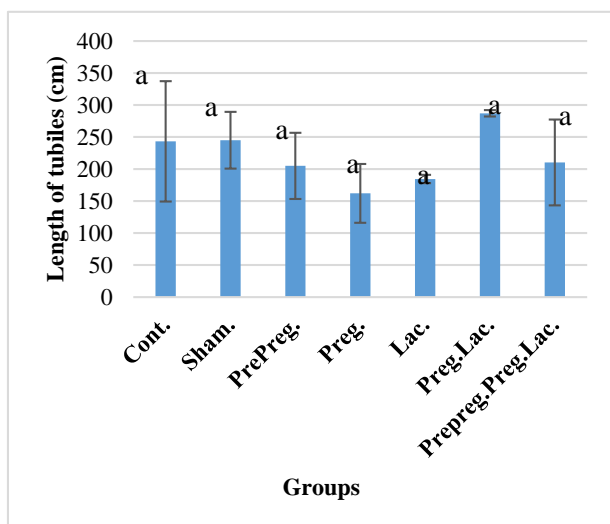


Figure 9. Indicates the results of data related to the length of seminiferous tubules in the testes of 63-day-old male offspring rats exposed to 0.2% lead acetate orally. The results are expressed as Mean \pm Std. There was no significant different.

3.3. The surface area of the epithelium of the seminiferous tubules and the height of the germinal epithelium

There was no significant difference in comparison of the means from different groups in the surface area of the seminiferous tubules epithelium of the testis of the experimental animals ($P > 0.05$) (fig. 10). Statistically, the height of the seminiferous tubules germinal epithelium of the testes showed a significant decrease in the pregnancy, lactation, pregnancy-lactation and pre-pregnancy-pregnancy-lactation groups compared with the control group ($P < 0.05$) (fig. 11).

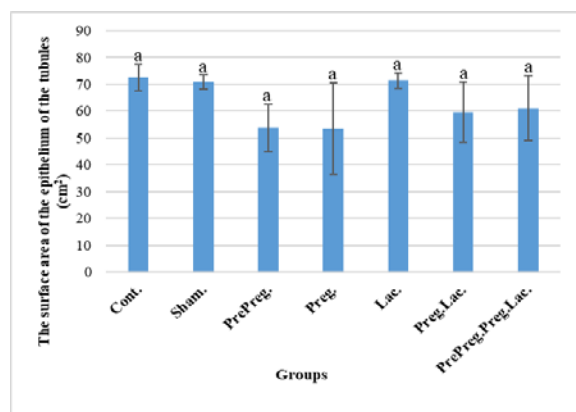


Figure 10. Indicates the results related to the surface area of the germinal epithelium of the seminiferous tubules of 63-day-old male offspring rats exposed to 0.2% lead acetate orally. The results are expressed as Mean \pm Std. There was no significant different.

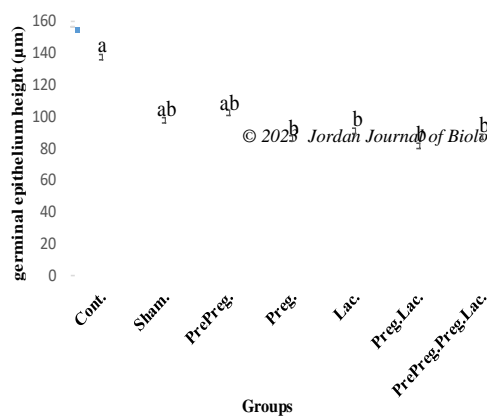
Figure 11. Indicates the results related to the height of the germinal epithelium of the seminiferous tubules of 63-day-old male offspring rats exposed to 0.2% lead acetate orally. The results are expressed as Mean \pm Std. Heterogeneous letters indicate a significant difference.

4. Discussion

Exposure to lead, causes several organs dysfunction including reproductive disorders. If not controlled, lead as an important environmental pollutant can cause serious damage. Recently, lead exposure has been highlighted as an important cause of testicular dysfunction and male infertility. Excessive exposure to lead derivatives reduces sperm quality and reproductive capacity and ultimately causes male infertility (El-Khadragy *et al.*, 2020).

In the present study, statistically, for the absolute weight and volume of testes in 63-day-old offspring, we saw a significant decrease between the means of the pregnancy, lactation, and pregnancy-lactation groups compared to control and sham groups ($P < 0.05$). Among the experimental groups, the mean obtained from the pre-pregnancy group showed a significant decrease compared to the means obtained from the lactation and pregnancy-lactation groups ($P < 0.05$). Also, the mean from the pregnancy-lactation group showed a significant decrease compared to the mean obtained for the pre-pregnancy-pregnancy-lactation group ($P < 0.05$). In this regard, Assi *et al.*, (2016) in their study stated that lead acetate (10 mg/kg/oral and daily) caused a significant reduction in testicular weight in the Sprague Dawley rats. Other researchers such as Allouche *et al.*, (2009) and Elgawish and Abdelrazek (2014) have also shown that different doses of lead acetate induce testicular weight and degenerative testicular changes. Dadkhah *et al.* (2017), in their study, stated that lead acetate caused a decrease in testicular weight in the studied rats, although this reduction was not significant. They mentioned the reason for this decrease as the decrease in germ cells and sperm cells.

Hassan *et al.*, (2019) and Offor *et al.* (2019) reported significant reductions in testicular weight and relative testicular weight during exposure of albino rats to lead acetate, respectively. In another study, Udefa *et al.* (2020) reported a significant reduction in absolute testicular weight of rats exposed to lead acetate. Dorostghoal *et al.* (2011) considered significant testicular weight loss due to high atrophy of the seminiferous tubules. It has been shown that the weight of reproductive organs is used as a basic criterion in toxicological studies (Crissman *et al.*, 2004; Yavasoglu *et al.*, 2008). Mruk and Cheng (2004) have stated that testicular weight is highly dependent on spermatogenic cell mass and that testicular weight loss may be due to impaired spermatogenesis.



Dorostghoal *et al.* (2011) reported a significant decrease in testicular volume in the offspring of Wistar rats following maternal exposure to lead acetate. The results of the present study on the change in absolute testicular volume in 63-day-old rat offspring following maternal exposure to lead acetate are consistent with the results of their study. It seems that anatomical changes in the testis, such as reduction in size and volume, depending on the amount of compound and the duration of exposure, occur due to the production of free radicals in spermatogenic cells and the consequent destruction of these cells. According to Sadeghinezhad *et al.* (2021), there is a positive correlation between testicular volume and the number of spermatogenic cells.

In the present study, comparing the means of the volume of seminiferous tubules and epithelial volume of these tubules showed that there was a significant difference only between control and sham groups with all experimental groups except lactation group, and pregnancy group with lactation group ($P < 0.05$). The volume of interstitial testicular tissue was significantly different ($P < 0.05$) in the control and sham groups compared with the pre-pregnancy group. These significant differences were recorded, while for the volume of seminiferous tubules the volume of the epithelium of these tubules, the volume of interstitial testicular tissue, and the means obtained from all experimental groups showed a decrease compared to the means of the control and sham groups.

In the study of Khodabandeh *et al.* (2021), no significant decrease in the volume of seminiferous tubules following exposure to lead acetate was reported. However, Asadpour *et al.* (2013) reported a decrease in the volume of seminiferous tubules in rats exposed to lead acetate. The results of the present study are in line with the results of their study that this volume reduction may be due to the shrinkage phenomenon in the seminiferous tubules. Sadeghinezhad *et al.* (2021) also considered the decrease in the volume of seminiferous tubules as the reason for the decrease in the number of germ cells due to apoptosis in these cells during the inhibition of calcium pumps in the endoplasmic reticulum.

Khodabandeh *et al.* (2021) stated that lead acetate did not have a significant effect on reducing the epithelial volume of seminiferous tubules. Asadpour *et al.* (2013) also reported a decrease in germ epithelial volume in rats exposed to lead acetate. The results of the present study are in line with the results of the above studies. In another study, Bouazza *et al.* (2018) stated that lead acetate created empty spaces between germ cells. Aftab and Abdul Rauf, (2014) attributed the vacancy between the germ cells to the Sertoli cell damage, which is caused by genotoxic and antiproliferative effects of compounds such as lead acetate. Kumar and Devi, (2018) in a review study stated that exposure to lead acetate destroys the structure of the

epithelium and disrupts the process of spermatogenesis. Hassan *et al.* (2019) also reported the loss of reproductive epithelial cells during exposure of albino rats to lead acetate. According to Oboma *et al.* (2018), lead has a cytotoxic effect on sertoli cells, secreting the sex hormone testosterone, and also inhibiting the expression of specific enzymes involved in the production of steroid hormones. They also stated that lead acetate causes hypertrophy of the seminiferous tubules and dilation of interstitial tissue, which in turn impairs the growth of leydig cells. According to their report, lead poisoning during spermatogenesis can decline sperm count as well as the release of immature spermatogenic cells into the seminiferous tubules. Also, lead acetate can accumulate in the cell nucleus and disrupt the process of cell proliferation and DNA synthesis in vivo. Thus, lead treatment can affect germ cells during the prenatal and postnatal periods, when pro-spermatogonia cells undergo mitosis or Leydig cells develop.

Akinola *et al.* (2015) reported that the interstitial connective tissue of the seminiferous tubules of rats did not change when exposed to an aqueous solution of 2.5% lead-acetate. BaSalamah *et al.* (2018) also reported interstitial tissue change (interstitial necrosis) in their study, using 1000 mg of lead acetate per liter of drinking water for four weeks in rats. In another study, Khodabandeh *et al.* (2021) stated that the volume of interstitial tissue in lead-treated animals increased compared to the control group, but the number of Leydig cells did not change, so it appears that this increase does not depend on the number of Leydig cells. Massanyi *et al.* (2007) have stated that lead causes dilation of capillaries in interstitial testicular tissue. Therefore, the increase in interstitial tissue volume in the present study may be due to changes in interstitial tissue components, especially dilation of blood vessels.

In the present study, it was found that maternal exposure to lead acetate during prenatal and lactation periods reduced the length of seminiferous tubules compared with the control and sham groups. Of course, this decrease was not statistically significant. The results of the present study on changes in the length of seminiferous tubules of rat testes were consistent with the results of Khodabandeh *et al.* (2021) who reported that the length of seminiferous tubules in the lead-acetate group decreased compared to the control group, but this decrease was not significant. In justifying the changes in the length of the tubules, it can be said that according to Mustafa (2015), shrinkage of the seminiferous tubules in rats treated with lead acetate is due to contractions of myoid cells. Also, according to Franca and Russell, (1998), three factors, testicular size, the diameter of seminiferous tubules, and the volumetric density of these tubules affect the length of seminiferous tubules. In the present study, it was found that testicular size and volumetric density of seminiferous tubules in experimental groups decreased compared to control and sham groups.

In the present study, despite the decrease in the statistical analysis of data obtained from all experimental groups, except the lactation group, there was no observed significant difference between the results of the studied groups for the surface area of the tubular epithelium. Despite the statistical decrease in the results of the data analysis, the height of the germinal epithelium did not

show a significant difference compared to the control and sham groups. Akinola *et al.* (2015) reported that the thickness of the epithelium of the seminiferous tubules of rats decreased significantly compared to the control group when exposed to an aqueous solution of 2.5% lead acetate. Zhang *et al.* (2014) stated that lead can bind directly to DNA through four binding sites and form the Pb-DNA complex, thereby damaging the DNA double helix structure. Therefore, the loss of germ cells that reduced the diameter of seminiferous tubules and germinal epithelium in adult rats in their study could be due to the genotoxic effect of lead on germ cell DNA and finally the death of these cells. In addition to the ability of lead to directly damage the DNA of germ cells, it can weaken the antioxidant system in the rat testis by increasing the production of free radicals. The results of the present study and related studies support the role of oxidative damage to germ cells due to lead exposure, and may also support thinning of the germinal epithelium of the seminiferous tubules in our study.

Asad *et al.* (2019) stated that lead acetate caused a significant decrease in the height of the reproductive epithelium compared to the control group. BaSalamah *et al.* (2018) in their study reported atrophy of the seminiferous tubules and destruction of germ cells and sertoli cells in the testis while exposed to rat lead acetate. In another study, Bouazza *et al.* (2018) stated that lead acetate reduced the height of the germ epithelium and created empty spaces between the germ cells. Dorostghoal *et al.* (2011) also reported a significant dose-dependent decrease in the height of the germinal epithelium during the neonatal, pre-pubertal, and post-pubertal periods of rats exposed to lead acetate. Udefa *et al.* (2020) attributed the significant decrease in the height of the reproductive epithelium of the seminiferous tubules to rats exposed to lead acetate due to oxidative stress and apoptosis due to lead acetate exposure. According to them, the decrease in the height of the germinal epithelium indicates the cessation of spermatogenesis in the spermatocyte stage while exposed to lead acetate.

5. Conclusion

It has been found that even in low amounts, lead acetate causes problems in different organs of the body, especially in both male and female reproductive system. The results of this study confirmed the results of previous studies about adverse effects of lead acetate on male reproductive system. The adverse effects of maternal exposure to lead acetate on the morphometric parameters of male offspring rats in this study confirm not only a part of wide range spectrum of adverse effects of this compound on the male reproductive system but also make it necessary to take important decisions to protect the mother and the fetus from exposure to heavy metals, especially lead acetate.

References

Aftab A, and Abdul Rauf S. 2014. Anti-proliferative and Genotoxic Effects of Arsenic and Lead on Human Cells in vitro. *Toxicol Environ Health Sci.* **6**: 148-154.

Akinola O B, Oyewopo A O, Aremu Sh A, Afolayan S T, Sanni G O and Biliaminu S A. 2015. Testicular histomorphometry and

semen quality of adult Wistar rats following juvenile oral lead intoxication. *Eur J Anat.* **19**(1): 65-72.

Allouche L, Hamadouche M and Touabti A. 2009. Chronic effects of low lead levels on sperm quality, gonadotropins and testosterone in albino rats. *Exp. Toxicol. Pathol.* **61**:503–510

Altunkaynak M E, Akgul N, Yahyazadeh A, Altunkaynak B Z, Turkmen A P, Anjum M R and Reddy DR P S. 2013. effect of prenatal exposure to lead acetate on testicular lipid peroxidation in adult rats. *Int. j. pharm. biol. sci.* **4**(1)(B): 893-898.

Apostoli P, Porru S and Bisanti L. 1999. Critical aspects of male fertility in the assessment of exposure to lead. *Scand J Work Environ Health.* **25**: 40 – 43.

Asad A, Hamid S and Qamar K. 2018. Effect of Lead Acetate on Basement Membrane of Seminiferous Tubules of Adult Rat Testis and Protective Effects of *Ficus carica*: A Histological Study. *J Coll Physicians Surg Pak.* **28**(10): 731–734.

Asadpour R, Azari M, Hejazi M, Tayefi H, and Zaboli N. 2013. Protective effects of garlic aqueous extract (*Allium sativum*), vitamin E, and N-acetylcysteine on reproductive quality of male rats exposed to lead. *Vet Res Forum.* **4**(4): 251–257.

Assi M A, Hezmee M N, Abba Y, Yusof M S, Haron A W, Rajion M A, and Al-Zuhairy M A. 2016. Prophylactic effect of *Nigella sativa* against lead steroidogenesis enzymes, and testicular damage in testes of diabetic rats. *Acta histochemica*, acetate induced changes in spermiogram, reproductive hormones and gonadal histology of rats. *Vet. World.* **9**(11): 1305–1311.

Baghurst P A, Robertson E F, Oldfield R K, King B M, McMichael A J, Vimpani G V and Wigg N R. 1991. Lead in placenta, membranes, and umbilical cord in relation to pregnancy outcome in a lead-smelter community. *Environ. Health Perspect.* **90**: 315 – 320.

BaSalamah M A, Abdelghany A H, El-Boshi M, Ahmad J, Idris Sh and Refaat B. 2018. Vitamin D alleviates lead induced renal and testicular injuries by immunomodulatory and antioxidant mechanisms in rats. *Sci. Rep.* **8**(4853): 1-13.

Benoff S, Jacob A, and Hurley I R. 2000. Male infertility and environmental exposure to lead and cadmium. *Hum. Reprod. Update.* **6**(2): 107–121.

Bouazza S, Demmouche A, Toumi-Benali F, Zouba M, Bahri R, Agher N, Merakchi N, and Ahmar El. 2018. Effect of bee pollen extract on lead-induced toxicity in rat testis. *South Asian J Exp Biol.* **8**(3): 91-102.

Boyce R W, Dorph-Petersen K A, Lyck L, Gundersen H J. 2010. Design-based stereology: introduction to basic concepts and practical approaches for estimation of cell number. *Toxicol. Pathol.* **38** (7): 1011-1025.

Brown D L. 2017. Practical Stereology Applications for the Pathologist. *Vet. Pathol.* **54**(3): 358–368.

Crissman J W, Goodman D G, Hildebrandt P K, Maronpot R R, Prater D A, Riley J H, Seaman W J and Thake D C. 2004. Best practices guideline: toxicologic histopathology. *Toxicol. Pathol.* **32**(1): 126–131.

Dadkhah N, Shahnazi M, Mesgari Abbasi M and Etemadifar S. 2017. Assessment of the protective effect of vitamin E on the quality of spermatogenesis and sperm parameters in rats exposed to lead. *Adv. Herb. Med.* **3**(2): 6-14.

Dehoff R T. 2000. Probes, populations, samples, measurements and relations in stereology. *Image Anal. Stereol.* **19**: 1-8.

Dorostghoal M, Dezfoolian A and Sorooshnia F. 2011. Effects of Maternal Lead Acetate Exposure during Lactation on Postnatal Development of Testis in Offspring Wistar Rats. *Iran J Basic Med Sci.* **14**(2): 122-131.

- Elgawish R AR and Abdelrazek H M A. 2014. Effects of lead acetate on testicular function and caspase-3 expression with respect to the protective effect of cinnamon in albino rats. *Toxicol. Rep.* **1**: 795-801.
- El-Khadragy M, Al-Megrin W A, AlSadhan N A, Metwally D M, El-Hennamy R E, Salem F, Kassab R B and Abdel Moneim A E. 2020. Impact of Coenzyme Q10 Administration on Lead Acetate-Induced Testicular Damage in Rats. *Oxid. Med. Cell.* 12p.
- Fair J M and Ricklefs R E. 2002. Physiological growth and immune responses of Japanese quail chicks to the multiple stressors of immunological challenge and lead shot. *Arch. Environ. Contam. Toxicol.* **42**: 77 – 87.
- Franca L R and Russell L D. 1998. *The testes of domestic animals. In: Male Reproduction. A Multidisciplinary Overview*, Madrid: Churchill Livingstone.
- Goyer R A. 1990. Transplacental transport of lead. *Environ. Health Perspect.* **89**: 101–105.
- Gundersen H J, Bagger P, Bendtsen T F, Evans S M, Korbo L, Marcussen N, Moller A, Nielsen K, Nyengaard J R and Pakkenberg B. 1988. The new stereological tools: disector, fractionator, nucleator and point sampled intercepts and their use in pathological research and diagnosis. *APMIS.* **96**(10): 857–881.
- Hassan E, El-Neweshy M, Hassan M, and Noreldin A. 2019. Thymoquinone attenuates testicular and spermatotoxicity following subchronic lead exposure in male rats: Possible mechanisms are involved. *Life Sci.* **230**: 132–140.
- Heidmets L T, Zharkovasky T, Jurgenson M, Jaako-Movits K and Zharkovasky A. 2006. early post-natal, low level lead exposure increase the number of PSA-NCAM expressing cells in the dentate gyrus of adult rat hippocampus. *Neurotoxicology.* **27**: 39-43.
- Howard C V and Reed M G. 2005. *Unbiased Stereology: Three-Dimensional Measurement in microscopy* (2nd ed). Garland Science/BIOS Scientific Publishers, UK.
- Jaako-Movits k, Zharkovasky T, Romantchik O, Jurgenson M, Mersalu E, Heidmets L T, and Zharkovasky A. 2005. Developmental lead exposure impairs contextual fear conditioning and reduces adult hippocampal neurogenesis in the rat brain. *Int J Dev Neurosci.* **23**: 350-627.
- Khodabandeh Z, Dolati P, Zamiri M J, Mehrabani D, Borsbar H, Alae S, Jamhiri I and Azarpira N. 2021. Protective Effect of Quercetin on Testis Structure and Apoptosis Against Lead Acetate Toxicity: An Stereological Study. *Biol. Trace Elem. Res.* 199: 3371–3381.
- Massanyi P, Massanyi M, Madeddu R, Stawarz R and Lukac N. 2020. Effects of Cadmium, Lead, and Mercury on the Structure and Function of Reproductive Organs. *Toxics.* **8**(4): 94.
- Morais S, Costa F G and Pereira M L. 2012. Heavy Metals and Human Health, Environmental Health - Emerging Issues and Practice, Prof. Jacques Oosthuizen (Ed.), ISBN: 978-953- 307-854-0.
- Mruk D and Cheng C Y. 2004. Sertoli-Sertoli and Sertoli-germ cell interactions and their significance in germ cell movement in the seminiferous epithelium during spermatogenesis. *Endocr. Rev.* **25**(5): 747–806.
- Mustafa H N. 2015. Potential alleviation of *Chlorella vulgaris* and *Zingiber officinale* on lead-induced testicular toxicity: an ultrastructural study. *Folia Biol.* **63**(4): 269–278
- Nyengaard J R. 1999. Stereologic Methods and Their Application in Kidney Research. *J. Am. Soc. Nephrol.* **10**: 1100-1123.
- Oboma Y I, Sylvanus B, Okara P N, Tamuno omie F A and Ibiang O E. 2018. Protective effect of combined aqueous extracts of *Allium sativum* and *Zingiber officinale* against lead acetate induced hepatotoxicity and testicular damage in *Rattus norvegicus*. *MOJ Anat & Physiol.* **5**(5):306-313.
- Offor S J, Mbagwu H O and Orisakwe O E. 2019. Improvement of Lead Acetate-Induced Testicular Injury and Sperm Quality Deterioration by *Solanum anomalum* Thonn. Ex. Schumach Fruit Extracts in Albino Rats. *J Family Reprod Health.* **13**(2): 98–108.
- Restanty D A, Soeharto S and Indrawan I W A. 2018. The effect of oral lead acetate exposure on bax expression and apoptosis index granulose cells antral follicle in female wistar rat (*Rattus norvegicus*). *Asian Pac. J. Reprod.* **6**(2): 54-57.
- Sadeghinezhad J, Dahmardeh M, Tootian Z, Bojarzadeh H and Yarmahmoudi F. 2021. Study on the effect of maternal administration of oxaliplatin on offspring testes. *J Exp Clin Med.* **38**(2): 99-106.
- Santhosh Kumar R and Asha Devi S. 2018. Lead Toxicity on Male Reproductive System and its Mechanism: A Review. *Res J Pharm Technol.* **11**(3): 1228-1232.
- Snoeijs T, Dauwe T, Pinxten R, Vandesande F and Eens M. 2004. Heavy metal exposure affects the humoral immune response in a free-living small songbird, the great tit (*Parus major*). *Arch. Environ. Contam. Toxicol.* **46**: 399 – 404.
- Taupeau C, Poupon J, Nome F and Lefevre B. 2001. Lead accumulation in the mouse ovary after treatment-induced follicular atresia. *Reprod. Toxicol.* **15**: 385–391.
- Treuting P M, Dintzis S M and Montine K S. 2017. *Comparative Anatomy and Histology a Mouse and Human Atlas*. Academic press.
- Udefa A L, Amama E A, Archibong E A, Nwangwa J N, Adama S, Inyang V U, Inyaka G U, Aju G J, Okpa S and Inah I O. 2020. Antioxidant, anti-inflammatory and anti-apoptotic effects of hydro-ethanolic extract of *Cyperus esculentus* L. (tigernut) on lead acetate-induced testicular dysfunction in Wistar rats. *Biomed. Pharmacother.* **129**: 110491.
- West M J. 2012. Introduction to stereology. Cold Spring Harbor Protocols. 843-851. *World Health Organization* (WHO). Lead poisoning and health. 2016; Available from: <http://www.who.int/mediacentre/factsheets/fs379/en/> [Accessed 2017 28/09].
- Yavasoglu A, Karaaslan M A, Uyanikgil Y, Sayim F, Ates U and Yavasoglu N U. 2008. Toxic effects of anatoxin- a on testes and sperm counts of male mice. *Exp. Toxicol. Pathol.* **60**(4-5): 391–396.
- Zhang H, Zhang M, Liu R and Chen Y. 2014. Assessing the mechanism of DNA damage induced by lead through direct and indirect interaction. *J. Photochem. Photobiol. B.* **136**: 46-53.

Bioefficacy of *Bacillus cereus* and its Three Mutants by UV Irradiation Against *Meloidogyne incognita* and Gene Expression in Infected Tomato Plants

Gazeia M. Soliman¹, Sameh M. El-Sawy², Rasha G. Salim³, Ghada M. El-Sayed³ and Walaa A. Ramadan^{4,*}

¹Plant Pathology Department, Nematology Unit, National Research Centre, Dokki, Giza, Egypt; ²Vegetable Research Department, National Research Centre, Dokki, Giza, Egypt; ³Microbial Genetics Department, National Research Centre, Dokki, Giza, Egypt; ⁴Genetics and Cytology Department, National Research Centre, Dokki, Giza, Egypt.

Received: June 10, 2022; Revised: November 5, 2022; Accepted: November 25, 2022

Abstract

Stress the use of safer options such as biological control to avoid the hazards of chemical nematicides. UV irradiation has been used to induce mutations and improve protease overproduction. All mutants recorded significant decreases in nematode-related parameters when compared with the wild type and control. Mutant number one (M1) achieved high protease activity about 2.5 fold. At two concentrations of the wild type *Bacillus cereus* and their mutants effect on percentage mortality of *Meloidogyne incognita* juveniles. M1 achieves the highest mortality, 99.33 %, and achieved greatest reductions in the number of juveniles in soil, juveniles/5 g root, galls, and egg-masses recorded 89.76 %, 90.16 %, 85.29 %, and 89.11 %, respectively. M1 achieved the best increase of the growth parameters of plant length, number of branches, number of leaves, and fresh weight of leaves recorded 54.35 %, 71.45 %, 169.44 %, and 256.17 %, respectively. These results are in harmony with those of leaves water soluble-protein electrophoretic patterns after one month and the end of the application, which showed that the plant exposed to M1 exhibited the highest number of bands in both stages of application and appeared unique band at M.W 55kDa after one month of application.

Keywords: Biological-control, *Bacillus cereus*, Mutation, UV irradiation, *Meloidogyne incognita*, SDS-protein electrophoresis, Tomato plants

1. Introduction

The world's human population is rapidly expanding, and as a result, food consumption is rising. Because of the rising demand for food, producers have turned to new techniques to produce more food in the same cultivation area. Tomato (*Solanum lycopersicum* L.) is regarded as one of Egypt's most important vegetable crops. The root-knot nematodes are one of the highly important pathogens that cause great damage and losses incurred to horticultural and field crops, and they are found all over the world; some species are found in tropical and subtropical areas of Africa, such as Egypt (Ismail *et al.*, 2018). These losses ranged between 24 and 38 % as a result of root-knot nematode infestation (El-Nagdi *et al.* 2019; Netscher and Sikora 1990).

Root-knot nematodes, *Meloidogyne* spp., have a diverse host range, attacking up to 5500 plant species (Trudgill and Blok, 2001). The traditional method of nematode management through the use of chemical nematicides is more effective, but it has drawbacks such as high costs and risks to human health and the environment (Mitiku, 2018; Migunova and Sasanelli, 2021). Concerns about public health and environmental safety are driving calls to reduce chemical nematicides used in plant-

parasitic nematode control. As a result, immediate changes in chemical control are required, as is encouraging scientists to look for natural compounds that are less toxic and more environmentally friendly. Biological control by plant-growth-promoting rhizobacteria is a safe alternative approach and promising tool for controlling plant-parasitic nematodes (Kumar and Arthurs, 2021; Lee and Kim, 2016; Rika *et al.*, 2017; Priyank *et al.*, 2018; Sidhu, 2018; Soliman *et al.*, 2020).

Several rhizosphere bacteria have been identified as having potential antagonistic activity against plant-parasitic nematodes by producing enzymes. Protease, chitinase, and lipase are among the lytic enzymes secreted by bacteria. For tylenchoid nematodes like *Meloidogyne* spp., the primary reasoning for their usage in plant nematodes control originates from the fact that the biochemical makeup of nematode structure comprises collagens and lipids during mobile phases, as well as protein, chitin and lipids during sedentary stages (Bird and McClure, 1976). In *in vitro* testing, when compared to the control, *B. cereus* culture filtrates has a nematocidal effect on *M. incognita* egg hatching and mortality (Soliman *et al.*, 2019). Extracellular enzymes, including proteases, are produced by *B. cereus* (Shumi *et al.*, 2004; Soliman *et al.*, 2019). *B. cereus* strain supernatant was used to treat *M. incognita*, which resulted in strong nematocidal activity

* Corresponding author. e-mail: walaanrc70@yahoo.com.

and 90.96 % death. *B. cereus* strain can create extracellular chemicals that kill nematodes (Gao *et al.*, 2016; Mohamed *et al.*, 2021). Eissa *et al.* (2010) used ultraviolet irradiation to increase the nematocidal effect of the chitinolytic bacterium, the wild type of *B. thuringiensis* against *M. incognita*, infecting sunflower. When compared to the wild type and the untreated control, the mutants employed reduced the number of juveniles, galls, and egg-masses while improving plant development parameters.

Usually, bacteria produce valuable products, such as enzymes, in the required amounts to benefit; thus, they tend not to overproduce their metabolites (Shafique *et al.*, 2021). A successful relationship between mutational genetics and industrial microbiology has been reported. Many studies have been published on the use of the strain improvement process through mutations to produce various industrial enzymes such as chitinase, lipase, cellulase, glucoamylase, and protease (Eissa *et al.*, 2010; Ismail *et al.*, 2019; Rakib, *et al.*, 2020). Mutation techniques are used to improve the biocontrol agents to manage phytopathogens. Physical and chemical mutagens have been applied by many researchers to generate new biotypes (Rey *et al.*, 2000). Ultraviolet irradiation (UV) was used to improve the enzyme activity of the original strains as a protease (Afifi *et al.*, 2014; Wang *et al.*, 2007).

Proteins represent the final product of gene expression in organisms; protein isolation and characterization have been one of the most important subjects for researchers. The biochemical markers which study the protein expression make more exact identification possible. The biochemical techniques are rapid, accurate, and dependable (Sammour, 2014). Many reports show that the protein pattern changes are accompanied by biological changes in the process of adaptation, making the organism more fit in the altered environment (Hurkman, *et al.*, 1998; Singh *et al.*, 1985). Polyacrylamide gel electrophoresis SDS-PAGE is commonly used in biological analysis to identify shifts in protein bands. These bands might be enzymes or proteins. Bio-stress, due to hormonal changes, could cause protein synthesis and enzymatic shifts (Ghasempour *et al.*, 2001; Ghasempour and Kianian, 2002; Ghasempour and Maleki, 2003). Increasing bands were detected in both cultivars upon transition from control to stress environment and the resistant cultivar showed more bands as compared to the susceptible cultivar (Vyomesh *et al.*, 2018; Ramadan and Soilman, 2020).

2. Material and Methods

2.1. Bacterial strain

The bacterial strain of *Bacillus cereus* NRC215, isolated and identified in the microbial genetic department, recorded under accession number MT229271 in the NCBI database, was used in this investigation and grown in Luria Broth medium (LB) according to (Davis *et al.*, 1980).

2.2. Genetic Improvement via Ultraviolet irradiation (UV) mutagenesis

One milliliter of eighteen hours old bacterial culture *B. cereus* (saturated culture), as wild type was re-suspended in 50 ml LB medium-containing flasks for 4 h to ensure that cells were in exponential phase and that according to (Alireza 2016). For UV treatment, 10 ml of saturated culture were centrifuged washed twice, and re-suspended

in an equal volume of 50 mM phosphate buffer, pH 7.0, and 2-ml sample was evenly placed in a sterile glass petri dish (5 cm in diameter). One plate was kept in dark which served as control and the rest were exposed to UV-light (A 30-w germicidal lamp at 254 nm (VL-130.G, Vilber, Germany) from a distance of 20 cm for 3, 5, and 10 min. After treatment, samples were immediately diluted 1:10 in LB medium-containing flasks wrapped in tin foil and grown to saturation. Then, appropriate cell dilutions from treated and control samples were spread on LB plates with and without RIF (100 µg/ml) to isolate induced and spontaneous RIF's resistant mutation, respectively.

2.3. Protease assay

Petri dishes 150 mm diameter each contains 50 ml of 0.4% gelatin medium were inoculated from the 24-hours age slants of the evaluated *B. cereus* and its mutants by UV irradiation. Inoculated plates were then incubated for 48 hours at 30 °C after which 7-10 ml of the test solution (100 ml Dist. Water + 15 g. HgCl₂ + 20 ml HCl) were pipetted on the surface of agar. Relationship between diameter of analysis zone and the bacterial growth zone, then, the difference between them divided by the diameter of the growth zone was calculated according to Smith *et al.*, (1952).

2.4. Preparation of Nematode, *M. incognita* culture

M. incognita, the nematode population employed in the bioassay experiment, was obtained from the Plant Pathology Department's greenhouse culture of tomato plants. The eggs were incubated at 27°C in an incubator and hatched out to second-stage juveniles (J2) using modified Baermann plates, which were counted under a stereoscopic microscope.

2.5. Identification of nematode from field area

Roots infected with root-knot nematode were collected from the research field. The perineal pattern of mature females was used to identify root- knot nematode species (Eisenback1985).

2.6. Nematocidal activity of *B. cereus* wild type and its mutants by UV irradiation on percentage mortality of *M. incognita* juvenile's in vitro bioassay

Effect of wild types and different mutants of lytic *B. cereus* (by UV irradiation) on percentage mortality of *M. incognita* juveniles, Two concentrations (100 and 50 %) from cell suspension of wild types (pre-genetic improvement bacteria) and 3 mutants from *B. cereus* were prepared by sterile water. 1 ml of freshly hatching juvenile suspension (50 juveniles±5 / 1 ml) with 2 ml of culture filtrate were transferred to test type. Juveniles that kept in 3 ml of distill water served as control. Five replicates of each treatment were used. The test types were incubated at room temperature (28± 2° C). The juveniles which did not regain their activities and do not move when probed with fine needle were considered "dead". On the other hand, the juveniles were considered active when they were visibly flexible. Handling tools were cleaned with sterilized water throughout the experiment. The percentages of juvenile survival were calculated under a microscope. The percentages of nematode mortality were calculated according to Abbott's Formula as follows:

Juvenile mortality (%) = $(m - n) / (100 - n) \times 100$, where m and n indicate the percentages of mortality in treatments and control, respectively.

2.7. Effect on *M. incognita* developmental parameters:

The initial population of *M. incognita* were estimated in field experiments before transplanting time by taking five samples of about 200 g soil subsamples of well-mixed soil collected from each row. Then, sieving and decanting nematodes were extracted from this soil by Barker (1985). Four months after transplanting, soil and root samples were collected and the numbers of juveniles (J2) of *M. incognita* in soil were counted using Hawksly slide under light microscope. Root samples were gently washed free of soil and an aliquot of 5 g per plot (5 plants) was cut into 2-cm-long pieces. At each sampling time, the root pieces were placed in Petri dishes with distilled water incubated under laboratory conditions (25 ± 5 °C) for a week to extract and count *M. incognita* J2. The numbers of nematode galls and egg-masses were also counted in another 5 g root. The percentages of nematode reduction in total nematode stages inside the roots J2, galls and egg-masses on roots per 5g were calculated with respect to untreated control. J2 in soil were calculated according to the formula of Henderson and Tilton (Puntener, 1981). Gall Index Measuring: The gall index of *Meloidogyne* infested roots was measured as described by Zeck, (1971) on a scale from 0-10.

2.8. Field experiment

Suppressive effect of wild type of *B. cereus* and its three mutants against *M. incognita* infected tomato plant was carried out at the Experimental and Production Station of National Research Centre, El-Noubaria region, Beheira Governorate, north of Egypt, during 2020 and 2021 season, to study the effect wild type of *B. cereus* and its three mutants (M1, M2, M3) on combination on growth, chemical composition, flowering, yield and fruit quality of tomato (*S. lycopersicum* L.) cv. CH7, tomato seedlings were transplanted to the field experiment at (September). The experiment was arranged in a randomized complete block design. The plot area was 10.5m² (3 x 3.5m) with five rows.

All agricultural practices for this plant were carried out as recommended by the Ministry of Agric., Egypt All of the treatments that were evaluated were used on the soil drench. The bacteria were applied by rate 100 ml / around plant root at two doses (1ml contains about 10^{12} cfu) after 3 and 30 days from transplanting date. Vydate was applied with a rate of 0.2 ml/plant, and 12.5 kg/fed, as recommended rates in Egypt by Ali and El-Ashry (2021). This experiment included the following treatments:

- 1- Untreated plants (Control).
2. Vydate® 24% L (Oxamyl)
3. Mutant 1(M1)
4. Mutant2 (M2)
5. Mutant3 (M3)

Five plants were randomly chosen from each replicate at 65 days from transplanting date to determine the following parameters:

2.8.1. Vegetative growth characteristics

Plant length (cm), number of leaves per plant, number of branches per plant and Fresh and dry weights of leaves per plant (g).

2.8.2. Flowering characteristics

Number of clusters per plant.

2.8.3. Fruit yield

Tomato fruits were hand harvested when reaching red ripe stage. Total marketable yield was calculated considering red and disease-free fruits. Number of fruits per plant, fruit yield per plant (g) and total marketable yield (ton/fed) were calculated.

2.8.4. Fruit quality

Random samples of fruits were taken from each experimental plot at the middle of harvesting stage to determine the following characteristics

2.8.5. Fruit physical quality characteristics

Average fruit weight (g) and Average diameter (cm)

2.8.6. Fruit chemical quality characteristics

Determination of total soluble solids (TSS %): Total soluble solids were measured in harvested fruits using hand refractometer, (Atago, U.S.A.).

2.9. SDS-Protein Electrophoresis

Samples of 1 g from leaves exposed to different applications were used to detect the induction of systemic resistance (ISR) in tomato plants infected with *M. incognita* via quantitative and determination of the soluble and non-soluble proteins. This method was done according to Laemmli (1970). Sample preparation and extraction of water-soluble and non-soluble2 proteins were performed according to Stegmann (1979). The gel was photographed and scanned by Gel Doc Bio-Rad System (Gel- Pro analyzer V.3). SDS-PAGE was as modified by Studier (1973).

2.10. Statistical analysis

All data collected were subjected to analysis of variance (ANOVA) and significant means separated with Duncan's Multiple Range Test (DMRT) at P <0.05 level according to Duncan (1955).

3. Results

3.1. Genetic improvement of *B. cereus* protease by UV irradiation

UV treatment of *B. cereus* for three minutes resulted from six rifampin-resistant mutants. There were no rifampin-resistant mutants after five and ten minutes. Only three of the six mutants have lytic activity and have generated protease, and their nematocidal activity against *M. incognita* has been tested under laboratory and field conditions.

3.2. Protease production

The protease activities of *B. cereus* and its three mutants were assessed using gelatin agar, and the diameter of the clear zone was measured. When compared to other mutants and the wild type, the results showed that mutant1 (M1) achieved high protease 250% about 2.5-fold followed by M3 and M2. Generally, the mutants produced

the maximum protease activity compared with the wild type Figure 1(A and B)

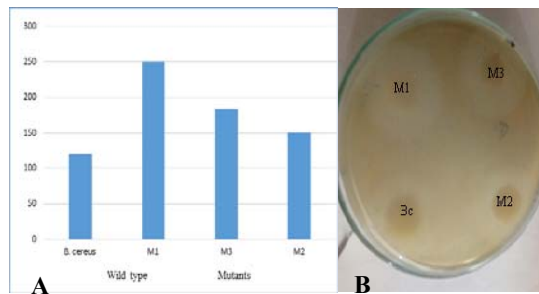


Figure 1. A: Protease activity of *B. cereus* and its three mutants M1, M2, and M3. B: Clear zone of protease activity of *B. cereus* and its three mutants M1, M2, and M3.

3.3. Effects of *B. cereus* and its three mutants on *M. incognita* J2 mortality

The results in (Table1) indicated that the effect of bacterial filtrate of *B. cereus* and its mutants on percentages mortality of *M. incognita* juveniles after 24 h at two concentrations 100 % and 50%. allowed to recover by their transferred to aerated water indicated that mortality percentages after 24 h significantly ($P < 0.05$) increased at using all mutants as compared to the wild type and control. Their percentages of mortality ranged from 99.33 % at M1 and 92.00% at using M3 compared to 87% when applied the wild type at the first concentration.

In the second concentration, percentages of mortality ranged from 96.33 % at M1 to 89.33 % at using M3 compared to 82 % at wild type. Also, there was a positive relationship between the nematode mortality and concentrations.

Also, there was a positive relationship between the nematode mortality and the protease production from the mutants and the wild type (Table 1).

Table 1. Effect of wild type of *B. cereus* and its three mutants by UV irradiation on percentage mortality of *M. incognita* juveniles after 24h.

<div>Concentrations</div> <div>Treatments</div>	Nematode Mortality			
	Wild type	Mutants		
	<i>B. cereus</i>	M 1	M2	M 3
100 %	87.00*d	99.33a	95.00b	92.00c
50%	82.00c	96.33a	91.66b	89.33b

* Means followed by the same letter(s) are not significantly ($P \leq 0.05$) different according to Duncan's Multiple Range Test

3.4. Nematicidal potential of *B. cereus* and its three mutants against *M. incognita* infecting tomato plants

Table 2 shows the effect of *B. cereus* and M1, M 2, and M3 on nematode parameters as compared to vydate and untreated plants (control). The tested wild type and mutant were more effective than the control at reducing the number of *M. incognita* J2 in soil, no. J2 in 5 g root, galls, and egg-masses /5 g root. The M1 treatment achieved the greatest reductions in the number of J2 in the soil J2 in the 5 g root, galls a number, and a number of egg-masses, with reductions of 89.76 %, 90.16 %, 85.29 %, and 89.11 %, respectively. It is followed by M2 with 78.40 %, 89.31 %, 81.51 %, and 86.14 % J2 in the soil, J2 in g root, galls number, and number of egg-masses, respectively. While the wild type had a reduction of 43.45 and, 26.56 & 62.18 %, and 65.94 % in the number of second-stage juveniles in the soil when compared to the untreated control, J2 had a reduction of 5 g root, galls, and egg-masses when compared to the untreated control.

Table 2. Effect of *B. cereus* wild type and its mutants on development of *M. incognita* parameters infected tomato plant under field conditions.

Treatments		Nematode parameters									
		No. J2 in soil (250g)	% R	No. J2 / 5 g root	% R	No. galls / 5 g root	% R	Root gall index**	No. egg-masses / 5 g root	% R	Egg-masses index**
Untreated plant	Control	475.33*a	--	315.00 a	---	79.33a	---	8	67.33a	---	7
Vydate	Nematicides	201.67c	50.75	214.33b	31.96	28.33 b	64.29	5	15.33c	77.23	4
<i>B. cereus</i>	Wild type	268.33b	43.45	231.33b	26.56	30.00b	62.18	5	23.00b	65.94	5
M 1	Mutants	48.67e	89.76	31.00d	90.16	11.67d	85.29	4	7.33e	89.11	3
M2		102.67d	78.40	33.67d	89.31	14.67d	81.51	4	9.33de	86.14	3
M 3		112.67d	76.30	102.00c	67.61	20.67c	73.94	4	11.33d	83.17	4

*Means followed by the same letter(s) are not significantly different according to Duncan's Multiple Range Test. **Root galls and egg-masses indexes were determined according to Zeck (1971) scale as follows: 1 = no galls or egg-mass, 2 = 1-5, 3 = 6-10, 4 = 11-20, 5 = 21-30, 6 = 31-50, 7 = 51-70, 8 = 71-100 and 9 >100 galls or egg-mass/plant . R % = % Reduction

3.5. The potential effect of *B. cereus* and its three mutants on improving tomato plants characteristics.

3.5.1. Vegetative growth of tomato plants

The effect of *B. cereus* and M1, M 2, and M3 compared to the vydate and untreated plant (control) on vegetative

growth of tomato plants grown in sandy soil was shown in (Table 3). The results revealed that tomato plants treated with M1 and M2 had the highest significant of plant length which increased by 54.35% and 47.22% respectively compared to the untreated plants, with non-significant differences between the two mutants. In the same trend,

M1 and M2 treatments produced the highest significance of number of branches per plant compared to the other treatments and increased by 71.45% than the control treatment. On the other hand, tomato plants treated by M1

had the maximum significant of number of leaves and fresh weight of leaves per plant, where the values increased by 169.44% and 256.17%, respectively, compared to the control plants.

3.5.2. Flowering and fruit yield of tomato plants

Regarding the effect of *B. cereus*, M1, M2, and M3, vydate and control treatments on flowering and fruit yield

Table 3. Effect of wild type of *B. cereus* and its three mutants by UV irradiation on vegetative growth of tomato plants#.

Treatments		Plant length (cm)	% Increase	Number of branches/ plant	% Increase	Number of leaves/ plant	% Increase	Fresh weight of leaves/ plant (g)	% Increase
Untreated plant	Control	108.00* e	---	2.33 c	----	36.00 f	---	226.80 f	----
Vydate	Nematicides	135.00 d	25.00	3.33 b	42.86	70.33 e	95.36	402.70 e	77.56
<i>B. cereus</i>	Wild type	143.00 cd	32.41	3.33 b	42.86	79.67 d	121.31	496.90 d	119.09
M1	Mutants	166.70 a	54.35	4.00 a	71.45	103.00 a	186.11	904.20 a	298.68
M 2		159.00 ab	47.22	4.00 a	71.45	97.00 b	169.44	807.80 b	256.17
M 3		150.00 bc	38.89	3.67 ab	57.18	90.67 c	151.86	689.50 c	204.01

*Means followed by the same letter(s) are not significantly ($P \leq 0.05$) different according to Duncan's Multiple Range Test. # Values are average of five replicates

3.5.3. Fruit quality of tomato plant

Regarding the effect of *B. cereus*, M1, M2, and M3, vydate and control treatments on the fruit quality of tomatoes, data in Table 4 showed that the highest significant values of tomatoes average fruit weight and fruit diameter were noticed with M1 and M2 treatments with non-significant differences between them. The results

of tomato plants, data in Table 3 illustrated that M1 and M2 treatments outperformed the other studied treatments with significant differences, where the number of clusters and number of fruits per plant increased by 188.51% and 185.60% and by 107.09% and 94.14% with M1 and M2 treatments, respectively, while the M1 treatment only achieved the highest significant for fruit per plant and fruit yield (ton/ fedden) with increasing by 35.49% and 35.48%, respectively, compared to the control treatment.

show that tomato plants treated by M1 and M2 treatments increased the mentioned characteristics by 135.55% and 126.77% and by 24.81% and 24.09%, respectively. On the other hand, there were no significant differences among *B. cereus*, M1, M2 and M3 treatments with superiority upon vydate and control treatments.

Table 4. Effect of wild type of *B. cereus* and its three mutants by UV irradiation on flowering and fruit yield of tomato plants.

Treatments		Number of clusters/ plant	% Increase	Number of fruits/ plant	% Increase	Fruit yield (g/plant)	% Increase	Fruit yield (ton/ fedden)	% Increase
Untreated Plant	Control	11.67 d		28.33 d		1905.00 d		28.58 d	
Vydate	Nematicides	17.00 c	45.67	36.00 c	27.04	2122.00 c	11.39	31.83 c	11.37
<i>B. cereus</i>	Wild type	18.33 c	57.07	34.33 cd	21.18	2217.00 c	16.38	33.26 c	16.37
M1	Mutants	33.67 a	188.51	58.67 a	107.09	2581.00 a	35.49	38.72 a	35.48
M 2		33.33 a	185.60	55.00 a	94.14	2426.00 b	27.35	36.40 b	27.36
M2 3		26.67 b	128.53	44.33 b	56.48	2351.00 b	23.41	35.27 b	23.41

Table 5. Effect of wild type of *B. cereus* and its three mutants by UV irradiation on fruit quality parameters of tomato plants.

Treatments		Average fruit weight (g)	% Increase	Fruit diameter (cm)	% Increase	TSS %	% Increase
Untreated plant	Control	59.18 e		4.57 d		3.70 c	
Vydate	Nematicides	86.93 d	46.89	5.00 c	9.48	4.72 b	27.49
<i>B. cereus</i>	Wild type	98.20 c	65.93	5.13 c	12.39	5.17 a	39.65
M 1	Mutants	139.40 a	135.55	5.70 a	24.81	5.00 ab	35.16
M 2		134.20 ab	126.77	5.67 a	24.09	5.00 ab	35.16
M 3		126.10 b	113.08	5.40 b	18.24	5.00 ab	35.14

3.6. Effect of wild type and different mutants of *B. cereus*, on Protein expression in infected tomato plants

3.6.1. after one month of application

Protein profile (soluble proteins and non-soluble proteins) was performed to detect the biochemical differences in infected tomato plants. The results revealed clear differences in the number and molecular weights of protein bands due to the different applications of wild type and different mutants of *B. cereus* as a bio-agent against *M. incognita*.

The results of water soluble proteins appeared in Table (6) and figure (2) the electrophoresis pattern showed 10 bands with molecular weight 12-140 kDa, four bands were monomorphic at M.W 62, 29, 17 and 12kDa while six bands were polymorphic. The infected plant exposed to mutant 1 exhibited the highest number of bands (10 bands) including unique band at M.W 55kDa. The lowest number four 4 bands appeared in infected plant exposed to wild type of *B. cereus*.

Table 6. Densitometric analysis represents leaves water soluble protein electrophoretic patterns for infected tomato plant under normal and different applications after one month.

B.N	M.W	Untreated plant	Vydate	Wild type of <i>B. cereus</i>	Mutant 1	Mutant 2	Mutant 3
1	140kDa	+	+	-	+	+	+
2	68kDa	+	+	-	+	+	+
3	62kDa	+	+	+	+	+	+
4	55kDa	-	-	-	+	-	-
5	50kDa	+	+	-	+	-	+
6	40kDa	-	-	-	+	-	+
7	32kDa	+	+	-	+	+	+
8	29kDa	+	+	+	+	+	+
9	27kDa	+	+	+	+	+	+
10	12kDa	+	+	+	+	+	+
Total Bands		8	8	4	10	7	9

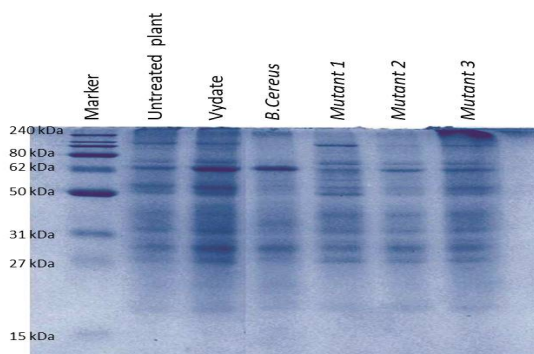


Figure 2. SDS-PAGE of leaves water soluble protein electrophoresis patterns for infected tomato plant under normal and different after one month.

Water non-soluble proteins presented in table (7) and finger (3) a total of seven bands were found in protein pattern ranging from 18 - 62 kDa, two bands were monomorphic while five bands were polymorphic. The lowest number was two bands appeared in the infected plant that were exposed to the wild type of *B. cereus*.

Table 7. Densitometric analysis represents leaves water non-soluble protein electrophoretic patterns for infected tomato plant under normal and different applications after one month

B.N	M.W	Untreated plant	Vydate	Wild type of <i>B. cereus</i>	Mutant 1	Mutant 2	Mutant 3
1	62 kDa	+	+	+	+	+	+
2	53 KDa	+	+	+	+	+	+
3	45KDa	+	+	-	+	+	+
4	31KDa	+	+	-	-	-	-
5	21KDa	+	+	-	+	+	+
6	20KDa	+	+	-	+	+	-
7	18KDa	+	+	-	+	-	-
Total Bands		7	7	2	6	6	4

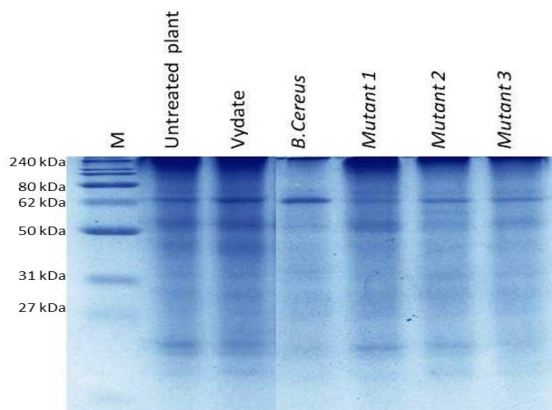


Figure 3. SDS-PAGE of leaves water non-soluble protein electrophoresis patterns for infected tomato plant under normal and different applications after one month.

3.6.2. End of experiment

The results of water soluble proteins of end of experiment presented in Table (8) and figure (4). Showed 13 bands with MW ranging from 18 – 240 kDa, with; seven bands were monomorphic while six bands were polymorphic. The highest number of bands (12 bands) appeared in plants exposed to M1 of *B. cereus*.

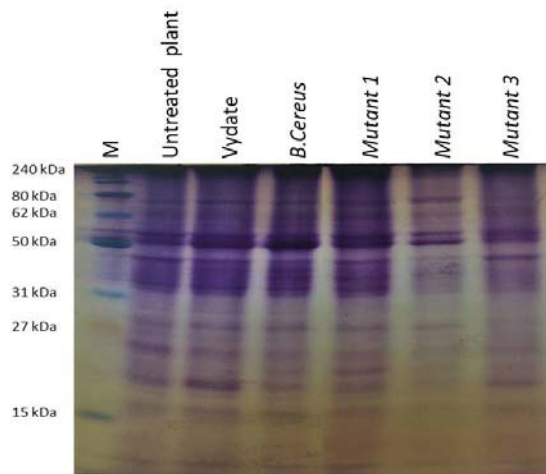
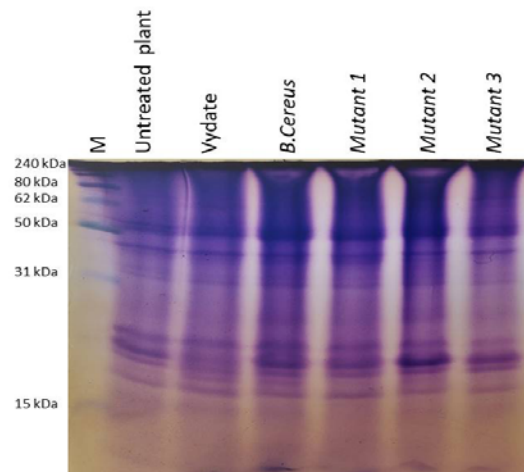
Table 8. Densitometric analysis represents leaves water soluble protein electrophoretic patterns for infected tomato plant under normal and different applications at end of experiment.

B.N	M.W	Untreated plant	Vydate	Wild type of <i>B. cereus</i>	Mutant 1	Mutant 2	Mutant 3
1	240kDa	-	-	-	-	+	-
2	90 kDa	+	+	+	+	+	-
3	62 kDa	+	+	+	+	+	-
4	57kDa	+	+	+	+	+	+
5	52kDa	+	+	+	+	+	+
6	45kDa	+	+	+	+	+	+
7	39kDa	+	+	+	+	+	+
8	32kDa	+	+	+	+	+	+
9	27kDa	+	+	+	+	+	+
10	25kDa	+	+	+	+	-	+
11	22kDa	-	-	-	+	-	-
12	20kDa	+	+	+	+	+	+
13	18kDa	+	+	+	+	-	+
Total Bands		11	11	11	12	9	9

Water non-soluble proteins Table (9) and figure 5 showed that a total of nine bands were found in protein pattern ranging from 29 – 115 kDa, eight bands were monomorphic while one band was polymorphic. Band at MW 115kDa appeared only in plants exposed to M1 and M3 of *B. cereus*.

Table 9. Densitometric analysis represents leaves water non-soluble protein electrophoretic patterns for infected tomato plant under normal and different applications at end of experiment.

B.N	M.W	Untreated plant	Vydate	Wild type of <i>B. cereus</i>	Mutant 1	Mutant 2	Mutant 3
1	115kDa	-	-	-	+	-	+
2	65kDa	+	+	+	+	+	+
3	62kDa	+	+	+	+	+	+
4	59kDa	+	+	+	+	+	+
5	51kDa	+	+	+	+	+	+
6	35kDa	+	+	+	+	+	+
7	31kDa	+	+	+	+	+	+
8	30kDa	+	+	+	+	+	+
9	29kDa	+	+	+	+	+	+
Total Bands		8	8	8	9	8	9

**Figure 4.** SDS-PAGE of leaves water soluble protein electrophoresis patterns for infected tomato plant under normal and different applications at end of experiment.**Figure 5.** SDS-PAGE of leaves water non-soluble protein electrophoresis patterns for infected tomato plant under normal and different applications at end of experiment.

4. Discussion

Plant-parasitic nematodes infect a wide range of agricultural crops around the world, causing significant losses. The root-knot nematode, *M. incognita* is the most common nematode related to low yield (Kayani *et al.*, 2017). Synthetic nematicides pose a risk to humans and the environment, emphasizing the importance of instruments like biological control in sustainable agricultural systems (Giannakou *et al.*, 2004). The use of biological control agents is considered to be safe (Mukhtar *et al.*, 2017; Soliman *et al.*, 2020). The antagonistic microorganisms, particularly those that produce lytic enzymes, are one of the most promising alternatives to chemical nematicides (El-Alfy and Schlenk 2002; Ashoub and Amara 2010; Kashyap *et al.*, 2022). Bacteria produced lytic enzymes when they come into contact with parasitic nematode, which helps to degrade the eggshell, prevent egg hatching, and/or inhibit juvenile activity (Xiang *et al.*, 2018). Biological control with rhizosphere bacteria has been shown to improve plant growth (Kashyap *et al.*, 2021) and reduce nematode reproduction through a variety of mechanisms including increased nitrogen-fixing ability and plant growth hormones production (Mohamed *et al.*, 2021; Saharan and Nehra 2011).

These enzymes have an important role in bacterial-nematode-plant interactions and could be used as a nematicidal to keep nematode populations suppression in the soil (Lian *et al.*, 2007). UV mutation was used to induce the generation of a protease-overproducing mutant from *B. cereus*, according to (Afifi *et al.*, 2014). In our result, when compared to other mutants and the wild type, mutant M1 had a 2.5-fold increase in protease. UV irradiation is being to increase protease overproduction by inducing mutations agreement (Afifi *et al.*, 2014).

Mutation achieved increasing in alkaline protease-over producing mutants, which produced two to three times more activity than the wild type of *S. marcescens* (Kassab *et al.*, 2017). There were positive relationships between the nematode mortality and each of the bacteria concentration and enzyme production from the mutants in bioassay; this result agrees with Kassab *et al.* (2017). The wild type of *B. cereus* and its mutants with their two concentrations show stronger nematicidal activity against second-stage juveniles (J2) of *M. incognita*, according to the results of the laboratory experiment. These results agreed with those of (Eissa *et al.*, 2010; Kassab *et al.*, 2017). All mutants recorded significant ($P < 0.05$) decreased nematode-related parameters and increased growth parameters of the plant when compared with the wild type and control this results in agreement (Kassab *et al.*, 2017; Ismail *et al.*, 2018).

Quantitative proteins of induced tomato plants infected with nematode were identified by using SDS- PAGE; our results indicated that the plant exposed to M1 exhibited the highest number of soluble protein bands (10 bands) including a unique band at M.W 55kDa, after one month of application, also gave The highest number of soluble protein bands (12 bands) at the end of the application. These results are in harmony with those of plants exposed to M1 products, which significantly increased all plan growth parameters and tomato yield. This indicates the importance of applying the M 1 of bacterium strain *B. cereus*, which helped the plant to produce increasing protein bands.

An increase in the number of protein bands refers to the induction of the resistance genes, and this change was reflected in plant growth. This result agreed with those of (Chen *et al.*, 2006; El-DougDoug *et al.*, 2014; Sofy *et al.*, 2014). They suggested that the induced proteins may help to limit the spread or multiplication of pathogens. Sharaf *et al.*, (2016) detected a new pattern of proteins, with different increase in the density of bands when they used antagonistic bacterial strains of *B. subtilis* against the root-knot nematode *M. incognita* infecting tomato plants.

Our results indicated that presence of leaves soluble protein bands with molecular weights 27and 32 KD (PR3 –Chitinase) in all plants treated with biotic inducers. Chitin is a major cell wall component of many bacteria, fungi and nematodes. Chitinase can hydrolyze the cell walls of the pathogen (Hassan, 2004; Kashyap *et al.*, 2020). Several investigators have indicated that induced resistance in plants has been associated with a significant increase in chitinase activity. These results agreed with those of Sharaf *et al.* (2016) who found that the presence of molecular weight 27and 32 KD (PR3 –Chitinase) of protein bands on all plants treated with biotic inducers; these induced proteins have been defined as pathogenesis-related proteins, and they are implicated in plant defense due to their anti-pathogenic activities (Van-Loon *et al.*, 1994).

The outcomes of this study demonstrate that *B. cereus* and its mutations can be employed as an alternative to nematicides in the biological control of *M. incognita*, which results in improved tomato quality and quantity as well as a contribution to the creation of more sustainable agriculture.

5. Conclusion

B. cereus and its mutations can be used as an alternate nematicide to manage *M. incognita* biologically. As a result, all mutants had significantly lower nematode-related parameters as compared to the wild type and control. The best mutant application was Mutant M1, which resulted in the highest juvenile mortality in soil, and achieved a reduction in juveniles in root, galls and egg-masses and improving the plant growth parameters. Also the plant who exposed to M1 exhibited the highest number of protein bands in both stages of application

Reference

- Abbot WS. 1925. A method for computing the effectiveness of insecticides. *J. Econ. Ent.*, **18**: 265-267.
- Afifi AF, Abo-Elmagd HI, Housseiny MM. 2014. Improvement of alkaline protease production by *Penicillium chrysogenum* NRRL 792 through physical and chemical mutation, optimization, characterization and genetic variation between mutant and wild-type strains. *Ann Microbiol.*, **64**:521–530. doi:10.1007/s13213-013-0685-y
- Ali AAI and El-Ashry RM. 2021. Potential effect of the nematicide oxamyl and surfactant combinations on root-knot nematode *Meloidogyne incognita* infecting tomato plants *Egypt Acad J Biolog Sci.*, **13**(1):159-176
- Alireza G. 2016. UV-Induced Mutagenesis in Lactic Acid Bacteria. *J. Genet. Genom.*, **4**: 1-4, doi: 10.11648/j.ijgg.20160401.11.

- Ashoub AH and Amara MT. 2010. Biocontrol activity of some bacterial genera against root-knot nematode, *Meloidogyne incognita*. *J AmrSci.*, **6**: 321-328.
- Barker KR. 1985. Nematode extraction and bioassay In: An advanced treatise on *Meloidogyne*, Volume 11- Methodology (Eds K. R. Barker, C. C. Carter and J. N. Sasser), **19**- 35. North Carolina State University Graphics: Raleigh. North Carolina, USA.
- Bird A and McClure M. 1976. The tylenchid (nematode) egg shell: structure, composition and permeability. *Paracitology.*, **72**:19-28.
- Chen M, Qiu DW, Liu Z, Yang XF and Cao KQ. 2006. Inhibition of RNA replication and coat protein synthesis in Tobacco mosaic virus by a plant activator protein. *Chinese Journal of Biological Control.*, **22**: 63-66. (English abstract).
- Davis RW, Botstein D, Rotho JR .1980. Transfection of DNA. In bacterial genetics: a manual for genetic engineering advanced bacterial genetic, vol **67**. Cold Spring Harbor laboratory cold spring harbor, New York., 134-137.
- Duncan DB. 1955. Multiple range and multiple F tests. *Biometrics.*, **11**: 1-42.
- Eisenback JD. 1985. Detailed Morphology and Anatomy of Second-Stage Juveniles, Males and Females of the Genus *Meloidogyne* (Root-Knot Nematodes). In: Advanced Treatise on *Meloidogyne*, Sasser, J.N. and C.C. Carter (Eds.). Vol. 1, North Carolina State University Graphics, Raleigh., 47-77.
- Eissa MFM, Ismail AE, Abd- El Bary NA, Yassin MY, Bader UM, Soliman GM. 2010. Control of *Meloidogyne incognita* using a wild type and its three mutants of the chitinolytic bacteria, *Bacillus thuringiensis* under greenhouse conditions. *Bull. NRC.*, **35** (2): 139-149.
- El-Alfy A and Schlenk D. 2002. Effect of 17{beta}-estradiol and testosterone on the expression of flavin-containing mono oxygenase and the toxicity of aldicarb to Japanese Medaka *Oryzias latipes*. *Toxicol Sci.*, **68**: 381-388.
- El-DougDoug KA, Sofy AR, Mousa AA and Refaey EE. 2014. Monitoring variability responses of cultivated potato varieties infected with Potato virus Y pepper isolate. *Egyptian J of Virology.*, **11**(2): 82-101.
- El-Nagdi MAW, Abd-El-Khair H, Soliman GM, Ameen HH and El-Sayed M G. 2019. Application of protoplast fusants of *Bacillus licheniformis* and *Pseudomonas aeruginosa* on *Meloidogyne incognita* in tomato and eggplant. *Middle East J of Appl Sci.*, **9** (2): 622-629.
- Gao GH, Qi G Yin R, Zhang H, Li C and Zhao X. 2016. *Bacillus cereus* strain S2 shows high nematocidal activity against *Meloidogyne incognita* by producing sphingosine. *Scientific Reports.*, **6**:28756 1-11. DOI: 10.1038/srep28756.
- Giannakou IO, Karpouzias DG, Prophetou-Athanasiadou D. 2004. A novel non-chemical nematicide for the control of root-knot nematodes. *Appl. Soil Ecol.*, **26**:69-79.
- Ghasempour HR and Kianian J. 2002. Drought stress induction of free proline, total proteins, soluble sugars and its protein profile in drought tolerant grass *Sporobolus elongates*. *J. Sci. Teacher Training Univ.*, **1**: 111-118.
- Ghasempour HR and Maleki M. 2003. A survey comparing desiccation tolerance in resurrection plant *Notholaena vellea* and studying its protein profile during drought stress against a non resurrection plant *Nephrolepis sp.* *Iranian J. Biol.*, **15**: 43-48.
- Ghasempour HR, Anderson EM and Gaff Donald F. 2001. Effects of growth substances on the protoplasmic drought tolerance of leaf cells of the resurrection grass, *Sporobolus stapfianus*. *Aust J Plant Physiol.*, **28**: 1115-1120.
- Hassan HM. 2004. Chitinase from the biocontrol agents: *Trichoderma* spp. *Afr. J. Mycol. Biotechnol.*, **12**: 45-58.
- Holbrook CC, Knauff DA, Dikson DW. 1983 A technique for screening peanut for resistance to *Meloidogyne arenaria*. *Plant Dis.*, **57**:957-958
- Hurkman WJ, Tanaka CK and Dupont FM. 1988. The Effects of Salt Stress on Polypeptides in Membrane Fractions from Barley Roots, *Plant Physiol.*, **88**: 1263-1273.
- Ismail AE, Soliman GM and Badr UM. 2018. Genetic improvement of nematotoxicity of *Serratia liquefaciens* against *Meloidogyne incognita* infected eggplant by gamma irradiation in Egypt. *Pakistan J of Parasitol.*, **66** (3): 28-38.
- Kashyap AS, Dinesh S, Amit KK and Ravinder PS. 2020. Characterization of plant growth-promoting rhizobacteria isolated from chilli rhizosphere of southern plateau and hills region. *Int. J. of Current Microbiology and Appl Sci.*, **9** (08): 3473- 3483, <https://doi.org/10.20546/ijemas.908.402>
- Kashyap AS, Manzar N, Nebapure SM, Rajawat MVS, Deo MM, Singh JP, Kesharwani AK, Singh RP, Dubey SC and Singh D. 2022. Unraveling microbial volatile elicitors using a transparent methodology for induction of systemic resistance and regulation of antioxidant genes at expression levels in chili against bacterial wilt disease. *Antioxidants.*, **11**: 404, <https://doi.org/10.3390/antiox11020404>.
- Kashyap AS, Manzar N, Rajawat MVS, Kesharwani AK, Singh RP, Dubey SC, Pattanayak D, Dhar S, Lal SK and Singh D. 2021. screening and biocontrol potential of rhizobacteria native to gangetic plains and hilly regions to induce systemic resistance and promote plant growth in chilli against bacterial wilt disease. *Plants.*, **10**: 2125, <https://doi.org/10.3390/plants10102125>
- Kassab SA, Eissa MFM, Bader UM, Ismail AE, Abdel Razik, BA, and Soliman, GM. 2017. The nematocidal effect of a wild type of *Serratia marcescens* and their mutants against *Meloidogyne incognita* juveniles. *Egypt J. Agronomatol.*, **16** (2):95-114.
- Kayani MZ, Mukhtar T and Hussain MA. 2017. Interaction between nematode inoculum density and plant age on growth and yield of cucumber and reproduction of *Meloidogyne incognita*. *Crop Prot.*, **92**: 207-212.
- Kumar K. K and Arthurs S. 2021. Recent advances in the biological control of citrus nematodes: A review. *Biological Control.*, **157**:10459.
- Laemmli UK. 1970. Cleavage of structural proteins during the assembly of the head of bacteriophage T4. *Nature.*, **227**: 680-685.
- Lee Y and Kim K. 2016. Antagonistic potential of *Bacillus pumilus* L1 against root-knot nematode, *Meloidogyne arenaria*. *J Phytopathol.*, **164**: 29-39.
- Lian LH, Tian BY, Xiong R, Zhu M Z, ZuJ and Zhang K Q. 2007. Proteases from *Bacillus*: a new insight into the mechanism of action for rhizobacterial suppression of nematode, *Letters in Applied Microbiology.*, **45**:262-269.
- Migunova VD and Sasanelli N. 2021. Bacteria as biocontrol tool against phytoparasitic nematodes. *Plants.*, **10**: 389.
- Mitiku M. 2018. Plant-parasitic nematodes and their management.. A review. *Agric. Res. Technol.*, **8**:30-38.
- Mohamed SAH, Ameen HH, Elkelany US, El Wakeel MA, Hammam MMA, Soliman, GM. 2021. Genetic improvement of *Pseudomonas aeruginosa* and *Bacillus cereus* for controlling root knot nematode and two weeds under laboratory conditions. *Jordan J Biol Sci.*, **14** (4): 859-865.
- Mukhtar T, Hussain MA and Kayani MZ. 2017. Interaction between nematode inoculum density and plant age on growth and yield of cucumber and reproduction of *Meloidogyne incognita*. *Bragantia.*, **75**: 108-112.

- Netscher C and Sikora RA. 1990. Nematode parasites of vegetables. Pp. 237-283 in M. Luc, R. A. Sikora, and J. Bridge, eds. Plant parasitic nematodes in subtropical and tropical agriculture, CAB International, Wallingford, Oxon, UK.
- Priyank H, Chinnannan K, Kadirvelu K, *et al.* 2018. Plant growth promoting rhizobacteria (PGPR): A potential alternative tool for Nematodes biocontrol. *Biocatal Agr Biotechnol.*, **17**: 119-128.
- Puntener W. 1981. Manual for field trials in plant protection. Agric. Div Geigy Limited, Basle, Switzerland, 205p.
- Rakib K, Nain Z, Ahammed B, Karim, M. 2020. Developing *Pseudomonas aeruginosa* mutants with hyperproteolytic activity through UV mutagenesis and characterization for optimized production. **3**: 135- 142, <https://doi.org/10.5455/jabet.2020.d118>.
- Rey M, Delgado JJ, Rincon AM, Limon CM, Benitez T, Perez EA. 2000. Improvement of *Trichoderma* strains for biocontrol. *Rev., Iberoam Micl.*, **17**:531-536
- Rika A, Nyoman P and Tati S. 2017.Role of Indigenous Rhizosphere Bacteria in Suppressing Root-knot Nematode and Improve Plant Growth Tomato. *Plant Pathol J.*, **16**: 25-32.
- Sammour RH. 2014. Cultivars identification based on biochemical markers. *RRBS.*, **8 (9)**:347-358.
- Mohamed SAH, El-Sayed GM, Elkelany US, Youssef MMA, El-Nagdi WMA, Soliman GM. 2021. A local *Bacillus* spp.: isolation, genetic improvement, nematode biocontrol, and nitrogen fixation. *Egyptian pharmaceutical journal.*, **20 (3)**:352-363.
- Shafique, T, Shafique J, Zahid S, Kazi M, Alnemer O, Ahmad A. 2021. Screening selection and development of *Bacillus subtilis* apr-IBL04 for hyper production of macromolecule alkaline protease. *Saudi Journal of Biological Sciences.*, **28**, 1494-1501, <https://doi.org/10.1016/j.sjbs.2020.11.079>.
- Sharaf AMA , Kailla AM , Mohamed S. Attia MS and Mohamed M, Nofa MM. 2016. Induced resistance in tomato plants against root knot nematode using biotic and abiotic inducers. *Int. J. Adv. Res. Biol. Sci.*, **3(11)**: 31-46
- Shumi W Hossain T and Anwar MN. 2004. Proteolytic Activity of a Bacterial Isolate *Bacillus. fastidiosus*. *J.B.S.*, **4**: 370-374.
- Sidhu H. 2018. Potential of plant growth-promoting Rhizobacteria in the management of nematodes: A review. *J Entomol Zoology Studies.*, **6**: 1536-1545.
- Singh NK, Handa AK, Hasegawa PM, and Bressan R. 1985. Proteins Associated with Adaptation of Cultured Tobacco Cells to NaCl, *Plant Physiol.*, **79**: 126–137.
- Smith H, Gallop R C, Patricia W, Harris-Smith and Stanley JL.1952.Sofy AR, Attia MS, Sharaf AMA and El-DougDoug KA. 2014. Potential impacts of seed bacterization or salix extract in faba bean for enhancing protection against bean yellow mosaic disease. *Nature and Science.*, **12(10)**: 67-82.
- Soliman GM, Mohamed HAH., Haggag LF, and El-Hady ES. 2020. Efficiency of biological control of root-knot nematodes in infected grapevines seedling by genetic Improved bacteria. *Plant Archives.*, **20 (1)**: 951-961.
- Soliman, GM, Ameen, HH, Abdel-Aziz, M. and E-Isayed, GM. 2019. In vitro evaluation of some isolated bacteria against the plant parasite nematode *Meloidogyne incognita*. *Bull. NRC.*, **43**:171, <https://doi.org/10.1186/s42269-019-0200-0>
- Stegmann H. 1979. Electrophoresis and focusing in slabs using the Pantaphor apparatus for analytical and preparative separations in gel (Polyacrylamide, Agarose, Starch, Sephadex). Messweg 11, D-3300, *Braunschweig Institute of Biochemistry*, West-Germany., pp: 1-29.
- Studier FW. 1973. Analysis of bacteriophage T7 early RNA and protein of slab gels. *Molecular. Biol.*, **79**:237-248.
- Trudgill DL and Blok VC. 2001. Apomictic, polyphagous root-knot nematodes: exceptionally successful and damaging biotrophic root pathogens. *Annual Review of Phytopathol.*, **39**: 53-77.
- Van Loon LC, Pierpoint WS, Boller T and Conejero V. 1994. Recommendations for naming plant pathogenesis related proteins. *Plant Molecular Biology Reporte.*, **12**: 245-264.
- Vyomesh SP, Pitambara and ShuklaYM. 2018. Proteomics study during root knot nematode (*Meloidogyne incognita*) infection in tomato (*Solanum lycopersicum* L.). *J of Pharmacognosy and Phytochemistry* ., **7 (3)**: 1740-1747
- Ramadan WA and. Soliman GM. 2020 Effect of different applications of bio-agent *Achromobacter xylosoxidans* against *Meloidogyne incognita* and gene expression in infected eggplant. *Jordan J of Biol Sci.*, **13(3)**: 363–370
- Wang H, Liu D, Liu Y, Cheng C, Ma Q, Huang Q, Zhang Y. 2007. Screening and mutagenesis of a novel *Bacillus pumilus* strain producing alkaline protease for dehairing. *Lett Appl Microbiol.*, **44**:1–6. doi:10.1111/j.1472-765X.2006.02039.x
- Xiang N Kathy S and Donald A. 2018. Biological control potential of plant growth-promoting rhizobacteria suppression of *Meloidogyne incognita* on cotton and *Heterodera glycines* on soybean: A review. *J Phytopathol.*, **166** :449-458.
- Zeck WM. 1971. A rating scheme for field evaluation of root-knot infestations. *Pflanzenschutz-Nachr.*, **24**: 141–144.

Skin-Cancer Protective Effect of *Ziziphus Spina-christi* Leaf Extract: *In vitro* and *In Vivo* Models

Omar F. Khabour^{1,*}, Karem H. Alzoubi², Ahmad S. Alkofahi³, Rafat M. Al-Awad¹

¹Department of Medical Laboratory Sciences, Faculty of Applied Medical Sciences, Jordan University of Science and Technology, Irbid, Jordan; ²Department of Clinical Pharmacy, Jordan University of Science and Technology, Irbid, Jordan; ³Department of Medicinal Chemistry and Pharmacognosy, Faculty of Pharmacy, Jordan University of Science and Technology, Irbid, 22110, Jordan.

Received: July 30, 2022; Revised: November 13, 2022; Accepted: December 1, 2022

Abstract

Cancer prevention includes approaches that can reduce the risk of developing cancer, such as maintaining a healthy diet and avoiding exposure to mutagenic agents. Plants with antimutagenic properties can be valuable as cancer-protective agents. This study aims to investigate the antimutagenic activity and cancer-protective effects of *Ziziphus spina-christi* using *in vitro* and *in vivo* human and animal models, respectively.

The antimutagenic activity of *Ziziphus spina-christi* leaf extract was examined in cultured human lymphocytes using sister-chromatid exchanges (SCEs) and 8-OHdG assays. In addition, the cancer-protective effect of the extract was investigated using a skin painting assay and 7,12-dimethylbenz(a) anthracene (DMBA)-induced cancer of Balb/c mice. Animals were treated with DMBA for 20 weeks with concurrent consumption of *Ziziphus spina-christi* leaf extract 100mg/kg daily, 5 days/week. The *Ziziphus spina-christi* leaf extract significantly reduced the levels of SCEs and the 8-OHdG levels in human lymphocytes in a dose-response manner ($P < 0.01$). In addition, leaf extract significantly reduced the incidence of skin tumors, tumor sizes, and frequency of DMBA-induced papilloma ($P < 0.05$). It also delayed the onset of tumor development compared to the DMBA group ($P < 0.05$). Finally, animals treated with *Ziziphus spina-christi* leaf extract had lower body weight compared to the control group ($P > 0.05$). In conclusion, the experimental investigation demonstrated the beneficial properties of *Ziziphus spina-christi* as an anticancer agent.

Keywords: plant extract, *Ziziphus*, carcinoma, skin cancer, cancer prevention.

1. Introduction

Skin cancer (SC) is a common disease affecting a large number of individuals in the world (Ahmed et al., 2020). The three most common types of SC are melanoma, basal cell carcinoma, and cutaneous squamous cell carcinoma (Collins et al., 2019). Although various therapies have been applied to cure cancer, researchers have been searching for more potent and simultaneously safer medications to beat the disease (Lalotra et al., 2020). Natural compounds such as plant products have been utilized as antitumor agents for different types of cancers (Sajadimajid et al., 2020; Sauter, 2020). In addition, many plant products have shown antimutagenic activities and thus can be used as protective agents against the development of cancer (Alzoubi et al., 2021; Fahmy et al., 2022; Nageen et al., 2021).

Among the promising medicinal plants is *Ziziphus spina-christi* which belongs to the plant family *Rhamnaceae* (Abdulrahman et al., 2022). More than 40 species have been classified within this family, with a wide range of medicinal uses including the management of chronic diseases, infectious diseases and malignancies (Al Omar et al., 2022). *Ziziphus spina-christi* is an evergreen plant that is native to north/tropical Africa, and

South/West Asia (Abdulrahman et al., 2022; Albalawi, 2021). Various studies have revealed the valuable components of *Ziziphus spina-christi* plant such as botulin, spinanine, tanines, sterols, rutin, quercetin derivatives, triterpenoids, sapogenins, and saponins (Bozicevic et al., 2017; Hussein, 2019; Soliman et al., 2019). *Ziziphus spina-christi* plant extracts have shown a potent function against cancer cell lines (El-Maksoud et al., 2021; Fahmy et al., 2022; Farmani et al., 2016; Jafarian et al., 2014). Additionally, the plant leaf extract has been reported to be effective in fighting bacterial and viral infections as well as reducing diarrhea symptoms and diabetes activity (Abdulrahman et al., 2022; Albalawi, 2021; Hussein, 2019; Zandiehvakili and Khadivi, 2021).

In the current study, the antimutagenic activity of *Ziziphus spina-christi* leaf extract was examined in cultured human lymphocytes using sister-chromatid exchanges (SCEs) and 8-hydroxy-2'-deoxyguanosine (8-OHdG) assays. In addition, the cancer-protective effect of the extract was investigated using mouse skin painting assay. The 8-OHdG assay is widely used to examine the level of DNA damage caused by oxidative stress in living cells. The SCEs assay is used as an indicator of DNA strand damage induced by various mutagenic agents. Finally, the skin painting assay is a valid and widely used model for examining the carcinogenic potential of

* Corresponding author. e-mail: khabour@just.edu.jo.

chemical agents. In addition, the model has also been used to investigate treatments that can be useful as protective agents against the development of cancer.

2. Materials and Methods

2.1. Animals

Young (7-8 weeks old) Balb/c mice were purchased from the Animal Care Facility of Jordan University of Science and Technology (JUST). Animals were housed in standard mice cages (4-6 animals per cage) and underwent 14 days of acclimatization to experimental conditions prior to the start of the experiments (Alzoubi et al., 2020). The animals were kept in optimal experimental conditions that included temperature ($24\pm1^{\circ}\text{C}$), humidity ($45\pm5\%$), light/dark cycle (12h/12h), and food/water (*ad libitum*). Animals were shaved in the interscapular region 3 days before the start of the experiment. The animal part of the study was approved by the Animal Care and Use Committee at JUST.

2.2. *Ziziphus spina-christi* leaf extract

Ziziphus spina-christi was collected from Jordan, Irbid region under the supervision of Professor Jamal Lahaam, a botanist from Yarmouk University (Irbid, Jordan). The leaves of the plant were dried, stored, and a gummy extract was prepared as previously described (Alkofahi et al., 2017). In brief, after drying, *Ziziphus spina-christi* leaves were mechanically stranded using a 2 mm mesh machine (Wiley grinder, Homas Scientific, USA). Stranded leaves were percolated in ethanol (80%) and then subjected to vacuum evaporation at 40°C . The extracts were stored in aliquots at -30°C until used (Alkofahi et al., 2016).

2.3. Skin paint assay

Animals were divided into 3 homogeneous groups of 15 mice each. Animals were assigned into groups according to their body weight using Xybion PATH/TOX software, Cedar Knolls, NJ, USA. The three groups were: the control group (treated with vehicle), DMBA group (100 μg of 7,12-dimethylbenz(a) anthracene, Sigma-Aldrich, Saint Louis, MO, USA) and DMBA/plant extract group (Alzoubi et al., 2021). DMBA, the tumor induction agent, was dissolved in acetone and immediately applied to the interscapular skin of animals using micropipettes. Animals in the DMBA/plant extract group were treated with DMBA as in group 2 plus *Ziziphus spina-christi* leaf extracts (administered using oral gavage, dose = 100 mg/kg). DMBA and the plant extract were administered daily except for Friday and Saturday of each week during the 20-week experimental period (Li and Brakebusch, 2021). The general health of the animals was checked regularly in each working day during the study period. Regarding tumor development, the skin of the animals was examined weekly. Papillomas with diameters of 2mm or larger were recorded (Roemer et al., 2010). In addition, the following measures were recorded: tumor incidence (% of tumor-bearing mice), multiplicity (% of tumors/mice), and tumor onset (Ghosh et al., 2015; Gopalakrishnan et al., 2019).

2.4. Blood Cultures

Blood was obtained from 5 health donors in heparin vacutainer tubes. The criteria for the selection of blood

donors were as previously described (Hendawi et al., 2022; Tarboush et al., 2022). For each 1mL blood culture, 9 mL of PB-Max media (Thermo Fisher Scientific, MA, USA) were used. Blood cultures were maintained at 37°C in a humid CO_2 incubator as described previously (Rababa'h et al., 2019). Cultures assigned to SCEs were treated with 5-bromodeoxyuridine (BrdU, 25 $\mu\text{g}/\text{mL}$ final concentration, Sigma-Aldrich, USA) to obtain differential staining of sister-chromatids (Al-Eitan et al., 2020).

2.5. *In vitro* sister-chromatid exchanges (SCEs) assay

Cultures assigned for SCEs were treated with leaf extracts (10, 100, and 500 $\mu\text{g}/\text{mL}$ final concentration) in the last 24 hours of the culture period. Lymphocytes at metaphase were harvested by treating the cultures with colcemid (10 $\mu\text{g}/\text{mL}$ final concentration). The cultures were then subjected to a hypotonic solution of KCl and then the cells were collected by centrifugation and fixed in methanol/acetic acid (3/1 respectively). Fixed cells were spotted on microscopic glass slides by dropping and then stained using the Fluorescence Plus Giemsa (FPG) method as previously described (Khabour et al., 2013). At least 250 metaphase II cells were scored for each treatment (Alqudah et al., 2018).

2.6. The 8-OHdG assay

At the end of the 72 hours incubation period, blood cultures assigned for 8-OHdG assay were centrifuged at 300xg, and the culture media was removed. The cells were then washed 5 times using RBMI media. The cells were then treated in RBMI media with different concentrations of leaf extracts (10, 100, and 500 in $\mu\text{g}/\text{mL}$ final concentration) for 6 hours (Daradka et al., 2018). The cell suspension was then centrifuged at 300 xg, and 8-OHdG in the supernatant was measured using a commercial ELISA assay obtained from Abcam (Cambridge, UK). ELISA plates were read at 405 nm using the ELx800 ELISA plate reader (BIO-TEK, USA) as previously described (Azab et al., 2017). A total of 8 replicates were used for each concentration.

2.7. Statistical analysis

Data were analyzed using GraphPad Prism Software (version 5, La Jolle, CA, USA). Groups were compared using one-way ANOVA followed by Tukey's post hoc test. A $p<0.05$ indicates statistical significance.

3. Results

Ziziphus spina-christi leaf extracts were tested for antimutagenic potential using SCEs and 8-OHdG assays in cultured human lymphocytes. Figure 1 shows SCEs levels in lymphocytes treated with different concentrations (10, 100, and 500 $\mu\text{g}/\text{mL}$) of the plant extract. *Ziziphus spina-christi* leaf extracts at 100 $\mu\text{g}/\text{mL}$ and 500 $\mu\text{g}/\text{mL}$ induced a significant decrease in the frequency of SCEs compared to the control group ($P<0.01$). However, *Ziziphus spina-christi* leaf extracts at 10 $\mu\text{g}/\text{mL}$ did not affect the frequency of SCEs compared to the control group ($P<0.05$). The magnitude of the decrease in the frequency of SCEs resulting from the 100 $\mu\text{g}/\text{mL}$ concentration is similar to that observed at 500 $\mu\text{g}/\text{mL}$. This indicates a saturation effect at the 100 $\mu\text{g}/\text{mL}$ concentration. Figure 2 shows the levels of 8-OHdG in cultures treated with different concentrations (10, 100, and 500 $\mu\text{g}/\text{mL}$) of the

leaf extract. A significant decrease in 8-OHdG levels was observed for all examined concentrations of *Ziziphus spina-christi* leaf extract. The magnitudes of the decrease in 8-OHdG caused by 100 µg/mL and 500 µg/mL were significantly higher than that induced by the 10 µg/mL concentration ($P<0.01$). In addition, both concentrations of 100 µg/mL and 500 µg/mL induced a similar reduction in the levels of the 8-OHdG marker, indicating a saturation effect. Results of sister-chromatid exchange and 8-OHdG assays indicate the antimutagenic effects of the *Ziziphus spina-christi* plant extract.

The protective effect of the leaf extract against cancer development was examined using the mouse skin painting assay (Figure 3). The results showed that *Ziziphus spina-christi* leaf extract significantly lowered the incidence of skin tumors, tumor sizes, and frequency of papilloma ($P<0.05$) induced by treating animal skin with DMBA (Figures 3C, 3E, and 3F respectively). Additionally, the *Ziziphus spina-christi* plant extract significantly retarded the onset of skin tumors ($P<0.05$) (Figure 3D). On the other hand, animals treated with *Ziziphus spina-christi* leaf extract showed marked decreases in body weight when compared with the control group (Figure 3A, $P>0.05$). Finally, leaf extract did not affect the number of tumors/animal (Figure 3B, $P>0.05$).

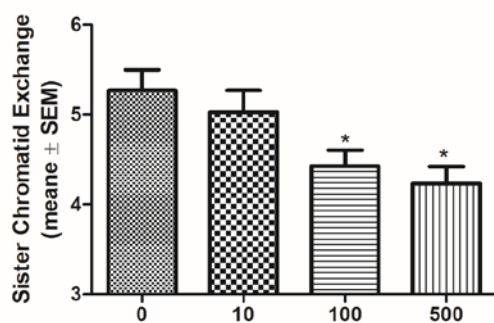


Figure 1. Antimutagenic activity of *Ziziphus spina-christi* leaf extract using sister-chromatid exchanges (SCEs) assay. *Ziziphus spina-christi* leaf extract significantly reduced levels of SCEs in cultured human lymphocytes at 100 µg/mL and 500 µg/mL concentrations (* indicates $P<0.01$).

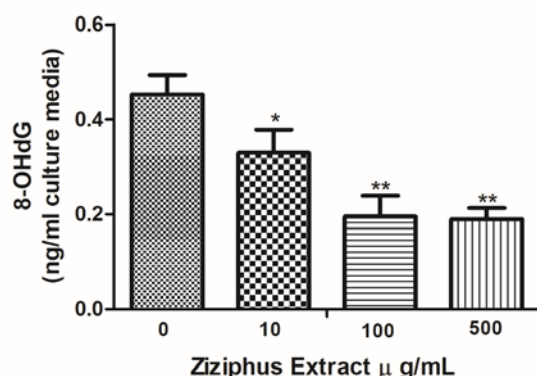


Figure 2. Antimutagenic activity of *Ziziphus spina-christi* leaf extract using 8-OHdG assay. *Ziziphus spina-christi* leaf extract significantly reduced levels of 8-OHdG in cultured human lymphocytes at 10 µg/mL, 100 µg/mL and 500 µg/mL concentrations (* indicates $P<0.05$, ** indicates $P<0.01$).

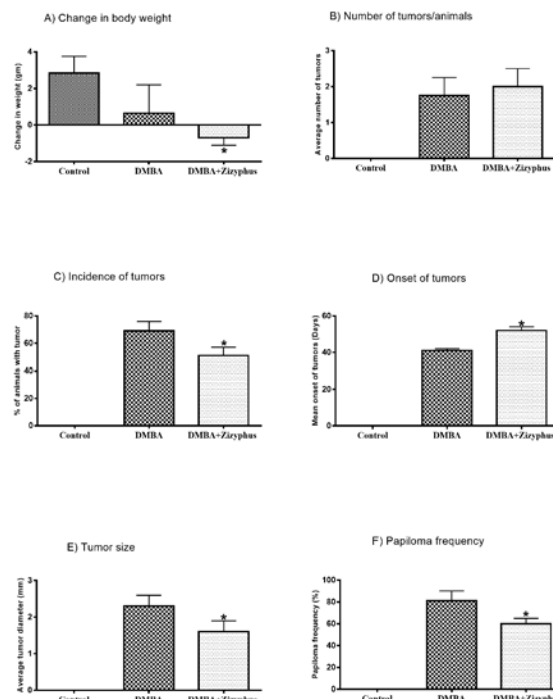


Figure 3. Cancer-prevention effect of *Ziziphus spina-christi* leaf extract.

Mouse skin-painting assay was used. *Ziziphus spina-christi* leaf extract was administered using oral gavage, once daily (100mg/kg) for 5 days/week until the end of the experiment. Skin tumor was induced using DMBA. *Ziziphus spina-christi* leaf extract significantly reduced the incidence of skin tumors (C), tumor sizes (E), and frequency of papilloma (F). *Ziziphus spina-christi* plant extract significantly delayed the onset of skin tumors (D) and lowered the body weight of animals (A). Finally, leaf extract did not affect the number of tumors/animal (B). * indicates $P<0.05$.

4. Discussion

Cancer remains among the leading causes of death worldwide despite the remarkable improvement in the treatment of most malignancies (Torre et al., 2016). Therefore, adopting a preventive strategy for cancer can reduce the burden and death associated with this disease. Natural products with antimutagenic and antioxidant potential are good candidates that can help in cancer prevention (Sanders et al., 2016).

In the current study, the antimutagenic activity and cancer-prevention effects of the medicinal plant *Ziziphus spina-christi* were examined. The results showed a strong antimutagenic activity of *Ziziphus spina-christi* in vitro in cultured human lymphocytes. In addition, consumption of *Ziziphus spina-christi* leaf extract significantly reduced the carcinogenicity of DMBA-induced skin cancer.

The antimutagenicity of *Ziziphus spina-christi* leaf extract was demonstrated in the current study using SCEs and the 8-OHdG assays. The antimutagenic effects of *Ziziphus spina-christi* leaf extract are dose-dependent ($P<0.01$). SCEs in mitotic cells reflect damage to DNA strands that are usually corrected using a recombination DNA repair system that utilizes the unaltered homologous

DNA to fix the damaged strand. The 8-OHdG biomarker reflects DNA damage induced by free radicals generated within cells during cellular respiration and by chemical/physical agents. Therefore, *Ziziphus spina-christi* leaf extract appears to protect cells from a spectrum of DNA damage through single/multiple mechanisms. Among these mechanisms is the potent antioxidant property of *Ziziphus spina-christi* leaf extract which has been shown to neutralize more than 90% of cellular-induced oxidative stress (Almeer et al., 2018; Hosny et al., 2022; Zandiehvakili and Khadivi, 2021). Among the known antioxidants of *Ziziphus spina-christi* leaf extract are glycosides, phenols, terpenoids, cyclopeptide alkaloids, and flavonoids (Elghaffar et al., 2022; Sakna et al., 2019). In addition, consumption of the leaf extract has been shown to reduce oxidative stress and improve recovery from brain injury via modulating aquaporin-4 and TLR4/NF- κ B/TNF- α signaling pathways (Safdari et al., 2021). Using a rat animal model, *Ziziphus spina-christi* leaf extract has been reported to attenuate mercuric chloride-induced liver and testicular injury via normalizing oxidative stress (Almeer et al., 2020; Ramadan et al., 2021). The antioxidative status of rabbits fed a diet supplemented with *Ziziphus spina-christi* leaves showed significant improvements in blood total antioxidative capacity and glutathione peroxidase, catalase and superoxide dismutase activities (Abduljawad, 2020). Therefore, using different animal models, *Ziziphus spina-christi* showed potent activity against the body's oxidative stress.

In the current study, the cancer-protective activity of *Ziziphus spina-christi* leaf extract was demonstrated using the mouse skin painting assay. A significant reduction in several measures of tumor development was observed in animals that consumed *Ziziphus spina-christi* leaf extract. These include the incidence of tumors, tumor sizes, and frequency of induced papilloma by the carcinogen. In addition, tumor onset was significantly delayed in the animals that received *Ziziphus spina-christi* leaf extract. Consistent with the current study, methanolic *Ziziphus spina-christi* leaf extract has been reported to protect Wistar rats from hepatocellular carcinoma induced by diethyl nitrosamine (El-Din et al., 2019). Similarly, *Ziziphus spina-christi* fruit extract has been shown to protect animals from azoxymethane-induced colon cancer (Guizani et al., 2013). The anticancer effects of *Ziziphus spina-christi* leaf extract were attributed to its high content of polyphenols, flavonoids, betulin derivatives, and cyclopeptide alkaloids compounds (Abdulrahman et al., 2022; Soliman et al., 2019).

Several mechanisms may mediate the cancer-protective effects of *Ziziphus spina-christi* leaf extract. *Ziziphus spina-christi* leaf extract contains numerous bioactive compounds with potent anticancer activity reported using human and animal cancer cell lines (Abdulrahman et al., 2022; El-Maksoud et al., 2021; Jafarian et al., 2014; Sakna et al., 2019; Soliman et al., 2019). For example, *Ziziphus spina-christi* leaf extract showed strong activity against human MCF7 breast cancer cells with an IC₅₀ of 40.25 μ g/mL (Hosny et al., 2022). Another mechanism by which *Ziziphus spina-christi* leaf extract can prevent the development of cancer is via promoting apoptosis in cancer cells by activating the Bax-independent apoptosis pathway (Farmani et al., 2016; Ghaffari et al., 2021). In

addition, *Ziziphus spina-christi* leaf extract can significantly reduce tissue inflammation, which is a predisposing factor for the development of cancer (Alajmi et al., 2019; Kadioglu et al., 2016). A human study showed the efficacy of *Ziziphus spina-christi* leaf extract in protecting against skin rashes associated with anticancer medications (Alzahrani et al., 2019). Finally, the antimutagenic activity of *Ziziphus spina-christi* leaf extracts reported in the current study may play an important role in protecting animals from skin cancer.

Animals that consumed *Ziziphus spina-christi* leaf extract showed a notable reduction in body weight. This observation is consistent with previous studies using other animal models. For example, a reduction in the body weight of obese rats has been reported after the consumption of *Ziziphus* tea (El Seedy et al., 2021). The mechanism by which *Ziziphus spina-christi* reduces body weight may involve promoting fatty acid oxidation in mitochondria and reducing adipokine secretions (Yagoub et al., 2021). However, in a goat breed, adding *Ziziphus spina-christi* leaves to the diet enhanced food intake and increased body weight (Ali et al., 2019). Therefore, further studies are needed to confirm the current findings on the effect of *Ziziphus spina-christi* leaf extract on animals' body weight.

Among the limitations of the current study is that the crude extract of the leaves was used. Fractionation of the crude extract and identification of active antimutagenic and anticancer compounds is recommended. In addition, future *in vitro* studies using skin cancer cell lines are needed to confirm the current findings.

Conclusion

Ziziphus spina-christi leaf extract is beneficial for cancer prevention by reducing the mutagenicity of cancer-inducing agents.

Acknowledgment

The authors thank the Scientific Research Funds, Ministry of Higher Education and Scientific Research, Amman, Jordan for funding the current research (MPH/02/07/2012). In addition, the authors thank the Deanship of Research at Jordan University of Science and Technology for its support.

References

- Abduljawad, S.H. 2020. Digestive Fermentation, Antioxidant Status, and Haemato-Biochemical Indices of Growing Rabbits Fed on Diets Supplemented with *Ziziphus spina-christi* Leaf. *J Nutr Metab.* **2020**:9046862.
- Abdulrahman, M.D., A.M. Zakariya, H.A. Hama, S.W. Hamad, S.S. Al-Rawi, S.W. Bradosty, and A.H. Ibrahim. 2022. Ethnopharmacology, Biological Evaluation, and Chemical Composition of *Ziziphus spina-christi* (L.) Desf.: A Review. *Adv Pharmacol Pharm Sci.* **2022**:4495688.
- Ahmed, B., M.I. Qadir, and S. Ghafoor. 2020. Malignant Melanoma: Skin Cancer-Diagnosis, Prevention, and Treatment. *Crit Rev Eukaryot Gene Expr.* **30**(4):291-297.
- Al-Eitan, L.N., K.H. Alzoubi, L.I. Al-Smadi, and O.F. Khabour. 2020. Vitamin E protects against cisplatin-induced genotoxicity in human lymphocytes. *Toxicol In Vitro.* **62**:104672.

- Al Omar, R., R. Micklewright, K. Masud, T. Naz, S. Vemulpad, and J. Jamie. 2022. The genus *Alphitonia* Reissek ex Endl. (Rhamnaceae): A review of its customary uses, phytochemistry and biological activities. *J Ethnopharmacol.* **294**:115168.
- Alajmi, R.A., W.A. Al-Megrin, D. Metwally, H. Al-Subaie, N. Altamrah, A.M. Barakat, A.E. Abdel Moneim, T.T. Al-Otaibi, and M. El-Khadragy. 2019. Anti-Toxoplasma activity of silver nanoparticles green synthesized with *Phoenix dactylifera* and *Ziziphus spina-christi* extracts which inhibits inflammation through liver regulation of cytokines in Balb/c mice. *Biosci Rep.* **39**(5):BSR20190379.
- Albalawi, A.E. 2021. Antileishmanial Activity of *Ziziphus spina-christi* Leaves Extract and Its Possible Cellular Mechanisms. *Microorganisms.* **9**(10):2113.
- Ali, A., F. Tegegne, B. Asmare, and Z. Mekuriaw. 2019. On farm evaluation of sun-dried *Ziziphus spina-christi* leaves substitution for natural pasture hay on feed intake and body weight change of Bati goat breeds in Ethiopia. *Trop Anim Health Prod.* **51**(2):457-463.
- Alkofahi, A.S., K.K. Abdul-Razzak, K.H. Alzoubi, and O.F. Khabour. 2017. Screening of the Anti-hyperglycemic activity of some medicinal plants of Jordan. *Pak J Pharm Sci.* **30**(3):907-913.
- Alkofahi, A.S., K.H. Alzoubi, O.F. Khabour, and N.M. Mhaidat. 2016. Screening of selected medicinal plants from Jordan for their protective properties against oxidative DNA damage. *Ind Crops Prod.* **88**:106-111.
- Almeer, R.S., G. Albasher, R.B. Kassab, S.R. Ibrahim, F. Alotibi, S. Alarifi, D. Ali, S. Alkahtani, and A.E. Abdel Moneim. 2020. *Ziziphus spina-christi* leaf extract attenuates mercury chloride-induced testicular dysfunction in rats. *Environ Sci Pollut Res Int.* **27**(3):3401-3412.
- Almeer, R.S., M.F. El-Khadragy, S. Abdelhabib, and A.E. Abdel Moneim. 2018. *Ziziphus spina-christi* leaf extract ameliorates schistosomiasis liver granuloma, fibrosis, and oxidative stress through downregulation of fibrinogenic signaling in mice. *PLoS One.* **13**(10):e0204923.
- Alqudah, M.A.Y., F.Y. Al-Ashwal, K.H. Alzoubi, M. Alkhatatbeh, and O. Khabour. 2018. Vitamin E protects human lymphocytes from genotoxicity induced by oxaliplatin. *Drug Chem Toxicol.* **41**(3):281-286.
- Alzahrani, A.M., A.A. Alzahrani, and A.A. Alsharm. 2019. The Use of *Ziziphus spina-christi* Extract in Treating Erlotinib (Tarceva®) Associated Rash: A Case Report. *Case Rep Oncol.* **12**(3):909-912.
- Alzoubi, K.H., L. Abdel-Hafiz, O.F. Khabour, T. El-Elimat, M.A. Alzubi, and F.Q. Alali. 2020. Evaluation of the Effect of *Hypericum triquetrifolium* Turra on Memory Impairment Induced by Chronic Psychosocial Stress in Rats: Role of BDNF. *Drug Des Devel Ther.* **14**:5299-5314.
- Alzoubi, K.H., O.F. Khabour, A.S. Alkofahi, N.M. Mhaidat, and A.A. Abu-Siniyeh. 2021. Anticancer and antimutagenic activity of *Silybum marianum* L. and *Eucalyptus camaldulensis* Dehnh. against skin cancer induced by DMBA: In vitro and in vivo models. *Pak J Pharm Sci.* **34**(3).
- Azab, M., O.F. Khabour, K.H. Alzoubi, H. Hawamdeh, M. Quttina, and L. Nassar. 2017. Assessment of genotoxicity of pyrethrin in cultured human lymphocytes. *Drug Chem Toxicol.* **40**(3):251-255.
- Bozicevic, A., M. De Mieri, A. Di Benedetto, F. Gafner, and M. Hamburger. 2017. Dammarane-type saponins from leaves of *Ziziphus spina-christi*. *Phytochem.* **138**:134-144.
- Collins, L., A. Quinn, and T. Stasko. 2019. Skin Cancer and Immunosuppression. *Dermatol Clin.* **37**(1):83-94.
- Daradka, H.M., O.F. Khabour, and M.K. Alotaibi. 2018. Potent antioxidative DNA damage of selected Saudi medicinal plants in cultured human lymphocytes. *Pak J Pharm Sci.* **31**(4(Supplementary)):1511-1517.
- El-Din, M.S., A.M. Taha, A.A. Sayed, and A.M. Salem. 2019. *Ziziphus spina-christi* leaves methanolic extract alleviates diethylnitrosamine-induced hepatocellular carcinoma in rats. *Biochem Cell Biol.* **97**(4):437-445.
- El-Maksoud, A.A.A., A.I.A. Makhlof, A.B. Altemimi, I.H.A. El-Ghany, A. Nassrallah, F. Cacciola, and T.G. Abdelmaksoud. 2021. Nano Milk Protein-Mucilage Complexes: Characterization and Anticancer Effect. *Molecules.* **26**(21).
- El Seedy, G.M., E.S. El-Shafey, and E.S. Elsherbiny. 2021. *Ziziphus spina-christi* (L.) fortified with *Camellia sinensis* mediates apoptosis, Notch-1 signaling, and mitigates obesity-induced non-alcoholic fatty liver. *J Food Biochem*:e13849.
- Elghaffar, R.Y.A., B.H. Amin, A.H. Hashem, and A.E. Sehim. 2022. Promising Endophytic *Alternaria alternata* from Leaves of *Ziziphus spina-christi*: Phytochemical Analyses, Antimicrobial and Antioxidant Activities. *Appl Biochem Biotechnol.* **194**(9):3984-4001.
- Fahmy, M.A., A.A. Farghaly, E.E. Hassan, E.M. Hassan, Z.M. Hassan, K. Mahmoud, and E.A. Omara. 2022. Evaluation of the Anti-Cancer/Anti-Mutagenic Efficiency of *Lavandula officinalis* Essential Oil. *Asian Pac J Cancer Prev.* **23**(4):1215-1222.
- Farmani, F., M. Moein, A. Amanzadeh, H.M. Kandelous, Z. Ehsanpour, and M. Salimi. 2016. Antiproliferative Evaluation and Apoptosis Induction in MCF- 7 Cells by *Ziziphus spina christi* Leaf Extracts. *Asian Pac J Cancer Prev.* **17**(1):315-321.
- Ghaffari, K., R. Ahmadi, B. Saberi, and P. Moulavi. 2021. Antiproliferative effects of *Ziziphus spina-christi* and *Phlomis russeliana* leaf extracts on HEK293 and MCF-7 Cell Lines and Evaluation of Bax and Bcl-2 Genes Expression Level in MCF-7 Cells. *Asian Pac J Cancer Prev.* **22**(S1):81-87.
- Ghosh, S., S. Sikdar, A. Mukherjee, and A.R. Khuda-Bukhsh. 2015. Evaluation of chemopreventive potentials of ethanolic extract of *Ruta graveolens* against A375 skin melanoma cells in vitro and induced skin cancer in mice in vivo. *J Integr Med.* **13**(1):34-44.
- Gopalakrishnan, T., S. Ganapathy, V. Veeran, and N. Namasivayam. 2019. Preventive effect of D-carvone during DMBA induced mouse skin tumorigenesis by modulating xenobiotic metabolism and induction of apoptotic events. *Biomed Pharmacother.* **111**:178-187.
- Guizani, N., M.I. Waly, V. Singh, and M.S. Rahman. 2013. *Nabag* (*Ziziphus spina-christi*) extract prevents aberrant crypt foci development in colons of azoxymethane-treated rats by abrogating oxidative stress and inducing apoptosis. *Asian Pac J Cancer Prev.* **14**(9):5031-5035.
- Hendawi, E.K., O.F. Khabour, L.N. Al-Eitan, and K.H. Alzoubi. 2022. Reduction of Genotoxicity of Carbamazepine to Human Lymphocytes by Pre-Treatment with Vitamin B12. *Curr Mol Pharmacol.*
- Hosny, M., A.S. Eltaweil, M. Mostafa, Y.A. El-Badry, E.E. Hussein, A.M. Omer, and M. Fawzy. 2022. Facile Synthesis of Gold Nanoparticles for Anticancer, Antioxidant Applications, and Photocatalytic Degradation of Toxic Organic Pollutants. *ACS Omega.* **7**(3):3121-3133.
- Hussein, A.S. 2019. *Ziziphus spina-christi*: Analysis of bioactivities and chemical composition. In *Wild Fruits: Composition, Nutritional Value and Products*. Springer. 175-197.
- Jafarian, A., B. Zolfaghari, and K. Shirani. 2014. Cytotoxicity of different extracts of arial parts of *Ziziphus spina-christi* on Hela and MDA-MB-468 tumor cells. *Adv Biomed Res.* **3**:38.

- Kadioglu, O., S. Jacob, S. Bohnert, J. Naß, M.E. Saeed, H. Khalid, I. Merfort, E. Thines, T. Pommerening, and T. Efferth. 2016. Evaluating ancient Egyptian prescriptions today: Anti-inflammatory activity of *Ziziphus spina-christi*. *Phytomed.* **23**(3):293-306.
- Khabour, O.F., O.A. Soudah, and M.H. Aaysh. 2013. Genotoxicity assessment in iron deficiency anemia patients using sister chromatid exchanges and chromosomal aberrations assays. *Mutat Res.* **750**(1-2):72-76.
- Lalotra, A.S., V. Singh, B. Khurana, S. Agrawal, S. Shrestha, and D. Arora. 2020. A Comprehensive Review on Nanotechnology-Based Innovations in Topical Drug Delivery for the Treatment of Skin Cancer. *Curr Pharm Des.* **26**(44):5720-5731.
- Li, H., and C. Brakebusch. 2021. Analyzing skin tumor development in mice by the DMBA/TPA model. *Methods Cell Biol.* **163**:113-121.
- Nageen, B., A. Rasul, G. Hussain, M.A. Shah, H. Anwar, S.M. Hussain, M.S. Uddin, I. Sarfraz, A. Riaz, and Z. Selamoglu. 2021. Jaceosidin: A Natural Flavone with Versatile Pharmacological and Biological Activities. *Curr Pharm Des.* **27**(4):456-466.
- Rababa'h, A.M., O.F. Khabour, K.H. Alzoubi, D. Al-Momani, and M. Ababneh. 2019. Assessment of Genotoxicity of Levosimendan in Human Cultured Lymphocytes. *Curr Mol Pharmacol.* **12**(2):160-165.
- Ramadan, S.S., R.S. Almeer, S. Alkahtani, S. Alarifi, G. Albasher, and A.E. Abdel Moneim. 2021. *Ziziphus spina-christi* leaf extract attenuates mercuric chloride-induced liver injury in male rats via inhibition of oxidative damage. *Environ Sci Pollut Res Int.* **28**(14):17482-17494.
- Roemer, E., T.H. Ottmueller, H.J. Urban, and C. Baillet-Mignard. 2010. SKH-1 mouse skin painting: a short-term assay to evaluate the tumorigenic activity of cigarette smoke condensate. *Toxicol Lett.* **192**(2):155-161.
- Safdari, M.R., F. Shakeri, A. Mohammadi, B. Bibak, P. Alesheikh, T. Jamialahmadi, T. Sathyapalan, and A. Sahebkar. 2021. Role of Herbal Medicines in the Management of Brain Injury. *Adv Exp Med Biol.* **1328**:287-305.
- Sajadimajd, S., R. Bahramsoltani, A. Iranpanah, J. Kumar Patra, G. Das, S. Gouda, R. Rahimi, E. Rezaeihamiri, H. Cao, F. Giampieri, M. Battino, R. Tundis, M.G. Campos, M.H. Farzaei, and J. Xiao. 2020. Advances on Natural Polyphenols as Anticancer Agents for Skin Cancer. *Pharmacol Res.* **151**:104584.
- Sakna, S.T., A. Mocan, H.N. Sultani, N.M. El-Fiky, L.A. Wessjohann, and M.A. Farag. 2019. Metabolites profiling of *Ziziphus* leaf taxa via UHPLC/PDA/ESI-MS in relation to their biological activities. *Food Chem.* **293**:233-246.
- Sanders, K., Z. Moran, Z. Shi, R. Paul, and H. Greenlee. 2016. Natural Products for Cancer Prevention: Clinical Update 2016. *Semin Oncol Nurs.* **32**(3):215-240.
- Sauter, E.R. 2020. Cancer prevention and treatment using combination therapy with natural compounds. *Expert Rev Clin Pharmacol.* **13**(3):265-285.
- Soliman, S., A.M. Hamoda, A.A. El-Shorbagi, and A.A. El-Keblawy. 2019. Novel betulin derivative is responsible for the anticancer folk use of *Ziziphus spina-christi* from the hot environmental habitat of UAE. *J Ethnopharmacol.* **231**:403-408.
- Tarboush, N.A., D.H. Almomani, O.F. Khabour, and M.I. Azzam. 2022. Genotoxicity of Glyphosate on Cultured Human Lymphocytes. *Int J Toxicol.* **41**(2):126-131.
- Torre, L.A., R.L. Siegel, E.M. Ward, and A. Jemal. 2016. Global Cancer Incidence and Mortality Rates and Trends--An Update. *Cancer Epidemiol Biomarkers Prev.* **25**(1):16-27.
- Yagoub, A.E.A., G.M. Alshammari, P. Subash-Babu, M.A.A. Mohammed, M.A. Yahya, and A.I. Alhosain. 2021. Synthesis of *Ziziphus spina-christi* (Jujube) Root Methanol Extract Loaded Functionalized Silver Nanoparticle (ZS-Ag-NPs); Physiochemical Characterization and Effect of ZS-Ag-NPs on Adipocyte Maturation, Adipokine and Vascular Smooth Muscle Cell Interaction. *Nanomaterials (Basel).* **11**(10): 2563.
- Zandiehvakili, G., and A. Khadivi. 2021. Identification of the promising *Ziziphus spina-christi* (L.) Willd. genotypes using pomological and chemical proprieties. *Food Sci Nutr.* **9**(10):5698-5711.

Induced Toxicity and Bioaccumulation of Chromium (VI) in Cluster Bean: Oxidative Stress, Antioxidative Protection Strategy, Accumulation and Translocation of Certain Nutrient

Kamlesh Kumar Tiwari^{1,*}, Manoj Kumar Bidhar¹, Naveen Kumar Singh²

¹Sophisticated Instrumentation Centre for Applied Research and Testing (SICART), Sardar Patel Centre for Science and Technology,

Vallabh Vidyanagar, Anand- 388120 (Gujarat), India; ²Department of Chemistry, Environmental Science Discipline

Manipal University Jaipur- 303007 (Rajasthan), India

Received: September 14, 2022; Revised: November 3, 2022; Accepted: December 2, 2022

Abstract

(Language note by the journal's language editor: the whole manuscript should be checked for accurate use of active and passive sentence structures!!!!)

The present investigation was carried out to examine the noticeable phytotoxicity symptoms, growth behavior, metabolic changes, sulfur, phosphorus, iron, chromium translocation and accumulation in the cluster bean (*Cyamopsis tetragonoloba* L.) plants under different concentration of Cr (VI) treatment. Initially plants were grown after sowing of seeds for 90 d with supplying essential nutrients solution. On the day 91 after plant growth, Cr treatment was given as potassium dichromate at 0.05 mM, 0.25 mM and 0.50 mM concentration along with a set of control (0.00 mM Cr). At 0.5 mM of Cr (VI), visual toxicity symptoms were noticed 8-9 days after exposure expressed as loss of turgor, old as well as central leaves became chlorotic, wilted and reductions in leaf dimension. Later phases of toxicity symptoms appear on newly young upper leaves followed by chlorosis and necrosis in patches at subsequent stages. After 15 days of Cr exposure, toxicity symptoms showed at lower levels (0.25 mM) with decreased leaf area, RWC, biomass, yield, concentration of chlorophyll, non-reducing sugar, protein nitrogen, total nitrogen, starch, protein, hill activity, glutathione reductase and non-protein thiol; however, the concentration of reducing sugar, total sugar, non-protein nitrogen, catalase activity, peroxidase, ribonuclease, acid phosphatase, proline and lipid peroxidation increased in the Cr treated plants. Excess levels of Cr concentration resulted in reduction of iron (Fe) accumulation in the leaves from 497 to 176 $\mu\text{g/g dw}$ along with sulfur (S) and phosphorus (P) translocation significantly at 0.50 mM Cr concentration. Maximum Cr accumulation recorded in the roots ($197 \mu\text{g g}^{-1} \text{ dw}$) and leaves ($142 \mu\text{g g}^{-1} \text{ dw}$) and minimum in the shoots ($69 \mu\text{g g}^{-1} \text{ dw}$) at higher concentration of Cr (0.50 mM) and 30 days of treatment duration. The present study concludes that uptake and accumulation of Cr at higher concentration affect the plant growth, metabolic processes, translocation of essential nutrients, crop yield and may lead to health hazards.

Keywords : Chromium; Phytotoxicity; RWC; Glutathione reductase; Non protein thiol

1. Introduction

The chromium (Cr) is a metal known for its toxic effects due to its detrimental effects on living organisms including human beings and persistent nature in the soil and water for a long time once contaminated (Kapoor et al., 2022). Cr (VI) and Cr (III) are more stable among several chromium oxidation state (Shanker et al., 2005), and hexavalent chromium causes more toxicity in the living being as compared to trivalent chromium due to its more reactivity and mobility (Cervantes et al., 2001; Von Handorf et al., 2021). Cr has been listed as one of the 14 most dangerous substances due to its toxic and detrimental effects on plants and other organisms (EPA 2000).

Chromium (Cr) in trace amount required in animals including human beings for certain metabolism (Mertz 1969), however, no known biological role reported in the plant metabolism (Reale et al., 2016). Presence of chromium in water bodies is largely due to discharge of industrial effluent particularly from tanneries (Nriagu, 1988) and electroplating industries. On average, 2000–3200 tons of Cr beings discharged in the aquatic environment by tanneries effluent annually in India (Chandra et al., 1997). Discharge of more Cr in the water and soil leads to serious health concern through environmental and food chain contamination (Dube et al., 2003; Ahmed et al., 2016; Singh et al., 2021).

Effects of chromium in relation to phytotoxicity have been investigated by Tiwari et al., (2008; 2009; 2013) on

* Corresponding author. e-mail: drkktiwari14@rediffmail.com; kkt@sicart.res.in.

The author K.K. Tiwari and N.K. Singh contributed equally to the paper.

***Abbreviations :** Cr Chromium, Cr (VI) Hexavalent chromium, RWC Relative Water Content, d Days

important crop plants due to its uptake from soil, water and subsequent accumulation in the plant tissues. Cr has detrimental impacts on the plant's growth due to imbalances in nutrients uptake and metabolic processes due to its competing uptake with other essential elements having similar structure and absorption pathway. Also, Cr uptake in plants leads to formation of more reactive oxygen species (ROS) due to oxidative damage of plant tissues, ultrastructural changes in the chloroplast, cell membrane and subsequent phytotoxicity (Sharma et al., 2020a). Phytotoxicity leads to retarded growth of plants, seed germination inhibition, degradation of photosynthetic pigments, nutrient imbalances, and oxidative injuries (Panda et al., 2003; Tiwari et al., 2009; Tiwari et al., 2013). Trivalent chromium (Cr III) treatment induces stunted growth and phytotoxicity with smaller leaves, wilting and chlorosis (Chatterjee and Chatterjee 2000). Similarly, Cr induced biochemical changes and enzyme activities in the crop plant under different concentrations leads to chlorosis and necrosis of leaves (Dube et al., 2003).

Cr effects nutrients and water uptake in plants leads to reduction in cell division, reduced translocation of essential elements, decrease uptake of selective inorganic nutrients, increase in generation of reactive radicals and oxidative stress, essential nutrients substitution with ligands and other key molecules, damage to plant tissues and organelles including chloroplasts, mitochondria and nucleic acids (Cervantes et al., 2001; Shanker et al., 2005; Tiwari et al., 2013). Although Cr induced stress may be alleviated by activities of antioxidants, it is more susceptible to Cr toxicity in plants at higher concentration (Dong et al., 2007). Toxicity of Cr basically depends on the oxidation state, mobility in rhizosphere, uptake, translocation, and accumulation in the plant tissues. Cr (VI) follows the same pathway of active transport for plant uptake as other anions like sulphate (Cervantes et al., 2001). Iron (Fe), Sulfur (S) and phosphorus (P) compete with chromium for binding sites of carriers (Wallace et al., 1976). Micronutrient deficiencies in different crops were reported from agricultural fields irrigated with tannery effluent (Sujatha and Gupta 1996; Broadway et al., 2010). Present study was undertaken to evaluate tolerance level of Cr (VI), visual toxicity symptoms, physiological and metabolic changes, nutrient uptake and translocation in the plant, cluster bean at different concentration of Cr (VI) exposures under sand pot culture growth condition.

2. Materials and Methods

2.1. Sand pot culture experimental setup

The plant Cluster bean (*Cyamopsis tetragonoloba* L) cv. Agaita Guara-112 grown in pre-washed sand as per procedure of Hewitt (1966) with slight modification (Agarwala and Chatterjee 1996) to maintain ambient temperature optimum ($25^{\circ}\text{--}30^{\circ}\text{C}$) under glasshouse-controlled condition for Indian climatic condition. Polyethylene made containers with 10 L size having a hole at center used to grow plants having roofed with a reversed watch glass and glass wool. Nutrient solution was prepared (control) with a composition of 4m MKNO_3 (Potassium nitrate), 4 mM $\text{Ca}(\text{NO}_3)_2$ (Calcium nitrate), 2 mM MgSO_4 (Magnesium sulfate), 1.33 mM NaH_2PO_4 (Sodium

dihydrogen phosphate), 100 μM Fe EDTA (Ferric Ethylene Diamine Tetra Acetic Acid), 10 μM MnSO_4 (Manganese sulfate), 30 μM H_3BO_3 (Boric Acid), 1 μM CuSO_4 (Copper sulphate), 1 μM ZnSO_4 (Zinc sulphate), 0.2 MNa_2MoO_4 (Sodium molybdate), 0.1 μM CaSO_4 (Calcium sulfate), 0.1 μM NiSO_4 (Nickel sulphate) and 0.1 Mm NaCl (Sodium chloride). Concentration of iron in the nutrient solution is maintained with Fe EDTA (Ferric ethylene diamine tetra acetic acid) chelate as per the recommendation of Jacobson (1951) and pH maintained to 6.8 ± 0.2 in the prepared nutrient solution during the entire treatment duration.

2.2. Plant growth and chromium treatment

Based on the growth condition, life cycle of test plant and assessed phytotoxic parameters under treatment of Cr (VI), plants were initially grown for 90 d along with complete nutrient solution after sowing of planting seeds in the pots to acclimatize and achieve uniform growth under sand culture experimental condition. Prepared nutrient solution was supplied on regular basis during the experiment duration except in case flushing of pots with deionized water removing the roots exudates and settled salts. After acclimatization under normal growth sand culture conditions, on the day 91, pots were kept in a group of three pots and three lots along with one lot to serve as the control, in which no Cr was added. In the remaining lots, Cr (VI) was supplied at 0.05, 0.25, 0.50 mM concentration superimposed along with base nutrient solutions. Nutrient solution was supplied to plant pots every day on a regular basis except during the removal of salts and other substances from the sand culture medium by flushing with deionized water. Visible phytotoxic symptoms and other phytotoxic parameters of Cr treatment were observed continuously for 30 d after Cr exposures with short treatment duration to complete the study before the achieving maturity stage of the test plant. Plant pots were regularly monitored and maintained under sand culture growth condition for 120 days throughout during the Cr treatment experiment.

2.3. Measurement of growth parameters and biochemical analysis

Cr induced effects on growth behavior, metabolic changes, imbalances in uptake and translocation of sulphur, phosphorus, iron and chromium were studied in detail in the present investigation. On 106 d (16 d of chromium treatment), the Relative Water Content (RWC) was analyzed in the analogous middle leaves as per procedure of Barrs and Weatherley (1962) during between 9.00 and 11.00 AM under waterlogged sand with nutrient solution in the pots. Temperature (Ambient) was recorded between $25\text{--}30^{\circ}\text{C}$ along with atmospheric humidity at the range of 65-75%. As an index of plant growth, leaf area (cm^2) deliberated by Delta-T leaf area dimension system was measured at d 16 after Cr treatment. At d 107 (17 d after Cr treatment), mature young leaves were harvested from the plants and processed with crude leaf extract for determination of chlorophyll (a, b and total) and Hill activity, sugars and starch content, nitrogen and phenol concentration, and enzyme activities (peroxidase, catalase, ribonuclease, and acid phosphatase), lipid peroxidation, proline, non-protein thiol and soluble protein by following the prescribed standard procedures. Chlorophyll a, b and

total content were determined in the leaves extracted from harvested fresh leaves by crushing in 80% acetone by following the procedure of Arnon (1949). Similarly, Hill activity was determined at 620 nm by using calorimeter with reaction of 2,4,6-Dichlorophenol Indo Phenol (DCPIP) and determined changes in optical density (O.D./10 min/100mg fw) by following the method of Brewer and Jogendorf 1965. Reducing, non-reducing and total sugar concentration in tested plants was determined by the method of Nelson (1944). Starch concentration was measured as per the method prescribed by Montgomery (1957). Nitrogen fraction was analyzed as per the method given by Chibnall et al. (1943). Phenols content is analyzed by using the method of Swain and Hillis (1959). *Enzymatic activities* of peroxidase, catalase, ribonuclease, and *acid phosphatase* were determined in the harvested fresh leaves extract after homogenizing leaf sample in the ice-cold glass distilled water (1:10) and grinding with help of pestle and mortar at 4°C. Peroxidase and catalase activity was assayed by the method of Luck (1963) and Bisht et al. (1989), respectively. Similarly, ribonuclease was assayed by the method of Tuve and Anfinsen (1960) and acid phosphatase by method of Schmidt (1955). Lipid peroxidation is determined in terms of malondialdehyde (MDA) content in the leaves by the reaction of Thiobarbituric Acid (TBA) as described by Heath and Packer, 1968. Proline content was determined by following the method of Bates *et al.*, 1973. Glutathione reductase was determined in the leaves extract by following the procedure of Smith *et al.*, 1988. Non protein thiol (NP-SH) and soluble protein were determined in leave homogenate precipitated in TCA following the method of Boyer (1954) and Bradford (1976) using bovine serum albumin (BSA) as standard, respectively.

2.4. Estimation of iron and chromium

At 120 d of growth (30 d after Cr treatment), Cluster Bean plants are harvested for analysis of tissue. Harvested treated plant samples, washed with tap water, were wiped with 0.01 N HCl and rinsed with deionized water then roots, shoots and leaves were separated, chopped, and kept in a forced-draught oven at 70°C for complete dryness. *For analysis of Fe and Cr, harvested dried plant sample was digested in a mixture of HClO₄: HNO₃ (1:4 v/v), up to dryness (Piper, 1942) to get clear digests samples and then diluted with distilled water (milli-Q grade) for estimation of iron and chromium using ICP-OES (Optima 3300 RL).*

2.5. Quality control and assurance

For quality control and quality assurance, the instrumental techniques and standard calibration reference materials of Cr (EPA, quality control samples from E-Merck, Germany) used, and for Iron (BND, 1101.02) from National Physical Laboratory (NPL), India used. Analytical data quality of the tested element was ensured by multiple analysis (n=5) of standard reference samples and data established about ±2.01% of certified value. Blanks were taken in triplicate for all sets of samples to ensure accuracy of the method with the detection limit of chromium (0.5 ppb) and iron (0.3 ppb). Mean resurgence was observed around 98 and 96 for chromium and iron, respectively.

2.6. Analysis of data

Experiment conducted in a randomized block design and all measurements were conducted in triplicate and twice. *All data was analyzed for two-way analysis of variance (ANOVA) to measure significance between treatments and to ensure variability and validity of results.* Standard deviation of the means was calculated and given along with the mean according to the method of Panse and Sukhatme (1954).

3. Results

3.1. Periodic observation of phytotoxic symptoms

To investigate Cr induced phytotoxicity, the plants of cluster bean grown under refined sand pot culture condition with Cr (VI) treatment at different concentration (0.05, 0.25, 0.50 mM) along with a set of control. The sand culture technique was very useful for specific symptoms-based study, plant nutrition, plant-metal interaction, plant physiology and plant biochemistry study of a single or mixed metal treatment under controlled conditions as it provides better growth conditions as soil without any interference of other elements. Phytotoxic effects of chromium treatment in the treated plants were observed in terms of grain yield production up to the maturity stage. After d 8 of Cr treatment, toxicity symptoms were observed as chlorosis on the middle leaves followed by wilting at 0.25 mM and 0.50 mM Cr of treatment. On 10th d of Cr treatment, older leaves changed into golden yellow color with reduced number and small size followed by chlorosis intensification and severe necrosis in subsequent days and formed large necrotic areas. Further after a few days, chlorotic leaves observed were permanently dried and wilted leading to leaf fall. Similarly, the next upper young leaf showed the same pattern of toxicity spread over a large area. After 15-16 d of Cr treatment, chlorosis symptoms are relatively delayed in the leaves of plants grown at low concentration of Cr.

3.2. Growth Responses of cluster bean under Cr treatment

Growth responses of cluster bean plant under chromium treatment in terms of biomass production, leaf area index and relative water content (RWC), grain yield are given in the Table 1. In the present study, dry biomass of cluster bean is recorded to decrease with increased chromium in the growth medium (Nutrient solution) from 0.05 mM to 0.50 mM. At 0.5 mM Cr (VI) concentration, and after 120 days of maturity, significant reduction (76.9%) in biomass was observed as comparison to the control plants. In term of grain yield, pods produced only in the pots treated with 0.05 mM and 0.25 mM Cr (VI), pods were not produced at higher level (0.50 mM). Similarly, grain weight decreased considerably from 0.05 mM and 0.25 mM of Cr treatment which was more pronounced at 0.25 mM Cr (VI) in comparison to control plant. Seed size and shape were found abnormal with more deformed and shriveled seed in plants treated with higher Cr concentration with reduction grain yield (85.94%) at 0.25 mM of Cr (VI) concentration. At d 118 (28 d after metal exposure), leaf area of cluster beans observed decrease with increasing Cr (VI) concentration in the solution in comparison to control plants and recorded a

depression of 55.58% in the plants treated with 0.50 mM of Cr (VI). Similarly, relative water content (RWC) was observed to decrease gradually in leaves with increasing Cr concentration as compared to control plants which showed a decrease of 4.26%, 42.9% and 60.3% at

0.05mM, 0.1 mM and 0.25mM Cr concentration, respectively. Biomass reduction in Cr treated cluster beans may be due to profound loss of moisture content and tissue damage.

Table 1. Effect of variable chromium exposure on biomass, grain yield, leaf area and relative water content of cluster bean plants.

Days of growth	Days after metal supply		mM chromium treatment				LSD (P=0.05)
			Control	0.05	0.25	0.50	
120	30	Biomass: g plant ⁻¹	28.52 ±1.80	21.75 ±1.03	10.46 ±0.48	6.58 ±0.21	0.81
120	30	Grains: g plant ⁻¹	9.75 ±0.14	5.21 ±0.11	1.37 ±0.01	-	0.27
118	28	Leaf area: cm ²	93.15 ±4.72	77.24 ±3.84	58.12 ±2.93	41.37 ±1.89	2.75
106	16	RWC: %	96.28 ±5.63	92.17 ±4.05	54.96 ±2.42	38.18 ±0.94	3.51

Values are means ± SE (n=5).

3.3. Chlorophyll content and biochemical changes in cluster bean

Effects of Cr treatment on the photosynthetic pigment and biochemical changes in the cluster bean under different concentrations of Cr (VI) are shown in Table 2. In the present study, concentration of chlorophyll total, a and b decreased variably and manifestly with increase of Cr (VI) concentration in the solution supplied to the treated plant. However, decrease in content of photosynthetic pigment in leaves of the cluster bean observed more at 0.25 mM and 0.50 mM of Cr treatment with 53.09 % reduction in total chlorophyll in comparison

to control plant. Decrease in chlorophyll content might be due to inhibition of chlorophyll biosynthesis enzymes or lipid peroxidation of chloroplast membrane by ROS exposed with high concentration of Cr (VI) treatment. Carotene content in fresh leaves of cluster bean plant recorded decreased with increasing concentration of Cr (VI) in the solution. Highest decline was observed at 0.50 mM treatment by 82.09%. Similarly, reducing sugars content was recorded appreciably in higher order. Compared to control leaves, Cr treated plants showed higher reducing sugars with increasing Cr (VI) concentration.

Table 2. Variable chromium exposure on concentration of chlorophyll, carbohydrate fraction, starch, nitrogen and phenol in leaves of cluster bean leaves (at d 107; 17 d after metal exposure).

Parameters	mM chromium treatment				LSD (P=0.05)
	Control	0.05	0.25	0.5	
Chlorophyll: mg g ⁻¹ fresh wt					
A	0.985 ±0.06	0.639 ±0.04	0.418 ±0.42	0.356 ±0.02	0.07
B	0.518 ±0.05	0.347 ±0.03	0.287 ±0.03	0.175 ±0.02	0.03
Total	1.503 ±0.13	0.986 ±0.11	0.705 ±0.09	0.531 ±0.03	0.09
Carotene (mg g ⁻¹ fw)	4.86±0.23	4.12±0.27	2.27±0.15	0.87±0.08	0.03
Sugars: % fresh weight					
Reducing	0.27 ±0.02	0.34 ±0.02	0.41 ±0.03	0.49 ±0.04	0.04
Non reducing	0.08 ±0.01	0.07 ±0.01	0.05 ±0.01	0.03 ±0.01	0.01
Total sugars	0.31± 0.02	0.45 ±0.03	0.49 ±0.05	0.49 ±0.04	0.03
Nitrogen: % fresh weight					
protein nitrogen	1.131 ±0.13	0.927± 0.12	0.655± 0.10	0.572± 0.06	0.08
non protein nitrogen	0.253± 0.01	0.288 ±0.02	0.396 ±0.04	0.465 ±0.03	0.04
total nitrogen	1.384 ±0.15	1.215 ±0.12	1.051 ±0.11	1.037 ±0.07	0.07
Starch: % fresh weight	1.175 ±0.13	0.962 ±0.11	0.537 ±0.07	0.381 ±0.02	0.06
Phenols: % fresh weight	0.002± 0.001	0.004± 0.001	0.005±0.001	0.007± 0.001	0.001

Values are mean ±SE (n=5).

In the same trend, total sugars content also increased gradually with increasing chromium in the treatment solution. In contrast, Cr treated plants showed a declining trend of non-reducing sugars with increasing concentration of Cr in the medium. Concentration of protein N decreased with an increasing Cr (VI) level in the nutrient medium, however, the value of non- protein N was recorded with increasing order as compared to non- treated plant. In case of total nitrogen content, a decreasing trend is observed

with increasing Cr concentration in comparison to control plant. The starch content decreased in the Cr (VI) treated plants and a maximum 67.57% reduction was recorded in the plant grown at 0.50 mM of chromium treatment. In the present study phenols level was found to increase with Cr (VI) concentration in the medium in cluster bean plants in comparison to non-treated plants and observed increase by 47% at higher Cr (VI) concentration (0.50 mM).

3.4. Protein content and antioxidant enzyme activities in cluster bean

In the present study, data of protein contents and antioxidant enzyme activities in the plant cluster bean under Cr (VI) treatment in the sand culture condition were quite evident (Fig.1). Results indicate that Cr (VI) treatment affects protein content which was observed to decrease gradually with increasing Cr (VI) concentration in the growth medium and maximum 32.2% and 47.9% reduction observed in the plants grown at 0.25mM and 0.50 mM of Cr (VI) treatment. At d 107 (17 d of treatment), catalase activity was found to decrease with

differential Cr (VI) concentration in treated plants. In contrast, peroxidase activity at the same treatment duration and concentration of Cr (VI) is recorded to increase in treated plants as compared to control plants. Excess treatment of Cr at 0.25 mM resulted in slight decrease of ribonuclease activity; however, the activity further increased gradually up to 0.50 mM. The present study showed an increasing trend of activity of acid phosphatase at 0.05mM to 0.50 mM of Cr treatment. Hill activity in fresh leaves of cluster beans was observed to decrease with increased Cr (VI) concentrations.

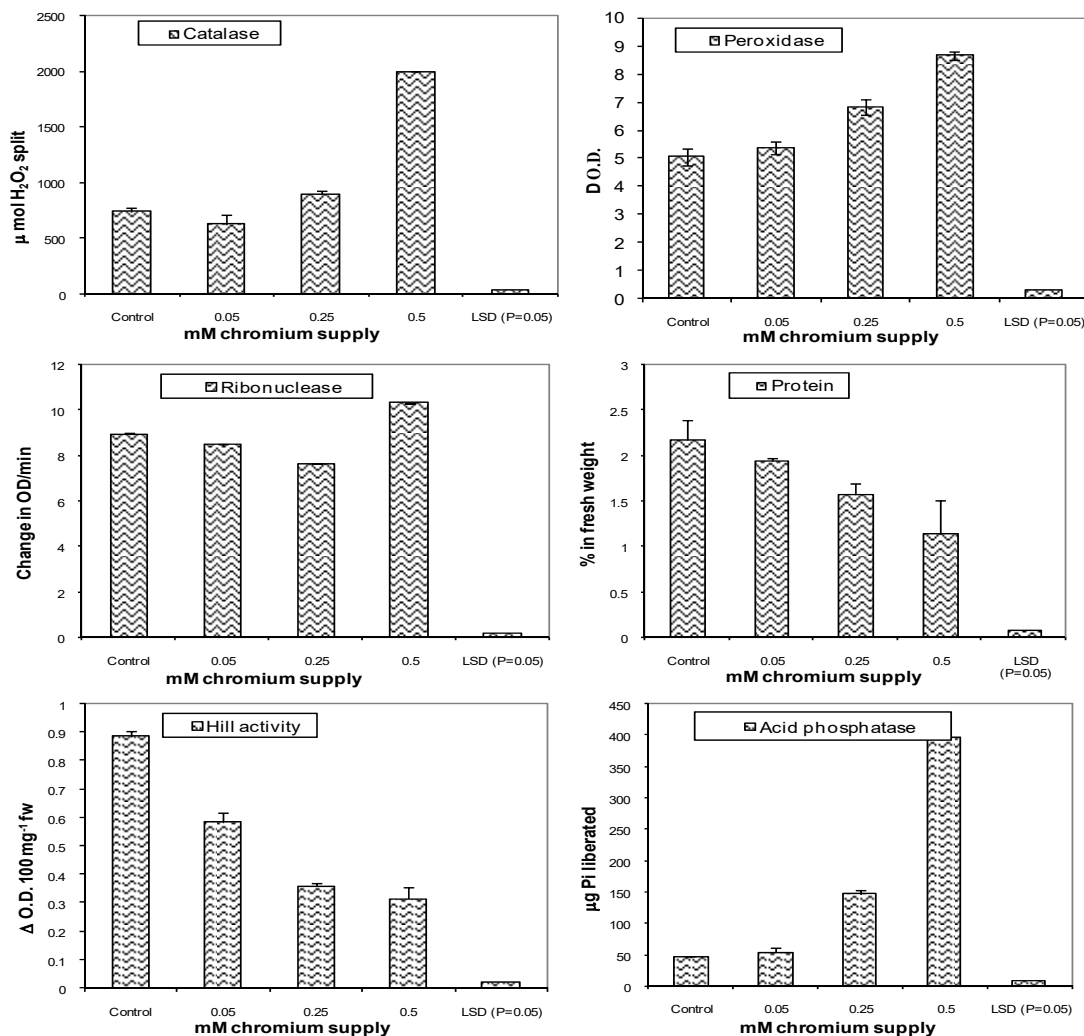


Figure 1. Variable chromium treatment and activities of enzymes, catalase, peroxidase, ribonuclease; hill reaction, acid phosphatase and protein concentration in leaves of cluster beans at 107 d (after 17 days of metal treatment). Values are means \pm SE (n=5)

3.5. Proline, glutathione reductase, non-protein thiol and lipid peroxidation

Proline content, activities of glutathione reductase, lipid peroxidation and non-protein thiol (NP-SH) in the leaves of cluster beans under different chromium treatment are depicted in Table 3. The present investigation data showed changes in proline content at higher concentration of chromium and increasing trend observed with Cr (VI)

concentration in the nutrient solution. However, activity of glutathione reductase in the Cr treated cluster bean is observed to decrease with increasing Cr concentration. At d 107 (17 days of metal supply), the activity of lipid peroxidation increased with increasing level of Cr (VI) from 0.05mM to 0.50 mM, as Cr generates induced phytotoxic results in the plant of cluster beans. The activity of non-protein thiol (NPSH) was found to decrease with excess of Cr (VI) supply in the growth medium.

Table 3. Variable chromium exposure on proline, glutathione reductase and lipid peroxidation and Non protein thiol in the Cluster Bean plant leaves (at d 107; 17 d after metal exposure).

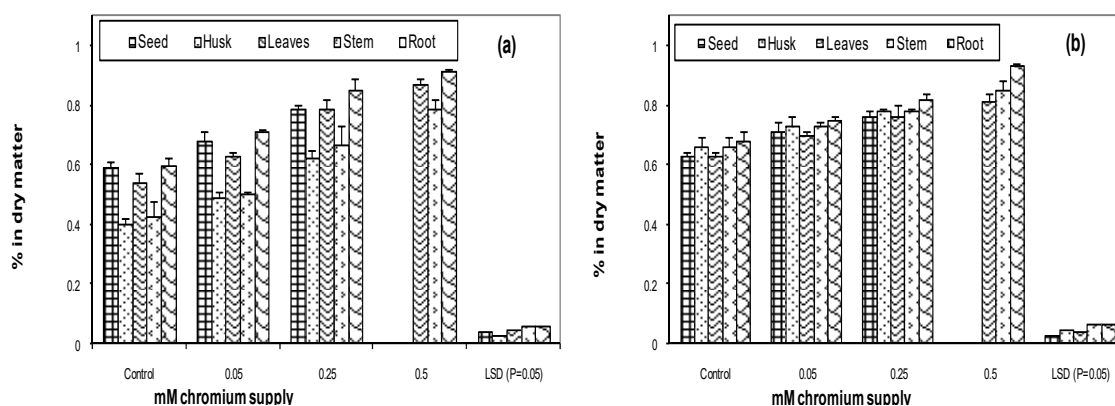
Parameters	mM chromium treatment				LSD (P=0.05)
	Control	0.05	0.25	0.5	
Proline ($\mu\text{g g}^{-1}\text{fw}$)	0.79 \pm 0.06	1.32 \pm 0.09	2.05 \pm 0.11	3.14 \pm 0.15	0.05
Glutathione reductase (GR) (unit/ min/ mg/ protein)	1.29 \pm 0.08	1.17 \pm 0.06	1.12 \pm 0.07	0.92 \pm 0.04	0.03
Lipid Peroxidation ($\mu\text{g g}^{-1}\text{fw}$)	26.74 \pm 2.75	33.62 \pm 3.18	39.54 \pm 2.54	51.21 \pm 4.71	0.09
Non protein thiol (NPSH) ($\mu\text{g g}^{-1}\text{fw}$)	98.61 \pm 4.82	91.53 \pm 3.86	72.19 \pm 4.19	57.42 \pm 3.07	0.07

Values are mean \pm SE (n=5).

3.6. Phosphorus, sulfur, iron and chromium concentration in cluster bean

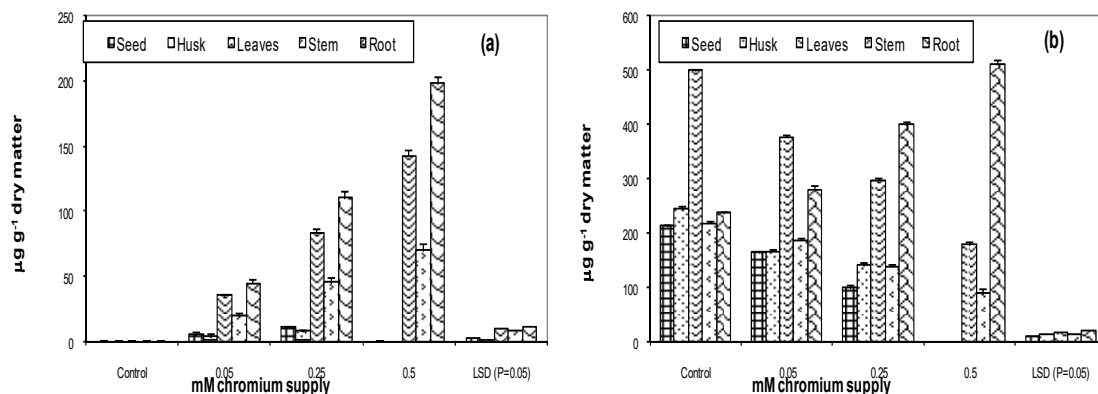
Translocation of phosphorus (P) and sulfur(S) from roots to other parts of the cluster beans is affected by higher concentration of Cr (VI) treatment. At higher

concentration of Cr, the plant cluster bean showed higher concentration of P and S in different plant parts as compared to the control plant; however, analytical results showed more accumulation of P and S considerably in the roots (Fig 2).

**Figure 2.** Variable chromium treatment and S (a) and P (b) uptake and accumulation in different parts of the plant of cluster beans at 120 d growth (after 30 days of chromium exposure). Values are means \pm SE (n=5)

Higher concentration of Cr (VI) treatment resulted in less accumulation of iron in the upper portion of the plant including stem, leaves, husk and seed and more accumulation in the roots (Fig 3). Chromium accumulation in different parts of cluster bean plants varied with response to Cr (VI) concentration in the medium (Fig 3) and roots, shoots, leaves and other parts of the tested plants. Maximum Cr accumulation observed in the roots,

followed by leaves at higher concentration of Cr treatment (0.50 mM). Cr induced toxicity as resulted in reduction of economic yields in terms of seed quality and quantity observed in the present study. High concentration of Cr ranged from 44 to 197 $\mu\text{g/g dw}$ recorded in the roots, however, least accumulation of Cr in the shoots observed with a range from 49 to 69 $\mu\text{g/g dw}$ at different concentration of Cr(VI) treatment.

**Figure 3:** Variable chromium supply and accumulation of chromium (a) and iron (b) in different parts of the plant of cluster beans at 120 d growth (after 30 days of chromium exposure). Values are means \pm SE (n=5)

4. Discussion

Various symptoms of phytotoxicity were observed in the plant cluster beans grown under different concentrations of Cr (VI) initially as chlorosis on middle leaves and subsequently, wilting of affected leaves appeared and finally leaf fall at higher concentration (0.25mM and 0.50 mM). The color of middle leaves of tested plants started to change from green to golden yellow in the Cr treated plant. Smaller size and lower number of leaves were observed in the Cr treated plants with severe chlorosis and necrosis in successive days of the treatment. Later, necrotic patches were spread with large areas over the entire leaves followed by wilted dry permanently and premature leaf fall. However, chlorosis observed delayed in the plants grown comparatively at low concentration of Cr treatment even after 15 d. The symptoms of high concentration Cr in cluster bean plants are new insight in ecotoxicological studies and more resemble as reported by Dube et al. (2003). Tiwari et al. (2013) reported on radish plants and recommend that the Cr may generate induced phytotoxic symptoms, reduction in leaf development, growth depression and changes in several biochemical activities as common characteristics under Cr stress. Cr treated plants showed reduced growth with gradual decrease of biomass of cluster bean at 0.05 mM to 0.50 mM concentration. Similar observation reported by many investigators with conclusion that Cr (VI) induces toxicity in the plants by effecting physiological and biochemical processes leading to reduced crop yield (Tiwari et al., 2009; Tiwari et al., 2013; Eleftheriou et al., 2015). In our finding, the crop yields produced only at 0.05 mM and 0.25 mM Cr (VI) treatment level; however, abnormal and deformed size and shape of seed observed with a noticeable reduction in grain yield in cluster beans under Cr treatment. Plant yield is reliant on leaf growth and leaf area; in our present observation the depression in leaf area is observed in treated plants at 0.50 mM as compared to control plants. Many studies examined the Cr and its interaction with plant growth and reported that Cr impedes plant growth, leaf development and yield production while going beyond the threshold levels (Arun et al., 2005; Tiwari et al., 2009). Reduced RWC observed at higher concentration of Cr (VI) treatment with respect to control plants. Reduction in the fresh biomass of cluster bean recorded due to loss of water as apparent from the low RWC of the leaves of plants resulted in wilting. Higher concentration of Cr (VI) exhibited lower water potential and relative water content which in agreement with the observation of Rauser and Dumbroff (1981). The extensively high levels of Cr (VI) exposures cause moribund the stomatal conductance might be owing to the higher oxidative ability of Cr (VI) in the nutrient medium, which in turn might be active in hurtful of the cells and membrane of stomatal protector cells.

Decreasing trends of concentration of chlorophyll content a, b and total in the leaves of cluster bean under Cr (VI) treatment observed, which indicates reduction in the photosynthetic synthesis under Cr treatment as compared to non-treated control plants. Reduction of chlorophyll content may be due to interference of chlorophyll biosynthesis (Lushchak, 2011; Sharma et al., 2020b; Guanet al., 2021), changes in the chloroplastic structure or

due to Cr (VI) competes with Mg at functional site of the porphyrin ring (Mengel and Kirkby, 2001). Similarly, carotene content was also found to decrease as compared with control plants which support comparable observations reported previously (Mondal et al., 2013; Mondal et al., 2015). Concentration of reducing sugars and total sugars in cluster bean plant leaves was appreciably recorded in higher order with increasing Cr (VI) supply; however, non-reducing sugars concentration recorded declining. Similarly, no significant effects of Cr on non-reducing sugars were reported (Agarwala et al., 1977); however, reducing sugars content was found to increase with Cr(VI) concentration in the growth solution. Increase in reducing sugars due to reduction in the vein and inhibition of photoassimilate export with more sugar accumulation (Rauser and Samarkoon, 1980). Reduction in protein nitrogen, total N and increase in non-protein N concentration in cluster bean leaves recorded in the Cr treated plant in comparison to the control plant. Sharma et al. (1995) reported that Cr affects nitrogen accumulation and absorption which is apparent in decline in protein N content in leaves of wheat plant as N is constituent element of protein as well as core element in the different biomolecules. In cluster bean leaves starch content is also found to decrease under different concentrations of Cr (VI) treatment. Similar observation of reduction in biosynthesis of starch was reported in citrullus plant (Tiwari et al., 2008). The concentration of phenols increased in cluster bean plant at 0.50 mM of Cr treatment as compared to control plants which related to previous study reported by Tewari et al. (2001) and reported same trend of increasing phenols level could be due to fast diffusion of H₂O₂ in the cytosol or due to accretion of high phenols and lower protein formation under Cr stress. The content of protein gradually decreased with increasing Cr (VI) concentration in the growth medium. Chatterjee and Chatterjee (2000) reported the reduced plant biomass in cauliflower might be due to low protein synthesis under stress of Cr, Co and Cu. Degradation of protein can also result in the inhibition of activity of nitrate reductase (Solomonson and Barber, 1990; Nazet al., 2021). In cluster bean leaves, the catalase activity was found to significantly decrease in Cr (VI) treated plants, and the observation agreed with the conclusion of Adrees et al. (2015). Catalase might be more susceptible to excess levels of Cr (VI) since it binds willingly to thiol groups and thereby inactivates the thiol-containing enzyme. The efficiency of catalase as an H₂O₂ scavenger is lowered; therefore, it would not play a significant role as an antioxidant (Luna et al., 1994). In cluster bean plant leaves, the activity of peroxidase is observed to increase with an increase in concentration of Cr (VI) in the growth medium. Peroxidase is an enzyme which catalyzes reduction of H₂O₂ into H₂O; however, ascorbate restricts the reduction of H₂O₂ (Luna et al., 1994; Tiwari et al., 2008; Shahid et al., 2016). In cluster bean plant leaves, treatment of Cr up to 0.25 mM reduced ribonuclease activity; however, further increased activity expressed at 0.50 mM of Cr treatment. Enhancement of ribonuclease activity contradicts with the earlier finding (Strakhov and Chazova, 1981) in the plant grapevines. However, some other findings by Tiwari et al. (2013) reported the enhanced ribonuclease activity and acid phosphatase activity seems similar as per our observation. This may be owing to reduced protein synthesis or uptake

of inorganic phosphorus (Marschner, 1995). In our present observation, the hill activity in cluster bean plant was found to decrease with increasing Cr concentration in the medium. Reduced chlorophyll content owing to chromium stress has an impact on the Hill activity in the tested plant. Krupa and Baszynski (1995) investigated that the Cr can also inhibit the Hill reaction disturbing together light and dark reaction. Proline content showed an increasing trend with increase of Cr (VI) concentration in the nutrient solution. Similarly, high levels of amino acids such as cysteine and enhanced synthesis of proline have been observed at high concentration of chromium (Vajpayee et al., 2001) and support other studies suggesting only proline accumulates in the plants grown under metal stress among other amino acids (Zdunek-Zastocka et al., 2021). In comparison to the non-treated plant, glutathione activity of reductase is recorded to decrease in the cluster bean due under higher concentration of Cr (VI). Cr (VI) treatment also affected antioxidant enzymes and inhibited activities of glutathione reductase (GR), catalase and peroxidase (Adrees et al., 2015; Ali et al., 2015). In cluster bean leaves, the activity of lipid peroxidation increased from 0.05 mM to 0.50 mM of Cr (VI). Various studies reported increased ROS generation in plants under Cr stress resulted in damage of DNA, pigments, proteins, lipids and initiate the process peroxidation of lipid leads to oxidative burst (Choudhury et al., 2005; Ullah et al., 2009). Similarly, lipid peroxidation and enhanced proline were reported in radish plants under Cr (VI) treatment (Azmat and Akhter 2010). Non-protein thiol (NPSH) activity decreased due to excess amount of Cr in nutrient solution. Cysteine, proline, nonprotein thiol acts as non-enzymatic antioxidants and assist in modulating tolerance under Cr toxicity to protect biomolecules from the free radicals generated during the oxidative stress (Hayat et al., 2012).

In plants, Cr (VI) treatment affects nutrient uptake by interfering uptake of essential nutrients. In excess Cr treatment resulted in increased phosphorus (P) and Sulphur (S) content in various plant parts of cluster bean. However, nutrients element accumulated more significantly in the roots and translocation of P and S from roots to shoot and leaves of plants affected by chromium treatment. Findings of Dube et al. (2003) indicated that high concentration of Cr affects translocation of P, S and other essential nutrients in the Citrullus plants. It is observed that high concentration of Cr (VI) treatment resulted in a decrease accumulation of iron in shoots and increase in the roots. Chlorosis due to Cr treatment has been normally associated with lower plant Fe mobilization and uptake from root to leaves via stems. In iron deficient conditions, leguminous plants enhance root Fe (III) reductase activity to increase the efficiency to reduce Fe (III) to Fe (II), which is more bioavailable and accumulates in the roots (Alcantara et al., 1994). It is also suggested that the excess levels Cr disturbs the nutrient uptake stability from the nutrient sources (Tiwari et al., 2009). This might specify poor utilization of vital nutrients due to Cr toxicity. Translocation and accumulation of Cr in different parts of cluster bean plant from the nutrient solution indicate tolerance responses, which somewhat coincides with an earlier study (Dube et al., 2003; Aoet al., 2022) and showed variable uptake and accumulation of Cr roots, shoot and leaves of plant. Our findings are in consonance

with the other studied conducted by Huffman and Allaway (1973) who recommended that the mobilization of chromium from roots to shoot and leaves is poor as Cr remains restricted in root.

5. Conclusion

In the present investigation chromium (VI) induced phytotoxicity emphasized in cluster beans with visible symptoms, inhibition of plant growth, reduction of biomass and yield quality. Cr (VI) stress involves particularly with plant metabolism through uptake, translocation, interference in enzymatic activities, and competing essential nutrients on binding sites. It is also concluded that the tolerance limit of Cr (VI) for cluster bean plant was monitored by 0.25 mM level of treatment along with essential nutrient solutions, above which the behind limit plant does not sustain the induced toxicity generated by Cr. Consequently, it is vital to understand the potential strategies to restrict Cr uptake and accumulation in edible parts of crop plants from contaminated sites and to minimize related detrimental effects in the other living beings due to Cr contamination. Further, physiological and biochemical aspects of Cr (VI) toxicity have not been as much considered for study on intact plants in detail. This might lead us to conclude that uptake of Cr from the contaminated agriculture field-grown crop plants may lead to serious health hazards and risk to environmental safety. Importance of present studies could be a new insight in ecotoxicological studies in assessing possible environmental concerns of chromium contamination and ensuring safe and sustainable agriculture.

Acknowledgements

Authors greatly acknowledge Sophisticated Instrumentation Centre for Applied Research & Testing, Vallabh Vidyanagar for utilization of sophisticated analytical instrumentation facility used for the present investigation. The author NKS is thankful to the Manipal University Jaipur for essential support and continuous encouragement.

Conflicts of interest

The authors declares no conflict of interests in this manuscript.

References

- Adrees M, Ali S, Iqbal M, Bharwana SA, Siddiqi Z, Farid M, Ali Q, Saeed R and Rizwan M. 2015. Mannitol alleviates chromium toxicity in wheat plants in relation to growth, yield, stimulation of anti-oxidative enzymes, oxidative stress and Cr uptake in sand and soil media. *Ecotoxicol Environ Saf.*, **122**: 1-8.
- Agarwala SC and Chatterjee C. 1996. Techniques in micronutrient research. In: Hemantranjan E (Ed), **Advancements in Micronutrients Research**. Scientific Publishers, Jodhpur, India, pp. 401-453.
- Agarwala SC, Bisht SS and Sharma CP. 1977. Relative effectiveness of certain heavy metals in producing toxicity and symptoms of iron deficiency in barley. *Can J Bot.*, **55**: 1299-1307.

- Ahmed F, Hossain M, Abdulla, AT, Akbor M and Ahsan M. 2016. Public health risk assessment of chromium intake from vegetable grown in the wastewater irrigated site in Bangladesh. *Pollution*, **2**: 425-432.
- Alcantara E, Romera FJ, Canete M and De la Guardia MD. 1994. Effects of heavy metals on both induction and function of root Fe (III) reductase in Fe-deficient cucumber (*Cucumis sativus* L.) plants. *J Exp Bot.*, **45**: 1983-1998.
- Ali S, Chaudhary A, Rizwan M, Anwar HT, Adrees M, Farid M, Irshad MK, Hayat T and Anjum SA. 2015. Alleviation of chromium toxicity by glycinebetaine related to elevated antioxidant enzymes and suppressed chromium uptake and oxidative stress in wheat (*Triticum aestivum* L.). *Environ Sci Pollut Res.*, **22**: 10669-10678.
- Ao M, Chen X, Deng T, Sun S, Tang Y, Morel JL, Qiu R and Wang S. 2022. Chromium biogeochemical behavior in soil-plant systems and remediation strategies: A critical review. *J Hazard Mater.*, **424**: 127233.
- Arnon DI. 1949. Copper enzyme in isolated chloroplasts. Polyphenol oxidase in *Beta vulgaris*. *Plant Physiol* 24:1-15.
- Arun KS, Cervantes C, Herminia LT and Avudainayagam D. 2005. Chromium toxicity in plants. *Environ Int.*, **31**: 739-753.
- Azmat R and Akhter H. 2010. Changes in some biophysical and biochemical parameters of mung bean (*Vigna radiata* L) Wilczek grown on chromium-contaminated soil treated with solid tea wastage. *Pak J Bot.*, **42**: 3065-3071.
- Barrs HD and Weatherley PE. 1962. A reexamination of the relative turgidity technique for estimating water deficits in leaves. *Aust J Biol Sci.*, **15**: 413-428.
- Bates LS, Waldren RP and Thomas CE. 1973. Rapid determination of free proline for water stress studies. *Plant Soil.*, **39**: 205-207.
- Bisht SS, Sharma D and Chaturvedi K. 1989. Certain metabolic lesions of chromium toxicity in radish. *Indian J Agri Biochem.*, **2**: 109-115.
- Boyer PD. 1954. Spectrophotometric Study of the Reaction of Protein Sulfhydryl Groups with Organic Mercurials. *J Amer Chem Soc.*, **76**: 4331.
- Bradford MN. 1976. A rapid and sensitive method for the quantitation of microgram quantities of protein utilizing the principle of protein-dye binding. *Anal Biochem.*, **72**: 248-254.
- Brewer J and Jogendorf AT. 1965. Damage to spinach chloroplast induced by dark preincubation with ferricyanide. *Plant Physiol.*, **40**: 303-311.
- Broadway A, Cave MR, Wragg J, Fordyce FM, Bewley RJ, Graham MC, Ngwenya BT and Farmer JG. 2010. Determination of the bioaccessibility of chromium in Glasgow soil and the implications for human health risk assessment. *Sci Total Environ.*, **409**: 267-277.
- Cervantes C, Garcia JC, Devars S, Corona FG, Tavera HL and Torres-Guzman JC. 2001. Interactions of chromium with microorganisms and plants. *FEMS Microbiol Rev.*, **25**: 335-347.
- Chandra P, Sinha S and Rai UN. 1997. Bioremediation of Cr from water and soil by vascular aquatic plants. In: Kruger EL, Anderson TA, Coats JR (Eds), **Phytoremediation of soil and water contaminants**. ACS Symposium Series 664. American Chemical Society, Washington, DC, pp. 274-282.
- Chatterjee J and Chatterjee C. 2000. Phytotoxicity of cobalt, chromium and copper in cauliflower. *Environ Pollut.*, **109**: 69-74.
- Chibnall AC, Rees MW and Williams EF. 1943. The total nitrogen content of egg albumin and other proteins. *Biochem J.*, **37**: 354-359.
- Choudhury S and Panda SK. 2005. Toxic effects, oxidative stress and ultrastructural changes in moss *Taxithelium nepalense* (Schwaegr.) Broth. under chromium and lead phytotoxicity. *Water Air Soil Pollut.*, **167**: 73-90.
- Dong J, Wu F, Huang R and Zang G. 2007. A Chromium tolerant plant growing in Cr-contaminated land. *Int J. of Phytoremedia.*, **9**: 167-179.
- Dube BK, Tewari K., Chatterjee J and Chatterjee C. 2003. Excess chromium alters uptake and translocation of certain nutrients in *citrullus*. *Chemosphere.*, **53**: 1147-1153.
- Eleftheriou EP, Adamakis IDS, Panteris E and Fatsiou M. 2015. Chromium-induced ultrastructural changes and oxidative stress in roots of *Arabidopsis thaliana*. *Int J Mol Sci.*, **16**: 15852-15871.
- EPA (Environmental Protection Agency). 2000. Effluent Limitations Guidelines, Pretreatment Standards, and New Source Performance Standards for the Commercial Hazardous Waste Combustor Subcategory of the Waste Combustors Point Source Category. *Fed Regist* 4360-4385.
- Guan X, Li Q, Maimaiti T, Lan S, Ouyang P, Ouyang B, Wu X and Yang ST. 2021. Toxicity and photosynthetic inhibition of metal-organic framework MOF-199 to pea seedlings. *J Hazard Mater.*, **409**: 124521.
- Hayat S, Khalique G, Irfan M, Wani AS, Tripathi BN and Ahmad A. 2012. Physiological changes induced by chromium stress in plants: An overview. *Protoplasma.*, **249**: 599-611.
- Heath RL and Packer L. 1968. Photoperoxidation in isolated chloroplasts. I. Kinetics and stoichiometry of fatty acid peroxidation. *Arch Biochem Biophys.*, **125**: 189-198.
- Hewitt EJ. 1966. Sand and water culture methods used in the Study of Plant Nutrition, Technical Communication 22. Commonwealth Agricultural Bureau, London.
- Huffman EWD and Allaway WH. 1973. Chromium in plants: distribution in tissues, organelles and extracts and availability of bean leaf chromium to animals. *J Agric Chem.*, **21**: 982-986.
- Jacobson L. 1951. Maintenance of iron supply in nutrient solutions by a single addition of ferric potassium ethylenediamine tetra acetate. *Plant Physiol.*, **26**: 411-413.
- Kapoor RT, Bani Mfarrej MF, Alam P, Rinklebe J and Ahmad P. 2022. Accumulation of chromium in plants and its repercussion in animals and humans. *Environ Pollut.*, **301**: 119044.
- Krupa Z. and Baszynski T. 1995. Some aspects of heavy metals toxicity towards photosynthetic apparatus-direct and indirect effects on light and dark reactions. *Acta Physiol Plant.*, **17**: 177-190.
- Luck H. 1963. Peroxidase. In: Hill B (Ed), **Methods in enzymatic analysis**. Academic, New York, pp. 895-897.
- Luna CM, Gonzalez CA and Trippi VS. 1994. Oxidative damage caused by an excess of copper in oat leaves. *Plant Cell Physiol.*, **35**: 11-15.
- Lushchak VI. 2011. Adaptive response to oxidative stress: Bacteria, fungi, plants and animals. *Comp Biochem Physiol C Toxicol Pharmacol.*, **153**: 175-90.
- Marschner H. 1995. **Mineral nutrition of higher plants**. Academic Press, New York.
- Mengel K and Kirkby EA. 2001. Elements with more toxic effects. In: Mengel, K., Kirkby, E.A., Kosegarten, H., Appel, T. (Eds), **Principles of plant nutrition**, Kluwer Academic Publishers, London, pp. 656-670.
- Mertz W. 1969. Chromium occurrence and functions in biological systems. *Physiol Rev.*, **49**: 163-239.

- Mondal NK, Das C and Datta JK. 2015. Effect of mercury on seedling growth, nodulation and ultrastructural deformation of *Vigna radiata* (L) Wilczek. *Environ Monit Assess.*, **187**: 1-14.
- Mondal NK, Das C, Roy S, Datta JK and Banerjee A. 2013. Effect of varying cadmium stress on chickpea (*Cicer Arietinum* L) seedlings: an Ultrastructural study. *Ann Environ Sci.*, **7**: 59-70.
- Montgomery R. 1957. Determination of glycogen. *Arch BiochemBiophys.*, **67**: 378-386.
- Naz R, Sarfraz A, Anwar Z, Yasmin H, Nosheen A, Keyani R, Roberts TH. 2021. Combined ability of salicylic acid and spermidine to mitigate the individual and interactive effects of drought and chromium stress in maize (*Zea mays* L.). *Plant PhysiolBiochem.*, **159**: 285-300.
- Nelson N. 1944. Photometric adaptation of Somogyi method for determination of glucose. *J Biol Chem.*, **153**: 375-380.
- Nriagu JO. 1988. Production and uses of chromium. In: NriaguJO, Nieboer E. (Eds), **Chromium in natural and human environment**. John Wiley and Sons, pp. 81-105.
- Panda SK, Chaudhury I and Khan MH. 2003. Heavy metals induce lipid peroxidation and affects antioxidants in wheat leaves. *Biol Plant.*, **46**: 289-294.
- Panse VG and Sukhatme PV. 1954. **Statistical Methods for Agriculture Workers**. ICAR, New Delhi.
- Piper CS. 1942. **Soil and plant analysis**. Monograph. Waite Agricultural Research Institute, The University, Adelaide, Australia.
- Rauser WE and Dumbroff EB. 1981. Effect of excess cobalt, nickel and zinc on the water relations of *Phaseolus vulgaris*. *Environ Expt Bot.*, **21**: 249-255.
- Rauser WE and Samarukoon AB. 1980. Vein loading in seedlings of *Phaseolus vulgaris* exposed to excess cobalt, nickel and zinc. *Plant Physiol.*, **65**: 578-583.
- Reale L, Ferranti F, Mantilacci S, Corboli M, Aversa S, Landucci F, Baldisserotto C, Ferroni L, Pancaldi S and Venanzoni R., 2016. Cyto-histological and morpho-physiological responses of common duckweed (*Lemna minor* L.) to chromium. *Chemosphere.*, **145**: 98-105.
- Schmidt, G. 1955. Acid prostatic phosphatase, In: Colowick N. and Kaplan O. (Eds.), **Methods in enzymology**, Academic Press, New York, 2: pp. 523-530.
- Shahid M, Dumat C, Khalid S, Niazi NK and Antunes PMC. 2016. Cadmium Bioavailability, Uptake, Toxicity and Detoxification in Soil-plant System. *Rev Environ ContamToxicol.*, **239**:1-65.
- Shanker AK, Cervantes C and Loza-Tavera H. 2005. Chromium toxicity in plants. *Environ Inter***31**: 739-753.
- Sharma A, Wang J, Xu D, Tao S, Chong S, Yan D, Li Z, Yuan H and Zheng B. 2020b. Melatonin regulates the functional components of photosynthesis, antioxidant system, gene expression, and metabolic pathways to induce drought resistance in grafted *Carya cathayensis* plants. *Sci Total Environ.*, **713**: 136675.
- Sharma A, Kapoor D, Wang J, Shahzad B, Kumar V, Bali AS, Jasrotia S, Zheng B, Yuan H and Yan D. 2020a. Chromium bioaccumulation and Its Impacts on Plants: An Overview. *Plants.*, **9**: 1-17.
- Sharma DC, Chatterjee C and Sharma CP. 1995. Chromium accumulation and its effect on wheat (*Triticum aestivum* L. cv. HD 2004) metabolism. *Plant Science.*, **111**: 145-151.
- Singh P, Itankar N and Patil Y. 2021. Biomangement of hexavalent chromium: Current trends and promising perspectives. *J Environ Manage.*, **279**: 111547.
- Smith IK, Vierhellaer TL and Thorne CA. 1988. Assay of glutathione reductase in crude tissue homogenates using 5,5-dithiobis (2-nitrobenzoic acid). *Anal Biochem.*, **175**: 408-413.
- Solomonson LP and Barbar MJ. 1990. Assimilatory nitrate reductase: functional properties and regulation. *Ann Rev Plant Mol Biol.*, **41**: 225-253.
- Strakhov VG and Chazova TP. 1981. Effect of chromium, molybdenum and tungsten on grapevine quality. *Sodovod Vinograd. Vinodel Mold.*, **36**: 58-60.
- Sujatha P and Gupta A. 1996. Tannery effluent characteristics and its effects on agriculture. *J Ecotoxicol Environ Monit.*, **6**: 45-48.
- Swain T and Hillis WE. 1959. The phenolic constituent of *Prunus domestica*. The qualitative analysis of phenolic constituents. *J Sci Food Agri.*, **10**: 63-68.
- Tewari RK, Kumar P, Sharma PN and Bisht SS. 2002. Modulation of oxidative stress responsive enzymes by excess cobalt. *Plant Science.*, **162**: 381-388.
- Tiwari KK, Dube BK, Sinha P and Chatterjee C. 2008. Phytotoxic effects of high chromium on oxidative stress and metabolic changes in *Citrullus*. *Ind J Horticult.*, **65**: 171-175
- Tiwari KK, Dwivedi S, Singh NK, Rai UN and Tripathi RD. 2009. Chromium (VI) induced phytotoxicity and oxidative stress in pea (*Pisum sativum* L.): Biochemical changes and translocation of essential nutrients. *J Environ Biol.*, **30**: 389-394.
- Tiwari KK, Singh NK and Rai UN. 2013. Chromium Phytotoxicity in Radish (*Raphanus sativus*): Effects on Metabolism and Nutrient Uptake. *Bull Environ Contam Toxicol.*, **91**: 339-344.
- Tuve TV and Anfinsen CB. 1960. Preparation and properties of spinach ribonuclease. *J Biol Chem.*, **235**: 3437-3441.
- Ullah A, Shahzad B, Tanveer M, Nadeem F, Sharma A, Lee DJ and Rehman A. 2019. Abiotic Stress Tolerance in Plants Through Pre-sowing Seed Treatments with Mineral Elements and Growth Regulators. In: Hasanuzzaman M, Fotopoulos V (Eds), **Priming and Pretreatment of Seeds and Seedlings: Implication in Plant Stress Tolerance and Enhancing Productivity in Crop Plants**; Springer, Singapore pp. 427-445.
- Vajpayee P, Rai UN, Ali M, Tripathi RD, Yadav V, Sinha S and Singh SN. 2001. Chromium-Induced Physiologic Changes in *Vallisneria spiralis* L. and Its Role in Phytoremediation of Tannery Effluent. *Bull Environ Contam Toxicol.*, **67**: 246-256.
- VonHandorf A, Zablon HA and Puga A. 2021. Hexavalent chromium disrupts chromatin architecture. *Semin Cancer Biol.*, **76**: 54-60.
- Wallace A, Soufi SM, Cha JW and Romney EM. 1976. Some effects of chromium toxicity on bush bean plants grown in soil. *Plant Soil.*, **44**: 471-473.
- Zdunek-Zastocka E, Grabowska A, Michniewska B and Orzechowski S. 2021. Proline Concentration and Its Metabolism Are Regulated in a Leaf Age Dependent Manner But Not by Absciscic Acid in Pea Plants Exposed to Cadmium Stress. *Cells.* **10**: 946.

Antifungal and Antiamoebic Activities, Cytotoxicity, and Toxicity of Aqueous and Ethanolic Extracts of Propolis Produced by Brunei Stingless Bees

Nadzirah Zullkiflee¹, Fatimah Hashim², Hussein Taha³, Anwar Usman^{1,*}

¹Department of Chemistry, Faculty of Science, Universiti Brunei Darussalam, Jalan Tungku Link, Gadong BE1410, Brunei Darussalam;

²Faculty of Science and Marine Environment, Universiti Malaysia Terengganu, 21030 Kuala Terengganu, Terengganu, Malaysia;

³Environmental and Life Sciences, Faculty of Science, Universiti Brunei Darussalam, Jalan Tungku Link, Gadong BE1410 Brunei Darussalam

Received: September 28, 2022; Revised: December 2, 2022; Accepted: December 6, 2022

Abstract

Antifungal activities of aqueous and ethanolic extracts of propolis produced by three different stingless bee species, namely *Heterotrigona itama*, *Geniotrigona thoracica*, and *Tetrigona binghami*, found in Brunei, against *Candida albicans* and *Saccharomyces cerevisiae* strains were evaluated. It was found that aqueous extract of the propolis displayed significant activities against the two fungal strains, whereas the antifungal activity of ethanolic extracts was not observed. *T. binghami* propolis had the highest antifungal activity, followed by *G. thoracica* and *H. itama* propolis. The MIC values also indicated that the aqueous extracts (2500–5000 µg/mL) have stronger antifungal activity than the ethanolic extracts (5000–10000 µg/mL), and all the propolis extracts were fungistatic. The brine shrimp nauplii lethality bioassay indicated that the propolis extracts are nontoxic and the cytotoxicity test suggested that the propolis extracts have low anti-amoebic activity against *Acanthamoeba* sp., much lower than that of chlorhexidine. This study revealed the low antifungal and antiamoebic activities of the aqueous and ethanolic propolis extracts from Brunei stingless bees.

Keywords: Propolis, propolis extract, antifungal, *T. binghami*, cytotoxicity, *Acanthamoeba* sp., toxicity

1. Introduction

Over the last few decades, antibiotic resistance in harmful bacteria, fungi, viruses, and parasites has received great attention (Prestinaci et al., 2015). In particular, fungal infections caused by a variety of fungi in our daily environment have become a significant occurrence in humans and are challenging to treat. *Candida* and *Cerevisiae* are some of the most common fungi that affect human health, and overgrowth of these fungi causes a wide variety of mucosal and dermal infections (Cockerill et al., 2012; Nobile and Johnson, 2015; Pappas et al., 2016; Abid et al., 2022). These fungi can also damage internal organs, including the gastrointestinal, respiratory, and urinary tracts (Abid et al., 2022), resulting in high-risk medical conditions, a weakened immune system, and body-wide systemic infections (Patricio et al., 2019). The emerging threat of drug-resistant fungal strains has increased due to the limited amount and efficacy of medical treatments (Wiederhold, 2017; Scorzoni et al., 2017). Therefore, natural products that can reduce the development of virulence factors have been of great interest for effective antifungal treatments (Roemer and Krysan, 2014; Al-Ghamdi et al., 2020; Bendjedid et al., 2022).

Among natural products, propolis, a natural product composed of lipophilic, solid, and resinous substances gathered by bees from various plants and soil combined

with their enzymatic saliva (Marcucci, 1995), has been demonstrated to possess a variety of biological and pharmacological properties, including anticancer, antioxidant, antibacterial, antifungal, anti-inflammatory, and antiseptic activities (Wagh, 2013; Lofty, 2006; Gucwa et al., 2018; Abdullah et al., 2020; Ożarowski et al., 2022; Ibrahim and Alqurashi, 2022; Zullkiflee et al., 2022a). Propolis has been reported to be effective against several fungal strains, including *Candida albicans* and *Saccharomyces cerevisiae*. Propolis originates from different countries such as Brazil, Malaysia, Iran, and Poland, present antifungal properties against several *Candida* and *Saccharomyces* strains (Moghim et al., 2021; Gucwa et al., 2018; Yusoff et al., 2016). In general, the bioactive compounds present in propolis have been attributed to their antifungal activity, including caffeic acid phenethyl esters, caffeic acid, flavanone, pinocembrin, p-coumaric acids, and pinobanksin-3-acetate (Anjum et al., 2019; Rivera-Yañez et al., 2021), which inhibit fungal cell division and DNA replication (Patton et al., 2001). Synergistic effects improve the fungicidal activity of the bioactive compounds present in propolis and reduce the development of resistant strains (Alves et al., 2012; Rivera-Yañez et al., 2021). However, the bioactive compounds of propolis vary depending on the bee species, geographical location, surrounding environment, harvesting season, and botanical species around the bee hive. Therefore, the antifungal activity of propolis

* Corresponding author. e-mail: anwar.usman@ubd.edu.bn (AU).

produced by different bee species and/or found in different geographical origins is still of research interest (Bankova et al., 2014).

In this study, the antifungal activities of aqueous and ethanolic extracts of *Tetrigona binghami*, *Heterotrigona itama*, and *Geniotrigona thoracica* propolis against *Candida albicans* and *Saccharomyces cerevisiae* strains were evaluated. The antifungal properties, including the fungal growth inhibition zone, minimum inhibitory concentration (MIC), and minimum fungicidal concentration (MFC) of the propolis extracts, were respectively evaluated using the agar well diffusion, broth microdilution, and inoculation methods. In addition, the cytotoxicity of the aqueous and ethanolic extracts of propolis produced by three different stingless bee species against *Acanthamoeba* sp. cells was investigated, and the toxicity of the propolis extracts was tested using a brine shrimp (*Artemia salina* L.) larvae lethality bioassay.

2. Materials and methods

2.1. Chemicals and reagents

All chemicals and reagents, including 3-(4,5-dimethylthiazol-2-yl)-2,5-diphenyltetrazolium bromide (MTT), Mueller-Hinton broth (MHB) microbiology, Mueller-Hinton agar (MHA), and ethanol (95%) were obtained from Merck (Darmstadt, Germany), and were used as received.

2.2. Propolis collection and preparation of propolis extracts

The raw *T. binghami*, *H. itama*, and *G. thoracica* propolis in this study were collected in August 2021 from the Tasbee Meliponiculture Farm in Tutong District, Brunei Darussalam. Thus, the propolis of the three stingless bee species used in this study was obtained from the same geographical location, surrounding environment, and botanical species around their hives. The stingless bee farm is situated in a suburban area, which is at least 20 km from active agricultural or industrial sites (Abdullah et al., 2020). The collected propolis was rinsed with distilled water, and dried using a dehumidifier at room temperature for 2–3 weeks. After drying, the propolis was ground into small pieces less than 1 millimeter in size.

The propolis extracts were prepared according to a previously reported procedure (Abdullah et al., 2019). Briefly, small pieces of propolis (5 g) were macerated with 125 mL of distilled aqueous or ethanol and the solutions were placed on a temperature-controlled shaker operating at 150 rpm for 18 h at 37 °C. After vacuum filtration, the filtrate was concentrated using a rotary evaporator, followed by drying under vacuum at 40 °C. The dried propolis extracts were then kept in sample vials and dissolved in the necessary solvent for further experiments, as described below.

2.3. Antifungal assay

Candida albicans (ATCC 10231) and *Saccharomyces cerevisiae* (NCPF 3178) strains were provided by the Department of Biodiversity and Environmental Research, Faculty of Science, Universiti Brunei Darussalam. The strains were regenerated from permanent cultures on a regular basis, according to the Clinical and Laboratory Standards Institute (CLSI) guidelines (Cockerill, 2012).

The antifungal activities of aqueous and ethanolic extracts of *T. binghami*, *H. itama*, and *G. thoracica* propolis against *C. albicans* and *S. cerevisiae* fungal strains were examined using an agar well diffusion test. Here, the fungal strains were prepared by culturing 100 µL of each fungal strain in 5 mL of sterile MHB, which was made by dissolving 19 g MHB in 0.5 L distilled water, and autoclaved at 121 °C for 2 h.

Subsequently, each culture was diluted with MHB, so that the absorbance of the prepared culture at 530 nm was measured to be within 0.08–0.13 OD, to produce a 0.5 McFarland standard culture which contains approximately 1.5×10^6 CFU/mL. The autoclaved MHA solution was added into petri dishes with a diameter of 9 cm and allowed to cool and solidify. A 200 µL of the standardized fungal culture was then uniformly spread over a thin layer of solidified sterile MHA using a sterile glass spreader and dried for a few minutes.

Four wells, each with a diameter of 6 mm, were prepared in Petri dishes. In each well, 40 µL of 80 mg/mL propolis extract in distilled water was added using a micropipette. The petri dishes were then incubated overnight for 48 h at 37 °C, and the diameter of the fungal growth inhibition zone in each well was measured and recorded.

2.4. Minimum inhibitory and fungicidal concentrations

The MIC value representing the lowest concentration of propolis extract to inhibit the growth of incubated *C. albicans* and *S. cerevisiae* fungal strains was evaluated using the broth microdilution method, according to the CLSI guidelines (Cockerill, 2012). Here, a 100 µL of the inoculated fungal cultures was diluted in a sterile MHB (5 mL), incubated for 24 h at 37 °C, and then adjusted to be 0.5 McFarland standard by dilution with MHB with an absorbance of 0.08–0.13 OD at 530 nm, and 0.5 mL of the standardized fungal suspension was further diluted with 74.5 mL of MHB.

On the other hand, 1 mL of each propolis extract (80 mg/mL) was prepared in distilled water, diluted with MHB in the test tube, and vigorously vortexed. By subsequent dilutions with MHB, a series of suspensions of propolis extracts with concentrations of 0.0156, 0.313, 0.625, 1.25, 2.5, 5, 10, 20, and 40 mg/mL were obtained. Finally, 1 mL of the standardized inoculated fungal culture was added into each test tube containing the propolis extract and mixed thoroughly to obtain a final concentration of 5×10^5 CFU/mL. The mixture was then incubated overnight at 37°C.

The MFC value, which is related to the lowest concentration of the propolis extracts showing no visible fungal growth on agar plates, was investigated against *C. albicans* and *S. cerevisiae* fungal strains. The propolis extracts were then swabbed onto the surface of agar plates, using a sterile inoculating loop, and incubated at 37 °C for 48 h. After incubation, the fungal growth on the plates was determined. The concentration of propolis extracts that exhibited no visible fungal growth was considered as the MFC value.

2.5. Cytotoxicity assay

The *in vitro* cytotoxicity of propolis extracts was evaluated against *Acanthamoeba* sp., which was isolated by corneal scraping from patients with keratitis in the

Hospital Kuala Lumpur Isolate, Malaysia. In this sense, protease yeast glucose (PYG) which was prepared by dissolving of protease (3.75 g), yeast extract (3.75 g), and D+ glucose (7.5 g) in 0.5 L of distilled water containing 1.5 mL of page amoeba solution, was used as the culture medium.

The isolated *Acanthamoeba* sp. was then cultured axenically in a T-25 tissue culture flask with 10 mL of PYG media, and was subcultured every four days while being incubated at 30 °C. A 30 µL of propolis extracts dissolved in dimethyl sulfoxide (DMSO) at different concentrations in the range of 35 µg/mL to 4500 µg/mL was mixed with 970 µL of PYG media containing *Acanthamoeba* sp. The mixture was vortexed, and kept in a refrigerator at 4 °C.

Interestingly, various *in vitro* tests have been developed to evaluate the proliferation and viability of *Acanthamoeba* sp. cells. The MTT assay is a common method for colorimetric determination of fungal cell metabolism due to its fast and reliable technique (Hussain et al., 1993). The MTT reagent was utilized to indicate the viability of *Acanthamoeba* cells when treated with the propolis extracts. The MTT assay has several advantages, and has been modified to metabolize the amoeba and other types of cells. Therefore, it is very beneficial to use this method to determine the remained amount of viable *Acanthamoeba* sp. cells following the exposure of cytotoxic agents.

In this study, the cytotoxicity of the propolis extracts was evaluated by determining the 50% inhibitory concentration (IC₅₀) value of *Acanthamoeba* cells based on the MTT assay. The MTT reagent was prepared by dissolving the MTT powder in 1 mL of PBS buffer solution according to the procedure reported by Mosmann (Mosmann, 1983). *Acanthamoeba* cells were first seeded in a 96-well microplate at 1×10⁵ cells/well and incubated at 30 °C for 8 h. After incubation, the culture media was removed and replaced with PYG media containing the prepared propolis extracts at various concentrations ranging from 35 µg/mL to 4500 µg/mL. Chlorohexidine was used as a positive control, whereas sterilized PYG media was used as a negative control. The mixtures were then incubated at 30 °C for 24 h. After incubation, 20 µL of the MTT solution was added to each sample and then incubated at 30 °C for 4 h. The purple-blue formazan crystals were then dissolved in 150 µL DMSO, and the absorbance at 570 nm was detected using a MicroElisa reader (Dynatech MR850).

2.6. Toxicity studies

It is essential to assess the toxicity of propolis extracts to determine whether propolis-derived medicines are safe for consumption. In this sense, the brine shrimp nauplii lethality assay was used to evaluate the toxicity and efficacy of phytochemicals found in most natural products. This test allows the determination of the intrinsic toxicity of propolis and the effects of its overdose.

The toxicity of aqueous and ethanolic propolis extracts was determined using the shrimp lethality bioassay in 12-well plate, according to the procedure reported by Kamyab et al. (Kamyab et al., 2020). Prior to this toxicity test, artificial seawater which was used as a medium in the culture was simulated by preparing a solution of commercial salt at a concentration of 34 g/L in distilled water. The seawater was then poured into a shallow

rectangular container which was divided into two compartments using Styrofoam with several 5 mm holes. The saltwater temperature was maintained at 30 °C. Approximately 3 g of brine shrimp eggs were soaked in a Clorox bleach solution for 5 minutes. The eggs were filtered and rinsed with distilled water for a few minutes, ground using filter paper, and then sprinkled into the larger compartment of the container covered with aluminum foil to protect it from light, while the smaller compartment was left under light. After 24 h, the brine shrimp started to hatch, and the larvae were left to mature for an additional 6 h. Once matured, the brine shrimp larvae (*Artemia nauplii* L.) were collected using a Pasteur pipette and kept in a container before being subjected to the toxicity tests.

Approximately, 0.5 mL of propolis extracts in distilled water and 2 mL of the prepared artificial seawater were mixed in 12-well plates, so that the concentrations of the propolis extracts were 100, 10, 1 and 0.1 mg/mL. In this test, instead of propolis extracts, 0.5 mL of distilled water was used as the negative control. Ten nauplii were transferred to each well of the 12-well plates, and artificial water was added to the wells to make a volume of 5 mL. The final concentrations of the propolis extracts were 10, 1, 0.1 and 0.01 mg/mL. The 12-well plates were then placed under a light source at 25–30 °C. After mixing with the propolis extracts for 24 h, the number of surviving and dead shrimp larvae was counted using a magnifying glass. Finally, the toxicity was represented by the LC₅₀ value which is the lethal concentration that resulted in the death of 50% of the brine shrimp larvae population, and the value of LC₅₀ of more than 1000 ppm suggested that the propolis extract was nontoxic.

2.7. Statistical analysis

All the antifungal, MIC, MFC, antiamoebic activity, cytotoxicity, and toxicity assays of the propolis extracts were performed at least in triplicate or quadruplicate. All collected data were included in the analyses. Statistical analysis, especially the unpaired t-test, was used to compare the significant differences between two means at a significance level of $p < 0.05$. The mean values and standard deviation errors are obtained from the statistical analysis.

3. Results

3.1. Antifungal activities of all propolis extracts

The inhibition zones associated with the antifungal activity of the aqueous and ethanolic extracts of stingless bees *T. binghami*, *H. itama*, and *G. thoracica* propolis against *C. albicans* and *S. cerevisiae* strains are displayed in Table 1. The results suggested that all aqueous extracts of the propolis have large inhibition zones. On the contrary, those of ethanolic extracts of the propolis were not observed. The aqueous extract of *T. binghami* propolis exhibited the strongest antifungal activity against both *C. albicans* and *S. cerevisiae* strains with inhibition zones of 33.0 mm and 29.7 mm, respectively. This was followed by those of *G. thoracica* and *H. itama* propolis with slightly smaller inhibition zones. The diameters of fungal growth inhibition of aqueous extract of *G. thoracica* propolis were 29.0 mm and 23.0 mm tested against *C. albicans* and *S. cerevisiae*, respectively, while the results for *H. itama* were 27.2 mm and 24.7 mm, respectively.

The MIC values of aqueous and ethanolic extracts of *T. binghami*, *H. itama*, and *G. thoracica* propolis are gathered in Table 1. Upon tested against *S. cerevisiae*, all aqueous propolis extracts have an MIC value of 5000 µg/mL, except for that of *G. thoracica* propolis (2500 µg/mL). This finding suggested that the aqueous extracts of propolis tend to be lower compared to ethanolic extracts.

Table 1. The diameters of inhibition zones of all aqueous and ethanolic propolis extracts tested against *C. albicans* and *S. cerevisiae* fungal strains after incubation for 48 h at 37 °C.

Stingless bee species	The diameter of inhibition zone (mm)			
	<i>C. albicans</i>		<i>S. cerevisiae</i>	
	Aqueous extract	Ethanolic extract	Aqueous extract	Ethanolic extract
<i>T. binghami</i>	33.0 ± 1.0	ND	29.7 ± 2.5	ND
<i>H. itama</i>	27.2 ± 1.4	ND	24.7 ± 2.5	ND
<i>G. thoracica</i>	29.0 ± 1.0	ND	23.0 ± 2.0	ND
Stingless bee species	MIC value (µg /mL)			
	Aqueous extract	Ethanolic extract	Aqueous extract	Ethanolic extract
	Aqueous extract	Ethanolic extract	Aqueous extract	Ethanolic extract
<i>T. binghami</i>	5000	>10000	5000	>10000
<i>H. itama</i>	5000	5000	5000	10000
<i>G. thoracica</i>	5000	>10000	2500	>10000

*ND = not detected

In the MFC tests, aqueous and ethanolic extracts of *T. binghami*, *H. itama*, and *G. thoracica* propolis showed fungal inhibition on all agar plates. These results indicated that propolis extracts inhibited fungal growth, suggesting that they were fungistatic rather than fungicidal in nature.

3.2. Cytotoxicity results of propolis extracts

The plots of the percentage of *Acanthamoeba* cell viability at different concentrations of aqueous and ethanolic extracts of *T. binghami*, *H. itama*, and *G.*

These MIC values might suggest that the aqueous extracts of propolis are better antifungal agents, supporting the observation of the fungal growth inhibition zones. However, high MIC values generally indicate that *T. binghami*, *H. itama*, and *G. thoracica* propolis found in Brunei have low antifungal activity.

thoracica propolis, along with chlorhexidine (positive control), are shown in Figure 1. The IC₅₀ values of all the propolis extracts were determined from their respective graphs. It was found that among the propolis extracts, only the aqueous extract of *T. binghami* propolis has the value of IC₅₀ (3635 µg/mL). This IC₅₀ value is much higher than that of chlorhexidine (36.75 µg/mL), suggesting that the efficacy of propolis extracts was very low, i.e. two orders of magnitude lower than that of chlorhexidine.

Table 2. The IC₅₀ values of all aqueous and ethanolic propolis extracts using the MTT assay

Stingless bee species	IC ₅₀ values (µg/mL)		Chlorhexidine
	Aqueous extract	Ethanolic extract	
<i>G. thoracica</i>	ND	ND	36.75
<i>H. itama</i>	ND	ND	
<i>T. binghami</i>	3635	ND	

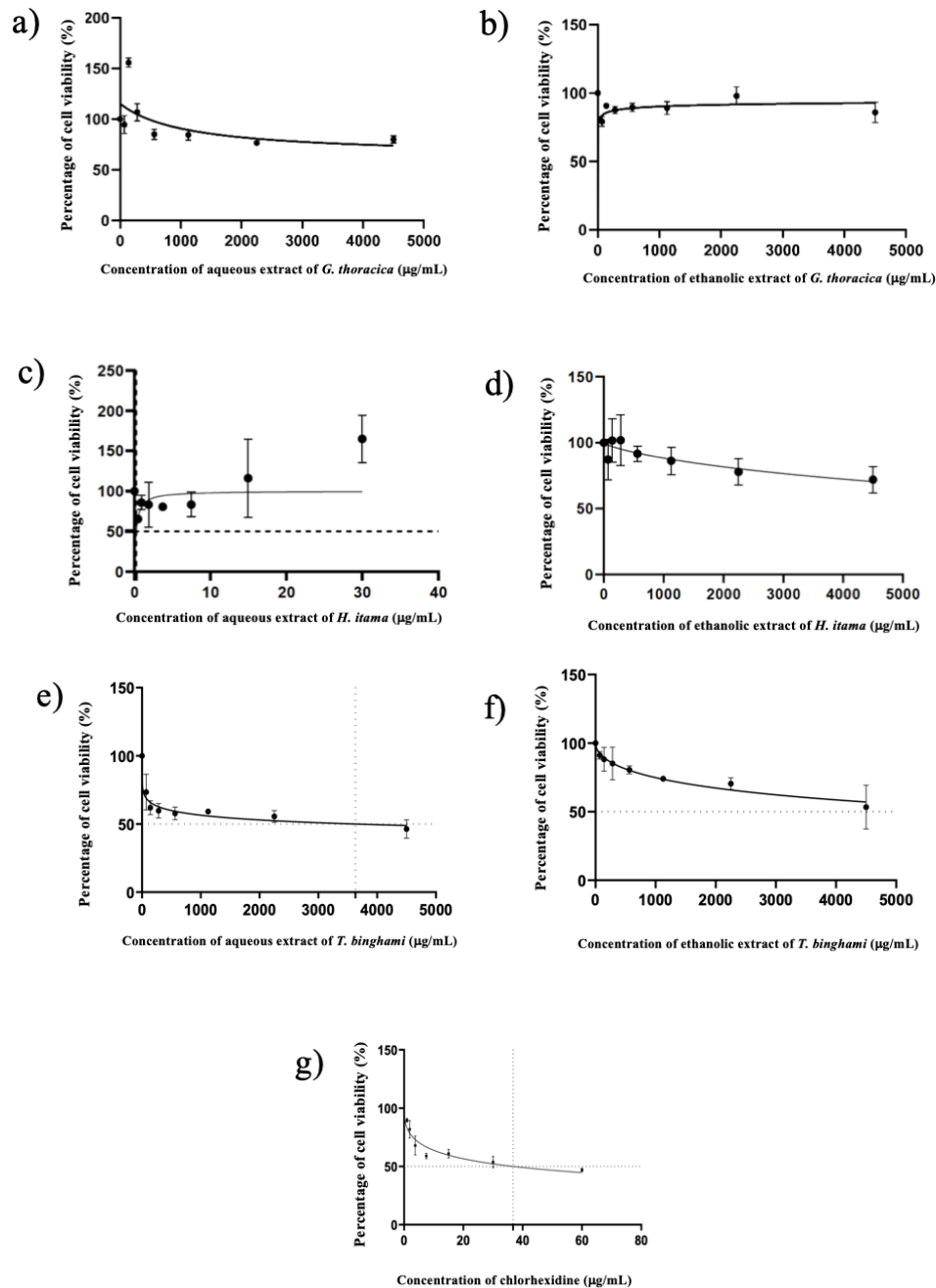


Figure 1. The plots of percentage of *Acanthamoeba* cells viability against the concentration of aqueous ethanolic extracts of stingless bees (a,b) *G. thoracica*, (c,d) *H. itama*, and (e,f) *T. binghami* propolis along with (g) chlorhexidine (positive control).

3.3. Toxicity tests

The results of the brine shrimp nauplii lethality tests of the aqueous and ethanolic extracts of *T. binghami*, *H. itama*, and *G. thoracica* propolis are gathered in Table 3. The LC_{50} was determined by plotting the percentage mortality against the logarithmic concentration of the propolis extracts, and was found to be higher than 1000 mg/mL. Therefore, in general, the brine shrimp nauplii lethality tests suggested that all propolis extracts in this

study are non-toxic or have low toxicity. Nevertheless, at concentrations as low as 0.1 mg/mL, the aqueous extracts of *T. binghami*, *H. itama*, and *G. thoracica* propolis resulted in 3–13% mortality of the nauplii. In comparison, the ethanolic extract of *H. itama* propolis at the same concentration showed higher mortality (20%), whereas that of *T. binghami* propolis exhibited the lowest percentage of mortality (0%).

Table 3. The LC₅₀ of all aqueous and ethanolic propolis extracts which resulted in death of 50% of nauplii at various concentration after 24 h

Bee species	Extract	Concentration (mg/mL)	No. of surviving nauplii (after 24 h)				Mortality (%)	LC ₅₀ (mg/mL)
			Test 1	Test 2	Test 3	Total		
<i>G. thoracica</i>	Aqueous	0.1	6	10	10	26	13	>1000
		1	10	7	9	26	13	
		10	10	6	9	25	13	
		100	9	10	10	29	3	
	Ethanolic	0.1	9	10	7	26	13	>1000
		1	9	10	10	29	3	
		10	8	9	10	27	10	
		100	10	9	10	29	3	
<i>H. itama</i>	Aqueous	0.1	9	10	10	29	3	>1000
		1	9	6	8	23	23	
		10	7	3	8	18	40	
		100	7	10	8	25	17	
	Ethanolic	0.1	9	8	7	24	20	>1000
		1	6	7	9	22	27	
		10	7	3	6	16	47	
		100	4	2	10	16	47	
<i>T. binghami</i>	Aqueous	0.1	9	10	10	29	3	>1000
		1	9	10	10	29	3	
		10	3	8	9	20	33	
		100	8	2	7	17	43	
	Ethanolic	0.1	10	10	10	30	0	>1000
		1	9	10	8	27	10	
		10	9	10	10	29	3	
		100	4	3	6	13	57	

4. Discussion

Propolis is rich in bioactive compounds with a variety of therapeutic potential that come from different sources including plants, microorganisms, etc. Propolis has been shown to be an excellent treatment option for a variety of diseases, as summarized in a recent review article (Zullkiflee et al., 2022b). Among the biological properties that have been studied worldwide, antimicrobial effects are the most commonly studied. However, due to the distinct flora in the surrounding area of bee hives being diverse in each region and country in the world, antimicrobial properties of stingless bee propolis depend on the origin from which the propolis samples are harvested. Moreover, the extraction method, osmotic effect, and phytochemical properties of propolis can also influence its antifungal activity.

In this study, the results showed that the aqueous extracts of *T. binghami*, *H. itama*, and *G. thoracica* propolis produced large inhibition zones, whereas the ethanolic extracts showed no antifungal activity. This was supported by the lower MIC values of *C. albicans* and *S. cerevisiae* in the presence of the aqueous extracts than the ethanolic extracts. This finding indicated that water could extract more antifungal compounds than ethanol. In other

words, the antifungal activities responsible for propolis extracts are highly polar organic compounds. The various antifungal activities of the aqueous extracts of *T. binghami*, *H. itama*, and *G. thoracica* propolis may be associated with their different chemical components. In other words, the different species of stingless bees might collect chemical components from different botanical plants that are available in the area surrounding their meliponi farm, and a large variety of the collected bioactive compounds could be attributed to the different antifungal activities (Sforcin and Bankova, 2011; Montero and Mori, 2012). In particular, in addition to the flavonoid and phenolic compounds present in propolis (Zullkiflee et al., 2022a), aromatic esters and acids present in the resins are also attributed to their antifungal activity (Montero and Mori, 2012). In this sense, the permeability of the cytoplasmic membrane of fungal cells is strongly affected by the phenolic acids present in propolis, causing leakage of intracellular components such as inorganic ions, nucleic acids, and proteins, which resulted in complete cell mortality (Montero and Mori, 2012; Farnesi et al., 2009). In comparison, the efficacy of propolis of the same bee species originated from different geographical locations to inhibit the development of yeasts may also differ, indicating that the botanical origin of propolis has a substantial impact on its antifungal activity.

The MFC tests suggested that propolis extracts are fungistatic, rather than fungicidal. A similar finding has been reported for the antifungal activity of *Trigona thoracica* propolis against *C. albicans* strains (Kačániová et al., 2013). It is worth noting that the fungistatic properties of propolis are of interest for the application of this bee glue in many different medicinal treatments including asthma, diabetes, ulcers, skin infections, and wound healing (Shehu et al., 2015).

In this study, the primary toxicity test using the brine shrimp nauplii lethality assay indicated that the aqueous and ethanolic extracts of *T. binghami*, *H. itama*, and *G. thoracica* propolis are not toxic. Although there have been numerous reports stating that propolis is relatively nontoxic and safe for consumption, there are still a few studies that state otherwise (Vakhonina et al., 2021). Nevertheless, despite the disparity in reported toxicities of propolis, some propolis extracts, irrespective of their stingless bee species, may have a very low intrinsic toxicity, which is likely caused by the preparation of the extracts or the presence of a small amount of the bioactive compounds in propolis. For example, it was reported that, propolis also contains flavonoids which are active ingredients and known for their relatively low toxicity (Burdock, 1998). Phytochemicals such as toxic metals (arsenic, lead, chromium, mercury, and cadmium) found in propolis can also greatly influence its toxicity (Ahangari et al., 2018; Hodel et al., 2020). These toxic metals are often associated with contamination, especially if the propolis originates around active sites such as industrial areas, mining, and active urbanization, or it is exposure to fertilizers and pesticides (González-Martín et al., 2015; Hodel et al., 2020). Overexposure to high amount of these metals can cause toxicity (Jaishankar et al., 2014).

5. Conclusion

The present study revealed that all aqueous extracts of *T. binghami*, *H. itama*, and *G. thoracica* propolis displayed significant antifungal activity against *Candida albicans* and *Saccharomyces cerevisiae* strains, supported by the lower MIC values of aqueous extracts compared to ethanolic extracts. The MFC values indicated that all the aqueous and ethanolic propolis extracts were fungistatic. The brine shrimp nauplii lethality bioassay indicated that the propolis extracts were non-toxic, and the cytotoxicity test suggested that the propolis extracts have a low anti-amoebic activity against *Acanthamoeba* sp., much lower than that of chlorhexidine. Overall, this study revealed that the aqueous and ethanolic propolis extracts of the three stingless bees found in Brunei showed low antifungal and anti-amoebic activities. A deeper understanding of the antifungal and anti-amoebic activities of these stingless bees propolis should be provided by comprehensive research to identify specific compounds present in propolis.

Acknowledgements

The authors thank Mitasby H. Mamit (Tasbee Meliponiculture Farm) for supplying the propolis.

References

- Abdullah NA, Ja'afar F, Yasin HM, Taha H, Petalcorin MIR, Mamit MH, Kusrini E and Usman A. 2019. Physicochemical analyses, antioxidant, antibacterial, and toxicity of propolis particles produced by stingless bee *Heterotrigona itama* found in Brunei Darussalam. *Heliyon* 5 (9): e02476.
- Abdullah NA, Zulkiflee N, Zaini SNZ, Taha H, Hashim F and Usman A. 2020. Phytochemicals, mineral contents, antioxidants, and antimicrobial activities of propolis produced by Brunei stingless bees *Geniotrigona thoracica*, *Heterotrigona itama*, and *Tetrigona binghami*. *Saudi J. Biol. Sci.* 27: 2902–2911.
- Abid R, Waseem H, Ali J, Ghazanfar S, Muhammad Ali G, Elsbali AM and Alharethi SH. 2022. Probiotic yeast *Saccharomyces*: Back to nature to improve human health. *J. Fungi* 8 (5): 444.
- Ahangari Z, Naseri M and Vatandoost F. 2018. Propolis: Chemical composition and its applications in endodontics. *Iran. Endod. J.* 13 (3): 285–292.
- Al-Ghamdi AY, Fadlilmula AA, Mohamed OM and Abdalla MOM. 2020. Total phenolic content, antioxidant and antimicrobial activity of *Ruta chalepensis* L. leaf extract in Al-Baha Area, Saudi Arabia. *Jordan J. Biol. Sci.* 13: 675–680.
- Alves IA, Bandeira LA, Mario DAN, Denardi LB, Neves LV, Santurio JM and Alves SH. 2012. Effects of antifungal agents alone and in combination against *Candida glabrata* strains susceptible or resistant to fluconazole. *Mycopathologia* 174 (3): 215–221.
- Anjum SI, Ullah A, Khan KA, Attaullah M, Khan H, Ali H, Bashir MA, Tahir M, Ansari MJ, Ghramh HA, Adgaba N and Dash CK. 2019. Composition and functional properties of propolis (bee glue): A review. *Saudi J. Biol. Sci.* 26 (7): 1695–1703.
- Bankova V, Popova M and Trusheva B. 2014. Propolis volatile compounds: Chemical diversity and biological activity: A review. *Chem. Cent. J.* 8: 28.
- Bendjedid S, Bazine I, Tadjine A, Djelloul R, Boukhari A and Bensouici C. 2022. Analysis of phytochemical constituents by using LC-MS, antifungal and allelopathic activities of leaves extracts of *Aloe vera*. *Jordan J. Biol. Sci.* 15: 21–28.
- Burdock GA. 1998. Review of the biological properties and toxicity of bee propolis (propolis). *Food Chem. Toxicol.* 36 (4): 347–363.
- Cockerill FR. 2012. Methods for Dilution Antimicrobial Susceptibility Tests for Bacteria That Grow Aerobically; Approved Standard—Ninth Edition. Vol. 32. Wayne, PA (USA): Clinical and Laboratory Standards Institute.
- Farnesi AP, Aquino-Ferreira R, De Jong D, Bastos JK and Soares AE. 2009. Effects of stingless bee and honey bee propolis on four species of bacteria. *Genet. Mol. Res.* 8 (2): 635–640.
- González-Martín MI, Escuredo O, Revilla I, Vivar-Quintana AM, Coello MC, Riocerezo CP and Moncada GW. 2015. Determination of the mineral composition and toxic element contents of propolis by near infrared spectroscopy. *Sensors* 15 (11): 27854–68.
- Gucwa K, Kusznierevicz B, Milewski S, Van Dijk P and Szveda P. 2018. Antifungal activity and synergism with azoles of Polish propolis. *Pathogens* 7 (2): 56.
- Hodel KVS, Machado BAS, Santos NR, Costa RG, Menezes-Filho JA and Umsza-Guez MA. 2020. Metal content of nutritional and toxic value in different types of Brazilian propolis. *Sci. World J.* 2020: 4395496.

- Hussain RF, Nouri AM and Oliver RT. 1993. A new approach for measurement of cytotoxicity using colorimetric assay. *J. Immunol. Methods* **160** (1): 89–96.
- Ibrahim MEE and Alqurashi RM. 2022. Anti-fungal and antioxidant properties of propolis (bee glue) extracts. *Int. J. Food Microbiol.* **361**: 109463.
- Jaishankar M, Tseten T, Anbalagan N, Mathew BB and Beeregowda KN. 2014. Toxicity, mechanism and health effects of some heavy metals. *Interdiscip. Toxicol.* **7** (2): 60–72.
- Kačániová M, Melich M, Kačániová V, Felšöciiová S and Sudzinová J. 2013. The antimicrobial activity of honey and propolis against yeasts *Candida* species. *Lucrari Stiintifice: Zootehnie si Biotehnologii* **42**(2): 167–173.
- Kamyab E, Rohde S, Kellermann MY and Schupp PJ. 2020. Chemical defense mechanisms and ecological implications of Indo-Pacific holothurians. *Molecules* **25**, 4808.
- Lofty M. 2006. Biological activity of bee propolis in health and disease. *Asian Pac. J. Cancer Prev.* **7** (1): 22–31.
- Marcucci MC. 1995. Propolis: Chemical composition, biological Properties and therapeutic activity. *Apidologie* **26** (2): 83–99.
- Moghim H, Taghipour S, Kheiri S, Khabbazi H and Baradaran A. 2021. Antifungal effects of Iranian propolis extract and Royal jelly against *Candida albicans in-vitro*. *Int. J. Prev. Med.* **12**, 163.
- Montero JC and Mori GG. 2012. Assessment of ion diffusion from a calcium hydroxide-propolis paste through dentin. *Braz. Oral Res.* **26** (4): 318–322.
- Mosmann T. 1983. Rapid colorimetric assay for cellular growth and survival: Application to proliferation and cytotoxicity assays. *J. Immunol. Methods* **65** (1–2): 55–63.
- Nobile CJ and Johnson AD. 2015. *Candida albicans* biofilms and human disease. *Annu. Rev. Microbiol.* **69**: 71–92.
- Ożarowski M, Karpiński TM, Alam R and Łochyńska M. 2022. Antifungal properties of chemically defined propolis from various geographical regions. *Microorganisms* **10** (2): 364.
- Pappas PG, Kauffman CA, Andes DR, Clancy CJ, Marr KA, Ostrosky-Zeichner L, Reboli AC, Schuster MG, Vazquez JA, Walsh TJ, Zaoutis TE and Sobel JD. 2016. Clinical practice guideline for the management of candidiasis: 2016 update by the infectious diseases society of America. *Clin. Infect. Dis.* **38** (2): 161–189.
- Patricio P, Paiva JA and Borrego LM. 2019. Immune response in bacterial and *Candida sepsis*. *Eur. J. Microbiol. Immunol.* **9** (4): 105–113.
- Patton LL, Bonito AJ and Shugars DA. 2001. A systematic review of the effectiveness of antifungal drugs for the prevention and treatment of oropharyngeal candidiasis in HIV-positive patients. *Oral Surg. Oral Med. Oral Pathol. Oral Radiol. Endod.* **92** (2): 170–179.
- Prestinaci F, Pezzotti P and Pantosti A. 2015. Antimicrobial resistance: a global multifaceted phenomenon. *Pathog. Glob. Health* **109** (7): 309–318.
- Rivera-Yañez N, Rivera-Yañez CR, Pozo-Molina G, Méndez-Catalá CF, Reyes-Realí J, Mendoza-Ramos MI, Méndez-Cruz AR and Nieto-Yañez O. 2021. Effects of propolis on infectious diseases of medical relevance. *Biology* **10** (5): 428.
- Roemer T and Krysan DJ. 2014. Antifungal drug development: Challenges, unmet clinical needs, and new approaches. *Cold Spring Harb. Perspect. Med.* **4** (5): a019703.
- Scorzoni L, de Paula E Silva AAC, Marcos CM, Assato PA, de Melo WCMA, de Oliveira HC, Costa-Orlandi CB, Mendes-Giannini MJS and Fusco-Almeida AM. 2017. Antifungal therapy: new advances in the understanding and treatment of mycosis. *Front. Microbiol.* **8**: 36.
- Sforzin JM and Bankova V. 2011. Propolis: is there a potential for the development of new drugs. *J. Ethnopharmacol.* **133** (2): 253–260.
- Shehu A, Rohin MAK, Aziz AA and Ismail S. 2015. Antifungal, characteristic properties and composition of bee glue (Propolis). *J. Chem. Pharm. Res.* **7** (3): 1992–1996.
- Vakhonina EA, Lapynina EP and Lizunova AS. 2021. Study of toxic elements in propolis. *IOP Conf. Series: Earth Environ. Sci.* **845** (1): 012122.
- Wagh VD. 2013. Propolis: a wonder bees product and its pharmacological potentials. *Adv. Pharmacol. Sci.* **2013**: 308249.
- Wiederhold NP. 2017. Antifungal resistance: current trends and future strategies to combat. *Infect. Drug Resist.* **10**: 249–259.
- Yusoff NYN, Mohamad S, Abdullah HN and Rahman NA. 2016. Antifungal activity of Malaysian honey and propolis extracts against pathogens implicated in denture stomatitis. *AIP Conf. Proc.* **1791**: 020006.
- Zullkiflee N, Taha H, Abdullah NA, Hashim F and Usman A. 2022a. Antibacterial and antioxidant activities of ethanolic and water extracts of stingless bees *Tetrigona binghami*, *Heterotrigona itama*, and *Geniotrigona thoracica* propolis found in Brunei. *Philipp. J. Sci.* **151** (4): 1455–1462.
- Zullkiflee N, Taha H and Usman A. 2022b. Propolis: its role and efficacy in human health and diseases. *Molecules* **27**: 6120.

Chemical and Functional Properties of Myofibrillar Protein from Selected Species of Trash Fish

Choirul Anam¹, Manar Fayiz Mousa Atoum², Noor Harini³, Damat Damat^{3,*},
Roy Hendroko Setyobudi³, Ahmad Wahyudi³, Agustia Dwi Pamujiati⁴,
Nita Kuswardhani⁴, Yuli Witono⁴, Rusli Tonda³, Hendro Prasetyo⁵, Ida Ekawati⁶,
Endang Dwi Purbajanti⁷, Zane Vincēviča-Gaile⁸, Taavi Liblik⁹, Ahmad Fauzi³,
Hadinoto Hadinoto¹⁰, Nico Syahputra Sebayang¹¹, Eni Suhesti¹⁰,
Asgami Putri¹⁰, and Fasal Munsif¹²

¹Universitas Islam Darul Ulum, Lamongan 62253, Indonesia; ²The Hashemite University, 13133 Zarqa, Jordan;

³University of Muhammadiyah Malang, Malang 65145, Indonesia; ⁴University of Jember, Jember 68121, Indonesia;

⁵University of Brawijaya, Malang 65145, Indonesia; ⁶Universitas of Wiraraja, Sumenep 69451, Indonesia; ⁷University of Diponegoro, Semarang 50275, Indonesia; ⁸University of Latvia, Riga LV-1004, Latvia; ⁹Tallinn University of Technology, 12616 Tallinn, Estonia;

¹⁰University of Lancang Kuning, Pekanbaru, Riau 28261, Indonesia; ¹¹University of Muhammadiyah Palembang, Palembang 30116, Indonesia; ¹²University of Agriculture Peshawar, 25130 Khyber Pakhtunkhwa, Pakistan.

Received: Feb 14, 2023; Revised: Apr 1, 2023; Accepted Apr 1, 2023

Abstract

Trash fish is a captured fish that has low economic value. Trash fish has a reasonably high protein. However, myofibrillar protein from trash fish cannot form gel properly. Therefore, it is necessary to modify it by adding a gelling agent. This study aimed to determine myofibrillar protein's chemical and functional characteristics from trash fish as a food ingredient. The research method is in the form of laboratory experiments. The types of fish used as samples in this study were Chacunda gizzard-shad (*Anodontostoma chacunda* Hamilton, 1822), Orange fin ponyfish (*Leiognathus bindus* Valenciennes, 1835), and Sardines (*Sardinella fimbriata* Valenciennes, 1847). Myo fibril modification was carried out by adding 10 % carrageenan (wv⁻¹) to each trash fish sample. The results showed that the myofibrillar protein from Chacunda gizzard-shad had higher protein content (84.77 %), water holding capacity (524.78 %), and emulsion activity (8.85 m g⁻²) than other samples. Chacunda gizzard-shad is characterized by more red meat than the others. This fish species also has the highest oil-holding capacity (620.35 %) and emulsion stability (4.58 h). The microstructure of the trash fish myofibrils is tighter and more hollow, so it has a better ability to absorb oil. Myofibrillar protein from another species, Orange fin ponyfish, has a relatively higher whiteness value (78.42) than other samples because white meat is dominant for this species. Modifying myofibrillar protein by adding agar and carrageenan can increase the hardness value of the sample due to the addition of agar. According to this study, the Chacunda gizzard-shad has the greatest potential to be an ingredient in high-value commercial food products.

Keywords: Chacunda gizzard-shad, Fish waste characterization, Fish proteins, Marine waste to food, Orange fin ponyfish, Rough fish, Sardine, Waste utilization

1. Introduction

In fishing operations, the fish catches contain not only high-economic value fish but also so-called trash fish (also known as rough fish or dirt fish) with lower economic value (Anam *et al.*, 2021; Raissa *et al.*, 2014). Uses of various marine waste, including trash fish, are broad – for feed and food production and a source for renewable energy production (Coppola *et al.*, 2012; Rudovica *et al.*, 2021; Susanto, *et al.*, 2020). Several studies indicate trash fish utilization as a source for biogas production due to the scarcity of fossil fuels (Abdullah *et al.*, 2020; Bucker *et al.*, 2020; Burlakovs *et al.*, 2022; Kafle and Kim, 2012; Setyobudi *et al.*, 2021). However, technological

difficulties must be overcome as a two-stage digester is recommended to avoid the non-homogeneity of trash fish (Adinurani *et al.*, 2013, 2014; Hendroko *et al.*, 2014). Facing the global problem of food shortage, trash fish should be considered a valuable raw material for food and feed production due to its considerable protein content, *i.e.*, 15 % to 20 % (Erbay dan Yeşilsu, 2021).

Trash fish in Lamongan Regency, one of the marine sector fisheries in East Java, Indonesia, is dominated mainly by two species: Chacunda gizzard-shad (*Anodontostoma chacunda*, Hamilton, 1822) and Orange fin ponyfish (*Photopectoralis bindus*, Valenciennes, 1835). However, currently the utilization of these trash fish is minimal as they only are used for feed and salted fish production, even though they are suitable to be applied as

*Corresponding author. e-mail: damat@umm.ac.id.

food ingredients leading to higher economic value (Coppola *et al.*, 2012; Hasan *et al.*, 2021; Rudovica *et al.*, 2021).

Protein-rich fish muscles are divided into three types: sarcoplasmic, myofibrillar, and stroma (Dara *et al.*, 2021). Myofibrillar protein (65 % to 75%) prevails over the other component and is soluble in salt solution (Deng *et al.*, 2021). Myofibrillar protein consists of myosin, actin, tropomyosin, and actomyosin and influences fish products' quality and functional properties. Furthermore, myofibrillar protein has a role in the formation of gel and the process of flesh coagulation (Liu *et al.*, 2022).

Based on preliminary research, myofibrillar protein from trash fish cannot be transferred into a gel but needs modification by adding a gelling agent such as agar and carrageenan (Leha and Moniharapon, 2013). Agar is a complex of polysaccharides (having two main components, agarose and agarpectin) with rigid, fragile, and malleable gelling characteristics. At the same time, carrageenan is a hydrocolloid compound that consists of ester-sulfate content in a mixture with galactose and 3,6-anhydrogalactose polymer characterized by elastic gelling properties (du Preez *et al.*, 2020).

Agar and carrageenan can make interaction with proteins influencing viscosity and gel formation. Therefore, adding agar and carrageenan is expected to improve the gelation of myofibrillar protein from trash fish, resulting in its use as a raw material for surimi production (Li *et al.*, 2022). Surimi is an intermediate product and can be processed into products that need flesh elasticity. Generally, cod fish (a common name for various marine fish of the genus *Gadus* of the family *Gadidae*) is used as a raw material for surimi production (Millan *et al.*, 2021), but modified myofibrillar protein from trash fish can be assessed as a potential substitute for cod fish. This research investigates the chemical and functional characteristics of myofibrillar protein from trash fish, including its color, texture, and microstructure characteristics after the modification of the protein.

2. Materials and Methods

2.1. Fish samples and reagents

Trash fish species such as Chacunda gizzard-shad (*A. chacunda*), Orangefin ponyfish (*P. bindus*) and Sardine (*Sardinella fimbriata* Valenciennes, 1847) were selected for this study. Fresh fishes (on average 100 g in each sample) of these species were purchased at the central fish market in Lamongan Regency, East Java Province, Indonesia. Samples were kept in an ice box and placed in cold storage while transported to the Department of Agro-industry Technology, Faculty of Agricultural Technology, University of Jember, Indonesia. Upon arrival, samples were immediately kept in a freezer. Before analysis, amount of 2 500 g fish samples were thawed at room

temperature, washed, filleted, and minced to uniformity by using a chopper.

Gelling agents (agar and *i*-carrageenan) were obtained from a chemical shop in Hiroshima, Japan. The gelling agent used was purchased from Sigma, with product code C1013. Reagents used in the research were NaCl, 0.1 M phosphate buffer solution (pH 7), HCl, NaOH, Lowry reagent, H₂SO₄, 4 % H₃BO₃, methanol, tris HCl buffer containing 0.1 % sodium dodecyl sulfate sucrose, urea, 2 % sodium dodecyl sulfate, 2 % 2-mercaptoethanol, 50 % glycerol, coomassie brilliant blue, staining solution, Na₂CO₃, CuSO₄, KNaC₄H₄O₆·4H₂O (sodium potassium tartrate), phenolic solution, glutaraldehyde, ethanol. All chemicals used were analytical grade from the manufacturer Merck, Germany.

2.2. Extraction of myofibrillar protein from trash fish

Myofibrillar protein samples were extracted from trash fish according to the method reported by (Dara *et al.*, 2021) with some modifications (Figure 1). First, fish mince was mixed with three volumes of 10 % NaCl in 0.1 M phosphate buffer (pH 7) and magnetic stirred (MYP11-2, Shanghai Meiyongpu Instrument Co., Ltd., China) at 4 °C for 3 min, followed by centrifugation (X1R, Thermo Fisher Technologies Co., Ltd., Waltham, MA, USA) at a speed of 4 000 rpm (1 rpm = 1/60 Hz) at 2 °C for 10 min. Obtained pellet decantation was repeated one time. Pellets were filtered through a filter cloth of four layers. Then the filtrate was added with three volumes of 10 % NaCl in 0.1M phosphate buffer (pH 7), followed by centrifugation at 4 000 rpm at 2 °C for 10 min. Finally, pellets obtained were wet myofibrillar protein. Next, the myofibrillar protein was added with 5 % sucrose (ww⁻¹) and dried by using freeze-drying. Samples were kept in an airtight chamber. All samples were prepared in triplicate.

The freezing process is carried out by adopting the method developed by Prosapio and Lopez-Quiroga (2020). The first stage of the product is frozen first at -50 °C. Then, the drying process (sublimation) is carried out by placing frozen products into a vacuum chamber. The pressure is maintained at about 0.036 psi (1 psi = 6.89 kPa) or about 0.0025 bar and the temperature is then raised in a controlled manner until it reaches about 100 °F (38 °C) so that the sublimation process occurs. In the mechanism of the freeze dryer, the water vapor produced is then sucked in and condensed so that it does not wet the product being dried. The drying process was carried out for 13 h.

2.3. Modification of myofibrillar protein from trash fish

Trash fish myofibrils could not form a gel. Then the myofibril modification was carried out using agar and carrageenan. First, myofibrillar protein samples from Chacunda gizzard-shad, Orangefin ponyfish, and Sardine were weighted 10 % (wv⁻¹) and added 1 % (wv⁻¹) of agar and carrageenan. Then, 20 mL of distilled water was added to the mixture. Afterward, the mixture was heated at 75 °C for 30 min and kept at room temperature until the solid gel was formed. Final solid gel samples were kept in the refrigerator until the analysis.

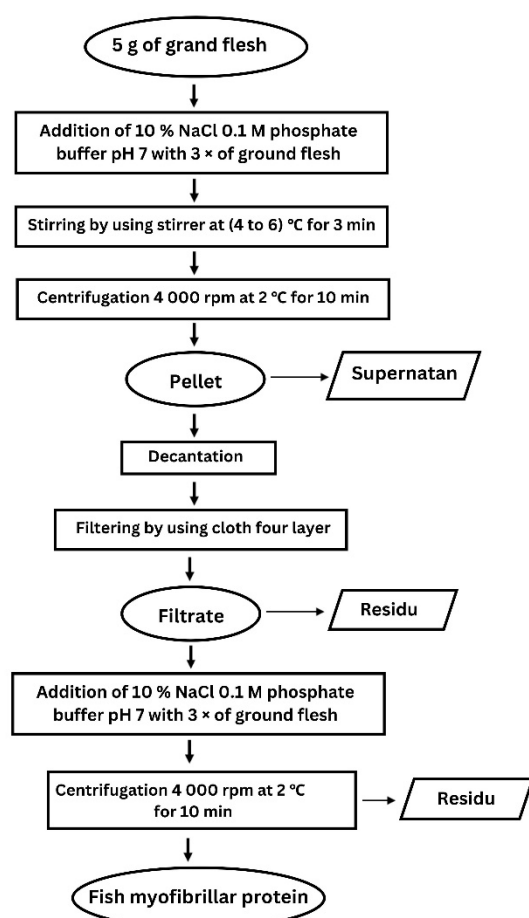


Fig. 1. The process of isolation of myofibrillar protein from trash fish

2.4. Analysis of chemical and functional properties

The chemical and functional properties of myofibrillar protein from trash fish *per se* and after modification were subjected to the detection of following parameters: protein content (AOAC, 2005); water holding capacity (WHC) (Zhang *et al.*, 2015); oil holding capacity (OHC) (Nguyen *et al.*, 2015); emulsion activity and stability (Najafian and Babji, 2015); color (Seighalani *et al.*, 2017); microstructure (Arfat and Benjakul, 2012; Shui *et al.*, 2021); molecular weight (Fowler and Park, 2015); and texture (Petcharat and Benjakul, 2017). The resulting data of chemical and functional parameters were averaged over each variable and subjected to descriptive statistics (Adinurani, 2022).

2.4.1. Analysis of protein content (AOAC, 2005)

Amount of 0.1 g sample was weighed and then put into the Kjeldahl flask. Into the flask was added 2 mL of concentrated H₂SO₄ (Sulfuric acid 95 % to 97 % (Merck for analysis) and 0.9 g of selenium. The solution was then heated using digestion for 45 min. After cooling, the solution was added as much as 5 mL of distilled water and then distilled. The distillate is put into an Erlenmeyer, given 15 mL of 4 % boric acid solution and two drops of indicator. After that, the solution was titrated with 0.02 N HCl solution (HCl Brand, for analysis) to change the color

to a slightly purplish-blue. Calculation on protein levels employed Equation (1):

$$\text{Protein (\%)} = \frac{(ts - tb) \times N \text{ HCl} \times 6.25 \times \text{MW Nitrogen}}{\text{Sample weight} \times 1000} \times 100 \% \quad (1)$$

Description:

ts = titrated volume of sample HCl (mL), tb = titrated volume of blank HCl (mL)

N HCl = 0.0858, 6.25 = conversion factor from nitrogen to protein
Molecular weight (MW) nitrogen = 14.008 (g mol⁻¹)

2.4.2. Water holding capacity (WHC) (Zhang *et al.*, 2015)

Analysis of water holding capacity (WHC) was carried out in the following way: The centrifuge tube was dried and then weighed (a gram). Next, a sample of 0.5 g (b gram) is put into a dry centrifugal tube whose weight is known. Into the centrifuge tube, 7× sample weight of distilled water was added. Each sample mixture was homogenized using a vortex (Vortex Mixer DLAB MX-S), and then separated using a centrifuge (Centrifuge HC-12A Microhematocrit) for 5 min (speed 2 000 rpm). Finally, the supernatant was poured, and the residue was weighed (c gram). After that, the calculation using Equation (2):

$$\text{WHC (\%)} = \frac{(c - a) - b}{a} \times 100 \% \quad (2)$$

Description:

a = weight of empty centrifuge tube

b = sample weight

c = weight of precipitate at the end of centrifugation

2.4.3. Oil holding capacity analysis (Nguyen *et al.*, 2015)

The sample's OHC (Oil Holding Capacity) analysis was carried out in the following way: The empty centrifuge tube was dried and weighed (a gram). Next, a 0.5 g (b-gram) sample is put into a centrifuge tube. The oil was added 7× the sample weight into the centrifuge tube. Next, the samples were homogenized using a vortex (Vortex Mixer DLAB MX-S). Then, the separation was performed using a centrifuge (Centrifuge HC-12A Microhematocrit) at 2 000 rpm for 5 min. Finally, the supernatant was poured, and the residue formed was weighed (c gram). After that, the OHC calculation was performed using Equation (3).

$$\text{OHC (\%)} = \frac{(c - a) - b}{b} \times 100 \% \quad (3)$$

Description:

a = weight of empty centrifuge tube

b = sample weight

c = weight of precipitate at the end of centrifugation

2.4.4. Stability and emulsion power (Najafian and Babji, 2015)

Emulsion power was measured as follows: 0.1 g of sample was added to 100 mL of 0.05M phosphate buffer pH 7, then stirred with a stirrer for 15 min. Furthermore, 25 mL of cooking oil was added to the sample and mixed using a blender (Philips Series 5000) for 3 min. The emulsion power of the samples was measured after mixing with a blender. Emulsion stability was measured by taking 1 mL with an interval of 10 min for sampling. The two samples were added with 5 mL of 0.1 % SDS and mixed with a vortex (Vortex Mixer DLAB MX-S). Measurements

were made using a spectrophotometer (UV Vis Spectrophotometer Shimadzu 1240) at a wavelength of 500 nm. The power and stability of the sample emulsion are calculated using Equation (4) and Equation (5):

Information:

$$EAI (m^2 g^{-1}) = \frac{2 \times 2.303}{c \times (1 - \phi) \times 10^4} \times \text{abs} \times \text{dilution} \quad (4)$$

EAI = Emulsifying activity index ($m^2 g^{-1}$)

c = protein concentration (gmL^{-1})

ϕ = oil volume fraction ($mL mL^{-1}$) of the emulsion

abs = absorbance

dilution = solution (SDS + emulsion)

$$ESI (\text{time}) = \frac{T \times \Delta t}{\Delta t} \quad (5)$$

Explanation:

ESI = Emulsifying Stability Index

T = absorbance for 0 hour

Δt = time reduction calculation Δ

T = absorbance reduction for 0 hour with the calculated absorbance

2.4.5. Color analysis (Seighalani *et al.*, 2017)

Myofibril protein color analysis was performed using Konica Minolta's CR-10 Plus. Brightness (L^*), redness/greenness (a^*), and yellowness/blueness (b^*) will be measured in the instrument. Color analysis is calculated using two formulas. First, the degree of whiteness will be calculated using Equation (6).

$$\text{Whiteness} = 100 - [(100 - L^*)^2 + a^{*2} + b^{*2}]^{1/2} \quad (6)$$

The second is to determine the color angle of the sample expressed in Hue. To calculate the degree of color using Equation (7):

$$H = \arctan \frac{b^*}{a^*} \quad (7)$$

Where,

$H = 180 - \tan^{-1} b/a$ (if a is positive and b is positive)

$H = 180 + \tan^{-1} b/a$ (if a is negative and b is positive)

$H = 180 - \tan^{-1} b/a$ (if a is negative and b is negative)

2.4.6. Miofibril protein microstructure (Arfat and Benjakul, 2012; Shui *et al.*, 2021)

The protein microstructure of trash fish myofibrils was determined using a Scanning Electron Microscope (SEM) (Arfat and Benjakul, 2012) with several modifications (Shui *et al.*, 2021). Freeze-dried trash fish myofibril samples were placed on a tip and mounted on an SEM device to view its microstructure. The first modified myofibril sample was cut with a size of $0.5 \text{ mm} \times 0.5 \text{ mm} \times 0.5 \text{ mm}$ and immersed in a 2.5 % ($v v^{-1}$) glutaraldehyde solution in 0.2 M phosphate buffer (pH 7.2) for 2 h. Next, samples were washed using distilled water. Samples that had been washed with distilled water were then immersed in ethanol with graded concentrations of 50 %, 70 %, 80 %, 90 %, 95 %, and 100 % ($v v^{-1}$) for 5 min each. The sample is plated with gold for a few minutes. Finally, the sample microstructure was viewed using Scanning Electron Microscopy (Hitachi TM 3000).

2.4.7. Molecular weight analysis (SDS-Page) (Fowler and Park, 2015)

The molecular weight of myofibril protein was analyzed by SDS-PAGE. Amount of 0.2 g of myofibril protein was dissolved in 3.75 mL of 20 mM Tris-HCl buffer pH 8 containing 8 M urea, 2 % SDS, and 2 % 2-mercaptoethanol. The sample added with buffer is heated at 99 °C for 2 min. After that, stirring was carried out using a shaker (Oregon orbital shaker I HSR-200) for more than 20 h at 30 °C to dissolve the sample. A volume of 200 μL of the dissolved sample was taken, and 50 mM of Tris-HCl pH 8 buffer was added containing 5 % SDS, 5 % 2-mercaptoethanol, and 50 % glycerol as much as 50 μL . Samples that had been added buffer were heated at 99 °C for 1 min. A sample of 2.5 μL and a standard of 5 μL were put into wells of 12.5 % polyacrylamide gel that had been installed in an electrophoresis apparatus (AE 6530 serial number 5009405) and flown with a constant current of 20 mA for 75 min. When finished, the gel was taken and added with coomassie brilliant blue R-250 0.125 g 100 mL^{-1} and rinsed using distilled water three times. Protein bands will appear on the gel and be compared with the standard molecular weight (XL-Lader Broad Range SP-2110).

2.4.8. Texture analysis (Petcharat and Benjakul, 2017)

The tested sample was formed into a cylinder with a diameter of 2.5 cm. Cylindrical samples can be analyzed using a Rheometer (Fudoh Rheometer, Model NRM-2002J). A needle with a round tip with a diameter of 7 mm was pressed perpendicularly to the sample's surface until a puncture was formed with a puncture depth of 1 cm. The results will appear on the graph and be plotted into the formula so that the Hardness, Cohesiveness, and Adhesiveness values by Equation (8), Equation (9), and Equation (10).

$$\text{Hardness (N cm}^{-2}\text{)} = \text{force (g)} \times 0.0098 \times \text{cross-section area of probe} \quad (8)$$

$$\text{Cohesiveness} = \frac{A_2 (\text{peak area of second time})}{A_1 (\text{peak area of first time})} \quad (9)$$

$$\text{Adhesiveness} = \text{peak area drawn at Y-axis neg. direction; } A_3 (\text{gf.mm}) \quad (10)$$

2.5. Data analysis

The data were analyzed using simple statistics ($\bar{x} \pm \sigma$) and continued with the Least Significant Difference test ($\alpha = 5 \%$) to determine the better physicochemical properties of myofibrils (Adinurani, 2016).

3. Results and Discussion

3.1. Chemical and functional properties

3.1.1. Myofibrillar protein content

The highest myofibrillar protein content was detected for Chacunda gizzard-shad (84.77 %), but lower for Orangefin ponyfish (65.08 %), with an average of 66.44 % for investigated Sardine (Table 1). According to Tahergorabi *et al.* (2011), myofibrillar protein content can reach 70 % to 80 % of the total protein content, depending

on the fish species. Moreover, the amount of red and white flesh in a fish affects myofibrillar protein content. Chacunda gizzard-shad contains a greater amount of red flesh than the other fish. Dale *et al.* (2021) claimed that myofibrillar protein content for red flesh is higher by 62.40 %, while for white flesh lower by 59.20 %. Furthermore, the freeze-drying process affects maintaining myofibrillar protein content, preventing denaturation. In his study, Novian (2005) stated that dried myofibrillar protein content from gold band goat-fish (*Upeneus moluccensis* Bleeker, 1855) could increase by after freeze-drying 38 % than if another drying method is applied.

3.1.2. Water Holding Capacity

Water Holding Capacity (WHC) determines the loss of water during transport, storage, processing, and cooking. The type of material generally influences Water Holding Capacity (Damat *et al.*, 2021). The WHC means the ability of proteins to trap water and hold it performing as an advantage property for the food system. According to Table 1, the highest value of WHC is attributed to Chacunda gizzard-shad (524.78 %).

Table 1. Physico-chemical properties of trash fish protein myofibrils

	Protein content (%)	WHC (%)	OHC (%)	EA (m ² g ⁻¹)	ESI(h)	Whiteness
MT	66.44±0.95a	511.13±2.44b	620.35±2.80c	8.61±0.88b	4.58±1.22c	75.17±0.47a
MO	65.08±2.61a	352.22±0.61a	455.30±3.79a	6.19±0.16a	1.53±0.17a	78.42±0.38b
MC	84.77±0.39b	524.78±3.45c	513.26±1.99b	8.85±0.28c	3.76±1.27b	75.24±0.20a

Note: Numbers followed by the same letter in the same column are not significantly different based on the Difference test ($\alpha=5\%$)

MT – Sardine; MO – Orangefin ponyfish; and MC – Chacunda gizzard-shad

The highest value of OHC is attributed to Sardine because its structure contains bigger pores and, therefore, can better trap oil (Phung *et al.* 2020). Furthermore, Ulloa *et al.* (2017) indicated that the protein structure is the decisive factor in oil absorption as more lipophilic structures have more nonpolar protein branches contributing to the increased oil absorption capacity.

3.1.4. Emulsion activity and stability

Emulsion activity can be defined as the ability of the material to assist in establishing an emulsion, whereas emulsion stability can be defined as the ability of a material to maintain an emulsion formed. These parameters are affected by total protein content and solubility. The emulsion activity and stability of a myofibrillar protein from trash fish are reflected in Table 1.

The highest emulsion activity value is detected for samples derived from Chacunda gizzard-shad (8.85 m² g⁻¹), and it is dependent on total myofibrillar protein content. Also, Najafian and Babji (2015) stated that increasing protein concentration levels could increase emulsion activity and stability. In addition, these parameters are influenced by pH, ionic strength, and heat treatment (de Castro *et al.*, 2017).

The highest relative emulsion stability for myofibrillar protein from trash fish is attributed to Sardine (4.58 h), followed by Chacunda gizzard-shad (3.76 h), and Orangefin ponyfish (1.53 h). Gao *et al.* (2018) indicated that the emulsion activity of proteins is inversely

Najafian and Babji (2015) showed in their study claimed that WHC is affected by total protein concentration, ionic strength, temperature, and other components such as the content of hydrophilic polysaccharides, fats, and salt. WHC also might be influenced by the duration of heating and protein storage conditions. For example, surimi with a weak gel structure reflects low water holding capacity (de Castro *et al.*, 2017). Also, the drying method affects the WHC as freeze-drying can lead to better outcomes because freeze-dried surimi powder has the highest WHC than spray-dried one (Shaviklo, 2015).

3.1.3. Oil holding capacity

The oil holding capacity (OHC) is the amount of oil trapped in the protein matrix at certain conditions. For example, Table 1 reveals the highest myofibrillar protein OHC from trash fish investigated for Sardine (620.35 %), followed by Chacunda gizzard-shad (513.26 %) and Orangefin ponyfish (455.30 %), respectively.

proportional to emulsion stability that is caused by the rupture of the protein membrane. Protein solubility will determine the resulting gel strength. Protein heating conditions cause denaturation and increase fragility, rupturing the protein membrane. According to Li *et al.* (2022), increasing the protein concentration can also improve the stability of the emulsion.

3.1.5. Protein color

The color of myofibrillar protein is stated by whiteness value (WV). Whiteness, an important indicator, is used to measure the character of meat (Wu *et al.*, 2022). The WV of myofibrillar protein depends on the fish species (Park *et al.*, 2012). According to Table 1, the WV for myofibrillar protein was highest for Orangefin ponyfish (78.42), followed by similar results for Chacunda gizzard-shad (75.24) and Sardine (75.17). The pigment content in flesh causes the difference in color – Orangefin ponyfish has dominant white flesh than red flesh while Chacunda gizzard-shad fish has dominant red flesh.

According to Cropotova *et al.* (2021), demersal (benthic) fish is characterized by lower myoglobin content than pelagic fish. For example, Orangefin ponyfish is demersal fish and has lower myoglobin content than Chacunda gizzard-shad, that is pelagic fish, and, therefore, the first one is whiter. Dara *et al.* (2021) explained that demersal fish gold band goat-fish (*Upeneus moluccensis* Bleeker, 1855) has the highest brightness level (78.7 ± 1.0) compared to big-eyed pelagic fish (*Selar crumenophthalmus* Bloch, 1793) amount 67.2 ± 0.7 . In addition, the autoxidation of myoglobin to metmyoglobin

(Mannino *et al.*, 2020) may cause a pigment change to less bright or brownish during fish storage (Harnkarnsujarit *et al.*, 2015; Niu *et al.*, 2022).

3.1.6. Microstructure of protein

The microstructure of myofibrillar protein varies by fish species (Figure 2): for Sardine, it is more tightly with small pores compared with Orangefin ponyfish and

Chacunda gizzard-shad. The microstructure of Chacunda gizzard-shad has larger pores. As it was mentioned previously, the microstructure of myofibrillar protein affects the oil-holding ability of proteins. Similar and compact protein microstructure can improve the gelation properties of surimi from silver carp (Gao *et al.*, 2021). In addition, protein microstructure is affected by the duration of fish storage at freeze conditions (Xu *et al.*, 2019).

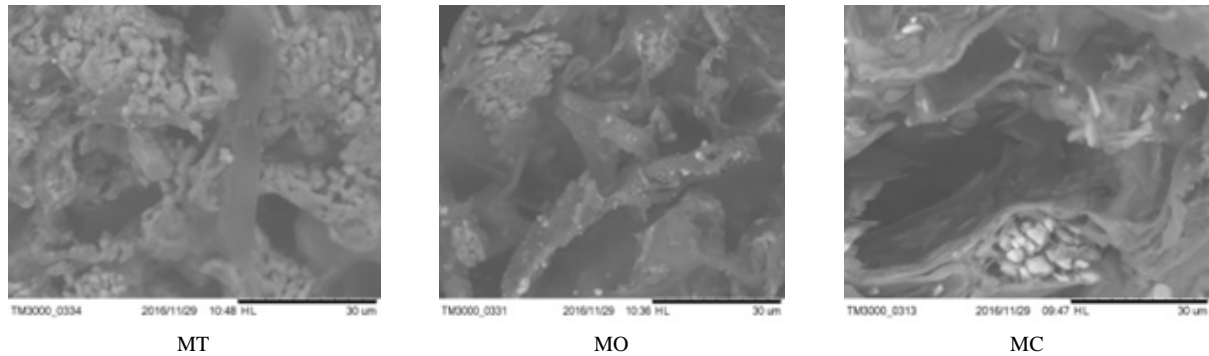


Fig. 2. Microstructure of myofibrillar protein from trash fish at a magnification of 2 000× (MT – average for Sardine; MO – Orangefin ponyfish; and MC – Chacunda gizzard-shad)

3.1.7. Molecular weight of protein

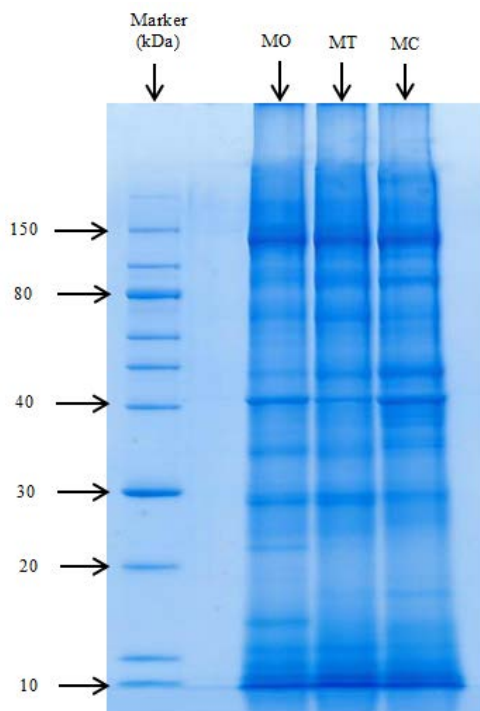


Fig. 3. Molecular weight (kDa) for fish myofibrillar protein from trash fish (MT – average for Sardine; MO – Orangefin ponyfish; and MC – Chacunda gizzard-shad; volume of marker = 5 µL and volume of a sample = 2.5 µL)

According to Figure 3, the myofibrillar protein of the fish has two major bands: 150 kDa and 40 kDa. In addition, the myofibrillar protein bands in Sardine fish (100, 60 to 80, 50), Orangefin ponyfish (100, 60 to 80, 50, 30 to 40, 15 to 20), and Chacunda gizzard-shad fish (100, 50, 30 to 40, 15 to 20) identified. Protein with a molecular weight of 140 kDa is C protein (a type of cod fish muscle

myofibrillar protein), while protein with a molecular weight of 165 kDa is M protein (Brenner, 2019).

Orangefin ponyfish and Chacunda gizzard-shad samples do not have the dominant band with a molecular weight of 60 kDa to 80 kDa. Troponin H has a molecular weight of 70 kDa to 78 kDa (Mukund and Subramaniam, 2020). The same samples also do not have a dominant band with a molecular weight of 30 kDa to 40 kDa, which can indicate myosin regulatory light chain at 24 kDa to 30 kDa, glutathione-S-transferase two at 32 kDa to 35 kDa, tropomyosin at 35 kDa to 37 kDa, and actin at 43 kDa (Mukund and Subramaniam, 2020). Moreover, Orangefin ponyfish and Chacunda gizzard-shad samples also have the dominant band with molecular weights of 15 kDa to 20 kDa. According to Yang *et al.* (2019), molecular weight in a range from 15 kDa to 20 kDa is attributed to troponin C (18 kDa), myosin essential light chain (18 kDa), and flight in (20 kDa).

3.1.8. Modification and comparison of myofibrillar protein

The myofibrillar protein from Orangefin ponyfish, Chacunda gizzard-shad, and Sardine cannot make a gel which might be caused by fish protein denaturation during the storage frozen before its isolation. It has been detected that storage frozen can negatively affect the protein content of surimi from threadfin bream (Setyawan *et al.*, 2017) and may induce degradation of gel strength (Zhang *et al.*, 2020). According to these results, protein modification is needed to improve gelling ability. It is expected that adding agar and carrageenan improves the gelation of myofibrillar protein from trash fish.

3.1.9. Protein color after modification

The color of modified myofibrillar protein from trash fish is described by the hue value (Binatha, 2016) that is compared to the hue of myofibrillar protein from cod fish (Table 2).

Table 2. Comparison of modified fish myofibrillar protein with cod fish myofibrillar protein

Modified fish myofibrillar protein	Parameters			
	Hue Value	Hardness (Nm ⁻²)	Cohesiveness (gfs ⁻¹)	Adhesiveness (gfmm)
CC: Carrageenan+MC	98.68	0.0005	0.35	879
CO: Carrageenan+MO	114.51	0.0006	0.62	963
CT: Carrageenan+MT	98.40	0.0004	0.58	570
AC: Agar+MC	103.40	0.0204	0.42	5.538
AO: Agar+MO	100.70	0.0197	0.37	5.303
AT: Agar+MT	93.79	0.0217	0.41	4.562
*)MCd: Cod fish myofibrillar protein	121.93	0.0713	0.26	116

*) Pamujiati *et al.*, 2020

Generally, the hue of modified myofibrillar protein from trash fish was lower than for protein from cod fish. However, Wei *et al.* (2012) stated that the hue value between 90 and 125 is attributed to yellow color, and, according to the table of hue conversion, all of the modified myofibrillar protein samples and cod fish myofibrillar protein have the same color – yellow that can be an advantage for surimi production from trash fish.

3.1.10. Texture after modification

The texture of modified myofibrillar protein has various results (Table 2). The texture is described by hardness, cohesiveness, and adhesiveness. Hardness is generally related to the texture of a product (Damat *et al.*, 2020). Hardness is defined as the necessary force to achieve deformation. Cohesiveness is defined as the ability of a material to receive stress. Adhesiveness means the need for force to overcome the attractive force between the surface of the material and the surface of the other material at their contact surface (Tee and Siow, 2017). Myofibrillar protein from cod has the highest hardness value (0.0713 Nm⁻²), whereas CT has the lowest detected hardness value (0.0004 Nm⁻²), which is affected by total protein content.

Protein content in cod fish is 16 % to 19 % (Oliveira *et al.*, 2012) – almost twice higher than in Orange-fin ponyfish (8.80 %), Chacunda gizzard-shadfish (9.30 %), and Sardine (10.10 %).

CO has the highest detected cohesiveness (0.62 gf s⁻¹), whereas MCd has the lowest (0.26 gf s⁻¹). On the other hand, AC has the highest adhesiveness (5.538 gf mm), whereas MCd has the lowest adhesiveness (116 gf mm). Moreover, gel texture depends on the fish species used for the preparation of surimi and the concentration of salt used for the protein solubilization. Also, temperature, time of heat treatment, and moisture content may play a role (de Oliveira *et al.*, 2017).

The addition of agar to myofibrillar protein increased hardness value remarkably, while carrageenan did not. Belova and Dyshlyuk (2016) stated that the gel from agar is characterized as rigid, fragile, and malleable, while the gel from carrageenan is predominantly elastic. Also, the cohesiveness values after adding carrageenan are higher than for the samples made with agar. According to Gao *et al.* (2016), combining soy protein isolate and carrageenan can increase the gel strength of salt-soluble meat protein caused by the molecular interaction of both. Adding carrageenan and protein isolate from legumes can improve the gel strength but may decrease the whiteness (Bashir *et al.*, 2017). On the other hand, the gel from carrageenan is more elastic. Therefore, adding agar resulted in a lower hardness value for myofibrillar protein from fish than at modification.

3.1.11. Microstructure after modification

Figure 4 shows modified AC (agar with protein from Chacunda gizzard-shad) has a more tightly porous structure than other samples. In contrast, modifying AO (agar with protein from Orange-fin ponyfish) leads to bigger pores and sprawls. Modified AT (agar with Sardine) has much smaller pores. A third of each sample creates a three-dimensional network with various densities. All myofibrillar protein trash fish modified by agar samples have different microstructures than MCd (cod fish myofibrillar protein). AC and AT have tightly porous structures, while MCd has bigger pores; AO tends to create a three-dimensional network, while MCd does not. The same thing happened in AT.

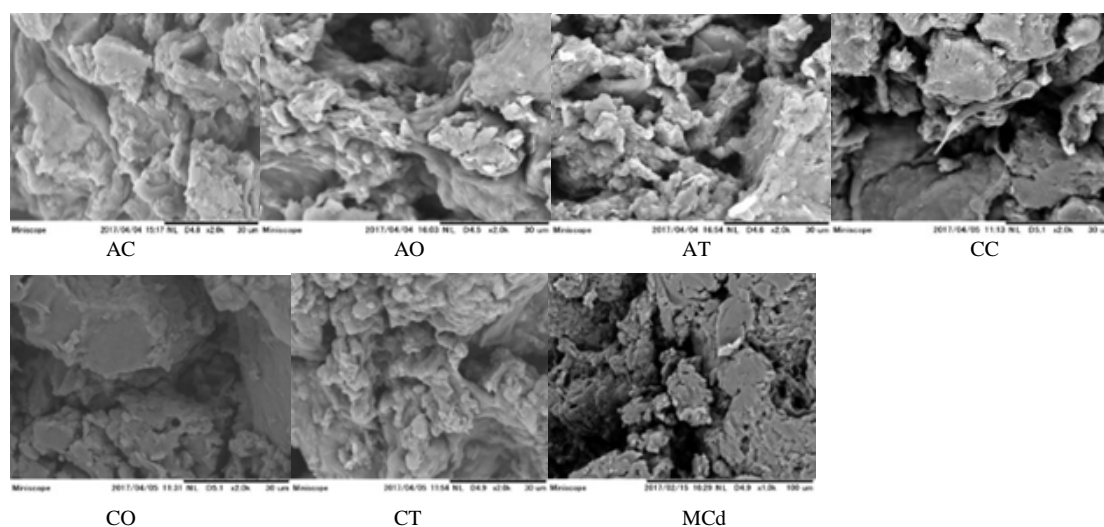


Figure 4. The microstructure of modified fish myofibrillar protein at a magnification of 2 000×, where AC means agar+MC; AO – agar+MO; AT – agar+MT; CC – carrageenan+MC; CO – carrageenan+MO; CT – carrageenan+MT; MCd – cod fish myofibrillar protein

According to the protein content, AC has the highest protein content (84.77 %), which affects the three-dimensional network formation. In general, the microstructure of fish myofibrillar protein changed by adding agar compared with the native microstructure of fish myofibrillar protein (Figure 4). Fish myofibrillar protein modified by adding carrageenan has a different microstructure. Modified CC (carrageenan with protein from Chacunda gizzard-shad) has a microstructure like a slab and large pores. The microstructure of CO (carrageenan with protein from Orangetin ponyfish) is tight and a little porous, and the surface tends to be a little surging. Modified CT (carrageenan with Sardine protein) has a porous structure and rough surface like a three-dimensional network. All myofibrillar protein samples modified by adding carrageenan have similarities with the microstructure of MCd. The microstructure of modified CC and CO has almost the same microstructure as MCd, but the microstructure of modified CT tends to create a three-dimensional network as for MCd. After adding carrageenan, the microstructure of fish myofibrillar protein tended to have a finer porous structure and create a three-dimensional network than the native microstructure of fish myofibrillar protein (Figure 4). The results are supported by the study of Liu *et al.*, (2023) who stated that the increase in carrageenan concentration up to 0.75 % may result in a finer gel matrix and also improve the compactness of protein gel network. Myofibrillar protein microstructure and texture are interrelated (Cheng *et al.*, 2014). Based on the results of this study, it can be concluded that the Chacunda gizzard-shad trash fish (*A. chacunda*) can be used as a raw material for various rich food products in protein and have high economic value.

4. Conclusions

The study revealed that the protein content of trash fish Chacunda gizzard-shad was higher (84.77 %) than for other samples. For this species, characteristics of myofibrillar protein were higher water-holding capacity (524.78 %) and more significant emulsion activity (8.85 mg^{-2}) than other samples. Sardine had a higher ability of oil holding capacity (620.35 %) and emulsion stability (4.58 h) than other fish myofibrillar protein samples, but Orangetin ponyfish had the highest whiteness value (78.42). Assessing the molecular weight of myofibrillar protein samples of trash fish, the dominant bands were at 150 kDa and 40 kDa, meaning that the protein band has a higher concentration than other bands.

Modifying fish myofibrillar protein by adding agar and carrageenan led to increased hardness values (up to 0.0217 N m^{-2}), although the value was still lower than for cod fish myofibrillar protein (0.0713 N m^{-2}). In addition, the hue value indicated that the color of all modified myofibrillar protein was the same – yellow. Based on the results of this study, it can be concluded that the Chacunda gizzard-shad trash fish (*A. chacunda*) can be used as a raw material for various rich food products in protein and have high economic value.

Acknowledgment

The authors would like to acknowledge the Ministry of Research, Technology and Higher Education, the Republic of Indonesia (166/SP2H/PPM/DRPM/III/2016–on behalf of Agustia Dwi Pamujiati), and the Faculty of Life and Environmental Sciences, Prefecture University of Hiroshima, Japan, for the support through the research grants, facilities, and joint supervision in the implementation of this research.

References

- Abdullah K, Saepul UA, Soegeng R, Suherman E, Susanto H, Setyobudi RH, Burlakovs J and Vincēviča-Gaile Z. 2020. Renewable energy technologies for economic development. *E3S Web Conf.*, **188(00016)**: 1–8. <https://doi.org/10.1051/e3sconf/202018800016>
- Adinurani PG, Liwang T, Salafudin, Nelwan LO, Sakri Y, Wahono SK and Hendroko R. 2013. The study of two stages anaerobic digestion application and suitable bio-film as an effort to improve bio-gas productivity from *Jatropha curcas* Linn capsule husk. *Energy Procedia* **32**: 84–89. <https://doi.org/10.1016/j.egypro.2013.05.011>
- Adinurani PG, Hendroko R, Wahono SK, Sasmito A, Nelwan LO, Nindita N and Liwang T. 2014. Optimization of concentration and EM4 augmentation for improving bio-gas productivity from *Jatropha curcas* Linn. capsule husk. *Int. J. Renew. Energy Dev.*, **3(1)**:73–78. <https://doi.org/10.14710/ijred.3.1.73-78>
- Adinurani PG. 2016. **Design and Analysis of Agrotorial data: Manual and SPSS**. Plantaxia, Yogyakarta, Indonesia
- Adinurani PG. 2022. **Non-Parametric Statistics (Agricultural Applications, Manuals, and SPSS)**. DeePublish, Yogyakarta, Indonesia
- Anam C, Harini N, Damat D, Wahyudi A, Witono Y, Kuswardhani N, Azar MAS, Anne O and Rachmawati D. 2021. Potential analysis of low economic value fish in Lamongan regency, East Java, Indonesia. *E3S Web Conf.*, **226(00011)**: 1–12. <https://doi.org/10.1051/e3sconf/202122600011>
- AOAC. 2005. **Official Method of Analysis**. 18th edition. Association of Officiating Analytical Chemists, Washington DC.
- Arfat YA and Benjaku S. 2012. Gelling characteristics of surimi from yellow stripe trevally (*Selaroides leptolepis*). *Int. Aquat. Res.*, **4**:5; 1–13.
- Bashir KMI, Kim JS, An JH, Sohn JH, and Choi JS. 2017. Natural food additives and preservatives for fish-paste products: A review of the past, present, and future states of research. *J. Food Qual.*, **9675469**:1–31. <https://doi.org/10.1155/2017/9675469>
- Belova DD and Dyshlyuk LS. 2016. The study of natural polysaccharides: Organoleptic, physical, chemical, microbiological properties, and thermodynamic characteristics of aqueous solutions. *Science Evolution*, **1(1)**: 72–79. <https://doi.org/10.21603/2500-1418-2016-1-1-72-79>
- Binatha C. 2016. Hue saturation value (HSV) color space for content-based image retrieval. *Int. J. Eng. Res. Technol.*, **5(4)**: 119–123.
- Bücker F, Marder M, Peiter MR, Lehn DN, Esquerdo VM, de Almeida Pinto LA and Konrad O. 2020. Fish waste: An efficient alternative to biogas and methane production in an anaerobic mono-digestion system. *Renew. Energy*, **147(1)**: 798–805. <https://doi.org/10.1016/j.renene.2019.08.140>

- Burlakovs J, Vincevica-Gaile Z, Bisters V, Hogland W, Kriipsalu M, Zekker I, Setyobudi RH, Jani Y, and Anne O. 2022. Application of anaerobic digestion for biogas and methane production from fresh beach-cast biomass. Proceedings EAGE GET 2022 – 3rd Eage Global Energy Transition, The Hague, Netherlands. <https://doi.org/10.3997/2214-4609.202221028>
- Brenner T. 2019. Aggregation behavior of cod muscle proteins. Ph.D. Thesis. Department of Chemistry Faculty of Physical Sciences the University of Iceland Reykjavík, Iceland.
- Cheng JH, Sun DW, Han Z and Zeng XA. 2014. Texture and structure measurements and analyses for evaluating fish and fillet freshness quality: A review. *Compr. Rev. Food Sci. Food Saf.*, **13**(1): 52–61. <https://doi.org/10.1111/1541-4337.12043>
- Coppola D, Lauritano C, Esposito FP, Riccio G, Rizzo C and de Pascale D. 2012. Fish waste: From problem to a valuable resource. *Mar Drugs*, **19**(2): 1–39. <https://doi.org/10.3390/md19020116>
- Cropotova J, Mozuraityte R, Standal IB, Szulecka O, Kulikowski T, Mytlewski A and Rustad T. 2021. Sensory and physicochemical quality characteristics of haddock fish cake enriched with Atlantic Mackerel. *Food Technol. Biotechnol.*, **59**(1): 4–15. <https://doi.org/10.17113/ftb.59.01.21.6695>
- Damat D, Setyobudi RH, Soni P, Tain A, Handjani H and Chasanah U. 2020. Modified arrowroot starch and glucomannan for preserving physicochemical properties of sweet bread. *Cienc. e Agrotecnologia*, **44**:e014820:1–9. <https://doi.org/10.1590/1413-7054202044014820>
- Damat D, Setyobudi RH, Burlakovs J, Gaile ZV, Siskawardani DD, Anggriani R and Tain A. 2021. Characterization properties of extruded analog rice developed from arrowroot starch with addition of seaweed and spices. *Sarhad J. Agric.*, **37**(Special issue 1):159–170. <https://dx.doi.org/10.17582/journal.sja/2021.37.s1.159.170>
- Dale HF, Madsen L and Lied GA. 2021. Fish-derived proteins and their potential to improve human health. *Nutr. Rev.*, **77**(8): 572–583. <https://doi.org/10.1093/nutrit/nuz016>
- Dara PK, Geetha A, Mohanty U, Raghavankutty M, Mathew S, Nagarajaro RC and Rangasamy A. 2021. Extraction and characterization of myofibrillar proteins from different meat sources: A comparative study. *J. Bioresour. Bioprod.*, **6**(4): 367–378. <https://doi.org/10.1016/j.jobab.2021.04.004>
- de Castro RJS, Domingues MAF, Ohara A, Okuro PK, dos Santos JG, Brexó RP and Sato HH. 2017. Whey protein as a key component in food systems: Physicochemical properties, production technologies, and applications, *Food Struct.*, **14**: 17–29. <https://doi.org/10.1016/j.foostr.2017.05.004>
- Deng X, Ma Y, Lei Y, Zhu X, Zhang L, Hu L, Lu S, Guo X, and Zhang J. 2021. Ultrasonic structural modification of myofibrillar proteins from Coregonus peled improves emulsification properties. *Ultrason Sonochem.*, **76**(105659): 1–10. <https://doi.org/10.1016/j.ultsonch.2021.105659>
- de Oliveira DL, Grassi TLM, Santo EFDE, Cavazzana JF, Marcos MTDS and Ponsano EHG. 2017. Washings and cryoprotectants for the production of Tilapia surimi, *Food Sci. Technol. Campinas*, **37**(3): 432–436. <http://dx.doi.org/10.1590/1678-457X.18716>
- du Preez R, Paul N, Mouatt P, Maizoub ME, Thomas T, Panchal SK and Brown L. 2020. Carrageenans from the red seaweed *Sarconema filiform* attenuate symptoms of diet-induced metabolic syndrome in rats, *Mar. Drugs*, **18**(2): 1–26. <https://doi.org/10.3390/md18020097>
- Erbay EA and Yeşilsu AF. 2021. Fish protein and its derivatives: Functionality, biotechnology, and health effects. *Aquatic Food Studies*, **1** (1)AFS13: 1–8. <https://doi.org/10.4194/AFS-13>
- Fowler MR and Park JW. 2015. Effect of salmon plasma protein on pacific whiting surimi gelation under various ohmic heating conditions. *LWT - Food Sci. Technol.*, **61**(2): 309–315. <http://dx.doi.org/10.1016/j.lwt.2014.12.049>
- Gao X, Hao X, Xiong G, Gea Q, Zhanga W, Zhoua G and Yueb X. 2016. Interaction between carrageenan/soy protein isolates and salt-soluble meat protein. *Food Bioprod. Process.*, **100**: 47–53. <https://doi.org/10.1016/j.fbp.2016.06.014>
- Gao X, Xiea Y, Yin T, Hua Y, Youa J, Xionga S and Liua R. 2021. Effect of high-intensity ultrasound on gelation properties of silver carp surimi with different salt contents. *Ultrason. Sonochem.*, **70**(105326): 1–8. <https://doi.org/10.1016/j.ultsonch.2020.105326>
- Gao Y, Fukushima H, Deng S, Jia R, Osako K, and Okazaki E. 2018. Effect of emulsifying stability of myofibrillar protein on the gel properties of emulsified surimi gel. *Food Sci. Nutr.*, **6**(5): 1229–1237. <https://doi.org/10.1002/fsn3.663>
- Harnkarnsujarit N, Kawai K and Suzuki T. 2015. Effects of freezing temperature and water activity on microstructure, color, and protein conformation of freeze-dried bluefin Tuna (*Thunnus orientalis*). *Food Bioprocess Technol.*, **8**(4): 916–925. <https://doi.org/10.1007/s11947-014-1460-1>
- Hasan MM, Sood V, Erkinbaev C, Paliwal J, Suman S and Rodas-Gonzalez A. 2021. Principal component analysis of lipid and protein oxidation products and their impact on color stability in bison longissimus lumborum and psoas major muscles. *Meat Sci.*, **178**: 1–11. <https://doi.org/10.1016/j.meatsci.2021.10852>
- Hendroko R, Wahono SK, Adinurani PG, Salafudin, Yudhanto AS, Wahyudi, and Dohong S. 2014. The study of optimization hydrolysis substrate retention time and augmentation as an effort to increase biogas productivity from *Jatropha curcas* Linn. capsule husk at two-stage digestion. *Energy Procedia*, **47**: 255–262. <https://doi.org/10.1016/j.egypro.2014.01.222>
- Kafle G K and Kim SH. 2012. Evaluation of the biogas productivity potential of fish waste: A lab-scale batch study. *J. Biosyst. Eng.*, **37**(5): 302–313. <https://doi.org/10.5307/JBE.2012.37.5.302>
- Leha MA and Moniharapon A. 2013. Fortification of trash fish surimi for the quality of wet noodles. *E-Jurnal Ambon Industrial Standardization Research and Industry Center*, **9**(1): 14–22.
- Li J, Yang Z, Li Z, Wu L, Shen J, Wang J and Wang P. 2022. Effects of tea polyphenol palmitate existing in the oil phase on the stability of myofibrillar protein O/W emulsion, *Foods*, **11**(1326): 1–13. <https://doi.org/10.3390/foods11091326>
- Li S, Lin S, Jiang P, Bao Z, Li S and Sun N. 2022. Insight into the gel properties of Antarctic krill and Pacific white shrimp surimi gels and the feasibility of polysaccharides as texture enhancers of Antarctic krill surimi gels, *Foods*, **11**(2917): 1–17. <https://doi.org/10.3390/foods11162517>
- Liu Q, Lin Z, Chen X, Chen J, Wu J, Chen H and Zeng X. 2022. Characterization of structures and gel properties of ultra-high-pressure treated-myofibrillar protein extracted from mud carp (*Cirrhinus molitorella*) and quality characteristics of heat-induced sausage products. *LWT - Food Sci. Technol.*, **165**(113691): 1–9. <https://doi.org/10.1016/j.lwt.2022.113691>
- Liu Y, Lei Y, Kang X, Ouyang H, Li X, Yu X, Gu Q and Li S. 2023. Walnut protein isolate-κ-carrageenan composite gels improved with synergetic ultrasound-transglutaminase: gelation properties and structure. *Gels*, **9**(91): 1–17. <https://doi.org/10.3390/gels9020091>
- Mannino MH, Patel RS, Eccardt AM, Janowiak BE, Wood DC, He F and Fisher JS. 2020. Reversible oxidative modifications in myoglobin and functional implications. *Antioxidants*, **9**(549): 1–22. <https://doi.org/10.3390/antiox9060549>

- Millan JC, Sarabia JLH, Carrera NR and Santos YQ. 2021. Hospital nutrition fish protein: Nutrition and innovation. *Nutrición Hospitalaria*, **38(2)**: 35–39. <http://dx.doi.org/10.20960/nh.03795>
- Mukund K and Subramaniam S. 2020. Skeletal muscle: A review of molecular structure and function, in health and disease. *Wiley Interdiscip Rev Syst Biol Med*, **12(1)**: e1462. <http://dx.doi.org/10.1002/wsbm.1462>
- Nguyen DQ, Mounir S and Allaf K. 2015. Functional properties of water holding capacity, oil holding capacity, wettability, and sedimentation of swell-dried soybean powder. *Sch. J. Eng. Tech.*, **4B**: 402–412
- Najafian L and Babji AS. 2015. Isolation, purification, and identification of three novel antioxidative peptides from patin (*Pangasius sutchi*) myofibrillar protein hydrolysates. *LWT*, **60(1)**: 452–461. <https://doi.org/10.1016/j.lwt.2014.07.046>
- Niu F, Ju M, Du Y, WANG M, Han X, Chen Q, Zhang B, Ritzoulis C and Pan W. 2022. Changes in properties of nano protein particles (NPP) of fish muscle stored at 4 °C and its application in food quality assessment. *LWT*, **155(112968)**: 1–10. <https://doi.org/10.1016/j.lwt.2021.112968>
- Novian U. 2005. Characteristics of goldband goat-fish (*Upeneus* sp.) dried myofibril extracted using papain enzyme with heat press method. Undergraduate Thesis. Faculty of Agriculture Technology, University of Jember, Indonesia.
- Oliveira H, Pedro S, Nunes ML, Costa R and Vaz-Pires P. 2012. Processing of salted cod (*Gadus* spp.): A Review. *Compr. Rev. Food Sci. Food Saf.*, **11(6)**: 546–564. <https://doi.org/10.1111/j.1541-4337.2012.00202.x>
- Pamujati AD., Witono Y and Lisanty N. 2020. Preparation and characteristics of pacific codfish (*Gadus macrocephalus*) myofibril for surimi. *Food ScienTech Journal*, **2(1)**: 25–30. <https://doi.org/10.33512/fsj.v2i1.8346>
- Park JW. 2012. Surimi and fish protein isolate, In Granata, L.A, Flick, G.J. Jr. and Martin, R.E. (Eds), **Chapter 10, The Seafood Industry: Species, Products, Processing, and Safety**, Second Edition. Blackwell Publishing Ltd. Hoboken, New Jersey, USA, pp. 118–127. <https://doi.org/10.1002/9781118229491.ch10>
- Petcharat T and Benjakul S. 2017. Effect of gellan and calcium chloride on properties of surimi gel with low and high setting phenomena. *RSC Adv.*, **7(83)**: 52423–52434.
- Phung AS, Bannenberg G, Vigor C, Reversat G, Oger C, Roumain M, Galano JM, Durand T, Muccioli GG, Ismail A and Wang SC. 2020. Chemical compositional changes in over-oxidized fish oils. *Foods*, **9(1501)**: 1–31. <https://doi.org/10.3390/foods9101501>
- Prosapio V and Lopez-Quiroga E. 2020. Freeze-drying technology in foods. *Foods*, **9(920)**: 1–3. <https://doi.org/10.3390/foods9070920>
- Raissa DV, Setiawan RP and Rahmawati D. 2014. Identification of indicators influencing sustainability of minapolitan area in Lamongan regency. *Procedia Soc Behav Sci.*, **135**: 167–171. <https://doi.org/10.1016/j.sbspro.2014.07.342>
- Rudovica V, Rotter A, Gaudêncio SP, Novoveská L, Akgül F, Akslen-Hoel LK, Alexandrino DAM, Anne O, Arbidans L, Atanassova M, Beldowska M, Beldowski J, Bhatnagar A, Bikovens O, Bisters V, Carvalho MF, Catalá TS, Dubnika A, Erdoğan A, Ferrans L, Haznedaroglu BZ, Setyobudi RH, Graca B, Grinfelde I, Hogland W, Ioannou E, Jani Y, Kataržytė M, Kikionis S, Klun K, Kotta J, Kriipsalu M, Labidi J, Bilela LL, Martínez-Sanz M, Oliveira J, Ozola-Davidane R, Pilecka-Ulcugaceva J, Pospiskova K, Rebours C, Roussis V, López-Rubio A, Safarik I, Schmieder F, Stankevica K, Tamm T, Tasdemir D, Torres C, Varese GC, Vincevica-Gaile Z, Zekker I and Burlakovs J. 2021. Valorization of marine waste: Use of industrial by-products and beach wrack towards the production of high added-value products. *Front. Mar. Sci.*, **8(723333)**: 1–39. <https://doi.org/10.3389/fmars.2021.723333>
- Seighalani FZB, Bakar J, Saari N and Khoddami A. 2017. Thermal and physicochemical properties of red tilapia (*Oreochromis niloticus*) surimi gel as affected by microbial transglutaminase. *Anim. Prod. Sci.*, **57**: 993–1000. <http://dx.doi.org/10.1071/AN15633>
- Setyawan F, Santoso H and Syaui A. 2017. Surimi protein of Kurisi fish (*Nemipterus hexodon*) due to the effect of frozen storage and its contribution in protein sufficiency fulfillment. *Biosaintropis*, **3(1)**: 31–38.
- Setyobudi RH, Yandri E, Atoum MFM, Nur SM, Zekker I, Idroes R, Tallei TE, Adinurani PG, Vincēviča-Gaile Z, Widodo W, Zalizar L, Van Minh N, Susanto H, Mahaswa RK, Nugroho YA, Wahono SK, and Zahriah Z. 2021. A healthy-smart concept as the standard design of kitchen waste biogas digester for urban households. *Jordan J. Biol. Sci.*, **14(3)**: 613–620. <https://doi.org/10.54319/jjbs/140331>
- Shaviklo AR. 2015. Development of fish protein powder as an ingredient for food applications: A review. *J. Food Sci. Technol.*, **52(2)**: 648–661. <https://doi.org/10.1007/s13197-013-1042-7>
- Shui S, Yao H, Jiang Z, Benjakul S, Aubourg SP and Zhang B. 2021. The differences of muscle proteins between neon flying squid (*Ommastrephes bartramii*) and jumbo squid (*Dosidicus gigas*) mantles via physicochemical and proteomic analyses. *Food Chem.*, **364(130374)**. <http://dx.doi.org/10.1016/j.foodchem.2021.130374>
- Susanto H, Uyun AS, Setyobudi RH, Nur SM, Yandri E, Burlakovs J, Yaro A, Abdullah K, Wahono SK, and Nugroho YA. 2020. Development of moving equipment for fishermen's catches using the portable conveyor system. *E3S Web of Conf.*, **190(00014)**: 1–10. <https://doi.org/10.1051/e3sconf/202019000014>
- Tahergorabi R, Hosseini SV and Jaczynski J. 2011. Seafood proteins. In: Phillips GO and Williams PA (Eds.), **Hand Book of Food Proteins**. Woodhead Publishing Limited., Cambridge, United Kingdom, pp.116–149.
- Tee ET and Siow LF. 2017. Effect of tapioca and potato starch on the physical properties of frozen Spanish mackerel (*Scomberomorus guttatus*) fish balls. *Int. Food Res. J.*, **24(1)**: 182–190.
- Ulloa JA, Barbosab MCV, Vazquez JAR, Ulloa PR, Ramírez JC, Carrillo YS and Torrese LG. 2017. Production, physicochemical and functional characterization of a protein isolate from jackfruit (*Artocarpus heterophyllus*) seeds. *CYTA - J. Food*, **15(4)**: 497–507. <http://dx.doi.org/10.1080/19476337.2017.1301554>
- Wei S, Ou L, Ming L and John H. 2012. Optimization of food expectations using product color and appearance. *Food Qual Prefer*, **23(1)**: 49–62. <https://doi.org/10.1016/j.foodqual.2011.07.004>
- Wu ZW, Zou XL, Yao PL, Kang ZL and Ma HJ. 2022. Changes in gel characteristics, rheological properties, and water migration of PSE meat myofibrillar proteins with different amounts of sodium bicarbonate. *Molecules*, **27(8853)**: 1–9. <https://doi.org/10.3390/molecules27248853>
- Xu Y, Song M, Xia W and Jiang Q. 2019. Effects of freezing method on water distribution, microstructure, and taste active compounds of frozen channel catfish (*Ictalurus punctatus*). *J. Food Process Eng.*, **42(1)**: 1–9. <https://doi.org/10.1111/jfpe.12937>

Yang F, Jia S, Liu J, Gao P, Yu D, Jiang Q, Xu Y, Yu P, Xia W and Zhan X. 2019. The relationship between degradation of myofibrillar structural proteins and texture of superchilled grass carp (*Ctenopharyngodon idella*) fillet, *Food Chem.*, **301(125278)**. <https://doi.org/10.1016/j.foodchem.2019.12527>

Zhang L, Li Q, Hong H and Luo Y. 2020. Prevention of protein oxidation and enhancement of gel properties of silver carp (*Hypophthalmichthys molitrix*) surimi by addition of protein hydrolysates derived from surimi processing by-products, *Food Chem.*, **316(126343)**. <https://doi.org/10.1016/j.FOODCHEM.2020.126343>

Zhang Z, Yang Y, Tang X, Chen Y and You Y. 2015. Effects of ionic strength on chemical forces and functional properties of a heat-induced myofibrillar protein gel. *Food Sci. Technol. Res.*, **21(4)**: 597–605. <https://doi.org/10.3136/fstr.21.597>

Biogenic Synthesis of Chitosan/Silver Nanocomposite by *Escherichia coli* D8 (MF062579) and its Antibacterial Activity

Mohamed M. El-Zahed^{*}, Zakaria A. M. Baka, Mohamed I. Abou-Dobara, and Ahmed K.A. El-Sayed

¹ Department of Botany and Microbiology, Faculty of Science, Damietta University, New Damietta, Egypt.

Received: October 18, 2022; Revised: December 12, 2022; Accepted: December 15, 2022

Abstract

Silver nanomaterials are usually applied as antimicrobial agents; however, they can cause toxic effects on human health. The current investigation was performed to study the combined effects of chitosan and silver nanoparticles (AgNPs) using the cell-free supernatant of *Escherichia coli* (MF062579). The produced chitosan/silver nanocomposite (CS/AgNC) showed good antibacterial activity and high stability. The biosynthesized CS/AgNC contained homogeneous spherical AgNPs with an average size of ~12.3 nm and a net surface charge of +30.9 ± 3.2 mV. CS/AgNC revealed a good minimum inhibitory concentration (MIC) result against Gram-negative (G-ve, *E. coli*) and Gram-positive (G+ve, *Bacillus cereus*) bacteria with inhibition ratios of 80.7% and 75.5%, respectively. Nanocomposite-treated cells displayed complete lysis of the bacterial cell, a low amount of DNA, and cell membrane and wall disruption. Glutamate dehydrogenase (GDH) and malate dehydrogenase (MDH) activities of tested bacterial strains were demonstrated using spectrophotometry and electrophoresis on a non-denaturing acrylamide gel. In CS/AgNC-treated strains, enzyme production and activity were fewer than in untreated strains. The obtained results suggested that CS/AgNC seems to be more effective against G-ve than G+ve bacteria.

Keywords: silver, chitosan, nanocomposite, biosynthesis, *Escherichia coli*, antibacterial

1. Introduction

Silver (Ag) is usually applied as a disinfectant in medical equipment, antimicrobial wound dressings, food containers, and other industrial applications (Natsuki *et al.*, 2015; Zhang *et al.*, 2016; Kate *et al.*, 2020). Continuous physical and chemical studies competed to synthesize new antimicrobial silver nanoparticles (AgNPs) as soon as nanotechnology was discovered, which proved that the properties of nanoscale materials can be very different from those at a larger scale (Bayda *et al.*, 2020). However, earlier techniques were expensive, risky, challenging, and potentially harmful to both humans and the environment. Recent advances in the field of nanobiotechnology, sometimes known as "biological techniques," offer novel, simple, and quick instruments for producing AgNPs that are affordable and environmentally benign (Iravani *et al.*, 2014). Microorganisms like bacteria, fungi, yeast, and algae are frequently used in biological approaches for producing AgNPs because of how easy they are to cultivate, how quickly they develop, how diverse they are, and how well they adapt to various environmental circumstances. To bio-reduce the silver ions (Ag⁺) to AgNPs, one of the biological agents, bacteria, responded differently with various metal solutions (Tsekhmistrenko *et al.*, 2020; Saravanan *et al.*, 2021). The production of nanoparticles (NP) involves a variety of reducing

biological elements, including proteins, enzymes, peptides, and pigments. Some bacteria can biosynthesize nanoparticles using either extracellular or intracellular methods with different efficiency, size, and shape. However, intracellular methods require more expensive and time-consuming extraction and additional purifying processes (Nguyen *et al.*, 2022, Singh *et al.*, 2020). In order to produce AgNPs and silver nanocomposites with special features, *Escherichia coli* is employed as one of the best nanofactories (El-Shanshoury *et al.*, 2011, Baltazar-Encarnación *et al.*, 2019, El-Zahed *et al.*, 2021b). Currently, the aggregation, agglomeration, and biocompatibility of nanomaterials hinder their applications in different biomedical fields (Restrepo and Villa, 2021). The combination of AgNPs with a polymer matrix could be considered as one of the most important solutions proposed to overcome these problems (Fan *et al.*, 2022).

The most prevalent and least expensive natural biopolymer, chitosan (CS), has surface functional groups that can bind with Ag⁺ and other heavy metal ions. CS was used as an antibacterial agent in medicines, biosensing devices, diagnostics, etc. (Youssef & Hashim, 2020). However, a variety of parameters, including concentration, bacterial species, pH, and others, can affect the antibacterial action of CS (Menazea *et al.*, 2020; Badi'ah, 2021). Combination between AgNPs and CS will enhance the composite biological, chemical, and physical qualities, including stability, catalytic activity, optical, and

^{*} Corresponding author. e-mail: : mohamed.marzouq91@du.edu.eg.

mechanical capabilities. Chitosan/silver nanocomposite (CS/AgNC) has recently been used in antimicrobial formulations against pathogens that are harmful to people, animals, and plants (Namasivayam *et al.*, 2022). CS/AgNC nanocomposite showed antibacterial activity against methicillin-resistant *Staphylococcus aureus* and found a high bactericidal impact at minimum inhibitory concentrations (MIC) of 0.25, 0.45, and 0.15 mg/mL for AgNPs, CS, and CS/AgNC solutions, respectively (Hassanen and Ragab, 2021). Additionally, Tripathi *et al.*, (2014) reported using the agar diffusion method that the composite had antibacterial efficacy against *Pseudomonas aeruginosa*, *E. coli*, and *Bacillus subtilis*. The molecular analysis of CS/antibacterial AgNC's action is still very evident and is of considerable interest for both fundamental research and the creation of pharmaceutical medicines.

Thus, AgNPs were prepared using biological synthesis, integrated into the polymeric matrix of CS, and tested *in vitro* for antibacterial activity. To our knowledge, this is the first study to use glutamate dehydrogenase (GDH) and malate dehydrogenase (MDH) as models for investigating the structure-function relationships in proteins of the CS/AgNC-treated bacteria.

2. Experimental methods

2.1. The bacterial strains and culture conditions

The bacterial strains of *Bacillus cereus* ATCC 6633 and *E. coli* ATCC 25922 were obtained from the American Type Culture Collection (ATCC), USA. While the *E. coli* D8 (MF062579) strain was obtained from the Microbiology Laboratory Culture Collection (MLCC), Egypt. All bacterial strains were cultivated on tryptic soy agar (TSA, Sigma-Aldrich, USA) for 48 h at 37°C.

2.2. Synthesis of chitosan/silver nanocomposite

The biological preparation of AgNPs was carried out according to El-Dein *et al.* (2021). Briefly, 4 ml of 0.001 M AgNO₃ (Panreac Quimica S.L.U, Spain) and 4 ml of the cell-free supernatant of *E. coli* D8 (MF062579) were mixed, adjusted to pH 7, and submitted to the sunlight at room temperature (25°C in our case) until the appearance of a dark brown suspension showing AgNPs formation. Then, the suspension was centrifuged at 10,000 rpm twice for 10 minutes each (Eppendorf 3H24RI intelligent high-speed refrigerated centrifuge, Herexi Instrument & Equipment Company, China), and the residue was rinsed thrice with distilled H₂O to eradicate excess impurities, and then centrifuged and dried. A solution of 1% CS (w/v, MW 50–190 KDa, deacetylation degree: ≥85%, Sigma-Aldrich, USA) was prepared in 1% acetic acid (pH 8), mixed with a solution of AgNPs (596 µg/ml) in a ratio of 1:1 v/v, and then exposed it to ultrasonication for 1 hr at 25°C by using an ultrasonic bath (Delta-sonic 920 N°484, Meaux, France, 28 kHz). A jacketed vessel containing circulated, cooled distilled water was used to maintain the temperature at 25°C (Price *et al.* 1995). After the ultrasonication time, the product was kept on a magnetic stirrer/hot plate (IKA, Germany) at 70°C with constant stirring (500 rpm) for 90 minutes. Finally, the pH of the CS/AgNC solution was adjusted to 7.5 with 0.001 M NaOH by using a pH-meter (Jenco Electronics Ltd., Micro-Computer pH Meter Model 6209), centrifuged at

10,000 rpm for 10 minutes, and then freeze-dried (Baka *et al.*, 2019).

2.3. Characterization of chitosan/silver nanocomposite

The spectrum of AgNPs formation was monitored using UV-Vis spectrophotometry (Beckman DU-40). CS/AgNC were analyzed using the Malvern Zetasizer Nano-ZS90 (Malvern, UK), X-ray diffractometer (Shimadzu, Japan), and transmission electron microscopy (TEM, JEM-2100, Japan).

2.4. Silver nanoparticles release from CS/AgNC

The release of Ag⁺ from CS was tested according to El-Zahed *et al.* (2021a). 50 µg/ml of AgNPs solution was prepared, added to dialysis tubes, and then submerged within 200 ml of double distilled water and incubated in a shaking incubator at 37°C/100 rpm (LSI-3016R, Daihan Lab Tech Co., Ltd., Namyangju, Kyonggi, South Korea). The released Ag⁺ was evaluated using atomic absorption spectroscopy (PerkinElmer, UK) (Sotiriou *et al.*, 2012).

The CS/AgNC solubility was investigated in several polar and non-polar solvents, including water, ethanol, methanol, dimethylformamide (DMF), acetone, n-butyl alcohol, toluene, and hexane (Sigma-Aldrich, USA). The Zeta average size (Zavg) and polydispersity index (PDI) were estimated using the Malvern Zetasizer.

2.5. In vitro antibacterial test using agar well diffusion method

Antibacterial experiments were conducted according to the Clinical and Laboratory Standards Institute (CLSI, Clinical and Laboratory Standards, 2007). 100 µl of each tested bacterial suspension (2.5×10^3 CFU.mL⁻¹); *B. cereus* ATCC 6633 and *E. coli* ATCC 25922 were added to cold melted Mueller-Hinton agar (MHA) medium (Oxoid, UK) at the time of pouring the plates in triplicate. After solidifying the agar plates, 100 µl of a unified concentration (150 µg/ml) of AgNO₃, CS, AgNPs, CS/AgNC and penicillin (as a positive control) was added separately into punched holes (5 mm) under aseptic conditions and incubated at 37°C for 48 hr. Then, the inhibition zones of bacterial growths were measured (mm).

2.6. Minimum inhibitory concentration

The MIC tests for treated bacteria were evaluated according to CLSI (Clinical Laboratory Standards, 2017). Different concentrations (1-30 µg/ml) of AgNO₃, CS, AgNPs and CS/AgNC were added into Mueller-Hinton broth (MHB) medium flasks inoculated by 2.5×10^3 CFU.mL⁻¹ tested bacteria and incubated at 37°C and 150 rpm for 24 hr. Untreated bacteria and penicillin were used as controls. Bacterial growth rates were measured spectrophotometrically (λ : 600 nm) against controls. The percentage growth inhibition was evaluated according to the formula: % growth inhibition = (OD_c-OD_t) × 100, where OD_c; the optical density of broth media (negative control) and OD_t is the optical density of CS/AgNC-treated bacteria.

2.7. Ultrastructural analysis of treated bacteria

The bacterial cell cultures were exposed to CS/AgNC (MIC value) for 2 hr at 37°C in MHB. Bacterial cells were washed, fixed with 2.5% glutaraldehyde and 0.1 M cacodylate buffer, pH 7, and sent to the Central Laboratory, Electron Microscope Unit, Faculty of

Agriculture, Mansoura University, Egypt, for observing and studying their ultrastructure.

2.8. Protein estimation

The bacterial protein concentration of untreated and CS/AgNC-treated strains was estimated according to Kruger (2009) method. Briefly, the bacterial strains; *B. cereus* ATCC 6633 and *E. coli* ATCC 25922 were subjected to MIC, 6 µg/ml of CS/AgNCs for 2 hr at 37°C. After that, they were harvested using a tabletop centrifuge (Centrifuge Model 800 by Xiangshui. FADA medical apparatus factory, China) for 20 minutes at 5000 rpm. The bacterial pellets were washed three times in sterile distilled water after the supernatants were discarded. The pellets were centrifuged at 10,000 rpm at 4°C after being sonicated for one minute at 750 W, 20 kHz. The supernatants were put into fresh, sterile eppendorf tubes for the upcoming assays and kept at 4°C. Additionally, untreated bacterial samples were included. The Bradford method was used to evaluate the concentration of bacterial proteins (Bradford, 1976).

2.9. Estimation of some of dehydrogenase activity

The GDH and MDH activities of the untreated and CS/AgNC-treated bacteria were assayed according to Robb *et al.* (2001) and Yoshida, (1965), respectively. Briefly, the activity of the GDH enzyme was measured spectrophotometrically by evaluation of the reduction rate of NAD⁺ in a reaction mixture of 0.2 ml of NAD⁺ (2 mg/ml), 0.1 ml of 1 M sodium glutamate (Oxoid, UK), 2.6 ml of 0.5 M phosphate buffer (pH 7.0) (Oxoid, UK) and 0.1 ml of bacterial enzyme solution. For the oxidation of L-malate; 2.5 ml of 0.5 M phosphate buffer (pH 7.0), 0.1 ml of 0.1 M sodium malate (Oxoid, UK), 0.1 ml of 10 mM NAD⁺, 0.1 ml of enzyme solution, and water to a final volume of 3.0 ml are placed in a quartz cuvette. By measuring optical density at 340 nm, the enzymatic processes were spectrophotometrically quantified (UV-1100, Shanghai Mapada Instruments Co., Ltd., Shanghai, China). A mole of NAD⁺ reduced to NADH for each unit time at 25°C was used to measure enzyme activity. The number of enzyme units per microgram of protein is how specific activity is measured.

2.10. Total Soluble protein profile by SDS-PAGE

SDS-PAGE was studied to clarify the protein profiles of untreated and CS/AgNC-treated *B. cereus* ATCC 6633 and *E. coli* ATCC 25922, according to Laemmli, (1970). Bacterial proteins were analyzed by SDS-PAGE (12% w/v polyacrylamide gel with 6% w/v stacking gel) at 150 mV in a miniprotein® 3 electrophoresis cell (BioRad, USA). Protein detection was typically done using Coomassie blue staining.

2.11. Isozymal profiles for MDH and GDH using native PAGE

Vertical PAGE was used. A 10% native polyacrylamide gel overlaid with a 6% polyacrylamide stacking gel was prepared using the electrode buffers according to Laemmli, (1970) without SDS. Electrophoresis was carried out at ~4°C (on an ice bath) with a constant voltage of 150 mV (about 2 hr). After electrophoresis, the gels were placed directly into substrate solutions for the visualization of specific activity. For GDH, 16.9 g of sodium glutamate was added to 100 ml of 0.5 M phosphate buffer, pH 7.0. About 5 ml of substrate solution and 60 mg of NAD⁺ were mixed well and completed into 100 ml by distilled water. For MDH, 1.34 g of L-malic acid was added to 4.9 ml of 2 M Na₂CO₃ and completed into 100 ml by distilled water. Then, 25 ml of phosphate buffer, 5 mL of substrate solution and 60 mg of NAD⁺ were mixed well and completed to 100 ml by distilled water. Then a staining solution (30 mg of nitroblue tetrazolium (NBT) and 2 mg of phenazine methosulphate (PMS)) was added into each enzymatic reaction mixture just before incubation in the dark at 37°C until a blue color appeared (Selander *et al.*, 1986). The gels were rinsed for 5 minutes in distilled water and proteins were fixed in glacial acetic acid/water (5%).

2.12. Statistical analysis

All the experiments were carried out in triplicate. Results (means ± standard deviation (SD)) were analyzed with ordinary one-way ANOVA tests (SPSS software, 18) with a statistically significant *P*-value < 0.05 (O'Connor, 2000).

3. Results

3.1. Synthesis and characterization of CS/AgNC

AgNPs physical-chemical properties were characterized. AgNPs caused a surface plasmon resonance (SPR) at ~424 nm, indicating a good dispersion of particles in the nanocolloids (Genç *et al.*, 2017, Figure 1A). Size distribution by intensity and by volume determined using dynamic light scattering (DLS) (Figure 1B) and Zeta potential (Figure 1E) results confirmed the monodispersity of the produced NPs (0.316 ± 0.11 PDI) and their positive net surface charge (+21 ± 1.9 mV). While the net surface charge of CS/AgNC was increased to +30.9 ± 3.2 mV (Figure 1D). The AgNPs XRD patterns showed characteristic diffraction peaks for Ag at 2θ = 32.25°, 38.25°, 46.3°, 57.6°, and 64.55° which resemble the crystallographic planes of (110), (111), (200), (210), and (220), respectively (Figure 1C). The TEM micrograph of AgNPs showed ~12.3 ± 2.3 nm uniform spherical particles (Figure 1F & G).

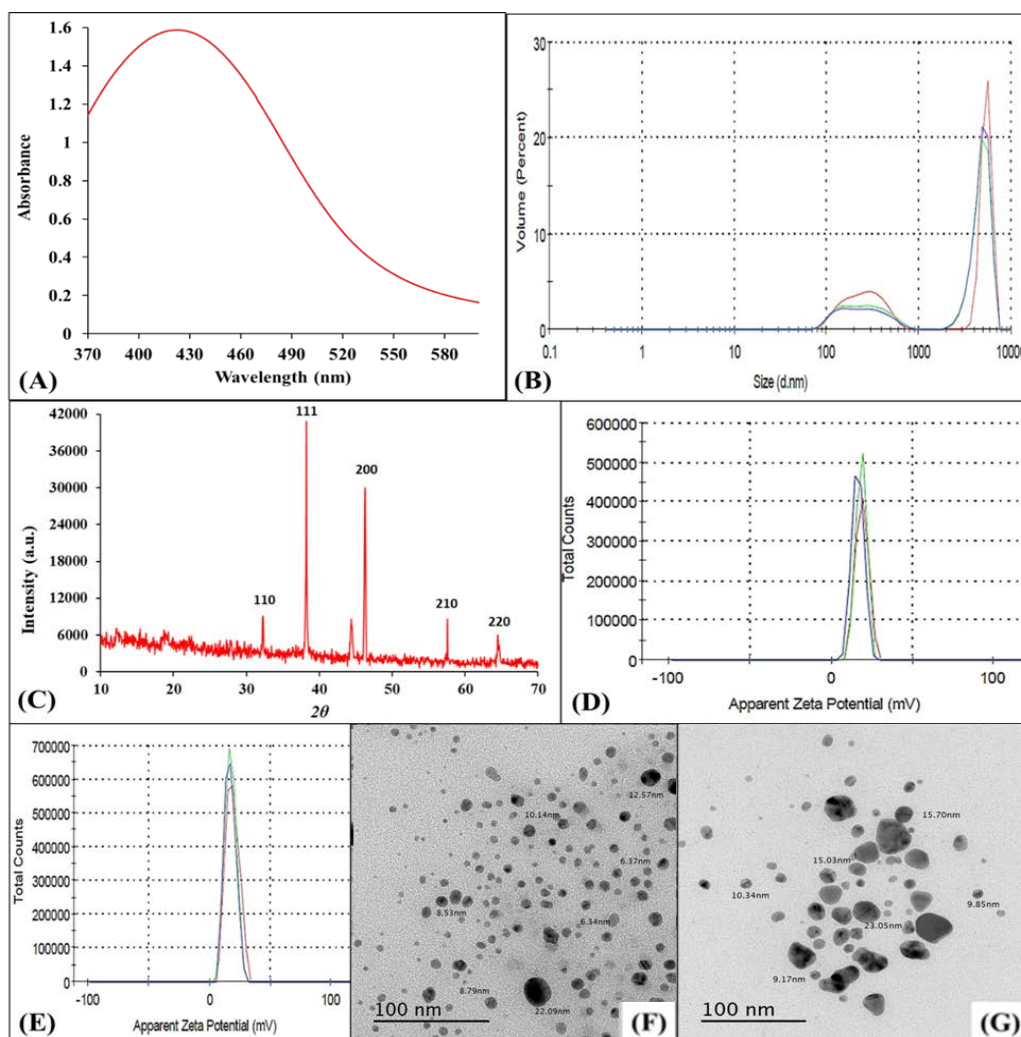


Figure 1. Chitosan/silver nanocomposite characterization. (A) UV-Vis spectrum of AgNPs. (B) Size distribution by intensity and by volume was determined using DLS measurements of AgNPs in deionized water. (C) X-ray diffraction (XRD). (D) Zeta potential of the AgNPs. (E) Zeta potential of CS/AgNC. (F) TEM micrograph of AgNPs. (G) CS/AgNC by TEM. Bars scale = 100 nm (F & G).

The presented work embedded the AgNPs into the CS, which played an important role in decreasing and delaying in silver release from the polymeric matrix (Figure 2). Zeta average size and PDI measurements for the solubility of CS/AgNC in polar and non-polar solvents confirmed that the release capacity of silver decreased in the tested non-polar solvents (Supplementary Table 1).

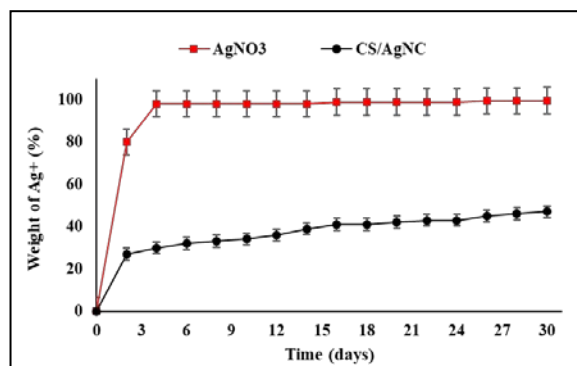


Figure 2. The release property of AgNO_3 and AgNPs from CS/AgNC at 37°C.

3.2. Antibacterial activity

The antibacterial activity of CS/AgNC was demonstrated and compared with the free AgNPs synthesized using the bacterial supernatant, as well as the solo polymer CS. Treatment with CS, AgNPs, and CS/AgNC inhibited the growth of all tested bacterial strains as shown in Supplementary Table 2. Results showed AgNPs and CS/AgNC had better bactericidal action against the G-ve than the G+ve bacteria.

CS/AgNC and penicillin showed the same MIC values (6 $\mu\text{g/ml}$) against *E. coli* and *B. cereus* besides complete inhibition at 25 $\mu\text{g/ml}$ exhibiting a dose-dependent behavior of CS/AgNC antibacterial potential (Figure 3). The MIC value of CS/AgNC inhibited the growth of *B. cereus* by 75.5% and *E. coli* by 80.7% (Figure 4).

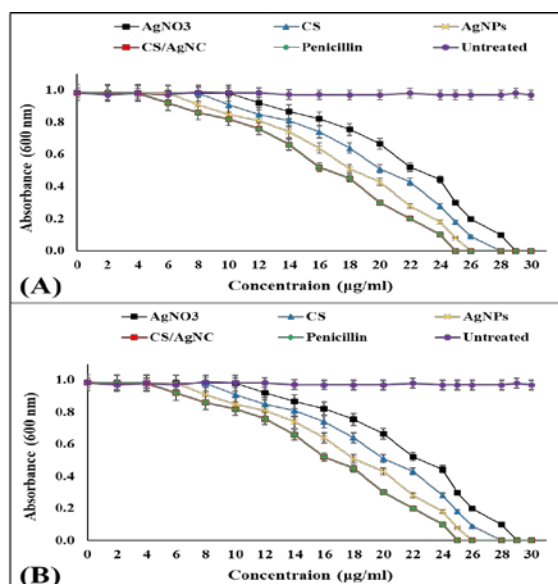


Figure 3. Effect of AgNO₃, CS, AgNPs, CS/AgNC and penicillin against the broth cultures of *B. cereus*; (A) and *E. coli*; (B).

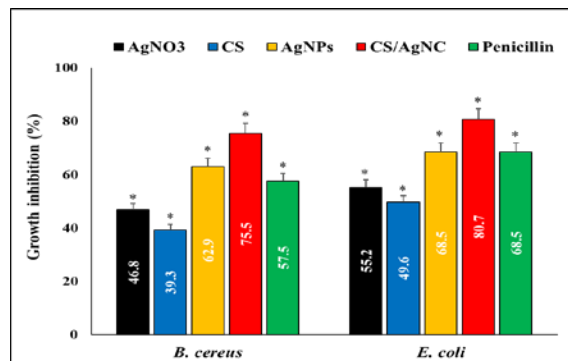


Figure 4. Growth inhibition percentage of AgNO₃, CS, AgNPs, CS/AgNC and penicillin against *B. cereus* and *E. coli* strains (Highly significant = * $P < 0.05$, $n = 3$). Ultrastructural changes in treated bacteria

3.3. Ultrastructural changes in treated bacteria

Morphological characteristics of the ultrastructure of *B. cereus* cells in MHB changed in response to their treatment with CS/AgNC (Figure 5). Native cells were identical rods with integral cell walls (Figure 5A). The CS/AgNC-treated cells showed damaged and crinkled cell walls, as well as a separation between them and the plasma membrane was observed (Figure 5B & C).

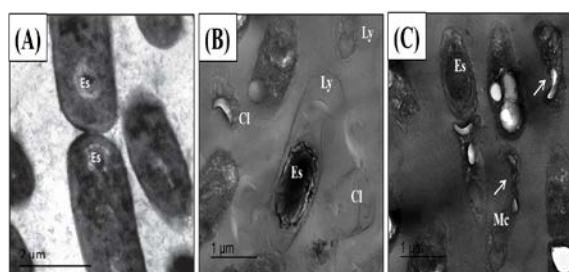


Figure 5. TEM micrograph of the bactericidal effect of CS/AgNCs on the ultrastructure of *B. cereus*. (A) A negative control (without CS/AgNCs). (B & C) A treated sample (at 6 µg/ml), there are irregular-shaped rods (arrows) with lysed cell walls (Ly), malformed cells (Mc), and complete cell lysis (Cl). Note the endospore formation (Es).

Figure 6 shows the negative effects of CS/AgNC on the ultrastructure of *E. coli*. Untreated cells appeared as uniformly dense rods. In contrast, the CS/AgNC-treated cells displayed damaged cells with irregular shapes in addition to an obvious rupture between their cell membrane and cell wall (Figure 6B).

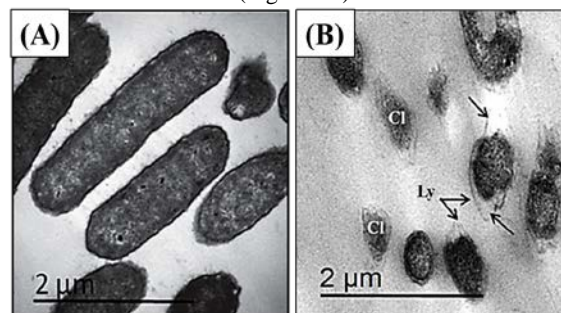


Figure 6. TEM micrograph of the bactericidal effect of CS/AgNC on the ultrastructure of *E. coli*. (A) A negative control (without CS/AgNC). (B) A treated sample (at 6 µg/ml), there are irregular-shaped rods with lysed cell walls (Ly). Also, note the separation that occurred between the bacterial cell wall membranes (arrows).

3.4. Impact of CS/AgNC on GDH and MDH enzymes and protein profiling

The effects of CS/AgNC on MDH and GDH activities of *B. cereus* and *E. coli* are shown in Figure 7 and Table 1. During the assay of MDH GDH and activities in intact and CS/AgNC-treated bacteria, it was found that the enzymatic activities and specific activities decreased after treatment. Moreover, *E. coli* was found to be more susceptible to CS/AgNC treatment than other bacterial strains. MDH activity was still present after the treatment with CS/AgNC, but it decreased from 356.9 and 566.0 to 307.1 and 36.4 µmol NADH.min⁻¹ for *B. cereus* and *E. coli*, respectively. Also, CS/AgNC showed vital effects on GDHs activities in the treated bacteria and decreased the specific activities of GDHs of *B. cereus* and *E. coli* from 0.274 and 0.625 to 0.250 and 0.054 µmol NADH.min⁻¹, respectively.

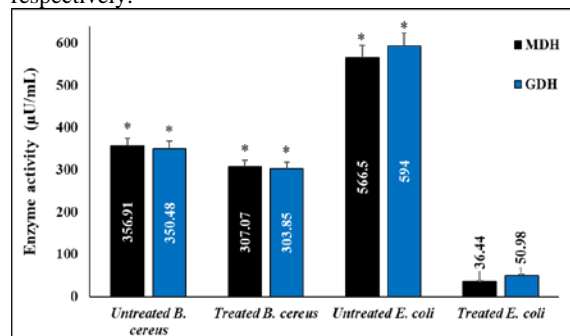


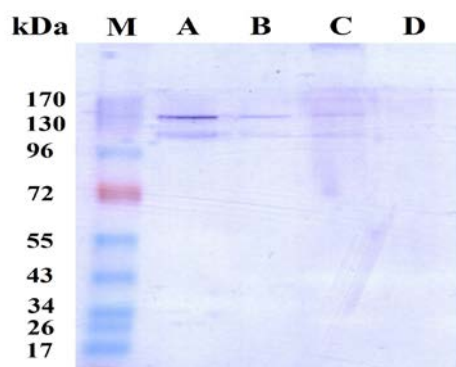
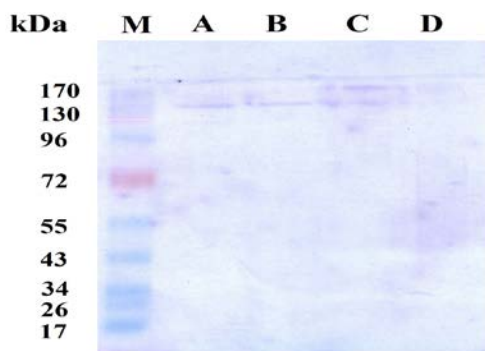
Figure 7. The enzymatic activities for MDH and GDH of the untreated and CS/AgNC-treated bacterial strains (Highly significant = * $P < 0.05$, $n = 3$).

Table 1. The enzymatic activities and specific activities for MDH and GDH of the untreated and CS/AgNC-treated bacterial strains (mean \pm SD).

Bacterial strain	Total protein concentration ($\mu\text{g/ml}$)	GDH		MDH	
		Units of enzyme ($\mu\text{U/ml}$)	Specific activity ($\mu\text{U}/\mu\text{g}$)	Units of enzyme ($\mu\text{U/ml}$)	Specific activity ($\mu\text{U}/\mu\text{g}$)
Untreated <i>B. cereus</i>	1760 \pm 0.03	350.5 \pm 0.03	0.274 \pm 0.03	356.9 \pm 0.03	0.279 \pm 0.03
Treated <i>B. cereus</i>	1900 \pm 0.03	303.9 \pm 0.03	0.250 \pm 0.03	307.1 \pm 0.03	0.253 \pm 0.03
Untreated <i>E. coli</i>	1277.6 \pm 0.03	549.0 \pm 0.03	0.625 \pm 0.03	566.0 \pm 0.03	0.596 \pm 0.03
Treated <i>E. coli</i>	1214.6 \pm 0.03	50.9 \pm 0.03	0.054 \pm 0.03	36.4 \pm 0.03	0.039 \pm 0.03

The profile of total soluble protein revealed several changes in the protein content of treated bacteria (*B. cereus* and *E. coli*) with CS/AgNC compared with the untreated ones (Supplementary Figure 1). It was noted that some protein bands were missed at different molecular weights for the treated *B. cereus* and more bands for *E. coli*.

The MDH pattern revealed two distinct bands with approximate molecular weights of 120 and 140 kDa for both *B. cereus* and *E. coli* (Figure 8). On the other hand, the GDH isozymal pattern showed two bands with approximate molecular weights of about 130 and 170 kDa for *E. coli* and only one band (130 kDa) for *B. cereus* (Figure 9). In the case of MDH detection, the intensity of the smaller band (120 kDa) was dramatically decreased when *B. cereus* was treated with CS/AgNC, while the two bands (120 and 140 kDa) totally disappeared for the treated *E. coli*. The single band (130 kDa) of GDH did not undergo any change when *B. cereus* was treated with CS/AgNC, while the two bands (130 and 170 kDa) almost disappeared for the treated *E. coli*.

**Figure 8.** MDH of *B. cereus* and *E. coli* after staining at 37°C. M: marker; A: untreated *B. cereus*; B: treated *B. cereus*; C: untreated *E. coli* and D: treated *E. coli*.**Figure 9.** GDH of *B. cereus* and *E. coli* after staining at 37°C. M: marker; A: untreated *B. cereus*; B: treated *B. cereus*; C: untreated *E. coli* and D: treated *E. coli*.

4. Discussion

AgNPs have been stabilized using CS in numerous investigations (Marková *et al.*, 2012; El-Sherbiny and Sedki, 2019; Bonilla *et al.*, 2021). AgNPs are tightly connected to the CS OH groups, forming a network of polymeric chains that reduces NP aggregation and boosts stability (Kumar, 2000). Due to CS's antibacterial capabilities, the combination with AgNPs increased its effectiveness (An *et al.*, 2018). In this study, silver nitrate was biologically reduced with *E. coli* D8 cell-free supernatant to biosynthesize AgNPs, which were then alternatively integrated into a chitosan matrix. Based on prior research demonstrating antibacterial efficacy, the bacterial supernatant was employed as reducing and stabilizing agents, respectively (Shahverdi *et al.*, 2007; El-Dein *et al.*, 2021). Furthermore, the presented work was also able to study the ultrastructure of CS/AgNC-treated bacteria as well as some of their enzymatic activity.

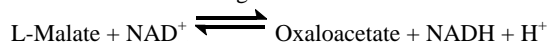
Characterization of the biosynthesized CS/AgNC, TEM, and DLS results confirmed the uniform spherical shape of AgNPs with small sizes and a high positive net surface charge that usually indicated higher antimicrobial activity, as reported previously (Ivask *et al.*, 2014). AgNPs' relevance and usage are greatly influenced by their shape and size. According to reports, spherical AgNPs are the smallest in size and have the strongest antibacterial effects (Hillaireau and Couvreur, 2009; Syu *et al.*, 2014). Nanomaterials' stability and propensity to aggregate are thought to be common problems that limit their potential for use in industrial and medical applications. By preventing their aggregation, the exterior capping agents are crucial in determining the shape, size, and stability of NPs (Duan *et al.*, 2015). According to Siddique *et al.*, (2013), the positive charge of nanometals may strengthen the attraction between particles, reducing the tendency for them to aggregate. Zeta average size and PDI values for CS/AgNC confirmed its high solubility in polar solvents, including water (Lee *et al.*, 2019). The small size of metallic NPs might have a cytotoxic effect on mammalian cells (El-Zahed *et al.*, 2021a). Consequently, the presented work embedded the AgNPs into the CS to decrease the silver toxicity. Also, CS participated in delaying and decreasing the silver release from its polymeric matrix.

The antibacterial activity of CS/AgNC showed a higher antibacterial action against the G^{-ve} bacteria than the G⁺ve bacteria. Owaid (2018) reported that AgNPs were more effective against the G^{-ve} than the G⁺ve bacteria. This difference may be due to the components and structure of the bacterial cell wall, mainly peptidoglycan thickness (Verma and Stellacci, 2010). The G^{-ve} bacterial cell wall includes thicker and several layers of acidic compounds and lipids than the G⁺ve cell wall. These

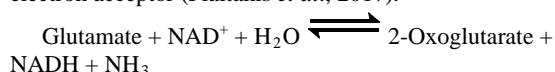
acidic compounds have a strong negative charge that could bind and trap the free Ag^+ and increase its action against G-ve bacteria (Kim *et al.*, 2007). The presented results agreed with previous reports confirming that the interaction of positively charged NP with cell contents has higher microbicidal action, which may be related to its easy cellular uptake and cell membrane penetration (Anas *et al.*, 2013; Li *et al.*, 2011). The large size of AgNO_3 particles might prevent its penetration throughout the bacterial cell wall, which decreased its antibacterial effects on the tested bacteria more than CS/AgNC.

CS/AgNC produced MIC values ranging from 6 $\mu\text{g/ml}$ to 25 $\mu\text{g/ml}$ against the tested bacterial strains in a dose-dependent manner. Nithya *et al.* (2015) reported that CS/AgNC possesses higher antibacterial activity than CS with MIC values ranging from 128 to 512 $\mu\text{g/ml}$ and 16 to 128 $\mu\text{g/ml}$ against *E. coli* and *S. aureus*, respectively. Arjunan *et al.*, (2016) found that the CS/AgNC MIC results ranged from 8 to $\mu\text{g/ml}$ against Gram-negative bacteria. MIC results of *Pongamia pinnata* seed extract-mediated green synthesized AgNPs against *S. aureus*, *E. coli*, and *B. cereus* reached to $\approx 250 \mu\text{g/ml}$ as documented by Paul *et al.* (2019). Also, the ultrastructure of *B. cereus* and *E. coli* after the treatment with CS/AgNC was negatively affected due to its being easily absorbed and trapped through the cell wall. The negative effects involved the inhibition of bacterial multiplication and the complete lysis of the bacterial cell or its encapsulation. Some treated cells showed a rupture between the bacterial cell membrane and its cell wall.

The negative effects of CS/AgNC on bacterial oxidative stress in its respiration were tested using two dehydrogenase enzyme behaviors; MDH and GDH (Sugimoto *et al.*, 2010). An enzyme of the tricarboxylic acid cycle, MDH, occurs in most living systems. MDH catalyzes the reversible conversion of malate to oxaloacetate while reducing NAD^+ to NADH:



GDH catalyzes the reversible oxidation of glutamate to generate α -ketoglutarate and ammonia using NAD^+ as an electron acceptor (Plaitakis *et al.*, 2017).



The dehydrogenase enzymes from animal cells have been extensively investigated, but information about them from bacterial sources needs more study. In *E. coli*, CS/AgNC strongly inhibited dehydrogenase activity, which was also documented by Luche *et al.* (2016). Eymard-Vernain *et al.* (2018) reported a decrease in GDH of *B. subtilis* after treatment with AgNPs and suggested that biomolecule-bearing carboxyl groups and those that are devoid of thiol groups can interact with AgNPs.

PAGE was considered one of the most sensitive methods for detecting protein and isozyme patterns. The intensity of the protein bands decreased for the treated bacteria, indicating that not only some types of protein were unexpressed, but also the level of protein expression decreased. The isozymal patterns for MDH and GDH were also performed. Selander *et al.* (1986) recorded MDH presence using electrophoresis techniques throughout different bacterial strains such as *E. coli*, *Pseudomonas aeruginosa*, *Bordetella* spp., *Hemophilus influenzae*, *Legionella pneumophila* and *Neisseria gonorrhoeae* in

addition to GDH in *L. pneumophila*, *P. aeruginosa*, *N. meningitidis*, *H. influenzae*, *N. gonorrhoeae*, *Streptococcus* spp. and *Bordetella* spp. MDH and GDH patterns of CS/AgNC-treated bacteria confirmed their harmful effects on the pathogenic bacteria's dehydrogenase activity, which could reduce the pathogenicity of the bacteria or cause its death. Vineela *et al.* (2017) documented the toxic effects of AgNPs on MDH and GDH activities based on their PAGE profiles.

Overall, although both controls of the tested bacterial strains (*B. cereus*, and *E. coli*) expressed higher values of enzymatic levels, the G-ve showed more susceptibility to CS/AgNC treatment compared to the G+ve. The elimination of the bacteria may be the cause of the CS/inhibitory AgNC's effect on the respiratory enzymes MDH and GDH. Additionally, it has been proposed that Ag^+ largely influences the performance of membrane-bound enzymes that are crucial to the respiratory chain (Holt and Bard 2005). Biomolecules in the cell that include sulfur or phosphorus are more likely to react with Ag. As a result, the preferred sites for AgNPs binding are likely to be acidic compounds or sulfur-containing proteins that are found in the bacterial plasma membrane or inside the cells (Krishnaraj *et al.*, 2010).

5. Conclusion

The free supernatant of *E. coli* D8 (MF062579) could act as a strong reducing agent and stabilizer in a one-step batch method to biosynthesize the CS/AgNC. This was done in the presence of sunlight. XRD, UV-visible spectrophotometry, Zeta potential, and TEM were used to confirm the synthesis of CS/AgNC. Long-term particle stability was indicated by the Zeta average size, PDI values, and AgNPs releasing properties of the CS/AgNC. With MIC values ranging from 6 to 25 $\mu\text{g/ml}$, the biosynthesized nanocomposite demonstrated significant antibacterial efficacy against different G+ve and G-ve bacteria. G-ve bacteria are more sensitive to CS/AgNC than G+ve bacteria in terms of total protein content, GDH and MDH enzymes, as well as the ultrastructure of the treated bacterial cells. The presented study assumed that the biosynthesized CS/AgNC might be suitable for use it as a bacterial growth inhibitor with relatively high efficacy and stability.

References

- An J, Guo G, Yin R, Luo Q, Li X, Liu F and Wang D. 2018. Facile preparation of silver/reduced graphene oxide/chitosan colloid and application of the nanocomposite in antibacterial and catalytic activity. *Polym Int.*, **67**: 515-527.
- Anas A, Jiya J, Rameez MJ, Anand PB, Anantharaman MR and Nair S. 2013. Sequential interactions of silver-silica nanocomposite (Ag-SiO₂NC) with cell wall, metabolism and genetic stability of *Pseudomonas aeruginosa*, a multiple antibiotic-resistant bacterium. *Lett Appl Microbiol.*, **56**(1): 57-62.
- Arjunan N, Kumari HLJ, Singaravelu CM, Kandasamy R and Kandasamy J. 2016. Physicochemical investigations of biogenic chitosan-silver nanocomposite as antimicrobial and anticancer agent. *Int J Biol Macromol.*, **92**: 77-87.
- Badi'ah HI. 2021. Chitosan as a capping agent of silver nanoparticles. *Indones J Chem.*, **9**(1): 21-25.

- Baka ZA, Abou-Dobara MI, El-Sayed AKA and El-Zahed MM. 2019. Synthesis, characterization, and antimicrobial activity of chitosan/Ag nanocomposite using *Escherichia coli* D8. *SJDFS*, **9(1)**: 1-6.
- Baltazar-Encarnación E, Escárcega-González CE, Vasto-Anzaldo XG, Cantú-Cárdenas ME and Morones-Ramírez JR. 2019. Silver nanoparticles synthesized through green methods using *Escherichia coli* top 10 (Ec-Ts) growth culture medium exhibit antimicrobial properties against nongrowing bacterial strains. *J Nanomater.*, **2019**: 4637325.
- Bayda S, Adeel M, Tuccinardi T, Cordani M and Rizzolio F. 2020. The history of nanoscience and nanotechnology: from chemical-physical applications to nanomedicine. *Molecules*, **25(1)**: 112.
- Bonilla JJA, Honorato L, Cordeiro de Oliveira DF, Araújo Gonçalves R, Guimarães A, Miranda K and Nimrichter L. 2021. Silver chitosan nanocomposites as a potential treatment for superficial candidiasis. *Med Mycol.*, **59(10)**: 993-1005.
- Bradford NB. 1976. A rapid and sensitive method for the quantitation microgram quantities of a protein isolated from red cell membranes. *Anal Biochem.*, **72(248)**: e254.
- Clinical and Laboratory Standards Institute. 2007. M100-S17. Performance standards for antimicrobial susceptibility testing; 17th informational supplement. Clinical and Laboratory Standards Institute, Wayne, PA, USA.
- Clinical and Laboratory Standards Document M100-S26. 2017. Performance standards for antimicrobial susceptibility testing: Approved standard-twenty-seven Edition, Clinical and Laboratory Standards Institute, Wayne, Pennsylvania, USA.
- Duan H, Wang D and Li Y. 2015. Green chemistry for nanoparticle synthesis. *Chem Soc Rev.*, **44(16)**: 5778-5792.
- El-Dein MMN, Baka ZA, Abou-Dobara MI, El-Sayed AK and El-Zahed MM. 2021. Extracellular biosynthesis, optimization, characterization and antimicrobial potential of *Escherichia coli* D8 silver nanoparticles. *JMBFS*, **10(4)**: 648-656.
- El-Shanshoury AERR, ElSilk SE and Ebeid ME. 2011. Extracellular biosynthesis of silver nanoparticles using *Escherichia coli* ATCC 8739, *Bacillus subtilis* ATCC 6633, and *Streptococcus thermophilus* ESh1 and their antimicrobial activities. *Int Sch Res Notices.*, **2011**: 385480.
- El-Sherbiny IM and Sedki M. 2019. Green synthesis of chitosan-silver/gold hybrid nanoparticles for biomedical applications. In: **Pharmaceutical nanotechnology**. Humana, New York, NY, pp. 79-84.
- El-Zahed MM, Baka ZA, Abou-Dobara MI, El-Sayed AK, Aboser MM and Hyder A. 2021a. *In vivo* toxicity and antitumor activity of newly green synthesized reduced graphene oxide/silver nanocomposites. *Bioresour Bioprocess.*, **8(1)**: 1-14.
- El-Zahed MM, Baka Z, Abou-Dobara MI and El-Sayed A. 2021b. *In vitro* biosynthesis and antimicrobial potential of biologically reduced graphene oxide/Ag nanocomposite at room temperature. *JMBFS*, **10(6)**: e3956-e3956.
- Eymard-Vernain E, Coute Y, Adrait A, Rabilloud T, Sarret G and Lelong C. 2018. The poly-gamma-glutamate of *Bacillus subtilis* interacts specifically with silver nanoparticles. *PLoS One*, **13(5)**: e0197501.
- Fan X, Wang X, Cai Y, Xie H, Han S and Hao C. 2022. Functionalized cotton charcoal/chitosan biomass-based hydrogel for capturing Pb²⁺, Cu²⁺ and MB. *J Hazard Mater.*, **423**: 127191.
- Genç A, Patarroyo J, Sancho-Parramon J, Bastús NG, Puentes V and Arbiol J. 2017. Hollow metal nanostructures for enhanced plasmonics: synthesis, local plasmonic properties and applications. *Nanophotonics*, **6(1)**: 193-213.
- Hassanen EI and Ragab E. 2021. *In vivo* and *in vitro* assessments of the antibacterial potential of chitosan-silver nanocomposite against methicillin-resistant *Staphylococcus aureus*-induced infection in rats. *Biol Trace Elem Res.*, **199(1)**: 244-257.
- Hillaireau H and Couvreur P. 2009. Nanocarriers' entry into the cell: relevance to drug delivery. *Cell Mol Life Sci.*, **66(17)**: 2873-2896.
- Holt KB and Bard AJ. 2005. Interaction of silver (I) ions with the respiratory chain of *Escherichia coli*: an electrochemical and scanning electrochemical microscopy study of the antimicrobial mechanism of micromolar Ag⁺. *Biochemistry*, **44(39)**: 13214-13223.
- Iravani S, Korbekandi H, Mirmohammadi SV and Zolfaghari B. 2014. Synthesis of silver nanoparticles: chemical, physical and biological methods. *Res Pharm Sci.*, **9(6)**: 385.
- Ivask A, Kurvet I, Kasemets K, Blinova I, Aruoja V, Suppi S. and Kahru A. 2014. Size-dependent toxicity of silver nanoparticles to bacteria, yeast, algae, crustaceans and mammalian cells *in vitro*. *PLoS one*, **9(7)**: e102108.
- Kate S, Sahasrabudhe M and Pethe A. 2020. Biogenic silver nanoparticle synthesis, characterization and its antibacterial activity against leather deteriorates. *JJBS.*, **13(4)**: 493 - 498.
- Kim JS, Kuk E, Yu KN, Kim JH, Park SJ, Lee HJ and Cho MH. 2007. Antimicrobial effects of silver nanoparticles. *Nanomed: Nanotechnol Biol Med.*, **3(1)**: 95-101.
- Krishnaraj C, Jagan EG, Rajasekar S, Selvakumar P, Kalaichelvan PT and Mohan NJCSBB. 2010. Synthesis of silver nanoparticles using *Acalypha indica* leaf extracts and its antibacterial activity against water borne pathogens. *Colloids Surf B Biointerfaces.*, **76(1)**: 50-56.
- Kruger NJ. 2009. The Bradford method for protein quantitation. In: Walker JM (eds) **The Protein Protocols Handbook**. Springer protocols handbooks. Humana Press, Totowa, NJ., pp. 17-24.
- Kumar MNR. 2000. A review of chitin and chitosan applications. *React Funct Polym.*, **46(1)**: 1-27.
- Laemmli UK. 1970. Cleavage of structural proteins during the assembly of the head of bacteriophage T4. *Nature*, **227(5259)**: 680-685.
- Lee SH and Jun BH. 2019. Silver nanoparticles: synthesis and application for nanomedicine. *Int J Mol Sci.*, **20(4)**: 865.
- Li WR, Xie X-B, Shi Q-S, Duan S-S, Ouyang Y-S and Chen Y-B. 2011. Antibacterial effect of silver nanoparticles on *Staphylococcus aureus*. *Biometals.*, **24(1)**: 135-141.
- Luche S, Eymard-Vernain E, Diemer H, Van Dorsselaer A, Rabilloud T and Lelong C. 2016. Zinc oxide induces the stringent response and major reorientations in the central metabolism of *Bacillus subtilis*. *J Proteom.*, **135(2016)**: 170-180.
- Marková Z, Šišková K, Filip J, Šafářová K, Prucek R, Panáček A and Zbořil R. 2012. Chitosan-based synthesis of magnetically-driven nanocomposites with biogenic magnetite core, controlled silver size, and high antimicrobial activity. *Green Chem.*, **14(9)**: 2550-2558.
- Menazea AA, Eid MM and Ahmed MK. 2020. Synthesis, characterization, and evaluation of antimicrobial activity of novel chitosan/tigecycline composite. *Int J Biol Macromol.*, **147**: 194-199.
- Namasivayam SKR, Pattukumar V, Samrat K, Kumar JA, Bharani RA, Alothman AA, Osman SM, Tran VA and Rajasimman M. 2022. Evaluation of methyl orange adsorption potential of green synthesized chitosan-silver nanocomposite (CS-AgNC) and its notable biocompatibility on freshwater Tilapia (*Oreochromis niloticus*). *Chemosphere*, **308(2)**: 135950.

- Natsuki J, Natsuki T and Hashimoto Y. 2015. A review of silver nanoparticles: synthesis methods, properties and applications. *Int j mater sci.*, **4(5)**: 325-332.
- Nguyen NTT, Nguyen LM, Nguyen TTT, Tran UP, Nguyen DTC and Van Tran T. 2022. A critical review on the bio-mediated green synthesis and multiple applications of magnesium oxide nanoparticles. *Chemosphere*, **312(1)**: 137301.
- Nithya A, JeevaKumari HL, Rokesh K, Ruckmani K, Jeganathan K and Jothivenkatachalam K. 2015. A versatile effect of chitosan-silver nanocomposite for surface plasmonic photocatalytic and antibacterial activity. *J Photochem Photobiol B: Biol.*, **153**: 412-422.
- O'connor BP. 2000. SPSS and SAS programs for determining the number of components using parallel analysis and Velicer's MAP test. *Behav Res Methods Instrum Comput.*, **32(3)**: 396-402.
- Owaid MN, Muslim RF and Hamad HA. 2018. Mycosynthesis of silver nanoparticles using *Terminia* sp. desert truffle, pezizaceae, and their antibacterial activity. *JJBS.*, **11(4)**: 401-405.
- Paul M and Londhe VY. 2019. *Pongamia pinnata* seed extract-mediated green synthesis of silver nanoparticles: Preparation, formulation and evaluation of bactericidal and wound healing potential. *Appl Organomet Chem.*, **33(3)**: e4624.
- Plaitakis A, Kalef-Ezra E, Kotzamani D, Zaganas I and Spanaki C. 2017. The glutamate dehydrogenase pathway and its roles in cell and tissue biology in health and disease. *Biology*, **6(1)**: 11.
- Price GJ, White AJ and Clifton AA. 1995. The effect of high-intensity ultrasound on solid polymers. *Polymer.*, **36(26)**: 4919-4925.
- Restrepo CV and Villa CC. 2021. Synthesis of silver nanoparticles, influence of capping agents, and dependence on size and shape: A review. *Environ Nanotechnol Monit Manag.*, 100428.
- Robb FT, Maeder DL, Diruggiero J, Borges KM and Tolliday N. 2001. Glutamate dehydrogenases from hyperthermophiles. In: **Methods in enzymology** (Vol. 331). Academic Press, pp. 26-41.
- Saravanan A, Kumar PS, Karishma S, Vo DVN, Jeevanantham S, Yaashikaa PR and George CS. 2021. A review on biosynthesis of metal nanoparticles and its environmental applications. *Chemosphere*, **264**: 128580.
- Selander RK, Caugant DA, Ochman H, Musser JM, Gilmour MN and Whittam TS. 1986. Methods of multilocus enzyme electrophoresis for bacterial population genetics and systematics. *Appl Environ Microbiol.*, **51(5)**: 873-884.
- Shahverdi AR, Minaeian S, Shahverdi HR, Jamalifar H and Nohi AA. 2007. Rapid synthesis of silver nanoparticles using culture supernatants of *Enterobacteria*: a novel biological approach. *Process Biochem.*, **42(5)**: 919-923.
- Siddique YH, Fatima A, Jyoti S, Naz F, Khan W, Singh BR and Naqvi AH. 2013. Evaluation of the toxic potential of graphene copper nanocomposite (GCNC) in the third instar larvae of transgenic *Drosophila melanogaster* (hsp70-lacZ) Bg9. *PloS One*, **8(12)**: e80944.
- Singh A, Gautam PK, Verma A, Singh V, Shivapriya PM, Shivalkar S, Sahoo AK and Samanta SK. 2020. Green synthesis of metallic nanoparticles as effective alternatives to treat antibiotics resistant bacterial infections: A review. *Biotechnol Rep.*, **25**: e00427.
- Sotiriou GA, Meyer A, Knijnenburg JT, Panke S and Pratsinis SE. 2012. Quantifying the origin of released Ag⁺ ions from nanosilver. *Langmuir*, **28(45)**: 15929-15936.
- Sugimoto S, Higashi C, Matsumoto S and Sonomoto K. 2010. Improvement of multiple-stress tolerance and lactic acid production in *Lactococcus lactis* NZ9000 under conditions of thermal stress by heterologous expression of *Escherichia coli* dnaK. *Appl Environ Microbiol.*, **76(13)**: 4277-4285.
- Syu YY, Hung JH, Chen JC and Chuang HW. 2014. Impacts of size and shape of silver nanoparticles on *Arabidopsis* plant growth and gene expression. *Plant Physiol Biochem.*, **83**: 57-64.
- Tripathi S, Mehrotra GK and Dutta PK. 2011. Chitosan-silver oxide nanocomposite film: Preparation and antimicrobial activity. *Bull Mater Sci.*, **34(1)**: 29-35.
- Tsekhmistrenko SI, Bitvutskyy VS, Tsekhmistrenko OS, Horalskyi LP, Tymoshok NO and Spivak MY. 2020. Bacterial synthesis of nanoparticles: A green approach. *Biosyst Divers.*, **28(1)**: 9-17.
- Verma A and Stellacci F. 2010. Effect of surface properties on nanoparticle-cell interactions. *Small*, **6(1)**: 12-21.
- Vineela D, Reddy SJ and Kumar BK. 2017. Impact of *Lihocin* and *Aeromonas veronii* on metabolic biomarkers of fish *Catla catla* against to immunostimulant silver nanoparticles. *Int J Pharma Bio Sci.*, **4(1)**: 38-46.
- Yoshida A. 1965. Enzymic properties of malate dehydrogenase of *Bacillus subtilis*. *JBC*, **240(3)**: 1118-1124.
- Youssef K and Hashim AF. 2020. Inhibitory effect of clay/chitosan nanocomposite against *Penicillium digitatum* on citrus and its possible mode of action. *JJBS*, **13(3)**: 349 - 355.
- Yuan Q, Hein S and Misra RDK. 2010. New generation of chitosan-encapsulated ZnO quantum dots loaded with drug: synthesis, characterization and *in vitro* drug delivery response. *Acta Biomater.*, **6(7)**: 2732-2739.
- Zhang XF, Liu ZG, Shen W and Gurunathan S. 2016. Silver nanoparticles: synthesis, characterization, properties, applications, and therapeutic approaches. *Int J Mol Sci.*, **17(9)**: 1534.

Supplementary

Table 1. The Zeta average size and poly dispersity index for CS/AgNC.

Solvent	Zavg (nm)	PDI (d.nm)
Water	313	0.394
Methanol	841	0.745
Ethanol	444	0.632
DMF	370	0.420
n-butyl alcohol	312	0.400
Acetone	1711	0.801
Toluene	1145	0.896
Hexane	647	0.688

Table 2. The Zeta average size and poly dispersity index for CS/AgNC.

Antibacterial agent	Zone of inhibition (n=3, mm, mean \pm SE)	
	<i>B. cereus</i> ATCC 6633	<i>E. coli</i> ATCC 25922
AgNO ₃	15 \pm 0.06	21 \pm 0.03
CS	13 \pm 0.14	25 \pm 0.06
AgNPs	19 \pm 0.06	26 \pm 0.03
CS/AgNC	25 \pm 0.06	35 \pm 0.03
Penicillin	20 \pm 0.14	39 \pm 0.03

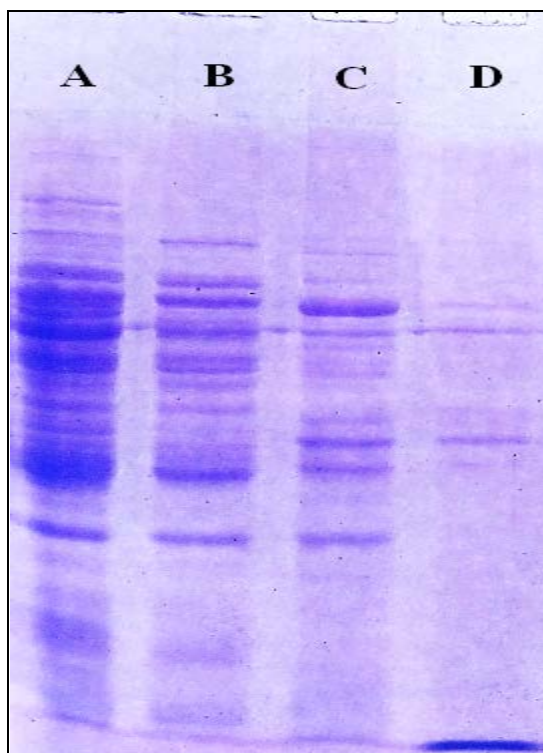


Figure 1. Protein expression profile on SDS-PAGE of *B. cereus* and *E. coli*. A: untreated *B. cereus*; B: treated *B. cereus*; C: untreated *E. coli* and D: treated *E. coli*. The gel was stained with Coomassie blue.

Plastic Particles in the Gastrointestinal Tract of Some Commercial Fish Species Inhabiting in the Gulf of Bejaia, Algeria

Z. Zeghdani^{1,*}, S. Mehdioui², Y. Mehdioui², R. Gherbi¹ and Z. Ramdane¹

¹ Laboratoire de Zoologie Appliquée et d'Ecophysiologie Animale, Faculté des Sciences de la Nature et de la Vie, Université de Bejaia, Bejaia 06000, Algérie ; ² Département des sciences biologiques de l'environnement, Faculté des Sciences de la Nature et de la Vie, Université de Bejaia, Bejaia 06000, Algérie

Received: September 10, 2022; Revised: November 26, 2022; Accepted: December 22, 2022

Abstract

In the present study we report for the first time, the presence of plastic particles on the gastrointestinal tracts of the examined commercial fish species: *Sardinella aurita* (n=60), *Sardina pilchardus* (n=60), *Pagellus acarne* (n=45), *Trachurus trachurus* (n=38), *Boops boops* (n=40), *Sparus aurata* (n=6). The sampled fish species (n=249) inhabiting in demersal, benthopelagic and pelagic marine ecosystems (Gulf of Bejaia) were examined to test eventual differences in micro and macro plastic particles. Overall, results showed that 58.63% of gastrointestinal tracts were contained plastic particles. An average 8.45 ± 14.69 items per fish were recorded. The most common morphotype particles were fiber (85%) whereas dominant colors of plastic debris were the blue and the red among three types of particle colors. Our results shows that there are no significant differences between females and males specimens in terms of ingested plastic particles. The highest abundance of plastic particles in fish gastrointestinal tracts was recorded in wet season.

Keywords: Plastic particles, Microplastics, Commercial fish species, Gulf of Bejaia.

1. Introduction

Plastics are the most widely used material (Millet *et al.*, 2018), inexpensive, lightweight, strong, durable, corrosion-resistant materials, with high thermal and electrical insulation properties (Thompson *et al.*, 2009), and this is why this material persists in the environment (Teuten *et al.*, 2009).

Sunlight, wind, and waves are the main natural factors transforming plastics into small particles (Matjasic *et al.*, 2021). When the size of these particles is less than 5 mm they are called microplastics (Hartmann *et al.*, 2019), some researchers use 0.5 or 1 mm as a maximum size for microplastics (Andrady, 2011; Cole *et al.*, 2011).

Microplastic particles can have either been manufactured purposely with that size (primary microplastic) or proceeding from fragmentation by different physical, chemical, and biological degradation (secondary microplastic) (Wright *et al.*, 2013; Rainieri *et al.*, 2018).

Plastics are emergent pollutants and have been found almost in every part of the planet (Mishra *et al.*, 2021) and their risk (macroplastics and microplastics) on the marine environment have been addressed by reporters as an emerging global problem that threatens marine organisms (Derraik, 2002). Regarding their size and form (fibers, fragments, etc.), this particle can be unfortunately ingested by biota (Galgani *et al.*, 2010; Andrady, 2011).

For these reasons many scientific works were conducted on microplastic ingestion by fish species (Takarina *et al.*, 2022; Piyawardhana *et al.*, 2022; Thiele *et al.*, 2021; Yin *et al.*, 2019), especially, in the Mediterranean Sea (Bellas *et al.*, 2016; Guven *et al.*, 2017; Pennino *et al.*, 2020), where researchers reported the occurrence of microplastic particles in the gastrointestinal tract of fish (Jabeen *et al.*, 2017; Jaafar *et al.*, 2021; Parvin *et al.*, 2021; Akhter and Panhwar, 2022).

The Mediterranean Sea recently classed as the most impacted regions of the world by plastic debris, demersal species from coastal zones ingest more plastic particles than other species (Murphy *et al.*, 2017), polymers can act as vector and adsorb heavy metals from the water column (Holmes *et al.*, 2014; Boucher *et al.*, 2016) which have a tendency to flow (Lagarde *et al.*, 2016).

Low-density microplastics are found in surface waters (Thompson *et al.*, 2004), they held some heavy metals (Brennecke *et al.*, 2016), then ingested by several species of zooplankton (Cole *et al.*, 2013) than by larvae and adults of fish (Browne *et al.*, 2013; Lusher *et al.*, 2013; Rochman *et al.*, 2013).

Researchers have reported that microplastics can enter the human body through the food chain and human exposure to microplastics could lead to harmful health (Couture, 2017), microplastics enriched bacterial pathogens (Junaid *et al.*, 2022) and can serve as carriers of antibiotic-resistant bacteria (Pham *et al.*, 2021).

The implications of the complex microplastics-heavy metals-bacterial pathogens to the human health are

* Corresponding author. e-mail: zeghdani1993@gmail.com; zouhir.zeghdani@univ-bejaia.dz.

significant (Wang et al., 2021). In effect, this complex seems to amplify the health risks for humans and animal.

In Algerian coasts, no studies were conducted on plastic particles containing in the gastrointestinal tracts of commercial fish species. The aim of the present study is to examine some commercial fish species (from Algerian coasts) for the presence of plastic debris (microplastics and macroplastics) in the gastrointestinal tract, to characterize the isolated plastic debris (form, color, size, etc.), and finally to analyze the variation of ingested plastic particles according to fish parameters, fish habitat and seasonal variation. These results may give us a clear idea on the presence of these toxic pollutants in the Algerian marine ecosystems, and the health risks that can induce to consumers of fish.

2. Materials and methods

A total of 249 specimens of fish belonging to six species (with high commercial value) were sampled in the port of Bejaia, Algeria (Figure.1) or from fish markets.

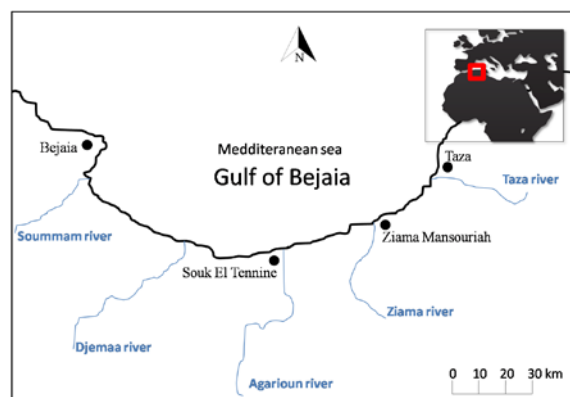


Figure 1. Location of the study area (Gulf of Bejaia)

In our sampling, we focused on fish species occupying various habitats (demersal, benthopelagic and pelagic) (Table.1).

In the laboratory, we worked in sterile space, in order to reduce the risk of air contamination using clean materials (disinfect with ethanol 70%), after identification of sampled fish specimens, total length (cm) and total weight (g) were measured for each specimen.

Table 1. Habitat and Biological parameters of examined fish species in the study (n = 249).

Fish species	(n)	Habitat	Mean weight (g) ± SD	Mean length (cm) ± SD
<i>Sardinella aurita</i>	60	Pelagic	26.95 ± 23.1	16.43 ± 4.1
<i>Sardina pilchardus</i>	60	Pelagic	25.43 ± 11.5	12.49 ± 3.9
<i>Pagellus acarne</i>	45	Benthopelagic	48.75 ± 18.4	14.61 ± 3.6
<i>Trachurus trachurus</i>	38	Pelagic	44.08 ± 12.31	16.84 ± 5.1
<i>Boops boops</i>	40	Demersal	56.91 ± 32.4	17.83 ± 2.7
<i>Sparus aurata</i>	6	Demersal	304.3 ± 11.2	25.67 ± 2.6

The protocol adapted by Baalkhuyur *et al.* (2018) was applied regarding its simplicity and feasibility. The different stapes devoted to detect the plastic particles in the examined fish individuals are: -Fish specimens were dissected and sexed (visual observations). After that, the gastrointestinal tract (GIT) was removed (from esophagus to the opening) and weighted; -The specimen's gut were rinsed with distilled water, and then carefully moved into cleaned Petri dishes. For each sample a code number was given; -After removal, the samples of GIT were placed in an oven for 1 hour at 60 °C; -To increase the efficacy of the extraction of plastic from the tissue, a digestion protocol was adapted from the procedure given by Cole *et al.* (2014). NaOH (1 M and 10 M), has been successfully applied to remove biogenic material; -30ml of a 1 M NaOH solution were added to reinforce the digestion (remove the remaining biological material and non-digestible residue) (Cole *et al.*, 2014; Catarino *et al.*, 2017); -Samples were manually shaken intermittently during the incubation period in order to facilitate complete digestion, and after the incubation, samples were inspected under binocular stereoscope visually (Hidalgo-Ruz *et al.*, 2012; Free *et al.*, 2014).

After identification, the plastic particles were counted, photographed and measured using the software "imagej" (ver: 1.4.3; <https://imagej.nih.gov/>), color and shape were also determined for each plastic particle (Jabeen *et al.*, 2017).

The occurrence of Frequency (FO %) of the collected microplastics in the digestive tracts was calculated using the following formula:

FO (%) = (Ni/N) × 100, where

FO% = frequency of occurrence of plastic particles;

Ni = number of gastrointestinal tracts that contained plastic particles;

N = total number of gastrointestinal tracts examined.

Data were analyzed using SPSS 14.0 software and EXCEL 2010. Independent t-test was performed to determine if there are differences on the abundance of plastic particles between wet season and dry season, and between males and females (95% confidence level). A significant difference in the abundance of plastics among individuals was tested applying one-way ANOVA. The Tukey test's HSD test was set at * = p < 0.05 and ** = p < 0.01 values.

3. Results

3.1. Biological parameters of fishes

A total of 249 specimens attached to 6 species were analyzed (Table.1). The body weight of fish specimens varies from 10.30 g to 328.20 g (31.74 g ± 20.42), and the total length varies from 10.90 cm to 24.20 cm (15.11 cm ± 2.5)

3.2. Intensity of plastic consumed by fishes

Evidence of plastic particles was appeared to be in 146 specimens from the total 249 (58.63%) examined in this study. These potential contaminants were found in the 6 species (Table.2), and therefore in pelagic, benthopelagic, and demersal species. The average number of particles

ingested was (8.45 ± 14.69 particles per specimen) ranging from 0 to 69 particles per gastrointestinal tract, the highest

average was recorded in *Boops boops* L. (21.03 ± 23.49 particles per specimen).

Table 2. Frequency of plastic particles ingestion by fish species.

Fish species	n of examined GIT	n of contaminated GIT	Rate (%)
<i>Sardinella aurita</i>	60	35	58.33
<i>Sardina pilchardus</i>	60	26	43.33
<i>Pagellus acarne</i>	45	33	73.32
<i>Trachurus trachurus</i>	38	24	63.16
<i>Boops boops</i>	40	22	55
<i>Sparus aurata</i>	6	6	100

GIT: Gastrointestinal Tract

Collected microplastics and mesoplastics from the examined fish specimens (2347 particles) recovered various morphotypes and colors of plastic particles.

3.3. Morphotype, size and color of the plastic particles retrieved

Two morphotypes of plastic particles were extracted (Figure.2), where the most observed were fibers with 85% ($p < 0.01$). In *Sardinella aurita*, *Sardina pilchardus* and *Trachurus trachurus* fibers reached 100%.

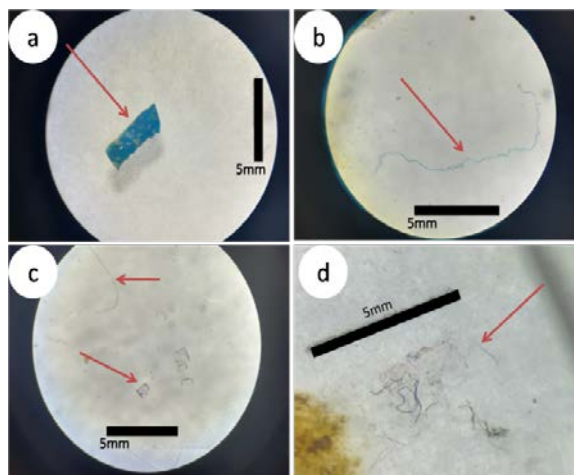


Figure 2. The morphotypes (a) fragment ingested by examined *Sparus aurata*; (b) mesoplastic fiber; (c) transparent fragments and a red fiber observed in the gut of *Boops boops*; (d) various fibers ingested by examined *Sardina pilchardus* (see red arrows).

Fragment morphotypes was exclusively extracted from *Boops boops*, *Sparus aurata* and *Pagellus acarne* with 15% of the total number of plastics (Figure.3a). The size of plastic particles varied from 0.1 mm to 5 mm for microplastics and the highest size of a mesoplastic was 18 mm, microplastics were the most observed with 94.58% of the total number of particles ($p < 0.01$) (Figure.3b).

Microplastics lower than 2 mm (size $< 2\text{mm}$) represent 71% of the number of analyzed plastics.

In the study region, the extracted plastics represent numerous colors (especially red, blue and transparent). The dominant color was the blue plastic particles with 56.4% followed by the red color with 41.3%. Transparent and other colors were not highly observed (Figure.3c).

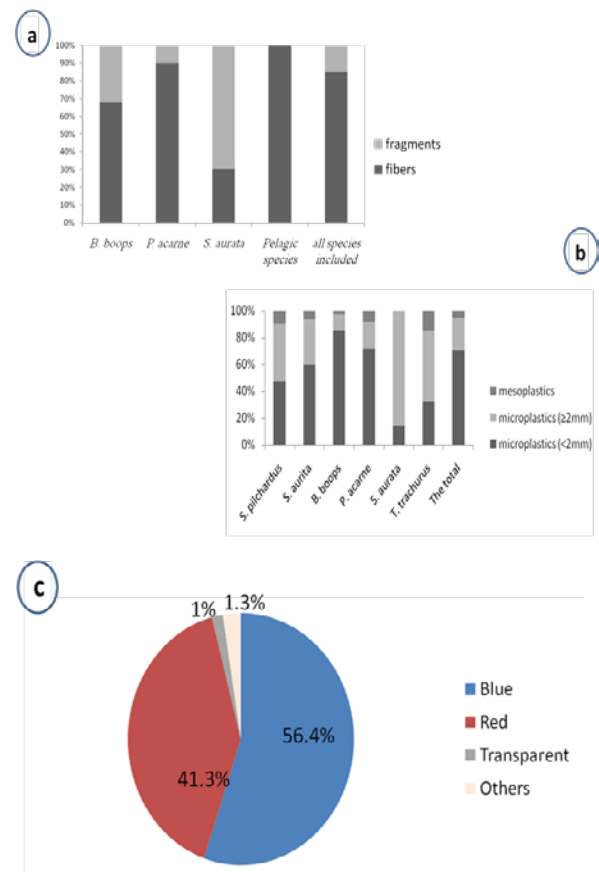


Figure 3. morphotypes (a), size (b) and color (c) of the ingested plastics by the contaminated fish species.

3.4. Occurrence and mean number of collected microplastics according to sex.

From the total of samples, 123 were females, 96 were males and 30 were undetermined individuals. The percentage of females with infected gastrointestinal tract reached 74.1% followed by males (FO reached 21%). When comparing the number of ingested plastics particles we found that females ingest slightly more than males (1055 and 1022 particles respectively) and for undetermined gender, a number of 270 particles was noted. According to sex, the mean number of plastic particles (Figure.4) shows no significant differences between the 3 genders (ANOVA, Tukey HSD $p\text{-value} > 0.05$).

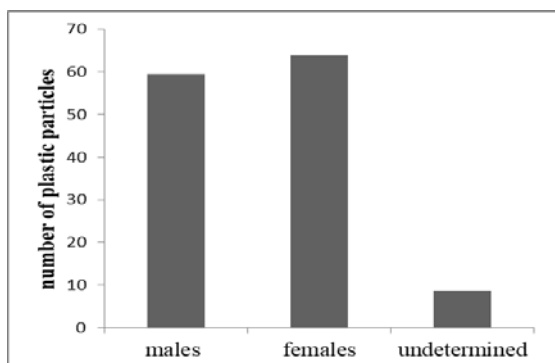


Figure 4. mean number of plastic particles ingested by sex (global examined fish species).

3.5. seasonal variation and plastic ingestion

Contaminated fish specimens by plastic particles were high in the wet season (Figure.5a), with a mean of 26.71 ± 4.2 individuals contain plastic. In the dry season the mean number of contaminated fish specimens was lower (8.71 ± 1.7). A one-way ANOVA test between the two seasons (wet and dry) confirms that the collected plastic debris was significantly higher in wet season than the dry season ($p < 0.01$).

Our results indicate a significant differences in the mean number of ingested plastics among the two seasons (one-way ANOVA; $F=6.99$; $p < 0.05$). The total number of plastic particles ingested by fish in wet season was 2092 particles (418.4 per species), in contrast, the dry season counted only 129 (25.8 per species) (Figure.5b).

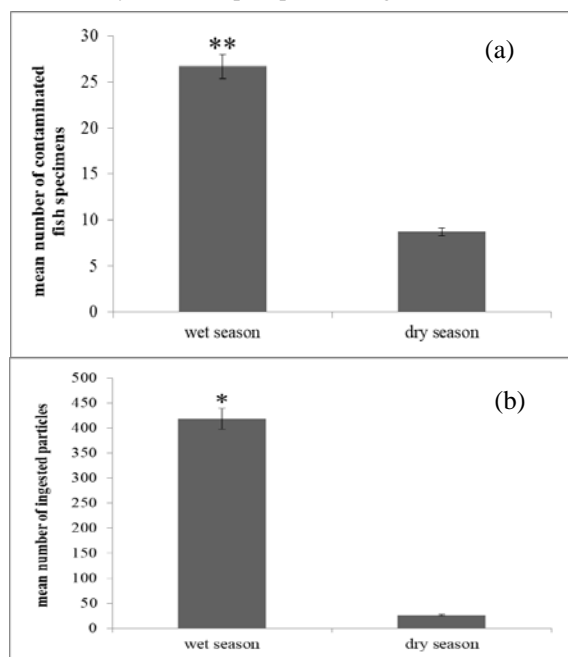


Figure 5 the mean number of contaminated fishes (a) and the mean number of ingested plastic particles (b) in the wet and the dry season. **: $p < 0.01$; *: $p < 0.05$

4. Discussion

In the present study, fishes from three regimes e.g. pelagic, benthopelagic and demersal were gathered to investigate the presence of plastic particles in the gastrointestinal tract. Our results revealed higher abundance of these potential contaminants in all examined

fishes especially in demersal fish species. These results confirm that plastic particles are present throughout the water column, and probably, a part of these plastic particles make complex with other organic or chemical elements (metallic contaminants) enhancing their sedimentation and their availability for benthopelagic and demersal fishes in deeper marine water. Lagarde *et al.* (2016) reported that these plastic particles adsorb heavy metals from the water column, which have a tendency to flow. In this context, a recent study conducted by Akhter and Panhwar (2022) revealed the presence of microplastic materials in crabs and fishes from pelagic and mesopelagic area in Pakistan. The authors stated that microplastics materials are present in pelagic regime than demersal and validate that low weight of plastic particles floats on ocean surfaces.

All examined fish species (*Sardinella aurita*, *Sardina pilchardus*, *Pagellus acarne*, *Trachurus trachurus*, *Boops boops* and *Sparusaurata*) consumed plastic particles. Our results showed that more than a half of the sampled fish specimens contain marine plastics. The recorded frequency of occurrence reaches 58.63%. Our results corroborate with the previous studies were high value were reported. For example, Ferreira *et al.* (2016) reported in *Cynoscion acoupa* from the Goiana Estuary 51%, in the Northwest Atlantic, Wieczorek *et al.* (2018) assessed the presence of microplastics in the stomachs of nearly three out of every four mesopelagic fish. Karbalaie *et al.* (2019) highlighted that 9 of 11 examined fish species from Malaysia (*Megalaspis cordyla*, *Epinephelus coioides*, *Rastrelliger kanagurta*, *Thunnus tonggol*, *Eleutheronema tridactylum*, *Clarias gariepinus*, *Colossoma macropomum*, *Nemipterus bipunctatus* and *Ctenopharyngodon idella*) were contaminated.

Neves *et al.* (2015) measured microplastics in stomach contents of 17 fish species from Portuguese coast (comprising *B.boops*, *P.acarne*, *T.trachurus* and *S.pilchardus*). In this study region, the authors reported relatively low rate (19.8% of 263 specimens) of fish contaminated with plastic particles regarding our results.

In addition, the mean number of plastic items ingested by specimens of *B. boops* was higher (21.03 ± 23.49) than those reported by Nadal *et al.* (2016) in the same fish species around the Balearic Islands (3.75 ± 0.25 microplastic items per fish). Many previous studies (Romeo *et al.*, 2015; Anastasopoulou *et al.*, 2013) have related the rate of marine debris or particles ingestion by fish to the variability of feeding habits.

Only two morphotypes of plastics were recorded (fibers with 85% and fragments with 15%) in the sampled specimens of all examined species. Our results corroborate with those of Neves *et al.* (2015), Ferreira *et al.* (2018), Sathish *et al.* (2020) and Merga *et al.* (2020) who reported clearly, the predominance of fibers as the most common particles ingested by fishes. These results maybe explained by the abundance of fibers in their ecosystems. After Valente *et al.* (2019) fibers are the most common in the environment. Fishing nets and textiles are possible sources of most fibers (Kane and Clare, 2019). They are similar in shape to the fish feed, which promote the ingestion by specimens (Walkinshaw *et al.*, 2020).

Fragments were extracted only from the gastrointestinal tracts of *B. boops*, *S. aurata* and *P. acarne*. *B. boops* which are semipelagic to demersal fishes and *P. acarne* a

benthopelagic species so they contact various plastic morphotypes than pelagic fishes when they are in movement (Sbrana *et al.*, 2020).

From the total of marine debris extracted, 94.58% were microplastics while mesoplastics represent a low percentage, all specimens contaminated ingest microplastics more than mesoplastics, the same results were reported in previous studies (Romeo *et al.*, 2015; Murphy *et al.*, 2017; Jabeen *et al.*, 2017). The obtained results confirm that the abundance of microplastics was higher than mesoplastics in all investigated fish species. Ingestion of small particles is maybe easier by small size of marine organisms (Neves *et al.*, 2015).

Our findings highlight that the blue particles were by far the most frequent plastics in the gastrointestinal tract contents; this is a result that was reported worldwide (Barboza *et al.*, 2019; Merga *et al.*, 2020). Some authors relate that (abundance blue particles) to their availability in the environment (Ferreira *et al.*, 2018) or because fishes mistake them more as they are like food (Barboza *et al.*, 2019). The red particles came second representing 41.3% of the total plastic debris, the source of red fibers is the fishing industry mainly fishing nets (Cole *et al.*, 2011; Lusher *et al.*, 2013; Nelms *et al.*, 2018).

The results show no significant differences in the ingestion of plastic debris between males, females and undetermined specimens ($p > 0.05$). Maybe the availability of these pollutants particles in the ecosystems (pelagic and benthic) offers the same chance for all these categories, although they have different feeding habits.

Contaminated fish specimens by plastic debris in gastrointestinal tract was significantly higher in wet season as compared to dry season ($p < 0.01$). The wet season showed a high contamination (2092 plastic particles) compared to dry season (129 plastic particles). Precipitation and strong winds during the wet season (63.7 mm in our study) stimulate the movement and degradation of plastic debris (Cheung *et al.*, 2016). In addition, rivers are important sources of plastic contamination (Rowley *et al.*, 2020; Xu *et al.*, 2020), many microplastics and mesoplastics are maybe introduced to the sea by many rivers connected to the gulf of Bejaia. This high input of marine debris into the coastal waters depends on the seasonal activity making therefore plastic particles available to fish species then to consumers of fish.

5. Conclusion

This study shows high ingestion of plastic particles by commercial fishes from the gulf of Bejaia (Algeria). Extracted plastic debris were analyzed for the first time in the gastrointestinal tract of examined fish species. These pollutants exhibit a variability in colors, morphotypes and size, their abundance is higher in the wet season and in fish species from different ecosystems (pelagic, benthopelagic and demersal), and particularly those having a benthopelagic and demersal behavior. The obtained results maybe give an insight on the state of the marine ecosystem health of Algerian coast (especially in the studied region).

We highly recommend using the digestion process by sex in the future investigations on plastic particles ingested by fish species. We also recommend substantial investigations on the impact of these potential toxic

pollutants on the health of consumers, and on depollution techniques reducing this kind of pollutants in the environment.

Acknowledgements

We warmly thank the fishermen for their help in getting fish samples. We would like to thank the anonymous reviewers, we believe that all their comments and remarks substantially improved our article.

References

- Akhter, N., & Panhwar, S. K. 2022. Baseline study of microplastics in the gastrointestinal tract of commercial species inhabiting in the coastal waters of Karachi, Sindh, Pakistan. *Front. Mar. Sci.*, **9**:855386.
- Anastasopoulou, A., Mytilineou, C., Smith, C. J., & Papadopoulos, K. N. 2013. Plastic debris ingested by deep-water fish of the Ionian Sea (Eastern Mediterranean). *Deep Sea Res. Part I Oceanogr. Res. Pap.*, **74**: 11-13.
- Andrady, A. L. 2011. Microplastics in the marine environment. *Mar. Pollut. Bull.*, **62**(8): 1596-1605.
- Baalkhuyur, F. M., Dohaish, E. J. A. B., Elhalwagy, M. E., Alikunhi, N. M., AlSuwailem, A. M., Røstad, A., & Duarte, C. M. 2018. Microplastic in the gastrointestinal tract of fishes along the Saudi Arabian Red Sea coast. *Mar. Pollut. Bull.*, **131**: 407-415.
- Barboza, L. G. A., Lopes, C., Oliveira, P., Bessa, F., Otero, V., Henriques, B., & Guilhermino, L. 2020. Microplastics in wild fish from North East Atlantic Ocean and its potential for causing neurotoxic effects, lipid oxidative damage, and human health risks associated with ingestion exposure. *Sci. Total Environ.*, **717**: 134625.
- Bellas, J., Martínez-Armental, J., Martínez-Cámara, A., Besada, V., & Martínez-Gómez, C. 2016. Ingestion of microplastics by demersal fish from the Spanish Atlantic and Mediterranean coasts. *Mar. Pollut. Bull.*, **109**(1): 55-60.
- Boucher C., Morin M. & Bendell L. I. 2016. The influence of cosmetic microbeads on the sorptive behavior of cadmium and lead within intertidal sediments: A laboratory study. *Reg. Stud. Mar. Sci.*, **3**: 1-7.
- Brennecke, D., Duarte, B., Paiva, F., Caçador, I., & Canning-Clode, J. 2016. Microplastics as vector for heavy metal contamination from the marine environment. *Estuarine, Cont. Shelf Res.*, **178**: 189-195.
- Browne, M. A., Niven, S. J., Galloway, T. S., Rowland, S. J., & Thompson, R. C. 2013. Microplastic moves pollutants and additives to worms, reducing functions linked to health and biodiversity. *Curr. Biol.*, **23**(23): 2388-2392.
- Catarino, A. I., Thompson, R., Sanderson, W., & Henry, T. B. 2017. Development and optimization of a standard method for extraction of microplastics in mussels by enzyme digestion of soft tissues. *Environ. Toxicol. Chem.*, **36**(4): 947-951.
- Cheung, P. K., Cheung, L. T. O., & Fok, L. 2016. Seasonal variation in the abundance of marine plastic debris in the estuary of a subtropical macro-scale drainage basin in South China. *Sci. Total Environ.*, **562**: 658-665.
- Cole, M., Lindeque, P., Halsband, C., & Galloway, T. S. 2011. Microplastics as contaminants in the marine environment: A review. *Mar. Pollut. Bull.*, **62**(12): 2588-2597.
- Cole, M., Lindeque, P., Fileman, E., Halsband, C., Goodhead, R., Moger, J., & Galloway, T. S. 2013. Microplastic ingestion by zooplankton. *Environ. Sci. Technol.*, **47**(12): 6646-6655.

- Cole, M., Webb, H., Lindeque, P. K., Fileman, E. S., Halsband, C., & Galloway, T. S. 2014. Isolation of microplastics in biota-rich seawater samples and marine organisms. *Sci. Rep.*, **4**(1): 1-8.
- Couture S.J. 2017. L'impact des microplastiques sur les organismes marins. Département des sciences et des applications nucléaires de l'AIEA (l'agence internationale de l'énergie atomique).
- Derraik, J. G. 2002. The pollution of the marine environment by plastic debris: a review. *Mar. Pollut. Bull.*, **44**(9): 842-852.
- Ferreira, G. V., Barletta, M., Lima, A. R., Dantas, D. V., Justino, A. K., & Costa, M. F. 2016. Plastic debris contamination in the life cycle of Acoupa weakfish (*Cynoscion acoupa*) in a tropical estuary. *ICES J. Mar. Sci.*, **73**(10): 2695-2707.
- Ferreira, G. V., Barletta, M., Lima, A. R., Morley, S. A., Justino, A. K., & Costa, M. F. 2018. High intake rates of microplastics in a Western Atlantic predatory fish, and insights of a direct fishery effect. *Environ. Pollut.*, **236**: 706-717.
- Free, C. M., Jensen, O. P., Mason, S. A., Eriksen, M., Williamson, N. J., & Boldgiv, B. 2014. High-levels of microplastic pollution in a large, remote, mountain lake. *Mar. Pollut. Bull.*, **85**(1): 156-163.
- Galgani, F., Fleet, D., Van Franeker, J. A., Katsanevakis, S., Maes, T., Mouat, J., & Janssen, C. 2010. Marine Strategy Framework Directive-Task Group 10 Report marine litter do not cause harm to the coastal and marine environment. Report on the identification of descriptors for the Good Environmental Status of European Seas regarding marine litter under the Marine Strategy Framework Directive. Office for Official Publications of the European Communities.
- Güven, O., Gökdağ, K., Jovanović, B., & Kideys, A. E. 2017. Microplastic litter composition of the Turkish territorial waters of the Mediterranean Sea, and its occurrence in the gastrointestinal tract of fish. *Environ. Pollut.*, **223**: 286-294.
- Hartmann, N.B., Hüffer, T., Thompson, R.C., Hassellöv, M., Verschoor, A., Daugaard, A.E., Rist, S., Karlsson, T., Brennholt, N., Cole, M., Herrling, M.P., Hess, M.C., Ivleva, N.P., Lusher, A.L., Wagner, M. 2019. Are we speaking the same language? recommendations for a definition and categorization framework for plastic debris. *Environ. Sci. Technol.*, **53**: 1039-1047.
- Hidalgo-Ruz, V., Gutow, L., Thompson, R. C., & Thiel, M. 2012. Microplastics in the marine environment: a review of the methods used for identification and quantification. *Environ. Sci. Technol.*, **46**(6): 3060-3075.
- Holmes L. A., Turner A. & Thompson R. C. 2014. Interactions between trace metals and plastic production pellets under estuarine conditions. *Mar. Chem.*, **167**: 25-32.
- Horton, A. A., Jürgens, M. D., Lahive, E., van Bodegom, P. M., & Vijver, M. G. 2018. The influence of exposure and physiology on microplastic ingestion by the freshwater fish *Rutilus rutilus* (roach) in the River Thames, UK. *Environ. Pollut.*, **236**: 188-194.
- Jaafar, N., Azfaralriff, A., Musa, S. M., Mohamed, M., Yusoff, A. H., & Lazim, A. M. 2021. Occurrence, distribution and characteristics of microplastics in gastrointestinal tract and gills of commercial marine fish from Malaysia. *Sci. Total Environ.*, **799**: 149457.
- Jabeen, K., Su, L., Li, J., Yang, D., Tong, C., Mu, J., & Shi, H. 2017. Microplastics and mesoplastics in fish from coastal and fresh waters of China. *Environ. Pollut.*, **221**: 141-149.
- Junaid, M., Siddiqui, J. A., Sadaf, M., Liu, S., & Wang, J. 2022. Enrichment and dissemination of bacterial pathogens by microplastics in the aquatic environment. *Sci. Total Environ.*, 154720.
- Kane, I. A., & Clare, M. A. 2019. Dispersion, accumulation, and the ultimate fate of microplastics in deep-marine environments: a review and future directions. *Front. Earth Sci.*, **7**: 80.
- Karbalaei, S., Golieskardi, A., Hamzah, H. B., Abdulwahid, S., Hanachi, P., Walker, T. R., & Karami, A. 2019. Abundance and characteristics of microplastics in commercial marine fish from Malaysia. *Mar. Pollut. Bull.*, **148**: 5-15.
- Lagarde F., Olivier O., Zanella M., Daniel P., Hiard S. & Caruso A. 2016. Microplastic interactions with freshwater microalgae: Hetero-aggregation and changes in plastic density appear strongly dependent on polymer type. *Environ. Pollut.*, **215**: 331-339.
- Lusher, A. L., Mchugh, M., & Thompson, R. C. 2013. Occurrence of microplastics in the gastrointestinal tract of pelagic and demersal fish from the English Channel. *Mar. Pollut. Bull.*, **67**(1-2): 94-99.
- Matjašič, T., Simčič, T., Medvešček, N., Bajt, O., Dreo, T., and Mori, N. 2021. Critical evaluation of biodegradation studies on synthetic plastics through a systematic literature review. *Sci. Total Environ.*, **752**: 141959.
- Merga, L. B., Redondo-Hasselerharm, P. E., Van den Brink, P. J., & Koelmans, A. A. 2020. Distribution of microplastic and small macroplastic particles across four fish species and sediment in an African lake. *Sci. Total Environ.*, **741**: 140527.
- Millet, H., Vangheluwe, P., Block, C., Sevenster, A., Garcia, L. and Antonopoulos, R. 2018. **The Nature of Plastics and Their Societal Usage**, in *Plastics and the Environment*, pp. 1-20.
- Mishra, S., & Das, A. P. 2021. **Current treatment technologies for removal of microplastic and microfiber pollutants from wastewater**. *Wastewater Treatment*. pp. 237-251
- Murphy, F., Russell, M., Ewins, C., & Quinn, B. 2017. The uptake of macroplastic & microplastic by demersal & pelagic fish in the Northeast Atlantic around Scotland. *Mar. Pollut. Bull.*, **122**(1-2): 353-359.
- Nadal, M. A., Alomar, C., & Deudero, S. 2016. High levels of microplastic ingestion by the semipelagic fish bogue *Boops boops* (L.) around the Balearic Islands. *Environ. Pollut.*, **214**: 517-523.
- Nelms, S. E., Galloway, T. S., Godley, B. J., Jarvis, D. S., & Lindeque, P. K. 2018. Investigating microplastic trophic transfer in marine top predators. *Environ. Pollut.*, **238**: 999-1007.
- Neves, D., Sobral, P., Ferreira, J. L., & Pereira, T. 2015. Ingestion of microplastics by commercial fish off the Portuguese coast. *Mar. Pollut. Bull.*, **101**(1): 119-126.
- Pennino, M. G., Bachiller, E., Lloret-Lloret, E., Albo-Puigserver, M., Esteban, A., Jadaud, A., & Coll, M. 2020. Ingestion of microplastics and occurrence of parasite association in Mediterranean anchovy and sardine. *Mar. Pollut. Bull.*, **158**: 111399.
- Pham, D. N., Clark, L., & Li, M. 2021. Microplastics as hubs enriching antibiotic-resistant bacteria and pathogens in municipal activated sludge. *J. Hazard. Mater. Lett.*, **2**: 100014.
- Piyawardhana, N., Weerathunga, V., Chen, H. S., Guo, L., Huang, P. J., Ranatunga, R. R. M. K. P., & Hung, C. C. 2022. Occurrence of microplastics in commercial marine dried fish in Asian countries. *J. Hazard. Mater.*, **423**: 127093.
- Rainieri, S., Conlledo, N., Larsen, B. K., Granby, K., & Barranco, A. 2018. Combined effects of microplastics and chemical contaminants on the organ toxicity of zebrafish (*Danio rerio*). *Environ. Res.*, 162: 135-143.
- Rochman, C. M., Hoh, E., Kurobe, T., & Teh, S. J. 2013. Ingested plastic transfers hazardous chemicals to fish and induces hepatic stress. *Sci. Rep.*, **3**(1): 1-7.
- Romeo, T., Pietro, B., Pedà, C., Consoli, P., Andaloro, F., & Fossi, M. C. 2015. First evidence of presence of plastic debris in stomach of large pelagic fish in the Mediterranean Sea. *Mar. Pollut. Bull.*, **95**(1): 358-361.

- Rowley, K. H., Cucknell, A. C., Smith, B. D., Clark, P. F., & Morritt, D. 2020. London's river of plastic: High levels of microplastics in the Thames water column. *Sci. Total Environ.*, **740**: 140018.
- Sathish, M. N., Jeyasanta, I., & Patterson, J. 2020. Occurrence of microplastics in epipelagic and mesopelagic fishes from Tuticorin, Southeast coast of India. *Sci. Total Environ.*, **720**: 137614.
- Sbrana, A., Valente, T., Scacco, U., Bianchi, J., Silvestri, C., Palazzo, L., de Lucia, G.A., Valerani, C., Ardizzone, G. and Matiddi, M., 2020. Spatial variability and influence of biological parameters on microplastic ingestion by Boops boops (L.) along the Italian coasts (Western Mediterranean Sea). *Environ. Pollut.*, **263**: 114429.
- Teuten, E. L., Saquing, J. M., Knappe, D. R. U., Barlaz, M. A., Jonsson, S., Björn, A., *et al.* 2009. Transport and release of chemicals from plastics to the environment and to wildlife. *Trans. R. Soc. B.*, **364**: 2027–2045.
- Thiele, C. J., Hudson, M. D., Russell, A. E., Saluveer, M., & Sidaoui-Haddad, G. 2021. Microplastics in fish and fishmeal: an emerging environmental challenge?. *Sci. Rep.*, **11**(1): 1-12.
- Thompson, R.C., Olsen, Y., Mitchell, R.P., Davis, A., Rowland, S.J., John, A.W.G., McGonigle, D., Russell, A.E. 2004. Lost at sea: Where is all the plastic? *Science.*, **304**: 838-838.
- Thompson, R. C., Moore, C., vom Saal, F. S., & Swan, S. H. 2009. Plastics, the environment and human health: Current consensus and future trends. *Trans. R. Soc. B.*, **364**: 2153–2166.
- Valente, T., Sbrana, A., Scacco, U., Jacomini, C., Bianchi, J., Palazzo, L., & Matiddi, M. 2019. Exploring microplastic ingestion by three deep-water elasmobranch species: A case study from the Tyrrhenian Sea. *Environ. Pollut.*, **253**: 342-350.
- Wang, Q., Xu, Y., Liu, L., Li, L.Y., Lin, H., Wu, X.Y., Bi, W.J., Wang, L.T., Mao, D.Q. and Luo, Y. 2021. The prevalence of ampicillin-resistant opportunistic pathogenic bacteria undergoing selective stress of heavy metal pollutants in the Xiangjiang River, China. *Environ. Pollut.*, **268**: 115362.
- Wieczorek, A. M., Morrison, L., Croot, P. L., Allcock, A. L., MacLoughlin, E., Savard, O., & Doyle, T. K. 2018. Corrigendum: Frequency of Microplastics in Mesopelagic Fishes from the Northwest Atlantic. *Frontiers in Marine Science.*, **5**: 127.
- Wright, S. L., Rowe, D., Thompson, R. C., & Galloway, T. S. 2013. Microplastic ingestion decreases energy reserves in marine worms. *Curr. Biol.*, **23**(23): R1031-R1033.
- Xu, Q., Xiang, J., & Ko, J. H. 2020. Municipal plastic recycling at two areas in China and heavy metal leachability of plastic in municipal solid waste. *Environ. Pollut.*, **260**: 114074.
- Yin, L., Jiang, C., Wen, X., Du, C., Zhong, W., Feng, Z., & Ma, Y. 2019. Microplastic pollution in surface water of urban lakes in Changsha, China. *Int. J. Environ. Res. Public Health.*, **16**(9): 1650.

Peptides from Casein Extend the Survival Rate and Protect *Drosophila melanogaster* from Oxidative Stress Via Interacting with the Keap1-Nrf2 Pathway

Idris Zubairu Sadiq^{1,*}, Babangida Sanusi Katsayal¹, Rashidatu Abdulazeez², Odunola Safiyyah Adedoyin¹, Yakubu Fatimat Omengwu¹, Abdullahi Garba Usman^{3,4}

¹Department of Biochemistry, Faculty of life sciences, Ahmadu Bello University, Zaria; ²Drosophila and Neurogenetics laboratory, Department of Zoology, Faculty of life sciences, Ahmadu Bello University, Zaria; ³Operational research Centre in healthcare, Near East University, Nicosia, Turkish Republic of Northern Cyprus; ⁴Department of Analytical Chemistry, Faculty of Pharmacy, Near East University, Nicosia, Turkish Republic of Northern Cyprus

Received: August 11, 2022; Revised: September 25, 2022; Accepted: December 23, 2022

Abstract

It is generally established that oxidative stress has a role in the etiology of diseases linked to the lifestyle, such as cancer, aging, diabetes mellitus, and neurological diseases, among others. This research aims to evaluate the effect of casein on the survival rate and oxidative stress markers in *Drosophila melanogaster*. 360 flies were divided into four groups, each containing 90 flies (30 flies in triplicate). The groups include: 1) the control group; 2) the H₂O₂ treated group; 3) the H₂O₂ induced + 1% Casein group; 4) the 1% Casein only group. Oxidative stress was induced in the flies and 1% Casein was used to protect the flies through enrichment of their diet and the effect of stress and Casein treatment was monitored on the mortality rate of the flies and selected oxidative stress markers. The results revealed that H₂O₂ significantly decreases the survival rate, GSH, total thiol and total protein while it increases the level of MDA, SOD and CAT. However, treatment with 1% Casein significantly reverses the effect of H₂O₂ on the oxidative stress biomarkers and increases flies' survival rate. In conclusion, Casein may increase the survival rate of the fruit flies under stress and modulate stress biomarkers via possible binding of the peptides AS29, AS14, K009, and K010 to the Keap1/Nrf2 signaling pathway.

Keywords: Antioxidants, fruit flies, hydrogen peroxide, casein, Keap1/Nrf2

Practical application

The oxidation process is thought to be the primary cause of human aging, degenerative diseases, and stress related diseases. Casein is a protein found in mammalian milk that accounts for roughly 20 to 60% of the proteins in human milk and 80% of the proteins in cow's milk. It represents a good source of antioxidants and bioactive peptides making it a promising candidate for preventing harmful stress, aging, immune boosting and preventing/treating disorders associated with oxidative stress.

1. Introduction

Oxidative stress is a typical situation in which the biological buffering capacity of the system is exceeded by production of reactive oxygen/nitrogen species (Tabima *et al.*, 2012). This reactive species often damages biological macromolecules (carbohydrates, DNA, proteins and lipids), thereby modifying the functions of these molecules (Roberts and Hubel, 2004). The genesis and/or progress of numerous diseases, including cardiovascular diseases, atherosclerosis, diabetes, cancer and metabolic disorders

were linked to oxidative stress (Taniyama and Griendling, 2003). Life of living organisms encounters reactive oxidants from internal metabolisms and environmental exposure to chemicals. The body's defense system responds via the Nrf2, which controls the expression of an array of antioxidant response element-dependent genes (Ma, 2013). As free radicals are extremely reactive, macromolecules in nearly all the cells are often prone to attack, causing irreversible damage. Therefore, the breakdown of excessive H₂O₂ is a prerequisite for survival of the living cells (Droge, 2002).

Natural antioxidants derived from foods have been studied and believed to have protective biological functions in preventing stress induce diseases and cell damage due to free radicals (Balsalobre-Fernández *et al.*, 2017). Milk, in particular, contains proteins with varied biological functions, and caseins are the major protein of ovine and bovine milks, which is present in the form of macromolecular aggregates.

Milk proteins and dairy products were reported to have antioxidant activity which can scavenge reactive oxygen species (Khan *et al.*, 2019). Casein possesses several bioactivities including antimicrobial, antioxidative, antithrombotic, antihypertensive, anti-carcinogenic, and immunomodulatory process (Shahidi and Zhong, 2008).

* Corresponding author. e-mail: izzsadiq@abu.edu.ng.

The basic structure of casein molecules works as a scavenger for free radicals since free individual amino acids may not quench these radicals (Suetsuna *et al.*, 2000). Owing to their chemical antioxidant capabilities, bioactive peptides have attracted a lot of attention these days. The properties of these bioactive peptides are demonstrated by their well-characterized properties, which include chelating transition pro-oxidant metals and hydrogen atom transfer (Aguilar-Toalá and Liceaga, 2021), inhibiting the lipoxygenase-catalysed lipid oxidation (Suetsuna *et al.*, 2000) as well as the ability to attract free radicals (Rocha-Decker, 2004). These well characterized properties make these peptides as potential antioxidants present in milk and dairy products.

2. Materials and methods

2.1. Chemicals and reagents

Casein from bovine milk and hydrogen peroxide were purchased from Sigma Aldrich. All other reagents were of analytical grades.

2.2. *Drosophila melanogaster* stock and culture

D. melanogaster wild type (Harwich strain) flies was obtained, maintained and reared from the Drosophila laboratory, Department of Zoology, Ahmadu Bello University, Zaria on a cornmeal medium at constant temperature and humidity (23 - 25°C) under 12 hrs dark/light cycle conditions.

2.3. Experimental protocol

Thirty (30) flies consisting of ten (10) males and twenty (20) females were segregated into twelve (12) vials each, and divided into four (4) groups, with each group in triplicate. The experimental design is presented in figure 1.

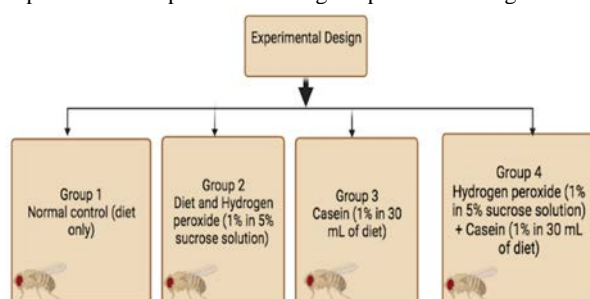


Figure 1. Experimental design

2.4. Stress induction in *Drosophila melanogaster*

Wild type (Harwich strain) of *D. melanogaster* was used for *in vivo* studies. The flies were induced by exposing 3 days old flies (both sexes) to a filter paper moistened with 1% H₂O₂ (in 5% sucrose solution) for 4 hours. The exposed flies were then placed in a culture media containing Casein for 3 days before subjecting the flies to biochemical analysis as described elsewhere (Subramanian *et al.*, 2014) with minor modifications. The control flies were only provided with the normal diet without exposure to H₂O₂ or administration of casein.

2.5. Survival rate of flies

The survival rate was determined as modified from (Chattopadhyay *et al.*, 2015). 10 male and 20 female (single-sex) flies were segregated into vials diet with the

treatment of Casein after exposure with H₂O₂. The flies were transferred into new vials with fresh diet every 5 days.

2.6. Preparation of samples and biochemical assays

2.6.1. Sample Preparations

Thirty (30) flies were anesthetized on ice for the biochemical experiments, weighed, homogenized in 0.1M phosphate buffer (PBS), and centrifuged for 10 min at 4,000 rpm and 4°C. Assays for total protein, GSH, catalase, superoxide dismutase, malondialdehyde, and total thiol (TSH) levels were performed using the supernatants that were obtained after separating the pellets from the supernatants.

2.6.2. Determination of Biochemical Parameters

A modified Lowry method was used to measure the protein concentration (Peterson, 1977). Glutathione and total thiol levels were estimated using the Ellman method (Ellman, 1959). Catalase activity was measured using the Aebi-reported technique (Aebi, 1984). Malondialdehyde level was measured using the method described by Niehaus & Samuelson (Niehaus & Samuelson, 1968), while superoxide dismutase activity was analyzed using the method described by Fridovich (Fridovich, 1989).

2.7. In silico Digestion and Bioactivity Prediction

Gastrointestinal enzymatic hydrolysis of casein was accomplished using BIOPEP Web server by simulating the action of different proteases found in the digestive tract of *Drosophila* such as chymotrypsin (EC3.4.21.1), trypsin (EC 3.4.21.4) and (pepsin, pH = 1.3) (Kose, 2021). The potential antioxidant bioactivities of the peptides were analyzed using FeptideDB and published research papers (<http://www4g.biotech.or.th/FeptideDB/>) (Panyayai *et al.*, 2019). FeptideDB represent bioactive peptide database which contain records from both available research articles and about 12 public bioactive peptide databases including BIOPEP-UWM, APD, BACTIBASE, CAMP, PenBase, RAPD, Hmrbase, PhytAMP, PeptideDB, ACEpepDB, Amper, and BAGEL3.

2.8. Molecular Docking Studies

The 3-Dimensional structure of Keap1 was retrieved from protein data bank with PDB Code 6TYM, and the selected bioactive peptide sequence was converted to 3D structure using a 3D peptide generator. By eliminating solvent molecules, the crystal structures of Keap1 and the peptides were formed, and then Chimera 1.11 was used to optimize them to mimic physiological conditions (Pettersen *et al.*, 2004). The standard residue was given polar hydrogen, and Gasteiger partial charge—which presumes that all hydrogen atoms are clearly represented—was used to assign partial charges to the standard residue. Utilizing AutoDock Vina v.1.1.2, molecular docking studies were used to identify the most advantageous binding interactions. With the assistance of Molegro Molecular Viewer 2.5, the interactions of the docked complexes were virtually examined.

3. Results

The result shows a significant decrease in the survival of flies exposed to hydrogen peroxide due to oxidative stress compared to those administered 1% casein. The survival assay graph shown below (Fig.2) indicates the survival rate of the flies as percentage survival against number of days.

PERCENTAGE SURVIVAL(%)

Figure 2: Effect of Hydrogen peroxide and Casein on survival of *Drosophila melanogaster*. Flies exposed to hydrogen peroxide had a 100% decreased survival at day 28, while 30%, 25% and 20% decrease in survival were observed in Casein-treated, control and casein only flies, respectively.

Essentially, we noted that oxidative stress significantly ($p < 0.05$) lowered the amount of total protein in the stress flies, but no statistical significant differences were observed in the 1% casein-treated, normal control, and negative control (1% casein alone) groups (Fig. 3a). We also observe that the activity of SOD considerably ($p < 0.05$) increased in the flies exposed to H_2O_2 , but no statistically significant difference ($p < 0.05$) was noted in the case of the flies treated with 1% casein and the control group (Fig. 3b). Flies subjected to hydrogen peroxide also showed a significant rise ($p < 0.05$) in the level of malondialdehyde (MDA), whereas in the 1% casein treatment and negative control (1% casein alone) groups, the MDA concentration did not differ significantly ($p < 0.05$) from that of the control group (Fig. 3c). In the stressed flies also, total thiol levels also decreased significantly ($p < 0.05$). However, neither the group treated with 1% casein nor the negative control (1% casein only) group showed a statistically significant decrease ($p < 0.05$) in comparison to the control (Fig. 3d). Additionally, stress was discovered to significantly ($p < 0.05$) lower the level of GSH in the flies (Fig. 3e), whereas the catalase activity in flies exposed to hydrogen peroxide considerably ($p < 0.05$) increased in comparison to the other groups (3f).

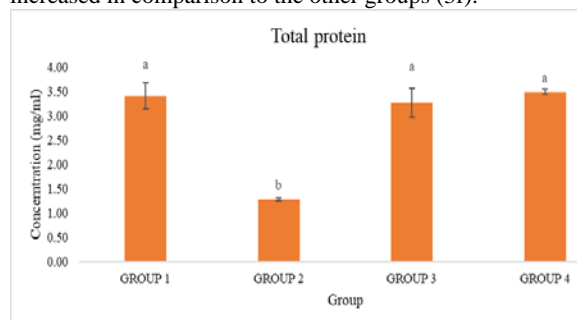


Figure 3a: Effect of Casein on total protein in hydrogen peroxide induced oxidative stress in *Drosophila melanogaster*. [All results are expressed as mean \pm standard deviation, and superscripts containing different letters (a, b) indicate significantly different results when at $p < 0.05$].

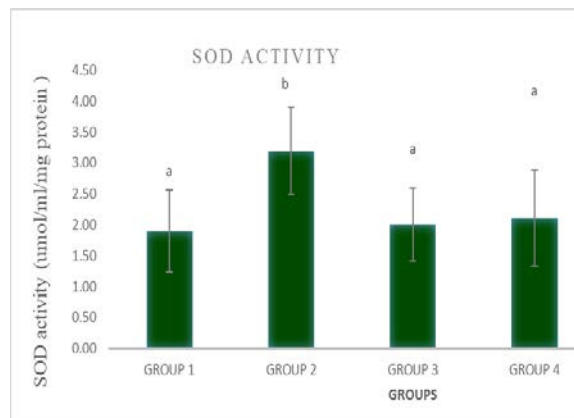


Figure 3b: Effect of Casein on SOD in hydrogen peroxide induced oxidative stress in *Drosophila melanogaster*. [All results are expressed as mean \pm standard deviation, and superscripts containing different letters (a, b) indicate significantly different results when at $p < 0.05$].

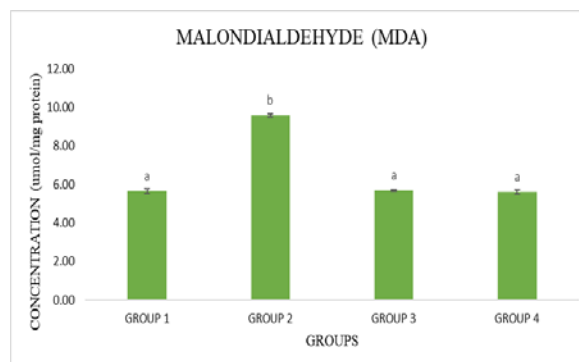


Figure 3c: Effect of Casein on MDA in hydrogen peroxide induced oxidative stress in *Drosophila melanogaster*. [All results are expressed as mean \pm standard deviation, and superscripts containing different letters (a, b) indicate significantly different results when at $p < 0.05$].

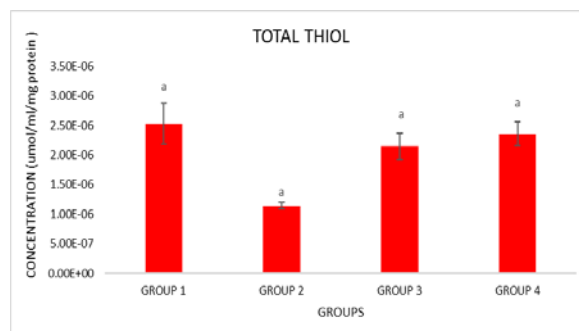


Figure 3d: Effect of Casein on total thiol in hydrogen peroxide induced oxidative stress in *Drosophila melanogaster*. [All results are expressed as mean \pm standard deviation, and superscripts containing different letters (a, b) indicate significantly different results when at $p < 0.05$].

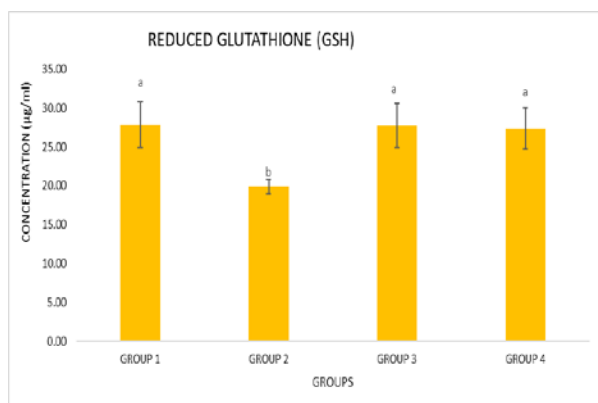


Figure 3e: Effect of Casein on GSH in hydrogen peroxide induced oxidative stress in *Drosophila melanogaster*. [All results are expressed as mean \pm standard deviation, and superscripts containing different letters (a, b) indicate significantly different results when at $p < 0.05$].

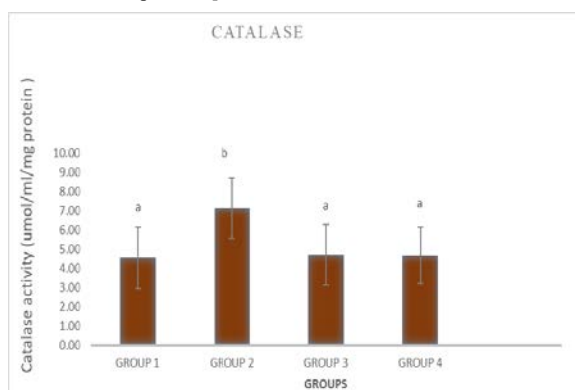


Figure 3f: Effect of Casein on CAT in hydrogen peroxide induce oxidative stress in *Drosophila melanogaster*. [All results are expressed as mean \pm standard deviation, and superscripts containing different letters (a, b) indicate significantly different results when at $p < 0.05$].

3.1. In silico Digestion and Bioactivity Prediction

Hydrolysis of casein proteins with cysteine/aspartic/serine type endopeptidases was accomplished using the BIOPEP website. These enzymes were reported to play most important role in producing bioactive peptides of 3-30 amino acid chains in the gastrointestinal tract of *Drosophila melanogaster* (Lemaitre & Miguel-Aliaga, 2013). The enzymes generate about 90 peptides 3-50 amino acid chains with different molecular weight and isoelectric points (Table 1). Four bioactive peptides were selected based on their antioxidant properties predicted from PeptideDB and literature search (written in red in Table.1). The selected bioactive peptides were converted into a 3D structure for molecular docking interaction with Keap1.

Table1. Digestion Product

S/N	Mass	PI	Peptide	Mass	PI	Peptide	Mass	PI	Peptide	Mass	PI	Peptide
	Alpha S2			Alpha S1			Beta Casein			Kappa Casein		
1.	348.46	8.80	AMK	351.4	5.52	LGY	407.51	5.52	LLY	402.45	8.75	QQK
2.	381.43	5.15	TVY	524.62	8.76	HIQK	388.46	6	IEK	330.43	8.75	IAK
3.	392.46	5.52	LNK	493.61	8.76	HPIK	373.45	8.75	INK	348.36	5.55	SDK
4.	422.48	5.52	LQY	667.76	4	YPELF	512.61	6.74	IHPF	418.41	4.37	DER
5.	403.44	6.00	QEK	614.76	8.76	LHSMK	750.85	4	YPVEPF	378.44	5.99	CEK
6.	490.60	5.49	VIPY	747.91	5.19	TTMPLW	747.91	6.1	EMPPFK	408.57	8.5	MMK
7.	484.60	8.75	IQPK	636.66	3.8	TDAPSF	645.77	6.1	EAMAPK	503.51	5.84	NQDK
8.	539.59	8.76	QHOK	770.93	6	LEQLLR	741.93	5.52	GPFPITV	465.51	5.52	GLNY
9.	502.57	9.75	ISQR	688.78	5.97	VNELSK	820.96	3.8	DMPAQF	528.56	5.52	YPSY
10.	488.54	5.84	DQVK	776.89	5.49	VPLGTQY	829.95	8.79	AVPYPQR	473.57	9.72	VLSR
11.	553.62	5.52	FPQY	830.85	4.14	EDVPSEK	779.98	8.72	VLPVPQK	512.61	10.18	PAAVR
12.	501.58	6.10	EVVR	910	6.85	EGHAQQK	994.16	6	QEPVLGPVR	651.76	5.52	LPYPY
13.	590.68	5.57	ALPQY	905.06	4	VAPFPEVF	1087.3	6	LQPEVMGVSK	632.76	5.52	IPQY
14.	747.80	4.25	LTEEEK	1107.19	3.8	QLDAYPSGAW	1438.88	8.22	VLILACLVALALAR	655.85	8.5	MAIPPK
15.	689.76	4.21	ITVDDK	1363.55	3.8	EPMIGVNQELAY	1834.82	3.77	QSEEQQTDELQDK	971.09	7.02	HPHPLSF
16.	867.82	3.67	NANEEY	1486.56	4.14	SDIPNPIGSENSEK	2735.09	4.13	TESQSLTLTDVENLHLP LPLQSW	942.08	5.24	SPAQLQW
17.	812.89	4.00	ENLCSTF	1580.76	4.25	VPQLEIVPNSAEER	2646.84	3.83	ELEELNVPGEIVSLSS EESITR	1015.18	5.96	PVALINNQF
18.	948.04	4.00	ALNEINQF	1468.9	8.25	LLILTCLVAVALAR	2912.42	8.54	MHQPHQPLPPTVMFPP QSVLSLSQSK	1056.23	8.75	QVLSNTVPAK
19.	874.02	8.75	NMAINPSK	1759.98	5.4	HQGLPQEVLENLLR	3755.37	5.57	AQTQSLVYPFGPIPNS LPQNIPPLTQTPVVVPPF	1193.36	7.96	SCQAQPTTMAR
20.	1023.20	5.52	QGPIVLNPW	1767.84	3.71	DIGSESTEDQAMEDIK				1299.66	5.52	LVVTILALTLPF
21.	1157.26	3.57	TVDMESTEVF	2321.5	3.98	QMEAEISSSEIVPNSVEQ K				1510.63	4.53	LGAQEQNQEQPIR
22.	1002.28	7.89	TCLLAVALAK							5455.92	3.28	TEIPTINTIASGEPT STPTTEAVESTVA TLEDSPEVIESPPEI NTVQVTSTAV
23.	251.27	4.25	EQLSTSEENSK									
24.	1195.38	9.75	NAVPTPTLNR									
25.	1838.90	3.98	SIGSSSESAEVA TEEVK									
26.	2171.27	4.09	NTMEHVSSSEES IISQETY									
27.	880.86	4.53	STSEENSK									
28.	752.69	3.79	GSSSEESA									

AS29 = Alpha S2 peptide 9, AS14 = Alpha S1 peptide 4, K009 = Kappa casein peptide 9 and K010 =Kappa casein peptide 1

3.2. Molecular Docking Studies

As presented in the Figures 4-7 below, the four bioactive peptides selected from table1 bind to Nrf2 binding pocket in Keap1 with a very strong binding energy (Table2). The interactions resulted from both polar and nonpolar amino acid residues found within the binding cavities of the proteins which include Tyr10, Arg36, Phe253, Tyr248, Gly231, Ala232, Val280, Gly275, Gly9, Ser39, Arg53, and Asn90 among many others (Fig.4-7).

Table 2. Binding energy of the selected bioactive peptides on Keap1.

Ligand/Peptides	Binding Energy (Kcal/mol)
AS29	-8.0
AS14	-8.4
K009	-8.6
K010	-9.7

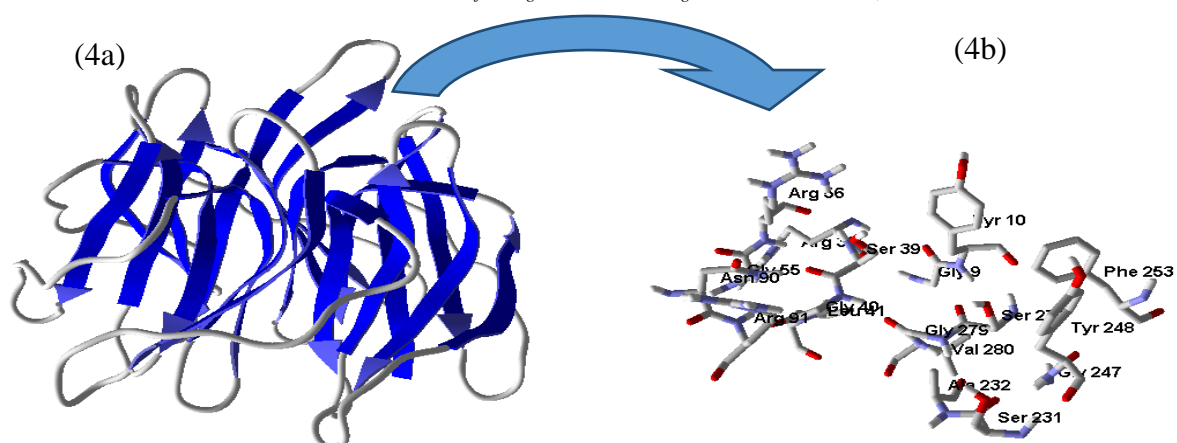


Figure 4. Keap1 (4a) cartoon structure (4b) 3D pocket amino acids residues.

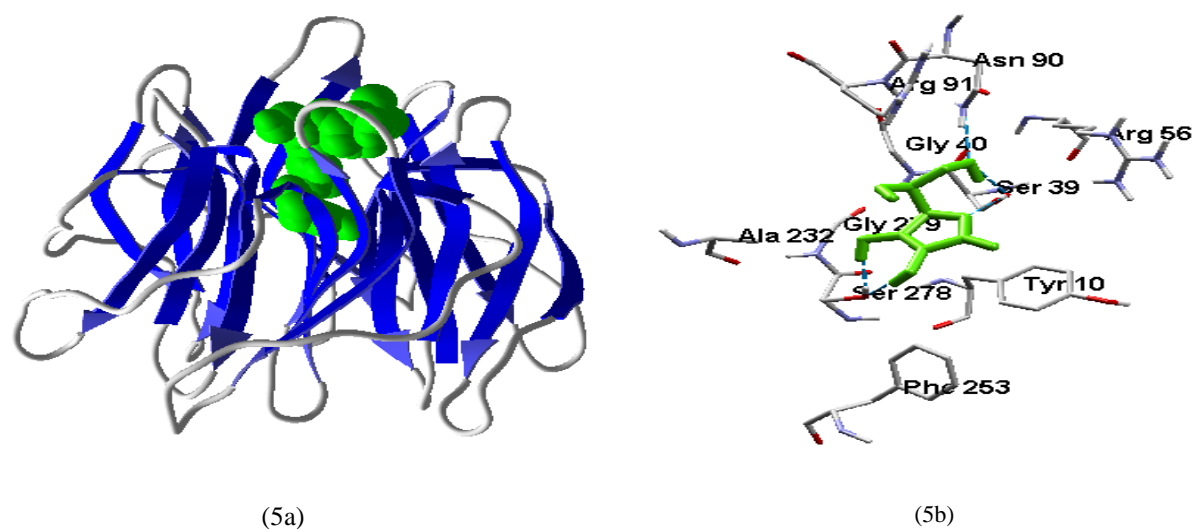


Figure 5. Keap1 bound to AS29 (5a) cartoon structure (5b) 3D interaction residues.

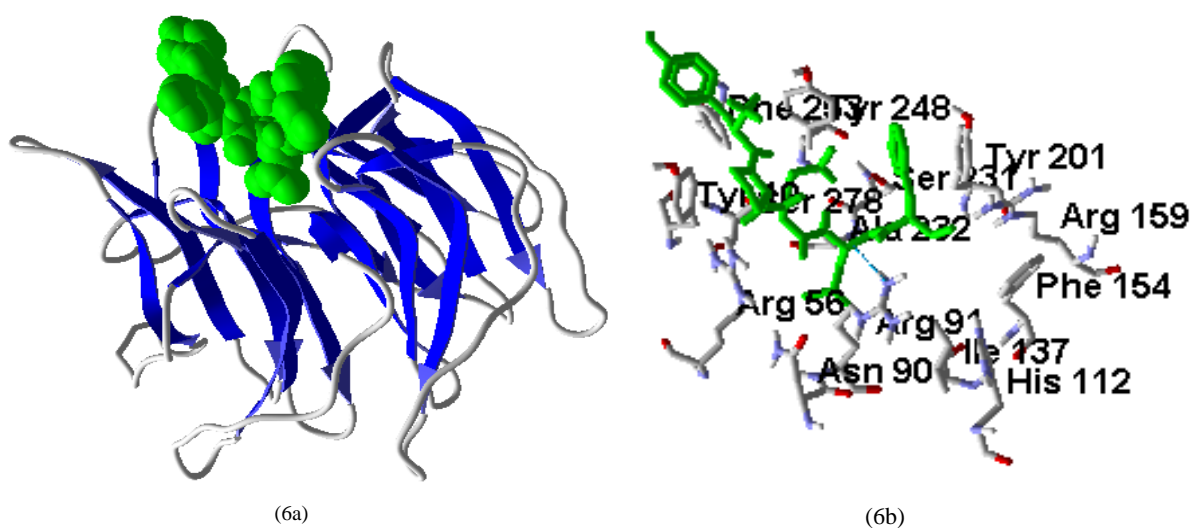


Figure 6. Keap1 bound to AS14 (6a) cartoon structure (6b) 3D interaction residues.

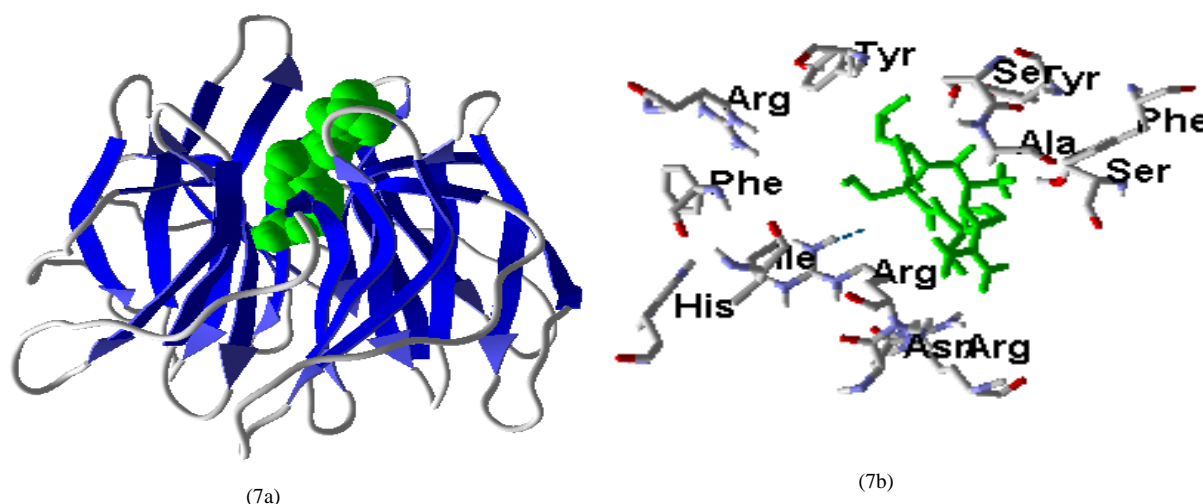


Figure 7: Keap1 bound to K010 (7a) cartoon structure (7b) 3D interaction residues.

4. Discussion

This research is aimed at exploring the possible use of peptides as potentially antioxidant agents for enhancing longevity as well as the amelioration of oxidative stress that is common in both aging process and stress related illnesses. In the cellular models, exposure to hydrogen peroxide (H_2O_2) is a common approach for inducing oxidative damage or stress (Gille & Joenje, 1992). Previous study indicated that casein had a clearly unfavorable effect on longevity at an acid pH, contrary to the finding obtained at a neutral pH (Van Herreweghe, 1974). Essentially, the current study uses a neutral pH and 5% sucrose which may likely play role in flies longevity (Van Herreweghe, 1974). Our survival assay results indicated that casein increase the survival rate of the flies by protecting the flies from oxidative stress. Our data thus showed that stress substantially reduced the level of some oxidative stress markers including total protein, total thiol, and reduced glutathione while increasing the level of malondialdehyde, superoxide dismutase and catalase ($p < 0.05$) when compared to the control. The increase in SOD activity in stressed fruit flies suggests that this enzyme is involved in reducing the presence of hydrogen peroxide free radicals. The critical antioxidant activity of SOD is to catalyzes the dismutation of superoxide anion radicals to hydrogen peroxide as well as involving in chain breaking reactions that protect against harmful effects of lipid peroxidation (Wang *et al.*, 2018). CAT safeguard cells by converting hydrogen peroxide to molecular oxygen and water, a crucial process for the development of tolerance and adaptive cellular response to oxidative stress (González-Párraga *et al.*, 2003). The increase in the activity of catalase in the stress flies indicates the presence of oxidative stress and antioxidant response by the system (Perkhulyn *et al.*, 2017).

A significant source of necessary amino acids that also function as intracellular antioxidants is dietary protein and a study has linked arginine and histidine oxidative stress and inflammation in obese and non-obese women (Niu *et al.*, 2012). Treatment with 1% casein to stress flies considerably increased the survival of *D. melanogaster* under stress conditions and reversed H_2O_2 induced

oxidative stress by modulating the levels of the oxidative stress biomarkers. According to a study, casein enrichment in the diet of flies can dramatically reduce oxidative damage and undo alterations in the activity of antioxidant enzymes (Venkareddy, 2015). Milk containing A1 β -casein was linked to slower and less accurate cognitive functioning, worsened PD3 symptoms, delayed transit and increased gastrointestinal inflammation (Jianqin *et al.*, 2016). Therefore, taking milk that solely contains the A2 form of beta casein could prevent those unwanted effects (Jianqin *et al.*, 2016).

A study has also evaluated the antioxidant activity of casein phosphoprotein in caco-2 cells and confirmed its cytoprotective effects (Laparra *et al.*, 2008). Another study also indicated the protective effects of casein and dairy products from breast, prostate and colon cancer (Khan *et al.*, 2019). The existence of a larger quantity of glutathione, which is widely known for its antioxidant activity, could be responsible for casein's anticancer properties (Khan *et al.*, 2019). Mammalian milk contains casein that makes up roughly 20% to 60% of the proteins in human milk and 80% of the proteins in cow's milk. Considering the exceptional properties of this peptide, casein may function as a co-adjuvant in conventional treatment for conditions like cardiovascular disease, metabolic disease, asthma and other stress-related diseases (Khan *et al.*, 2019). Casein could also be hydrolyzed using different enzymes to produce a vast number of bioactive peptides having physiological activities in the endocrine, cardiovascular, immunological, and neurological systems (Mohanty *et al.*, 2016). Antioxidant peptides have become increasingly popular as they have the ability to remove excess free radicals (Zhao *et al.*, 2021). From this study, we observed that four bioactive peptides from casein, AS29, AS14, K009, and K010 had antioxidant activity and may help the flies live longer by reversing oxidative stress markers.

The Nrf2 is a master transcription factor tasked with guarding against oxidative cell damage by controlling the production of antioxidant proteins (Zhang, 2006). An essential signaling pathway for controlling the antioxidant system is provided by the interaction between Keap1 and Nrf2, which also maintains the cell's redox balance and metabolism (Zhang, 2006). When under normal

circumstances, Nrf2 is located within the cytoplasm and rapidly broken down by a group of proteins. However, when under conditions of oxidative stress, Nrf2 binds to the antioxidant response element (ARE) in the nucleus and starts the transcription of antioxidant genes such as catalase, glutathione S-transferase, superoxide dismutase, heme oxidase (heme oxygenase), thioredoxin reductase, glutathione reductase/peroxidase, NAD(P)H dehydrogenase, thioredoxin reductase, heme oxygenase, glutathione S-transferase. As numerous conditions were linked to oxidative stress, including cancer, Alzheimer's disease, Parkinson's disease, and diabetes, study have shown that the Keap1-Nrf2 signaling pathway to be involved (Tkachev *et al.*, 2011). Selected bioactive peptides from casein were reported in the literature to conferred antioxidant activities by stimulating the activities of CAT, GSH, SOD and GSH-Px (Xiao *et al.*, 2021). According to a recent study, bioactive peptides derived from milk have an antioxidant effect through activating the Nrf2 pathway (Tonolo *et al.*, 2020). Molecular docking from this study reveals that the selected bioactive peptides (AS29, AS14, K009, and K010) fits exactly in the binding pocket of Keap1 (Fig. 4-7), and these will facilitate its binding to the antioxidant response element and subsequent activation of antioxidant enzymes.

5. Conclusion

Casein increased the survival rate of *Drosophila melanogaster* under oxidative stress conditions. Casein was also found to modulate the selected oxidative stress markers by acting as an antioxidant.

Conflict of interest

None

Acknowledgement

The team appreciates the assistance of Mal. S. Muhammad, the research assistant of the *Drosophila* and Neurogenetics laboratory, Department of Zoology, A.B.U. Zaria. We thank Prof. D.M. Shehu, Department of Zoology A.B.U. Zaria for his mentorship during this research.

Authors Contributions

IZS. Conception, supervision, financial contribution and manuscript writing. RA. Supervision of the lab work and edited the manuscript. O. S. A. and Y. F. O. carried out the research and manuscript writing. BSK. Supervision, molecular docking and manuscript writing. AGU. Statistics, graphs, and final manuscript version.

References

Aebi, H. (1984). Catalase in vitro. *Meth Enzymol.*, 105, 121–126.

Aguilar-Toalá, J. E., & Liceaga, A. M. (2021). Cellular antioxidant effect of bioactive peptides and molecular mechanisms underlying: beyond chemical properties. *International Journal of Food Science & Technology*, 56(5), 2193–2204.

Balsalobre-Fernández, C., Marchante, D., Baz-Valle, E., Alonso-Molero, I., Jiménez, S. L., & Muñoz-López, M. (2017). Analysis of wearable and smartphone-based technologies for the measurement of barbell velocity in different resistance training exercises. *Front Physiol.*, 8, 649.

Chattopadhyay, D., James, J., Roy, D., & Sen, S. (2015). Effect of semolina-jaggery diet on survival and development of *Drosophila melanogaster*. *Fly (Austin)*, 9(1), 16–21. <https://doi.org/10.1080/19336934.2015.1079361>

Droge, W. (2002). Free radicals in the physiological control of cell function. *Physiol Rev*, 82(1), 47–95.

Ellman, G. L. (1959). Tissue sulfhydryl groups. *Arch Biochem Biophys*, 82(1), 70–77.

Fridovich, I. (1989). Superoxide dismutases: an adaptation to a paramagnetic gas. *J Biol Chem*, 264(14), 7761–7764.

Gille, J. J. P., & Joenje, H. (1992). Cell culture models for oxidative stress: superoxide and hydrogen peroxide versus normobaric hyperoxia. *Mut Res/DNAging*, 275(3–6), 405–414.

González-Párraga, P., Hernández, J. A., & Argüelles, J. C. (2003). Role of antioxidant enzymatic defences against oxidative stress (H₂O₂) and the acquisition of oxidative tolerance in *Candida albicans*. *Yeast*, 20(14), 1161–1169.

Jianqin, S., Leiming, X., Lu, X., Yelland, G. W., Ni, J., & Clarke, A. J. (2016). Effects of milk containing only A2 beta casein versus milk containing both A1 and A2 beta casein proteins on gastrointestinal physiology, symptoms of discomfort, and cognitive behavior of people with self-reported intolerance to traditional cows' milk. *Nutr J.*, 15, 35. <https://doi.org/10.1186/s12937-016-0147-z>

Khan, I. T., Nadeem, M., Imran, M., Ullah, R., Ajmal, M., & Jaspal, M. H. (2019). Antioxidant properties of Milk and dairy products: a comprehensive review of the current knowledge. *Lipids Health Dis.*, 18(1), 1–13.

Kose, A. (2021). In Silico Bioactive Peptide Prediction from The Enzymatic Hydrolysates of Edible Seaweed Rubisco Large Chain. *Turkish J Fish Aquat Sci.*, 21(12), 615–625.

Laparra, J. M., Alegra, A., Barber R., & Farr, R. (2008). Antioxidant effect of casein phosphopeptides compared with fruit beverages supplemented with skimmed milk against H₂O₂-induced oxidative stress in Caco-2 cells. *Food Res Int.*, 41(7), 773–779.

Lemaitre, B., & Miguel-Aliaga, I. (2013). The digestive tract of *Drosophila melanogaster*. *Ann Rev Genet.*, 47, 377–404.

Ma, Q. (2013). Role of nrf2 in oxidative stress and toxicity. *Ann Rev Pharmacol Toxicol.*, 53, 401–426. <https://doi.org/10.1146/annurev-pharmtox-011112-140320>

Mohanty, D. P., Mohapatra, S., Misra, S., & Sahu, P. S. (2016). Milk derived bioactive peptides and their impact on human health – A review. *Saudi J Biol Sci.*, 23(5), 577–583. <https://doi.org/https://doi.org/10.1016/j.sjbs.2015.06.005>

Niehaus, W. G., & Samuelson, B. (1968). Formation of malondialdehyde from and glucose 6-phosphate dehydrogenase from fermenting yeast and phospholipids arachidonate during microsomal lipid peroxidation. *Eur J Biochem.*, 6, 126–130.

Niu, Y.-C., Feng, R.-N., Hou, Y., Li, K., Kang, Z., Wang, J., Sun, C.-H., & Li, Y. (2012). Histidine and arginine are associated with inflammation and oxidative stress in obese women. *British J Nutr.*, 108(1), 57–61.

Panyayai, T., Ngamphiw, C., Tongsim, S., Mhuanong, W., Limsripraphan, W., Choowongkamon, K., & Sawatdichaiakul, O. (2019). PeptideDB: A web application for new bioactive peptides from food protein. *Heliyon*, 5(7), e02076.

- Perkhulyn, N. V., Rovenko, B. M., Lushchak, O. V., Storey, J. M., Storey, K. B., & Lushchak, V. I. (2017). Exposure to sodium molybdate results in mild oxidative stress in *Drosophila melanogaster*. *Redox Rep.*, **22**(3), 137–146.
- Peterson, G. L. (1977). A simplification of the protein assay method of Lowry et al. which is more generally applicable. *Anal Biochem.*, **83**(2), 346–356.
- Roberts, J. M., & Hubel, C. A. (2004). Oxidative stress in preeclampsia. *American Journal of Obstetrics & Gynecology*, **190**(5), 1177–1178.
- Rocha-Decker, M. S. (2004). *The development and validation of the Proactive Assessment of Social Skills for preschool children*. University of Oregon.
- Shahidi, F., & Zhong, Y. (2008). Bioactive peptides. *J AOAC Int.*, **91**(4), 914–931.
- Subramanian, P., Prasanna, V., Jayapalan, J. J., Rahman, P. S. A., & Hashim, O. H. (2014). Role of *Bacopa monnieri* in the temporal regulation of oxidative stress in clock mutant (cryb) of *Drosophila melanogaster*. *J Insect Physiol.*, **65**, 37–44.
- Suetsuna, K., Ukeda, H., & Ochi, H. (2000). Isolation and characterization of free radical scavenging activities peptides derived from casein. *J Nutr Biochem.*, **11**(3), 128–131.
- Tabima, D. M., Frizzell, S., & Gladwin, M. T. (2012). Reactive oxygen and nitrogen species in pulmonary hypertension. *Free Rad Biol Med.*, **52**(9), 1970–1986.
- Taniyama, Y., & Griending, K. K. (2003). Reactive oxygen species in the vasculature: molecular and cellular mechanisms. *Hypertension*, **42**(6), 1075–1081.
- Tkachev, V. O., Menshchikova, E. B., & Zenkov, N. K. (2011). Mechanism of the Nrf2/Keap1/ARE signaling system. *Biochem (Moscow)*, **76**(4), 407–422.
- Tonolo, F., Folda, A., Cesaro, L., Scalcon, V., Marin, O., Ferro, S., Bindoli, A., & Rigobello, M. P. (2020). Milk-derived bioactive peptides exhibit antioxidant activity through the Keap1-Nrf2 signaling pathway. *J Funct Foods*, **64**, 103696. <https://doi.org/https://doi.org/10.1016/j.jff.2019.103696>
- Van Herrewege, J. (1974). Nutritional requirements of adult *drosophila melanogaster*: The influence of the casein concentration on the duration of life. *Exp Gerontol.*, **9**(4), 191–198.
- Venkareddy, L. K. (2015). Potential of casein as a nutrient intervention to alleviate lead (Pb) acetate-mediated oxidative stress and neurotoxicity: first evidence in *Drosophila melanogaster*. *Neurotoxicol.*, **48**, 142–151.
- Wang, Y., Branicky, R., Noë, A., & Hekimi, S. (2018). Superoxide dismutases: Dual roles in controlling ROS damage and regulating ROS signaling. *J Cell Biol.*, **217**(6), 1915–1928. <https://doi.org/10.1083/jcb.201708007>
- Zhang, D. D. (2006). Mechanistic studies of the Nrf2-Keap1 signaling pathway. *Drug Metab Rev.*, **38**(4), 769–789.
- Zhao, X., Cui, Y.-J., Bai, S.-S., Yang, Z.-J., Megrou, S., Aziz, T., Sarwar, A., Li, D., & Yang, Z.-N. (2021). Antioxidant activity of novel casein-derived peptides with microbial proteases as characterized via Keap1-Nrf2 pathway in HepG2 cells. *J Microbiol Biotechnol.*, **31**(8):1163–1174.

The Impact of Selected Ecological Factors on the Growth and Biochemical Responses of Giza Faba Bean (*Vicia faba* L.) Seedlings

Mohammad Abo Gamar^{1,*}, Riyadh Muhaidat¹, Tareq Fhely¹, Fatima Abusahyoun¹, and Taghleab Al-Deeb²

¹Department of Biological Sciences, Faculty of Science, Yarmouk University, Irbid 21163, Jordan; ²Department of Biological Sciences, Faculty of Science, Al al-Bayt University, Mafrq 25113, Jordan.

Received: October 5, 2022; Revised: December 23, 2022; Accepted: December 25, 2022

Abstract

The climate is changing, warming and drying, and how plants will fare under such deteriorating climate is presently a prime question in plant ecology research. Giza faba bean (*Vicia faba* L.) is one essential crop of the world, and reductions in its biomass and yield are expected in response to global climate change, particularly in stressful habitats. A greenhouse study was conducted from March to April 2022 to examine the impacts of the main components of climate change: temperature, elevated CO₂, and water stress on the growth and biochemical responses of Giza faba bean seedlings. Seedlings were grown under two temperature regimes (22/18°C and 28/24°C), 12/12h light/dark photoperiod, two CO₂ concentrations (400 and 800 µmol mol⁻¹), and two watering regimes (well-watered and water stressed). Twelve-day-old seedlings were assigned in random to experimental conditions where they were grown for 14 days. Upon harvest, growth and biochemical parameters were measured. Overall, higher temperatures and water stress, individually, decreased growth parameters, leaf moisture content, dry and fresh matter of all plant parts, leaf mass area, nitrogen balance index and anthocyanin, but increased electrolyte leakage, chlorophyll measured by Dualex, flavonoid content, and Chl *a*, carotenoids, total chlorophyll, and Chl *a/b* ratio. Moreover, higher temperatures increased proline content and water stress increased malondialdehyde (MDA) content. Elevated CO₂ increased growth parameters, leaf moisture content, fresh matter of stems and leaves and dry matter of all plant parts, leaf area ratio, flavonoid content, but decreased MDA and electrolyte leakage. Interactions among the three components of climate change primarily affected leaf number, moisture content, root dry mass, MDA and flavonoid contents. Elevated CO₂ alleviated the negative impacts of temperature and water stress on Giza faba bean seedlings through decreasing oxidative stress and increasing plant water status. Our study showed that Giza faba bean has the potential to decrease negative impacts of the main components of climate change in the future.

Keywords: Abiotic stress, Climate change, Elevated CO₂, Giza faba bean (*Vicia faba* L.), Plant growth, Temperature, Water stress.

1. Introduction

For more than a decade, climate change has been considered as a chief issue of international concern because of increased emissions of greenhouse gases (primarily CO₂) and warming of the Earth (Triacca *et al.*, 2014; Kesaulya and Vega, 2019). Human modifications of the global environment, through burning of fossil fuels and destruction of plants natural habitats, are key causes of climate deterioration and altered behavior and distribution of organisms at the individual, population and community levels of ecological organization (Kesaulya and Vega, 2019). For this reason, climate change ecology has become a core research topic in different laboratories of life sciences around the world (Timpane-Padgham *et al.*, 2017).

Since plant growth and food production, as measured by plant biomass, are generally enhanced by atmospheric CO₂ enrichment, a central question in plant ecology today

is, “how will plants fare under increases in atmospheric CO₂ in the future?” Attentions have thus been turned toward investigating how unavoidable increases in atmospheric CO₂ affects plants performance and structure of the Earth’s vegetation, particularly in stressful environments (Marcilly *et al.*, 2021). The main components of climate change (temperature, drought) associated with elevated atmospheric CO₂ influence plants growth and productivity on a global scale and so have received special research attention by plant ecologists (IPCC, 2013). Global warming and a drier climate result from increased emissions and accumulation of greenhouse gases in the atmosphere (Triacca *et al.*, 2014). With such drastic climatic changes, plants have to develop the ability to adapt to external and frequently harmful environmental stresses of increased temperatures and decreased soil water availability associated with increased levels of greenhouse gases in the atmosphere (Moretti *et al.*, 2010; Lacis *et al.*, 2013).

* Corresponding author. e-mail: mohammad.abogamar@yu.edu.jo.

Temperature stress can cause plants to go through morphological and biochemical changes in order to adapt to adverse conditions (Moretti *et al.*, 2010; Qaderi *et al.*, 2012; Xu *et al.*, 2012; Prash and Sonnewald, 2015; Martel and Qaderi, 2016; Abo Gamar *et al.*, 2019, 2021). DaMatta *et al.* (2010) stated that, in regions of low latitude, a modest increase of 1-2°C would have negative impacts on the yield of crops. Rising atmospheric temperature is continuous due to the amount of carbon dioxide present in the atmosphere and could bring a temperature increase in earth's temperature from 1-6°C, depending on the climate model (DaMatta *et al.*, 2010; IPCC, 2013).

Carbon dioxide concentrations rise by an average of 0.005 ppm per year; in our current climate they rise by an average of 2 ppm per year (Sukumaran *et al.*, 2018). Anthropogenic activities have quickly increased the concentration of CO₂ in the atmosphere, and the present concentration of CO₂ is 400 ppm is likely to reach to 700 ppm by 2100 (IPCC, 2013). However, on the basis of the current anthropogenic emission rates of CO₂ to the atmosphere, other studies suggested that it may exceed 1000 µmol mol⁻¹ by 2100 (Solomon, 2007; Diatta *et al.*, 2020). This places stress on existing ecosystems, and allows forest lines to retreat while other species move into their former territory (Jiang *et al.*, 2013). This elevation in the concentration of CO₂ in the atmosphere could positively and negatively affects plants (Qaderi *et al.*, 2006).

Water stress is a major abiotic stress inhibiting plant growth and development and causing enormous losses in many crops (Mishra and Singh, 2010). Global warming has been shown to increase its incidence in many parts of the world, particularly in the warm regions of the globe (Qaderi *et al.*, 2012; Okorie *et al.*, 2019; Abo Gamar *et al.*, 2021). This poses a problem for areas that are already dry, and may lead to a need for frequent irrigation in agricultural areas (Liu *et al.*, 2013). Previous studies have shown that plant growth and biomass are considerably retarded during periods of water stress (Sangtarash *et al.*, 2009; Qaderi and Reid, 2009; Qaderi *et al.*, 2012; Prash and Sonnewald, 2015; Abo Gamar *et al.*, 2021). Water stress enhances plants to make adjustment for their physiological processes to help them make an adaption to moderate levels of stress factors (Sangtarash *et al.*, 2009; Kaur *et al.*, 2015).

Earlier studies have looked at temperature (Cline, 2007; Kaur *et al.*, 2015; Mekonnen *et al.*, 2016) or carbon dioxide (Taub, 2010; Munir *et al.*, 2014; Váry *et al.*, 2015) or watering regime (Hu *et al.*, 2006; Ihuoma and Madramootoo, 2019); some have examined a combination of two of them (Farrar and Gunn, 2017; Ulfat *et al.*, 2021); and only few studies examined the interactive effects of the main components of climate change on plant (Qaderi *et al.*, 2011; Padhy *et al.*, 2018; Abo Gamar *et al.*, 2019, 2021; Singh *et al.*, 2021; Fallah *et al.*, 2022).

Faba bean (*Vicia faba* L.) belongs to the family Fabaceae or Leguminosae, and it is among the oldest crops grown worldwide (Osman *et al.*, 2010). Faba bean (*Vicia faba* L.) is also known as broad bean, horse bean and field bean and it is the fourth most main crop in the world (Tiwari and Singh, 2019). The seeds of faba bean contain high protein content of 24-33% (Tiwari and Singh, 2019). In Jordan, the crop is cultivated either under irrigation or

rained for the purposes of fresh pod utilization and dry seed production (Thalji, 2015).

We hypothesized that growth of Giza faba bean seedlings would be negatively influenced by high temperature and water stresses, but positively enhanced by elevated CO₂, and that the elevated CO₂ could alleviate the detrimental impacts of high temperature and water stresses on Giza faba bean seedlings. The objectives of this study were to: (1) examine how Giza faba bean plants respond to the single and interactive effects of temperature, carbon dioxide and water stress and (2) find if stress responses in Giza faba bean plants are alleviated by elevated CO₂.

2. Materials and methods

2.1. Plant materials and growth conditions

A greenhouse study was conducted from March to April 2022 at Yarmouk University to investigate the effects of the main climate change components; temperature, CO₂, and watering regimes and their interactions on growth and biochemical responses of Giza faba bean (large seed) seedlings. In this study, Giza faba bean seeds (obtained from the National Agricultural Research Center [NARC] in Amman, Jordan) were sown in 200 cm³ pots containing a mixture of vermiculite, perlite and peat moss (1:1:1, by volume). One faba bean seed was sown in each pot and left for germination in a naturally illuminated greenhouse under the conditions of 12/12h light/dark photoperiod, photon flux density (PPFD) of 600 photons m⁻² s⁻¹, relative humidity (RH) 45.9% ± 6.5%, and 22/18°C day/night thermoperiod. Each pot was given 60 mL of tap water to begin germination; afterwards, seedlings were watered using a fine-spray watering, which was gradually increased in spray amount as plants grow larger and hardier. The germination process, in total, was lasted roughly 7 days. After germination, seedlings were left to grow under the previous mentioned greenhouse conditions for a period of 5 days until established and produced their first foliage leaves. Seedlings were fertilized with NPK fertilizer (18-18-18, Type 100, Chissor-Asahi® Fertiliser Co. Ltd., Tokyo, Japan). After that, seedlings were randomly placed in four equal size Plexiglas cabinets of 60 cm depth, 65 cm width, and 50 cm height built up in the greenhouse. Same previous conditions were established inside cabinets in terms of light density, photoperiod, thermoperiod and relative humidity. However, two cabinets were selected to represent the normal temperature treatment (22/18°C day/night; the greenhouse normal temperature) and the other two to represent the high temperature treatment (28/24°C day/night; the high temperature was established and maintained by lamps covered with aluminum foil connected to heat sensors). Temperatures were chosen to represent the current average temperature values (22/18°C) in Jordan from March to April, whereas the higher temperatures represent the expected average temperature by 2100 if temperatures increase by the highest expected value of 6.4°C (28/24°C, IPCC, 2013). Under each temperature treatment, one cabinet was supplied with ambient CO₂ (400 ppm) and the other one with elevated CO₂ (800 ppm), and half of the seedlings were watered to field capacity (well-watered) and the other half was water-stressed. A split-split-plot design with three factors

(temperature, CO₂, and watering regime) was applied to get eight experimental conditions as shown in table 1. An electrical fan was used to keep CO₂ circulation constant in each cabinet and the relative humidity was kept at 45.9% ± 6.5% based on the greenhouse relative humidity. The flow

of gas from the CO₂ cylinder to the Plexiglas cabinet was regulated by pressure gauge, solenoid valve and flow meter, and regularly monitored by a pSense portable CO₂ meter (CO₂ Meter, Inc., Ormond Beach, FL, USA).

Table 1. Experimental conditions under which Giza faba bean seedlings were grown.

Normal temperatures regime (22°C/18°C)				High temperatures regime (28°C/24°C)			
Ambient CO ₂ (400 µmol mol ⁻¹)		Elevated CO ₂ (800 µmol mol ⁻¹)		Ambient CO ₂ (400 µmol mol ⁻¹)		Elevated CO ₂ (800 µmol mol ⁻¹)	
Well-watered	Water-stressed	Well-watered	Water-stressed	Well-watered	Water-stressed	Well-watered	Water-stressed

Seedlings were grown under their respective treatment for 14 days in cabinets. Pots were rotated within the cabinets every second day to minimize the variation in growth due to placement within the cabinets and shading effects of the greenhouse. The experiment was replicated three times in order to show reproducibility.

2.2. Determination of growth parameters

After 14 days of growth, the following growth parameters for all experimental conditions were measured: stem length and diameter, dry and fresh mass of leaves, stems and roots, and leaf area and moisture content. Measurement of stem length was performed from the surface of soil to apical meristem of each plant using a ruler, whereas stem diameter was measured using a Digimatic caliper (Mitutoyo Corp. Kanagawa, Japan) placed at the midway point between soil and the apical meristem. Three plants, per condition, were harvested to determine leaf, stem, and root fresh masses using a digital electronic balance (Model GD603, Sartorius, Gottingen, Germany). Then, same plants were dried at 60 °C for 72 h in a forced air oven in order to determine leaf, stem, and root dry masses using the same balance. To assess leaf moisture content, an average-sized leaf from each plant was removed and weighed before and after drying using the previous mentioned balance. Leaf area of each dried plant was determined using an image J software (<http://rsb.info.nih.gov/ij/>).

2.3. Stress indicators

2.3.1. Measurement of proline content

Proline content of three different samples per treatment for each experimental condition were estimated according to Bates *et al.* (1973). Proline concentrations were measured using a standard curve of proline on a fresh mass basis (µmol g⁻¹ FM).

2.3.2. Measurement of lipid peroxidation

Lipid peroxidation was determined by measuring the malondialdehyde (MDA) using 2-thiobarbituric acid assay procedure following Abo Gamar *et al.* (2019). Three fresh leaf samples (50 mg) from three separate plants were collected from each treatment, frozen in liquid nitrogen and homogenized using a mortar and a pestle in a solution composed of 1.5 ml 0.5% 2-thiobarbituric acid and 1.5 ml 0.1% trichloroacetic acid. Following centrifugation at 4000g for 15 min at 4°C, the supernatant was boiled for 10 min and cooled on ice. Afterwards, the absorbance at 532

nm and 600 nm using A UV/visible spectrophotometer (Olympus, Tokyo, Japan). The 0.5% 2-thiobarbituric acid and 0.1% trichloroacetic acid were used as a blank. The concentration of MDA (nmol g⁻¹ FM) was calculated by using the following formula: $[(A_{532} - A_{600}) \times v] \times 1000 / (\epsilon \times M)$. 'ε' represents the specific extinction coefficient (= 155 mM⁻¹ cm⁻¹), 'v' is the volume of extraction medium, 'M' is the leaf fresh mass, and 'A₆₀₀' and 'A₅₃₂' are absorbance at 600 and 532 nm, respectively.

2.3.3. Measurement of membrane permeability

Membrane permeability was estimated by measuring the electrical conductivity of three samples per treatment according to Abo Gamar *et al.* (2019). Three leaf samples (100 mg) from three different plants per treatment were washed thoroughly and soaked in 15 ml distilled water at room temperature for 24 h. The initial conductivity (C1) of the fresh tissue was measured using an HI 98311 DiST@ 5 EC/TDS/Temperature Tester. Samples were then boiled for 1 hour at 100°C to release the electrolytes. The maximum conductivity of the dead tissue (C2) was measured, and the electrolyte leakage was calculated as a ratio of C1 and C2 expressed in percentage.

2.4. Measurement of nitrogen balanced index (NBI), chlorophyll, flavonoids and anthocyanins by duallex machine

Three leaves from separate plants per treatment were used for determination of nitrogen balance index (NBI), chlorophyll, flavonoids, and anthocyanins contents using Duallex Scientific® (Duallex Scientific, Force-A, Orsay Cedex, France).

2.5. Analysis of photosynthetic pigments

The concentrations of chlorophyll (Chl) *a*, Chl *b*, and carotenoids, as well as total Chl and Chl *a/b* ratio were measured according to Hiscox and Israelstam (1979). For each treatment, three leaf samples (~ 50 mg) were harvested from three different plants and were incubated in 5 ml of dimethylsulfoxide at room temperature for 24 h in the dark until the pigments were completely bleached. The absorbance of Chl *a*, Chl *b*, and carotenoids was then measured at 664 nm, 648 nm, 470 nm using a UV-visible spectrophotometer (model V5800, Shanghai Metash Instruments Co. Ltd (China), respectively). The concentrations of Chl *a*, Chl *b*, carotenoids, as well as total Chl, and Chl *a/b* ratio were calculated per gram of fresh weight according to Chappelle *et al.* (1992).

2.6. Data analysis

The impacts of temperature, CO₂, and watering regime on growth and biochemical features of Giza faba bean were analyzed, using ANOVA for split-split-plot design (SAS Institute, 2011). For the split-split-plot analysis, temperature, CO₂, watering regime and cabinets were considered, respectively, as the main plot, subplot, split-subplot, and replications. A one-way ANOVA was used to find variations among single factors, using Scheffé's test at the 5% probability level (SAS Institute 2011). For all parameters, three trials were used.

3. Results

3.1. Plant growth

Elevated CO₂ significantly increased stem length, leaf area and number, leaf moisture content and root length of Giza faba bean seedlings, while water and high temperature stresses significantly decreased them, in addition to the stem diameter (Table 2; Figure 1A-F).

Temperature, CO₂, watering regime and the two-way interactions between T × W significantly affected stem height (Table 3). Temperature, watering regime and the two-way interactions between T × W were significantly affected stem diameter (Table 3). The T × W interaction revealed that seedlings grown under normal temperatures and well-watered had the highest and thickest stem, while those grown under high temperatures and water-stressed had the shortest and thinnest stem (Figure 1A,B). Temperature, carbon dioxide, watering regime, and the two-way interactions between T × CO₂ and T × W significantly affected leaf area (Table 3). For the T × CO₂ interaction, seedlings grown under low temperatures and elevated CO₂ had significantly the highest leaf area, whereas seedlings grown under high temperatures and ambient CO₂ had significantly the lowest leaf area (Figure 1C). The T × W interaction revealed that seedlings grown under normal temperatures and well-watered had significantly the highest leaf area, while those grown under

high temperatures and water-stressed had significantly the lowest leaf area (Figure 1C). Leaf number was significantly affected by the main factors and their interactions with exception to the two-way interaction between T × CO₂ (Table 3). The T × W interaction revealed that seedlings grown under normal temperatures and well-watered had the highest leaf number, while those grown under high temperatures and water-stressed had the lowest leaf number (Figure 1D). The CO₂ × W interaction showed that leaf number was significantly the highest for well-watered seedlings at elevated CO₂, but significantly the lowest for water-stressed seedlings at ambient CO₂ (Figure 1D). Based on the T × CO₂ × W interaction, leaf number was significantly highest for seedlings grown under the combination of normal temperature, elevated CO₂ and well-watered, but significantly lowest for seedlings grown under the combination of high temperatures, ambient CO₂ and water-stressed (Figure 1D). Leaf moisture content was significantly affected by the main factors and their interactions except for the two-way interactions between T × CO₂ and CO₂ × W (Table 3). The T × W interaction indicated that seedlings grown under normal temperatures and well-watered had significantly the highest leaf moisture content, whereas seedlings grown under high temperatures and water-stressed had significantly the lowest leaf moisture content (Figure 1E). On the basis of the T × CO₂ × W interaction, leaf moisture content was significantly highest for seedlings grown under normal temperatures, elevated CO₂ and well-watered, but significantly lowest for seedlings grown under high temperatures, ambient CO₂ and water-stressed (Figure 1E). Root length was significantly affected by the carbon dioxide and the two-way interaction between T × W (Table 3). The T × W interaction showed that seedlings grown under high temperatures and water-stressed had significantly the tallest root, while those grown under normal temperatures and water-stressed had significantly the shortest root (Figure 1F).

Table 2. Individual impacts of temperature, CO₂ and watering regime on growth and biochemical parameters of Giza faba beans (*Vicia faba* L.) seedlings.

Parameter	Temperature		Carbon dioxide		Watering regime	
	Normal	High	Ambient	Elevated	Well-watered	Water-stressed
Stem length (cm)	37.3 ± 3.6A	26.1 ± 1.4B	29.9 ± 3.1B	33.4 ± 3.3A	39.7 ± 2.9A	23.7 ± 0.8B
Stem diameter (mm)	0.47 ± 0.04A	0.27 ± .02B	0.38 ± 0.03A	0.36 ± 0.04A	0.46 ± 0.04A	0.29 ± 0.02B
Leaf area (cm ² plant ⁻¹)	107.7 ± 12A	73.9 ± 8.6B	74.7 ± 9.3B	107.1 ± 11.6A	119.9 ± 9.3A	61.8 ± 5.5B
Leaf number (plant ⁻¹)	11.7 ± 1.3A	6.9 ± 0.4B	8.04 ± 0.8B	10.5 ± 1.4A	11.6 ± 1.3A	6.9 ± 0.4B
Leaf moisture (%)	81.4 ± 2.8A	70.9 ± 4.8B	72.9 ± 4.5B	79.5 ± 3.7A	88.1 ± 1.3A	64.3 ± 2.9B
Root length (cm)	25.5 ± 1.48A	27.4 ± 1.5A	24.2 ± 1.2B	28.7 ± 1.5A	26.5 ± 1.04A	26.4 ± 1.9A
Stem fresh mass (g)	3.9 ± 0.4A	2.5 ± 0.2B	2.8 ± 0.3B	3.7 ± 0.5A	4.2 ± 0.4A	2.3 ± 0.1B
Leaf fresh mass (g)	3.9 ± 0.5A	2.5 ± 0.4B	2.8 ± 0.4B	3.6 ± 0.6A	4.6 ± 0.4A	1.9 ± 0.2B
Root fresh mass (g)	4.34 ± 0.3A	4.11 ± 0.1A	4.1 ± 0.2A	4.38 ± 0.3A	4.8 ± 0.2A	3.7 ± 0.1B
Total fresh biomass (g)	12.2 ± 1.3A	9.2 ± 0.6B	9.7 ± 0.8B	11.7 ± 1.3A	13.6 ± 0.9A	7.8 ± 0.2B
Stem dry mass (g)	2.3 ± 0.2A	1.2 ± 0.1B	1.67 ± 0.2B	1.98 ± 0.2A	2.2 ± 0.3A	1.4 ± 0.1B
Leaf dry mass (g)	1.6 ± 0.24A	0.89 ± 0.16B	1.1 ± 0.2B	1.4 ± 0.2A	1.9 ± 0.2A	0.6 ± 0.1B
Root dry mass (g)	1.3 ± 0.1A	0.85 ± 0.1B	0.98 ± 0.1B	1.2 ± 0.1A	1.4 ± 0.08A	0.78 ± 0.09B
Total dry biomass (g)	5.3 ± 0.5A	2.9 ± 0.3B	3.7 ± 0.5B	4.5 ± 0.6A	5.4 ± 0.5A	2.8 ± 0.3B
Proline (μmole g ⁻¹ FM)	34.9 ± 4.6B	55.6 ± 2.2A	45.7 ± 5.1A	44.8 ± 4.3A	40.9 ± 4.4A	49.5 ± 4.7A
MDA (μmole g ⁻¹ FM)	0.23 ± 0.03A	0.3 ± 0.04A	0.3 ± 0.1A	0.18 ± 0.01B	0.16 ± 0.01B	0.32 ± 0.04A
Electrical conductivity (%)	16.9 ± 1.4B	31.4 ± 1.8A	27.5 ± 2.6A	20.9 ± 2.4B	20.8 ± 2.2B	27.7 ± 2.8A
Nitrogen balance index	80.8 ± 8.1A	69.1 ± 1.9B	77.7 ± 7.3A	72.3 ± 4.6A	85.9 ± 6.7A	64.1 ± 3.03B
Chlorophyll (μg cm ⁻² FM)	25.7 ± 1.08B	29.5 ± 1.05A	26.7 ± 0.8A	28.5 ± 1.4A	24.9 ± 0.86B	30.2 ± 0.96A
Flavonoids (μg cm ⁻² FM)	0.37 ± 0.04B	0.54 ± 0.01A	0.4 ± 0.03B	0.52 ± 0.01A	0.32 ± 0.02B	0.59 ± 0.04A
Anthocyanin (nmol/cm ²)	0.07 ± 0.005A	0.05 ± 0.004B	0.06 ± 0.004A	0.05 ± 0.006A	0.07 ± 0.005A	0.04 ± 0.003B
Chl <i>a</i> (μg mg ⁻¹ FM)	1.9 ± 0.2B	2.6 ± 0.1A	2.28 ± 0.2A	2.29 ± 0.1A	2.5 ± 0.17A	2.1 ± 0.2A
Chl <i>b</i> (μg mg ⁻¹)	1.3 ± 0.1A	1.8 ± 0.2A	1.8 ± 0.2A	1.3 ± 0.1A	1.7 ± 0.21A	1.4 ± 0.17A
Carotenoids (μg mg ⁻¹ FM)	0.42 ± 0.06B	0.65 ± 0.07A	0.48 ± 0.07A	0.6 ± 0.08A	0.54 ± 0.07A	0.54 ± 0.08A
Total Chl (μg mg ⁻¹ FM)	3.2 ± 0.4B	4.4 ± 0.3A	4.1 ± 0.4A	3.6 ± 0.3A	4.2 ± 0.35A	3.5 ± 0.4A
Chl <i>a/b</i>	1.5 ± 0.1B	2.1 ± 0.2 A	1.7 ± 0.17A	1.9 ± 0.15A	1.77 ± 0.15A	1.8 ± 0.17A

Giza faba bean seedlings were grown under normal (22/18°C) or high (28/24°C) temperatures, ambient CO₂ (400 ppm) or elevated CO₂ (800 ppm) and well-watered or water-stressed conditions. Plants were grown under experimental conditions in Plexiglas cabinets for 14 days, following an initial germination period of 7 days and

growth period of 5 days under greenhouse conditions. Data are means ± SE of at least 9 samples from three different experiments. Means (± SE) followed by different upper-case letters within rows and factors are significantly different ($P < 0.05$) according to Scheffé's test.

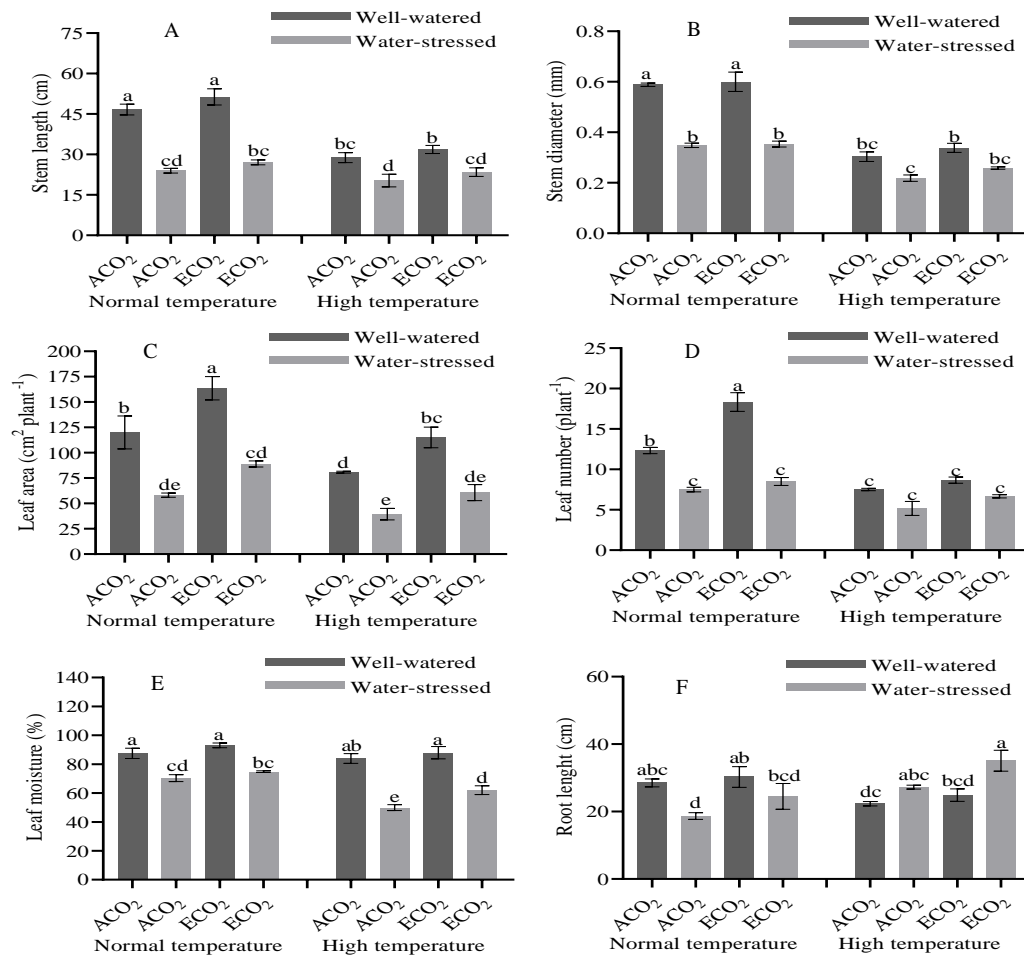


Figure 1. Stem height (A), stem diameter (B), leaf area (C), leaf number (D), moisture content (E) and root length (F) for 26-day-old Giza faba bean (*Vicia faba* L.) seedlings grown in Plexiglas cabinets for 14 days under eight experimental conditions after 12 days of initial germination and growth under greenhouse conditions. Error bars denote standard error (n = 9). Means followed by different letters are significantly different at $P < 0.05$ according to Scheffé's test. ACO₂ ambient CO₂, ECO₂ elevated CO₂.

Table 3. Analysis of variance for the individual impacts of temperature, CO₂ and watering regime and their interactions on stem height, stem diameter, leaf area, leaf number, moisture content and root length of Giza faba bean (*Vicia faba* L.) seedlings.

		Stem height (cm)	Stem diameter (mm)	Leaf area (cm ² plant ⁻¹)	Leaf number (plant ⁻¹)	Moisture content (%)	Root length (cm)
Source	df						
Temperature (T)	1	2240.22***	590.55**	43.04*	609.19**	31.43*	3.44
Main plot error	2	-	-	-	-	-	-
Carbon dioxide (CO ₂)	1	12.49*	3.56	765.26****	31.76**	20.86*	68.89**
T x CO ₂	1	0.19	1.44	15.87*	5.08	1.11	1.66
Subplot error	4	-	-	-	-	-	-
Watering regime (W)	1	376.60****	169.55****	250.63****	96.49****	725.49****	0.01
T x W	1	83.28****	41.31***	7.58*	31.51***	48.66***	52.40****
CO ₂ x W	1	0.20	0.00	3.11	6.92*	3.86	4.89
T x CO ₂ x W	1	0.25	0.05	0.00	6.92*	6.49*	0.08
Split-subplot error	8	-	-	-	-	-	-

Note: * $P < 0.05$; ** $P < 0.01$; *** $P < 0.001$; **** $P < 0.0001$. Giza faba bean seedlings were grown under normal (22/18°C) or high (28/24°C) temperatures, ambient CO₂ (400 ppm) or elevated CO₂ (800 ppm) and well-watered or water-stressed conditions. Plants were grown under experimental conditions in Plexiglas cabinets for 14 days, following an initial germination period of 7 days and growth period of 5 days under greenhouse conditions.

3.2. Biomass accumulation

3.2.1. Fresh mass accumulation

High temperatures and water stress reduced stem (Table 2; Figure 2A), leaf (Table 2; Figure 2B), and total (Table 2; Figure 2D) fresh biomass. Water stress also decreased root fresh mass (Table 2; Figure 2C). On the other hand, elevated CO₂ increased stem (Table 2; Figure 2A), leaf (Table 2; Figure 2B) and total (Table 2; Figure 2D) fresh biomass.

All measured fresh biomass parameters were significantly affected by the three main factors (Table 4). Stem and total fresh biomass were significantly affected the two-way interactions between T × W and CO₂ × W (Table 4). The T × W interaction revealed that seedlings grown under normal temperatures and well-watered had significantly the highest stem and total fresh biomass, whereas seedlings grown under high temperatures and

water-stressed had significantly the lowest stem and total fresh biomass (Figure 2A,D). The CO₂ × W interaction showed that well-watered seedlings at elevated CO₂ had the highest stem and total fresh biomass, whereas water-stressed seedlings at ambient CO₂ had the lowest stem and total fresh biomass (Figure 2A,D). Root fresh mass was significantly affected the two-way interactions between T × CO₂ and T × W (Table 4). The T × CO₂ interaction showed that elevated CO₂ significantly caused the highest root fresh mass for seedlings grown under normal temperatures, but ambient CO₂ significantly caused the lowest root fresh mass for seedlings grown under normal temperatures (Figure 2C). For the T × W interaction, well-watered seedlings grown under normal temperatures had significantly the highest root fresh mass, whereas water-stressed seedlings grown under normal temperatures had significantly the lowest root fresh mass (Figure 2C).

Figure 2. Stem fresh mass (A), leaf fresh mass (B), root fresh mass (C) and total fresh mass (D) for 26-day-old Giza faba bean (*Vicia faba* L.) seedlings grown in Plexiglas cabinets for 14 days under eight experimental conditions after 12 days of initial germination and growth under greenhouse conditions. Error bars denote standard error (n = 9). Means followed by different letters are significantly different at P < 0.05 according to Scheffé's test. ACO₂ ambient CO₂, ECO₂ elevated CO₂.

Table 4. Analysis of variance for the individual impacts of temperature, CO₂ and watering regime and their interactions on stem fresh mass,

Stem fresh mass (g)					
A					
Well-watered					
Water-stressed					
Normal temperature					
High temperature					
Leaf fresh mass (g)					
B					
Well-watered					
Water-stressed					
Normal temperature					
High temperature					
Root fresh mass (g)					
C					
Well-watered					
Water-stressed					
Normal temperature					
High temperature					
Total fresh biomass (g)					
D					
Well-watered					
Water-stressed					
Normal temperature					
High temperature					
Main plot error					
Carbon dioxide (CO ₂)					
T × CO ₂					
Subplot error					
Watering regime (W)					
T × W					
CO ₂ × W					
T × CO ₂ × W					
Split-subplot error					

leaf fresh mass, root fresh mass and total fresh biomass of Giza faba bean (*Vicia faba* L.) seedlings.

Note: *P < 0.05; **P < 0.01; ***P < 0.001; ****P < 0.0001. Giza faba bean seedlings were grown under normal (22/18°C) or high (28/24°C) temperatures, ambient CO₂ (400 ppm) or elevated CO₂ (800 ppm) and well-watered or water-stressed conditions. Plants were grown under experimental conditions in Plexiglas cabinets for 14 days, following an initial germination period of 7 days and growth period of 5 days under greenhouse conditions.

3.2.2. Dry mass accumulation

High temperature and water stresses decreased stem, leaf, root and total dry, while elevated CO₂ increased them (Table 2; Figure 3A,B,C,D). All measured dry biomass parameters were significantly affected by the three main factors (Table 4). Moreover, stem dry mass was significantly affected by the two-way interactions between T × W (Table 5). The T × W interaction showed that seedlings grown under high temperatures and water-stressed had significantly the highest stem dry mass, whereas those grown under normal temperatures and well-watered had significantly the lowest stem dry mass (Figure 3A). Leaf dry mass and total dry biomass were significantly affected by the two-way interactions between T × CO₂ and T × W (Table 5). The T × CO₂ interaction revealed that seedlings grown under normal temperatures at elevated CO₂ resulted in significantly the highest leaf

dry mass and total dry biomass, but high temperatures at ambient CO₂ resulted in significantly the lowest leaf dry mass and total dry biomass in seedlings (Figure 3B,D). The T × W interaction indicated that seedlings grown under normal temperatures and well-watered had significantly the highest leaf dry mass and total dry biomass, whereas seedlings grown under high temperatures and water-stressed had significantly the lowest leaf dry mass and total dry biomass (Figure 4B,D). Root dry mass was significantly affected by the three-way interaction among T × CO₂ × W (Table 5). On the basis of the three-way interaction among the three main factors, seedlings grown under normal temperatures, elevated CO₂, and well-watered conditions had significantly the highest root dry mass, whereas those grown under high temperatures, ambient CO₂ and water-stressed conditions had significantly the lowest root dry mass (Figure 3C).

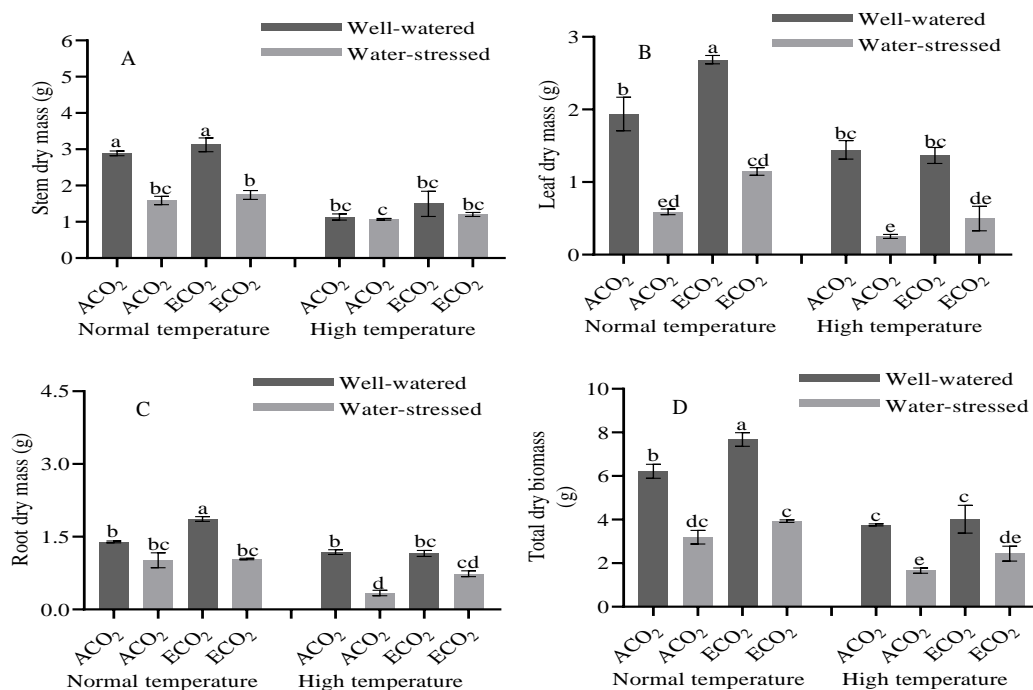


Figure 3. Stem dry mass (A), leaf dry mass (B), root dry mass (C) and total dry mass (D) for 26-day-old Giza faba bean (*Vicia faba* L.) seedlings grown in Plexiglas cabinets for 14 days under eight experimental conditions after 12 days of initial germination and growth under greenhouse conditions. Error bars denote standard error (n = 9). Means followed by different letters are significantly different at P < 0.05 according to Scheffé's test. ACO₂ ambient CO₂, ECO₂ elevated CO₂.

Table 5. Analysis of variance for the individual impacts of temperature, CO₂ and watering regime and their interactions on stem dry mass, leaf dry mass, root dry mass and total dry biomass of Giza faba bean (*Vicia faba* L.) seedlings.

Source	Df	Stem dry mass (g)	Leaf dry mass (g)	Root dry mass (g)	Total dry biomass (g)
Temperature (T)	1	2005.35***	286.21**	88.72*	4539.80***
Main plot error	2	-	-	-	-
Carbon dioxide (CO ₂)	1	17.28*	62.71**	147.55***	85.81***
T × CO ₂	1	0.26	37.15**	3.29	11.05*
Subplot error	4	-	-	-	-
Watering regime (W)	1	213.27****	196.97****	107.84****	229.58****
T × W	1	125.24****	5.50*	0.06	20.19**
CO ₂ × W	1	2.24	0.14	0.01	0.09
T × CO ₂ × W	1	0.49	2.15	13.45**	3.24
Split-subplot error	8	-	-	-	-

Note: *P < 0.05; **P < 0.01; ***P < 0.001; ****P < 0.0001. Giza faba bean seedlings were grown under normal (22/18°C) or high (28/24°C) temperatures, ambient CO₂ (400 ppm) or elevated CO₂ (800 ppm) and well-watered or water-stressed conditions. Plants were grown under experimental conditions in Plexiglas cabinets for 14 days, following an initial germination period of 7 days and growth period of 5 days under greenhouse conditions.

3.2.3. Proline, lipid peroxidation and electrical conductivity

Proline content was increased by high temperatures Giza faba bean seedlings (Table 2; Figure 4A). Significant effect of the two-way interaction between $T \times CO_2$ was observed on proline content (Table 6). For the $T \times CO_2$ interaction, seedlings grown under high temperatures at ambient CO_2 had significantly the highest proline content, while those grown under normal temperatures at ambient CO_2 had significantly the lowest proline content (Figure 6A).

Malondialdehyde (MDA) generation increased under water-stressed, but decreased by elevated CO_2 in Giza faba bean seedlings (Table 2; Figure 4B). MDA generation was significantly affected by carbon dioxide, watering regime, the two-way interactions between $T \times CO_2$, $CO_2 \times W$ and the three-way interactions among $T \times CO_2 \times W$ (Table 6). The $T \times CO_2$ interaction revealed that seedlings grown under high temperatures at ambient CO_2 resulted in significantly the highest MDA content, but high temperatures at ambient CO_2 resulted in significantly the least MDA content in Giza faba bean seedlings (Figure

4B). The $CO_2 \times W$ interaction showed that seedlings grown at ambient CO_2 and water-stressed had significantly the highest MDA content, whereas seedlings grown at ambient CO_2 and well-watered had significantly the lowest MDA content (Figure 4B). On the basis of the $T \times CO_2 \times W$ interactions, seedlings grown under high temperatures, ambient CO_2 , and water-stressed conditions had significantly the highest MDA content, whereas those grown under high temperatures, ambient CO_2 and well-watered conditions had significantly the lowest MDA content (Figure 4B).

Electrical conductivity was increased by high temperatures and water stresses, but decreased by elevated CO_2 in Giza faba bean seedlings (Table 2; Figure 4C). Effects of temperature, CO_2 , watering regime and the two-way interactions between $CO_2 \times W$ were significant on the electrical conductivity (Table 6). The $CO_2 \times W$ interaction showed that seedlings grown at ambient CO_2 and water-stressed conditions had significantly the highest electrical conductivity, whereas those grown at ambient CO_2 and well-watered conditions had significantly the lowest electrical conductivity (Figure 4C).

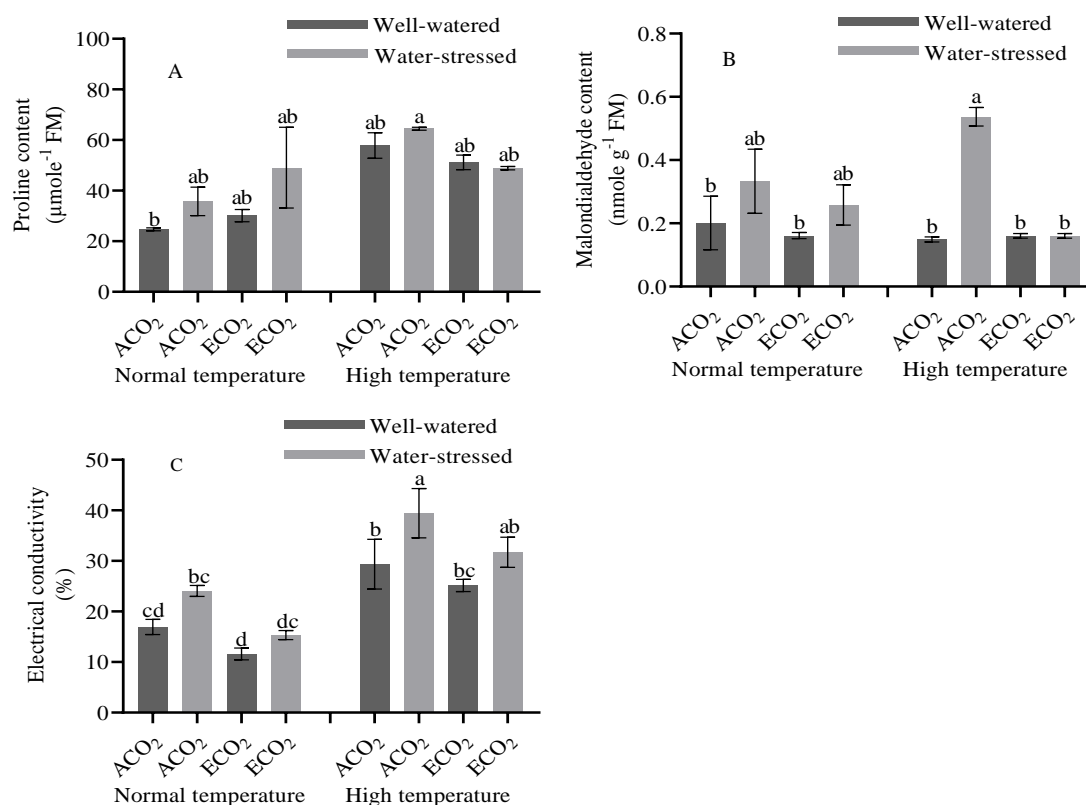


Figure 4. Proline content (A), Malondialdehyde content (B) and electrical conductivity (C) for 26-day-old Giza faba bean (*Vicia faba* L.) seedlings grown in Plexiglas cabinets for 14 days under eight experimental conditions after 12 days of initial germination and growth under greenhouse conditions. Error bars denote standard error ($n = 9$). Means followed by different letters are significantly different at $P < 0.05$ according to Scheffé's test. ACO_2 ambient CO_2 , ECO_2 elevated CO_2 .

Table 6. Analysis of variance for the individual impacts of temperature, CO₂ and watering regime and their interactions on proline content, MDA content and electrical conductivity of Giza faba bean (*Vicia faba* L.) seedlings.

Source	Df	Proline content (μmole g ⁻¹ FM)	MDA content (μmole g ⁻¹ FM)	Electrical conductivity (%)
Temperature (T)	1	11.27	0.10	99.86**
Main plot error	2	-	-	-
Carbon dioxide (CO ₂)	1	0.08	46.14**	15.43*
T x CO ₂	1	11.98*	12.52*	0.10
Subplot error	4	-	-	-
Watering regime (W)	1	4.69	23.89**	108.16****
T x W	1	2.64	1.61	4.74
CO ₂ x W	1	0.00	11.27*	6.85*
T x CO ₂ x W	1	1.13	7.83*	0.00
Split-subplot error	8	-	-	-

Note: * $P < 0.05$; ** $P < 0.01$; *** $P < 0.001$; **** $P < 0.0001$. Giza faba bean seedlings were grown under normal (22/18°C) or high (28/24°C) temperatures, ambient CO₂ (400 ppm) or elevated CO₂ (800 ppm) and well-watered or water-stressed conditions. Plants were grown under experimental conditions in Plexiglas cabinets for 14 days, following an initial germination period of 7 days and growth period of 5 days under greenhouse conditions.

3.2.4. Nitrogen balance index (NBI), chlorophyll, flavonoids and anthocyanin

NBI decreased under high temperatures and water-stressed condition in seedlings (Table 2; Figure 7A). NBI was significantly affected by watering regime and the two-way interactions between T × CO₂ and T × W (Table 7). The T × CO₂ interaction revealed that seedlings grown under normal temperatures at ambient CO₂ resulted in significantly the highest NBI, but normal temperatures at elevated CO₂ resulted in significantly the lowest NBI in Giza faba bean seedlings (Figure 7A). The T × W interaction indicated that seedlings grown under normal temperatures and well-watered had significantly the highest NBI, whereas seedlings grown under normal temperatures and water-stressed had significantly the lowest NBI (Figure 7A).

Chlorophyll content was significantly increased by high temperatures and water stresses (Table 2; Figure 7B). Chlorophyll content was only significantly affected by temperature and watering regime (Table 7).

Flavonoid content was significantly increased by the three main factors (Table 2; Figure 7C). Flavonoid content

was significantly affected by the three main factors, the two-way interaction between CO₂ × W and the three-way interaction among T × CO₂ × W (Table 7). The CO₂ × W interaction showed that flavonoid content was significantly highest for water-stressed seedlings at elevated CO₂, but significantly lowest for well-watered seedlings at ambient CO₂ (Figure 7C). On the basis of the T × CO₂ × W interaction, flavonoid content was significantly highest for seedlings grown under high temperatures, elevated CO₂ and water-stressed, but significantly lowest for seedlings grown under normal temperatures, ambient CO₂ and well-watered (Figure 7C).

Anthocyanin was significantly decreased by high temperatures and water stresses (Table 2; Figure 7D). Anthocyanin was significantly affected by watering regime and the two-way interaction between T × CO₂ (Table 7). The T × CO₂ interaction revealed that seedlings grown under normal temperatures at elevated CO₂ resulted in significantly the highest anthocyanin, but high temperatures at elevated CO₂ resulted in significantly the lowest anthocyanin in Giza faba bean seedlings (Figure 7A).

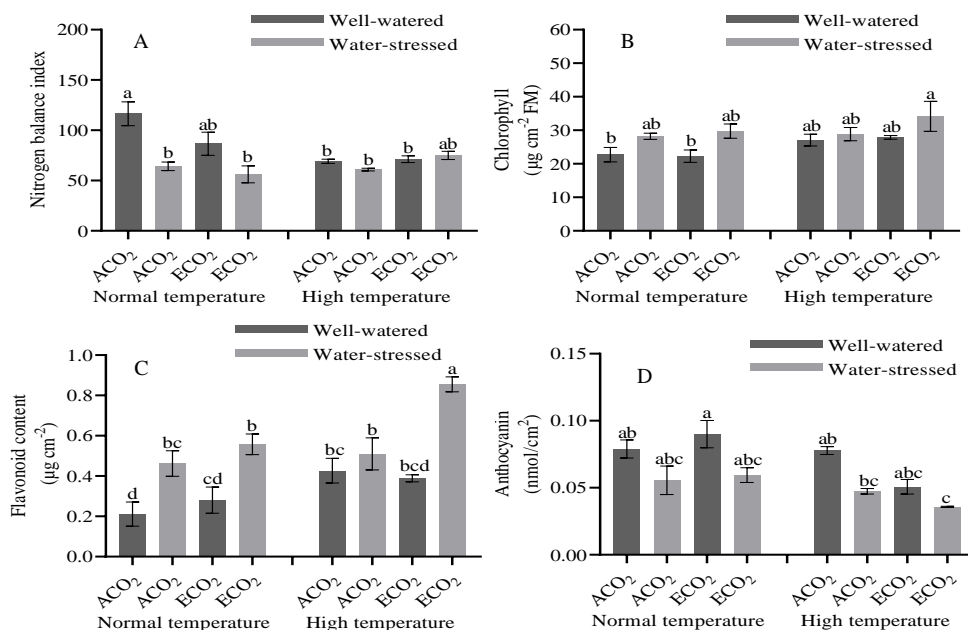


Figure 5. NBI (A), chlorophyll content (B) flavonoid content (C) and anthocyanin (D) measured by Dualex machine for 26-day-old Giza faba bean (*Vicia faba* L.) seedlings grown in Plexiglas cabinets for 14 days under eight experimental conditions after 12 days of initial germination and growth under greenhouse conditions. Error bars denote standard error ($n = 9$). Means followed by different letters are significantly different at $P < 0.05$ according to Scheffé's test. ACO_2 ambient CO_2 , ECO_2 elevated CO_2 .

Table 7. Analysis of variance for the individual impacts of temperature, CO_2 and watering regime and their interactions on NBI, chlorophyll, flavonoids and anthocyanin of Giza faba bean (*Vicia faba* L.) seedlings.

		NBI	Chlorophyll ($\mu g\ cm^{-2}\ FM$)	Flavonoids ($\mu gcm^{-2}\ FM$)	Anthocyanin($nmol/cm^2$)
Source	df				
Temperature (T)	1	9.91	113.72**	45.07*	4.60
Main plot error	2	-	-	-	-
Carbon dioxide (CO_2)	1	1.54	3.81	24.71**	2.42
T x CO_2	1	9.64*	1.87	2.25	12.50*
Subplot error	4	-	-	-	-
Watering regime (W)	1	14.14**	43.91***	186.61****	63.33****
T x W	1	11.33**	2.40	0.07	0.47
CO_2 x W	1	2.13	4.17	26.82***	0.43
T x CO_2 x W	1	0.18	0.63	20.53**	3.29
Split-subplot error	8	-	-	-	-

Note: * $P < 0.05$; ** $P < 0.01$; *** $P < 0.001$; **** $P < 0.0001$. Giza faba bean seedlings were grown under normal (22/18°C) or high (28/24°C) temperatures, ambient CO_2 (400 ppm) or elevated CO_2 (800 ppm) and well-watered or water-stressed conditions. Plants were grown under experimental conditions in Plexiglas cabinets for 14 days, following an initial germination period of 7 days and growth period of 5 days under greenhouse conditions. NBI, chlorophyll content, flavonoids and anthocyanin were measured by Dualex machine.

3.2.5. Photosynthetic pigments

High temperatures significantly increased Chl *a*, carotenoids, total Chl and Chl *a/b* ratio (Table 2; Figure 8A,C,D,E). Chl *a* was significantly affected by watering

regime, while Chl *b* and Chl *a/b* ratio were significantly affected by CO_2 (Table 8). However, none of the interactions among the three main factors had significant effect on the photosynthetic pigments (Table 8).

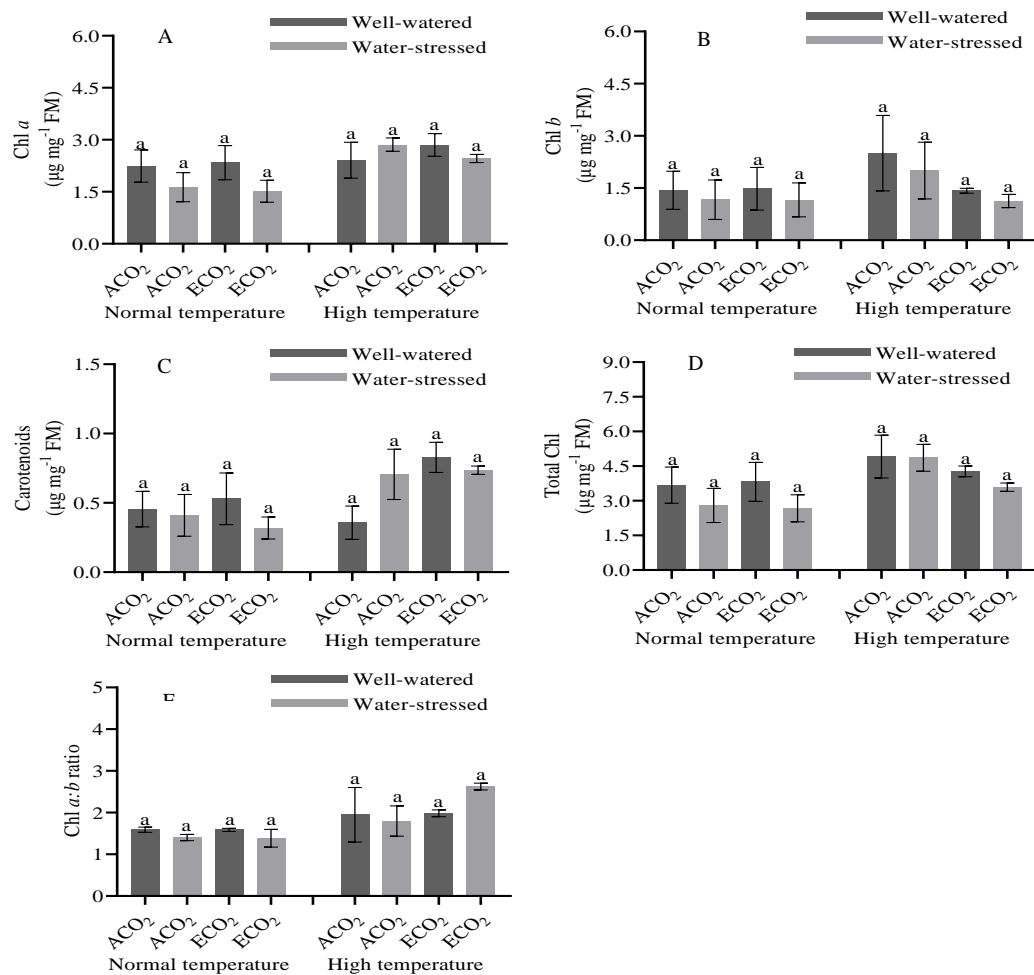


Figure 6. Chl *a* (A), Chl *b* (B), carotenoids (C), total Chl (D) and Chl *a*:*b* ratio (E) for 26-day-old Giza faba bean (*Vicia faba* L.) seedlings grown in Plexiglas cabinets for 14 days under eight experimental conditions after 12 days of initial germination and growth under greenhouse conditions. Error bars denote standard error (n = 9). Means followed by different letters are significantly different at P < 0.05 according to Scheffé's test. ACO₂ ambient CO₂, ECO₂ elevated CO₂.

Table 8. Analysis of variance for the individual impacts of temperature, CO₂ and watering regime and their interactions on Chl *a*, Chl *b*, carotenoids, total Chl and Chl *a*/*b* ratio of Giza faba bean (*Vicia faba* L.) seedlings.

		Chl <i>a</i> (µg mg ⁻¹ FM)	Chl <i>b</i> (µg mg ⁻¹ FM)	Carotenoids (µg mg ⁻¹ FM)	Total Chl (µg mg ⁻¹ FM)	Chl <i>a</i> / <i>b</i> ratio
Source	df					
Temperature (T)	1	3.53	2.10	3.03	2.86	15.69
Main plot error	2	-	-	-	-	-
Carbon dioxide (CO ₂)	1	0.00	30.09**	5.70	2.90	12.63*
T x CO ₂	1	0.01	32.45	6.52	3.01	13.78
Subplot error	4	-	-	-	-	-
Watering regime (W)	1	5.95*	1.53	0.00	2.91	0.01
T x W	1	7.01	0.03	2.00	0.63	0.71
CO ₂ x W	1	3.50	0.02	2.82	0.31	0.56
T x CO ₂ x W	1	1.19	0.05	0.58	0.05	0.60
Split-subplot error	8	-	-	-	-	-

Note: *P < 0.05; **P < 0.01; ***P < 0.001; ****P < 0.0001. Giza faba bean seedlings were grown under normal (22/18°C) or high (28/24°C) temperatures, ambient CO₂ (400 ppm) or elevated CO₂ (800 ppm) and well-watered or water-stressed conditions. Plants were grown under experimental conditions in Plexiglas cabinets for 14 days, following an initial germination period of 7 days and growth period of 5 days under greenhouse conditions.

4. Discussion

There is still a gap in our understanding about the adaptability or plasticity of species regarding their growth

behavior in response to the short-term combination effect of main ecological components of climate change. The purpose of this study was to examine the effects of the individual and combined impacts of temperature, CO₂, and watering regime on growth and biochemical responses of Giza faba bean (*Vicia faba* L.).

4.1. Effects of temperature

Seedlings grown under high temperatures exhibited lower stem height, stem diameter, leaf area, leaf number, leaf moisture than those grown under normal temperatures (Table 2; Figure 1A-F). This coincides with the results of previous research showing declines on growth parameters and leaf moisture content under high temperatures in *Arabidopsis thaliana* (Abo Gamar *et al.*, 2019, 2021). Fresh and dry biomass accumulation except root fresh mass were negatively affected by high temperatures (Table 2; Figures 2A-D, 3A-D), which are consistent with earlier findings on different plant species (Hamidou *et al.*, 2013; Sehgal *et al.*, 2017; Qaseem *et al.*, 2019) including faba bean (Qaderi and Reid, 2009). Seedlings accumulated more proline under high temperatures (Table 2; Figure 4A). This result is consistent with previous findings related to the effects of high temperature on *Prunus persica* (Shin *et al.*, 2016). Proline has a role in protecting and stabilizing different antioxidant enzymes and plasma membranes (Abo Gamar *et al.*, 2019). High temperatures increased electrolyte leakage in seedlings (Table 2; Figure 4C). Electrolyte leakage is an indication of an enhancement in membrane permeability and reduction in cell abilities to tolerate temperature (Cottee *et al.*, 2007). Chlorophyll (measured by Dualox) (Table 2; Figure 5B) and flavonoids (Table 2; Figure 5C) were increased in seedlings grown under high temperatures, while nitrogen balance index (NBI) (Table 2; Figure 5A), which measures the ratio between chlorophyll to flavonoids, decreased. This is an indication that nitrogen nutrition is an important factor in regulating growth of plants, as nitrogen is an important constituent in the structure of chlorophyll molecule (Taiz *et al.*, 2014). Plants under stress conditions produce different antioxidant compounds, including flavonoids, to protect them against ROS (Fini *et al.*, 2011; Naheed *et al.*, 2022; Akhter *et al.*, 2022). We found that high temperature caused a reduction in anthocyanin concentration (Table 2; Figure 5D), which is consistent with previous studies on Jaguar' rose (Dela *et al.*, 2003). Chl *a*, carotenoids, total Chl and Chl *a/b* ratio were all increased by high temperatures (Table 2, Figure 6A, C, D, E). In contrast to our results, chlorophyll content has been found to decrease in mulberry plants grown under high temperature (Chaitanya *et al.*, 2001). On the other hand, other reports reported that, total chlorophyll content was increased in plants grown under stress factors (Romero-Aranda *et al.*, 2001). Synthesizing more carotenoids under high temperatures might be an indicative of the increase in the antioxidant abilities of plants (Abo Gamar *et al.*, 2019).

4.2. Effects of CO₂

In our study, elevated CO₂ increased growth parameters (Table 2; Figure 1A, B, C, D, F), leaf moisture content (Table 2; Figure 1E), and fresh and dry biomass (Table 2; Figures 2A-D, 3A-D). Elevated CO₂ has been shown to increase growth and biomass accumulation in plants by increasing leaf photosynthetic rate and the efficiency of water usage by plants (Jones, 1992). The reduction in MDA content (Table 2; Figure 4B) and electrolyte leakage (Table 2; Figure 4C) in seedlings grown under elevated CO₂ is consistent with a previous study on *Arabidopsis thaliana* (Abo Gamar *et al.*, 2019). Elevated CO₂ increased flavonoid content (Table 2; Figure 5C), which indicated that elevated CO₂ helps plants to accumulate more

antioxidant materials, such as flavonoids (Abo Gamar *et al.*, 2019). Furthermore, this explained the reduction in the MDA content and electrolyte leakage in faba bean seedlings grown at elevated CO₂.

4.3. Effects of watering regime

Our results showed that water stress decreased growth parameters (Table 2; Figure 1A, B, C, D, F), leaf moisture content (Table 2; Figure 1E) and fresh and dry biomass (Table 2; Figures 2A-D, 3A-D). These significant effects on growth parameters and biomass might be due to stomatal closure, which has been shown to reduce photosynthesis in water-stressed plants, including faba bean (Qaderi and Reid, 2009; Sangtarash *et al.*, 2009; Prasad and Sonnewald, 2015). Our results showed an increase in MDA content (Table 2; Figure 4B) and electrolyte leakage (Table 2; Figure 4C) in water-stressed seedlings. This agrees with past research, which showed that water stress increased lipid peroxidation, which caused damage in the plasma membrane and, in turn, increased electrolyte leakage and MDA content (Hajhashemi and Ehsanpour, 2013). Water stress decreased NBI (Table 2; Figure 5A), which is consistent with a previous study on pea (*Pisum sativum*) seedlings (Abdulmajeed *et al.*, 2018). Anthocyanin content was reduced in water-stressed plants (Table 2; Figure 5D). During water stress, the usage of antioxidant enzymes to anthocyanin as co-substrates molecules to capture for ROS resulting in decreased anthocyanin content (Maritim *et al.*, 2021).

4.4. Effects of the combination of the climate change main components.

In this study, from 38 cases, 33 of two-way (see Tables 3, 4, 5, 6 and 7) and 5 of three-way interactions (Tables 3, 5, 6 and 7) were significant. Plant parameters were significantly affected by T × CO₂ in 12 cases (see Tables 3, 4, 5 and 6), by T × W in 14 cases (see Tables 3, 4, 5 and 7), by CO₂ × W in 7 cases (see Tables 3, 4, 6 and 7), and by T × CO₂ × W in 5 cases (Tables 3, 5, 6 and 7).

The interaction among the three main factors (T × CO₂ × W) had significant effects on leaf number (Table 3; Figure 1D), moisture content (Table 3; Figure 1E), root dry mass (Table 5; Figure 3C), MDA (Table 6; Figure 4B) and flavonoids (Table 7; Figure 5C). Water-stressed plants grown under higher temperatures at elevated CO₂ had highest leaf number, moisture content and root dry mass, whereas well-watered plants grown under lower temperatures at elevated CO₂ had lowest leaf number (Table 3; Figure 1D), moisture content (Table 3; Figure 1E) and root dry mass (Table 5; Figure 3D). Seedlings grown under higher temperature, elevated CO₂, and water stress conditions had the highest flavonoid content (Table 7; Figure 5C). Moreover, higher temperature and water stress, individually and together, increased MDA content (Table 6; Figure 4B), but elevated CO₂ decreased it under stress conditions. These results indicated that the stress-reducing effect of elevated CO₂ was clearly observed for biomass, plant water status and stress indicator parameters, as shown by increasing some growth and biomass parameters, moisture content and flavonoids and decreasing MDA. Moreover, these results are consistent with previous study on *Arabidopsis thaliana* (Abo Gamar *et al.*, 2019). Thus, it is important to study the effects of the main ecological climate change factors (temperature,

CO₂ and watering regime) associated with climate change along with their combined effects on plants.

5. Conclusions

This study showed that higher temperature and water stress had negative effects, while elevated CO₂ had positive effects, on Giza faba bean seedlings. Elevated CO₂ decreased stresses on Giza faba bean seedlings by increasing their growth, water content and antioxidant activity. The capability shown in Giza faba bean to potentially survive under climate change main components may predict that this plant will resist such conditions in the future.

Funding

The authors thank the deanship of research at Yarmouk University/Jordan for funding this project.

Conflicts of Interest

Authors declare no conflict of interests.

References

- Abdulmajeed AM, Abo Gamar MI and Qaderi MM. 2018. Inter- and intra-varietal variation in aerobic methane emissions from environmentally stressed pea plants. *Botany*, **96**: 837-850.
- Abo Gamar MI, Dixon SL and Qaderi MM. 2021. Single and interactive effects of temperature, carbon dioxide and watering regime on plant growth and reproductive yield of two genotypes of *Arabidopsis thaliana*. *Acta Physiol. Plant.*, **43**: 1-16.
- Abo Gamar MI, Kisiala A, Emery R, Yeung EC, Stone SL and Qaderi MM. 2019. Elevated carbon dioxide decreases the adverse effects of higher temperature and drought stress by mitigating oxidative stress and improving water status in *Arabidopsis thaliana*. *Planta*, **250**: 1191-1214.
- Akhter N, Habiba O, Hina M *et al.* 2022. Structural, biochemical, and physiological adjustments for toxicity management, accumulation, and remediation of cadmium in wetland ecosystems by *Typha domingensis* Pers. *Water Air Soil Pollut.*, **233**: 151.
- Bargali K and Tewari A. 2004. Growth and water relation parameters in drought-stressed *Coriaria nepalensis* seedlings. *J. Arid Environ.*, **58**: 505-512.
- Bates LS, Waldren RP and Teare I. 1973. Rapid determination of free proline for water-stress studies. *Plant Soil*, **39**: 205-207.
- Chaitanya K, Sundar D and Reddy AR. 2001. Mulberry leaf metabolism under high temperature stress. *Biol. Plant.*, **44**: 379-384.
- Chappelle EW, Kim MS and McMurtrey III JE. 1992. Ratio analysis of reflectance spectra (RARS): an algorithm for the remote estimation of the concentrations of chlorophyll a, chlorophyll b, and carotenoids in soybean leaves. *Remote Sens. Environ.*, **39**: 239-247.
- Cline WR. 2007. Global warming and agriculture: impact estimates by country (center for global development, peterson institute for international economics. Washington, DC. pp. 178.
- Cottee N, Tan D, Bange M and Cheetham J. 2007. Simple electrolyte leakage protocols to detect cold tolerance in cotton genotypes. Proceedings 4th World Cotton Research Conference.
- DaMatta FM, Grandis A, Arenque BC and Buckeridge MS. 2010. Impacts of climate changes on crop physiology and food quality. *Food Res. Int.*, **43**: 1814-1823.
- Dela G, Or E, Ovadia R, Nissim-Levi A, Weiss D and Oren-Shamir M. 2003. Changes in anthocyanin concentration and composition in 'Jaguar' rose flowers due to transient high-temperature conditions. *Plant Sci.*, **164**: 333-340.
- Diatta AA, Fike JH, Battaglia ML, Galbraith JM and Baig MB. 2020. Effects of biochar on soil fertility and crop productivity in arid regions: a review. *Arab. J. Geosci.*, **13**: 1-17.
- Fallah S, Azizi K, Eisvand HR, Akbarpour O, and Akbari N. 2022. Effect of zinc sulfate foliar application on morphological characteristics and yield of red beans (*Phaseolus vulgaris* L.) under different carbon dioxide-temperature and water stress. *Env. Stresses Crop Sci.*, **15**: 641-56.
- Farrar JF and Gunn S. 2017. Effects of temperature and atmospheric carbon dioxide on source-sink relations in the context of climate change. In: **Photoassimilate distribution in plants and crops**. Routledge, pp. 389-406.
- Fini A, Brunetti C, Di Ferdinando M, Ferrini F and Tattini M. 2011. Stress-induced flavonoid biosynthesis and the antioxidant machinery of plants. *Plant Signal. Behav.*, **6**: 709-711.
- Granda E, Rossatto DR, Camarero JJ, Voltas J and Valladares F. 2014. Growth and carbon isotopes of Mediterranean trees reveal contrasting responses to increased carbon dioxide and drought. *Oecologia*, **174**: 307-317.
- Hajihashemi S and Ehsanpour A. 2013. Influence of exogenously applied paclobutrazol on some physiological traits and growth of *Stevia rebaudiana* under *in vitro* drought stress. *Biologia*, **68**: 414-420.
- Hamidou F, Halilou O and Vadez V. 2013. Assessment of groundnut under combined heat and drought stress. *J. Agron. Crop. Sci.*, **199**: 1-11.
- Hiscox J and Israelstam G. 1979. A method for the extraction of chlorophyll from leaf tissue without maceration. *Canad. J. Bot.*, **57**: 1332-1334.
- Hu Y, Burucs Z and Schmidhalter U. 2006. Short-term effect of drought and salinity on growth and mineral elements in wheat seedlings. *J. Plant Nutr.*, **29**: 2227-2243.
- Ihuoma SO and Madramootoo CA. 2019. Sensitivity of spectral vegetation indices for monitoring water stress in tomato plants. *Comput. Electron. Agric.*, **163**: 104860.
- IPCC. 2013. Climate change 2013: Summary for policymakers. Contribution of working groups I, II, and III to the fifth assessment report of the Intergovernmental Panel on Climate Change. IPCC, Geneva, Switzerland.
- Jiang X, Rauscher SA, Ringler TD, Lawrence DM, Williams AP, Allen CD, Steiner AL, Cai DM and McDowell NG. 2013. Projected future changes in vegetation in western North America in the twenty-first century. *J. Clim.*, **26**: 3671-3687.
- Jones, HG. 1992. Plants and microclimate. In: **a quantitative approach to environmental plant physiology**. Cambridge University Press, Cambridge, UK.
- Kaur R, Bains T, Bindumadhava H and Nayyar H. 2015. Responses of mungbean (*Vigna radiata* L.) genotypes to heat stress: effects on reproductive biology, leaf function and yield traits. *Sci. Hortic.*, **197**: 527-541.
- Kesaulya I and Vega R. 2019. Effects of hypersaline conditions on the growth and survival of larval red drum- (*Sciaenops ocellatus*). *Jordan J. Biol. Sci.*, **12**: 119-122.
- Lacis AA, Hansen JE, Russell GL, Oinas V and Jonas J. 2013. The role of long-lived greenhouse gases as principal LW control knob that governs the global surface temperature for past and future climate change. *Tellus B: Chem. Phys. Meteorol.*, **65**: 19734.
- Liu J, Folberth C, Yang H, Röckström J, Abbaspour K and Zehnder AJ. 2013. A global and spatially explicit assessment of climate change impacts on crop production and consumptive water use. *PLoS One*, **8**: e57750.

- Marcilly CM, Torsvik TH, Domeier M and Royer DL. 2021. New paleogeographic and degassing parameters for long-term carbon cycle models. *Gondwana Res.*, **97**: 176-203.
- Martel AB and Qaderi MM. 2016. Does salicylic acid mitigate the adverse effects of temperature and ultraviolet-B radiation on pea (*Pisum sativum*) plants? *Environ. Exp. Bot.*, **122**: 39-48.
- Maritim TK, Korir RK, Nyabundi KW, Wachira FN, Kamunya SM and Muoki RC. 2021. Molecular regulation of anthocyanin discoloration under water stress and high solar irradiance in pluckable shoots of purple tea cultivar. *Planta*, **254**: 1-17.
- Mekonnen ZA, Grant RF and Schwalm C. 2016. Contrasting changes in gross primary productivity of different regions of North America as affected by warming in recent decades. *Agric. For. Meteorol.*, **218**: 50-64.
- Mishra AK and Singh VP. 2010. A review of drought concepts. *J. Hydrol.*, **391**: 202-16.
- Moretti C, Mattos L, Calbo A and Sargent S. 2010. Climate changes and potential impacts on postharvest quality of fruit and vegetable crops: a review. *Food Res. Int.*, **43**: 1824-1832.
- Munir T, Xu B, Perkins M and Strack M. 2014. Responses of carbon dioxide flux and plant biomass to water table drawdown in a treed peatland in northern Alberta: a climate change perspective. *Biogeosciences*, **11**: 807-820.
- Naheed R, Zahid M, Aqeel M *et al.* 2022. Mediation of growth and metabolism of *Pisum sativum* in salt stress potentially be credited to thiamine. *J. Soil Sci. Plant Nutr.*, **22**: 2897-2910.
- Okorie VO, Mphambukeli TN and Amusan SO. 2019. Exploring the political economy of water and food security nexus in BRICS. *Afr. Insight*, **48**: 21-38.
- Osman AG, Elaziz FI and ElHassan GA. 2010. Effects of biological and mineral fertilization on yield, chemical composition and physical characteristics of faba bean (*Vicia faba* L.) cultivar *Seleim*. *Pak. J. Nutr.*, **9**: 703-8.
- Padhy GK, Wu CS and Gao S. 2018. Friction stir based welding and processing technologies-processes, parameters, microstructures and applications: A review. *J. Mater. Sci. Technol.*, **34**: 1-38.
- Prasch CM and Sonnewald U. 2015. Signaling events in plants: stress factors in combination change the picture. *Environ. Exp. Bot.*, **114**: 4-14.
- Qaderi MM, Kurepin LV and Reid DM. 2006. Growth and physiological responses of canola (*Brassica napus*) to three components of global climate change: temperature, carbon dioxide and drought. *Physiol. Plant.*, **128**: 710-721.
- Qaderi MM, Kurepin LV and Reid DM. 2012. Effects of temperature and watering regime on growth, gas exchange and abscisic acid content of canola (*Brassica napus*) seedlings. *Environ. Exp. Bot.*, **75**: 107-113.
- Qaderi MM and Reid DM. 2009. Crop responses to elevated carbon dioxide and temperature. In: **climate change and crops**. Springer, pp. 1-18.
- Qaderi MM and Reid DM. 2011. Stressed crops emit more methane despite the mitigating effects of elevated carbon dioxide. *Funct. Plant Biol.*, **38**: 97-105.
- Qaseem MF, Qureshi R and Shaheen H. 2019. Effects of pre-anthesis drought, heat and their combination on the growth, yield and physiology of diverse wheat (*Triticum aestivum* L.) genotypes varying in sensitivity to heat and drought stress. *Sci. Rep.*, **9**: 1-12.
- Romero-Aranda R, Soria T and Cuartero J. 2001. Tomato plant-water uptake and plant-water relationships under saline growth conditions. *Plant Sci.*, **160**: 265-272.
- Sangtarash M, Qaderi M, Chinnappa C and Reid D. 2009. Differential sensitivity of canola (*Brassica napus*) seedlings to ultraviolet-B radiation, water stress and abscisic acid. *Environ. Exp. Bot.*, **66**: 212-219.
- SAS Institute. 2011. SAS/STAT User's Guide. Version 9.3. SAS Institute, Cary, North Carolina.
- Sehgal A, Sita K, Kumar J, Kumar S, Singh S, Siddique KH and Nayyar H. 2017. Effects of drought, heat and their interaction on the growth, yield and photosynthetic function of lentil (*Lens culinaris* Medikus) genotypes varying in heat and drought sensitivity. *Front. Plant Sci.*, **8**: 1776.
- Shin H, Oh S, Arora R and Kim D. 2016. Proline accumulation in response to high temperature in winter-acclimated shoots of *Prunus persica*: a response associated with growth resumption or heat stress? *Can. J. Plant Sci.*, **96**: 630-638.
- Singh H. 2021. Building effective blended learning programs. In: **challenges and Opportunities for the Global Implementation of E-Learning Frameworks**. pp. 15-23.
- Solomon S. 2007. Climate change the physical science basis. In: **agu fall meeting abstracts**, pp. U43D-01.
- Sovacool BK. 2021. Who are the victims of low-carbon transitions? Towards a political ecology of climate change mitigation. *Energy Res. Soc. Sci.*, **73**: 101916.
- Sukumaran P, Bin Omar H, Nulit RB, Halimoon NB, Simoh SB and Bin Ismail A. 2018. The prospects of the cultivation of *Arthrospira platensis* under outdoor conditions in Malaysia. *Jordan J. Biol. Sci.*, **11**: 419-426.
- Taduri S, Lone AA, Meyers MS, Shankle MW and Reddy KR. 2017. Sweetpotato cultivar responses to interactive effects of temperature, drought, and carbon dioxide. Poster session presented at the Managing Global Resources for a Secure Future Meeting, Tampa, FL. Retrieved from <https://scisoc.confex.com/crops/2017am/webprogram/Paper107834.html> (accessed August 2022).
- Taiz L, Zeiger E, Møller IM and Murphy A. 2014. Plant physiology and development. Sunderland, MA, USA: Sinauer Associates.
- Taub D. 2010. Effects of rising atmospheric concentrations of carbon dioxide on plants. *Nat. Sci. Educ.*, **3**: 21.
- Timpane-Padgham BL, Beechie T and Klinger T. 2017. A systematic review of ecological attributes that confer resilience to climate change in environmental restoration. *PLoS One*, **12**: e0173812.
- Tiwari JK and Singh AK. 2019. Principal component analysis for yield and yield traits in faba bean (*Vicia faba* L.). *J. Food Legume.*, **32**: 13-5.
- Triacca U, Pasini A, Attanasio A, Giovannelli A and Lippi M. 2014. Clarifying the roles of greenhouse gases and ENSO in recent global warming through their prediction performance. *J. Clim.*, **27**: 7903-7910.
- Ulfat A, Shokat S, Li X, Fang L, Großkinsky DK, Majid SA, Roitsch T and Liu F. 2021. Elevated carbon dioxide alleviates the negative impact of drought on wheat by modulating plant metabolism and physiology. *Agric. Water Manag.*, **250**: 106804.
- Váry Z, Mullins E, McElwain JC and Doohan FM. 2015. The severity of wheat diseases increases when plants and pathogens are acclimatized to elevated carbon dioxide. *Glob. Change Biol.*, **21**: 2661-2669.
- Xu W, Ren X, Johnston T, Yin Y, Klein K and Smith A. 2012. Spatial and temporal variation in vulnerability of crop production to drought in southern Alberta. *Can. Geogr.*, **56**: 474-491.

Investigation of Seagrass-Associated Fungi as Antifouling Candidates with Anti-Bacterial Properties

Wilis Ari Setyati^{1,*}, Sri Sedjati¹, Alun Samudra¹, and Dafit Ariyanto²

¹Department of Marine Science, Faculty of Fisheries and Marine Science, Diponegoro University, Semarang, Central Java, 50275, Indonesia; ²Research Center for Oceanography, National Research and Innovation Agency (BRIN), Jakarta, 14430, Indonesia

Received: August 24, 2022; Revised: December 9, 2022; Accepted: December 29, 2022

Abstract

The aim of this study was to test seagrass-associated fungi that have antibacterial activity against *Vibrio alginolyticus* and *Vibrio parahaemolyticus*. Seagrass sampling, fungi isolation, antibacterial screening, and molecular identification were used in this study. The antibacterial screening found that 2 out of 10 isolates were positive for antibacterial activity. This includes a seagrass-associated fungi of *Thalassia hemprichii*, which has green colonies. This isolate has no exudates and has a green reverse. The other isolate TA.EA.1.3 was a seagrass-associated fungi of *Enhalus acoroides*, white in color, with exudates and a brown reverse. The isolate extracts weighed 256 mg and 2017.9 mg, respectively. The antibacterial activity of the TA.TH.1.1 fungal isolate extract against *V. alginolyticus* and *Vibrio parahaemolyticus* was classified as strong because of the inhibition zone produced, which was 10-20 mm. The antibacterial activity of the TA.EA.1.3 isolate, classified as moderate, produced 5-10 mm of inhibition zone. Molecular identification showed that isolate TA.TH.1.1 was *Aspergillus unguis* (100% homology) and TA.EA.1.3 was *Aspergillus versicolor* (100% homology). In conclusion, *A. unguis* and *A. versicolor* have antibacterial ability against *Vibrio alginolyticus* and *V. parahaemolyticus* as antifouling bacteria.

Keywords: Antibacteria, Antifouling, Association, Fungi, Seagrass

1. Introduction

Marine ecosystems have high biodiversity, including a large population of bacteria. One liter of seawater can contain more than 20,000 bacterial cells (Sogin et al., 2006). *Vibrio* spp. survive in warm-brackish water, even in Indonesia (Baker-Austin et al., 2018). *Vibrio* spp. bacteria can cause a lot of losses in the marine sector, by leading to, for instance, the formation of a biofilm layer on some marine organisms (Ashrafudoulla et al., 2021). In addition, marine organisms contaminated by *Vibrio* spp. can get vibriosis, which causes huge economic losses in the aquaculture (Liu et al., 2013). This species reportedly also forms biofilms on the surface of ship hulls and marine infrastructure (Waturangi et al., 2017). Antifouling technology is used in controlling biofouling, for example, biofouling paint. Antifouling often used chemicals, such as tributyltin (TBT), Cu, Zn, Ba, Cd, Cr, Ni, and Pb, which are toxic to non-target objects. As a result, International Maritime Organization (IMO) banned the use of TBT and heavy metals for antifouling in 2008 (Qian et al., 2010).

Seagrasses are plants that have adapted to a life immersed in shallow seas. These higher plants have a high tolerance to salt levels in their habitat and reproduce by seeds (Touchette, 2007). Seagrasses have different kinds of associations with various organisms, one of which is fungi. Seagrass species, such as *Posidonia oceanica*, *Thalassia hemprichii*, and *Halophila ovalis*, accumulate large amounts of fungi in their bodies, (Ling et

al., 2015). Seagrass-associated fungi have a bioactive compound that allows their host to defend themselves from insects and pathogenic microorganisms (Gono et al., 2022). Such fungi can inhibit the formation of *Staphylococcus aureus*, *Pseudomonas aeruginosa*, and *Escherichia coli* bacteria (Supaphon et al., 2013; Rabbani et al., 2021). Activities of marine-derived fungi (MDF) isolated from seagrasses had potency in antibacterial, cytotoxic, and trypanocidal and salinity may influence the bioactivities of some species of MDF (Notarte et al., 2018).

Vibrio spp. is a kind of gram-negative bacteria and is comma-shaped. This bacteria is a natural constituent in freshwater, estuary, and warm marine ecosystems (Baker-Austin et al., 2018). The key factor supporting the survival of *Vibrio* spp. in marine ecosystems is its ability to form biofilms (Yildiz & Visick, 2009). Biofilm is a collection of microbial cells attached irreversibly to a surface, both biotic and abiotic, and encased in a matrix formed from polysaccharide material (Donlan & Costerton, 2002). *Vibrio* bacteria can form biofilms on the surface of some marine organisms, such as crabs, oysters, clams, and shrimp. They can also infect marine organisms and cause diseases, both for these organisms themselves and for humans who consume these organisms (Ashrafudoulla et al., 2021). Marine organisms contaminated by *Vibrio* can get vibriosis which causes huge economic losses in the aquaculture industry (Liu et al., 2013). Humans who consume marine organisms contaminated by *Vibrio* bacteria can complain from gastrointestinal diseases with

* Corresponding author. e-mail: wilisarsetyati@yahoo.co.id.

various symptoms, such as vomiting, headache, and nausea (Xi et al., 2012). This study aims to explore the potential of extracts of seagrass-associated fungi as an antibacterial product against *Vibrio alginolyticus* and *Vibrio parahaemolyticus*.

2. Materials and Methods

2.1. Site Research

Samples of the seagrass species *Cymodocea serrulata*, *Enhalus acoroides*, and *Thalassia hemprichii* from Teluk Awur, Jepara, Central Java, Indonesia were used in this research. Fresh samples were isolated in order to maximize the number of associated fungi. The isolation process was carried out at the Integrated Laboratory, Diponegoro University. Potato Dextrose Agar (PDA) and Malt Extract Agar (MEA) were used for fungal isolation (Sibero et al., 2018). The isolated samples were then incubated and observed for seven days. Bacterial screening was carried out to determine potential isolates for antibacterial activity. The screening was carried out based on the and cultured in a nutrient agar medium at room temperature (Sibero et al., 2017).

2.2. Sample Preparation

The extraction of seagrass-associated fungi was carried out by the maceration method (Payangan, 2018). The cultured fungi were macerated using ethyl acetate (EtOAc) solvent for 72 hours, and the solvent was changed every 24 hours. The maceration results were filtered using filter paper. The remaining solvent in the filter was evaporated using a rotary evaporator with nitrogen gas.

2.3. Antibacterial activity

The agar diffusion method (or the Kirby-Bauer disc diffusion method) was used to test the antibacterial

activity. The pathogens used were *V. alginolyticus* and *V. parahaemolyticus*. The fungal extract was diluted with dimethyl sulfoxide (DMSO) into three different concentrations, which were 100 g/disc, 250 g/disc, and 500 g/disc. Extracts from each concentration were then diffused on paper discs (Ø 6 mm Oxoid™) as much as 10 l/disc. Chloramphenicol was used as a positive control and DMSO was used as a negative control in the test (Sibero et al., 2018).

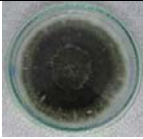
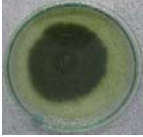





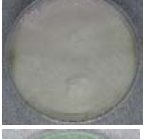
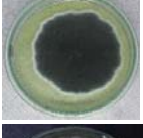

2.4. Molecular identification

DNA extraction was carried out using the Zymo® DNA Extraction Kit. Pure isolates of fungi were grown in an agar medium for seven days and used for DNA extraction. Amplification was carried out using the Internal Transcribed Spacer (ITS) as a primer for fungi barcoding when using polymerase chain reaction (PCR). The quality of PCR products was checked using electrophoresis with tris base buffer, acetic acid, and EDTA (TAE) 1X. The sequences obtained were processed using the MEGA X software and then formed a phylogenetic tree.

3. Results

The seagrasses associated with fungi, particularly *E. acoroides*, *T. hemprichii* and *C. serrulata*, showed several results (Table 1). There were 4 isolates of fungi isolated from *C. serrulata*, 3 isolates of fungi from *T. hemprichii*, and 3 isolates of fungi with different colors, mycelium, exudates, and reverse. Isolate TA.TH 1.1 from *T. hemprichii* had green colonies with white mycelium. This isolate had no exudates and had a green reverse. Isolate TA.EA.1.3 from *Enhalus acoroides* was white in color, white in mycelium, had exudates and a brown reverse. The screening was carried out before the isolate extract process.

Table 1: Results of Morphological Identification of Seagrass-associated Fungi

No	Seagrass	Isolate code	Results	Colony colour	Miselium	Exudates	Reverse
1	<i>Cymodocea serrulata</i>	TA.CS.1.1		black	black	No	black
2	<i>C. serrulata</i>	TA.CS.1.2		black	white	No	white
3	<i>C.serrulata</i>	TA.CS.1.3		black	white	no	brown
4	<i>C. serrulata</i>	TA.CS.1.4		white	white	No	pink
5	<i>T. hemprichii</i>	TA.TH.1.1		green	white	No	green
6	<i>T. hemprichii</i>	TA.TH.1.2		green	green	No	red
7	<i>T. hemprichii</i>	TA.TH.1.3		green -white	white	No	brown
8	<i>E. acoroides</i>	TA.EA.1.1		white	white	No	yellow
9	<i>E. acoroides</i>	TA.EA.1.2		blue	white	exist	blue
10	<i>E. acoroides</i>	TA.EA.1.3		white	white	No	brown

The screening results showed that 2 isolates of seagrass-associated fungi had the potential for antibacterial activity against *Vibrio alginolyticus* and *Vibrio parahaemolyticus* bacteria, namely isolates TA.TH.1.1 and TA.EA.1.3. The isolates were then extracted, yielding results that can be seen in Table 2.

Table 2: Seagrass Associated fungi Isolate Extract Weight

No	Isolate code	Weight (mg)
1	TA.TH.1.1	256
2	TA.EA.1.3	207.9

The TA.TH.1.1 isolate had an extract weight of 256 mg and the TA.EA.1.3 isolate had an extract weight of 207.9 mg. The results of the antibacterial activity test of the isolates of fungi-associated seagrass TA.TH.1.1 and TA.EA.1.3 against *V. alginolyticus* and *V.*

parahaemolyticus bacteria were observed over an incubation period of 24 hours and can be seen in Table 3.

Table 3: Seagrass Associated fungi Isolate Antibacterial Activity Test Results

No	Isolate Code	Concentration (µg/disc)	Avg. Inhibition Zone Diameter (mm)	
			<i>V. alginolyticus</i>	<i>V. parahaemolyticus</i>
1	TA.TH.1.1	500	15.47 ± 0.40	15.37 ± 0.19
		250	14.13 ± 0.33	12.46 ± 0.28
		100	11.10 ± 0.32	8.70 ± 0.23
		500	9.02 ± 0.49	8.60 ± 0.45
2	TA.EA.1.3	250	10.10 ± 0.48	10.19 ± 0.26
		100	5.8 ± 0.17	5.92 ± 0.21
3	Positive Control (Chloramphenicol)	30	15.15 ± 0.23	18.77 ± 0.24
4	Negative Control (DMSO)	-	-	-

The average diameter of the largest inhibition zone produced by isolates TA.TH.1.1 against *V. alginolyticus* was 15.47 mm at a concentration of 500 g/disc, while that produced by isolates TA.TH.1.1 against *V. parahaemolyticus* was 15.37 mm at a concentration of 500 g/disc. The average diameter of the largest inhibition zone produced by isolate TA.EA.1.3 against *V. alginolyticus* was 10.10 mm at a concentration of 250 g/disc, and by isolate TA.EA.1.3 against *V. parahaemolyticus* was 10.19 mm at a concentration of 250 g/disc. Potential isolates that had been amplified using PCR were characterized by the formation of a single band from each fungal DNA. Gene amplification results were used for further identification. The results of visualization of the DNA of fungi isolates TA.TH.1.1 and TA.EA.1.3 can be seen in Figure 1.

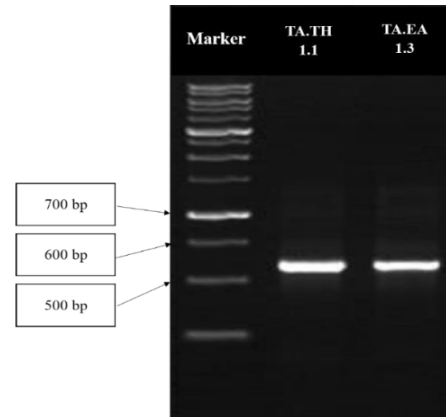


Figure 1: Result of Isolates TA.TH.1.1 dan TA.EA.1.3 DNA Visualization

The DNA visualization was followed by a homology BLAST search. According to the results obtained, isolate TA.TH.1.1 had a close kinship level (100%) with *Aspergillus unguis* (Acc Number MT582759.1), while isolate TA.EA.1.3 had a very close relationship (100%) with *Aspergillus versicolor* (Acc Number MK140698.1).

Table 4: Homology BLAST Search Results

No	Isolate Code	Identification Result	Query Cover	Percent Identify	E Value	Acc Number
1	TA.TH.1.1	<i>Aspergillus unguis</i>	100%	100%	0.0	MT582759.1
2	TA.EA.1.3	<i>Aspergillus versicolor</i>	100%	100%	0.0	MK140698.1

The results of processing base pair data for making a phylogenetic tree can be seen in Figure 2.

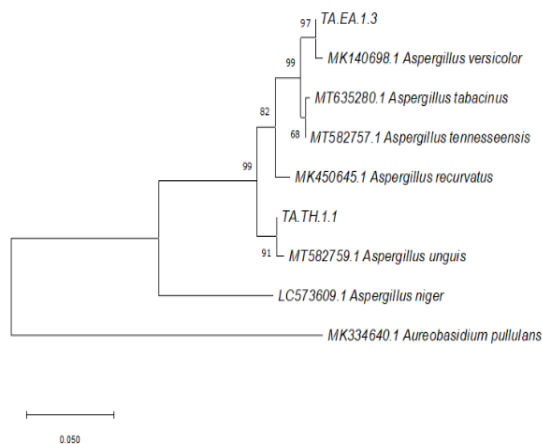


Figure 2: Phylogenetic tree of TA.TH.1.1 and TA.EA.1.3 fungi isolate

The results of data processing showed that there was a clustering of seagrass-associated fungi isolates with other organisms in the closest to farthest kinship levels. The level of kinship in the isolate TA.TH.1.1 showed a very close relationship with *Aspergillus unguis* while the isolate TA.EA.1.3 showed a very close relationship with *Aspergillus versicolor*. The out group used was the fungus *Aureobasidium pullulans* (MK334640.1) because it is a species that has no close relationship with the fungi isolates TA.TH.1.1 and TA.EA.1.3.

4. Discussion

The obtained results showed 7 isolates on PDA media and 3 isolates on MEA media. Isolation code naming and morphological characteristics PDA and MEA media were used in the growth of associated fungi. PDA increases fungi sporulation and pigment production (Fitriana et al., 2018). The MEA medium was used to grow fungi mycelia and to perfect its morphological characters (Abdullah &

Saadullah, 2018). The TA.TH.1.1 fungal isolate extract was heavier than the TA.EA.1.3 yeast isolate extract, due to the different media used, which led to differences in spore growth. This statement is supported by Abdullah and Saadullah (2018), who show that the PDA medium is generally used to accelerate fungi sporulation.

The results showed that the extract with a high concentration showed better antibacterial activity against the test bacteria. The antibacterial activity was high against microbes if the minimum inhibitory concentration is low but the inhibitory power is high (Balouiri et al., 2016). The antibacterial activity of the extract of the fungal isolate TA.TH.1.1 against the bacteria *V. alginolyticus* and *V. parahaemolyticus* was strong, while the antibacterial activity of the extract of the fungus isolate TA.EA.1.3 against the bacteria *V. alginolyticus* and *V. parahaemolyticus* was moderate. According to Davis and Stout (1971), an inhibition zone with a diameter of >20 mm can be categorized as having very strong activity.

The results showed that the isolate TA.TH.1.1 had a very close relationship with the fungus *Aspergillus unguis* with a query cover of 100% and homology (percent identify) of 100%. Isolate TA.EA.1.3 had a very close relationship with the fungus *Aspergillus versicolor* with a query cover of 100% and homology (percent identify) of 100%. The results of the analysis obtained are categorized as similar because they have a similarity percentage above 97%. As Hagström et al. (2000) have stated, isolates that had a similarity percentage of more than 97% could be said to represent the same species.

5. Conclusions

Fungi-associated seagrasses have antibacterial potential against *V. alginolyticus* and *V. parahaemolyticus* that cause fouling. *Aspergillus unguis* and *Aspergillus versicolor* were identified by molecular identification based on ITS region sequences and were known to form inhibition zones against *V. alginolyticus* and *V. parahaemolyticus*.

Contribution of authors

All authors are equal in contribution to the paper.

References

Abdullah B, and Saadullah A. 2018. Effect of types cultures media on isolation of fungi from indoor swimming pools. *Conference Portal ICPAS*, 23–27.

Ashrafudoulla M, Mizan MFR, Park SH, Ha SD. 2021. Current and future perspectives for controlling *Vibrio* biofilms in the seafood industry: a comprehensive review. *Crit Rev Food Sci Nutr*, **61**(11):1827–1851.

Baker-Austin C, Oliver JD, Alam M, Ali A, Waldor MK, Qadri F and Martinez-Urtaza J. 2018. *Vibrio* spp. infections. *Nat Rev Dis Primers*, **4** (8): 1–19.

Balouiri M, Sadiki M and Ibsouda SK. 2016. Methods for in vitro evaluating antimicrobial activity: A review. *J Pharm Anal*, **6**: 71–79.

Davis WW and Stout TR. 1971. Disc plate method of microbiological antibiotic assay. *Appl Microbiol*, **22**(4): 666–670.

Donlan RM and Costerton JW. 2002. Biofilms: survival mechanisms of clinically relevant microorganisms. *Clin Microbiol Rev*, **15**: 167–193.

Gono CMP, Ahmadi P, Hertiani T, Septiana E, Putra MY and Chianese G. 2022. A comprehensive update on the bioactive compounds from seagrasses. *Marine Drugs*, **20**(406):1–37.

Hagström Å, Pinhassi J and Li ZU. 2000. Biogeographical diversity among marine bacterioplankton. *Aquatic Microbial Ecol*, **21**: 231–244.

Ling J, Zhang Y, Wu M, Wang Y, Dong J, Jiang Y, Yang Q and Zeng S. 2015. Fungal community successions in rhizosphere sediment of seagrasses *Enhalus acoroides* under PAHs stress. *Int J Mol Sci*, **16**: 14039–14055.

Liu H, Srinivas S, Gong G, He X, Dai C, Feng Y, Chen X and Wang S. 2013. Quorum sensing in *Vibrio* and its relevance to bacterial virulence. *J Bacteriol Parasitol*, **4**(3): 1000172.

Notarte KI, Yaguchi T, Suganuma K, Cruz TE and Dela. 2018. Antibacterial, cytotoxic and trypanocidal activities of marine-derived fungi isolated from Philippine macroalgae and seagrasses. *Acta Botanica Croatica*, **77**(2): 141–151.

Payangan GE. 2018. Uji aktivitas antimikroba jamur laut yang berasosiasi *Phyllospongia lamellose*. *Pharmakon*, **7**(3): 266–275.

Qian P, Xu Y and Fusetani N. (2010). Natural products as antifouling compounds : recent progress and future perspectives. *Biofouling*, **26**(2): 223–234.

Rabbani G, Yan BC, Lee NLY, Ooi JLS, Lee JN, Huang D, and Wainwright BJ. 2021. Spatial and structural factors shape seagrass-associated bacterial communities in Singapore and Peninsular Malaysia. *Frontiers Mar Sci*, **8**: 1–11.

Sibero MT, Sabdaningsih A, Cristianawati O, Nuryadi H, Radjasa OK, Sabdono A, and Trianto A. 2017. Preface: International Conference on Recent Trends in Physics (ICRTP 2016). *JPCS*, **55**(012028): 1–12.

Sibero MT, Herdikiawan D, Radjasa OK, Sabdono A, Trianto A, and Triningsih DW. 2018. Antibacterial activity of sponge associated fungi against vibriosis agents in shrimp and its toxicity to *Litopenaeus vannamei*. *AACL Bioflux*, **11**(1): 10–18.

Sibero MT, Trianto A, Frederick EH, Wijaya AP, Ansori ANM, Igarashi Y. 2022. Biological activities and metabolite profiling of *Polycarpa aurata* (Tunicate, Ascidian) from Barrang Caddi, Spermonde Archipelago, Indonesia. *Jordan J Biol Sci*, **15**(1): 15–20.

Sogin ML, Morrison HG, Huber JA, Welch DM, Huse SM, Neal PR, Arrieta JM and Herndl GJ. 2006. Microbial diversity in the deep sea and the underexplored “rare biosphere. *Proc Natl Acad Sci USA*, **103**(32): 12115–12120.

Supaphon P, Phongpaichit S, Rukachaisirikul V, and Sakayaroj J. 2013. Antimicrobial potential of endophytic fungi derived from three seagrass species: *Cymodocea serrulata*, *Halophila ovalis* and *Thalassia hemprichii*. *PLoS ONE*, **8**(8): 1–9.

Touchette BW. 2007. Seagrass-salinity interactions: Physiological mechanisms used by submersed marine angiosperms for a life at sea. *J Exp Mar Biol Ecol*, **350**(1–2): 194–215.

Waturangi DE, Purwa HJ, Lois W, Hutagalung RA, and Hwang JK. 2017. Inhibition of marine biofouling by aquatic Actinobacteria and coral-associated marine bacteria. *Malays J Microbiol*, **13**(2): 92–99.

Xi D, Liu C, and Su YC. 2012. Effects of green tea extract on reducing *Vibrio parahaemolyticus* and increasing shelf life of oyster meats. *Food Control*, **25**: 368–373.

Yildiz FH, and Visick KL. 2009. *Vibrio* biofilms: so much the same yet so different. *Trends Microbiol*, **17**(3): 109–118.

Moringa oleifera (Lam) Root Extracts Elevate Catecholamine Levels in Experimental Rats: Potential Role of Ethnopharmacology in Combating Depressive Conditions

Auwal Adamu^{1,*}, Mahmoud S. Jada², Umar Saidu¹, Yahaya I. Usha¹, Emmanuel G. Favour¹ and Mohammed N. Shuaibu¹

¹Department of Biochemistry, Faculty of Life Sciences, Ahmadu Bello University, Zaria, Nigeria; ²Department of Biochemistry, Faculty of Life Sciences, Modibbo Adama University, Yola, Nigeria.

Received: August 27, 2022; Revised: December 10, 2022; Accepted: December 29, 2022

Abstract

Rising cases of neurodegenerative disorders negatively impact human and economic resources of the globe, hence the need to search for safe, affordable, and effective psychotherapeutic interventions. In the present study, the effect of extracts from roots of *Moringa oleifera* (*M. oleifera*) on norepinephrine and epinephrine levels in brain and serum of seemingly healthy rats was investigated.

Fresh roots of *M. oleifera* were collected, dried, ground and subjected to aqueous, methanol and diethyl-ether extractions. Median lethal dose (LD₅₀) of *M. oleifera* aqueous root extract was determined. Animal experimental groups received 100- and -200 mg/kg body weights of the different root extracts of *M. oleifera*. The animals were sacrificed after anesthesia on the eleventh day, and blood and brain samples were taken and tested for total proteins and catecholamines. All data were analysed using one-way-analysis of variance and Tukey tests. Value less than 0.05 was considered for statistical significance.

High doses of aqueous, methanol, and diethyl ether root extracts of *M. oleifera* significantly ($p < 0.05$) reduced brain total protein concentration. Level of serum epinephrine was not significantly ($p > 0.05$) altered by the aqueous, methanol and diethyl-ether root extracts, whilst brain epinephrine concentration was significantly ($p < 0.05$) raised by the diethyl-ether root extract. Norepinephrine levels in the brains and serum of rats that appeared to be in good condition were only marginally elevated by high and low dosages of the plant's aqueous and methanol root extracts, but they were markedly elevated ($p < 0.05$) by both doses of the di-ethyl-ether extract.

The present study reveals that di-ethyl-ether root extract of *M. oleifera* can dose dependently alter norepinephrine and epinephrine levels in brain and serum of apparently healthy rats. Consequently, it is crucial to investigate the mechanism by which the administration of di-ethyl-ether root extract of the plant to animals modulate catecholamine production.

KeyWords: Root-extracts, *M. oleifera*, Brain, Epinephrine and Norepinephrine

1. Introduction

Neurodegenerative diseases (NDs) and depressive disorders (DDs) are heterogeneous groups of disorders characterized by progressive deterioration of structures and functions of central and peripheral nervous systems (Harris *et al.*, 2014; Dawson *et al.*, 2018). NDs and DDs are life threatening clinical conditions affecting humans worldwide (Solomon, 2019). Cases of depression are alarmingly rising because of pandemic and insecurity challenges bedeviling the globe (Dadi *et al.*, 2020). Recent reports have shown that DDs manifest in patients with other underlying medical conditions (Almeida *et al.*, 2017; Alexopoulos, 2019). A number of medical conditions, such as Parkinson's disease, seizures, and Alzheimer's disease, have been linked to depressive symptoms (Solomon, 2019; Hussain *et al.*, 2020). The unpleasant symptoms of the diseases reveal a complex pathological state that develops

in later life, when chronic inflammation and oxidative stress cause proteins to change, leading to eventual malfunction (Crocco *et al.*, 2010).

In the central nervous system (CNS), NDs and DDs are frequently restricted to particular cells, such as dopaminergic neurons in Parkinson's disease or hippocampal neurons in Alzheimer's disease (Leonelli *et al.*, 2009; Cassano *et al.*, 2017). Reports have shown that DDs linked to NDs can conveniently be studied by targeting active structures within the CNS (Cai *et al.*, 2016; Pinto-almazán *et al.*, 2022). The pathophysiology of DDs and NDs is not clearly understood, but some studies have associated malfunctioning of adrenergic neurotransmitters to increased incidence of the diseases. DDs and NDs have been shown to involve mechanisms of neuro-inflammation and aggregation/deposition of misfolded proteins, which are presumably the cause of progressive CNS diseases (Sweeney *et al.*, 2017; Hussain *et al.*, 2020).

* Corresponding author. e-mail: auwaladamu@abu.edu.ng.

Catecholamines are a class of biogenic amines that are produced from the precursor L-tyrosine. Norepinephrine (also called noradrenalin), epinephrine (also called adrenalin), dopamine, and L-dopa serve as neurotransmitters in the brain and as hormones in the muscles, respectively. It has been reported that catecholamine levels are dysregulated in illnesses such as Parkinson's disease, bronchial asthma, hypertension, and some conditions leading to heart surgery (Qureshi, 2019). L-tyrosine is primarily converted to L-noradrenalin in the sympathetic nervous system and some parts of the brain. Changes in serum catecholamine levels have recently been utilized to diagnose a number of medical problems (Goldstein *et al.*, 2018).

For ages, several Asian and African nations have used the edible plant *Moringa oleifera*, a member of the *Moringaceae* family, for both food and medicinal purpose. Potassium, calcium, phosphorus, iron, vitamins A and D, vital amino acids, antioxidants including beta-carotene, vitamin C, and flavonoids have all been shown to be abundant in this plant's leaves (Abd-alwahab, 2018). Alkaloids, tannins, phenolics, saponins, and steroids are additional antinutrients that were found (Bisong *et al.*, 2019). Zeatin, quercetin, β -sitosterol, caffeoylquinic acid, and kaempferol are abundantly and commonly found in the *Moringa* plant (Milla *et al.*, 2021). As cardiac and circulatory stimulants, they also have antitumor, antipyretic, antiepileptic, anti-inflammatory, antiulcer, antispasmodic, diuretic, antihypertensive, cholesterol-lowering, antidiabetic, hepatoprotective, antibacterial, and antifungal properties. Various parts of this plant, including the leaves, roots, seed, bark, fruit, flowers, and immature pods, are used for the treatment of various illnesses (Hodas *et al.*, 2021). It has been shown in previous studies that several parts of plants possess neuroprotective and antidepressant activities (Es-Safi *et al.*, 2021). The antidepressant activity of *M. oleifera* leaf extract was recently reported in experimental animals (Yunusa and Musa, 2018). In an effort to search for potential neuroprotective properties of *M. oleifera* root extracts, the levels of norepinephrine and epinephrine in the brain and serum of apparently healthy rats were currently examined.

2. Materials and methods

2.1. Chemicals and reagents

Every chemical and reagent utilized in this study was of the analytical grade. The following items were obtained from Sigma Aldrich: Bovine serum albumin (BSA), Copper sulphate (CuSO_4), Potassium iodide (KI), Sodium potassium tartarate (NaK-tartarate), Silver nitrate (AgNO_3), Polyvinylpyrrolidone (PVP), Sodium hydroxide (NaOH), Epinephrine, and Norepinephrine.

2.2. Collection of plant

M. oleifera's fresh roots were harvested from its native environment in Nigeria's Chikaji, Sabon-Gari, Zaria, and Kaduna. Mr. Namadi Sunusi of the Department of Biological Science at Ahmadu Bello University (A.B.U), Zaria, certified the plant's authenticity, and a voucher specimen was added to the department's herbarium (number 571). Immediately after being chopped into small pieces, the fresh roots were cleaned and dried in the shade

at room temperature (25°C). Using a mortar, the dried root was pounded into powder.

2.3. Preparation of root extracts

Exactly one hundred and fifty grams (150 g) of the fine powdered root of *M. oleifera* was weighed and transferred into a sample bottle and about 750 ml of each of the extracting solvent (water, diethyl-ether and methanol) was added separately and then allowed to stand for 48 hours. After 48 hours, the soaked *M. oleifera* powder was filtered and filtrate transferred into an evaporating dish. The filtrate on the dish was then put on a water bath at 60°C for about 35 hours until a solid extract was obtained.

2.4. Experimental animals

Forty-eight adult albino Wistar rats of either sex weighing 100-150 g were obtained from Nigeria Institute for Trypanosomiasis and Onchocerciasis Research, Kaduna, Nigeria. They were divided into 2 main groups: thirteen and thirty-five rats for the conduct of acute toxicity study and experimental study, respectively. The rats were kept at room temperature (25 °C) with 5 per cage and 12-hour light/dark cycles, as well as open access to food and water. Prior to the experiment, the rats were given three weeks to acclimatize in the animal home of the Biochemistry Department of Ahmadu Bello University Zaria.

2.5. Acute toxicity study

To assess the acute toxicity of *M. oleifera*'s aqueous root extract, Lorke's method (1983) was employed. In accordance with this, for phases one and two, thirteen rats of either sex were split into three groups of three rats each and three groups of one rat each. The last rat served as normal control. Each group in the phase one was administered different doses of 10 mg/kg body weight (b.w.), 100 mg/kg b.w., and 1000 mg/kg b.w., respectively, of *M. oleifera* aqueous root extract, but in the second phase, each group was differently administered 1600 mg/kg b.w., 2900 mg/kg b.w., and 5000 mg/kg b.w. of the of the plant aqueous root extract, respectively. The behavior and potential for mortality were tracked and observed for 24 hours in each phase. The formula below was used to calculate median lethal dose (LD_{50}) of the aqueous root extract of *M. oleifera*.

$$\text{LD}_{50} = \sqrt{(D_0 \times D_{100})}$$

Where D_0 represents the highest dosage from phase one that didn't cause mortality,

D_{100} represents the lowest dose from phase two that caused mortality.

Accordingly, safety margin of the aqueous, methanol and diethyl-ether root extracts of *M. oleifera* was decided to be any value close or equal to 0.1 of their LD_{50} s.

2.6. Animal groupings

Thirty-five Wistar rats that appeared to be in good health were split into seven subgroups of five rats each. For ten days, the first subgroup—which acted as the normal control (NC)—received food and distilled water at their leisure. Two subgroups separately received low and high doses from *M. oleifera*'s aqueous root extract (AL and AH) as 100 and 200 mg/kg rat b.w., while two further subgroups separately received low and high doses from *M. oleifera*'s methanol root extract (ML and MH) as 100 and

200 mg/kg rat b.w. The last two subgroups separately received low and high doses from *M. oleifera*'s diethyl-ether root extract (DL and DH) as 100 and 200 mg/kg rat b.w. The extracts were administered orally to animals in all groups for an experimental period of ten days using syringe and cannula.

2.7. Sample collection

Animals of all groups were sacrificed by anaesthetizing them with chloroform on the eleventh day of the experiment. Separate blood samples were taken from rats' tail veins, transferred into clean, dry and plain tubes, allowed to clot for around 30 minutes, then spun at 3000 rpm for 10 minutes to separate sera. After excision of whole brain samples from rats, exactly 0.08 g of each brain tissue was homogenized in 5ml HCl-butanol, spun at 3000 rpm for 10 minutes. 1 ml of resulting supernatant was transferred into a centrifuge containing 2 ml of heptane and 0.3 ml of 0.1 M HCl. Following vigorous shaking for 10 minutes, each tube was spun at 3000 rpm for 10 minutes, giving rise to two phases (organic and aqueous phases), the organic phase was thrown off while the aqueous phase served as sample for catecholamine assay.

2.8. Spectrophotometric determination of total protein

The Biuret method, created by Gornall *et al.* (1949) was used to measure the amount of total protein in serum and brain homogenate. The working standard, 5 mg/ml BSA, was transferred in exactly 0.0, 0.2, 0.4, 0.6, 0.8, and 1 ml increments into five test tubes with labels. A test tube was filled with one milliliter (1 ml) of the serum or brain homogenate (unknown). Each test tube's capacity was adjusted to 1 ml, and a 1 ml tube filled with distilled water served as the blank. The test tubes, including the blank and unknown, received four milliliters (4 ml) of Biuret reagent. Shaking and 30 minutes of heat at 37°C were used to combine the contents of the tubes. The resultant mixes were cooled to room temperature and their absorbance was measured at 540 nm in comparison to a blank. Standard curve was plotted, and concentrations of total protein in either the serum or brain homogenates were calculated from the curves.

2.9. Spectrophotometric determination of norepinephrine and epinephrine

Hormozi-Nezhad *et al.* (2010) approach was used to determine the levels of norepinephrine and epinephrine. One milliliter of each of the epinephrine and norepinephrine solutions with concentrations of 0.1, 0.01, 0.001, and 0.0001 mg/ml, as well as one milliliter each of water, serum, or brain homogenate, were placed individually into two sets of five test tubes with the labels blank and unknown. 1 ml, 0.7 ml, and 1 ml of 0.01 M AgNO₃, 9.09 x 10⁻⁶ M PVP, and 0.001 M NaOH, respectively, were added to each of these tubes, slowly mixed, and incubated at 37°C for 7 minutes.

After reaching room temperature, the resultant mixes were tested for absorbance at 440 nm in comparison to a blank. The concentration of epinephrine and norepinephrine in the solution was determined using standard curves for both substances.

2.10. Statistical analysis

GraphPad-Instat (v3) was used to analyze all of the data. For the purpose of comparing group means and performing statistical comparisons between groups, Tukey's test and one-way analysis of variance were used. A p-value of less than 0.05 was used to establish the statistical significance of the data, which were presented as Mean ± Standard Deviation (SD).

3. Results

3.1. Acute toxicity result of aqueous root extract of *M. oleifera*

The acute toxicity result of the aqueous root extract of *M. oleifera* is shown in Table 1. There was no record of animal mortality in the first phase, but in the second phase, all the animals of the first group "13 rats" died after acute exposure to 1600 and 5000 -mg/kg b.w. of the aqueous root extract of *M. oleifera*. The LD₅₀ was calculated as 1264.91 mg/kg b.w.

Table 1. The acute toxicity result of aqueous root extract of *M. oleifera* base on Lorke method (1983).

Phase	Group	No. of animals	Dose of extract (mg/kg)	Number of mortality recorded
One	1	3	10	0/3
	2	3	100	0/3
	3	3	1000	0/3
Two	1	1	1600	1/1
	2	1	2900	1/1
	3	1	5000	1/1

3.2. Serum and brain total protein levels

Table 2 depicts the effects of *M. oleifera* root extracts on serum and brain total protein levels. Rats that had received a high dose of *M. oleifera*'s aqueous root extract had their brain total protein levels significantly ($p < 0.05$) lowered, whereas rats which had received a low dose had their serum total protein levels significantly ($p < 0.05$) increased. The serum total protein level was not substantially affected by the two dosages of *M. oleifera*'s methanol root extract ($p > 0.05$), but the high dose significantly ($p < 0.05$) decreased the total protein level in the brains of apparently healthy Wistar rats. While the two doses of di-ethyl-ether extract of *M. oleifera* had significantly lessened serum total protein level, only high dose of the di-ethyl-ether extract was observed to cause significant ($p < 0.05$) reduction in the animals' brain total protein level.

Table 2. Effect of *M. oleifera* root extracts on serum and brain total protein levels of apparently healthy rats.

Animal Groups	Serum Total Protein (mg/ml)	Brain Total Protein (mg/ml/g)
NC	34.86 ± 3.95 ^a	4.22 ± 1.26 ^a
AH	39.00 ± 0.71 ^a	2.78 ± 0.23 ^b
AL	118.17 ± 3.53 ^c	3.15 ± 0.54 ^a
MH	32.90 ± 7.91 ^a	2.64 ± 0.59 ^b
ML	41.52 ± 5.02 ^a	3.33 ± 0.18 ^a
DH	26.82 ± 5.63 ^b	2.28 ± 0.49 ^b
DL	24.24 ± 1.83 ^b	3.52 ± 1.18 ^a

Data are expressed as mean ± SD of 5 rats. Values bearing different superscript alphabets (a – c) along the respective vertical columns are significantly different (Tukey's HSD multiple range post hoc test, $P < 0.05$). NC represents normal control group; AH represents group of rats administered 200 mg/kg b.w. *M. oleifera* aqueous root extract; AL represents group of rats administered 100 mg/kg b.w. *M. oleifera* aqueous root extract; MH represents group of rats administered 200 mg/kg b.w. *M. oleifera* methanol root extract; ML represents group of rats administered 100 mg/kg b.w. *M. oleifera* methanol root extract; DH represents group of rats administered 200 mg/kg b.w. *M. oleifera* diethyl-ether root extract, and DL represents group of rats administered 100 mg/kg b.w. *M. oleifera* diethyl-ether root extract.

3.3. Serum and brain epinephrine levels

The effects of several *M. oleifera* root extracts on epinephrine levels in the serum and brain are shown in Table 3. Rats' serum levels of epinephrine were significantly ($p < 0.05$) raised by the high dose of *M. oleifera* aqueous root extract, while their brain levels were not significantly ($p > 0.05$) affected. Both the high and low doses of *M. oleifera* methanol root extract that were given to rats which appeared to be in good health did not significantly ($p > 0.05$) change the levels of epinephrine in their serum and brains. Similar to this, both high and low doses of *M. oleifera*'s diethyl-ether root extract did not significantly ($p > 0.05$) change the amount of epinephrine in the rats' serum, but they did significantly ($p < 0.05$) raise it in their brains.

Table 3. Effect of *M. oleifera* root extracts on serum and brain epinephrine levels of apparently healthy rats.

Animal Groups	Serum Epinephrine (mg/ml)	Brain Epinephrine (mg/ml/g)
NC	1.13 ± 0.05 ^a	0.89 ± 0.14 ^a
AH	2.02 ± 0.17 ^b	1.18 ± 0.23 ^a
AL	1.47 ± 0.25 ^a	1.12 ± 0.08 ^a
MH	1.74 ± 0.48 ^a	1.13 ± 0.08 ^a
ML	1.89 ± 0.56 ^a	1.01 ± 0.14 ^a
DH	1.43 ± 0.23 ^a	2.30 ± 0.48 ^b
DL	1.79 ± 0.79 ^a	2.34 ± 0.18 ^b

Data are expressed as mean ± SD of 5 rats. Values bearing different superscript alphabets (a – b) along the respective vertical columns are significantly different (Tukey's HSD multiple range post hoc test, $P < 0.05$). NC represents normal control group; AH represents group of rats administered 200 mg/kg b.w. *M. oleifera* aqueous root extract; AL represents group of rats administered 100 mg/kg b.w. *M. oleifera* aqueous root extract; MH represents group of rats administered 200 mg/kg b.w. *M. oleifera* methanol root extract; ML represents group of rats administered 100 mg/kg b.w. *M. oleifera* methanol root extract; DH represents group of rats administered 200 mg/kg b.w. *M. oleifera* diethyl-ether root extract, and DL represents group of rats administered 100 mg/kg b.w. *M. oleifera* diethyl-ether root extract.

3.4. Serum and brain norepinephrine levels

Table 4 depicts how various *M. oleifera* root extracts affected the levels of norepinephrine in the serum and the brain. Norepinephrine levels in serum and brain of apparently healthy Wistar rats were not significantly ($p > 0.05$) changed by the issuance of aqueous and methanol root extracts of *M. oleifera*. Similar to this, the two doses of *M. oleifera* diethyl-ether root extract did not significantly ($p > 0.05$) modify the serum norepinephrine level, but they did significantly ($p < 0.05$) increase the norepinephrine level in the rats' brains.

Table 4. Effect of *M. oleifera* root extracts on serum and brain norepinephrine levels of apparently healthy rats.

Animal Groups	Serum Norepinephrine (mg/ml)	Brain Norepinephrine (mg/ml/g)
NC	0.049 ± 0.002 ^a	0.039 ± 0.010 ^a
AH	0.075 ± 0.027 ^a	0.051 ± 0.010 ^a
AL	0.053 ± 0.038 ^a	0.049 ± 0.003 ^a
MH	0.076 ± 0.021 ^a	0.049 ± 0.004 ^a
ML	0.072 ± 0.030 ^a	0.044 ± 0.005 ^a
DH	0.062 ± 0.010 ^a	0.100 ± 0.021 ^b
DL	0.078 ± 0.019 ^a	0.102 ± 0.010 ^b

Data are expressed as mean ± SD of 5 rats. Values bearing different superscript alphabets (a – b) along the respective vertical columns are significantly different (Tukey's HSD multiple range post hoc test, $P < 0.05$). NC represents normal control group; AH represents group of rats administered 200 mg/kg b.w. *M. oleifera* aqueous root extract; AL represents group of rats administered 100 mg/kg b.w. *M. oleifera* aqueous root extract; MH represents group of rats administered 200 mg/kg b.w. *M. oleifera* methanol root extract; ML represents group of rats administered 100 mg/kg b.w. *M. oleifera* methanol root extract; DH represents group of rats administered 200 mg/kg b.w. *M. oleifera* diethyl-ether root extract, and DL represents group of rats administered 100 mg/kg b.w. *M. oleifera* diethyl-ether root extract.

4. Discussion

Mental disorders including depression and anxiety have been partly associated with loneliness, social media use, and insecurity challenges (Escobar-Viera *et al.*, 2018; Okruszek *et al.*, 2020). Hence, these disorders are not only common amongst diseased subjects but can be observed in some apparently healthy individuals. Recent reports have revealed rising cases of depression and other mental disabilities around the globe (Lim *et al.*, 2018; Dadi *et al.*, 2020); there is therefore an urgent need to search for safe, effective, and affordable psychotherapies. Several studies have examined the tissue-protection and psychotherapeutic potentials of plants preparations (Cai *et al.*, 2016; Es-Safi *et al.*, 2021). In fact, Hegazy *et al.* (2020) have recently reported the nephro-protective ability of *M. oleifera* seed preparation. Thus, in a bid to extend the search for plant-based remedy against mental disorders, the ability of *M. oleifera* root extracts to alter catecholamines levels in apparently healthy rats was investigated where different root extracts of *M. oleifera* dose dependently lessened brain total protein level while diethyl-ether root extract of the plant elevated norepinephrine and epinephrine levels. The findings from the present study inform the need to replicate same study in an established animal depressed model. Since the present study was not gender specific, the

impact of reproductive hormones on the changes in catecholamine levels was not investigated. In this context, Hegazy *et al.* (2018) have reported the potential influence of sex hormones in vitamin E protection of hepatic injury.

The safeness of different plant parts must be established prior to consumption by experimental animals. This is in view of the reports that certain herbs possess the ability to cause toxicity *in vivo* (Vengal Rao *et al.*, 2018). In the present study, only LD₅₀ of aqueous root extract of *M. oleifera* was determined, and the result was suggestive of a high toxicity at 1264.91 mg/kg b.w. Previously, Bisong *et al.* (2019) and Kadam and Gaykar (2017) reported the LD₅₀s of methanol- and -diethyl-ether root extracts of *M. oleifera* to be greater than 5000 mg/kg and 2000 mg/kg, respectively.

The activities of dopamine-β-hydroxylase, monoamine oxidase, phenylalanine hydroxylase, catalase, tryptophan hydroxylase-2, xanthine oxidase, L-amino acid decarboxylase, and some RNA binding proteins have been reported to change during depression and other neurodegenerative disorders (Berguig *et al.*, 2019; Ding *et al.*, 2020; Sun *et al.*, 2021). Moreover, *in vivo* administrations of excess phenylalanine and phytochemicals including chalcones, coumarins, alkaloids, and isothiocyanates were shown to competitively block L-amino decarboxylase and monoamine oxidase, respectively (Engelbrecht *et al.*, 2018; Kamal *et al.*, 2022). Thus, the observed reduction in brain total protein concentration may be attributed to down-regulation of some genes and inhibition of some enzymes by the plant-borne metabolites.

The primary neurotransmitters involved in neuro-motor control, cognition, emotion, memory processing, and endocrine regulation are catecholamines (Ranjbar-Slamloo *et al.*, 2020; Cai *et al.*, 2021). Although adrenaline is crucial to metabolic processes, especially fat and glucose metabolisms, noradrenaline is largely involved in the sympathetic control of blood pressure and flow in peripheral tissues, while both can be released in response to stress and arousal induced-stimuli (Chen *et al.*, 2019). Reports have linked reduced synthesis of neurotransmitters, oxidative stress, and abnormal ubiquitination to severity of DDs and NDs (Karim *et al.*, 2018; Menghani *et al.*, 2021). The increase in brain noradrenalin and adrenalin levels caused by the di-ethyl-ether root extract of *M. oleifera* could be linked to the presence of β-sitosterol which possibly served as an allosteric modulator of phenylalanine hydroxylase, the enzyme catalyzing the committed step in catecholamines biosynthetic pathway. Contrastingly, the aqueous and methanol root extracts of the plant could not elevate the levels of adrenalin and noradrenalin, possibly due to absence of activators for phenylalanine hydroxylase. The work of Mokler *et al.* (2019) had associated prenatal protein malnutrition to reduction in noradrenalin and dopamine levels in ventral prefrontal and infralimbic cortices of rats brains. Thus, the observed increase in noradrenalin level may have occurred following a steady concentration of phenylalanine in rats' brain after administration of the di-ethyl-ether root extract. Berguig *et al.* (2019) reported that elevated level of phenylalanine could impair transportation of tyrosine via large amino transporter 1 of the brain, competitively inhibit the activity of L-amino acid decarboxylase, and increase the

biosynthesis of phenethylamine as well as cause a decrease in the synthesis of noradrenalin. It can thus be suggested that the diethyl-ether extract of the plant raised brain noradrenalin level of apparently healthy rats because of the absence of inhibition of L-amino acid decarboxylase by phenylalanine.

Furthermore, DDs and NDs have been reported to be managed with plants possessing antioxidant activities (Asif *et al.*, 2019; Cai *et al.*, 2021). Given the established phytochemical contents of *M. oleifera* (Hodas *et al.*, 2019), it could be possible to link the neurotransmitter-enhancement function of the plant via antioxidative mechanism. Bioactive compounds such as alkaloids and flavonoids have been recently reported to confer neuroprotective effect, and these compounds were hugely traced to the extracts of the plant (Abdel-Rahman *et al.*, 2019), suggesting that the root extracts could truly be neuroprotective by raising catecholamine levels in brain.

5. Conclusion

The present study reveals that di-ethyl-ether root extract of *M. oleifera* can dose dependently alter norepinephrine and epinephrine levels in brain and serum of apparently healthy rats, which suggests a possibility of the extract to confer protection against depressive and neurodegenerative symptoms in animals.

Acknowledgements

We thank the Head of the Biochemistry Department at Ahmadu Bello University Zaria for providing us with a workbench and some chemicals.

Ethical consent

The consent of Ahmadu Bello University Zaria Ethics Committee on Animal Use and Care was sought before commencement of the study. Approval was granted with the following number: ABUCAUC/2022/066.

References

- Abd-alwahab WIA. 2018. Identifying and study of some of phytochemical compounds and anti-jaundice activity for powder of leaves and seeds of *Moringa oleifera* in male albino rats. *Tikrit J Pure Sci.*, **23**(9): 1813–1662.
- Abdel-Rahman MA, Metwally MM, Khalil M, Salem SR and Ali HA. 2019. *Moringa oleifera* extract attenuates the CoCl₂ induced hypoxia of rat's brain: expression pattern of HIF-1α, NF-κB, MAO and EPO. *Biomed Pharmacother.*, (2019)109: 1688–1697.
- Alexopoulos GS. 2019. Mechanisms and treatment of late-life depression. *Transl Psychiatry*, **9**(188): 1-16.
- Almeida OP, Hankey GJ, Yeap BB, Gollidge J and Flicker L. 2017. Depression as a modifiable factor to decrease the risk of dementia. *Transl Psychiatry*, **7**(5): 1–6.
- Asif HM, Hayee A, Aslam MR, Ahmad K and Hashmi AS. 2019. Dose-dependent, antidepressant, and anxiolytic effects of a traditional medicinal plant for the management of behavioral dysfunctions in animal models. *Dose-Response*, **17**(4): 1–6.
- Berguig GY, Martin NT, Creer AY, Xie L, Zhang L, Murphy R, Pacheco G, Bullens S, Olbertz J and Weng HH. 2019. Of mice and men: plasma phenylalanine reduction in PKU corrects neurotransmitter pathways in the brain. *Mol Genet Metab.*, **128**(4): 422–430.

- Bisong SA, Ajiwhien IO, Nku CO and Uruakpa KC. 2019. Phytochemical and neurotoxicity evaluation of methanolic leaf-extract of *Moringa oleifera*. *J Phytopharm.*, **8(5)**: 210–215.
- Cai L, Wang C, Huo XK, Dong PP, Zhang BJ, Zhang HL, Huang SS, Zhang B, Yu SM, Zhong M and Ma XC. 2016. Effect of alkaloids isolated from *Phyllodium pulchellum* on monoamine levels and monoamine oxidase activity in rat brain. *Evid Based Complement Alternat Med.*, **2016**: 1–7.
- Cai Y, Xing L, Yang T, Chai R, Wang J, Bao J, Shen W, Ding S and Chen G. 2021. The neurodevelopmental role of dopaminergic signaling in neurological disorders. *Neurosci Lett.*, **741** (2021): 135540.
- Cassano T, Calcagnini S, Pace L, Marco FDe, Romano A and Gaetani S. 2017. Cannabinoid receptor 2 signaling in neurodegenerative disorders: from pathogenesis to a promising therapeutic target. *Front Neurosci.*, **11(30)**: 1–10.
- Chen J, Zhang C, Wu Y and Zhang D. 2019. Association between hypertension and the risk of parkinson's disease: a meta-analysis of analytical studies. *Neuroepidemiology*, **26021(38)**: 181–192.
- Crocco EA, Castro K and Loewenstein DA. 2010. How late-life depression affects cognition: Neural mechanisms. *Curr Psychiatry Rep.*, **12(1)**: 34–38.
- Dadi AF, Wolde HF, Baraki AG and Akalu TY. 2020. Epidemiology of antenatal depression in Africa: A systematic review and meta-analysis. *BMC Pregnancy Childbirth*, **20(1)**: 1–13.
- Dawson TM, Golde TE and Lagier-tourenne C. 2018. Animal models of neurodegenerative diseases. *Nat. Neurosci.* **2018**: 1–10.
- Ding Q, Tian Y, Wang X, Li P, Su D, Wu C, Zhang W and Tang B. 2020. Oxidative damage of tryptophan hydroxylase-2 mediated by peroxisomal superoxide anion radical in brains of mouse with depression. *J Am Chem Soc.*, **142(49)**: 20735–20743.
- Engelbrecht I, Petzer JP and Petzer A. 2018. Nitrocatechol derivatives of chalcone as inhibitors of monoamine oxidase and catechol-o-methyltransferase. *Cent Nerv Syst Agents Med Chem.*, **18(2)**: 115–127.
- Escobar-Viera CG, Shensa A, Bowman ND, Sidani JE, Knight J, James AE and Primack BA. 2018. Passive and active social media use and depressive symptoms among United States adults. *Cyberpsychology, Behav Soc Netw.*, **21(7)**: 437–443.
- Es-Safi I, Mechchate H, Amaghnoije A, Elbouzidi A, Bouhrim M, Bencheikh N, Hano C and Bousta D. 2021. Assessment of antidepressant-like, anxiolytic effects and impact on memory of *Pimpinella anisum* L. total extract on swiss albino mice. *Plants*, **10(8)**: 1–16.
- Goldstein DS and Kopin IJ. 2018. Linking stress, catecholamine autotoxicity, and allostatic load with neurodegenerative diseases: a focused review in memory of Richard Kvetnansky. *Cell Mol Neurobiol.*, **38(1)**: 13–24.
- Gornall AG, Bardawill CJ and David MM. 1949. Determination of serum proteins by means of the biuret reaction. *J Biol Chem.*, **177(2)**: 751–766.
- Harris KD, Weiss M and Zahavi A. 2014. Why are neurotransmitters neurotoxic? An evolutionary perspective. *F1000Research*, **179(3)**: 1–10.
- Hegazy AA, Ahmed MM, Shehata MA and Abdelfattah MM. 2018. Changes in rats' liver structure induced by zinc oxide nanoparticles and the possible protective role of vitamin E. *IJHA*, **1(3)**: 1–16.
- Hegazy AA, Abd Al Hameed EA, El-Wafacy DI and Khorshed OA. 2020. Potential role of *Moringa oleifera* in alleviating paracetamol-induced nephrotoxicity in rat. *Eur. J. Anat.*, **24(3)**: 179–91.
- Hodas F, Zorzenon MRT and Milani PG. 2021. *Moringa oleifera* potential as a functional food and a natural food additive: a biochemical approach. *An Acad Bras Cienc.*, **93(4)**: 1–18.
- Hormozi-Nezhad MR, Tashkhourian J and Khodaveisi J. 2010. Sensitive spectrophotometric detection of dopamine, levodopa and adrenaline using surface plasmon resonance band of silver nanoparticles. *J Iran Chem Soc.*, **7(2)**: 83–91.
- Hussain M, Kumar P, Khan S, Gordon DK and Khan S. 2020. Similarities between depression and neurodegenerative diseases: pathophysiology, challenges in diagnosis and treatment options. *Cureus*, **12(11)**: 1–8.
- Kadam AB and Gaykar BM. 2017. Assessment of acute oral toxicity of synergistic formulation extract of traditional contraceptive plants. *Int J Pharmacogn Phytochem Res.*, **9(3)**: 313–318.
- Kamal RM, Razis AFA, Sukri NSM, Perimal EK, Ahmad H, Patrick R, Djedaini-Pilard F, Mazzon E and Rigaud S. 2022. Beneficial health effects of glucosinolates-derived isothiocyanates on cardiovascular and neurodegenerative diseases. *Molecules*, **27(3)**: 1–49.
- Karim N, Abdelhalim H, Gavande N, Khan I and Khan H. 2018. Natural products as an emerging therapeutic alternative in the treatment of neurological disorders. *Evidence-based Complement Altern Med.*, **2018**: 10–12.
- Leonelli M, Torráo AS and Britto LRG. 2009. Unconventional neurotransmitters, neurodegeneration and neuroprotection. *Brazilian J Med Biol Res.*, **42(1)**: 68–75.
- Lim GY, Tam WW, Lu Y, Ho CS, Zhang MW and Ho RC. 2018. Prevalence of depression in the community from 30 countries between 1994 and 2014 /692/699/476/1414 /692/499 article. *Sci Rep.*, **8(1)**: 1–10.
- Lorke D. 1983. A new approach to practical acute toxicity testing. *Arch Toxicol.*, **54(4)**: 275–287.
- Menghani YR, Bhattad DM, Chandak KK, Taksande JR and Umekar MJ. A review: pharmacological and herbal remedies in the management of neurodegenerative disorder (Alzheimer's). *Int J Pharmacogn Life Sci.*, **2(1)**: 18–27.
- Milla PG, Peñalver R and Nieto G. 2021. Health benefits of uses and applications of moringa oleifera in bakery products. *Plants*, **10(2)**: 1–17.
- Mokler DJ, McGaughy JA, Bass D, Morgane PJ, Rosene DL, Amaral AC, Rushmore RJ and Galler JR. 2019. Prenatal protein malnutrition leads to hemispheric differences in the extracellular concentrations of norepinephrine, dopamine and serotonin in the medial prefrontal cortex of adult rats. *Front Neurosci.*, **2019(13)**: 1–11.
- Okruszek Ł, Aniszewska-Stańczuk A, Piejka A, Wiśniewska M and Żurek K. 2020. Safe but lonely? loneliness, anxiety, and depression symptoms and COVID-19. *Front Psychol.*, **11**: 1–11.
- Pinto-almazán R, Farfán-garcía ED and Morales-gonzález JA. 2022. Polyphenols as potential enhancers of stem cell therapy against neurodegeneration. *NEURAL Regen Res.*, **17(10)**: 2093–2101.
- Qureshi HJ. 2019. Role of Neurotransmitters in The Human Body. *JAMDC*, **01(03)**: 117–120.
- Ranjbar-Slamloo Y and Fazlali Z. 2020. Dopamine and noradrenaline in the brain; overlapping or dissociate functions? *Front Mol Neurosci.*, **2020(12)**: 1–8.
- Solomon CG. 2019. Depression in the primary care setting. *N Engl J Med.*, **380(6)**: 559–568.
- Sun Z, Bo Q, Mao Z, Li F, He F, Pao C, Li W, He Y, Ma X and Wang C. 2021. Reduced plasma dopamine-β-hydroxylase activity is associated with the severity of bipolar disorder: a pilot study. *Front Psychiatry*. **2021** (12): 1–10.
- Sweeney P, Park H, Baumann M, Dunlop J, Frydman J, Kopito R, McCampbell A, Leblanc G, Venkateswaran A, Nurmi A and Hodgson R. 2017. Protein misfolding in neurodegenerative diseases: implications and strategies. *Transl Neurodegener.*, **6(6)**: 1–13.
- Vengal Rao P, Krishnamurthy PT, Dahapal SP and Chinthamaneni PK. 2018. An updated review on "Miracle tree": *Moringa oleifera*. *Res J Pharmacogn Phytochem.*, **10(1)**: 101.
- Yunusa S and Musa A. 2018. Evaluation of antidepressant effect of ethanol extract and chloroform fraction of *Moringa oleifera* Lam. (*Moringaceae*) leaf in mice. *J Drug Res Dev.*, **4(1)**: 1–6.

Carbon Footprint Calculation of Net CO₂ in Agroforestry and Agroindustry of Gayo Arabica Coffee, Indonesia

Rahmat Pramulya^{1*}, Tajuddin Bantacut², Erliza Noor², Mohamad Yani²,
Moh Zulfajrin², Yudi Setiawan², Heru Bagus Pulunggono², Sudrajat Sudrajat²,
Olga Anne³, Shazma Anwar⁴, Praptiningsih Gamawati Adinurani⁵, Kiman Siregar^{6,7},
Hendro Prasetyo⁸, Soni Sisbudi Harsono⁹, Elida Novita⁹, Devi Maulida Rahmah¹⁰,
Nguyen Ngoc Huu¹¹, Devi Agustia¹, and Maya Indra Rasyid¹

¹Teuku Umar University, Meulaboh 23681, Indonesia; ²Institut Pertanian Bogor University, Bogor 16680, Indonesia; ³Klaipėda University, 92294 Klaipėda, Lithuania, EU; ⁴University of Agriculture Peshawar, 25130 Khyber Pakhtunkhwa, Pakistan; ⁵Merdeka University of Madiun, Madiun 63133, Indonesia; ⁶Syah Kuala University, Banda Aceh 23111, Indonesia; ⁷Indonesian Life Cycle Assessment Network (ILCAN), Serpong Tangerang, 15314, Indonesia; ⁸Brawijaya University, Malang 65145, Indonesia; ⁹Jember University, Jember 68121, Indonesia; ¹⁰Padjadjaran University, Sumedang 45363, Indonesia; ¹¹University of Tay Nguyen, 63100 Buon Ma Thuot City, Dak Lak Province, Vietnam

Received: Dec 25, 2022; Revised: Apr 1, 2023; Accepted Apr 2, 2023

Abstract

Carbon dioxide (CO₂) in the atmosphere occurs as the result of various chemical, physical, and biological processes. The presence of CO₂ around atmosphere greatly affects the agroforestry and agroindustry of coffee. This study aimed to describe the CO₂ cycle in agroforestry and agroindustry of Gayo Arabica coffee (*Coffea arabica*) and net CO₂ ha⁻¹ of coffee plantation. CO₂ cycle was analyzed based on the movement of CO₂ around the agroforestry and agroindustry of coffee. CO₂ cycle model describes net CO₂, CO₂ emission, CO₂ reduction, and CO₂ sequestration. Net CO₂ ha⁻¹ of coffee plantation was 162.75×10^{-2} t CO₂ e ha⁻¹, with CO₂ emission was 203.84×10^{-2} t CO₂ e ha⁻¹, CO₂ reduction was 3.10×10^{-2} t CO₂ e ha⁻¹, and CO₂ sequestration was 363.49×10^{-2} t CO₂ e ha⁻¹. This research formulates the calculation of equivalent carbon emissions in the arabica coffee production system in the field and primary processing, using various methods (remote sensing analysis and calculation of direct and indirect equivalent carbon emissions). The CO₂ cycle positively impacts the sustainability of agroforestry and agroindustry of Gayo Arabica coffee.

Keywords: Climate change, Environmentally-friendly, Global warming, Green coffee industry, Greenhouse gases, Life cycle assessment, Life cycle thinking, Waste utilization

1. Introduction

Coffee is one of the most important agricultural commodities commercialized worldwide (Sachs *et al.*, 2019), supplied by approximately 25×10^6 farmers living in around 50 developing countries (ICO, 2022). Drinking coffee, particularly arabica coffee (*Coffea arabica* L.), is considered a lifestyle thanks to its distinct and unique sensory characteristics while serving as beverage (Cheng *et al.*, 2016). Meanwhile, its waste materials (*e.g.*, pulp, husk, silver skin, and parchment) can also potentially be recycled to produce value-added products (Damat *et al.*, 2019; Reichembach and de Oliveira Petkowicz, 2020; Serna-Jiménez *et al.*, 2022; Setyobudi *et al.*, 2018, 2019).

Arabica coffee production is based on primary processing methods (Sanz-Urbe *et al.*, 2017). Farmers' reasons for developing plantation types and processing methods follow the availability of production factors and value chain institutions (*e.g.*, certification). Coffee production from major producing countries such as Brazil

and Vietnam applies intensive coffee cultivation without other vegetation and post-harvest using agricultural mechanization. This system contrasts with Indonesia and other countries in the neotropical region, such as Mexico, Guatemala, and Costa Rica. In the latter countries, coffee production is based on various plantation models, *e.g.*, semi-intensive and agroforestry. The complexity of the production model of the agricultural sector causes the assessment of sustainability and environmental performance to have opportunities to develop measurement and assessment methods.

Currently, the priority of sustainable agriculture is essential due to the challenges ahead, where consumers are likely to demand coffee beans produced with sustainability principles (Bockel and Schiettecatte, 2018). From 2008 to 2016, conventional coffee production decreased by 8 % and certified sustainable coffee increased by 24 % (Voora *et al.*, 2019). Sustainable agriculture in coffee production uses Weil's terminology (Abbasi *et al.*, 2014; Sudrajat, 2019; Weil, 1990) as agriculture that maintains the quality of the garden and landscape environment and is based on available resources. Sustainable agriculture has economic viability, and provides welfare for farmers and society as a

*Corresponding author. e-mail: rahmatpramulya@utu.ac.id

whole. Hence, sustainable studies require a holistic approach, using and integrating knowledge-action-methods that become solutions to problems (Sala *et al.*, 2013). One agricultural model promoted based on a comprehensive study of ecosystem services in the coffee plantation landscape is agroforestry.

The agroforestry model of arabica coffee production as compared with monoculture coffee has many ecological benefits. The advantages involve providing ecosystem services and maintaining biodiversity (Sala *et al.*, 2013), storing carbon in coffee biomass and shading plants (Negash *et al.*, 2013), increasing soil carbon stocks (Tumwebaze *et al.*, 2016), and supplying plant nutrients through mineralization (Sauvadet *et al.*, 2019) and N fixation (Munroe and Isaac, 2014). The study of bee-pollination ecosystem services on coffee plants mentions the economic value range of (USD 16.5 to USD 129.6) ha⁻¹ of coffee plantation based on pollination value modeling (Bravo-Monroy *et al.*, 2015). However, many coffee bean products are traded in accordance with environmentally friendly coffee standards. Calculation of the carbon footprint indicates the source of GHG emissions from several activities, namely chemicals used on plantations, fossil fuels used on plantations and primary and secondary processing, fossil fuels used on transportation, and electricity used.

Hotspots that impacted the environment (midpoint and endpoint) are determined based on potential global warming indicators. The parameter used is CO₂ e (carbon dioxide equivalent) (BSI, 2011). The first step in the carbon emissions study of coffee was to calculate the carbon footprint of the entire activity (Motta, 2022). Carbon footprint indicators were used to compare the production models between organic and conventional cultivation (Trinh *et al.*, 2020), variations in carbon stock and plantation management in coffee agroforestry (van Rikxoort *et al.*, 2014), and productivity level of coffee grounds (Maina *et al.*, 2015). Calculating the carbon footprint has different assessment results and depends on the evaluated production model.

Carbon footprint studies are based on life cycle thinking (LCT). LCT provides benefits and calculates the trade-offs of all activities throughout the life cycle of products and services and then identifies opportunities for environmental improvement in each activity (Nazir, 2017). Therefore, the studies of carbon footprint can be expanded to include multidisciplinary considerations (ecological and socio-economic) and interdisciplinary considerations (engineering and environmental) for agricultural sustainability purposes (Henriksson *et al.*, 2015).

Several studies of coffee production's carbon footprint include agroforestry's potential to mitigate climate change (van Rikxoort *et al.*, 2014). Agroforestry of coffee has the potential for carbon sequestration (Goodall *et al.*, 2015) and provides socio-economic advantages from wood and fruit plants (Pinoargote *et al.*, 2016). Harsono *et al.* (2021) utilize energy balance and green house gas emission calculation and found the potential measures to replacing

gasoline with biofuel, utilising liquid waste with chemical processing, and solid wastes (briquettes and bio-pellets) of coffee production for renewable energy. Another study evaluated the net balance of GHG by including agroforestry potential in N mineralization and N fixation (Hergouale'h *et al.*, 2012). Bockel and Schiettecatte (2018) review the LCA method and the calculation of carbon footprints in the production models of various coffee in producer countries and then formulate a calculation of carbon footprint in agricultural production based on carbon balance. The development of knowledge and modeling of the carbon cycle is required to calculate the carbon footprint in controlling agricultural activities under climate change mitigation.

The most significant Arabica coffee production in Indonesia comes from Aceh Province of Indonesia. The province reportedly had moderate to low environmental conditions compared to other provinces in Indonesia (Hariyanti *et al.*, 2021). Gayo arabica coffee is known as Sumatran coffee. This type of coffee has a geographical indication certificate from the Indonesian government in 2008 (Damayanti and Setiadi, 2019) and received geographical indication recognition from the European Union in 2021 as an agricultural commodity from a specific geographical area – Gayo highlands and major river basins in Aceh province 3°45'0" to 4°59'0" North latitude and 96°16'10" to 97°55'10" East longitude (Ellyanti *et al.*, 2012). Gayo Arabica coffee has a unique and strong cupping character (body, aroma and flavor image of dark chocolate, clean). Gayo Arabica coffee cultivation has a shade plant of the lamtoro species [*Leucaena leucocephala* (Lam.) De Wit] and the cultivation is done organically (Siahaan *et al.*, 2023). Organic materials from primary processing waste, *i.e.* pulper and huller, are used (Setyobudi, 2022). Most farmers in cooperative organizations follow organic certification institutions and fair trade practices. Some of them become farmers who have rainforest alliance certificates. The main exports of Gayo Arabica coffee beans are to the European Union and the United States. Currently, an assessment of the carbon footprint that includes the potential for carbon sequestration of plants has not been carried out, so calculating the carbon balance per unit area (ha) is impossible. Thus, it is considered necessary to carry out a thorough calculation of the carbon balance in the form of a CO₂ balance. This study aims to describe the CO₂ cycle in agroforestry and Gayo Arabica coffee agro-industry and uses carbon footprint calculations using the reference unit of each coffee plantation area (ha).

2. Materials and Methods

2.1. Study area

This study was conducted in Gayo Highlands at Bener Meriah and Central Aceh Regency, Aceh Province, Indonesia as shown Figure 1. The study lasted for 9 mo, starting from December 2016 to August 2017.

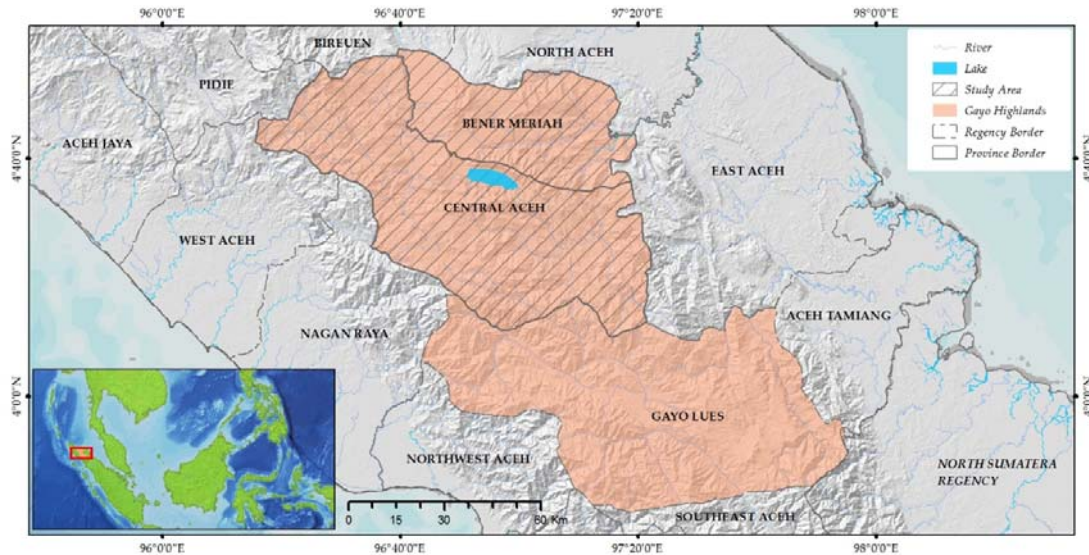


Figure 1. Location of study site

2.2. CO₂ cycle model

The CO₂ cycle explains the movement of CO₂ from various sources connecting the biosphere, atmosphere, geosphere, and hydrosphere (Grace, 2013) through photosynthesis, decomposition, respiration, and mineralization (Marchi *et al.*, 2015). Sources of CO₂ come from natural processes and human activities that are dynamic and temporal (Prentice *et al.*, 2011). Increasing the concentration of CO₂ in the atmosphere will cause an increase in the earth's surface temperature which has the potential to global warming. A controlled CO₂ cycle should be able to reduce deforestation, obtain alternative energy, and implement geo engineering (Grace, 2013).

The CO₂ cycle in this study was analyzed based on GHG's potential for storage and production (sink and sources). Calculating net CO₂ sourced from direct and indirect GHG emissions throughout coffee production activities, estimates of carbon sequestration (above and below biomass) in coffee agroforestry, and potential reduction of direct emissions through GHG conversion from waste. CO₂ is emitted from activities in plantations, transportation, primary processing, and final handling in coffee agroforestry and agroindustry cooperatives. CO₂ reduction in agroforestry and agroindustry of coffee is sourced from energy estimates from by-products. CO₂ sequestration in agroforestry and agroindustry of coffee sourced from CO₂ sequestration activities by plants.

2.3. Net CO₂

The net CO₂ analyzed is based on the net CO₂ present in the agroforestry and agroindustry of coffee [Equation (1)] as follow (Lacis *et al.*, 2010):

$$\text{Net CO}_2 = [\text{CO}_2 \text{ emissions} - \text{CO}_2 \text{ reduction} - \text{CO}_2 \text{ sequestration}] \quad (1)$$

Note:

Net CO₂: Total CO₂ who entering and leaving in the systems of agroforestry and agroindustry of coffee calculated based on CO₂ cycle.

CO₂ emissions: Total CO₂ determined from fuel and electricity used and the decomposition of organic matter.

CO₂ reduction: Total CO₂ from converting of wastewater, pulp, and parchment were producing in the agroforestry and agroindustry of coffee.

CO₂ sequestration: Total CO₂ sequestered during photosynthesis and respiration process.

The "plus" value of CO₂ accumulation in the agroforestry and agroindustry of coffee is expressed as CO₂ net.

2.3.1. CO₂ emissions

The CO₂ emissions are estimated by multiplying the amount of material by the value of the conversion factor (IPCC, 2006) in Equation (2).

$$\text{CO}_2 \text{ emissions} = [\text{M}] \times [\text{CF}] \quad (2)$$

Note:

CO₂ emissions: Total of CO₂ emissions (t CO₂ e ha⁻¹)

M: Total of materials (t C ha⁻¹)

CF: Conversion factor of materials (IPCC, 2006)

2.3.2. CO₂ reduction

CO₂ reduction is estimated by calculating the potential of electrical energy multiplied by the electric emission and conversion factors (IPCC, 2006) in Equation (3).

$$\text{CO}_2 \text{ reduction} = [\text{E}] \times [\text{EF}] \times [\text{CF}] \quad (3)$$

Note:

CO₂ reduction: Total of CO₂ reduction (t CO₂ e ha⁻¹)

E: Total electric potential from the conversion of waste (kWh)

EF: Emission factor from the production of electricity kWh⁻¹ in Indonesia = 0.867 CO₂-e

CF: Conversion factor of materials (IPCC, 2006)

2.3.3. CO₂ sequestration

CO₂ sequestration is estimated using Equation (4) (Guillaume *et al.*, 2018).

$$\text{CO}_2 \text{ sequestration} = [C_n] \times [3.67] \quad (4)$$

Note:

CO₂ sequestration: Total of CO₂ sequestration (t CO₂ e ha⁻¹)

C_n: C content per unit area (t C ha⁻¹)

3.67: The equivalent number or the conversion of element C to CO₂

3. Results and Discussion

3.1. CO₂ cycle model

In the CO₂ cycle, four main reservoirs of carbon are connected by exchange pathways. These reservoirs are the

atmosphere, the terrestrial biosphere (including freshwater systems and non-biological material such as soil carbon), the oceans (including dissolved inorganic carbon and biological and non-biological marine biota), and sediments (including fossil fuels). The movement or exchange of CO₂ between reservoirs occurs due to various chemical, physical, geological, and biological processes. The oceans contain the largest pools of activated carbon close to the earth's surface, but the slow exchange of CO₂ between the ocean and the atmosphere.

The results of these studies showed the CO₂ cycle in agroforestry and agroindustry of Gayo Arabica coffee contains several sources of CO₂. The sources include the decomposition of organic matters, coffee processing industries, coffee transportation, and CO₂ in the atmosphere, which will later be absorbed by coffee and shading plants (*L. leucocephala*) to photosynthetic and respiratory processes (Figure 2).

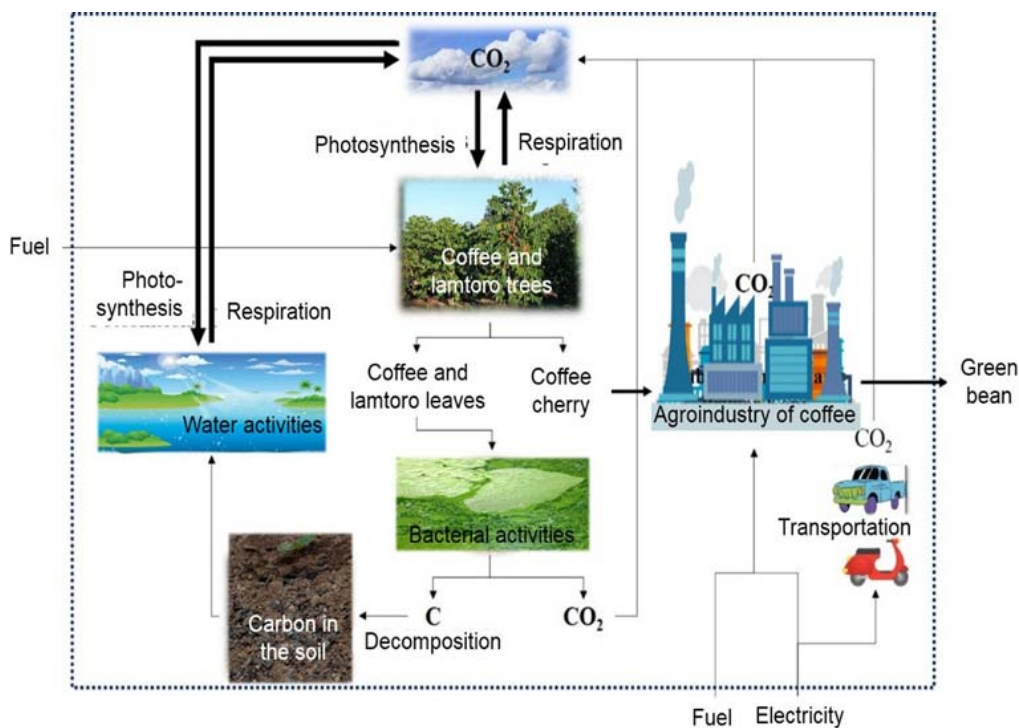


Figure 2 . CO₂ cycle in agroforestry and agroindustry of coffee

3.2. Net CO₂

Estimation of net CO₂ based on data obtained from 41 farmers; whom the cooperative members that possess 46.1 ha of agroforestry plantations in different locations in the Gayo area. The consideration factors in coffee agroforestry and agroindustry are the emitted, diminished, and sequestered CO₂ quantities. The estimated net CO₂ can be seen in Table 1.

The net CO₂ estimates based on Table 1 showed a positive CO₂ equilibrium. This indicates that the total CO₂ sequestration under coffee agroforestry was more prominent than its emissions from agroforestry and agroindustry.

Table 1. Net CO₂ in agroforestry and agroindustry of coffee

CO ₂ cycle	Amounts (t CO ₂ e ha ⁻¹)	Percentages
<u>CO₂ emissions</u>		
Atmosphere:		
(i) Land clearing activities	4.52×10^{-2}	2.22 %
(ii) Primary processing activities	20.54×10^{-2}	10.08 %
(iii) Transportation activities	0.57×10^{-2}	0.28 %
(iv) Decomposition activity	178.22×10^{-2}	87.43 %
Total of CO ₂ emission	203.84×10^{-2}	
<u>CO₂ reduction</u>		
Electrical energy production potential from:		
(i) Wastewater	1.84×10^{-2}	59.35 %
(ii) Pulps	1.25×10^{-2}	40.32 %
(iii) Parchments	0.01×10^{-2}	0.32 %
Total CO ₂ reduction	3.10×10^{-2}	
<u>CO₂ sequestration</u>		
Agroforestry of coffee:		
(i) Conversion of carbon stocks from coffee agroforestry	363.49×10^{-2}	100 %
Total of CO ₂ sequestration	363.49×10^{-2}	
Net CO ₂	162.75×10^{-2}	

CO₂ emissions are determined from emission sources that can be controlled from land clearing activities, indirect emissions from using fuel and electricity in primary processing and transportation machines, and indirect emissions that occur on-site. Oppositely, it cannot be controlled by the decomposition of coffee and *L. leucocephala* leaves. The emission data for 1 kg of green beans was determined from the calculation of the carbon footprint of Gayo Arabica coffee production in 2016.

Land clearing is an activity to clear the weeds on the coffee plantation using a pruning machine with 88 % iso-octane fuel (premium fuel). Cleaning is done thrice yearly, requiring a 7 L fuel ha⁻¹. The emission factor of 1 L of premium was 2.152 kg CO₂e. Total land clearing emissions ha⁻¹ yr⁻¹ was $2.1515 \times 21 \text{ L} = 45.18 \text{ kg CO}_2 \text{ e ha}^{-1} \text{ yr}^{-1}$

Primary processing changes cherry coffee into green beans through various activities by farmers, collectors, huller owners, and cooperatives. Its activities include preparing water requirements for pulping in the plantation, using pulper and huller machines with diesel fuel, completion of green bean handling in cooperatives, disposal of waste that causes decomposition, and burning of parchment at huller facilities. The emissions from all primary processing activities were calculated from the carbon footprint of Gayo Arabica coffee production in 2016. The emissions from activities per hectare are determined from the emission value of primary processing activities multiplied by the productivity.

Emissions from each preparation of water requirements, use of pulper machines, use of huller machines, final handling in cooperatives, decomposition of wastewater and pulp, and burning of parchment were (1.3×10^{-2} , 3×10^{-3} , 10^{-3} , 2.3×10^{-2} , 12.5×10^{-2} , 14.3×10^{-2} ,

and 5×10^{-3}) kg CO₂ e kg⁻¹ green bean, respectively. Thus, the emission from the activities ha⁻¹ were (13.9, 2.98, 0.81, 23.93, 2.90, 148.70, and 12.55) kg CO₂e ha⁻¹, respectively. The total emission from primary processing was 205.35 kg CO₂e ha⁻¹ yr⁻¹.

Transportation is an activity of moving materials (coffee beans processed by pulpers and hullers) with four routes: farmers to collectors, collectors to huller owners, huller owners to collectors, and collectors to the cooperative. Transportation uses premium and diesel fuels so that it produces direct emissions. The calculation of emissions from all transportation was determined from the carbon footprint of Gayo Arabica coffee production in 2016. Emissions from each route were (10^{-3} , 10^{-3} , 10^{-3} , and 2×10^{-3}) kg CO₂e ha⁻¹, respectively. Hence, emissions from each route per ha were (1.22, 1.40, 1.22, and 1.86) kg CO₂e ha⁻¹. The total emission from kg CO₂e ha⁻¹ was 5.697 kg CO₂e ha⁻¹ yr⁻¹.

The decomposition of coffee and *L. leucocephala* leaves breaks down the organic matter from coffee and *L. leucocephala* leaves that fall on the surface of the coffee fields. The emission factor of biomass from the plantation is 0.44 kg CO₂e. The fallen coffee and *L. leucocephala* leaves were estimated to be weighed at 248.969 kg ha⁻¹ (using 75 % dry base ha⁻¹). Thus, 1 782.210 kg CO₂e ha⁻¹ yr⁻¹ were totally emitted from the decomposition of both biomass components.

Reducing energy usage in the primary process of green bean production is a challenge for green bean producers. Minimizing energy usage in the primary process of green bean production will positively impact reducing CO₂ emissions because the highest energy usage will be contributed to CO₂ emissions. Energy reduction can be made in several ways by increasing efficiency in energy usage and using the energy from waste (Harsono *et al.*, 2015; Siregar *et al.*, 2020; Setyobudi *et al.*, 2021a, 2022; Yandri *et al.*, 2021a).

The efficiency of energy usage during the primary process of green bean production can be done by optimizing energy usage. All its stages depend primarily on energy. Therefore, optimization of energy usage can be carried out at every step. Optimizing energy usage during the process can be done by: i) reducing the distribution distance, ii) reducing water usage, and iii) reducing electricity usage (Novita *et al.*, 2021; Yandri *et al.*, 2020, 2021b).

Energy production from the waste of primary green bean production is one technological innovation to improve the company's performance based on an environmental management system. Several wastes, such as pulp, wastewater, and parchment, can be used as raw materials for energy production. All mentioned wastes can be used as raw material for biogas production through anaerobic fermentation (Adinurani *et al.* 2013; Novita *et al.*, 2021; Setyobudi *et al.*, 2018, 2021b, 2022; Syarief *et al.*, 2012) and bio briquettes through pyrolysis processes (Harsono *et al.*, 2019; Tandiono and Endah, 2020; Yandri *et al.*, 2021b), which can be used directly as fuels.

Recycling coffee waste into bio briquettes and biogas has advantages and disadvantages. Bio briquette requires resources and funds to make it happen. However, bio briquettes are energy materials that can be transported to generate energy in other locations. Biogas also requires financial resources, but relatively zero in terms of

resources. However, biogas's weakness is relative energy that cannot be transported, especially small and medium-scale biogas digesters (Adinurani *et al.* 2014, 2017). The advantage of the biogas digester is that it can simultaneously handle liquid and solid coffee waste (Setyobudi, 2022).

Biogas technology is recommended because the volume of coffee processing liquid waste is more significant than solid waste (Setyobudi *et al.* 2022). With a biogas digester, a double benefit is obtained, namely obtaining renewable energy —clean energy, minimizing the release of CO₂ into the air, minimizing environmental pollution in water and soil, and producing solid and liquid organic fertilizers (Abdullah *et al.*, 2020; Setyobudi, 2022; Susanto *et al.*, 2020a). Besides being able to generate electricity, biogas energy can also be used as drying energy in the coffee bean process, as a substitute for sunlight, or as a substitute for fossil drying energy, for example, liquid propane gas (LPG).

In order to increase the quantity of biogas production and the quality of the environment, several researchers recommend the combination of the biogas digester with the latrine system for the disposal of excreta from each household (Susanto *et al.*, 2020a, 2020b; Zhou *et al.*, 2022). Further research can be applied using renewable hybrid energy, *i.e.* biogas and solar panels, such as heating/drying energy in the coffee bean process (Novianto *et al.*, 2020; Setyobudi, 2022). Through this hybrid energy, coffee agroforestry and agroindustry can maximise CO₂ reduction.

Similarly, research on sustainable coffee production requires hybrid methods, one of which is remote sensing and geospatial methodologies (Hunt *et al.*, 2020) linked to life cycle thinking systems (Bockel and Schiettecatte 2018, Pramulya *et al.*, 2022). The renewable hybrid method aims to analyse several parameters of sustainability and provide implications for improving coffee production and supply chains (Hamdan *et al.*, 2018; Pramulya *et al.*, 2021). In addition, the hybrid method addresses coffee production that is sensitive to deforestation and land expansion.

The carbon footprint calculation in this study succeeded in calculating the actual carbon emissions from Arabica coffee production activities in the farm and primary processing using the land reference unit. The use of the land reference unit is necessary to estimate the amount of carbon emissions produced on each farmer's farm. This helps to formulate mitigation strategies for each farmer. Referring to the Land-based Carbon Dioxide Removal method (Gvein *et al.* 2023), calculating carbon footprint at farm level helps to understand the choice of mitigation scenarios in local environmental and social contexts.

4. Conclusion

The CO₂ cycle in agroforestry and agroindustry of Gayo Arabica coffee contains several sources of CO₂, such as the decomposition of organic matters, coffee processing industries, coffee transportation, and CO₂ in the atmosphere, which later will be absorbed by coffee and shading plants (*L. leucocephala*) to photosynthetic and respiratory process.

When comparing with the carbon stock calculations of Solis *et al.* (2020) in two regions in Peru, the carbon

sequestration data of agroforestry coffee plantations in the Gayo highlands is lower. This is because the vegetation type of the study site is relatively small (2 to 3 species) compared to the Peruvian region (18 species). Meanwhile, there was an additional soil carbon calculation in the Peruvian research.

However, the calculation of the overall carbon footprint of the coffee production system with the restriction from farm to processing stage shows that the carbon emissions of one kilo gram of green bean in the Gayo Highlands are lower (Pramulya *et al.* 2021) than the carbon emissions of coffee produced in Costa Rica at 1.93 kg CO₂-e (Killian *et al.* 2013), Mesoamerica at (6.2 to 10.8) kg CO₂-e (van Rikxoort *et al.* 2014) and Kenya at 4 kg CO₂-e (Maina *et al.* 2015).

Estimation of net CO₂ showed that the CO₂ equilibrium is positive. This indicates that the total CO₂ emissions in coffee agroforestry and agroindustry were smaller than the total CO₂ sequestration in coffee agroforestry. Net CO₂ ha⁻¹ in the coffee plantation was 162.75×10^{-2} t CO₂ ha⁻¹, with CO₂ emission, reduction, and sequestration being $(203.84 \times 10^{-2}$, 3.10×10^{-2} , and 363.49×10^{-2}) t CO₂ ha⁻¹. The CO₂ cycle positively impacts the sustainability of agroforestry and agroindustry of Gayo Arabica coffee.

Acknowledgements

The author would like to thank Prof. Tajuddin Bantacut for discussion on deep ecology, Prof. Lilik Budi Prasetyo – Dr. Yudi Setiawan – Dr. Aryo Adhi Condro (Laboratory of Environmental Analysis and Spatial Modeling – IPB University) for facilities and discussions during paper writing, Dr. Heru Bagus Pulunggono and Moh. Zulfajrin (Soil Science and Land Resource Department – IPB University) for discussion about data analysis, Dr. Roy Hendroko Setyobudi (Universitas Muhammadiyah Malang) for constructive discussion, and Teuku Umar University for supporting the publication of the article.

References

- Abbasi N, Torkashvan AM and Rahanandeh, H. 2014. Evaluation of mushroom compost for the bio control root-knot nematode., *Int. J. Biosci.* **5**(8): 147–153.
<https://doi.org/10.12692/ijb/5.8.147-153>.
- Abdullah K, Uyun AS, Soegeng R, Suherman E, Susanto H, Setyobudi RH, Burlakovs J and Vincēviča-Gaile Z. 2020. Renewable energy technologies for economic development. *E3S Web of Conf.* **188**(00016): 1–8 (2020).
<https://doi.org/10.1051/e3sconf/202018800016>
- Adinurani PG, Liwang T, Salafudin, Nelwan LO, Sakri Y, Wahono SK and Hendroko R. 2013. The study of two stages anaerobic digestion application and suitable bio-film as an effort to improve bio-gas productivity from *Jatropha curcas* Linn capsule husk. *Energy Procedia* **32**: 84–89.
<https://doi.org/10.1016/j.egypro.2013.05.011>
- Adinurani PG, Hendroko R, Wahono SK, Sasmito A, Nelwan LO, Nindita A and Liwang T. 2014. Optimization of concentration and EM4 augmentation for improving bio-gas productivity from *Jatropha curcas* Linn. capsule husk. *Int. J. Renew. Energy Dev.*, **3**(1) : 73–78.
<https://doi.org/10.14710/ijred.3.1.73-78>
- Adinurani PG, Setyobudi RH, Wahono SK, Mel M, Nindita A, Purbajanti E, Harsono SS, Malala AR, Nelwan LO and Sasmito A. 2017. Ballast weight review of capsule husk *Jatropha curcas*

- Linn. on acid fermentation first stage in two-phase anaerobic digestion. *Proc. Pakistan Acad. Sci. B.*, **54**(1): 47–57.
- Bockel L and Schiettecatte LS. 2018. Life cycle analysis and the carbon footprint of coffee value chains Organization (FAO) of the United Nations, Italy. In: Lashermes (Ed.), **Achieving Sustainable Cultivation of Coffee, 3rd Edition**. Burleigh Dodds Science Publishing. Cambridge, Cambridgeshire, United Kingdom
- Bravo-Monroy L, Tzanopoulos J and Potts SG. 2015. Ecological and social drivers of coffee pollination in Santander, Colombia. *Agric. Ecosyst. Environ.*, **211**: 145–154. <https://doi.org/10.1016/j.agee.2015.06.007>
- [BSI] British Standard Institute. 2008. PAS 2050:2008 Specification for the assessment of the life cycle greenhouse gas emissions of goods and services. London (UK): British Standard Institute.
- Cheng B, Furtado A, Smyth HE and Henry RJ. 2016. Influence of genotype and environment on coffee quality. *Trends Food Sci Technol.*, **57**: 20–30. <https://doi.org/10.1016/j.tifs.2016.09.003>
- Damat D, Anggriani R, Setyobudi RH and Soni P. 2019. Dietary fiber and antioxidant activity of gluten-free cookies with coffee cherry flour addition. *Coffe Sci.* **14**(4):493–500.
- Damayanti T and Setiadi H. 2019. The influence of certification of Gayo coffee geographical indication against value added of coffee in Gayo highlands, Aceh. *IOP Conf. Ser.: Earth Environ. Sci.*, **338** (012028): 1–9. <https://doi.org/10.1088/1755-1315/338/1/012028>
- Ellyanti, Karim A and Basri H. 2012. Analysis of geographical indication of Gayo coffee based on spatial planning of districts. *Agrista* **16** (2): 46–61
- Goodall KE, Bacon CM and Mendez VE. 2015. Shade tree diversity, carbon sequestration, and epiphyte presence in coffee agroecosystems: A decade of smallholder management in San Ramón, Nicaragua. *Agric. Ecosyst. Environ.*, **199**: 200–206. <https://doi.org/10.1016/j.agee.2014.09.002>
- Grace J. 2013. Carbon cycle. In: Levin SA (Ed.). **Encyclopedia of Biodiversity (Second Edition)**. Academic Press, Amsterdam.
- Guillaume T, Kotowska M.M, Hertel D, Knohl A, Krashevskaya V, Murtillaksono K, Stefan Scheu S and Kuzyakov Y. 2018. Carbon costs and benefits of Indonesian rainforest conversion to plantations. *Nat Commun* **9**. <https://doi.org/10.1038/s41467-018-04755-y>
- Gvein MH, Hu X, Næss JS, Watanabe MD, Cavalett O, Malbranque M, Kindermann G and Cherubini F. 2023. Potential of land-based climate change mitigation strategies on abandoned cropland. *Commun. Earth Environ.*, **4**(39):1–16. <https://doi.org/10.1038/s43247-023-00696-7>
- Hamdan, Fauzi A M, Rusli MS and Rustiadi E. 2019. A study of the smallholder coffee agroindustry sustainability condition using the life cycle assessment approach in Bengkulu province, Indonesia. *J. Ecol. Eng.*, **20**(6): 153–160. <https://doi.org/10.12911/22998993/108637>
- Hardjana AK. 2010. Biomass and carbon potential of forest plantation of *Acacia mangium* in HTI PT. Surya Hutani Jaya, East Kalimantan. *Jurnal Penelitian Sosial dan Ekonomi Kehutanan*, **7**(4): 237–249. <https://doi.org/10.20886/jpsek.2010.7.4.237-249>
- Harsono SS, Fauzi M, Purwono GS and Soemarno D. 2015. Second generation bioethanol from Arabica coffee waste processing at smallholder plantation in Ijen Plateau region of East Java. *Procedia Chem.*, **14**: 408–413. <https://doi.org/10.1016/j.proche.2015.03.055>
- Harsono SS, Dila R and Mel M. 2019. Coffee husk biopellet characteristics as solid fuel for combustion stove. *J Environ Sci Curr Res.*, **2**(004): 1–6.
- Harsono SS, Wibowo RKK and Supriyanto E. 2021. Energy balance and green house gas emission on smallholder Java coffee production at slopes Ijen Raung plateau of Indonesia. *J. Ecol. Eng.*, **22**(7):271–283 <https://doi.org/10.12911/22998993/138997>
- Hunt DA, Tabor K, Hewson JH, Wood MA, Reymondin L, Koenig K, Schmitt-Harsh M and Follett F. 2020. Review of remote sensing methods to map coffee production systems. *Remote Sens* **12**(2041): 1–23. <https://doi.org/10.3390/rs12122041>
- Hariyanti F, Indasari B, Syahza A, Zulkarnain and Nofrizal. 2021. Environmental disparity index (EDI): The new measurement to assess Indonesia environmental conditions for supporting sustainable development. *Jordan J. Biol. Sci.*, **14**(3): 571 – 579. <https://doi.org/10.54319/jjbs/140325>
- Henriksson PJ, Heijungs R, Dao HM, Phan LT, de Snoo GR and Guinée JB. 2015. Product carbon footprints and their uncertainties in comparative decision contexts. *PloS one*, **10**(3), e0121221. <https://doi.org/10.1371/journal.pone.0121221>
- Hergoualc'h K, Blanchart E, Skiba U, Hénault C and Harmand J-M. 2012. Changes in carbon stock and greenhouse gas balance in a coffee (*Coffea arabica*) monoculture versus an agroforestry system with *Inga densiflora*, in Costa Rica. *Agric. Ecosyst. Environ.*, **148**: 102–110. <https://doi.org/10.1016/j.agee.2011.11.018>
- ICO. [International Coffee Organization]. 2022. Historical data on the global coffee trade. International Coffee Organization. http://www.ico.org/new_historical.asp?section=Statistics. 11/22/2022.
- IPCC. [Intergovernmental Panel on Climate Change]. 2006. IPCC guidelines for national greenhouse gas inventories volume 2: Energy; chapter 3: Stationary combustion. Task Force on National Greenhouse Gas Inventories. <https://www.ipcc-nggip.iges.or.jp/public/2006gl/vol2.html>
- Lacis AA, Schmidt GA, Rind D and Ruedy RA. 2010. Atmospheric CO₂: Principal control knob governing earth's temperature. *Science*, **330**(6002): 356–359. <https://doi.org/10.1126/science.1190653>
- Maina JJ, Mutwiwa UN, Kituu GM and Githiru M. 2015. Evaluation of greenhouse gas emissions along the small-holder coffee supply chain in Kenya. *J. Sustain. Research Eng.*, **2**(4):111–120.
- Marchi M, Pulselli RM, Marchettini N, Pulselli FM and Bastianoni S. 2015. Carbon dioxide sequestration model of a vertical greenery system. *Ecol. Model.*, **306**: 46–56. <https://doi.org/10.1016/j.ecolmodel.2014.08.013>
- Motta WH. 2022. Carbon footprint as a first step towards LCA usage. In: Klos ZS, Kalkowska J and Kasprzak J. (Eds.) **Towards a Sustainable Future - Life Cycle Management**. Springer, Switzerland. pp.265–275. https://doi.org/10.1007/978-3-030-77127-0_24
- Munroe JW and Isaac ME. 2014. N₂-fixing trees and the transfer of fixed-N for sustainable agroforestry: A review. *Agron. Sustain. Dev.*, **34**(2): 417–427. <https://doi.org/10.1007/s13593-013-0190-5>
- Nazir N. 2017. Understanding life cycle thinking and its practical application to agri-food system. *Int. J. Adv. Sci. Eng. Inf. Technol.*, **7**(5):1861–1870.
- Negash M, Starr M, Kanninen M and Berhe L. 2013. Allometric equations for estimating aboveground biomass of *Coffea arabica* L. grown in the Rift Valley escarpment of Ethiopia. *Agrofor. Syst.*, **87**(4): 953–966. <https://doi.org/10.1007/s10457-013-9611-3>

- Novianto B, Abdullah K, Uyun AS, Yandri E, Nur S M, Susanto H, Vincēviča-Gaile Z, Setyobudi RH and Nurdiansyah Y. 2020. Smart micro-grid performance using renewable energy. *E3S Web of Conf.*, **188(00005)**: 1–11. <https://doi.org/10.1051/e3sconf/202018800005>
- Novita E, Khotijah, Purbasari D and Pradana HA. 2021. The application of cleaner production in Wulan coffee agroindustry Maesan sub district Bondowoso regency. *Jurnal Teknik Pertanian Lampung* **10(2)**: 263–273. <http://dx.doi.org/10.23960/jtep-l.v10.i2.263-273>
- Pinoargote M, Cerda R, Mercado L, Aguilar A, Barrios M and Somarriba E. 2016. Carbon stocks, net cash flow and family benefits from four small coffee plantation types in Nicaragua. *For. Trees Livelihoods*, **26(3)**: 183–198. <https://doi.org/10.1080/14728028.2016.1268544>
- Pramulya R. 2021. Design of agricultural system and sustainable Gayo Arabica coffee agroindustry in Aceh Province. PhD. Dissertation. Sekolah Pascasarjana, Institut Pertanian Bogor, Indonesia.
- Pramulya R, Bantacut T, Noor E, Yani M and Romli M. 2022. Life cycle assessment of Gayo Arabica coffee green bean at Aceh Province. *Habitat*, **33(03)**: 308–319. <https://doi.org/10.21776/ub.habitat.2022.033.3.29>
- Reichembach LH and de Oliveira Petkowicz CL. 2020. Extraction and characterization of a pectin from coffee (*Coffea arabica* L.) pulp with gelling properties. *Carbohydr Polym*, **245**:116473. <https://doi.org/10.1016/j.carbpol.2020.116473>
- Sachs JD, Cordes KY, Rising J, Toledano P and Maennling N. 2019. **Ensuring Economic Viability and Sustainability of Coffee Production**. Columbia Center on Sustainable Investment. Jerome Greene Hall. New York, USA.
- Sala S, Farioli F and Zamagni A. 2013. Progress in sustainability science: lessons learnt from current methodologies for sustainability assessment: Part 1. *Int. J. Life Cycle Assess.*, **18(9)**: 1653–1672. <https://doi.org/10.1007/s11367-012-0508-6>
- Sanz-Urbe JR, Yusianto, Menon SN, Peñuela A, Oliveros C, Husson J, Brando C and Rodriguez A. 2017. Postharvest processing—revealing the green bean. In: Folmer B (Ed.), **The Craft and Science of Coffee**. Academic Press, Cambridge UK. pp.51–79.
- Sauvadet M, den Meersche KV, Allinne C, Gay F, de Melo Virginio Filho E, Chauvat M, Becquer T, Tixier P and Harmand J-M. 2019. Shade trees have higher impact on soil nutrient availability and food web in organic than conventional coffee agroforestry. *Sci. Total Environ.*, **649**: 1065–1074. <https://doi.org/10.1016/j.scitotenv.2018.08.291>
- Serna-Jiménez JA, Siles JA, de los Ángeles M M and Chica AF. 2022. A review on the applications of coffee waste derived from primary processing: Strategies for revalorization. *Processes* **10(2436)**: 1–24. <https://doi.org/10.3390/pr10112436>
- Setyobudi RH, Wahono SK, Adinurani PG, Wahyudi A, Widodo W, Mel M, Nugroho YA, Prabowo B and Liwang T. 2018. Characterisation of Arabica coffee pulp – hay from Kintamani - Bali as prospective biogas feedstocks. *Matec Web of Conf.*, **164 (01039)**:1–13. <https://doi.org/10.1051/matecon/201816401039>
- Setyobudi RH, Zalazar L, Wahono SK, Widodo W, Wahyudi A, Mel M, Prabowo B, Jani Y, Nugroho YA, Liwang T and Zaebudin A. 2019. Prospect of Fe non-heme on coffee flour made from solid coffee waste: Mini review. *IOP Conf. Ser. Earth Environ. Sci.*, **293 (012035)**:1–24. <https://doi.org/10.1088/1755-1315/293/1/012035>
- Setyobudi RH, Yandri E, Atoum MFM, Nur SM, Zekker I, Idroes R, Tallei TE, Adinurani PG, Vincēviča-Gaile Z, Widodo W, Zalazar L, Van Minh N, Susanto H, Mahaswa RK, Nugroho YA, Wahono SK, and Zahriah Z. 2021a. Healthy-smart concept as standard design of kitchen waste biogas digester for urban households. *Jordan. J. Biol. Sci* **14(3)**, 613–620. <https://doi.org/10.54319/jjbs/140331>
- Setyobudi RH, Yandri E, Nugroho YA, Susanti MS, Wahono SK, Widodo W, Zalazar L, Saati EA, Maftuchah M, Atoum MFM, Massadeh MI, Yono D, Mahaswa RK, Susanto H, Damat D, Roeswitawati D, Adinurani PG and Mindarti S. 2021b. Assessment on coffee cherry flour of Mengani Arabica coffee, Bali, Indonesia as iron non-heme source. *Sarhad J. Agric.*, **37(Special Issue1)**:171–183. <https://doi.org/10.17582/journal.sja/2022.37.s1.171.183>
- Setyobudi RH, Atoum MFM, Damat D, Yandri E, Nugroho YA, Susanti MS, Wahono SK, Widodo W, Zalazar L, Wahyudi A, Saati EA, Maftuchah M, Hussain Z, Yono D, Harsono SS, Mahaswa RK, Susanto H, Adinurani PG, Ekawati I, Fauzi A and Mindarti S. 2022. Evaluation of coffee pulp waste from coffee cultivation areas in Indonesia as iron booster. *Jordan. J. Biol. Sci.*, **15(3)**: 475 – 488. <https://doi.org/10.54319/jjbs/150318>
- Setyobudi RH. 2022. Potential of coffee pulp as biogas — renewable energy and functional food source of Fe to overcome iron nutrient anemia. PhD. Dissertation University Muhammadiyah Malang, Malang, Indonesia
- Solis R, Vallejos-Torres G, Arévalo L, Marín-Díaz J, Ñique-Alvarez M, Engedal T, Bruun TB 2020. Carbon stocks and the use of shade trees in different coffee growing systems in the Peruvian Amazon. *J. Agric. Sci.* **158 (6)** : 450–460. <https://doi.org/10.1017/S002185962000074X>
- Siahaan ASA, Harahap EM, Hanum C, Karim A and Vincēviča-Gaile Z. 2023. The taste of Arabica coffee in several altitude and shading condition. *E3S Web of Conf.*, **374 (00001)**: 1–6. <https://doi.org/10.1051/e3sconf/202337400001>
- Siregar K, Machsun AL, Sholihati S, Alamsyah R, Ichwana I, Siregar NC, Syafriandi S, Sofiah I, Miharza T, Nur SM, Anne O and Setyobudi RH. 2020. Life cycle impact assessment on electricity production from biomass power plant system through life cycle assessment (LCA) method using biomass from palm oil mill in Indonesia. *E3S Web Conf.*, **188(00018)**: 1–11. <https://doi.org/10.1051/e3sconf/202018800018>
- Sudrajat IS. 2019. Sustainable farming system reviewed from perspective of Ki Hadjar Dewantara's noble teaching and Tamansiswa philosophy values. Proceedings Intercultural Collaboration Indonesia – Malaysia "Implementation of Tamansiswa Philosophy". Universitas Sarjanawiyata Tamansiswa, Yogyakarta, Indonesia. pp. 81–97.
- Susanto H., Setyobudi RH., Sugiyanto D, Nur SM, Yandri E, Herianto H, Jani Y, Wahono SK., Adinurani PG, Nurdiansyah Y and Yaro A. 2020a. Development of the biogas-energized livestock feed making machine for breeders. *E3S Web Conf.*, **188 (00010)**: 1–13. <https://doi.org/10.1051/e3sconf/202018800010>
- Susanto H , Uyun AS, Setyobudi RH, Nur SM, Yandri E, Burlakovs J, Yaro A, Abdullah K, Wahono SK, and Nugroho YA. 2020b. Development of moving equipment for fishermen's catches using the portable conveyor system. *E3S Web of Conf.* **190(00014)**: 1–10. <https://doi.org/10.1051/e3sconf/202019000014>
- Syarief R, Novita E, Noor E and Mulato S. 2012. Smallholder coffee processing design using wet technology based on clean production. *Journal of Applied Sciences in Environmental Sanitation*, **7(2)** : 93–102. <https://www.cabdirect.org/cabdirect/abstract/20133091387>

- Tandiono JL and Endah AS. 2020. The potential utilization of coffee waste of PT Javabica into bio-briquette as environmentally-friendly fuel. *Majalah Ilmiah Pengkajian Industri*. **14 (3)**: 203–210. <https://doi.org/10.29122/mipi.v14i3.4225>
- Trinh LTK, Hu AH, Lan YC and Chen ZH. 2020. Comparative life cycle assessment for conventional and organic coffee cultivation in Vietnam. *Int. J. Environ. Sci. Tech.*, **1**:1–18. <https://doi.org/10.1007/s13762-019-02539-5>
- Tumwebaze SB and Byakagaba P. 2016. Soil organic carbon stocks under coffee agroforestry system and coffee monoculture in Uganda. *Agric. Ecosyst. Environ.*, **216** : 188–193. <https://doi.org/10.1016/j.agee.2015.09.037>
- Van Rikxoort H, Schroth G, Läderach P and Rodríguez-Sánchez B. 2014. Carbon footprints and carbon stocks reveal climate-friendly coffee production. *Agron. Sustain. Dev.*, **34(4)**: 887–897. <https://doi.org/10.1007/s13593-014-0223-8>
- Voora V, Bermúdez S Larrea C and Baliño S. 2019. Global market report: Coffee. In: Baliño S (Ed.) **Sustainable Commodities Marketplace Series 2019**. The International Institute for Sustainable Development, Manitoba, Canada.
- Weil RR. 1990. Defining and using the concept of sustainable agriculture. *J. Agron. Educ.*, **19(2)**: 126–130. <https://doi.org/10.2134/jae1990.0126>
- Yandri E, Ariati R, Uyun AS, Setyobudi RH, Susanto H, Abdullah K, Wahono SK, Nugroho YA, Yaro A, and Burlakovs J. 2020. Potential energy efficiency and solar energy applications in a small industrial laundry: A practical study of energy audit *E3S Web of Conf.*, **190(00008)**: 1–9. <https://doi.org/10.1051/e3sconf/202019000008>
- Yandri E, Novianto B, Fridolini F, Setyobudi RH, Wibowo H, Wahono SK, Abdullah K, Purba W and Nugroho YA. 2021a. The technical design concept of hi-tech cook stove for urban communities using non-wood agricultural waste as fuel sources. *E3S Web of Conf.*, **226(00015)**: 1–9. <https://doi.org/10.1051/e3sconf/202122600015>
- Yandri E, Idroes R, Setyobudi RH, Rudationo CB, Wahono SK, Mahaswa RK, Burlakovs J and Susanto H. 2021b. Reducing energy and water consumption in textile dyeing industry with cleaner production by inlet-outlet modification to reuse wastewater. *Proc. Pak. Acad. Sci.: A* **58 (S)**: 49–58. [https://doi.org/10.53560/PPASA\(58-sp1\)732](https://doi.org/10.53560/PPASA(58-sp1)732)
- Zhou X, Simha P, Perez-Mercado LF, Barton MA, Lyu Y, Guo S, Nie X, Wu F and Li Z. 2022. China should focus beyond access to toilets to tap into the full potential of its rural toilet revolution. *Resour Conserv Recycl.*, **178**: 106100. <https://doi.org/10.1016/j.resconrec.2021.106100>

Immunomodulatory Effects of Unripe Sapodilla (*Manilkara zapota*) Fruit Extract Through Inflammatory Cytokine Regulation in Type 1 Diabetic Mice

Fikriya Novita Sari¹, Rizky Senna Samoedra¹, Setyaki Kevin Pratama¹, Sri Rahayu¹,
Aris Soewondo¹, Yoga Dwi Jatmiko¹, Muhammad Halim Natsir², Hideo Tsuboi³,
Muhaimin Rifa'i^{1,*}

¹Department of Biology, Faculty of Mathematics and Natural Sciences, Brawijaya University, Malang, Indonesia; ²Faculty of Animal Science, Brawijaya University, Malang, Indonesia ; ³Department of Immunology, Nagoya University, Nagoya 466-8550, Japan

Received: August 16, 2022; Revised: December 19, 2022; Accepted: December 31, 2022

Abstract

Background: One of the most prevalent metabolic disorder in the world is diabetes mellitus (DM), marked by chronic inflammation of pancreatic β -cells. To alleviate this disease, the response of the immune system can be manipulated to produce anti-inflammatory molecules. This research aims to evaluate the immunomodulatory activities of unripe sapodilla fruit (USF) extract according to the profile of TNF- α and IFN- γ that expressed from CD4 T cells, CD4⁺CD25⁺IL-10⁺, and malondialdehyde (MDA) in type 1 diabetes mellitus (T1DM). **Methods:** Unripe Sapodilla Fruit (USF) was extracted with water by maceration and freeze-drying process. Liquid Chromatography High Resolution Mass Spectrophotometry (LC-HRMS) was used to identify the phytochemical content of USF extract. Twenty-five male BALB/c mice were randomized into five groups (n=5). A single high dose (145 mg/kgBW) of streptozotocin (STZ) was administered intraperitoneally to induce T1DM. USF extract was administered orally once a day for 14 days. Blood glucose levels and body weight were assessed once every three days for 15 days. Splenic cells were immunostained with antibodies. The sample underwent a flow cytometric analysis and ANOVA was used to statistically assess all the data with p-value of ≤ 0.05 were significant. **Results:** LC-HRMS revealed that there were 12 major bioactive compounds in aqueous USF extract, which have activity of anti-diabetic, anti-inflammatory, free radical scavenging, and NF- κ B inhibitor. The results of USF administration showed that glucose levels in diabetic mice were reduced but not significant. CD4⁺TNF- α ⁺, CD4⁺IFN- γ ⁺ and MDA expression in diabetic mice decreased after USF administration. Meanwhile, CD4⁺CD25⁺IL-10⁺ expression in diabetic mice increased after USF administration. **Conclusion:** USF extract acts as an immunomodulator by regulating inflammatory cytokines in a non-dose-dependent manner. The ability to regulate inflammatory cytokines is shown by enhancing IL-10 as an anti-inflammatory cytokine to suppress TNF- α and IFN- γ . We also show a decrease in MDA expression as a result of USF's antioxidant activity, which aids in the suppression of inflammatory cytokines in diabetic mice.

Keywords: diabetes mellitus, anti-inflammatory, proinflammatory, streptozotocin, unripe sapodilla

1. Introduction

A metabolic disorder known as diabetes mellitus (DM) is marked by hyperglycemia or abnormally high blood glucose levels. Defects in insulin secretion, insulin action, or both contribute to hyperglycemia. One of the most common metabolic diseases in the world, it is constantly expanding. Based on International Diabetes Federation (IDF) data, people with DM reached 463 million in 2019 and increased to 537 million in 2021. If this condition is not properly treated, it is predicted that there would be 643 million sufferers in 2030 and 783 million persons in 2045 (IDF Diabetes Atlas, 2022).

Chronic hyperglycemia in DM patients could cause an energy metabolism disorder, early aging, and cell death. These lead to various microvascular and macrovascular complications (Cicimil *et al.*, 2018). Patients with DM,

particularly those with type 1 diabetes mellitus (T1DM), are characterized by the death of the insulin-producing pancreatic islet cells. Hyperglycemia promotes reactive oxygen species (ROS) production such as H₂O₂, O₂^{•-} and NO. The increase of ROS in T1DM is a side effect of glucose uptake control failure in muscle and fat tissue. Insufficient insulin causes intracellular glucose concentration, which accelerates glycolysis. Through the tricarboxylic acid (TCA) cycle, the rate of glycolysis contributes to the production of superoxide (O₂^{•-}) in the body (Rahangdale *et al.*, 2009). The accumulation of ROS is shown by malondialdehyde (MDA) expression. ROS will interact with polyunsaturated fatty acids that generate lipid peroxidation to produce MDA and other compounds. MDA is a reactive aldehyde produced by lipid peroxidation that acts as a warning sign that the body is under oxidative stress (Yonny *et al.*, 2016). High expression of MDA can cause cell damage and trigger

* Corresponding author. e-mail: immunobiology@ub.ac.id.

inflammation (Budiwiyono *et al.*, 2021). The increase of ROS will activate nuclear factor kappa B (NF- κ B) to trigger pro-inflammatory cytokine expression in T1DM (Fatima *et al.*, 2016). Excessive inflammation would speed up the loss of pancreatic islet cells and worsen immune cell infiltration, which would attack and cause pancreatic cell apoptosis. This mechanism is initiated by enhancing NF- κ B activation from proinflammatory cytokines induction (Szablewski, 2014). NF- κ B is a transcription factor that also targets proinflammatory cytokines such as TNF- α and IFN- γ as its target genes to amplify the inflammatory response by the body. The amplification of inflammatory response could worsen the condition of autoimmune diseases such as T1DM (Bacher and Schmitz, 2004). Proinflammatory cytokines like TNF- α and IFN- γ have been linked to cell destruction in DM patients (Karshenase, 2018). β cell destruction by immune cells is what makes DM considered to be an autoimmune disease. Hence, immunosuppressive activities are needed to maintain homeostasis within the immune system.

Regulatory T cells (T-reg) are lymphocytes known for their suppressive ability. T-reg are generally marked with CD4+CD25+ biomarkers, which modulate immune system with suppress or downregulate effector cell. T-reg are necessary because immune system suppression is critical for preserving immune system homeostasis, particularly in autoimmune disorders like DM. Treg play an immunosuppressive role by secreting IL-10 as one of the cytokine with potent anti-inflammatory properties. IL-10 can reduce the presentation of antigen and the production of proinflammatory cytokines by other immune cells (Bijjiga and Martino, 2013).

Sapodilla (*Manilkara zapota* (L.) P. Royen) comes from Sapotaceae family. It is a popular edible fruit, and it is common in tropical countries such as Indonesia, Brunei, China, India, Malaysia, Singapore, Thailand and Vietnam (Rojas-sandoval & Praci, 2017). The sapodilla fruit contains many phytochemicals with high antioxidant and anti-inflammatory activities, such as epigallocatechin, catechin, 4-o-galloylchlorogenic acid, methyl chlorogenate, chlorogenic acid, and gallic acid (Baky *et al.*, 2016). The aforementioned compounds have strong antioxidant properties, can scavenge free radicals such as H₂O₂, O₂⁻, and NO, and can also reduce lipid peroxidation. The flavonoids within the extract can also inhibit NF- κ B, which is crucial because it is the transcription factor for proinflammatory cytokines (Leelayungrayub *et al.*, 2019). In this experiment, we used unripe sapodilla fruits with higher polyphenol contents than ripe ones (Shui *et al.*, 2004). This experiment aims to assess the immunomodulatory activities of sapodilla fruit extract in controlling ROS and inflammatory cytokines production.

2. Methods

2.1. Herb extraction

Unripe sapodilla fruits with the specimen number 074/223A/102.7/2020 were collected in Nganjuk City and determined by UPT Materia Medica in Batu City, Indonesia. The extraction of unripe sapodilla fruit refers to (Tamsir *et al.*, 2020) with few modifications. Unripe sapodilla fruits (USF) were peeled and dried before

grounded until they became powder. Sapodilla powder was dissolved in distilled water at a 1:10 ratio (sapodilla:solvent, w/v) for the extraction in an Erlenmeyer flask covered with aluminum foil. The solution was mixed at 200 rpm for 24h with a magnetic stirrer. A freeze-drying method was used to remove the water after filtering the homogenate extract using Whatman filter paper.

2.2. Phytochemical content screening

The previously prepared sample was put into an autosampler, then injected into the liquid chromatography-high-resolution mass spectrometry (LC-HRMS). To determine the phytochemical composition of the USF aqueous extract, Thermo Scientific Dionex Ultimate 3,000 RSLC nano liquid chromatography (LC) and Thermo Scientific Q Exactive Mass Spectrometry (MS) was used (Thermo Fisher Scientific Inc., USA). Hypersil GOLD aQ serves as the LC instrument's stationary phase, and solvents A and B, which together make up the mobile phase, contain 0.1% formic acid in water and acetonitrile, respectively. The LC was operated at a flow rate of 40 μ L/min, a run period of 30 min, and a column temperature of 30 °C (Purwanti *et al.*, 2021). The obtained data were analyzed using MZmine with KEGG Library database. Compound was selected with PASS Online database, if compound has probability to be active (Pa) was more than 0.3, indicating that compound has anti-diabetic, anti-inflammatory, free radical-scavenging, and NF-inhibitory properties.

2.3. Experimental design

All methods in this research were reviewed and verified by the Animal Care and Use Committee of Brawijaya University with ethical approval number 016-KEP-UB-2021. Seven-week-old male BALB/c mice (n=25) were taken from Maulana Malik Ibrahim State Islamic University in Malang, Indonesia. Each mouse was maintained in a pathogen free environment in the Animal Physiology Laboratory at Brawijaya University while being fed a nutritional pellet diet and given proper water hydration. The animals were separated into five groups after acclimatization. Normal mice group (N) is the group of mice that are not injected with STZ nor given any USF treatment (n=5); diabetic mice group (DM) is the group of mice exposed to streptozotocin (STZ) without any USF treatment (n=5); while in DM treated group, mice were exposed to STZ and were given 3 doses of USF extract 150 mg/kgBW (DM-D1), 250 mg/kgBW (DM-D2), and 400 mg/kgBW (DM-D3) (n=5 for each respective dose). USF extract was given orally once daily for 14 days. Blood sugar levels and body weight were evaluated every three days for 15 days.

2.4. Induction of Diabetes Model

Mice were acclimatized for a week before the experiment. A single high dosage (SHD) of the diabetogenic agent streptozotocin (BioWorld, USA) was injected to induce T1DM. Intraperitoneal (i.p.) injections of STZ at a dose of 145 mg/kgBW were used to generate diabetic mice (Lestari *et al.*, 2022). Prior to receiving STZ injection, mice were fasted for 4 hours. STZ was freshly dissolved in citrate buffer with pH 4.5 for quick infusion within 10 minutes (Lestari *et al.*, 2022). Blood glucose levels were assessed using an Easy Touch glucometer (Biopetik Technology Inc., Taiwan) on the fourth and

seventh day after STZ injection. When the mice's blood glucose level exceeded 200 mg/dL, they were considered in T1DM condition. Previous experiment reported that T1DM in male mice BALB/c could be induced with a single high-dose injection of STZ (Adharini *et al.*, 2020).

2.5. Immunostaining and flow cytometry

The antibodies used in this study include anti-CD4 and anti-MDA conjugated FITC, the others such anti-CD25, anti-TNF- α , anti-IFN- γ , and anti-IL-10 conjugated PE (BioLegend, USA). Spleen and liver were isolated, and then homogenized with phosphate buffer saline (PBS). Spleen cells were isolated to analyze cytokine-secreting lymphocytes, while hepatocytes were isolated to obtain the MDA production. Homogenate was centrifuged at 2500 rpm and 10°C for 10 minutes. The pellet was resuspended in PBS for a second centrifugation after the supernatant from previous centrifugation was discarded. Extracellular antibodies were used to stain the cells at a concentration of 5 μ g/100 μ L (CD4 and CD25 antibody). Intracellular flow cytometry staining was carried out by using 50 μ L Cytofix™. The suspension was incubated for 20 minutes (4°C). Wash buffer solution (BioLegend, USA) was added for permeabilization. TNF, IFN, IL-10, and MDA antibodies as intracellular antibodies were used to stain the cells after centrifugation. The samples were prepared for analysis using flow cytometry (BD FACS-

Calibur, USA) by adding 400 μ L of PBS to the cuvette (Adharini *et al.*, 2020).

2.6. Statistical analysis

Statistical analysis was accomplished by SPSS 21.0 software for the ANOVA and Duncan Multiple Range tests. The probability value of 0.05 was regarded as significant between the two groups. The statistical analysis was done to analyze the blood glucose levels, CD4⁺TNF- α ⁺, CD4⁺IFN- γ ⁺, CD4⁺CD25⁺IL-10⁺, and MDA expressions. All data were shown in mean \pm standard deviation (SD).

3. Results

3.1. Phytochemical content screening of USF extract

This research identifies the bioactive compounds of unripe sapodilla fruit extract. LC-HRMS analysis revealed that there were 12 major bioactive compounds in aqueous USF extract, based on the results of the MZmine library analysis, which have biological activities including anti-diabetic, anti-inflammatory, free radical scavenger, and NF- κ B inhibitors. The compounds identified were mostly polyphenolic compounds including chlorogenic acid, caffeic acid, flavonols, luteoliflavan, ampelopsin, luteone, biflorin, catechins, and their derivatives (epicatechin, gallic catechin, leucocyanidin), then proanthocyanidins as derivatives of tannins (Figure 1).

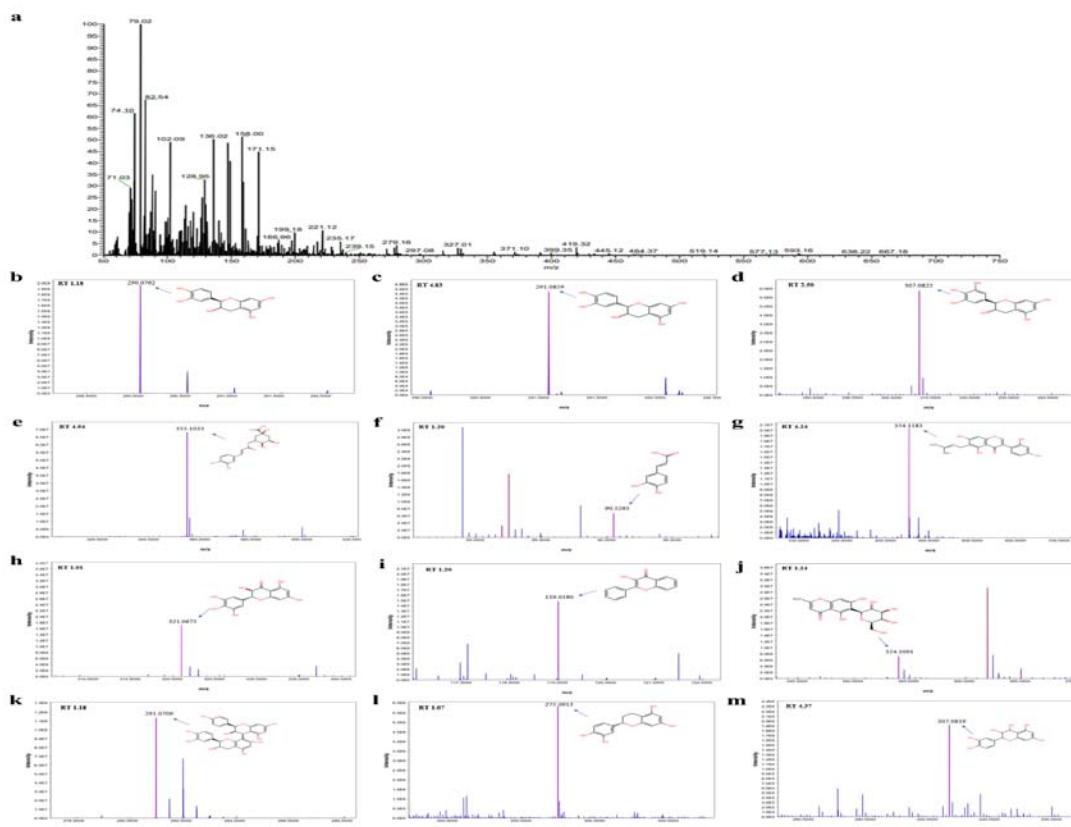


Figure 1. LC-HRMS spectrum of bioactive compounds in the aqueous extract of USF. (a) The LC-HRMS total ion chromatogram was carried out using Thermo Scientific Dionex Ultimate 3,000 RSLC nano liquid chromatography (LC) and Thermo Scientific Q Exactive Mass Spectrometry (MS). Twelve mass spectra are shown b-m. (b) catechin, (c) epicatechin, (d) gallic catechin, (e) chlorogenic acid, (f) caffeic acid, (g) luteone, (h) ampelopsin, (i) flavonol, (j) biflorin, (k) proanthocyanidin, (l) luteoliflavan, and (m) leucocyanidin.

3.2. USF treatment has effect as anti-diabetic in diabetic mice

The glucose level of diabetic mice (DM, DM-D1, DM-D2, DM-D3) was 386 mg/dL in the first measurement, and the glucose level in DM group mice was increased to 432 mg/dL after 15 days (Figure 2). The glucose level in the normal mice group (N) was constantly lower than all groups in 15 days, around 138-154 mg/dL, and greatly lower than DM mice group ($p < 0.05$). The administration of USF extract has given an anti-hyperglycemic effect in diabetic mice, as shown by the decrease in glucose level after treatment of 14 days. USF treatment had successfully

decreased glucose levels in DM-D1 and DM-D3 group compared to the diabetic control group (DM). However, the glucose levels of DM-D1 and DM-D3 group were still significantly higher than normal group. The DM-D2 mice group's blood glucose level did not differ significantly from that of the normal and DM mice group. This means that USF extract treatment in DM-D2 has a higher anti-hyperglycemic effect than other treated groups. Despite the fact that the value had not yet reached the normal level, the final glucose level in the USF treatment group (DM-D1, DM-D2, DM-D3) was lower.

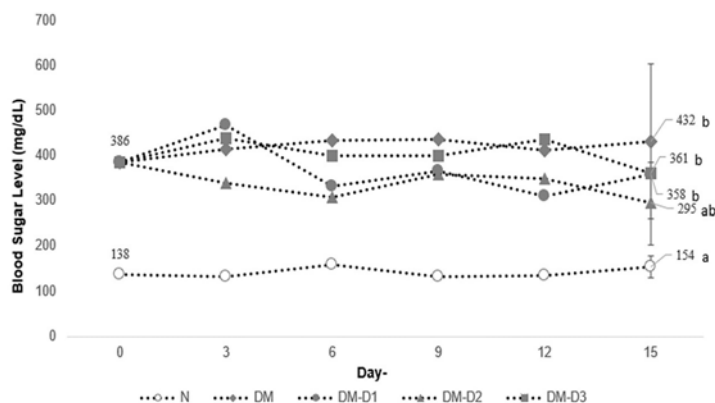


Figure 2. The administration of USF extract has given an anti-diabetic effect, as shown at the decreased blood glucose levels after 14 days of treatment.

3.3. MDA expression levels in diabetic mice are decreased after USF treatment

The expression levels of free radicals in diabetic mice are shown by the MDA expression level (Figure 3). The MDA expression level in the DM mice group increased from 23.65% to 40.87% ($p < 0.05$) compared to the N group. The administration of USF extract has given an antioxidant effect in DM-treated mice groups, as shown by the decrease of MDA expression in each treatment group after 14 days. All groups of USF treated mice had

significant lower level of MDA ($p < 0.05$) with value of 21.75%, 30.81%, 34.14% in DM-D1, DM-D2, and DM-D3, respectively. Among these three groups, DM-D1 was the most effective dosage to reduce MDA level. When compared to the normal mice group, the MDA expression level on DM-D1 treated group was still higher but not significant. However, the two others, DM-D2 and DM-D3 groups were significantly higher. These results implied that USF extract had an antioxidant effect in diabetic mice, and DM-D1 treatment has the highest antioxidant effect.

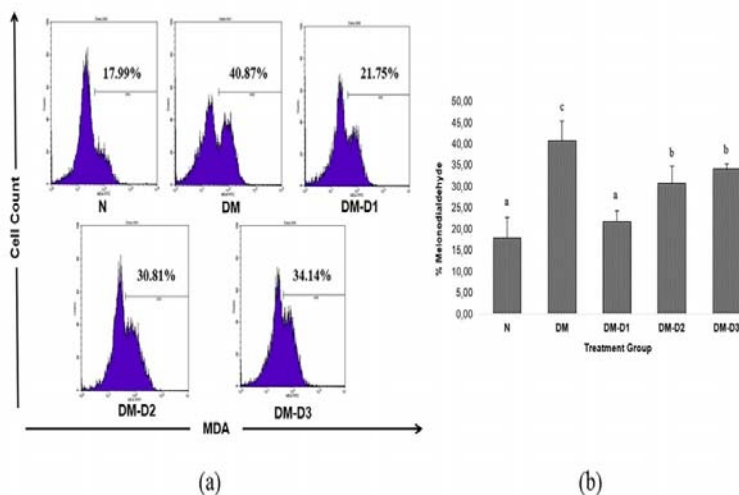


Figure 3. The relative number of MDA in each mice group. (a). Flow cytometry analysis and (b). Results of statistical analysis (p -value ≤ 0.05). N= Normal group; DM= Diabetic mice group (145 mg/kgBW STZ i.p injection/ SHD STZ); DM-D1 group (SHD STZ + 150 mg/kg BW USF treatment); DM-D2 group (SHDSTZ + 250 mg/kg BW USF treatment); DM-D3 group (SHD STZ + 400 mg/kg BW USF treatment).

3.4. $CD4^+TNF-\alpha^+$ and $CD4^+IFN-\gamma^+$ expression levels in diabetic mice were decreased after USF treatment

This study has shown that the levels of $TNF-\alpha$ (Figure 4a & 4c) and $IFN-\gamma$ (Figure 4b & 4d) secreted by $CD4^+$ T cells between normal (N) and diabetic mice (DM) groups are significantly different ($p < 0.05$). DM group had a more incredible amount of $TNF-\alpha$ and $IFN-\gamma$ expression levels than normal mice (N). Additionally, when compared to the

DM mice group without receiving treatment, oral administration of USF extract at all doses for 14 days in diabetic mice significantly lowers the expression levels of $CD4^+TNF-\alpha^+$ and $CD4^+IFN-\gamma^+$ ($p < 0.05$). These results imply that USF extract treatments with doses 1 (150 mg/kg) and 2 (250 mg/kg) were assessed as effective doses to restore the expressions of $TNF-\alpha$ and $IFN-\gamma$ close to normal conditions.

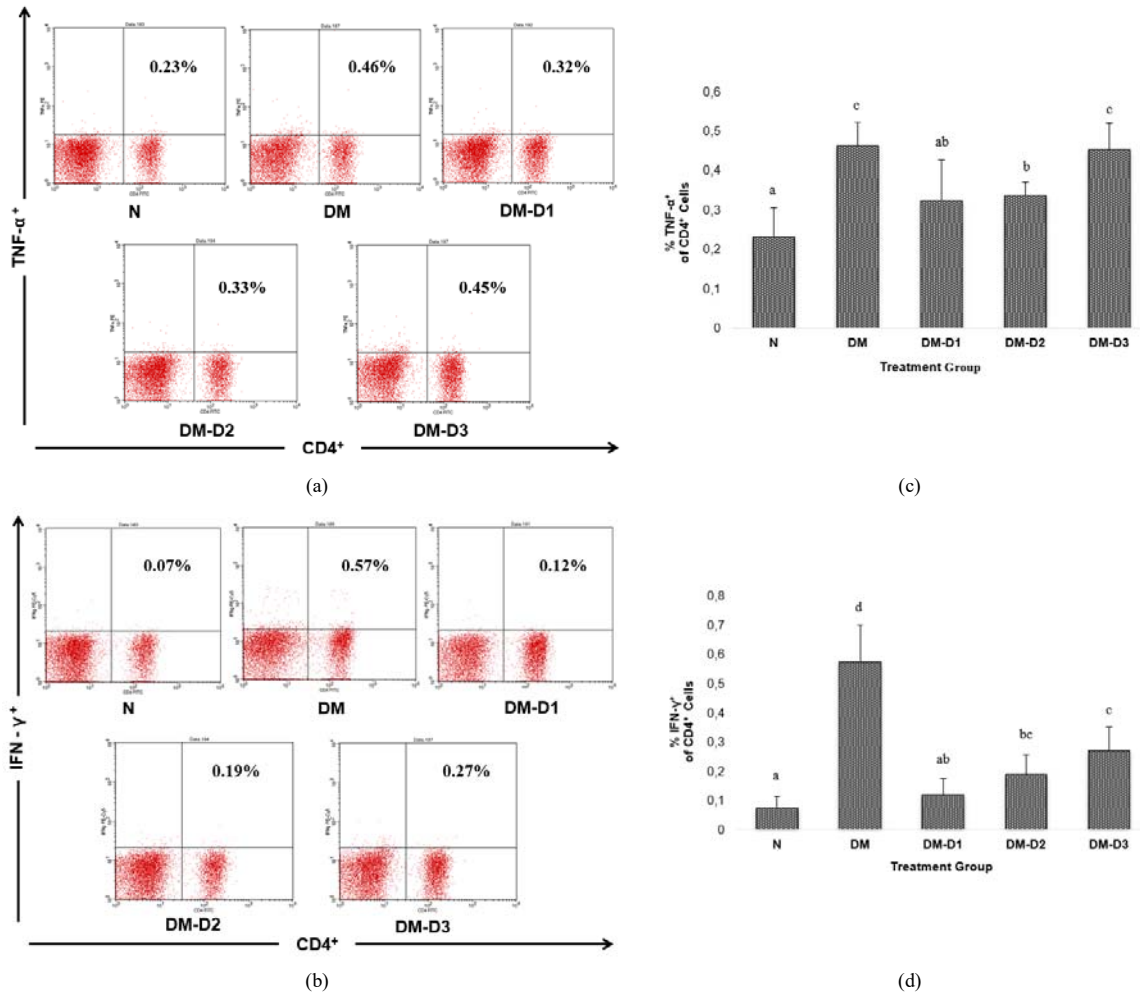


Figure 4. The relative number of $CD4^+TNF-\alpha^+$ and $CD4^+IFN-\gamma^+$ cells in each mice group. (a,b) Plot flow cytometry analysis of $TNF-\alpha$ and $IFN-\gamma$ by $CD4^+$ T cells, (c,d) Results of statistical analysis (p -value ≤ 0.05). N= Normal group; DM= Diabetic mice group (145 mg/kg BW STZ i.p injection/ SHD STZ); DM-D1 group (SHD STZ + 150 mg/kg BW USF treatment); DM-D2 group (SHD STZ + 250 mg/kg BW USF treatment); DM-D3 group (SHD STZ + 400 mg/kg BW USF treatment).

3.5. $CD4^+CD25^+IL-10^+$ expression levels in diabetic mice are increased after USF treatment

The expression levels of regulatory T (T-reg) cells secreting IL-10 in the DM mice group are significantly lower ($p < 0.05$) when compared to normal mice group (Figure 5). Meanwhile, all doses of USF treatments result in a significantly higher production of T-reg cells that secrete IL-10 when compared to the group of diabetic mice

($p < 0.05$). Dose 1 and 3 have significantly increased expression levels compared to the animals in the normal group ($p < 0.05$). Dose 2 of USF treatment manages to recover the expression of IL-10 secreting T-reg cells near-normal mice group levels ($p < 0.05$). These results imply that USF extract can increase the IL-10 expression of regulatory T cells, with dose 2 being the best dose to recover IL-10 secreting T-reg cells to near-normal levels.

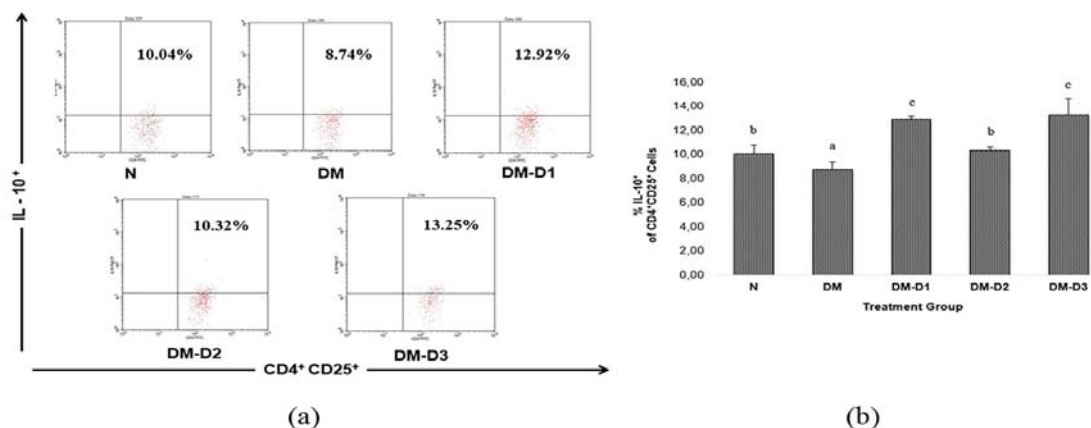


Figure 5. The expression of CD4⁺CD25⁺IL-10⁺ T cells in each mice group. (a). Plot flow cytometry analysis IL-10 by T-reg cells and (b). Results of statistical analysis (p -value ≤ 0.05). N= Normal group; DM= Diabetic mice group (145 mg/kg BW STZ i.p injection/ SHD STZ); DM-D1 group (SHD STZ + 150 mg/kg BW USF treatment); DM-D2 group (SHD STZ i.p injection + 250 mg/kg BW USF treatment); DM-D3 group (SHD STZ + 400 mg/kg BW USF treatment).

4. Discussion

Streptozotocin (STZ) is a diabetogenic agent in several studies using mice. STZ induces diabetes by selectively entering the pancreatic β cells through the glucose transporter receptor (GLUT2) and attacking pancreatic β cells. STZ had a structure similar to glucose that could enter the cell through GLUT2 (Graham *et al.*, 2011). We selected strain BALB/c mice because this strain is a widely used animal model in diabetes mellitus research (Adharini *et al.*, 2020). The liver regulates glucose level homeostasis through glycolysis, gluconeogenesis, and glycogen synthesis. In T1DM, the body lacks insulin due to pancreatic -cell destruction, which disrupts glucose level homeostasis. The increase in glucose level also causes the liver to produce excess glucose because the body cannot absorb and process glucose. Homeostasis of glucose levels could be improved by using phenolic compounds (Rajappa *et al.*, 2019).

This study found that USF extract has an anti-diabetic effect by decreasing the glucose level in diabetic mice (Figure 2). The decrease in glucose level in diabetic mice with USF treatment could be associated with phenolic compounds activity within the USF. Sapodilla is rich in polyphenol, and the USF is an excellent source of flavonoid and polyphenol compounds such as, catechin and derivatives, chlorogenic acid, caffeic acid, luteone, ampelopsin, biflorin, flavonol, luteoliflavan, leucocyanidin and proanthocyanidin. Based on previous research, unripe sapodilla had a higher total antioxidant capacity (TAC) value and total phenolic content (TPC) than ripe sapodilla. This value decreases during fruit maturation (Shui *et al.*, 2004). Based on the research from Shui *et al.* (2004) and Wang *et al.* (2012), several contents of polyphenols that are reported are the same as the results of this research. Composition of extract act to several mechanism to reduce glucose level in DM condition. Tannin increased glucose uptake through insulin signalings, such as increasing the activation of protein phosphoinositide 3-kinase (PI3K) and p38 mitogen-activated protein kinase (MAPK). All the protein activation will increase GLUT-4 translocation to absorb blood glucose (Kumari and Jain, 2012). Moreover, tannins also increase insulin expression by repairing and regenerating pancreatic β cells (Velayutham *et al.*, 2012).

Catechin and their derivatives were able to decrease the blood glucose levels by inhibiting the glucose absorption in intestine (Kumari and Jain, 2012). Epicatechin increased insulin production and secretion by modulating cellular signaling on CaMKII activation at GPR40 receptors (Yang and Chan, 2018). Chlorogenic acid is similar to metformin by increasing cells' sensitivity to insulin and glucose uptake in the liver. Chlorogenic acid lowered blood sugar levels by stopping G6-phase activity in glycogenolysis and gluconeogenesis in hepatic cells (Meng *et al.*, 2013).

MDA expression in the DM group is increased because of the hyperglycemia effect in diabetic mice (Facchini *et al.*, 2000). The presence of MDA in the body causes toxicity, changes in DNA, and oxidation of mutagenic lesions leading to cell death and inflammation. ROS accumulation should be suppressed to lower MDA expression (Luzcaj and Skrzydlewska, 2003). MDA expression in USF-treated diabetic mice is shown to be decreased because the compounds in USF could have an antioxidant effect on scavenging ROS (Xie *et al.*, 2017). The decrease in MDA expression is due to USF's phytochemical content that can capture free radicals. Their antioxidant potentials refer to a natural compound's capacity to neutralize free radicals and bind metal ions through functional grouping of their structure (Dehimat *et al.*, 2021). It is possible that the chlorogenic acid and caffeic acid contained in this extract can act as antioxidants by releasing hydrogen atoms to scavenge free radicals (Liang & David, 2016). Chlorogenic acid also reported that can generate an endogenous antioxidant enzyme (Stefanello *et al.*, 2015). The decrease of ROS is linked with β cell survival and the reduction of β cell deaths by reducing proinflammatory cytokines.

After 14 days of treatment with USF extract, CD4⁺ effector T cells expressed lower proinflammatory molecules like TNF- α and IFN- γ , indicating that USF extract was effective in lowering the risk of complications caused on by the high levels of TNF- α and IFN- γ expression associated with diabetes mellitus. Excessive TNF- α production will increase microvascular complications such as increased chronic inflammation of the eye (Gonzalez *et al.*, 2012). High levels of IFN- γ will trigger more severe pancreatic cell destruction (Suarez *et al.*, 1996). The ability to reduce proinflammatory

cytokines expression occurs due to the presence of polyphenolic and flavonoid compounds in the water extract of unripe sapodilla fruit (*Manilkara zapota*). The reduction of oxidative stress contributes to the mechanism of reducing inflammation in the body because the increased expression of proinflammatory cytokines is induced by the increase of ROS (Alipour et al., 2018). Polyphenol compounds, especially tannins derivatives such as proanthocyanidin, have anti-inflammatory effects that play an essential role in cellular protection against inflammation, as well as inhibiting the expression of iNOS genes and NF- κ B transcription factors (Hussain et al., 2016).

Bioactive contents of USF, such as chlorogenic acid, are also reported to have a role in controlling the expression of NF- κ B, which releases proinflammatory cytokines IL-6, IL-1 β and TNF- α and reduces AGE-RAGE overexpression by inhibiting ROS formation. Other compounds such as catechins and their derivatives have also been reported to prevent complications in diabetes by reducing the expression of proinflammatory molecules including TNF- α , IFN- γ , IL-18, IL-6, IL-1 β and MCP-1. However, high doses of catechins are not recommended because they have side effects that do not have a good impact on the body. This also answers the results of this study which shows that treatment with the water extract of unripe sapodilla fruit (*Manilkara zapota*) is not dose-dependent. Low dose (150 mg/kgBW) is considered more effective because it shows a more significant reduction in TNF- α and IFN- γ inflammation when compared to the use of high doses such as dose 3 (400 mg/kgBW) in this study. Other compounds such as chlorogenic acid are also able to contribute in this mechanism of reducing oxidative stress and inflammation. According to earlier studies, chlorogenic acid is known to contribute to the recovery of DM rats by lowering the lipid content of hydrogen peroxide and enhancing the concentration of non-enzymatic antioxidants such as glutathione (GSH), vitamin C, and vitamin E in the blood. This suggests that chlorogenic acid contributes to maintaining homeostasis in STZ-induced DM (Yan et al., 2020) and reduces the production of proinflammatory molecules, such as TNF- α , LPS, IL-1 β , and IFN- γ (Liang and Kitts, 2015).

Furthermore, this study shows that USF treatment can increase the anti-inflammatory cytokine expression represented by regulatory T cells secreting IL-10 (Figure 5). The compounds of USF support an anti-inflammatory response (Qiao et al., 2016). The expression of IL-10 secreted by regulatory T cells that increase after USF treatment has strengthened the ability of the compounds within the USF extract as an anti-inflammatory. IL-10 secreted by T-reg cells acts as an anti-inflammatory cytokine responsible for inhibiting inflammation. Previous research has reported that the role of T-reg cells associated with the effect of suppressive cytokines, including TGF- β and IL-10. Suppressive cytokine therapy is essential to prevent the onset of inflammatory diseases. (Lestari and Rifa'i, 2018).

It is known that DM has lower levels of CD4⁺CD25⁺IL-10⁺ expression (Qiao et al., 2016). Another study has shown that higher IL-10 expression in T1DM patients has better glucose control prediction (Sanda et al., 2008). IL-10 and TGF- β are the two central

cytokines secreted by regulatory T cells for immunosuppression. IL-10 can limit the activation of proinflammatory cytokines and decrease immune response mediated by other T cells (Hartati et al., 2017). Unfortunately, higher IL-10 expression does not mean that it is always better. Excessive IL-10 expression could cause diseases related to Th2 cell hypersensitivity, such as systemic lupus erythematosus (SLE) (Bijiga and Martino, 2013). This is why we suggested that dose 2 (250 mg/kg BW) is the best dose to increase IL-10 expressing regulatory T cells. In this experiment dose 2, CD4⁺CD25⁺IL-10⁺ expression significantly increased in the near-normal mice group compared to dose 1 (150 mg/kgBW) and dose 3 (400 mg/kgBW) which CD4⁺CD25⁺IL-10⁺ expression was significantly elevated than normal healthy mice group. Furthermore, this result is also analogous to blood glucose levels data shown previously (Figure 2), demonstrating that dose 2 is the best dose to reduce blood glucose levels in this research.

5. Conclusions

According to this study's findings, USF extract can modulate the immune system by non-dose-dependently regulating inflammatory cytokines. The regulation ability of USF on inflammatory cytokines is shown by the decrease of TNF- α and IFN- γ secreted by helper T cells and the increase of IL-10 as an anti-inflammatory cytokine secreted by T-reg cells. The decreasing expression levels of MDA showed ROS scavenging ability after USF treatment in diabetic mice and supported the regulation of inflammatory cytokines in diabetic mice. Further research is required to verify and confirm the results.

Acknowledgement

We acknowledge LPPM UB for funding this research through the HPU grant and Bambang Pristiwanto, Wahyu Isnia Adharini, and Ruri Vivian Nilamsari for assisting and giving us insight into this research.

References

- Adharini WI, Nilamsari RV, Lestari ND, Widodo N and Rifa'i M. 2020. Immunomodulatory effects of formulation of *Channa micropeltes* and *Moringa oleifera* through anti-inflammatory cytokines regulation in type 1 diabetic mice. *Pharm Sci.*, **26**(3):270-278.
- Alipour M, Reza M, Seyed AH, Amir A, Abed G, Hedayat AS and Matin G. 2018. The effect of catechin on related risk factor with type 2 diabetes: A review. *Prog Nutr.* **20**(1):12-20.
- Bacher S and Schmitz ML. 2004. The NF-kappaB pathway as a potential target for autoimmune disease therapy. *Curr Pharm Des.*, **10**(23):2827-2837.
- Baky MH, Kamal AM, Elgindi MR, and Haggag EG. 2016. A review on phenolic compounds from family Sapotaceae. *J Pharmacogn Phytochem.*, **5**(2):280-287.
- Bijiga E, Martino AT. 2013. Interleukin 10 (IL-10) regulatory cytokine and its clinical consequences. *J Clin Cell Immunol.*, **S1**(007):1-6.
- Budiwiyono I, Purwanto AP, Widyastiti NS and Hadian KDK. 2021. Correlation between ferritin levels with malondialdehyde and neutrophil-lymphocyte ratio on iron overload. *Indones J Clinical Pathol Med Laboratory.*, **27**:147-151.

- Cicmil S, Mladenovic I, Krunić J, Ivanović D and Stojanović N. 2018. Oral alterations in diabetes mellitus. *Balk J Dent Med.*, **22(1)**:7-14.
- Dehimat A, Azizi I, Baraggan-Montero V, Bachra K. 2021. In vitro antioxidant and inhibitory potential of leaf extracts of *Varthemia sericea* against key enzymes linked to type 2 diabetes. *Jordan J Biol Sci.*, **14(1)**:97-104.
- Facchini FS, Humphreys MH, DoNascimento C, Abbasi F and Reaven GM. 2000. Relation between insulin resistance and plasma concentrations of lipid hydroperoxides, carotenoids, and tocopherols. *Am J Clin Nutr.*, **72(3)**:776-779.
- Fatima N, Faisal SM, Zubair S, Ajmal M, Siddiqui SS, Moin S and Owais M. 2016. Role of proinflammatory cytokines and biochemical markers in the pathogenesis of type 1 Diabetes: correlation with age and glycemic condition in diabetic human subjects. *PLoS One.*, **11(8)**:1-17.
- Gonzalez Y, Herrera MT, Soldevila G, Garcia-Garcia L, Fabián G, Pérez-Armentariz EM, Bobadilla K, Guzmán-Beltrán S, Sada E, and Torres M. 2012. High glucose concentrations induce TNF- α production through the down-regulation of CD33 in primary human monocytes. *BMC Immunol.*, **13(19)**:1-14.
- Graham ML, Janecek JL, Kittredge JA, Hering BJ and Schuurman HJ. 2011. The streptozotocin-induced diabetic nude mouse model: differences between animals from different sources. *Comp Med.*, **61(4)**: 356–360.
- Hartati FK, Widjanarko SB, Widyarningsih TD and Rifa'i M. 2017. Anti-Inflammatory evaluation of black rice extract inhibits TNF- α , IFN- γ , and IL-6 cytokines produced by immunocompetent cells. *Food Agric Immunol.*, **28(6)**:1116-1125.
- Hussain T, Tan B, Yin Y, Blachier F, Tossou MC and Rahu N. 2016. Oxidative stress and inflammation: What polyphenols can do for us?. *Oxid Med Cell Longev.*, **2016(7432797)**:1-9.
- IDF Diabetes Atlas. <https://diabetesatlas.org/#:~:text=Diabetes%20around%20the%20world%20in%202021%3A,%2D%20and%20middle%2Dincome%20countries>. Accessed 18 May 2022.
- Karshenase MS. 2018. Evaluating the level of IFN gamma in diabetic patients. *J Adv Pharm Res.*, **8(S2)**: 186-188.
- Kumari M, Jain S. 2012. Tannins: An antinutrient with positive effect to manage diabetes. *Res J Recent Sci.*, **1(12)**: 1-8
- Leelayungrayub J, Pothasak Y, Kuntain R, Kaju J and Izhar AM. 2019. Potential health benefits of thai seasonal fruits; sapodilla and star fruit for elderly people. *Am J Biomed Sci.*, **5(1)**:49-53.
- Lestari ND, Rahmah AC, Adharini WI, Nilamsari RV, Jatmiko YD, Widodo N, Rahayu S, Rifa'i M. 2022. Bioactivity of *Moringa oleifera* and Albumin Formulation in Controlling TNF- α and IFN- γ Production by NK Cells in Mice Model Type 1 Diabetes. *Jordan J Biol Sci.*, **15(2)**: 205-208.
- Lestari SR and Rifa'i M. 2018. Regulatory T cells and anti-inflammatory cytokine profile of mice fed a high-fat diet after single-bulb garlic (*Allium sativum* L.) oil treatment. *Trop J Pharm Res.*, **17(11)**:2157-2162
- Liang N and Kitts DD. 2015. Role of chlorogenic acids in controlling oxidative and inflammatory stress conditions. *Nutrients.*, **8(1)**:1-20.
- Luzcaj W and Skrzydlewska E. 2003. DNA damage caused by lipid peroxidation products. *Cell Mol Biol Lett.*, **8(2)**: 391-413.
- Meng S, Cao J, Feng Q, Peng J and Hu Y. 2013. Roles of chlorogenic acid on regulating glucose and lipids metabolism: a review. *Evid Based Complementary Altern Med.*, **2013(801457)**:1-11.
- Purwanti E, Hermanto FE, Souhaly JW, Prihanta W and Permana TI. 2021. Exploring public health benefits of *Dolichos lablab* as a dietary supplement during the COVID-19 outbreak: A computational study. *J Appl Pharm Sci.*, **11(2)**:135-140.
- Qiao Y-C, Shen J, Hong X-Z, Liang L, Bo C-S, Sui Y, and Zhao H-L. 2016. Changes of regulatory T cells, transforming growth factor-beta and interleukin-10 in patients with type 1 diabetes mellitus: A systematic review and meta-analysis. *Clin Immunol.*, **170**: 61-69.
- Rahangdale S, Yeh SY, Malhotra A and Veves A. 2009. Therapeutic interventions and oxidative stress in diabetes. *Front Biosci (Landmark Ed.)*, **14(1)**:192-209.
- Rajappa R, Sireesh D, Salai MB, Ramkumar KM, Sarvajayakesavulu S and Madhunapantula SV. 2019. Treatment with naringenin elevates the activity of transcription factor Nrf2 to protect pancreatic β -cells from streptozotocin-induced diabetes in vitro and in vivo. *Front Pharmacol.*, **9(1562)**: 1-20.
- Rojas-Sandoval J and Praci. 2017. *Manilkara zapota* (Sapodilla). CABI Compendium.
- Sanda S, Roep BO and Herrath MV. 2008. Islet antigen-specific IL-10+ immune responses but not CD4+CD25+FOXP3+ cells at diagnosis predict glycemic control in type 1 diabetes. *Clin Immunol.*, **127(2)**:138-143.
- Shui G, Wong SP and Leong LP. 2004. Characterization of antioxidants and change of antioxidant levels during storage of *Manilkara zapota* L. *J Agric Food Chem.*, **52(26)**:7834-7841.
- Stefanello N, Pereira LB, Schamatz R, Passamontib S, Faccos G, Zaninia D, Abdalla FH, Vieira JM, Castro VSP, de Oliveira VA, MI de UM da Rochad, Kastend J, Morscha VM and Schetinger MRC. 2015. Chlorogenic acid, caffeine, and coffee reverse damage in liver, kidney, and pancreas parameters of diabetic rats. *J Diabetes Health.*, **108**:214-228.
- Suarez-Pinzon W, Rajotte RV, Mosmann TR and Rabinovitch A. 1996. Both CD4⁺ and CD8⁺ T-cells in syngenic islet grafts in NOD mice produce interferon during cell destruction. *Diabetes.*, **45(10)**:1350–1357.
- Szablewski L. 2014. Role of immune system in type 1 diabetes mellitus pathogenesis. *Int Immunopharmacol.*, **22(1)**:182-191.
- Tamsir NM, Esa NM, Omar SNC, and Shafie NH. 2020. *Manilkara zapota* (L.) P. Royen: potential source of natural antioxidants. *Malaysian J Med Health Sci.*, **16(6)**:196-204.
- Velayutham R, Nirmala S and Ahmed KFHN. 2012. Protective effect of tannins from *Ficus racemosa* in hypercholesterolemia and diabetes induced vascular tissue damage in rats. *Asian Pac J Trop Med.*, **5(5)**: 367-373.
- Wang H, Liu T, Song L and Huang D. 2012. Profiles and α -amylase inhibition activity of proanthocyanidins in unripe *Manilkara zapota* (chiku). *J Agric Food Chem.*, **60(12)**: 3098–3104.
- Xie Z, Wu B, Shen G, Li X and Wu Q. 2017. Curcumin alleviates liver oxidative stress in type 1 diabetic rats. *Mol Med Rep.*, **17(1)**:103-108.
- Yan Y, Zhou X, Guo K, Zhou F and Yang H. 2020. Use of chlorogenic acid against diabetes mellitus and its complications. *J Immunol Res.*, **2020(9680508)**:1-6.
- Yang K and Chan CB. 2018. Epicatechin potentiation of glucose-stimulated insulin secretion in INS-1 cells is not dependent on its antioxidant activity. *Acta Pharmacol.*, **39(5)**: 893–902.
- Yonny ME, EM Garcia, A Lopez, JI Arroquy and MA Nazareno. 2016. Measurement of malondialdehyde as an oxidative stress biomarker in goat plasma by HPLC-DAD. *Microchem J.*, **129**:281-285.

Activity of lactic acid-producing *Streptomyces* strain CSK1 against *Staphylococcus aureus*

Shahad Al Nuaimi¹, Ismail Saadoun^{1,*}, Ban Al Joubori¹, and Sofian Kanan²

¹Department of Applied Biology, College of Sciences, University of Sharjah, P.O. Box 27272, Sharjah, UAE. ²Department of Biology, Chemistry & Environmental Sciences, College of Sciences, American University of Sharjah, Sharjah, UAE.

Received: October 5, 2022; Revised: December 20, 2022; Accepted: January 4, 2023

Abstract

This study aimed to evaluate an active *Streptomyces* strain CSK1 previously isolated from UAE soils to produce inhibitory bioactive compounds under different nutritional and growth conditions against Gram positive *Staphylococcus aureus*. Using a One Strain Many Compounds (OSMAC) strategy, specifically media optimization on *Streptomyces* strain CSK1 to enhance antibacterial activity against *S. aureus*, results indicated an average inhibition zone diameter ranging between 13 and 20 mm after 7 days of growth in ISP4 broth. Moreover, the minimum inhibitory concentration (MIC) and minimum bactericidal concentration (MBC) of the water soluble of evaporated ethyl acetate crude extract revealed values of 0.79 and 6.29 mg mL⁻¹, respectively. GC-MS analysis of the crude ethyl acetate extract confirmed three compounds namely lactic acid, butyl lactate and lactide. The production of these compounds by *Streptomyces* strain CSK1 may stress their valuable importance in food and pharmaceutical industries.

Keywords: GC-MS; Lactic acid; MIC; *Staphylococcus aureus*; *Streptomyces*.

1. Introduction

Streptomyces are Gram positive filamentous bacteria that belong to Actinobacteria that are abundant in soil. They are known to produce many natural products that are important for the biotechnology industry. They produce various compounds that have been commercialized such as antibiotics, antifungal and anti-parasite, and antitumor agents (Moore *et al.*, 2022). *Streptomyces* have a complex life cycle that includes vegetative and reproductive growths. The cycle starts with spore germination, then substrate mycelium develops followed by the aerial mycelium, the apical aerial hypha grows and sporulates, upon maturation, the spores are dispersed. The synthesis of secondary metabolites is tightly linked to the *Streptomyces* complex life cycle (Khushboo *et al.*, 2021; Manteca and Yagüe, 2018).

Secondary metabolites are chemicals that exhibit biological activity and produced in small concentrations. They are not essential for bacterial growth, which distinguishes them from primary metabolites (Keswani *et al.*, 2019). Their diversity contributes to the microorganisms' ecological role. Secondary metabolites were found to have a significant influence on human health and are used in the pharmaceutical and food industries. *Streptomyces* produce secondary metabolites like cyclic and linear peptides and linear polyketides that are known for their antibacterial activity (Lacey and Rutledge, 2022). Genetic analysis has identified that up to 30 secondary metabolite pathways can be found in *Streptomyces* strains that are mostly not expressed when

grown in culture (Choudoir *et al.*, 2018; de Rop *et al.*, 2022; Otani *et al.*, 2022).

One of the methods used to activate the silent secondary metabolites pathways in *Streptomyces* is One Strain Many Compounds (OSMAC) approach. This strategy uses different culture conditions to induce and maximize the production of secondary metabolites. Cultural conditions include media chemical compositions, fermentation, and environmental factors. Secondary metabolites can be expressed or repressed through media chemical composition such as carbon and nitrogen sources. Fermentation and incubation conditions such as temperature and incubation period affect the quality of the natural products. pH is an environmental factor that is important for secondary metabolites synthesis and cellular metabolism. Developing high-quality natural products at an industrial scale with the use of affordable substrates is facilitated by optimizing the production conditions (Al Farraj *et al.*, 2020; Chen *et al.*, 2022; Hug *et al.*, 2018; Khattab *et al.*, 2016; Yun *et al.*, 2018).

The aim of this study is to optimize the cultural conditions of an active *Streptomyces* strain CSK1 previously isolated from UAE soil to produce inhibitory bioactive compounds against *Staphylococcus aureus*. The crude extract of *Streptomyces* strain CSK1 was analyzed using GC-MS to identify the active substrates.

* Corresponding author. e-mail: isaadoun@sharjah.ac.ae.

2. Materials and methods

2.1. Microbial test organisms

Test organisms that were used for the antimicrobial activity test included six bacterial strains and *Candida albicans* (ATCC® 66027). The bacterial Gram-positive strains are *Staphylococcus aureus* (ATCC® 29213), *Staphylococcus epidermidis* (ATCC® 14990), *Streptococcus pneumoniae* (ATCC® 6301) and *Bacillus subtilis* (ATCC® 6051). The bacterial Gram-negative strains are *Escherichia coli* (ATCC® 25922) and *Pseudomonas aeruginosa* (ATCC® 55638).

2.2. Isolation and Characterization of the *Streptomyces* CSK1 strain

The *Streptomyces* strain CSK1 was isolated previously from a cultivated soil sample from Dubai, United Arab Emirates (Al-Joubori, 2020). It was characterized according to the International *Streptomyces* project (ISP) (Shirling and Gottlieb, 1966). The isolate was grown on oatmeal agar (Himedia, India) and incubated at 28 °C for fourteen days. The colour of the aerial mycelium, substrate mycelium and diffusible soluble pigments was determined.

2.3. Antimicrobial activity of the *Streptomyces* CSK1 strain

The antimicrobial activity of the *Streptomyces* strain CSK1 was tested using the well diffusion method (Bauer *et al.*, 1966; Hudzicki, 2009). The microbial test organisms illustrated above were inoculated on nutrient agar (Himedia, India) plate at 37 °C for 24 hours. Bacterial suspension was prepared using direct colony transfer and the turbidity was adjusted to 0.5 McFarland standard. The adjusted test bacterial suspension was cultured on fresh Mueller Hinton agar (Himedia, India) plate using sterile cotton swab. Six mm diameter wells were made using a sterile Pasteur pipette in the Mueller Hinton agar plate. The wells were filled with 55 µL of the supernatant culture broth. The plates were incubated overnight at 37 °C then the inhibition zones were recorded after 24 hours.

2.4. Optimization of cultural conditions

Streptomyces strain CSK1 culture conditions were optimized for the highest antibiotic production. The conditions that were tested were the following: Culture media broth (Nutrient media (Himedia, India), Tryptone - yeast extract media or ISP1 (Himedia, India), Inorganic salts-starch media or ISP4 [Ingredients per Liter; Starch 10g, K₂HPO₄ 1g, MgSO₄.7H₂O 1g NaCl 1g, CaCO₃ 2g, (NH₄)₂SO₄ 2g, Trace salts solution 1mL], Carbon sources [concentration of 1%] (Glucose, Arabinose, xylose, sucrose, fructose, mannitol, sorbitol, starch, inositol, glycerol, carboxymethylcellulose, and Glucosamine), Nitrogen sources [concentration of 0.2%] (Ammonium sulphate, Casein, yeast extract, sodium nitrate, potassium nitrate, and Glycine), pH (5.0, 6.0, 7.2, 8.0 and 9.0) and temperature (25, 28, 31, 34, and 37 °C). *Streptomyces* strain CSK1 was grown in submerged cultures in 250 mL containing 50 mL culture broth. A seed culture of the *Streptomyces* isolate was prepared by growing the isolate on oatmeal agar plate for 4 days. The whole aerial mycelium was scrapped and suspended in sterile water. Flasks were inoculated with 1.0 mL of the spore suspension and incubated in an orbital shaker

incubator at 100 rpm for 7 days. During the growth period, 1.0 mL of the culture broth was taken on days 0, 1, 2, 3, 4, 6, and 7 for antimicrobial activity testing.

2.5. Fermentation, extraction of metabolites

A seed culture of the *Streptomyces* strain CSK1 was prepared as described above where 5.0 mL of the spore suspension of the seed culture are inoculated in four 1.0 L flasks containing 250 mL of the optimal culture media. The flasks were incubated in an orbital shaker at 100 rpm for 4 days .

After incubation, cell free broth was obtained through filtration using 0.22 µm filter unites (Millipore, USA). The metabolites were extracted through liquid-liquid extraction using ethyl acetate as the organic solvent. Ethyl acetate was added to the cell free broth (v/v) and mixed vigorously. The mixture was shaken for 30 minutes and then was allowed to stand in a separatory funnel to settle into two layers. The organic layer was evaporated using a rotary evaporator (Rotavapor R-300, Buchi) at 45 °C with 200 rpm at 200 mbar. The crude ethyl acetate extract was collected and used for further analysis.

2.6. Antimicrobial activity of the ethyl acetate crude extract

The ethyl acetate crude extract was dissolved in 1.0 mL distilled water and filter-sterilized using 0.22 µm syringe filter. The antimicrobial activity of the ethyl acetate crude extract was performed using well diffusion method as described above. The crude extract was tested against *S. aureus*. Lactic acid was used as a positive control, and pure ethyl acetate and ISP4 broth were used as negative controls. The antibacterial activity of the crude extract against *S. aureus* was tested using the microbroth dilution according to the clinical and laboratory standards institute (CLSI) (CLSI, 2006; Elshikh *et al.*, 2016). In a 96 well plate, the crude extract was serially diluted with Mueller Hinton broth starting from well one at 37.73 mg/mL followed by two-fold dilutions from 25.15 to 0.025 mg/mL in wells 2 through 12 performed in triplicates (columns A, B, and C). Positive control of tested *S. aureus* growth and negative control presenting only Mueller Hinton medium were assessed in columns G and H. The crude extract was incubated with 100 µL Mueller Hinton broth containing (5.0 x 10⁵ CFU/mL) of *S. aureus* overnight at 37 °C. The minimum inhibitory concentration (MIC) was detected using resazurin (0.015%) as an indicator of bacterial growth. The minimum bactericidal concentration (MBC) was assessed using 10 µL of crude extract with concentrations ranging from 0.196 to 6.29 mg/mL that showed inhibition of growth of *S. aureus* in the MIC method.

2.7. GC-MS analysis of the ethyl acetate crude extract

The GC-MS analysis of the ethyl acetate crude extract was performed using a GC-MS QP2010 ultra, Shimadzu-Japan. The carrier gas used was helium at a flow rate of 0.9 mL/min. The column used is Rxi-5ms, Restek with 30 m length, 0.25 mm thickness and 0.25 mm diameter. The process was as following: hold 2 minutes at 70 °C, followed by 300 °C with heating rate 5°C/min, holding for 8.4 min at 300 °C. The temperature of the injector was 280 °C. Mass spectrum was determined at 70 eV with a scan interim of 1666 U/sec and the fractions between 35 and 500 amu. The component spectrums were compared to

a database of known component spectrums stored in the GC-MS. The mass results were analyzed according to

Streptomyces Strain CSK1

Aerial Mycelium	White
Substrate Mycelium	Grey
Soluble pigment	No pigments
Antimicrobial Activity	
<i>Escherichia coli</i> (ATCC® 25922)	-
<i>Pseudomonas aeruginosa</i> (ATCC® 55638)	-
<i>Staphylococcus aureus</i> (ATCC® 29213)	19.67 mm ± 1.15
<i>Staphylococcus epidermidis</i> (ATCC® 14990)	25.67 mm ± 0.58
<i>Streptococcus pneumoniae</i> (ATCC® 6301)	-
<i>Bacillus subtilis</i> (ATCC® 6051)	-
<i>Candida albicans</i> (ATCC® 66027)	-

three libraries namely Wiley9, NIST14, and NIST14s.

2.8. Statistical Analysis

Analyses of variance (ANOVA) for all data were performed. Two-way ANOVA was used to compare between the means ($\alpha = 0.05$).

3. Results

3.1. Characterization and antimicrobial activity of the *Streptomyces* CSK1 strain

The *Streptomyces* strain CSK1 was grown on oatmeal agar for 14 days. The mature *Streptomyces* colonies have white aerial mycelium and grey substrate mycelium, with no soluble pigments produced (Figure 1). The isolate was

screened for antimicrobial activity using well diffusion method against various organisms (Table 1). The isolate showed an inhibitory activity against Gram positive organisms mainly *Staphylococcus aureus* and *Staphylococcus epidermidis* (Figure 2).

Table 1. *Streptomyces* strain CSK1 characteristics and antimicrobial activity.

(-) indicates that there is no antimicrobial activity against the organism. The data in the positive antimicrobial activity are represented by the average zone of inhibition of triplicate samples (mm) ± the standard deviation.

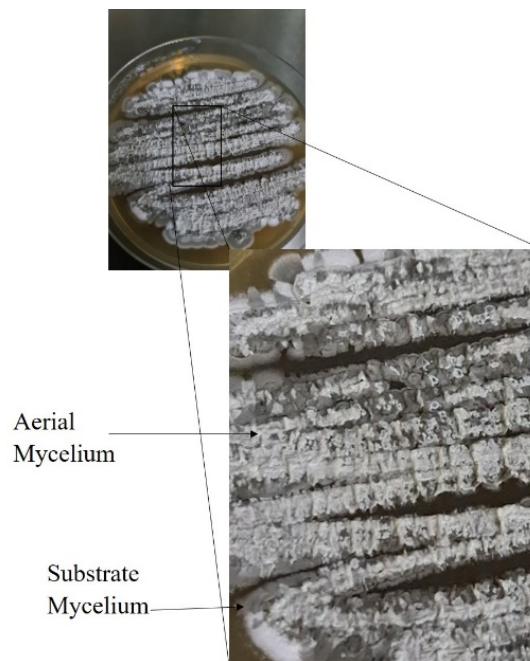


Figure 1. *Streptomyces* strain CSK1 grown on oatmeal agar for 14 days.

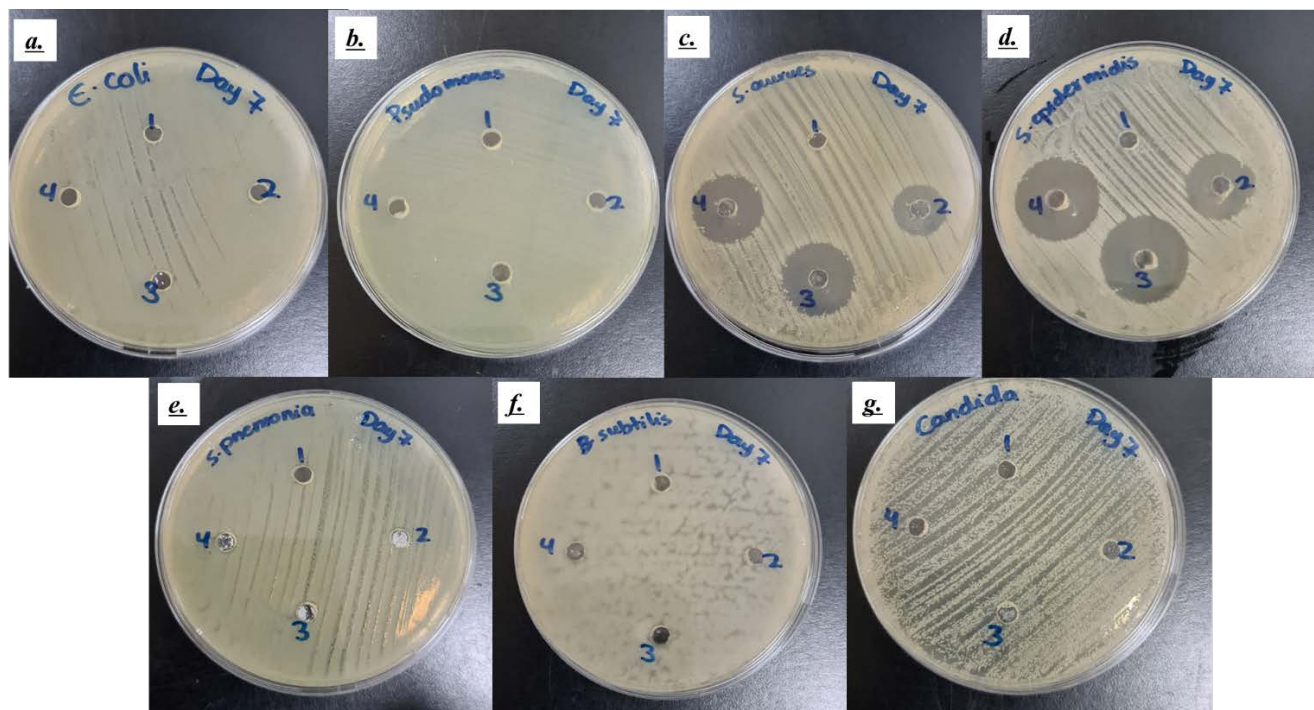


Figure 2. Antimicrobial activity of the *Streptomyces* strain CSK1 against various organisms (a) *Escherichia coli* (ATCC® 25922), (b) *Pseudomonas aeruginosa* (ATCC® 55638), (c) *Staphylococcus aureus* (ATCC® 29213), (d) *Staphylococcus epidermidis* (ATCC® 14990), (e) *Streptococcus pneumoniae* (ATCC® 6301), (f) *Bacillus subtilis* (ATCC® 6051), (g) *Candida albicans* (ATCC® 66027).

3.2. Optimal conditions for antimicrobial activity production

The Optimal physical and chemical conditions for production of the active inhibitory metabolites by *Streptomyces* CSK1 strain against *S. aureus* were investigated. The isolate was grown in three types of culture media and was tested for antimicrobial activity against *S. aureus*. Figure 3 showed that all three culture media broths were suitable for antimicrobial production. The average zone of inhibition in all three culture media broths ranged from 13.5 mm and 16 mm. Results indicated that there was no statistical significant difference ($P \geq 0.05$) between the antimicrobial activity in the three types of culture media after performing the statistical analysis. The culture medium used for further analysis was the inorganic salts starch media broth (ISP4).

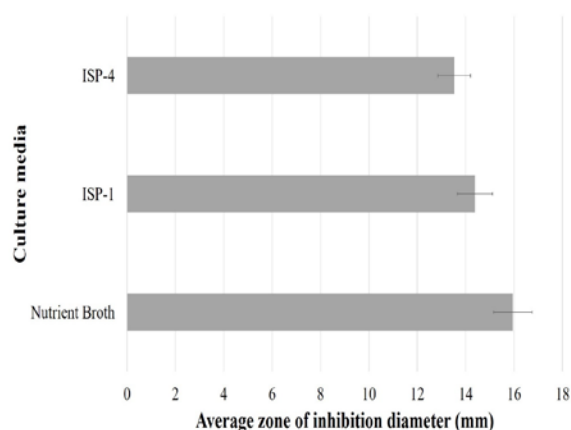


Figure 3. *Streptomyces* strain CSK1 antimicrobial activity against *S. aureus*. The isolate was cultured in three types of broth media: nutrient broth (NB), tryptone-yeast extract broth (ISP-1), and inorganic salts starch broth (ISP-4).

The carbon sources that affect the production of the inhibitory compounds was also tested. Inorganic salts starch media broth was used as a basal media and the starch was substituted with different carbon sources. No carbon source added to the basal media was considered the negative control and starch was used as the positive control. Results in Figure 4 showed that starch, fructose, and glucose produced the highest antimicrobial activity (average zone of inhibition >19 mm) while sorbitol produced the lowest antimicrobial activity (average zone of inhibition < 8 mm) against *S. aureus*. There was no significant difference ($P \geq 0.05$) between the carbon sources that produced high antimicrobial activity. The carbon source used for further analysis was starch.

The nitrogen sources were tested next for antimicrobial activity. Inorganic salts starch broth was used as a basal media and ammonium sulfate was substituted with

different nitrogen sources. The nitrogen sources selected for the test were from different organic and inorganic nitrogen sources and amino acids. No nitrogen source added to the basal media broth was considered the negative control and ammonium sulfate was considered the positive control. The nitrogen source affected the production of inhibitory compounds against *S. aureus* as illustrated in Figure 5. The highest antimicrobial activity was when ammonium sulfate or yeast extract were used as nitrogen sources (average zone of inhibition > 16 mm). There was almost no antimicrobial activity in the negative control (average zone of inhibition > 4 mm). There was no significant difference ($P \geq 0.05$) between the nitrogen sources that produced the highest antimicrobial activity. The ammonium sulfate was used for the analysis of the physical conditions of the inhibitory compounds production.

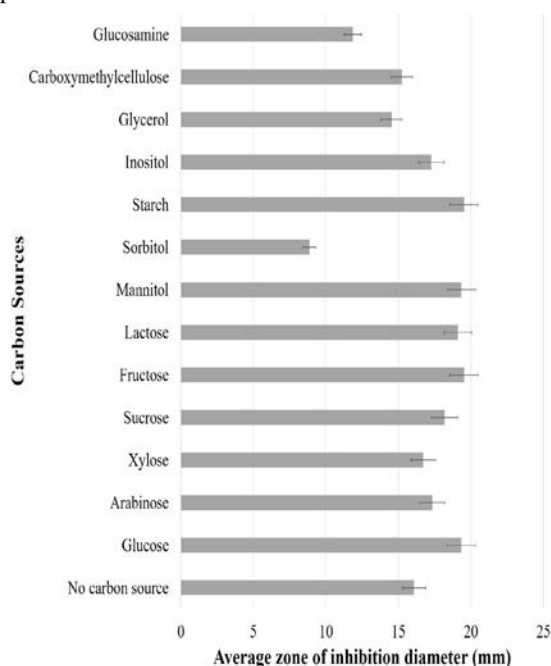


Figure 4. *Streptomyces* strain CSK1 antimicrobial activity against *S. aureus* using different carbon sources added to the optimal culture media (ISP4 as a basal media). No carbon was added to the negative control, and starch was added as the positive control.

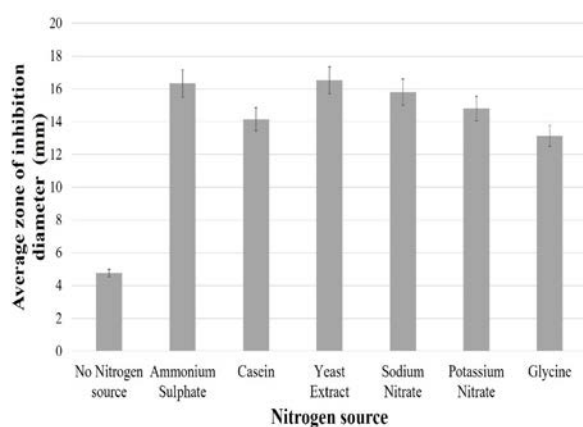


Figure 5. *Streptomyces* strain CSK1 antimicrobial activity against *S. aureus* using different nitrogen sources added to the optimal culture media (ISP4 as a basal media) and the optimal carbon source (Starch). No nitrogen source was added to the negative

control while ammonium sulphate was considered as the positive control.

The antimicrobial activity against *S. aureus* were tested at various temperatures and pH values ranged from 25 °C to 37 °C and 5.0 to 9.0, respectively. The controls of the temperature and pH were 28 °C and 7.2. The highest antimicrobial activity against *S. aureus* was observed at temperatures 28 °C and 31 °C, while the lowest was at temperature 34 °C (Figure 6). As for the pH, the antimicrobial activity against *S. aureus* was higher in alkaline conditions rather than acidic conditions (Figure 7). The highest antimicrobial activity was observed in pH 7.2. There was no antimicrobial activity when the initial pH of the broth was adjusted to pH 5.0. There was a significant difference ($P \leq 0.05$) between the results, so the temperature and pH used for further analysis and extraction of metabolites was 28 °C and pH 7.2.

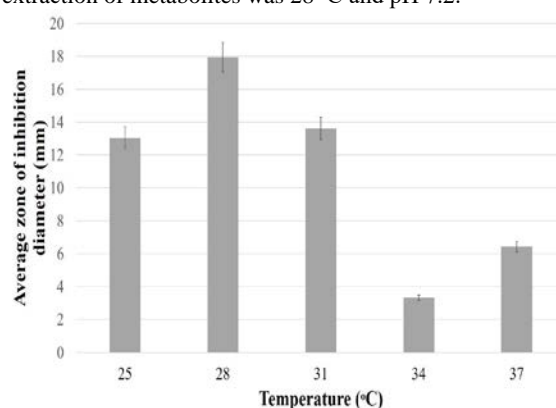


Figure 6. *Streptomyces* strain CSK1 antimicrobial activity against *S. aureus* cultured in the optimal culture media (ISP4, starch and ammonium sulphate) at different temperatures.

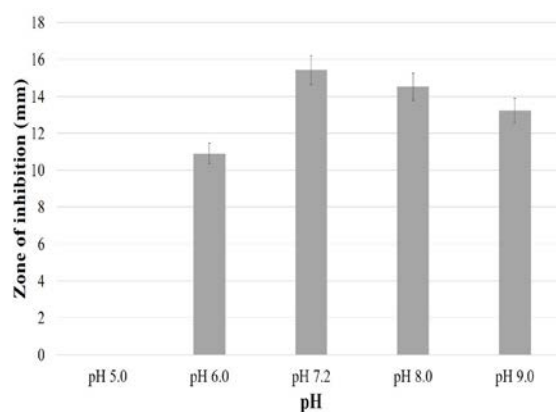


Figure 7. *Streptomyces* strain CSK1 antimicrobial activity against *S. aureus* cultured in the optimal culture media (ISP4, starch and ammonium sulphate, 28 °C) at different pH values.

GC-MS analysis of the ethyl acetate crude extract

After optimizing the conditions, *Streptomyces* strain CSK1 was grown in a larger scale. The metabolites were extracted using ethyl acetate as an organic solvent. The crude extract was collected and analyzed using Gas Chromatography Mass Spectrometry (GC-MS) for identification of metabolites. The samples were filtered using 0.25 µm filters to remove any solid particulates. The GC chromatogram (Figure 8) revealed three major products that appeared after 9.46, 11.60, and 17.93 minutes. The GC profile was completed in 43 minutes, and

no products were identified after 20 minutes. The peak at 9.46 showed a mass spectrum that match the identified compound 3,6-dimethyl-1,4-dioxane-2,5-dione commonly known as lactide. The major peak appeared at 11.6 minutes corresponds to the presence of lactic acid. Finally, the third product appears after 17.93 minutes, which showed a mass profile that corresponds to the presence of n-butyl lactate derivative. The GC peak areas indicated that lactic acid is the major product that is present in 5 times the abundance of the two other products where the relative ratio between the three compounds is 1: 5 : 1. Figure 9 shows the mass spectrum associated to the 11.6 min GC peak with all major ion fragments identified and presented within the figure.

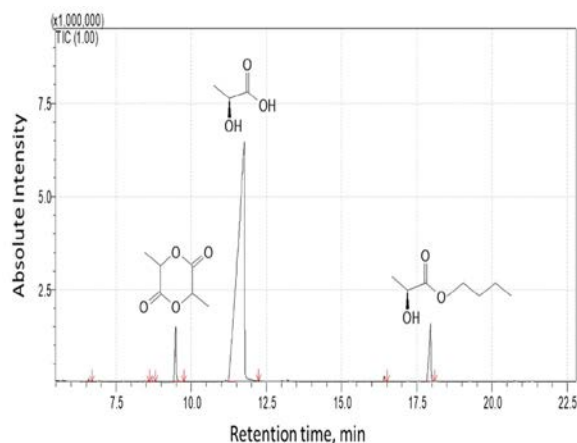


Figure 8. GC chromatogram of the ethyl acetate crude extract. The chromatogram shows three compounds were found in the ethyl acetate crude extract: Lactide appeared at minute 9.46, lactic acid appeared at 11.60 minutes and the last one is butyl lactate at 17.93 minute.

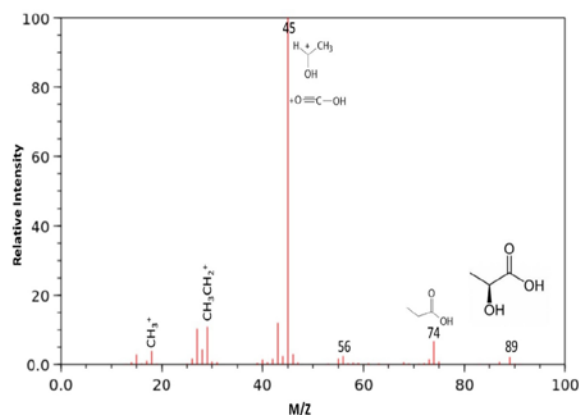


Figure 9. Mass spectrum of the 11.60 min GC peak along with all identified fragments.

3.3. Antimicrobial Activity analysis of the ethyl acetate crude extract

The ethyl acetate crude extract was used for antimicrobial activity analysis against *S. aureus*. The crude extract was dissolved in 1.0 mL distilled water and filter sterilized through 0.22 μ m syringe filters. The concentration of the ethyl acetate crude extract was 50.3 mg/mL. Antimicrobial activity of the ethyl acetate crude extract was carried out using well diffusion method. The crude extract was tested for antimicrobial activity against *S. aureus*. The controls used in this test were pure lactic acid as a positive control, pure ethyl acetate and ISP4 broth as negative controls. The antimicrobial activity of the ethyl acetate crude extract as illustrated in Table 2 resulted in a 21 mm zone of inhibition diameter, while the positive control generated a 36 mm zone of inhibition against *S. aureus* (Figure 10). The minimum inhibitory concentration (MIC) of the crude extract was 0.79 mg/mL, which is the lowest concentration to prevent the bacterial growth, and the minimum bactericidal concentration (MBC) is 6.29 mg/mL, which is the lowest concentration to kill the bacteria.

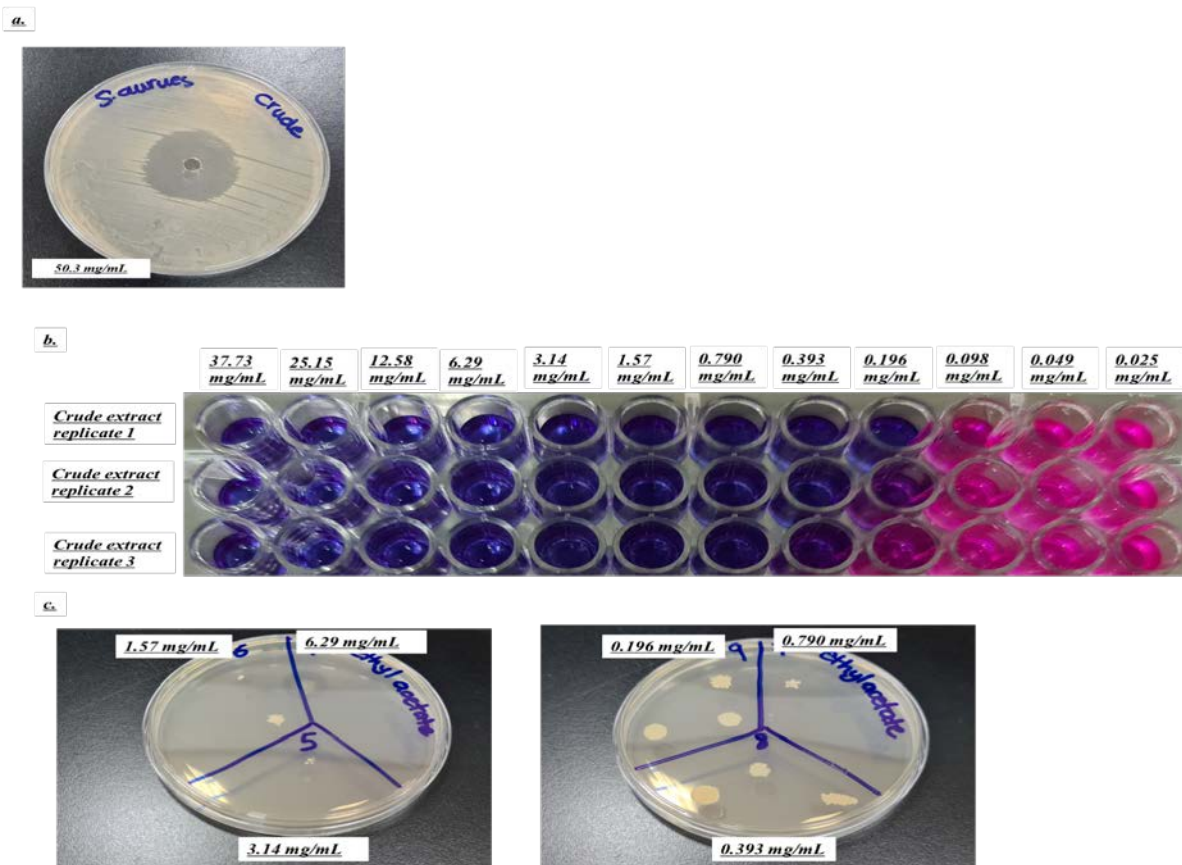


Figure 10: Antimicrobial activity of the ethyl acetate crude extract on *S. aureus*. (a) well diffusion test results using crude extract concentration of 50.3 mg/mL. (b) Minimum Inhibitory Concentration (MIC) test was performed in a 96 well plate, the crude extract was serially diluted with Mueller Hinton broth starting from well one at 37.73 mg/mL followed by two-fold dilutions from 25.15 to 0.025 mg/mL in wells 2 through 12 performed in triplicates (columns A, B, and C). Positive control of tested *S. aureus* growth and negative control presenting only Mueller Hinton medium were assessed in columns G and H (data not shown). (c) Minimum bactericidal concentration (MBC) assessed using 10 μ L of crude extract with concentrations ranging from 0.196 to 6.29 mg/mL.

Table 2. Antimicrobial activity of the ethyl acetate crude extract against *S. aureus*.

	Antimicrobial activity (Zone of inhibition in mm)				MIC	MBC
	Crude extract	Control				
		Lactic acid	ISP4 broth	Ethyl acetate		
<i>S. aureus</i>	23.3 ± 2.08	39.7 ± 3.5	0	0	0.79 mg/mL ± 0.00	6.29 mg/mL ± 0.00

4. Discussion

Streptomyces are important microorganisms for the biotechnology industry. They are known producers of many natural products that are beneficial to the human health. Genetic analysis showed that not all secondary metabolites can be activated in a lab setting (Del Carratore *et al.*, 2022). One of the strategies that are used to activate the cryptic metabolic pathways of the *Streptomyces* is through the optimization of the cultural conditions (Maithani *et al.*, 2022). In our study, *Streptomyces* strain CSK1 that has been recovered previously from the UAE soil showed an inhibitory activity against the Gram-positive bacteria. The antimicrobial activity was optimized to achieve the highest antimicrobial activity against the tested organism and then proceeded to identify the crude extract through GC-MS.

Streptomyces are known producers of many natural products. The diversity of natural products produced by *Streptomyces* are due to environment and their natural habitat conditions (Donald *et al.*, 2022). One of the methods that is used to optimize the production of

secondary metabolites and discover new metabolites is the modification of the contents and types of culture conditions. It is important to optimize the culture media components as it was found in some studies that the optimization of the culture media increases the production of secondary metabolites (Kalaiyarasi *et al.*, 2020; Norouzi *et al.*, 2019). In this study, the cultural conditions that were optimized are culture media broth, carbon sources, nitrogen sources, temperature, and pH. The culture media composition contributes to the activation of the silent metabolic pathways for secondary metabolites production (Antoraz *et al.*, 2015). In this study, three different culture media broths were used to check and optimize the production of antimicrobial activity against *S. aureus*. The optimal culture medium that was chosen for further analysis was the inorganic salts starch broth or ISP4 (ISSB). Similarly, Sholkamy *et al.* (2020) demonstrated that the best culture medium for producing an antibacterial and antinematicidal from a *Streptomyces* strain was inorganic salts starch broth. Carbon and nitrogen sources affect the production of secondary metabolites in *Streptomyces*. Some carbon sources are found to suppress the secondary metabolites production such as glucose and

glycerol. *Streptomyces* are found in soil where the carbon sources available are the polysaccharides, so they secrete enzymes to break them down and they do not affect the production of secondary metabolites. Nitrogen sources are important in the production of primary metabolites and secondary metabolites (Romero-Rodríguez *et al.*, 2018). In other studies, ISP4 broth media was also utilized for the synthesis of antimicrobial compounds, but after the carbon and nitrogen sources were optimized, the starch and ammonium sulphate were replaced with maltose and casein, respectively (Sebak *et al.*, 2021).

In our study, the optimal culture medium that produced high activity against *S. aureus* is the inorganic salts starch media broth (ISP4) that is supplied with starch as a carbon source and ammonium sulphate as a nitrogen source. Previous studies found that using starch as a carbon source yielded the best antibacterial secondary metabolites, which is consistent with our findings (Da Silva *et al.*, 2012; Mary *et al.*, 2021; Rakesh *et al.*, 2014). However, Leulmi *et al.* (2019) reported that starch was not a suitable carbon source for their microorganism's secondary metabolites production since it suppressed their product completely. This shows the importance of the optimization of the carbon sources and their effects on the production of secondary metabolites. The highest antimicrobial activity against *S. aureus* was achieved in our study when ammonium sulphate or yeast extract was used as a nitrogen source, which is consistent with the optimal nitrogen sources for secondary metabolites production in previous studies by Ahmad *et al.* (2017) and Al Farraj *et al.* (2020).

Environmental factors such as pH and temperature were found to affect secondary metabolites production, therefore an optimization step is required (Al-Ansari *et al.*, 2020). In the present study, pH 7.2 and 28 °C provided the highest levels of antibacterial activity against *S. aureus*. Chandrakar and Gupta (2019) and Khattab *et al.* (2016) reported various results for their optimal temperature and initial pH optimization analysis. Temperatures ranged between 25 and 30 °C, and initial pH in between 7.0 and 7.5, achieved the highest antimicrobial activity depending on the environment and habitat from which the *Streptomyces* isolates were obtained.

The chromatography profile of the crude extract showed three compounds produced by *Streptomyces* strain CSK1. The compounds are lactic acid, butyl lactate and lactide. The lactic acid was the most abundant compound in the crude extract. *Streptomyces lacticiproducens* sp. nov. was also a lactic acid producer (Zhu *et al.*, 2011), while this strain produced lactic acid in the cell free broth when cultured on Gause synthetic medium containing similar ingredients to inorganic salts starch broth (Zhu *et al.*, 2014). Christensen *et al.*, 2021 confirmed that bacteria producing lactic acid have antibacterial activity against *S. aureus*. Butyl lactate is a derivative of lactic acid. It is a lactate ester that is used in the food, cosmetic and pharmaceutical industry. It has been used as a food additive as it is considered safe by the Food and Drug administration. Butyl lactate has antimicrobial activity against various organisms that causes food spoilage, which is important to extend the shelf life of food while avoiding the use of toxic chemicals for disinfecting food (Kavčič *et al.*, 2014). Lactide is an important compound for the medical industry. It is a cyclic ester that is used to

synthesize polylactic acid (PLA). PLA is used to produce bio-based polymeric materials and medical products such as prostheses and membranes in surgery and prosthetics. It is also used in drug delivery and hydrogels due to its biodegradation and safety to human body. Lactide is an expensive dimer due to its difficult and time-consuming synthesis process (Cunha *et al.*, 2022).

Using *Streptomyces* bacteria to produce compounds that are important for the industry will certainly reduce the use of harsh chemicals and their high costs. Further exploration of conditions affecting the production of lactic acid, butyl lactate and lactide are necessary for the food and pharmaceutical industries.

5. Conclusions

Using a one strain many compounds (OSMAC) strategy, specifically media optimization on *Streptomyces* strain CSK1 to enhance antibacterial activity against *S. aureus*, the produced compounds (lactic acid, butyl lactate and lactide) may have valuable significance in food and pharmaceutical industries.

Acknowledgments

This research was funded by University of Sharjah and Sandooq AlWatan (Grant No.0045).

References

- Ahmad MS, El-Gendy AO, Ahmed RR, Hassan HM, El-Kabbany HM, Merdash AG. 2017. Exploring the antimicrobial and antitumor potentials of *Streptomyces* sp. AGM12-1 isolated from Egyptian soil. *Front Microbiol.*, **8**(438):1-11
- Al Farraj DA, Varghese R, Vágvölgyi C, ElshikhMS, Alokda AM, Mahmoud AH. 2020. Antibiotics production in optimized culture condition using low-cost substrates from *Streptomyces* sp. AS4 isolated from mangrove soil sediment. *J King Saud Univ Sci.*, **32**(2): 1528-1535.
- Al-Ansari M, KalaiyarasiM, AlmalkiMA, VijayaraghavanP. 2020. Optimization of medium components for the production of antimicrobial and anticancer secondary metabolites from *Streptomyces* sp. AS11 isolated from the marine environment. *J King Saud Univ Sci.*, **32**(3): 1993-1998.
- Al-Joubori BM. 2020. Identification of novel *Streptomyces* strains with antimicrobial and antitumor activity isolated from terrestrial habitats. Ph.D dissertation. University of Birmingham. Birmingham, United Kingdom.
- Antoraz S, SantamaríaRI, Díaz M, Sanz D, Rodríguez H. 2015. Toward a new focus in antibiotic and drug discovery from the *Streptomyces* arsenal. *Front Microbiol.*, **6**(461): 1-8.
- Bauer AW, Kirby WM, Sherris JC, Turck M. 1966. Antibiotic susceptibility testing by a standardized single disk method. *Am J Clin Pathol.*, **45**(4): 493-6.
- Chandrakar S, Gupta AK. 2019. Actinomycin-Producing Endophytic *Streptomyces parvulus* Associated with Root of Aloe vera and Optimization of Conditions for Antibiotic Production. *Probiotics &Antimicro. Prot.*, **11**(3):1055-1069.
- Chen J, Lan X, Jia R, Hu L, Wang Y. 2022. Response surface methodology (RSM) mediated optimization of medium components for mycelial growth and metabolites production of *Streptomyces alfalfae* XN-04. *Microorganisms*, **10**(9): 1854. <https://doi.org/10.3390/microorganisms10091854>

- Choudoir MJ, Pepe-Ranney C, Buckley DH. 2018. Diversification of secondary metabolite biosynthetic gene clusters coincides with lineage divergence in *Streptomyces*. *Antibiotics*, **7**(1): 1-15.
- Christensen IB, Vedel C, Clausen ML, Kjærulff S, Agner T, Nielsen DS. 2021. Targeted screening of lactic acid bacteria with antibacterial activity toward *Staphylococcus aureus* clonal complex type 1 associated with atopic dermatitis. *Front. Microbiol.*, **12**:733847. <https://doi.org/10.3389/fmicb.2021.733847>
- Clinical and Laboratory Standards Institute (CLSI). 2006. **Methods for Dilution Antimicrobial Susceptibility Tests for Bacteria That Grow Aerobically (M07)**, Seventh Ed. Clinical and Laboratory Standards Institute, Wayne, PA.
- Cunha BLC, Bahú JO, Xavier LF, Crivellin S, de Souza SDA, Lodi L, Jardim AL, Filho RM, Schiavon MIRB, Concha VOC, Severino P, Souto EB. 2022. Lactide: Production Routes, Properties, and Applications. *Bioengineering*, **9**(4):1-21.
- Da Silva IR, Martins MK, Carvalho CM, De Azevedo JL, De Lima Procópio RE. 2012. The Effect of Varying Culture Conditions on the Production of Antibiotics by *Streptomyces* spp., Isolated from the Amazonian Soil. *Ferment Technol.*, **1**(3): 1-5.
- De Rop A, Rombaut J, Willems T, de Graeve M, Vanhaecke L, Hulpiau P, De Maeseneire SL, De Mol ML, Soetaert WK. 2022. Novel alkaloids from marine actinobacteria: Discovery and characterization. *Mar Drugs*, **20**(1):1-23.
- Del Carratore F, Hanko EKR, Breitling R, Takano E. 2022. Biotechnological application of *Streptomyces* for the production of clinical drugs and other bioactive molecules. *Curr Opin Biotechnol.*, **77**: 102762. <https://doi.org/10.1016/j.copbio.2022.102762>
- Donald L, Pipite A, Subramani R, Owen J, Keyzers RA, Taufat. 2022. *Streptomyces*: Still the Biggest Producer of New Natural Secondary Metabolites, a Current Perspective. *Microbiol. Res.*, **13**(3): 418-465.
- Elshikh M, Ahmed S, Funston S, Dunlop P, McGaw M, Marchant R, Banat IM. 2016. Resazurin-based 96-well plate microdilution method for the determination of minimum inhibitory concentration of biosurfactants. *Biotechnol. Lett.*, **38**: 1015-1019.
- Hudzicki J. 2009. Kirby-Bauer Disk Diffusion Susceptibility Test Protocol. *American Society for Microbiology*, **15**: 55-63.
- Hug JJ, Bader CD, Remškar M, Cirsinski K, Müller R. 2018. Concepts and methods to access novel antibiotics from actinomycetes. *Antibiotics*, **7**(2): 1-47.
- Kalaiyarasi M, Ahmad P, Vijayaraghavan P. 2020. Enhanced production antibiotics using green gram husk medium by *Streptomyces* sp. SD1 using response surface methodology. *J King Saud Univ Sci.*, **32**(3): 2134-2141.
- Kavčič S, Knez Ž, Leitgeb M. 2014. Antimicrobial activity of n-butyl lactate obtained via enzymatic esterification of lactic acid with n-butanol in supercritical trifluoromethane. *J. Supercrit. Fluids*, **85**:143-150.
- Keswani C, Singh HB, Hermosa R, García-Estrada C, Caradus J, He YW, Mezaache-Aichour S, Glare TR, Borriss R, Vinale F, Sansinenea E. 2019. Antimicrobial secondary metabolites from agriculturally important fungi as next biocontrol agents. *Appl. Microbiol. Biotechnol.*, **103**(23-24): 9287-9303. <https://doi.org/10.1007/s00253-019-10209-2>
- Khattab AI, Babiker EH, Saeed HA. 2016. *Streptomyces*: isolation, optimization of culture conditions and extraction of secondary metabolites. *Int. Curr. Pharm. J.*, **5**(3): 27-32.
- Khushboo, Kumar P, Dubey KK, Usmani Z, Sharma M, Gupta VK. 2021. Biotechnological and industrial applications of *Streptomyces* metabolites. *Biofuel Bioprod. Biorefin.*, **16**(1): 244-264. <https://doi.org/10.1002/bbb.2294>
- Lacey HJ, Rutledge PJ. 2022. Recently discovered secondary metabolites from *Streptomyces* species. *Molecules*, **27**(3): 887. <https://doi.org/10.3390/molecules27030887>
- Leulmi N, Sighel D, Defant A, Khenaka K, Boulahrouf A, Mancini I. 2019. Enhanced Production and Quantitative Evaluation of Nigericin from the Algerian Soil-Living *Streptomyces youssoufiensis* SF10 Strain. *Fermentation*, **5**(1): 1-9.
- Maithani D, Sharma A, Gangola S, Chaudhary P, Bhatt P. 2022. Insights into applications and strategies for discovery of microbial bioactive metabolites. *Microbiol. Res.*, **261**: 127053. <https://doi.org/10.1016/j.micres.2022.127053>
- Manteca Á, Yagüe P. 2018. *Streptomyces* differentiation in liquid cultures as a trigger of secondary metabolism. *Antibiotics*, **7**(2): 1-13.
- Mary TR, Kannan RR, Iniyan AM, Vincent SG. 2021. Statistical optimization of fermentation media for beta lactamase inhibitor kalafungin production from marine *Streptomyces* sp. SBRK1. *J Appl Biol Biotechnol.*, **9**(3): 89-97
- Moore SJ, Lai HE, Li J, Freemont PS. 2022. *Streptomyces* cell-free systems for natural product discovery and engineering. *Nat. Prod. Rep.*, <https://doi.org/10.1039/d2np00057a>
- Norouzi H, Rabbani khorasgani M, Danesh A. 2019. Anti-MRSA activity of a bioactive compound produced by a marine *Streptomyces* and its optimization using statistical experimental design. *Iran J Basic Med Sci*, **22**(9): 1073-1084.
- Otani H, Udway DW, Mouncey NJ. 2022. Comparative and pangenomic analysis of the genus *Streptomyces*. *Sci. Rep.*, **12**(1): 1 - 6. <https://doi.org/10.1038/s41598-022-21731-1>
- Rakesh KN, Dileep N, Junaid S, Prashith KT. 2014. Optimization of culture conditions for production of antibacterial metabolite by bioactive *Streptomyces* species srdp-tk-07. *Int. J. Adv. Pharm. Sci.*, **5**(1): 1809-1816.
- Romero-Rodríguez A, Maldonado-Carmona N, Ruiz-Villafán B, Koirala N, Rocha D, Sánchez S. 2018. Interplay between carbon, nitrogen and phosphate utilization in the control of secondary metabolite production in *Streptomyces*. *Antonie van Leeuwenhoek*, **111**(5): 761-781.
- Sebak M, Saafan AE, Abdelghani S, Bakeer W, Moawad AS, El-Gendy AO. 2021. Isolation and optimized production of putative antimicrobial compounds from Egyptian soil isolate *Streptomyces* sp. MS. 10. *Beni Suef Univ J Basic Appl Sci*, **10**: 1 - 12.
- Shirling EB, Gottlieb D. 1966. Methods for characterization of *Streptomyces* species. *Int J Syst Bacteriol.*, **16**(3): 313-340.
- Sholkamy EN, Muthukrishnan P, Abdel-Raouf N, Nandhini X, Ibraheem IB, Mostafa AA. 2020. Antimicrobial and antinematocidal metabolites from *Streptomyces cuspidosporus* strain SA4 against selected pathogenic bacteria, fungi and nematode. *Saudi J. Biol. Sci.*, **27**(12): 3208-3220.
- Yun TY, Feng RJ, Zhou DB, Pan YY, Chen YF, Wang F, Yin LY, Zhang YD, Xie JH. 2018. Optimization of fermentation conditions through response surface methodology for enhanced antibacterial metabolite production by *Streptomyces* sp. 1-14 from cassava rhizosphere. *PloS one*, **13**(11): e0206497. <https://doi.org/10.1371/journal.pone.0206497>
- Zhu H, Guo J, Yang S, Sun X, Li Z. 2014. *Streptomyces lactis* and application thereof. *Patent*, CN101619296B.
- Zhu H, Yao Q, Yang S, Li Z, Guo J. 2011. *Streptomyces lacticiproducens* sp. nov., a lactic acid-producing streptomycete isolated from the rhizosphere of tomato plants. *Int J Syst Evol Microbiol.*, **61**(1): 35-39.

Bacteroides fragilis Induce Apoptosis and subG₁/G₁ Arrest Via Caspase and Nrf2 Signaling Pathways in HT-29 Cell Line

Samin Loniakan, Aras Rafiee^{*}, Alireza Monadi

Department of Biology, Central Tehran Branch, Islamic Azad University, Tehran, Iran

Received: July 4, 2022; Revised: December 30, 2022; Accepted: January 9, 2023

Abstract

Background: Although the link between the human microbiome and colorectal cancer has been elucidated over recent years, its underlying mechanisms for various bacteria such as nontoxigenic *Bacteroides fragilis* (NTBF) are still unclear.

Methods: HT29 cells were treated with Non-toxigenic *B. fragilis* Sonicated Extract (NBF-SE), strain ATCC-23745, in the dose (10⁸ and 10⁹ CFU/ml) - and time (24 and 72 hours)-dependent manners. To investigate the cytotoxic impact of NBF-SE on HT29 along with apoptosis-induction and cell cycle distribution, MTT assay and flow cytometry was carried out.

Changes in the expression level of Keap1/NRF2/Caspase3/caspase10/GCLM proposed signaling pathway were conducted by real time PCR analyses.

Results: We found that the NBF-SE had an antiproliferative effect on HT29 cells. In addition, NBF-SE induced sub-G₁ cell cycle cessation and an increment in cell apoptosis, all in a dose- and time-dependent manner. Further, NBF-SE significantly up-regulated Caspase10 and Caspase3 genes, correlated to increased apoptosis. However, Kelch-like ECH-associated protein 1 (KEAP1) and Nuclear factor erythroid 2-related factor 2 (Nrf2) as well as Glutamate-cysteine ligase modulator (GCLM) - mediated antioxidation and anti-apoptosis pathway genes were upregulated, which was in contradiction with apoptosis activation.

Conclusions: We revealed NTBF as a new inducer of cell death confirmed by cytotoxic activity, cell cycle arrest and, increased apoptosis together with NTBF's greater potency in the activation of caspase apoptotic signaling pathway over NRF2/ GCLM antioxidant response. Moreover, NTBF strain ATCC-23745 may be a hidden probiotic and be used for further studies in CRC treatment.

Keywords: non-toxigenic *Bacteroides fragilis*; Colorectal cancer (CRC), apoptosis; cell cycle; Nrf2 Pathway

1. Introduction

The incidence of Colorectal cancer (CRC) ranks third among the most common cancers worldwide and the gut microbiome plays a vital role in its commencement and development. The microbiome is involved in CRC by modulating different cell signaling pathways or by producing metabolites causing tumor progression or suppression (M. Li *et al.*, 2021; Rebersek, 2021). One major gut microbiota species in the human colon is *Bacteroides fragilis*. Based on the existence of *bft* gene which is located on a pathogenicity island and encoded enterotoxin (BFT) or fragilysin, *B. fragilis* strains may be divided into two groups. (I) enterotoxigenic *B. fragilis* (ETBF) strains, containing *bft* gene and, (II) nontoxigenic *B. fragilis* (NTBF) strains, lacking *bft* gene (Claros *et al.*, 2006).

Still, *B. fragilis* plays an intricate role in a way that enterotoxigenic *B. fragilis*-derived toxins induced Diarrhea, inflammatory bowel disease (IBD) and CRC, while non-toxigenic *B. fragilis* (NTBF) promoted mucosal

immune development or suppress colitis and inflammation-associated CRC (Chan *et al.*, 2019; Ryu *et al.*, 2020). NTBF also has a beneficial relationship with the host through modulation of the host's immune response by secreting outer membrane vesicles (OMVs) containing polysaccharide A (PSA). For instance, the T helper cells stimulated by PSA produce interleukin-10 (IL-10), which can prevent IBD or other inflammatory responses (Lee *et al.*, 2018; Wexler, 2007). Besides, some *Bacteroides* spp. like *Bacteroides thetaiotaomicron* (BT) ferment comestible fibers into some short-chain fatty acids (SCFAs) like propionate that repressed several histone methyltransferases which were presumed to have a functional role in CRC growth and metastasis (Okugawa *et al.*, 2015; Ryu *et al.*, 2020). SCFAs can also suppress the expression of proinflammatory cytokines and decrease colonic inflammation in colitis-associated colorectal cancer model (Tian *et al.*, 2018) and offers some protection against *Salmonella* (Jacobson *et al.*, 2018).

B. fragilis extract has a broad spectrum of molecules such as lipopolysaccharide (LPS) also known as endotoxin, amyloids, lipoprotein (LP), and non-coding

^{*} Corresponding author. e-mail: aras_rafiee@yahoo.com, ara.rafiee@iauctb.ac.ir.

^{**} **List of abbreviations** :CRC: colorectal cancer; NBF-SE: *B. fragilis* sonicated extract; nontoxigenic *B. fragilis* (NTBF); KEAP1: Kelch-like ECH-associated protein 1; Nrf2: Nrf-(erythroid-derived 2)-like 2; GCLM: Glutamate-cysteine ligase modulator; LPS: lipopolysaccharide; OMVs: outer membrane vesicles; Casp10: Caspase-10; casp3: caspase-3; PSA: polysaccharide A; AREs: antioxidant response elements; ROS: reactive oxygen species; DISC: death-inducing signaling complex

RNAs (Lukiw *et al.*, 2019; Zamani *et al.*, 2020) that raise the generation of reactive oxygen species (ROS) (Ko *et al.*, 2020; Zhao *et al.*, 2014), leading to oxidative stress-induced cell damage. Thereby, multiple antioxidant defense systems may be activated. For instance, ROS overproduction oxidizes cysteines within KEAP1 which causes segregation of KEAP1 from NRF2. Hence, NRF2 activates without its suppressor (KEAP1) and interacts with antioxidant response elements (AREs) in the regulatory regions of over 200 genes to mediate cellular antioxidant responses (Liu *et al.*, 2021; Schieber *et al.*, 2014). Moreover, antioxidant pathways associated with NRF2 also increase the synthesis of endogenous antioxidant glutathione (GSH). GSH synthesis requires Glutamate Cysteine Ligase (GCL) enzyme which is comprised of 2 sub-units defined as catalytic (GCLC) and modifier (GCLM) subunits. The promoters for both GCLC and GCLM consist of AREs (Bea *et al.*, 2003; Saha *et al.*, 2020). Also, there is evidence that ROS overproduction disrupts mitochondrial membrane integrity, accompanied by the dislodge of cytochrome c from mitochondria into the cytoplasm to recruit cell initiator caspases. Caspase-10 is a key initiator caspase that cleaves and activates caspases 3 and 7. Over-activation of some caspases such as caspase-3 can lead to abrupt cell death (Bell *et al.*, 2017).

Therefore, we discussed the effects of non-toxicogenic *B. fragilis* sonicated extract on cell viability, cell cycle and apoptosis of HT-29 cells in addition with the underlying Keap1/NRF2/Caspase3/caspase10/GCLM molecular pathway.

2. Materials and Methods

2.1. Bacterial culture and preparation of sonication-assisted extraction

NTBF *B. fragilis* (ATCC 23745) was obtained in a freeze-dried form (Pasteur Inst., Iran). The culture was performed in an anaerobe chamber. 1.0 mL of brain heart infusion (BHI) broth (Merck) was poured on a lyophilized bacterial pellet to rehydrate the entire content, then the aliquot was transferred into the tube containing 9 mL of BHI broth. Several drops of the suspension were inoculated on BHI agar, to check for purity. The cultures were placed in the anaerobe chamber at 37°C. At the exponential phase, bacterial cells were centrifuged. The bacterial pellet was washed and re-suspended with PBS to OD₆₀₀ = 1.0 (equivalent to approximately 10⁹ CFU/ml). Other needed concentrations were also adjusted using PBS. 10⁹ CFU per ml concentration of *B. fragilis* was lysed using an ultrasonic homogenizer (Hielscher) and then was directly sterilized by a 0.22-µm filter membrane (Bioyfil). Filtrates were stocked in aliquots at -80 °C until required (Li *et al.*, 2017).

2.2. Cell culture

HT-29 human colorectal adenocarcinoma cells (National Cell Bank, Iran) were cultured in RPMI 1640 (Bioidea) with 1% penicillin/streptomycin (Invitrogen) and 10% fetal bovine serum (Bioidea) in a CO₂ incubator (HEPA, Thermo Fisher Scientific, Inc).

2.3. MTT cytotoxicity assay

The toxicity effect of *B. fragilis* sonicated extract (NBF-SE) was analyzed by using MTT assay (Sigma-

Aldrich, Merck). Briefly, the 5×10⁴ HT-29 cells/well were cultured in 96-well plates overnight and then treated with 10% (10⁸ CFU/ml) and 100% (10⁹ CFU/ml) concentrations of NBF-SE for 24 and 72 h. Negative controls were treated with equal volumes of BHI containing RPMI1640 medium. After this time of incubation, cells were further incubated with MTT solution (Merck, Germany) for one hour. Thereafter, DMSO was added and the plates were shaken for 20 minutes on a shaker. The absorbance of well plates was read by microplate reader (BIO-RAD) at 570 nm. All the experiments were replicated three times. Below is the formula used to calculate the survival percentage:

$$\% \text{ Cell viability} = \frac{(\text{Mean OD}_{\text{Sample}} - \text{Mean OD}_{\text{blank}})}{(\text{Mean OD}_{\text{Negative control}} - \text{Mean OD}_{\text{blank}})} \times 100.$$

2.4. Quantitative Real-Time PCR

After treatment of HT-29 cells with 10⁹ CFU/ml NBF-SE for 24h, total RNA was isolated using the Cinnagen RNX extraction kit (Iran). RNA concentration and purity were assessed by measuring the absorbance at 260/280nm with the Spectrophotometer (BioTeck). The cDNA was synthesized utilizing the easy cDNA synthesis kit (Parstous, Iran) following the manufacturer's guideline. qRT-PCR was performed using RealQ Plus 2x Master Mix Green kit (Ampliqon). The reactions were carried out in MyGo Pro real-time PCR Thermocycler (IT-IS Life Science). Primers were designed using IDT, and Primer 3 online software and were synthesized by Sinaclon. The primer sequences are reported in Table 1.

Table 1. Sequence of used primer pairs in qPCR.

Primer sequence (5'→3')		
KEAP1	Forward	AGACGTGGACTTTCGTAGCC
	Reverse	CCAGGAACGTGTGACCATCA
NRF-2	Forward	AGCCCTGTGTGATTAGACGG
	Reverse	TGTCAGTTTGGCTTCTGGACT
GCLM	Forward	ACAGCCTTACTGGGAGGAATTA
	Reverse	ACCTGTGCCCCACTGATACA
CASP 3	Forward	TGGAGGCCGACTTCTGTATG
	Reverse	GCACAAAGCGACTGGATGAAC
CASP 10	Forward	CCGACAAAGGGTTTCTCTGT
	Reverse	TTGGGAAGCGAGTCTTTCAG
Gapdh	Forward	GTGGTCTCTCTGACTTCAAC
	Reverse	GGAAATGAGCTTGACAAAGTGG
Hprt1	Forward	AAGGGTGTATTATCCTCATGGAC
	Reverse	AGCACACAGAGGGCTACAA

The qPCR data was analyzed by Livak method ($2^{-\Delta\Delta CT}$) (Livak *et al.*, 2001) and normalized by the expression levels of housekeeping gene, GAPDH and HPRT.

2.5. Apoptosis analyses

In order to confirm whether the cytotoxicity induced by NBF-SE is indeed due to apoptosis,

Annexin-V Apoptosis Detection kit (BioLegend) was used. Briefly, HT29 Cells were seeded in 6-well plates and

incubated with 10^8 and 10^9 CFU/ml of NBF-SE for 24 and 72 h. The RPMI media containing BHI was used as a negative control. Following treatment, the cells were incubated with Annexin V/ propidium iodide (5 μ l each) for 15 min under room temperature. Finally, the apoptotic cells were detected by a flow cytometer (BD FACSCalibur) and analyzed by FLOWJO software (USA).

2.6. Apoptotic index (AI) percentage

AI was measured by dividing the % apoptotic cells (AnnexinV⁺) over the % total cells (AnnexinV⁺ plus AnnexinV⁻) using the following formula: %AnnexinV⁺ cells (apoptotic cells) / (%AnnexinV⁺ cells + %AnnexinV⁻ (Q1)) (Prieto *et al.*, 2002).

2.7. Cell Cycle Analysis

HT-29 cells were plated on 6-well plates. The following day, cells were treated with 10^8 CFU/ml of NBF-SE for 24 and 72 h. The RPMI media containing BHI was used as a negative control. After the specified time, cells were trypsinized, then harvested and rinsed with PBS and finally fixed in 70% ethanol. The fixed cells were suspended in staining solution containing PI/RNase A (50 μ g/mL of each) for 20 min. The relative proportions of cells distributed in each cycle regions were calculated by flow cytometer (BD Biosciences).

2.8. Statistical analysis

Scientific software, Graphpad Prism 7.0, was used for analysis, graphing and statistical evaluation. Significant differences among multiple groups were determined using an unpaired Student's t-test, one-way analysis of variance (ANOVA) and, tukey's multiple comparisons test evaluate the main effect of NBF-SE on HT-29 cells. Data were reported as the mean \pm standard error of the mean (SEM) and were considered statistically significant when the P value was * $p < 0.05$, ** $p < .01$, and *** $p < .001$ and, **** $p < .0001$ and indicated in the figures.

3. Results

3.1. Declines in HT-29 cell viability following NBF-SE exposure

With the intention of investigating the cytotoxicity of the obtained NBF-SE, the MTT assay was performed in two different concentrations (10^8 and 10^9 CFU/ml) and times (24 and 72h). As shown in figure 1, cell survival of

HT-29 cells treated with NBF-SE was significantly decreased in comparison with the control group in a time and dose-related manner compared to the control group. The inhibitory concentration (IC₅₀) of NBF-SE was $\sim 10^9$ CFU/ml after 24 h.

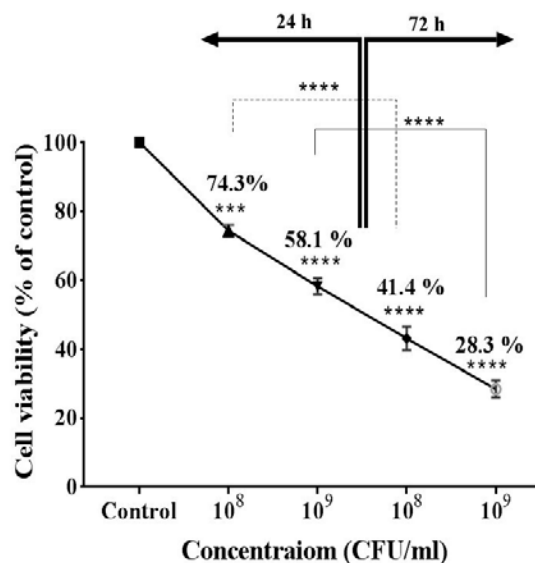


Figure 1. HT29 cells were treated with two different concentration of NBF-SE (10^8 and 10^9 CFU/ml) for 24 and 72h, then the cytotoxicity effect was measured by MTT assay. NBF-SE decreased the cell survival in a dose- time dependent manner. The results are reported as survival percentages compared with the control ($p < 0.05$, * $p < .05$, ** $p < .01$, *** $p < .001$ and, **** $p < .0001$). The lines drawn at the top of the charts indicate a significant comparison between the different groups.

3.2. Apoptotic induction in HT-29 Cells treated with NBF-SE

To examine whether NBF-SE has an apoptotic effect on HT29 over time and dose, annexin V/PI double staining was performed.

As shown by Fig 2A-F, NBF-SE clearly induced early and late apoptosis from a dose and time-dependent aspect compared with the control groups. Additionally, in both cases, increasing the concentration of NBF-SE from 10^8 to 10^9 CFU/ml and increasing the duration of exposure from 24 h to 72 h, has raised the percentage of the apoptotic index (AI) (Fig 2G, H).

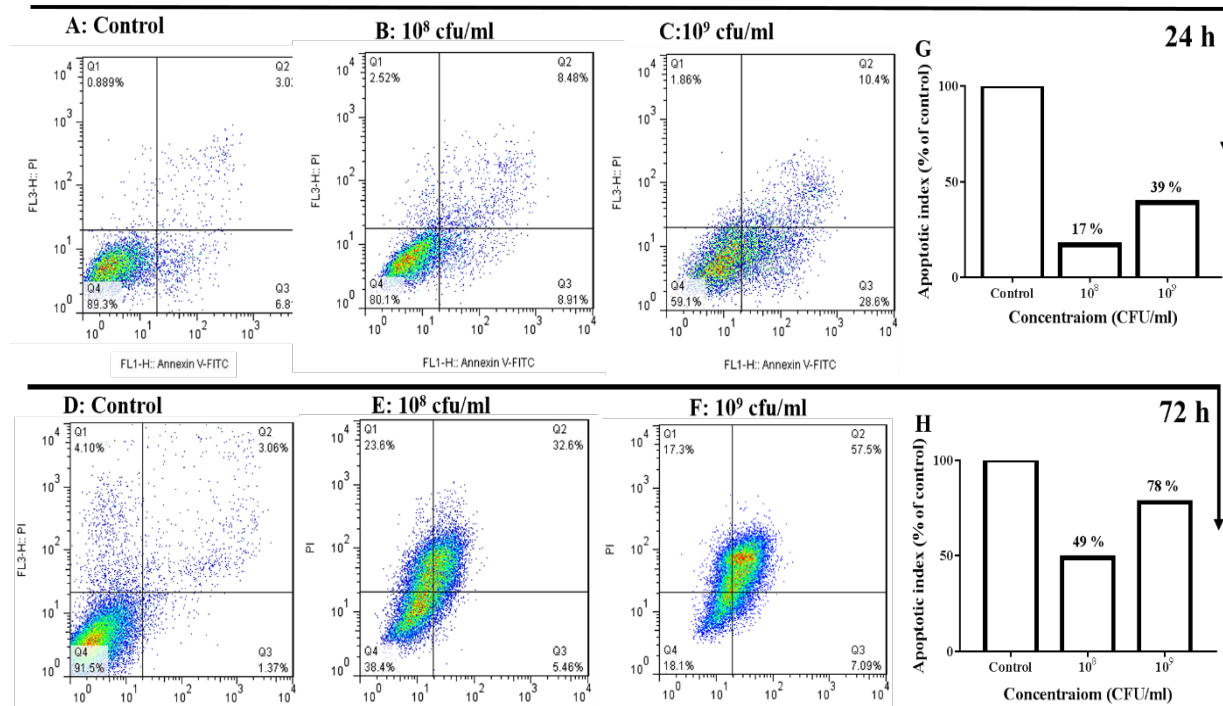


Figure 2. NBF-SE led to a significant increase in the percentage of apoptotic cells from a concentration and duration-dependent aspect. (A-F) Flow cytometry analysis was carried out after HT29 cells were treated with 10^8 and 10^9 CFU/ml NBF-SE for 24 and 72 h. The quadrants are as follows: Lower left belongs to viable cells, upper left shows necrotic cells, and lower right and upper right belongs to early and late apoptosis respectively. Apoptotic index (%) of HT-29 cells after 24 and 72, respectively (G, H).

3.3. NBF-SE induces subG1/G1 cell cycle arrest

Since cell cycle progression is one of the effective mechanisms in cell proliferation, any ingredient that arrests the cell cycle can be considered a possible candidate for an anti-cancer substance.

So, to better clarify the NBF-SE inhibitory effect, HT-29 cells were subjected to 10^8 CFU/ml NBF-SE for 24 and 72 h. Then cell subpopulations in sub-G1, G1, S and G2 phases were defined by flow cytometry. Percentage of cells in each phases of cell cycle showed a time-dependent Sub-G1 arrest. During 24h, NBF-SE treated cells showed a higher SubG1- G1 cell population (2.8%) compared to the control (subG1:0.9%), even though it was not statistically significant (Fig. 3). A concomitant reduction in S and G2 phase after 24h was also observed. Meanwhile, the extent of changes at 72h was more evident so that the ratio of treated cells in the sub-G1 phase (apoptotic cell population) was significantly increased from 2.8% to 42.2%. The significant observable decreases in cells at the G, S and, G2 illustrated no cell cycle arrest in those phases. This experiment suggested that NBF-SE induces growth arrest in subG1-phase.

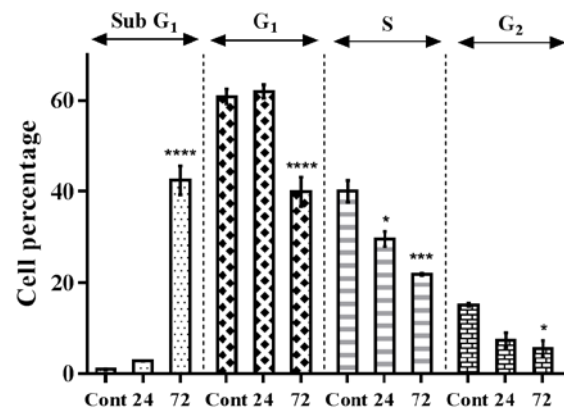


Figure 3. NBF-SE induces subG1-phase cell cycle arrest in HT-29 cells. Cells were treated with 10^8 CFU/ml NBF-SE for 24 h and 72 h, then the percentage of cells in each sub-G1, G1, S, and G2 phases of the cell cycle was calculated. Control groups are indicated as (Cont) and treated cells are indicated as 24 (24 h treatment) and 72 (72 h treatment). Each of the phases of the cell cycle is marked with an arrow at the top of the corresponding columns. Each data point represents the mean (\pm SEM) of three independent experiments ($P < 0.05$: *, $P < 0.01$: **, $P < 0.001$: *** and, $p < 0.0001$: ****).

3.4. Effect of NBF-SE on the expression of apoptosis-related genes

It was noticed in our previous test that the NBF-SE led to the subG1-phase cessation, which was conducted towards apoptotic cell death. In order to discover the cellular pathway which led to apoptosis, we investigated the NBF-SE effect on the expression of a hypothetical path consisting of Keap1/NRF2/ GCLM/Casp10/Casp3 genes. The relative expression of genes was measured by $2^{-\Delta\Delta Ct}$ method using GAPDH (Figure 4A) and HPRT (Figure 4B) housekeeping genes as normalizers. However, due to the lower variation in GAPDH expression (lower ΔCt values) compared to HPRT, GAPDH was chosen to report the results.

As shown in figure 4, significant over expression of 5 mediated apoptotic genes was observed after HT-29 cells were incubated with NBF-SE (10^8 CFU/ml) for 24 h. These results indicate that NBF-SE stimulated the transcriptional induction of NRF2 and its antioxidant response gene, GCLM. Additionally, increased expression levels of *initiator caspase-10* and executioner caspases-3 were observed.

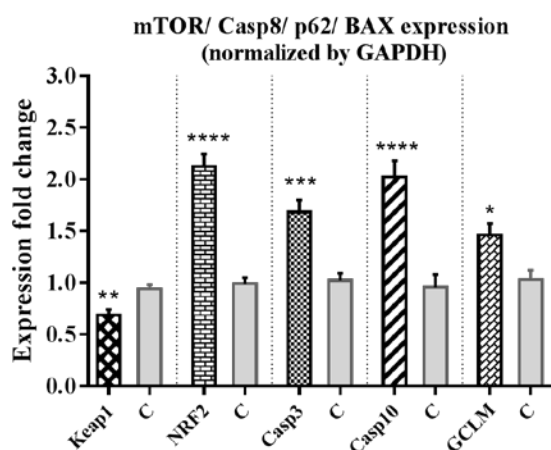


Figure 4. NBF-SE effect on the expression of hypothetical path consisting of the Keap1/NRF2/ GCLM/Casp10/Casp3-mediated apoptotic genes. HT-29 cells were exposed to 10^8 CFU/ml NBF-SE for 24 h. The relative expression of target genes was computed using A) GAPDH and B) HPRT as normalizers. The expression changes compared with control (denoted as 'C') are mentioned in diagrams as fold change. Data are represented as means (\pm SEM) of three independent experiments ($P < 0.05$: *, $P < 0.01$: **, $P < 0.001$: *** and $P < 0.0001$: ****). HT-29 cells treated with NBF-SE didn't show a significant change in Keap1 expression ($P > 0.05$).

4. Discussion

Commensal gut microbiota actuates the immune system of the host, resulting in protective responses against pathogens (Bae *et al.*, 2022), supplied the host with essential nutrients, metabolize indigestible carbohydrates, and produce certain nutrients such as short-chain fatty acids (Sánchez-Alcoholado *et al.*, 2020). *B. fragilis* can be considered a friendly commensal. The capsular Polysaccharide A (PSA) of *B. fragilis* is capable of stimulating T helper cells to produce anti-inflammatory cytokine IL-10, which is essential to mediate the generation of a normal mature immune system and

preventing abscess formation (Chang *et al.*, 2017; Lee *et al.*, 2018; Wexler, 2007). It has been shown that the treatment of CRC cells with purified PSA from *B. fragilis* inhibited the proliferation of CRC cells via the production of the IL-8 pro-inflammatory cytokine and suppressed cell migration and progression of the cell cycle (Sittipo *et al.*, 2018). Furthermore, most approved probiotics based on intestinal microbiota belong to lactic acid bacteria (LAB), but new species and genera are being assessed for future use. Recently, a new strain of *B. non-toxigenic fragilis* named ZY-312 is shown to exert beneficial probiotic effects and was recommended as the first probiotic candidate from the phylum Bacteroidetes (Deng *et al.*, 2016; Wang *et al.*, 2017).

Therefore, we believe non-toxigenic *B. fragilis* strain ATCC-23745 can be a fine choice to explore its capability as probiotic bacteria on growth inhibition, apoptosis induction, and blocking the cell cycle. Hence, in the present study, we assessed the impact of non-toxigenic *B. fragilis* strain ATCC-23745 sonicated extract (NBF-SE) on the colorectal adenocarcinoma HT29 cells. Our findings revealed a significant reduction of viable cells after co-incubation of HT29 cells with NBF-SE over time- and dose-dependent manner. Similarly, NBF-SE was associated in triggering early and late apoptosis of HT-29 cells depending over the time and dose of exposure, also could raise apoptotic index (AI) about 1.5-2-fold more than the control. This was also confirmed using qRT-PCR analysis. We observed greater expression of caspase-10 and caspase-3 genes, which indicated the caspase-dependent apoptosis following NBF-SE treatment.

In a relevant work using nontoxigenic *B. fragilis* ATCC 23745 strain (Miranda *et al.*, 2008) similar to that of our study, the phenylacetic acid (PA) of the sonicated extract could both induced vacuolating effect on Vero cells and peritoneal macrophages and increased apoptotic cell death (Falcão *et al.*, 2015).

Since excessive proliferation is a well-recognized hallmark of human cancer, therefore any agent that can arrest cancer cell cycles may be an efficient anticancer substance. By using flow cytometry analyses, we noted a time-dependent inhibitory effect of NBF-SE on HT-29 cells which was reliant on the cell cycle (sub-G1 phase) arrest. The percentage of sub-G1 cells increased significantly (42.2%) after 72 h, while the percentage of cells decreased about 2-3 fold at S and G2 phases after both 24 and 72 h.

Genetic research on *B. fragilis* suggested the downregulation of cell cycle-activating genes in HT29 cells treated with e those effective concentrations of *B. fragilis* PSA (Sittipo *et al.*, 2018).

However, there is something that contradicts the probiotic bacteria property in favor of human health. LPS, the major component of non-toxigenic *B. fragilis* outer membrane, is capable of stimulating apoptosis-inducing receptors. These transmembrane receptors then bind to other proteins to stablish DISC assembly and ROS overproduction. Upon the formation of DISC, apical initiator caspase 8 activates effector caspase 3, leading to apoptosis (Wachmann *et al.*, 2010). Also, these byproducts result in antioxidant pathways induced by NRF2 for maintaining the stability of cell's internal environment. There was also a report that LPS increased the expression of proapoptotic factor (BAX) and Nrf2 in wild-type (WT)

mice. Nrf2 then separates from its inhibitor, Keap1 and targets its downstream antioxidant response elements (AREs) such as GCLC and GCLM (two subunits of glutamate cysteine ligase) (Y. Li *et al.*, 2021).

Therefore, we detected the levels of Keap1/Nrf2/Caspase3/caspase10/GCLM to estimate the intracellular homeostasis state. Significant upregulation of Nrf2 and GCLM (Nrf2 target gene) and downregulation of Keap1 (Nrf2 inhibitor), reveals the activation of the antioxidant and anti-apoptosis pathway. The implementation of this protective path was against NBF-SE -induced oxidative damage. However, by looking at the results of casp10 and casp3 overexpression, increased cell apoptosis and, greater cell populations in sub-G1 phase (apoptotic cells), we speculate that the induction of Nrf2/GCLM expression was blunted by NBF-SE. This may be due to greater potency of caspase apoptotic signaling over NRF2/GCLM antioxidant pathway (Fig 5).

non-toxicogenic *B. fragilis* sonicated extract (NBF-SE)

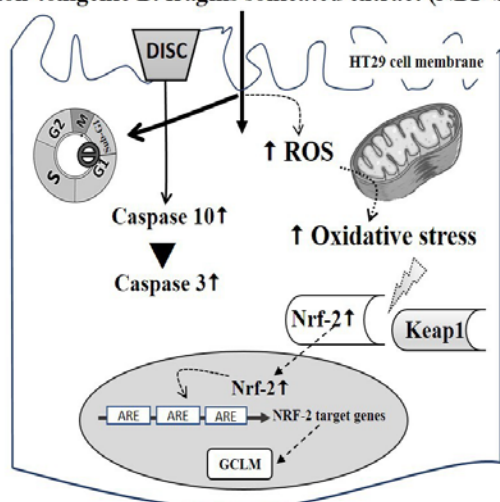


Figure 5. Possible mechanism of NBF-SE- induced apoptosis in HT29 cells. Stimulation of extrinsic death receptor-dependent pathways triggers the activation of the death-inducing signaling complex (DISC). This complex may then recruit a caspase-dependent cell execution pathway via the caspase-10 caspase-3 route, leading directly to apoptosis. Furthermore, during the stressed conditions, the amount of cellular NRF2 increased upon exposure to oxidative stress, ROS overproduction and oncogenic signaling. ROS reaction with sensor cysteines of KEAP1 protein disrupts the KEAP1-NRF2 complex. Nrf2 then translocates into the nucleus and targets its downstream antioxidant response elements (AREs) such as GCLC and GCLM (two subunits of glutamate cysteine ligase) to address oxidant stress. Dotted lines (---) indicate the weak path and continuous lines (—) indicate the main dominant pathway.

To clarify the validity, it is suggested to re-measure the apoptosis level and expression of caspases after increasing the expression of Nrf2 mRNA in cells by the Nrf2 expression vector. We also suggest 1- finding more involved apoptosis signaling pathways correlated to CRC, 2- scanning of effective apoptotic substances in NBF-SE and 3- examining additional cancer and normal cell lines along with untried recent microbiota.

5. Conclusions

In conclusion, we have demonstrated that NBF-SE eventuates in an antiproliferative and apoptotic effect on

human CRC cell line along with arresting the cell cycle progression in the subG₁ phase dependent over the time and dose of exposure. We have also uncovered that NBF-SE promoted apoptosis through the Casp10/Casp3 signaling pathway while making the antiapoptotic Keap1/Nrf2/ GCLM path less effective.

Funding

No funding to declare.

Acknowledgements

We thank Shoheila Zamanlui Benisi, Zahra Shahi, Arash Abednezhad, and Mohammad Daroon parvar for their skilled technical assistance. The authors are grateful to the Microbiology, Molecular biology laboratories and, Tissue Engineering Research Institute of the Islamic Azad University of Central Tehran Branch.

References

- Bae J, Park K, and Kim Y-M. 2022. Commensal microbiota and cancer immunotherapy: harnessing commensal bacteria for cancer therapy. *Immune Netw.*, **22**(1).
- Bea F, Hudson F N, Chait A, Kavanagh T J, and Rosenfeld M E. 2003. Induction of glutathione synthesis in macrophages by oxidized low-density lipoproteins is mediated by consensus antioxidant response elements. *Circ. Res.*, **92**(4):386-393.
- Bell R A, and Megeney L A. 2017. Evolution of caspase-mediated cell death and differentiation: twins separated at birth. *Cell Death Differ.*, **24**(8):1359-1368.
- Chan J L, Wu S, Geis A L, Chan G V, Gomes T A, Beck S E, Wu X, Fan H, Tam A J, and Chung L. 2019. Non-toxicogenic *Bacteroides fragilis* (NTBF) administration reduces bacteria-driven chronic colitis and tumor development independent of polysaccharide A. *Mucosal immunol.*, **12**(1):164-177.
- Chang Y-C, Ching Y-H, Chiu C-C, Liu J-Y, Hung S-W, Huang W-C, Huang Y-T, and Chuang H-L. 2017. TLR2 and interleukin-10 are involved in *Bacteroides fragilis*-mediated prevention of DSS-induced colitis in gnotobiotic mice. *PLoS One.*, **12**(7):e0180025.
- Claros M, Claros Z, Hecht D, Citron D, Goldstein E, Silva Jr J, Tang-Feldman Y, and Rodloff A. 2006. Characterization of the *Bacteroides fragilis* pathogenicity island in human blood culture isolates. *Anaerobe.*, **12**(1):17-22.
- Deng H, Li Z, Tan Y, Guo Z, Liu Y, Wang Y, Yuan Y, Yang R, Bi Y, and Bai Y. 2016. A novel strain of *Bacteroides fragilis* enhances phagocytosis and polarises M1 macrophages. *Sci. Rep.*, **6**(1):1-11.
- Falcão L S, Antunes E N, Ferreira E O, Pauer H, Romanos M T V, Vommaro R C, Seabra S H, Alviano D S, Alviano C S, and da Silva A J R. 2015. *Bacteroides fragilis* Supernatant Extracts Enriched in Phenylacetic Acid Induce a Cytotoxic Effect in Mammalian Cells. *Adv. Appl. Microbiol.*, **5**(10):730.
- Jacobson A, Lam L, Rajendram M, Tamburini F, Honeycutt J, Pham T, Van Treuren W, Pruss K, Stabler S R, and Lugo K. 2018. A gut commensal-produced metabolite mediates colonization resistance to *Salmonella* infection. *Cell host microbe.*, **24**(2):296-307. e297.
- Ko S H, Jeon J I, Woo H A, and Kim J M. 2020. *Bacteroides fragilis* enterotoxin upregulates heme oxygenase-1 in dendritic cells via reactive oxygen species-, mitogen-activated protein kinase-, and Nrf2-dependent pathway. *WJG, World J Gastroenterol.*, **26**(3):291.

- Lee Y, Mehrabian P, Boyajian S, Wu W, Selicha J, Vonderfecht S, and Mazmanian S. 2018. The protective role of *Bacteroides fragilis* in a murine model of colitis-associated colorectal cancer. *mSphere* 3: e00587-18. In).
- Li M, and Wang F. 2021. Role of Intestinal Microbiota on Gut Homeostasis and Rheumatoid Arthritis. *J. Immunol. Res.*, **2021**.
- Li Y, Shao J, Hou P, Zhao F-Q, and Liu H. 2021. Nrf2-ARE Signaling Partially Attenuates Lipopolysaccharide-Induced Mammary Lesions via Regulation of Oxidative and Organelle Stresses but Not Inflammatory Response in Mice. *Oxid. Med. Cell. Longev.*, **2021**.
- Li Z, Deng H, Zhou Y, Tan Y, Wang X, Han Y, Liu Y, Wang Y, Yang R, and Bi Y. 2017. Bioluminescence imaging to track *Bacteroides fragilis* inhibition of *Vibrio parahaemolyticus* infection in mice. *Front. cell. infect.*, **7**:170.
- Liu H, Xu X, Wu R, Bi L, Zhang C, Chen H, and Yang Y. 2021. Antioral Squamous Cell Carcinoma Effects of Carvacrol via Inhibiting Inflammation, Proliferation, and Migration Related to Nrf2/Keap1 Pathway. *Biomed Res. Int.*, **2021**.
- Livak K J, and Schmittgen T D. 2001. Analysis of relative gene expression data using real-time quantitative PCR and the 2- $\Delta\Delta CT$ method. *methods.*, **25**(4):402-408.
- Lukiw W J, Li W, Bond T, and Zhao Y. 2019. Facilitation of gastrointestinal (GI) tract microbiome-derived lipopolysaccharide (LPS) entry into human neurons by amyloid beta-42 (A β 42) peptide. *Front. Cell. Neurosci.*, **13**:545.
- Miranda K R, Dias M F, Guimarães P L, Boente R F, Pauer H, Ramos P Z, Falcão L S, Ferreira E d O, Balassiano I T, and Ferreira L Q. 2008. Enterotoxigenic and nontoxigenic *Bacteroides fragilis* strains isolated in Brazil. *Mem. Inst.*, **103**(7):734-735.
- Okugawa Y, Grady W M, and Goel A. 2015. Epigenetic alterations in colorectal cancer: emerging biomarkers. *Gastroenterology.*, **149**(5):1204-1225. e1212.
- Prieto A, Díaz D, Barcenilla H, García-Suárez J, Reyes E, Monserrat J, San Antonio E, Melero D, de la Hera A, and Orfao A. 2002. Apoptotic rate: a new indicator for the quantification of the incidence of apoptosis in cell cultures. *Cytom: j. Int. Soc. Anal. Cytol.*, **48**(4):185-193.
- Rebersek M. 2021. Gut microbiome and its role in colorectal cancer. *BMC cancer.*, **21**(1):1-13.
- Ryu T Y, Kim K, Han T-S, Lee M-O, Lee J, Choi J, Jeong E-J, Jung C-R, Jung J, and Park K. 2020. Histone methyltransferase EHMT2 degradation by propionate derived from *Bacteroides thetaiotaomicron* induced colon cancer apoptosis via epigenetic regulation of TNFAIP1.
- Saha S, Buttari B, Panieri E, Profumo E, and Saso L. 2020. An overview of Nrf2 signaling pathway and its role in inflammation. *Molecules.*, **25**(22):5474.
- Sánchez-Alcoholado L, Ramos-Molina B, Otero A, Laborda-Illanes A, Ordóñez R, Medina J A, Gómez-Millán J, and Queipo-Ortuño M I. 2020. The role of the gut microbiome in colorectal cancer development and therapy response. *Cancers.*, **12**(6):1406.
- Schieber M, and Chandel N S. 2014. ROS function in redox signaling and oxidative stress. *Curr.* **24**(10):R453-R462.
- Sittipo P, Lobionda S, Choi K, Sari I N, Kwon H Y, and Lee Y K. 2018. Toll-like receptor 2-mediated suppression of colorectal cancer pathogenesis by polysaccharide A from *Bacteroides fragilis*. *Front Microbiol.*, **9**:1588.
- Tian Y, Xu Q, Sun L, Ye Y, and Ji G. 2018. Short-chain fatty acids administration is protective in colitis-associated colorectal cancer development. *J. Nutr. Biochem.*, **57**:103-109.
- Wachmann K, Pop C, van Raam B J, Drag M, Mace P D, Snipas S J, Zmasek C, Schwarzenbacher R, Salvesen G S, and Riedl S J. 2010. Activation and specificity of human caspase-10. *Biochem.*, **49**(38):8307-8315.
- Wang Y, Deng H, Li Z, Tan Y, Han Y, Wang X, Du Z, Liu Y, Yang R, and Bai Y. 2017. Safety evaluation of a novel strain of *Bacteroides fragilis*. *Front Microbiol.*, **8**:435.
- Wexler H M. 2007. *Bacteroides*: the good, the bad, and the nitty-gritty. *Clin. Microbiol. Rev.*, **20**(4):593-621.
- Zamani S, Taslimi R, Sarabi A, Jasemi S, Sechi L A, and Feizabadi M M. 2020. Enterotoxigenic *Bacteroides fragilis*: a possible etiological candidate for bacterially-induced colorectal precancerous and cancerous lesions. *Front. cell. infect.*, **9**:449.
- Zhao C, Gillette D D, Li X, Zhang Z, and Wen H. 2014. Nuclear factor E2-related factor-2 (Nrf2) is required for NLRP3 and AIM2 inflammasome activation. *JBC.*, **289**(24):17020-17029.

Effects of Spirulina on Some Oxidative Stress Parameters and Endurance Capacity in Regular and Strenuous Exercises

Mehmet OZ^{1,*}, Hakkı GOKBEL²

¹Department of Physiology, Faculty of Medicine, University of Aksaray, Aksaray, Turkey; ²Department of Physiology, Faculty of Medicine, University of Selçuk, Konya, Turkey

Received: September 28, 2022; Revised: December 30, 2022; Accepted: January 10, 2023

Abstract

Objective: We examined the effects of spirulina supplementation on oxidative status in plasma, liver and muscle tissue and endurance capacity in moderate and exhaustive swimming exercise in rats.

Method: Animals were divided into six groups: control, spirulina (SP), chronic exercise (CE), chronic exercise with spirulina (CES), exhaustive exercise (E), and exhaustive exercise with spirulina (ES). Spirulina was administered orally to rats in the SP, CES and ES groups at a dose of 750 mg/kg per day for 6 weeks. The chronic exercise groups underwent swimming exercise for 1 hour/day for 6 weeks. Animals from groups E and ES were subject to exhaustive exercise stress. Creatine kinase (CK), CK-MB, lactate dehydrogenase activities, and uric acid levels were determined in the plasma, whereas malondialdehyde levels and MPO, XO, SOD, CAT, GPx and antioxidant activities were measured in plasma, liver and muscle tissues.

Results: Spirulina supplementation attenuated the increase in plasma CK activity induced by exhaustive exercise. Although chronic exercise increased plasma SOD activity, it promoted decreases in liver tissue XO activities and MDA levels as well as muscle tissue MDA levels. Exhaustive exercise reduced liver CAT activities, whereas plasma CAT activities increased. Spirulina supplementation had no effect on endurance capacity in a single session of exhaustive swimming exercise.

Conclusion: We concluded that spirulina platensis, ameliorates increases in the plasma activities of CK, probably by decreasing pre-oxidative MDA levels in skeletal muscle.

KeyWords: Exercise, oxidative stress, antioxidant status, spirulina, muscle damage, endurance capacity

1. Introduction

The production of reactive oxygen species (ROS) is an inevitable result of cellular metabolism. Organisms protect themselves against the harmful effects of ROS via the “antioxidant defense” system that serves to scavenge free radicals. The defense system utilizes several enzymatic and nonenzymatic antioxidant modalities such as superoxide dismutase (SOD), glutathione peroxidase (GPx), catalase (CAT), reduced glutathione (GSH), vitamin E, and vitamin C. In stressful situations, ROS production increases with a concomitant decrease in the efficacy of the antioxidant defense system, resulting in “oxidative stress,” which is defined as a disturbance of the balance between prooxidative and antioxidative processes in favor of prooxidation (Fisher-Wellman and Bloomer, 2009). Intense physical exercise is a factor that provokes oxidative stress. Exhaustive physical exercise, which dramatically increases oxygen consumption, escalates free radical production, resulting in the lipid peroxidation of polyunsaturated fatty acids in cellular membranes, and reduces antioxidant activities in blood and various tissues (Minato *et al.*, 2003; Chang *et al.*, 2007; Choi and Cho, 2009). Malondialdehyde (MDA) and thiobarbituric acid-reactive substances (TBARS) are widely used indicators of exercise-induced tissue injury (Fisher-Wellman and

Bloomer, 2009). Exhaustive exercise also leads to increments of plasma and skeletal muscle xanthine oxidase (XO) and myeloperoxidase (MPO) activities (Liu *et al.*, 2005). Although a single session of exhaustive exercise can generate excessive amounts of ROS due to intense oxygen consumption (Davies *et al.*, 1982), regular exercise has numerous health benefits including reduced risks of cancer, diabetes, and cardiovascular disease (Blair *et al.*, 2001; Powers and Jackson, 2008). The antioxidant defense capacity of sedentary people can be easily overburdened under conditions such as acute physical exercise; therefore, the consumption of products containing exogenous antioxidants (i.e. foods or supplements) may help sedentary individuals manage oxidative stress during exercise (Bucioli *et al.*, 2011).

Spirulina is a spiral-shaped microscopic blue-green alga that lives in both freshwater and saltwater and contains approximately 60%–70% protein. It is widely used as a human and animal supplement because of its high-grade protein, iron, gamma-linolenic acid, carotenoid, vitamin B1, vitamin B2, vitamin B12, provitamin A (beta-carotene), vitamin C, vitamin E, selenium, C-phycocyanin, and flavonoid content. In addition, dietary supplementation of spirulina has been reported to attenuate exercise-induced muscle injury. In a study of spirulina supplementation in 16 college students for 3 weeks, Lu *et al.* (2006) found that spirulina is protective against

* Corresponding author. e-mail: ozmhmt@gmail.com.

exhaustive exercise-induced skeletal muscle damage, probably by decreasing prooxidative activity. Kalafati *et al.* (2010) administered 6 g/day spirulina to nine moderately trained male athletes and reported that this supplementation boosted fat oxidation and exercise performance while decreasing lipid peroxidation. Spirulina supplementation improves antioxidant capacity and inflammation markers and decreases lipid peroxidation in rats subjected to strength training (Brito *et al.*, 2020). It has healing effects on intense exercise-induced muscle damage and inflammation in elite rugby players (Chaouachi *et al.*, 2022) and increases the amount of hemoglobin in submaximal exercise with arm cycling. It also improves oxygen consumption and heart rate during exercise (Gurney and Spendiff, 2020), and spirulina supplementation improves plasma lipid profile (Hernández-Lepe *et al.*, 2019b), maximal oxygen consumption and body composition in both young sedentary men and overweight obese individuals (Hernández-Lepe *et al.*, 2019a). However, the exact mechanism of spirulina in reducing exercise-induced oxidative stress and supporting exercise performance is not entirely clear, and there are some conflicting reports in the literature; no positive effects on plasma lipid peroxidation (Ferreira *et al.*, 2021), muscle damage and endurance capacity (Pappas *et al.*, 2021), and some metabolic parameters (Mohammad *et al.*, 2022). In this context, we evaluated the effects of spirulina on oxidative stress, antioxidant defense activity and endurance capacity due to acute exhaustive and chronic swimming exercise in this study. We aimed to clarify the utility of spirulina as a supplement to protect against exercise-induced oxidative stress.

2. Materials and Methods

2.1. Animals

Forty-eight healthy male Wistar strain albino rats (mean initial weight, 352 ± 27 g) were purchased from Selcuk University Experimental Medicine Research and Application Center. Rats were housed in polycarbonate/stainless steel cages (four rats/cage; base area, 1820 cm²) under controlled temperature ($20^\circ\text{C} \pm 2^\circ\text{C}$) and relative humidity ($50\% \pm 5\%$), with a 12-h/12-h light/dark cycle. Standard rat chow (Bilyem A.S. Ankara, Turkey) and tap water were provided ad libitum. All experimental procedures were approved by the Selcuk University Experimental Animals Local Ethical Commission.

2.2. Experimental Design and Supplementation

The 48 rats were randomly and equally divided into six groups. The study was organized to last for 6 weeks. All treatments were administered by oral gavage. The control group (C) received 2 mL/day tap water. Spirulina group (SP) was administered orally daily 750 mg/kg spirulina dissolved in tap water. Rats in the chronic exercise (CE) group were subjected to swimming exercise sessions in specially designed pools for 1 h/day for 5 days each week. Rats in the CE group also received 2-mL/day tap water. The chronic exercise + spirulina (CES) group was subjected to swimming exercise similar to the CE group, but unlike the CE group, the animals in this group were given 750 mg/kg/day spirulina. Rats in the exhaustion (E)

group received 2-mL/day tap water and performed exhaustive exercise on the last day of the study. The exhaustion + spirulina group (ES) received 750 mg/kg/day spirulina dissolved in tap water during the study period (6 weeks) and performed exhaustive exercise on the last day of the study. High-purity ($\geq 99\%$) Spirulina platensis powder was purchased from Egert Natural Products Ltd. (Bornova/Izmir). Spirulina, which was dissolved in cold tap water (10°C) using a magnetic stirrer, was freshly prepared before each administration.

2.3. Aerobic Exercise Procedure

We preferred swimming exercise to avoid prolonged exercise-induced muscle injury, electrical shock-stimulated exercise, plyometric contractions because these factors alone can provoke oxidative stress (Misra *et al.*, 2009). Endurance exercise was executed in temperature-controlled (30°C) pools ($120 \times 80 \times 80$ cm³). A maximum of four animals simultaneously swam in the same pool. The experiments were conducted at the same time each day. Chronic swimming exercise was performed for 60 min/day for 5 days each week over the course of 6 weeks. Rats were acclimatized for 3 consecutive days prior to testing sessions via swimming for 10, 20, and 30 min, respectively, on the 3 days.

2.4. Exhaustive Exercise Procedure

On the last day of the study, the swimming endurance time test was applied to evaluate the effects of Spirulina platensis on the exercise endurance of rats. Rats in groups E and ES were subjected to a single session of exhaustive exercise, and animals that were not able to keep their noses above water surface for more than 10 s or that lost motor coordination were considered to be exhausted (Buciolli *et al.*, 2011).

2.5. Sample Collection

Rats in the C and SP groups were sacrificed at the completion of treatment with tap water or spirulina. CE and CES rats were sacrificed 24 h after the last exercise session, and E and ES rats were sacrificed after exhaustion. In the course of the experiments, five rats (two SP rats, one CES rat, and two ES rats) died as a result of aspiration. Rats were anesthetized with ketamine/xylazine (60 mg/kg /10 mg/kg, i.p.). Cardiac blood (8–10 mL) was obtained from each animal via puncture and poured into EDTA-containing sterile tubes after confirming deep anesthesia. Plasma was acquired by cold centrifugation (NUVE NF 1200R) of blood at 3000 rpm for 10 min. Following exsanguination, the liver and skeletal muscle (gastrocnemius) were excised and gently washed with cold (4°C) distilled water to remove excess blood and residual tissue. Plasma and tissue samples were stored at -80°C (SANYO MDF-U5386S) until analysis.

2.6. Biochemical Analysis

The plasma activities of creatine kinase (CK), the MB isoform of CK (CK-MB), lactate dehydrogenase (LDH), and uric acid (UA) levels were analyzed using an autoanalyzer (Siemens Dimension EXL). CK, CK-MB, and LDH activities were expressed as U/L, whereas UA levels were expressed as mg/dL. MDA levels, XO, MPO, SOD, CAT, and GPx activities and antioxidant activity (AOA) were evaluated to assess tissue and plasma oxidative stress and antioxidant defense status. Tissue lipid

peroxidation was measured with a commercial assay kit, which measures TBARS, according to the manufacturer's instructions (Cayman Chemical Co., Ann Arbor, MI, USA). MDA levels were expressed as $\mu\text{mol/g}$ of wet tissue. Activities of XO, which is a generator of ROS, were measured using a commercial assay kit (Cayman Chemical) based on H_2O_2 production during hypoxanthine oxidation. Tissue and plasma XO activities were expressed as U/mg and $\mu\text{U/mL}$, respectively. The SOD, CAT, GPX, and AOA analyses were performed using commercial kits (Cayman Chemical) in accordance with the manufacturer's instructions. Tissue and plasma SOD activities were expressed as U/mg protein and U/mL, respectively. Tissue and plasma CAT and GPx activities were expressed as nmol/mg/min protein and nmol/mL/min, respectively. Tissue and plasma AOAs were expressed as mM/g and mM/mL, respectively. Tissue protein was measured by the Lowry method (Lowry *et al.*, 1951).

2.7. Statistical Analysis

The results were expressed as the mean \pm SD. The obtained data were subjected to one-way analysis of variance (ANOVA) and compared by Tukey's test, with $p < 0.05$ indicating significance, using SPSS.

3. Results

The initial weights of the animals were similar among the groups (one-way ANOVA, $p > 0.05$). The mean weight gain was 12.8% for spirulina-treated groups versus 12.5% for control groups. The smallest weight gain was observed in the CE group (3.8%), but there were no statistically significance differences in weight gain among the groups (one-way ANOVA, $p > 0.05$). The mean swimming time for the E and ES groups in the exhaustive swimming test on the final day of the study was 162 ± 8 and 164 ± 9 min, respectively. Despite the fact that the ES group had a longer swimming time, the contribution of spirulina supplementation was not statistically significant ($p > 0.05$).

Table 1 shows the effects of spirulina supplementation on plasma creatine kinase, CK-MB, and LDH activities, as well as UA levels, at the end of the six-week study. At the end of the study, there was no significant difference in plasma CK, CK-MB, LDH activities, or UA levels between the CON, SP, CE, and CES groups ($p > 0.05$). The exhausting swimming exercise performed on the rats in Group E and Group ES on the last day of the study caused an increase in plasma CK, CK-MB and LDH activities in the rats ($p < 0.05$). In addition, spirulina supplementation for 6 weeks caused a significant decrease in plasma CK activity ($p < 0.05$), which is the most important finding of our study. Plasma UA levels were found to be increased in E group compared to SP, CE and CES groups ($p < 0.05$).

Table 1. Effects of spirulina on biochemical parameters after swimming exercise challenge in the plasma.

	CON	SP	CE	CES	E	ES
CK (U/L)	220,50 \pm 127,26 ^{a,b}	239,67 \pm 104,69 ^{a,b}	161,38 \pm 50,13 ^{a,b}	268,17 \pm 183,98 ^{a,b}	963,57 \pm 342,69	610,33 \pm 222,69 ^b
CK-MB (U/L)	253,38 \pm 94,07 ^{a,b}	288,67 \pm 84,86 ^{a,b}	199,50 \pm 40,59 ^{a,b}	298,00 \pm 136,68 ^{a,b}	818,57 \pm 153,29	658,33 \pm 111,98
LDH (U/L)	128,63 \pm 59,77 ^{a,b}	113,83 \pm 34,12 ^{a,b}	96,88 \pm 19,93 ^{a,b}	159,50 \pm 125,03 ^b	366,57 \pm 122,57	293,17 \pm 121,69
UA (mg/dl)	0,70 \pm 0,71	0,45 \pm 0,08 ^b	0,38 \pm 0,07 ^b	0,38 \pm 0,04 ^b	1,26 \pm 0,43	0,82 \pm 0,27

Data are shown as means \pm S.D. CK= Creatin kinase, CK-MB= Creatin kinase-MB, LDH= Lactate dehydrogenase, UA= Uric acid.

^a $p < 0.05$ versus ES. ^b $p < 0.05$ versus E.

The effects of spirulina supplementation on liver and skeletal muscle MDA levels in animals subjected to chronic exercise are presented in Figure 1. Compared with the CON group, liver and muscle MDA levels were lower in the SP, CE, and CES groups ($p < 0.05$). Exhaustive exercise did not alter liver MDA levels (data not shown). The effect of chronic exercise on MPO activities in the liver, skeletal muscle, and plasma was not significant ($p > 0.05$, data were not shown). Nonetheless, it was discovered that XO activity in the liver tissue of chronically exercised rats (rats in the CE and CES groups) was increased compared to the CON group ($p < 0.05$, Table 2). We discovered that XO activity was lower in the CE group than in the CON and SP groups ($p < 0.05$) in skeletal muscle. Exhaustive exercise had no effect on plasma or skeletal muscle MPO and XO activities ($p > 0.05$), but it did reduce liver MPO and XO activities ($p < 0.05$).

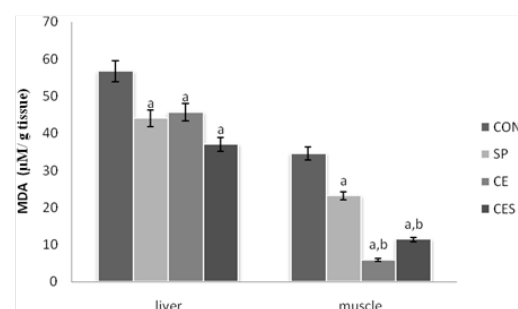


Figure 1. Effects of chronic exercise and spirulina supplementation on MDA concentrations in liver and muscle tissues. CON: control group; SP: spirulina treated group; CE: moderate, long-term exercised group; CES: exercise performed plus spirulina group. Data are expressed as mean \pm SD. ^a $p < 0.05$ versus CON. ^b $p < 0.05$ versus SP.

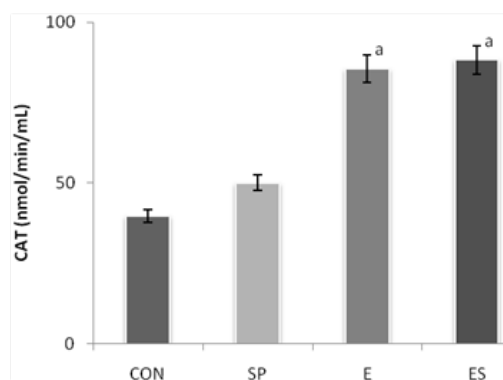
Table 2. Myeloperoxidase (ng/mg of protein) and xanthine oxidase (U/mg of protein) in liver and muscle tissues after exercise and spirulina supplementation.

		CON	SP	CE	CES	E	ES
MPO	Liver	54,48±15,58	57,40±10,68	41,38±15,03	36,59±16,70	28,58±11,64 ^{a,b}	23,16±6,46 ^{a,b}
	Muscle	12,54±2,29	13,95±7,30	9,55±2,34	12,53±4,83	10,03±2,63	6,80±5,78
XO	Liver	94,82±31,43	64,99±3,62	61,07±22,01 ^a	60,40±10,35 ^a	52,42±12,03 ^a	42,19±5,38 ^a
	Muscle	20,66±7,41	22,76±12,00	12,14±1,87 ^b	20,53±4,59	18,15±3,62	19,06±4,55

Data are shown as means±S.D. MPO= Myeloperoxidase,XO= Xanthine oxidase.

^a*p*<0.05 versus CON. ^b*p*<0.05 versus SP.

Changes SOD, CAT and GPx activities in liver and skeletal muscle were not significant in the chronic exercise groups (CE and CES groups) compared to the CON group (*p*>0.05). However, skeletal muscle AOA activity in the CE group was lower than in the CON group (*p*<0.05). Plasma CAT activities were found to be higher in E and ES groups compared to CON group (Figure 2, *p*<0.05). Plasma SOD activities were found to be statistically higher in CE and CES groups compared to SP group (*p*<0.05, Figure 3), while plasma GPx activities were observed to be lower in CES group compared to CON group (*p*<0.05). **The changes in SOD and GPx activities and AOA levels were not statistically significant (data not shown, *p*>0.05) in exhaustive exercised rats (E and ES groups).**

**Figure 2.** Effects of exhaustive exercise and spirulina supplementation on CAT activities in the plasma. CON: control**Table 3.** Effects of spirulina supplementation on hepatic antioxidant enzyme activities after exhaustive swimming exercise.

	SOD	CAT	AOA	GPx
CON	3,59±1,01	44,90±6,67	1,34±0,23	1,45±1,34
SP	3,55±1,30	43,70±9,94	1,23±0,27	1,19±1,10
E	2,05±0,61 ^{a,b}	32,92±6,49 ^{a,b}	0,88±0,31 ^a	1,14±0,74
ES	1,81±0,41 ^{a,b}	25,98±4,93 ^{a,b}	0,71±0,12 ^{a,b}	2,21±2,44

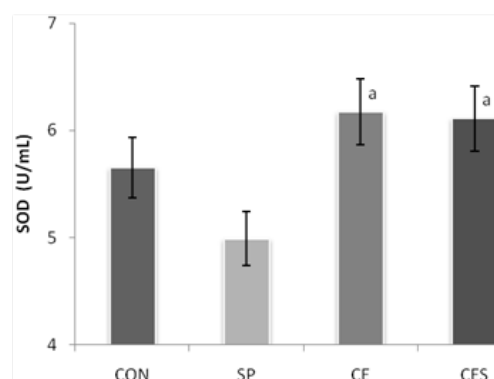
Data are shown as means±S.D. SOD (U/mg of protein)=Superoxide dismutase, CAT (nmol/min/mg of protein)=Catalase, AOA (mM/g tissue)=Antioxidant activity, GPx (nmol/min/mg of protein)=Glutathione peroxidase.

^a*p*<0.05 versus CON. ^b*p*<0.05 versus SP.

4. Discussion

The aim of the present study was to examine the effects of long-term/exhaustive exercise and spirulina intake on the oxidative status of plasma, liver tissue, and muscle tissue and endurance capacity in adult male rats. We found that exhaustive exercise alone increased the plasma activities of CK, CK-MB, and LDH. An important finding

group; SP: spirulina treated group; E: exhaustive swimming exercise group; CES: exhaustive swimming exercise performed plus spirulina group. Data are expressed as mean ± SD. ^a *p* <0.05 versus CON and SP

**Figure 3.** Effects of chronically exercise and spirulina supplementation on SOD activities in the plasma. Data are expressed as mean ± SD. ^a *p* <0.05 versus SP

SOD and CAT activities in liver tissue were found to be lower in the E and ES groups than in the CON and SP groups, and AOA levels were found to be lower only in the CON group (Table 3, *p*<0.05). The changes observed in skeletal muscle SOD, CAT and GPx activities and AOA levels after exhaustive exercise were not significant (data not shown, *p*>0.05).

of our study was that spirulina attenuated the exhaustive exercise-induced increment of CK activities in plasma. In addition, spirulina supplementation and acute or chronic exercise induced changes in antioxidant status and oxidative stress parameters. MDA levels, which are an end product of lipid peroxidation in the liver and skeletal muscle, were decreased by both spirulina supplementation and chronic exercise.

Although the influence of exercise on metabolism is well defined, the weight gain of exercised rats was not different from that of control rats. This finding is in concordance with previous studies (Lima *et al.*, 2013; Barcelos *et al.*, 2014). Thus, it can be suggested that swimming-based exercise has no major impact on the weight of rats, probably due to the intensity and duration of the exercise. In addition, 750 mg/kg/day (p.o.) spirulina supplementation for 6 weeks did not alter the weight of rats compared with that of the control animals. We could not locate any study in the medical literature that reports the direct effects of spirulina on body weight. However, there are several studies consistent with our findings that describe mechanisms by which spirulina influences weight (Khan *et al.*, 2006; Ismail *et al.*, 2009; Moura *et al.*, 2011). Therefore, in summary, it can be deduced that spirulina supplementation has no effect on the weight of rats. Moderate exercise or personal training programs improve pulmonary and cardiac function and decrease the incidence of chronic illness as a primary treatment while enhancing athletic performance (Pedersen and Saltin, 2006). Meanwhile, strenuous exercise has been demonstrated to provoke oxidative injury, particularly in skeletal muscle and the liver, as a result of free radical accumulation due to increased oxygen consumption (Huang *et al.*, 2009; Kan *et al.*, 2013). Modest amounts of ROS in tissues are essential for homeostatic harmony, but excess ROS production causes oxidative stress. There is bi-directional knowledge in the medical literature about exercise-induced ROS production. A study in laboratory animals revealed that prolonged moderate exercise reduces levels of MDA, which is widely accepted as a marker of oxidative stress (Viboolvorakul *et al.*, 2009). Thus the emergence of desirable adaptive responses to chronic exercise-induced oxidative stress is the most feasible explanation of the aforementioned decrement. Intermittent stimulation by modest amounts of ROS promotes exercise-related adaptations. In the present study, significant decreases in both liver and skeletal muscle MDA levels were noted (Figure 1). This result indicates that our exercise protocol is sufficient in intensity and duration to reverse the preoxidative status in skeletal muscle and liver tissues. In contrast, provocation of oxidative stress has been reported after regular exercise (Barcelos *et al.*, 2014). These diversities in study results may be associated with the usage of varying animal species or strains and the application of different exercise protocols primarily in terms of intensity and duration. Furthermore, in contrast to the aforementioned studies, a weight pendant (expressed as a percentile of body weight) was not attached to tails of swimming rats in our study. However, it is obvious that the increases in ROS and free radical generation in tissues as a result of acute/exhaustive exercise exceed the endogenous defense capacity and lead to oxidative stress, ultimately resulting in damage to multiple tissues. Exhaustive exercise increases whole-body oxygen consumption, resulting in increased electron escape from the mitochondrial transport system and disturbances of prooxidant-antioxidant homeostasis (Ji, 1999). Numerous animal studies reported an increase in lipid peroxidation, as evaluated by MDA levels, following exhaustive exercise (Huang *et al.*, 2009; Kan *et al.*, 2013). In our study, a single session of exhaustive exercise increased plasma activities of CK, which is frequently used for

assessing muscle injury, and previous studies suggested that elevated CK activities are associated with oxidative stress (Huang *et al.*, 2009; Kan *et al.*, 2013). In our study, we found that spirulina diet regimen ameliorated the exhaustive exercise-induced increase in plasma CK activity (Table 1, $p < 0.05$). Similarly, Lu *et al.* (2006) observed that the administration of 7.5 g/day spirulina for 3 weeks decreased CK activities by 28.77%, suggesting that the administered dose of spirulina in this study was adequate to protect against skeletal muscle injury after exhaustive exercise. A recent study of elite rugby athletes reported that muscle damage was prevented as a result of reduced plasma CK and LDH increases due to intense exercise with spirulina supplementation (Chaouachi *et al.*, 2022). However, in our study, despite this healing effect of spirulina against muscle damage, no significant difference was found between the groups in the endurance test performed on the last day ($p > 0.05$). Kalafati *et al.* (2010) reported that 6 g/day spirulina supplementation for 4 weeks did not significantly change serum CK activities compared with placebo in moderately trained men, but this supplementation increased the time to exhaustion. Consistent with this study, Franca *et al.* (2010) noted that 7.5 g/day spirulina administration to cyclists for 4 weeks did not induce a significant alteration in CK activities, and similar to our findings, did not exert an ergogenic effect. The variance of the results may be associated with the different training grades and exercise protocols used in the different studies.

Antioxidants are radical-scavenging molecules that prevent cellular damage caused by oxidative stress. Controversial results exist in the literature regarding the response of endogenous antioxidant defense mechanisms to exercise. This variance may be a consequence of the differences in exercise protocols used in the studies, as the response is dependent on the type, duration, and intensity of exercise. In the present study, plasma SOD activities were higher in the CE and CES groups than in the SP group (Figure 3). The lack of an increment of SOD activities in the SP group indicates that the stated effect of chronic exercise in the CES group is independent of spirulina. However, no change in CAT activities in the liver tissue was reported in a study utilizing a model of 4 weeks of moderate exercise, but the researchers noted a more significant decrease in CAT activities in the sedentary group following exhaustive exercise relative to that in trained subjects (Choi and Cho, 2007). Aydın *et al.* (2009) reported a decline in GPx and CAT activities after a single exercise session. Yu *et al.* (2012) observed a decrement of skeletal muscle SOD activities following exhaustive swimming exercise. Nevertheless, other studies noted an increment (Saborido *et al.*, 2011), maintenance (Caillaud *et al.*, 1999), or a decrement (You *et al.*, 2010) in SOD activities after exhaustive exercise. In our study, exhaustive exercise resulted in an augmentation of plasma CAT activities relative to the findings in the CON and SP groups (Figure 2). This effect was noted in both the E and ES groups. Taysi *et al.* (2008) reported a decline of CAT activities after exhaustive exercise in liver tissue, whereas Huang *et al.* (2009) stated that the levels of antioxidant enzymes such as SOD, GPx, and CAT were increased as a compensatory response to oxidative stress induced by exhaustive exercise in muscle tissue. However, no changes in the aforementioned enzyme activities in the liver and

kidneys were observed in that study (Huang *et al.*, 2009). In humans, spirulina supplementation did not alter GPx activities (Lu *et al.*, 2006), while this supplementation was associated with increased plasma SOD activities (Lu *et al.*, 2006) and GSH concentrations (Kalafati *et al.*, 2010), independent of exercise. The results of recent human and animal studies evaluating spirulina supplementation are conflicting. Three different doses of spirulina resulted in an improvement in antioxidant capacity and inflammation, as well as a dose-dependent decrease in lipid peroxidation assessed by MDA (Brito *et al.*, 2020), while in another animal study, it was reported that spirulina supplementation improved oxidative stress parameters and strengthened the antioxidant defense system of intestinal tissue in rats subjected to strength training (Araujo *et al.*, 2020). Furthermore, it was shown that the increase in the uterine tissue MDA level in female rats due to exercise was statistically reduced by spirulina supplementation, while spirulina improved the total antioxidant activity (Ferreira *et al.*, 2021). Spirulina supplementation was shown to improve body composition as assessed by free fat mass and immune system as assessed by IgA in overweight and obese women performing high-intensity interval training, but no positive contribution to exercise performance has been evaluated (Nobari *et al.*, 2022). Moreover, the contribution of spirulina to the metabolic functions of individuals with different physical characteristics is noteworthy in some recent studies. Spirulina supplementation has been reported to improve body composition, maximal oxygen consumption and plasma lipid profiles, especially in dyslipidemic obese men and overweight obese women; and spirulina supplementation has a synergistic effect with exercise on these parameters (Hernández-Lepe *et al.*, 2019a, 2019b). In order to fully explain the mechanism of these positive contributions reported in human studies, studies in experimental animals and tissue level analyses are significant. In this regard, our study is the first to demonstrate the effect of spirulina on plasma, liver and muscle tissue oxidative status, plasma muscle damage markers and endurance capacity due to regular and exhaustive swimming exercise in rats. However, the main limitations of our study include the fact that spirulina supplementation was not applied at different doses (less than or higher than 750 mg/kg), which could be more effective, and that some inflammation markers were not evaluated.

5. Conclusions

In conclusion, we suggest that *Spirulina platensis*, a blue-green alga and food supplement, ameliorates increases in plasma CK levels, which are a marker of exhaustive exercise-related muscular breakdown, probably by decreasing preoxidative MDA levels in skeletal muscle. However, it is apparent that spirulina supplementation in adult male rats had no positive effect on antioxidant activity and ergogenic status with our exercise protocol. Few studies have investigated the effects of spirulina supplementation on exercise-induced oxidative stress and exercise endurance capacity, and the mechanism by which spirulina alleviates oxidative stress during exercise is not yet well understood. Future studies are needed for satisfactory comprehension of the mechanism.

References

- Araujo LCC, Brito AF, Souza ILL, Ferreira PB, Vasconcelos LHC, Silva AS and Silva BA. 2020. Spirulina Platensis Supplementation Coupled to Strength Exercise Improves Redox Balance and Reduces Intestinal Contractile Reactivity in Rat Ileum. *Mar Drugs*, **18**(2): 89.
- Aydin C, Sonat F, Sahin SK, Cangul IT and Ozkaya G. 2009. Long term dietary restriction ameliorates swimming exercise-induced oxidative stress in brain and lung of middle-aged rat. *Indian J Exp Biol*, **47**: 24–31.
- Barcelos RP, Souza MA, Amaral GP, Stefanello ST, Bresciani G, Figuera MR, Soares FAA and Barbosa NV. 2014. Caffeine supplementation modulates oxidative stress markers in the liver of trained rats. *Life Sci*, **96**: 40–5.
- Blair SN, Cheng Y and Holder JS. 2001. Is physical activity or physical fitness more important in defining health benefits? *Med Sci Sports Exerc*, **33**: S379–99.
- Brito AF, Silva AS, de Oliveira CVC, de Souza AA, Ferreira PB, de Souza ILL, da Cunha Araujo LC, da Silva Félix G, de Souza Sampaio R, Tavares RL, de Andrade Pereira R, Neto MM and da Silva BA. 2020. Spirulina platensis prevents oxidative stress and inflammation promoted by strength training in rats: dose-response relation study. *Sci Rep*, **10**: 6382.
- Bucoli SA, de Abreu LC, Valenti VE, Leone C and Vannucchi H. 2011. Effects of vitamin E supplementation on renal non-enzymatic antioxidants in young rats submitted to exhaustive exercise stress. *BMC Complement Altern Med*, **11**: 133.
- Caillaud C, Py G, Eydoux N, Legros P, Prefaut C and Mercier J. 1999. Antioxidants and mitochondrial respiration in lung, diaphragm, and locomotor muscles: effect of exercise. *Free Radic Biol Med*, **26**: 1292–9.
- Chang WH, Chen CM, Hu SP, Kan NW, Chiu CC and Liu JF. 2007. Effect of purple sweet potato leaf consumption on the modulation of the antioxidative status in basketball players during training. *Asia Pac J Clin Nutr*, **16**: 455–61.
- Chaouachi M, Gautier S, Carnot Y, Guillemot P, Pincemail J, Moison Y, Collin T, Groussard C and Vincent, S. 2022. Spirulina supplementation prevents exercise-induced lipid peroxidation, inflammation and skeletal muscle damage in elite rugby players. *J Hum Nutr Diet*, **35**(6): 1151–1163.
- Choi EY and Cho YO. 2009. Effect of vitamin B(6) deficiency on antioxidative status in rats with exercise-induced oxidative stress. *Nutr Res Pract*, **3**: 208–11.
- Choi EY and Cho YO. 2007. The effects of physical training on antioxidative status under exercise-induced oxidative stress. *Nutr Res Pract*, **1**: 14.
- Davies KJ, Quintanilha AT, Brooks GA and Packer L. 1982. Free radicals and tissue damage produced by exercise. *Biochem Biophys Res Commun*, **107**: 1198–205.
- Ferreira PB, Diniz AFA, Lacerda Júnior FF, Silva MCC, Cardoso GA, Silva AS and da Silva B.A. 2021. Supplementation with Spirulina platensis Prevents Uterine Diseases Related to Muscle Reactivity and Oxidative Stress in Rats Undergoing Strength Training. *Nutrients*, **13**(11): 3763.
- Fisher-Wellman K and Bloomer RJ. 2009. Acute exercise and oxidative stress: a 30 year history. *Dyn Med*, **8**: 1.
- Franca GAM, Silva AS, Costa MJC, Moura Junior JS, Nóbrega TKS, Gonçalves MCR and Asciutti ISR. 2010. Spirulina does not Decrease muscle damage nor oxidative stress in cycling athletes with adequate nutritional status. *Biology of Sport*, **27**: 249–253.
- Gurney T and Spendiff O. 2020. Spirulina supplementation improves oxygen uptake in arm cycling exercise. *Eur J Appl Physiol*, **120**: 2657–2664.

- Hernández-Lepe MA, Olivas-Aguirre FJ, Gómez-Miranda LM, Hernández-Torres RP, Manríquez-Torres JJ and Ramos-Jiménez A. 2019a. Systematic Physical Exercise and Spirulina maxima Supplementation Improve Body Composition, Cardiorespiratory Fitness, and Blood Lipid Profile: *Correlations of a Randomized Double-Blind Controlled Trial. Antioxidants (Basel)*, **8(11)**: 507.
- Hernández-Lepe MA, Wall-Medrano A, López-Díaz JA, Juárez-Oropeza MA, Hernández-Torres RP and Ramos-Jiménez A. 2019b. Hypolipidemic Effect of Arthrospira (Spirulina) maxima Supplementation and a Systematic Physical Exercise Program in Overweight and Obese Men: A *Double-Blind, Randomized, and Crossover Controlled Trial. Mar Drugs*, **17(5)**: 270.
- Huang CC, Lin TJ, Lu YF, Chen CC, Huang CY and Lin WT. 2009. Protective effects of L-arginine supplementation against exhaustive exercise-induced oxidative stress in young rat tissues. *Chin J Physiol*, **52**: 306–15.
- Ismail MF, Ali DA, Fernando A, Abdraboh ME, Gaur RL, Ibrahim WM, Raj MHG and Ouhtit A. 2009. Chemoprevention of rat liver toxicity and carcinogenesis by Spirulina. *Int J Biol Sci*, **5**: 377–87.
- Ji LL. 1999. Antioxidants and oxidative stress in exercise. *Proc Soc Exp Biol Med*, **222**: 283–92.
- Kalafati M, Jamurtas AZ, Nikolaidis MG, Paschalis V, Theodorou AA, Sakellariou GK, Koutedakis Y and Kouretas D. 2010. Ergogenic and antioxidant effects of spirulina supplementation in humans. *Med Sci Sports Exerc*, **42**: 142–51.
- Kan NW, Huang WC, Lin WT, Huang CY, Wen KC, Chiang HM, Huang CC and Hsu MC. 2013. Hepatoprotective effects of Ixora parviflora extract against exhaustive exercise-induced oxidative stress in mice. *Molecules*, **18**: 10721–32.
- Khan M, Shobha JC, Mohan IK, Rao Naidu MU, Prayag A and Kutala VK. 2006. Spirulina attenuates cyclosporine-induced nephrotoxicity in rats. *J Appl Toxicol*, **26**: 444–51.
- Lima FD, Stamm DN, Della-Pace ID, Dobrachinski F, de Carvalho NR, Royes LFF, Soares FA, Rocha JB, González-Gallego J and Bresciani G. 2013. Swimming training induces liver mitochondrial adaptations to oxidative stress in rats submitted to repeated exhaustive swimming bouts. *PLoS One*, **8(2)**: e55668.
- Liu CC, Huang CC, Lin WT, Hsieh CC, Huang SY, Lin SJ and Yang SC. 2005. Lycopene supplementation attenuated xanthine oxidase and myeloperoxidase activities in skeletal muscle tissues of rats after exhaustive exercise. *Br J Nutr*, **94**: 595–601.
- Lowry OH, Rosebrough NJ, Farr AL and Randall RJ. 1951. Protein measurement with the Folin phenol reagent. *J Biol Chem*, **193**: 265–75.
- Lu HK, Hsieh CC, Hsu JJ, Yang YK and Chou HN. 2006. Preventive effects of Spirulina platensis on skeletal muscle damage under exercise-induced oxidative stress. *Eur J Appl Physiol*, **98**: 220–6.
- Minato K, Miyake Y, Fukumoto S, Yamamoto K, Kato Y, Shimomura Y and Osawa T. 2003. Lemon flavonoid, eriocitrin, suppresses exercise-induced oxidative damage in rat liver. *Life Sci*, **72**: 1609–16.
- Misra DS, Maiti R and Ghosh D. 2009. Protection of swimming-induced oxidative stress in some vital organs by the treatment of composite extract of Withania somnifera, Ocimum sanctum and Zingiber officinale in male rat. *Afr J Tradit Complement Altern Med*, **6**: 534–43.
- Mohammad M, Karim D, Mehdi M, Marziyeh S, Hadi S and Shila N. 2022. The Combinatory Effect of Spirulina Supplementation and Resistance Exercise on Plasma Contents of Adipolin, Apelin, Ghrelin, and Glucose in Overweight and Obese Men. *Mediators Inflamm*, **13**: 2022,9539286.
- Moura LP, Puga GM, Beck WR, Teixeira IP, Ghezzi AC, Silva GA and Mello MAR. 2011. Exercise and spirulina control non-alcoholic hepatic steatosis and lipid profile in diabetic Wistar rats. *Lipids Health Dis*, **10**: 77.
- Nobari H, Gandomani EE, Reisi J, Vahabdelshad R, Suzuki K, Volpe SL and Pérez-Gómez J. 2022. Effects of 8 Weeks of High-Intensity Interval Training and Spirulina Supplementation on Immunoglobulin Levels, Cardio-Respiratory Fitness, and Body Composition of Overweight and Obese Women. *Biology (Basel)*, **11(2)**: 196.
- Pappas A, Tsiokanos A, Fatouros IG, Poullos A, Kouretas D, Goutzourelas N, Giakas G and Jamurtas AZ. 2021. The Effects of Spirulina Supplementation on Redox Status and Performance Following a Muscle Damaging Protocol. *Int J Mol Sci*, **22(7)**: 3559.
- Pedersen BK and Saltin B. 2006. Evidence for prescribing exercise as therapy in chronic disease. *Scand J Med Sci Sports*, **16 Suppl 1**: 3–63.
- Powers SK and Jackson MJ. 2008. Exercise-induced oxidative stress: cellular mechanisms and impact on muscle force production. *Physiol Rev*, **88**: 1243–76.
- Saborido A, Naudí A, Portero-Otín M, Pamplona R and Megías A. 2011. Stanazolol treatment decreases the mitochondrial ROS generation and oxidative stress induced by acute exercise in rat skeletal muscle. *J Appl Physiol (1985)*, **110**: 661–9.
- Taysi S, Oztasan N, Efe H, Polat MF, Gumustekin K, Siktir E, Canakci E, Akcay F, Dane S and Gul M. 2008. Endurance training attenuates the oxidative stress due to acute exhaustive exercise in rat liver. *Acta Physiol Hung*, **95**: 337–47.
- Viboolvorakul S, Niimi H, Wongeak-in N, Eksakulkla S and Patumraj S. 2009. Increased capillary vascularity in the femur of aged rats by exercise training. *Microvasc Res*, **78**: 459–63.
- You Y, Kim K, Yoon HG, Lee KW, Lee J, Chun J, Shin DH, Park J and Jun W. 2010. Chronic effect of ferulic acid from Pseudosasa japonica leaves on enhancing exercise activity in mice. *Phytother Res*, **24**: 1508–13.
- Yu SH, Huang HY, Korivi M, Hsu MF, Huang CY, Hou CW, Chen CY, Kao CL, Lee RP, Lee SD and Kuo CH. 2012. Oral Rg1 supplementation strengthens antioxidant defense system against exercise-induced oxidative stress in rat skeletal muscles. *J Int Soc Sports Nutr*, **9(1)**: 23.

Jordan Journal of Biological Sciences

An International Peer – Reviewed Research Journal

Published by the Deanship of Scientific Research, The Hashemite University, Zarqa, Jordan



Name: الاسم:
 Specialty: التخصص:
 Address: العنوان:
 P.O. Box: صندوق البريد:
 City & Postal Code: المدينة: الرمز البريدي:
 Country: الدولة:
 Phone: رقم الهاتف:
 Fax No.: رقم الفاكس:
 E-mail: البريد الإلكتروني:
 Method of payment: طريقة الدفع:
 Amount Enclosed: المبلغ المرفق:
 Signature: التوقيع:
 Cheque should be paid to Deanship of Research and Graduate Studies – The Hashemite University.

I would like to subscribe to the Journal

For

- ☐ One year
☐ Two years
☐ Three years

One Year Subscription Rates

	Inside Jordan	Outside Jordan
Individuals	JD10	\$70
Students	JD5	\$35
Institutions	JD 20	\$90

Correspondence

Subscriptions and sales:

The Hashemite University
 P.O. Box 330127-Zarqa 13115 – Jordan
 Telephone: 00 962 5 3903333
 Fax no. : 0096253903349
 E. mail: jjbs@hu.edu.jo

المجلة الأردنية للعلوم الحياتية
Jordan Journal of Biological Sciences (JJBS)

<http://jjbs.hu.edu.jo>

المجلة الأردنية للعلوم الحياتية: مجلة علمية عالمية محكمة ومفهرسة ومصنفة، تصدر عن الجامعة الهاشمية وبدعم من صندوق دعم البحث العلمي والإبتكار – وزارة التعليم العالي والبحث العلمي.

هيئة التحرير

رئيس التحرير

الأستاذ الدكتورة منار فايز عتوم
الجامعة الهاشمية، الزرقاء، الأردن

مساعد رئيس التحرير

الدكتور مهند عليان مساعدة
الجامعة الهاشمية، الزرقاء، الأردن

الأعضاء:

الأستاذ الدكتور خالد محمد خليفات
جامعة مؤتة

الأستاذ الدكتور ليث ناصر العيطان
جامعة العلوم و التكنولوجيا الأردنية

الأستاذ الدكتورة طارق حسن النجار
الجامعة الأردنية / العقبة

الأستاذ الدكتور وسام محمد هادي الخطيب
الجامعة اليرموك

الأستاذ الدكتور عبد اللطيف علي الغزاوي
الجامعة الهاشمية

الأستاذ الدكتور نضال احمد عودات
جامعة البلقاء التطبيقية

فريق الدعم:

المحرر اللغوي

الدكتور شادي نعامنة

تنفيذ وإخراج

م. مهند عقده

ترسل البحوث الى العنوان التالي:

رئيس تحرير المجلة الأردنية للعلوم الحياتية
الجامعة الهاشمية

ص.ب , 330127 , الزرقاء , 13115 , الأردن

هاتف: 0096253903333

E-mail: jjbs@hu.edu.jo, Website: www.jjbs.hu.edu.jo



المملكة الأردنية الهاشمية



المجلة الأردنية



للعلوم الحياتية

مجلة علمية عالمية محكمة

تصدر بدعم من صندوق دعم البحث العلمي والابتكار



<http://jjbs.hu.edu.jo/>